

N71-20460

NASA CR-117351

NATIONAL AERONAUTICS AND SPACE ADMINISTRATION

*Technical Report 32-1460*

*Volume II*

*Mariner Mars 1969 Project Report*

*Performance*

**CASE FILE  
COPY**

**JET PROPULSION LABORATORY  
CALIFORNIA INSTITUTE OF TECHNOLOGY  
PASADENA, CALIFORNIA**

March 1, 1971

NATIONAL AERONAUTICS AND SPACE ADMINISTRATION

*Technical Report 32-1460*  
*Volume II*  
*Mariner Mars 1969 Project Report*  
*Performance*

JET PROPULSION LABORATORY  
CALIFORNIA INSTITUTE OF TECHNOLOGY  
PASADENA, CALIFORNIA

March 1, 1971



Prepared Under Contract No. NAS 7-100  
National Aeronautics and Space Administration

## Preface

The work described in this report was performed by the technical divisions of the Jet Propulsion Laboratory, under the cognizance of the *Mariner* Mars 1969 project.

This is Volume II of the three volumes that constitute the final report of the *Mariner* Mars 1969 project. The three volumes correspond, in chronological order, to the three principal activities of the project.

The preparation and preflight phase for the dual-spacecraft mission, *Mariners VI* and *VII*, from December 1965 through March 1969 is described in Volume I. The project management, planning, and mission analysis are presented in Part 1; the development, design, and testing of the spacecraft system and subsystems are detailed in Part 2; and the launch and Earth-based systems are covered in Part 3.

The conduct of the flight phase of the mission from February–March to October 1969 is presented in Volume II. A summary of the events of the entire flight phase and the flight-path report are given in Part 1; the launch phase is discussed in Part 2; and Part 3 covers the space flight phase, including details of spacecraft system and subsystem performance.

Postflight scientific analysis of the mission scientific data is given in Volume III. The project scientist's report is provided in Part 1 and some experimenters' interpretations are included in Part 2.

A comprehensive report of the tracking and data system support to the mission will be provided in a separate report.

## Acknowledgment

Various sections and contributions to this volume were prepared by, among others, the following:

L. A. Adams	H. J. Gordon	W. I. Purdy
W. N. Apel	D. Griffith	S. Reinbold
C. M. Ashley	L. Hershey	R. Rowley
J. Ball	R. Josephs	D. Schofield
D. L. Brunn	C. C. La Baw	J. P. Slonski
J. E. Campbell	D. W. Lewis	R. Spriestersbach
W. Chitty	J. C. Mahoney	M. Trubert
M. C. Clary	M. Mansour	J. H. Wilson
R. L. Crabtree	N. Medici	A. Wiltsey
G. E. Cunningham	D. Montgomery	J. Wolf
G. E. Danielson	B. Mulhall	S. K. Wong
T. Duxbury	J. A. Plamondon	

## **Contents**

### **Part 1. Mission**

<b>Introduction . . . . .</b>	<b>3</b>
<b>Mission Summary . . . . .</b>	<b>4</b>
<b>Flight Path/Navigation . . . . .</b>	<b>13</b>

### **Part 2. Launch Phase Performance**

<b>Mission Considerations . . . . .</b>	<b>63</b>
<b>Launch Operations . . . . .</b>	<b>66</b>
<b>Launch Vehicle Performance . . . . .</b>	<b>69</b>
<b>Spacecraft Dynamic Environment . . . . .</b>	<b>76</b>

### **Part 3. Space Flight Performance**

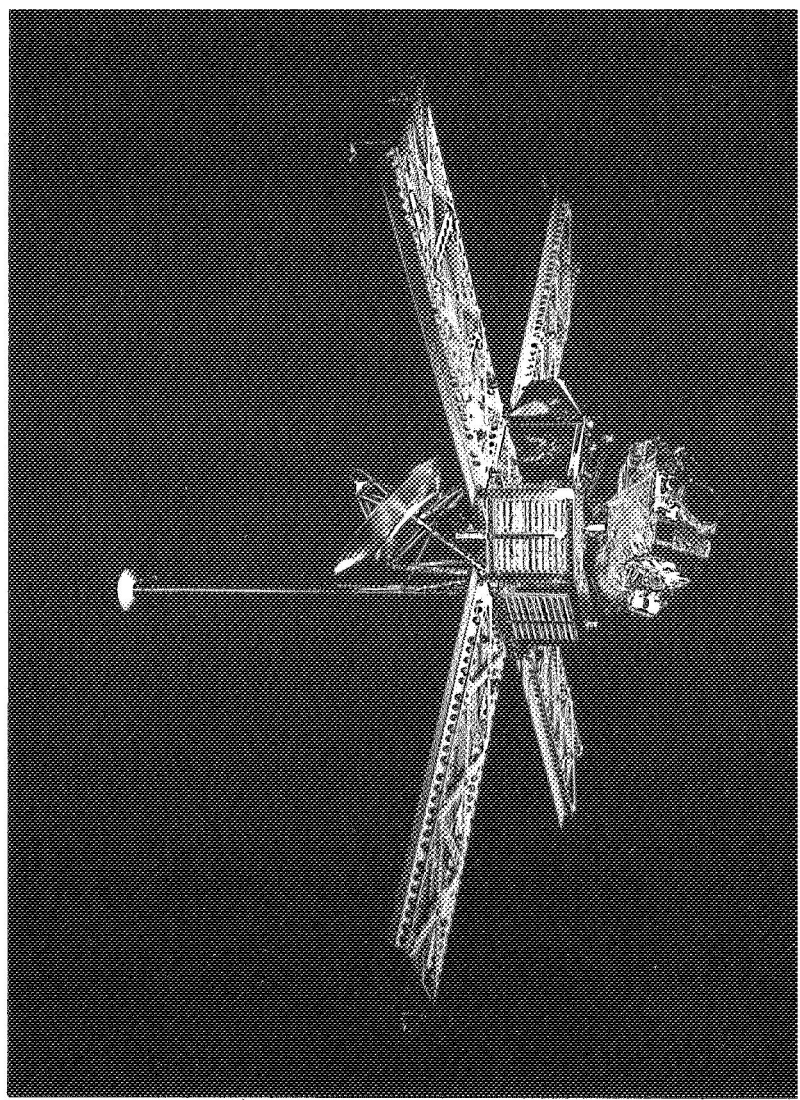
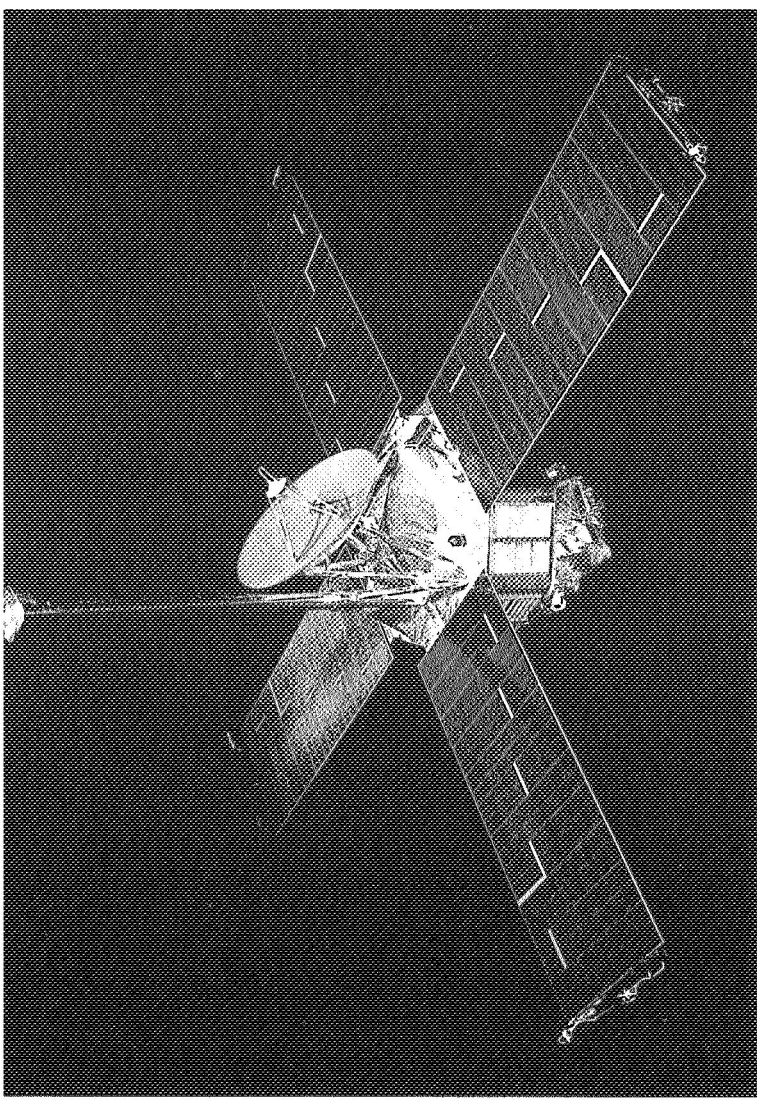
<b>Spacecraft System Performance . . . . .</b>	<b>87</b>
<b>Spacecraft Engineering Subsystem Performance . . . . .</b>	<b>127</b>
<b>Scientific Instrument Performance . . . . .</b>	<b>279</b>
<b>Glossary . . . . .</b>	<b>311</b>

## Abstract

This second of three volumes of the *Mariner* Mars 1969 Project Report describes the performance of the mission by flight and Earth-based elements during the launch and space flight phases. The first volume describes the pre-operational activities, including planning, development and design, manufacture, and testing; the third volume deals with the scientific program, including experiment results.

The dual-spacecraft (*Mariners VI and VII*) Mars flyby mission was successfully conducted according to plan. A number of flight anomalies were observed, including a major incident involving the *Mariner VII* spacecraft shortly before its Mars encounter, but these difficulties were overcome. The performance of all elements was generally excellent, and copious scientific data were returned to the Earth, including television pictures, ultraviolet and infrared spectral data, surface-temperature measurements, and other information.

The flight performance of each element is analyzed, problems are discussed, and recommendations based on the experience are presented.



## Part 1. Mission



## Introduction

The *Mariner* Mars 1969 mission consisted of the launch, transit, and flyby encounter of two identical spacecraft between February and August 1969. This dual spacecraft (designated *Mariner VI* and *Mariner VII*) mission to the planet Mars was both for furthering scientific investigations and space technology capabilities.

The scientific operations planned for the mission were concentrated upon study of the planet Mars, except for the celestial mechanics experiment, which analyzed navigation data in an examination of the gravitational fields through which the spacecraft passed. The Mars encounter sequences, which included long-range television observation and multiple close-range surface scans, were programmed into the spacecraft computers before launch, but could be—and were—modified by reprogramming during flight.

The dual mission, as successfully flown, returned many times more scientific data on the planet than had been conceived at the inception of the *Mariner* Mars 1969 project. (The scientific program, results, and interpretations are discussed in Volume III of the project

report.) In addition, they provided ample demonstration of the on-board programmable computer, the large two-degree-of-freedom scan platform, the high-rate telemetry link, and other design features and operational techniques that were used for the first time in this mission and exhibited great potential for future planetary flights.

The performance shown in this dual mission and described in this report was of generally high caliber, not because no difficulties occurred, but because none remained unsolved.

The *Mariner VI* and *Mariner VII* flights were conducted virtually simultaneously; actually they were interlaced, with corresponding critical events scheduled apart (the launches were separated by 31 days, the Mars encounters by 5 days) to facilitate the operational task and provide time to respond to anomalies. The specific flight events, navigation, and performance of both spacecraft are discussed together in this volume, except for those events that occurred separately or did not interlace, such as the launch phase.



## Mission Summary

The two spacecraft were launched February 25 and March 27, respectively, from Cape Kennedy aboard two *Atlas/Centaur* vehicles, and flew within approximately 3430 km of the surface of Mars on July 31 and August 5, then continued in solar orbit. Mars mission operations were formally terminated November 1, 1969 with both spacecraft still operating and with an extended mission, based on a new scientific experiment, already underway. This is the report of the dual Mars mission.

The principal postlaunch operations were completed on *Mariner VI* before the launch of *Mariner VII*, to provide for last-minute spacecraft modifications if necessary; this did not prove to be the case, however.

Both launches were entirely successful and highly accurate, requiring very small spacecraft thrust maneuvers to take out the injection bias and bring the flyby points to the selected target regions. *Mariner VI* was to fly close to the equator, permitting observation of the varied light and dark features near Meridiani Sinus; *Mariner VII* was targeted further south, to allow for scanning down as far as the south polar cap.

The Earth–Mars transit phase between the completion of the postlaunch activities and the beginning of pre-encounter preparations had been expected to be relatively inactive, in view of the lack of inflight scientific operations. However, a number of minor performance or design anomalies, and the need to respond to

these, resulted in the maintenance of a moderate level of activity throughout the period. The general soundness and flexibility of the spacecraft design, together with the ingenuity of the operations team, made it possible to overcome these difficulties and complete the dual mission in spite of them.

On July 29, the *Mariner VI* encounter sequence began when the spacecraft scan platform pointed the instruments at the distant planet Mars and imaging and other scientific data acquisition started. Some data were returned to the Earth in real-time over the high-rate telemetry link; television pictures were recorded aboard the spacecraft and played back, at high rate, at the end of each day.

During the second day of the *Mariner VI* far-encounter operations, the *Mariner VII* spacecraft suffered a major anomaly, sustaining temporary and permanent damage and losing telecommunications contact with the Earth three times. Again, however, the problems could be solved or worked around, and the *Mariner VII* encounter sequence was successfully conducted shortly afterward.

After acquiring and returning to the Earth many images and other observations in the far-encounter phase, each spacecraft received final reprogramming and carried out a complex near-encounter sequence, observing surface regions and features agreed upon by the

scientific investigators. The *Mariner VII* near-encounter was redesigned and reprogrammed to increase the polar cap coverage at the request of the investigators on the basis of data returned by *Mariner VI*.

After the instrument fields of view had moved off the planet, each spacecraft passed behind Mars (as seen from the Earth) to conduct the S-band occultation experiment, and, in the subsequent days, repeatedly played back the stored records of near-encounter observation.

The flight events of *Mariners VI* and *VII* are shown, in parallel to permit comparison, in Table 1. Since the

flight sequences were considered separately, had been designed and tested separately, and were to a large extent governed by the contents of separate spacecraft computer and sequencer subsystems, the chronological listings of events in Table 1 are given in a separate column for each spacecraft flight with common discussions or comments.

It should be noted that the maneuver and scan-platform unlatch of *Mariner VI* were conducted closer to launch than those of *Mariner VII*. This timing was deliberately planned so that these activities could be cleared before the second launch and to permit, if necessary, holding the launch for hardware changes based on experience with the first spacecraft.

**Table 1. *Mariner* Mars 1969 flight chronology**

Event	<i>Mariner VI</i>		<i>Mariner VII</i>		Comment
	Date (1969)	Time, GMT <sup>a</sup>	Date (1969)	Time, GMT <sup>a</sup>	
Launch	Feb 25	01:29:02	Mar 27	22:22:01	Liftoff
Mark 1, Atlas BECO <sup>b</sup>		01:31:33.2		22:24:31	
Mark 2, Atlas booster jettison		01:31:36.2		22:24:34	
Mark 3, insulation jettison		01:32:18.9		22:25:16	
Mark 4, nose fairing jettison		01:32:54.6		22:25:53	
Mark 5, Atlas SECO <sup>c</sup> /VECO <sup>d</sup>		01:33:33.2		22:26:16	
Mark 6, Atlas/Centaur separation		01:33:40.0		22:26:18	
Mark 7, Centaur main engine start		01:33:48.9		22:26:27	
Injection (Mark 8, Centaur MECO <sup>e</sup> )		01:41:11.6		22:33:53	Very accurate injections of both spacecraft
Spacecraft separation (Mark 9)		01:42:43		22:35:28	Separation rate from spacecraft: 0.7 m/s
Launch-phase spacecraft anomalies		—		—	<i>Mariner VI</i> : low-gain antenna drive drops at 01:43:02, 02:23:08; RF lock anomalies 19:19:42–19:48:57. <i>Mariner VII</i> : low-gain antenna drive drops at 22:26:50, returns 22:35:56; anomalous CC&S <sup>f</sup> readout 22:35:28–22:37:27; Canopus tracker Sun shutter closed (properly) 22:34:32–22:35:48; 11-W 2.4-kHz power spike at 22:39:26
Earth-shadow passage					<i>Mariner VI</i> launched in Earth shadow
Entry		—		22:38:27	
Exit		01:55:12		23:12:45	
Solar panels deployed		01:46:45		22:39:22	
<sup>a</sup> Received times at Earth; spacecraft event and command receipt shown at receipt of telemetry. <sup>b</sup> BECO = booster engine cutoff. <sup>c</sup> SECO = sustainer engine cutoff. <sup>d</sup> VECO = vernier engine cutoff. <sup>e</sup> MECO = main engine cutoff. <sup>f</sup> CC&S = central computer and sequencer.					

Table 1 (contd)

Event	Mariner VI		Mariner VII		Comment
	Date (1969)	Time, GMT <sup>a</sup>	Date (1969)	Time, GMT <sup>a</sup>	
<i>Centaur</i> retromaneuver					
Mark 10, begin reorientation	Feb 25	01:47:17	Mar 27	22:40:01	
Mark 11, begin blowdown		01:55:24		22:48:04	
DSS 51 initial acquisition		01:55:13		22:45:02	
DSS 62 initial acquisition	Mar 12	03:23:00		22:40:39	
Sun acquisition by spacecraft	Feb 25	01:58:35		23:14:33	
Initial roll-reference star acquisition		05:42:20	Mar 28	02:18:01	<i>Mariner VI</i> acquired Canopus; <i>Mariner VII</i> acquired Vega
DSS 12 initial acquisition		10:18:00		05:40:00	
DSS 41 initial acquisition		14:23:15		10:58:09	
<i>Mariner VII</i> roll search and Canopus acquisition			Apr 1	16:47:07 16:57:03	DC-21 command
Initial ranging on		03:04:56		19:56:06	DC-9 command
<i>Mariner VII</i> CC&S checkout sequence				17:32:07	Coded command word to clear flags, memory check; command word to revise executive program. Second memory check. Sequence completed 19:03:12
Battery charger off	Mar 1	02:21:03	Apr 4	18:46:13	DC-38 command (charger on at launch)
Maneuver sequence					
Roll reference change			Apr 8	15:46:25	DC-21 command; <i>Mariner VII</i> acquired Sirius at 15:48:11 as planned
Maneuver parameters loaded	Feb 28	20:20:04		16:51:25	20 coded commands; sequence took 20 min
CC&S memory verified		21:08:16		17:03:30	
Maneuver enabled		22:21:34		18:26:25	DC-14 command
Maneuver start		23:19:44		18:52:38	DC-27 command
Pitch turn	Mar 1	00:27:59— 00:30:09		20:00:55— 20:04:09	CC&S commands
Roll turn		00:38:41— 00:46:15		20:12:14— 20:13:51	CC&S commands
Motor burn		00:54:48— 00:54:53		20:22:23— 20:22:31	CC&S commands; bright particles observed
Reacquisition initiated		01:03:24		20:31:03	CC&S commands
Sun acquired		01:05:13		20:33:16	
Star acquired		01:10:50		20:44:15	<i>Mariner VI</i> acquired Canopus, <i>Mariner VII</i> acquired Vega
Roll search and Canopus acquisition				21:01:22 21:12:35	DC-21 command
Maneuver inhibit sequence	Mar 1	01:46:06— 01:48:04		21:31:24— 22:01:26	Minimum-effect maneuver loaded; maneuver inhibit (DC-13) and tandem maneuver (DC-33) commanded (not until Mar 4 on <i>Mariner VI</i> )
<i>Mariner VI</i> Canopus tracker	Mar 1	01:40:43		—	
Brightness transients	Mar 4	11:46:24		—	

Table 1 (contd)

Event	Mariner VI		Mariner VII		Comment
	Date (1969)	Time, GMT <sup>a</sup>	Date (1969)	Time, GMT <sup>a</sup>	
Mariner VI scan platform unlatch commanded	Mar 6	19:11:47		—	DC-45 command; squib fired
Canopus lock lost		19:12:25		—	Apparently caused by bright particles (up to 8 × Canopus); Canopus reacquired at 19:37:50
Platform unlatched		19:15:55		—	Anomalous delay from receipt of command (30–60 s expected)
DSS 14 initial acquisition	Mar 18	10:08:28	Apr 1	08:58:00	
Mariner VI radio self-lock anomaly	Mar 19– Mar 22	00:46:40		—	Sporadic occurrences individually solved by uplink power application or when ranging turned off
Mariner VII ranging anomalies and tests		—	Apr 21– Apr 25	17:45:00	Ranging channel performance found to be 5–7 dB below predicts. Receiver AGC <sup>§</sup> erratic (Apr 24)
Near-Earth ranging ended	Mar 19	06:25:44		17:18:54	CC&S Y1 command following last DC-9. Mariner VII ranging ended earlier than predicted because of reduced receiver sensitivity
Canopus cone angle to position 3	Mar 23	22:25:52	(prelaunch)		Mariner VI cone angle stepped by CC&S C1 command
Mariner VII scan unlatch (inertial)		—	May 8	15:27:48– 20:19:22	20 coded commands plus direct commands set inertial mode, platform unlatched by CC&S C5 command
Inertial encounter sequence loaded, encounter parameters updated	Apr 18	12:02:29– 14:15:50	May 9	16:32:15– 19:55:04	Two quantitative commands, 28 coded commands, direct commands, CC&S memory readout
Canopus cone angle to position 4	Apr 20– May 3	22:26:43– 23:28:09	Apr 21	01:18:44	CC&S C1, Mariner VII responded normally, Mariner VI stepped anomalously to position 2; 3 DC-17 commands toggled between positions 2 and 3. Gyro drift test, Apr 28–30. Following extensive commanded operations Apr 30–May 3, in attempt to find and hold alternate sources (Large Magellanic cloud, etc.), second DC-17 sequence initiated, position 4 achieved, Canopus reacquired
Encounter updates for Magellanic cloud as roll reference, etc.	Apr 30	19:47:56– 21:20:09		—	Quantitative command, 45 coded commands, CC&S memory readout (corrected after solution of cone-angle problem)
Mariner VII receiver tests		—	May 12– May 22	14:32:00	Threshold tests from DSSs 41, 62, 51; command threshold 7 dB lower than predicted. Testing continued for several days
Canopus cone angle to position 5	May 26	21:28:09– 23:51:21	May 29	23:34:11	Mariner VII stepped by DC-17 command. Mariner VI CC&S issued C1, angle stepped anomalously to position 3; Canopus lock lost. Eight DC-17

<sup>§</sup>AGC= automatic gain control.

Table 1 (contd)

Event	Mariner VI		Mariner VII		Comment
	Date (1969)	Time, GMT <sup>a</sup>	Date (1969)	Time, GMT <sup>a</sup>	
Canopus cone angle to position 5 (contd)					commands cycled angle through all steps to position 5; DC-18 placed spacecraft in roll inertial hold, DC-19 removed inertial hold, Canopus acquired on May 27 at 00:11:11
Encounter parameter update, TV-AAC <sup>b</sup> reprogramming	Jun 5	19:34:03– 23:15:04	May 27	19:23:58– 20:46:14	Many coded commands, CC&S memory readout
Spacecraft traveling-wave tube amplifier to high power	Jun 16	19:36:01	Jun 9	19:05:03	DC-42 command. CC&S C2 (bit rate change to 8 1/3) deleted because of high-power performance
Planetary ranging test	Jun 26	14:54:12– 21:30:08	Jun 20– Jun 27	17:56:14	Ranging turned on and off with DC-9, conditions checked, terminated with Y1 command
DSS 11 first tracking pass	Jun 17	01:18:10	Jul 24	23:46:51	DSN <sup>1</sup> encounter configuration checkout
Planetary ranging begun	Jul 7	01:08:17	Jul 8	00:48:09	DC-9 command at beginning of pass, ranging turned off by CC&S Y1 command after each pass
Radio to high-gain antenna	Jul 10	21:31:06	Jul 7	19:22:40– 20:38:06	CC&S C3; Mariner VI responded normally, Mariner VII did not switch, DC-11 command switched antennas. Mariner VII C1 source driver failure deduced; all encounter-sequence programming nullified
Encounter sequence update, etc.		—	Jul 8	02:00:55– 04:58:08	160 coded commands, quantitative command
Pre-encounter data-storage/HRT <sup>1</sup> test sequence	Jul 12	02:01:57– 05:27:59	Jul 9	01:56:13– 05:37:17	Many direct commands, tape playback over channels B and C to DSS 14 (CTA-21 <sup>k</sup> , in Pasadena) ATR <sup>1</sup> erased and verified by playback; CC&S clock check
	Jul 15	06:31:33– 08:22:59	Jul 15	00:44:00– 03:49:01	
CC&S checkout after C1 driver failure of Jul 8	Jul 15	08:25:22– 08:53:35	Jul 9	05:48:17– 05:30:37	Coded commands transmitted, CC&S events monitored; Mariner VI CC&S fully functional, Mariner VII problem only in C1 driver logic. Mariner VII reprogrammed in view of failure. Minor operational difficulties in taking CC&S readout (Jul 15)
	Jul 25	19:50:47– 21:25:46	Jul 10	00:59:03– 05:44:15	
			Jul 15	02:26:31– 05:17:40	
			Jul 26		
Pre-encounter battery conditioning					
Battery charger cycled	Jul 23	06:25:28– 06:40:28	Jul 25	04:00:21– 04:15:24	DC-38 command toggles charger on/off; DC-50 toggles test load in/out. Mariner VI charge cycle normal. Mariner VII abnormal
Battery test load in circuit		07:18:15– 17:49:41		04:29:50– 18:55:08	
Battery charge cycle	Jul 29	18:10:28– 00:56:14	May 1	19:10:28– 07:01:26	
<sup>b</sup> AAC = automatic aperture control. <sup>1</sup> DSN = Deep Space Network. <sup>1</sup> HRT = high-rate telemetry link. <sup>k</sup> CTA-21 = compatibility test area. <sup>1</sup> ATR = analog tape recorder.					

Table 1 (contd)

Event	Mariner VI		Mariner VII		Comment
	Date (1969)	Time, GMT <sup>a</sup>	Date (1969)	Time, GMT <sup>a</sup>	
Mariner VI pre-encounter reprogramming	Jul 25 Jul 26	21:35:47— 01:03:04		—	
Mariner VII major anomaly					
Battery-charge current fluctuations		—	Jul 26 Jul 31	14:12:00— 05:25:21	
Last good engineering telemetry			Jul 30	22:10:58.45	Many abnormal readings, etc., until loss of signal
Spacecraft signal level drops				22:11:10	Drops from -140.5 to -166.5 dBm in 40 s
Ground receiver out of lock (DSS 51)				22:11:41.3	Intermittent weak periodic signals for next 7 h
First antenna-switch command			Jul 31	05:10:00	DC-10 transmitted from DSS 11; arrives at spacecraft 5 min 37 s later
Acquisition by ground receiver (DSS 41)				05:21:15	DSS 11 acquisition 8 s later; velocity change indicated
Telemetry acquisition (DSS 41)				05:25:21	Spacecraft functioning, many anomalies indicated
DSS 11 receiver out of lock				06:33:25	Ground receivers in and out of lock for next 1/2 h
Loss of engineering data				06:36:27	Data returns 07:43:01, many anomalies indicated
Roll search				09:56:16	Repeated DC-21 commands, acquisitions; Canopus acquired 11:38:01
Tests and engineering checkout			Aug 1	05:00:00— 23:26:31	CC&S readout, various modes tested
Scan recalibration			Aug 2	00:21:33— 07:04:58	Direct, quantitative commands, two analog TV frames to position camera
CC&S operation checkout and far-encounter reprogramming			Aug 2	07:26:32— 08:43:49	Coded commands, CC&S memory readout
Far-encounter					
Science on	Jul 29	01:27:40	Aug 1	22:24:01	DC-25 command, followed by near-, far-encounter check. Sequence initiated early on Mariner VII for scan recalibration sequence
Far-encounter initiated		04:55:47	Aug 2	09:11:36	DC-32, DC-13 commands; CC&S initiates sequence C for Mariner VI, sequence D for Mariner VII
First TV picture		05:32:40		09:37:35	CC&S F2
HRT real-time science data, channel C (encounter II data mode)	Jul 29	03:35:16— 08:26:17	Aug 2	23:16:41— 01:05:41	DC-44 on, DC-3 off. Mariner VII also in encounter II for scan recalibration (above). TV (every seventh bit), IRR <sup>m</sup> , UVS <sup>n</sup> data via HRT to DSS 14
First ATR/HRT far-encounter playback	Jul 30	01:36:22— 04:28:05	Aug 3	01:05:41— 03:59:47	DC-3, DC-44 commands; ATR playback to DSS 14; ended by DC-25 (backed up by CC&S N1)
<sup>m</sup> IRR = infrared radiometer. <sup>n</sup> UVS = ultraviolet spectrometer.					

Table 1 (contd)

Event	Mariner VI		Mariner VII		Comment
	Date (1969)	Time, GMT <sup>a</sup>	Date (1969)	Time, GMT <sup>a</sup>	
Near-encounter sequence/slew update, <i>Mariner VI</i>	Jul 30	01:56:24— 02:38:36	Aug 3	—	12 coded commands, two CC&S memory readouts during playback
ATR erase cycles		04:53:26— 05:38:48		04:56:41— 05:04:40	DC-39 on CC&S F3. Starts cycle, AEOT <sup>o</sup> ends it. Two cycles
HRT real-time science data, channel C (encounter II data mode)		04:34:28— 08:26:27		04:55:43— 07:33:42	DC-44 on, DC-44 off. Science data via HRT to DSS 14 (CTA-21, TV-1 <sup>p</sup> )
Second-day far-encounter recording sequence initiated		05:16:28		05:28:41	DC-32, DC-13 commands; sequence B for <i>Mariner VI</i> , sequence C for <i>Mariner VII</i>
HRT real-time science data, channel C (encounter II data mode)	Jul 30— Jul 31	23:00:31— 01:01:33	Aug 4	23:16:48— 02:24:49	DC-44 on, DC-3 off; science data via HRT to DSS 14 (CTA-21, TV-1)
Second ATR/HRT far-encounter playback	Jul 31	01:01:33— 02:27:56		02:24:49— 05:18:47	DC-3, DC-44 commands; ATR playback to DSS 14 ended (CTA-21, TV-1); by DC-25 (backed up by CC&S N1)
Far-, near-encounter sequence update, <i>Mariner VII</i> ; near-encounter expanded, third day far-encounter re-timed		—		02:31:47— 04:44:04	60 coded commands, two CC&S memory readouts
Near-encounter angle update, <i>Mariner VII</i>				06:31:52— 06:36:50	Two quantitative commands (platform angle references) during playback
ATR erase cycles	Jul 31	02:44:36— 02:50:37	Aug 4	05:30:49— 05:45:02	DC-39 on starts cycle, AEOT ends it. Two cycles
HRT real-time science data, channel C (encounter II data mode)	(See near-encounter sequence below)			05:25:51— 07:36:54	DC-44 on, DC-44 off. Science data via HRT to DSS 14 (CTA-21, TV-1)
Third-day far-encounter recording sequence initiated		—		05:51:49	DC-32, DC-13 commands. Modified sequence B, <i>Mariner VII</i> ( <i>Mariner VI</i> far-encounter completed)
HRT real-time science data, channel C (encounter II data mode)		—	Aug 5	23:16:58— 00:13:53	DC-44 on, DC-3 off. Science data via HRT to DSS 14
Third ATR/HRT far-encounter playback		—		00:13:53— 02:24:35	DC-3, DC-44 commands; ATR playback to DSS 14 ended, by DC-25 (backed up by CC&S N1)
ATR erase cycle		—		02:30:57— 03:50:37	DC-39/CC&S F3 starts cycle, AEOT ends it; two cycles
Final near-encounter sequence/slew updates		01:11:33— 01:53:43		00:57:50— 03:53:00	Coded, quantitative commands for <i>Mariner VII</i> , CC&S, memory readout, during final far-encounter playback
Far-encounter ended, near-encounter started		02:27:56		02:24:52	Last far-encounter playback ended (by DC-25 for <i>Mariner VI</i> , CC&S N1 for <i>Mariner VII</i> )
Near-encounter (overlapping playback from far-encounter)					
HRT real-time science data, channel C (encounter II data mode)		02:34:35— 05:42:41		02:25:59— 05:21:43	DC-44 command

<sup>o</sup>AEOT = analog end of tape.<sup>p</sup>TV-1 = picture processing area.

Table 1 (contd)

Event	Mariner VI		Mariner VII		Comment
	Date (1969)	Time, GMT <sup>a</sup>	Date (1969)	Time, GMT <sup>a</sup>	
Inertial-hold attitude control	Jul 31	03:32:49	Aug 5	02:00:59	CC&S M2 (three axis inertial) for Mariner VI, DC-18 (roll-axis inertial) for Mariner VII
TV camera A cover deployed	Jul 29	06:06:16		02:36:56	DC-46 command, backed up by CC&S N7. Cover deployed at start of far-encounter for Mariner VI
IRS <sup>a</sup> cooldown and encounter enabled	Jul 31	04:39:36		03:42:00	DC-26 command, backed up by CC&S N6. Sensors and data automation subsystem near-encounter sequence enabled
IRS cooldown start				04:20:39	DC-49 command, backed up by sensor NAMG-1. This is the only irreversible encounter event. Mariner VI cooldown unsuccessful
Near-encounter recording starts		05:10:10		04:45:42	Sensor NAMG-2 (backed up by DC-16 commands) for Mariner VI, DC-16 command for Mariner VII
First slew by scan platform		05:15:31		04:51:39	CC&S N3 commands after eighth picture shuttered on Mariner VI, after ninth on Mariner VII
Second slew by scan platform		05:19:01		04:59:26	CC&S N3 and N4 commands (backed up by DC-41). After thirteenth picture for Mariner VI, after twentieth for Mariner VII
Third slew by scan platform		05:21:49		05:04:24	CC&S N3 and N4 commands. After seventeenth picture for Mariner VI, after twenty-seventh for Mariner VII (clock slew)
Closest approach to Mars (Earth observed)		05:24:26		05:06:26	
Analog recording stopped		05:22:19		05:10:25	CC&S N4 for Mariner VI, fourth end-of-tape for Mariner VII
Fourth slew by scan platform		05:32:23		05:11:27	CC&S N3 and N4 commands. No pictures
Digital recording stopped		05:34:46		05:10:04	Fourth end-of-tape, backed up by CC&S N9
Occultation behind Mars		05:39:52– 05:59:42		05:19:35– 05:49:12	Communications (command and telemetry) cut off. Experimental data taken at entry and emergence
Digital tape playback begins (playback 1 mode, during occultation)		05:42:41		05:21:43	CC&S P2 (assumed time)
Science preconditioned for turn-off		07:10:36		06:23:34	DC-48 command
Science turned off		09:32:51		06:29:02	CC&S N5 for Mariner VI, DC-1 command for Mariner VII
Attitude control on sensors		12:32:50		08:09:00	CC&S M1 and M2 for Mariner VI; DC-19 for Mariner VII. Canopus reacquired normally by both
HRT playback of near-encounter pictures	Aug 1	00:37:43– 05:51:45	Aug 6	00:29:57– 06:11:09	DC-44 commands. Two full playbacks of analog tape recorder, interrupting

<sup>a</sup>IRS = infrared spectrometer.



Table 1 (contd)

Event	Mariner VI		Mariner VII		Comment
	Date (1969)	Time, GMT <sup>a</sup>	Date (1969)	Time, GMT <sup>a</sup>	
HRT playback of near-encounter pictures (contd)					digital playback. Two more playbacks conducted Aug 6-7 ( <i>Mariner VII</i> ) and Aug 7-8 ( <i>Mariner VI</i> ); two more conducted on <i>Mariner VI</i> Aug 9-10
<i>Mariner VI</i> to cruise mode for <i>Mariner VII</i> encounter	Aug 1	05:51:45		—	DC-1 command
<i>Mariner VI</i> returned to playback mode	Aug 7	16:17:38		—	DC-3 command. Playback resumed on DTR <sup>†</sup> track 4
Spacecraft CC&S conditioned for postencounter cruise	Aug 7	22:47:41— 23:19:57	Aug 5	22:27:06— 23:09:18	23 coded commands, CC&S memory readout
End of playback 1 digital playback	Aug 9	16:17:00	Aug 8	00:13:42	Two playbacks of digital recorder
Analog/digital transfer		16:17:00— 16:41:26		00:13:42— 00:38:12	Initiated by ninth end-of-tape; transfer begins at start of analog track 2
Digital playback of analog data (playback 1 mode)	Aug 9— Aug 10	16:41:26	Aug 8— Aug 9	00:38:12	Two playbacks to verify quality of HRT data
<i>Mariner VII</i> battery testing			Aug 12 Aug 13	23:43:09— 03:13:09	Battery charge and test-load cycles. Battery condition determined: open-circuited
<sup>†</sup> DTR= digital tape recorder.					

# Flight Path/Navigation

## I. Introduction

The flight paths of the *Mariner VI* and *Mariner VII* spacecraft were affected principally by the conditions of the launch operations, the effects of the spacecraft trajectory-refining maneuvers, and the gravitational fields through which the spacecraft flew. In addition, they were affected by nongravitational environmental effects such as the pressure of sunlight, and by the small thrusts resulting from certain spacecraft events.<sup>1</sup>

The mission was designed (see Volume 1, Part 1, Mission Design, Analysis, and Engineering) to use *Atlas/Centaur* launches from Cape Kennedy in the period February 16—April 18, to separate the two launches by about a month, and to launch toward aiming points biased away from Mars. The spacecraft thrust maneuvers were to remove the bias and the injection error simultaneously. Acquisition parameters for the stations of the Deep Space Instrumentation Facility (DSIF), especially the initial acquisitions after launch, were based on orbit data. The spacecraft were to fly by Mars at points separated in latitude and arrival time (by five days), with very small error. The early flight events of *Mariner VI* (maneuver, scan platform unlatch) were to occur in time for corrective action, if necessary, to be applied to *Mariner VII* before its launch. Certain Mars-encounter parameters were to be updated on the basis of flight-

path information as close as a few hours before closest approach to the planet. These factors conditioned the manner in which the flight paths of *Mariners VI* and *VII* were determined.

Thus, *Mariner VI* was launched and injected into heliocentric orbit by the *Atlas/Centaur* vehicle, and its trajectory near the Earth (for station acquisition) and Mars flyby parameters (for maneuver determination) were calculated repeatedly, with converging solutions. After about four days, the maneuver was conducted, bringing the flyby parameters close to those desired by the scientific experimenters. About 10 days after launch, the scan platform was unlatched by a pressurized device whose effluent affected the flight path.

Next, *Mariner VII* was launched. A longer interval could be taken for orbit determination before the maneuver than on *Mariner VI*, and the maneuver was not conducted until about 12 days after launch. Early in April 1969, both spacecraft were in heliocentric cruise, accurately aimed for their respective flyby target zones; no further maneuvers were planned. However, *Mariner VI* operations in connection with the search for a roll reference (see Part 3, Spacecraft System Performance) resulted in a small perturbation to the flight path, and unlatching the scan platform of *Mariner VII* affected its flight path.

Turnaround ranging operations in the Mark 1A near-Earth mode had terminated on schedule for *Mariner VI*, but some days earlier than expected for *Mariner VII*

<sup>1</sup>The radio tracking data from which the flight paths were determined were affected by phenomena in space along the ray path of the signal, including charged particles in interplanetary space and the ionosphere of the Earth.

because of a reduction in the spacecraft receiver sensitivity. Ranging was resumed, in the R&D planetary mode, early in July. As the spacecraft approached planetary encounter, the increasing tracking data base and resulting precision in the orbit had led to updating of the encounter parameters in the spacecraft computer.

*Mariner VI* began its far-encounter operations about two days before closest approach to the planet, and progressive updates were carried out, the last one 4 h before the limb of Mars appeared in view of the scientific instruments.

During the final approach of *Mariner VI*, the *Mariner VII* spacecraft, still more than five days from closest approach, experienced a pre-encounter anomaly (see Part 3, Spacecraft System Performance). One effect of this unexpected series of events was a perturbation of the trajectory (analysis of which proved important in the investigation of the spacecraft anomaly), which increased the uncertainty in orbit determination and affected the flight path input updating of the encounter parameters. However, the essential functions were recovered with some improvisation and the encounter was successfully carried out.

One scientific instrument employed during encounter used a nitrogen-hydrogen cryostat whose effluent also perturbed the trajectory. In the case of *Mariner VI*, the device malfunctioned, and the jetting continued over several days.

Flight-path data were used in the celestial mechanics experiment to measure the gravitational fields that influenced the flight paths in an effort to improve knowledge of the masses and the positions and motions of the bodies involved.

Geocentric, heliocentric, and areocentric orbital elements at various stages of flight are given for *Mariners VI* and *VII* in Tables 1 and 2, respectively.

Following the dual Mars encounter, flight-path studies continued, and postencounter orbits were determined as tracking data became available. Postencounter tracking and navigation then became involved in the celestial mechanics experiment of the *Mariner* Mars 1969 extended mission, which is beyond the scope of this report.

The use of optical data for navigation was originally proposed as the function of an approach guidance subsystem, which was not able to be flown on the *Mariner* Mars 1969 mission. However, the use of optical data for navigation was attempted on an experimental basis with available data from the far-encounter planet sensor and far-encounter television pictures.

The material contained herein has been arranged in phases of the flight sequence, which permits comparison of *Mariners VI* and *VII* data but ignores the delay between respective phases of the two flights. Thus, the

**Table 1. *Mariner VI* orbital elements throughout flight**

Orbital parameter	At injection (geocentric)	Postmaneuver (heliocentric)	After scan unlatch (heliocentric)	After Magellanic operation (heliocentric)	Pre- encounter <sup>a</sup> (areocentric)	Encounter (areocentric)	Post- encounter <sup>b</sup> (areocentric)
Periapsis, km	6863	$148.11 \times 10^6$	$148.10 \times 10^6$	$148.10 \times 10^6$	6169.9	6842	7228.7
Semimajor axis, km	-35820	$194.44 \times 10^6$	$193.40 \times 10^6$	$192.86 \times 10^6$	-824.4	-825.8	-824.20
Longitude of ascending node, deg	318.27 <sup>c</sup>	335.94 <sup>d</sup>	335.82 <sup>d</sup>	335.60 <sup>d</sup>	163.10 <sup>d</sup>	148.21 <sup>d</sup>	139.04 <sup>d</sup>
Argument of periapsis, deg	135.99 <sup>c</sup>	179.91 <sup>d</sup>	179.91 <sup>d</sup>	180.02 <sup>d</sup>	16.70 <sup>d</sup>	30.89 <sup>d</sup>	40.29 <sup>d</sup>
Eccentricity	1.18	0.2383	0.2342	0.2321	8.48	9.29	9.77
Inclination, deg	43.33 <sup>c</sup>	1.99 <sup>d</sup>	1.96 <sup>d</sup>	1.94 <sup>d</sup>	6.35 <sup>d</sup>	6.92 <sup>d</sup>	7.94 <sup>d</sup>
Time of periapsis, GMT							
Date	Feb 25	Feb 24	Feb 24	Feb 24	Jul 31	Jul 31	Jul 31
Time	01:40:40.6	15:25:49	12:50:17	09:44:29	05:16:21	05:19:06.2	05:21:59.3
<sup>a</sup> Spacecraft approaching vicinity of Mars ( $\sim 2 \times 10^6$ km). <sup>b</sup> Spacecraft leaving vicinity of Mars ( $\sim 2 \times 10^6$ km). <sup>c</sup> With respect to Earth equatorial plane and vernal equinox. <sup>d</sup> With respect to ecliptic plane and vernal equinox.							

**Table 2. Mariner VII orbital elements throughout flight**

Orbital parameter	At injection (geocentric)	Post- maneuver (heliocentric)	After scan unlatch (heliocentric)	Pre- encounter <sup>a</sup> (areocentric)	Encounter (areocentric)	Post- encounter <sup>b</sup> (areocentric)
Periapsis, km	6884	$145.18 \times 10^6$	$145.21 \times 10^6$	6238.8	6812	7107.7
Semimajor axis, km	-23639	$190.01 \times 10^6$	$189.88 \times 10^6$	-857.3	-858.8	-857.12
Longitude of ascending node, deg	325.85 <sup>c</sup>	6.73 <sup>d</sup>	6.66 <sup>d</sup>	259.05 <sup>d</sup>	258.14 <sup>d</sup>	254.95 <sup>d</sup>
Argument of periapsis, deg	119.32 <sup>c</sup>	148.81 <sup>d</sup>	148.88 <sup>d</sup>	282.72 <sup>d</sup>	282.98 <sup>d</sup>	286.11 <sup>d</sup>
Eccentricity	1.27	0.2383	0.2353	8.28	8.96	9.29
Inclination, deg	31.01 <sup>c</sup>	1.60 <sup>d</sup>	1.60 <sup>d</sup>	32.20 <sup>d</sup>	28.15 <sup>d</sup>	24.43 <sup>d</sup>
Time of periapsis, GMT						
Date	Mar 27	Feb 27	Feb 28	Aug 5	Aug 5	Aug 5
Time	22:30:10.0	20:36:48	20:06:42	04:57:58	05:00:49.5	05:03:44.6

<sup>a</sup>Spacecraft approaching vicinity of Mars ( $\sim 2 \times 10^6$  km).  
<sup>b</sup>Spacecraft leaving vicinity of Mars ( $\sim 2 \times 10^6$  km).  
<sup>c</sup>With respect to Earth equatorial plane and vernal equinox.  
<sup>d</sup>With respect to ecliptic plane and vernal equinox.

near-Earth flight-path phenomena are compared, the maneuvers are compared, the heliocentric orbits are compared, and the near-Mars phase and postencounter trajectories are discussed together.

## II. Near-Earth Phase

The near-Earth phase was characterized by the spacecraft velocity profile showing high sensitivity to its position relative to the Earth. Under these conditions, the orbit could be very well determined after four or five days of continuous tracking.

Results of premaneuver tracking showed how the trajectory would have appeared if no maneuver had been performed. Based upon these results, maneuvers were performed to attain the desired terminal conditions.

### A. Mariner VI Launch

After *Mariner VI* was launched on a direct-ascent trajectory, a programmed 13-s roll brought the vehicle to an inertial azimuth 108 deg east of north. The pitch program was then initiated and completed. Eight seconds after booster engine cutoff, the initial yaw maneuver was begun. The yaw maneuver actually consisted of two separate maneuvers. The first yaw had a "yaw index" of 9.25. The term "yaw index" is used to describe the magnitude of the yaw maneuver and is a function of the trajectory inclination at *Centaur* main engine cutoff (MECO). If the desired inclination requires a planar azimuth heading greater than 115 deg,

an initial yaw is made to a 115-deg parallel azimuth heading, and then a final yaw maneuver is initiated shortly after *Centaur* main engine start to align the vehicle with the desired final heading. Yaw index equals the yaw rates multiplied by the yaw times, and is thus approximately equal to the total yaw angle turned during powered flight (Figs. 1 and 2).

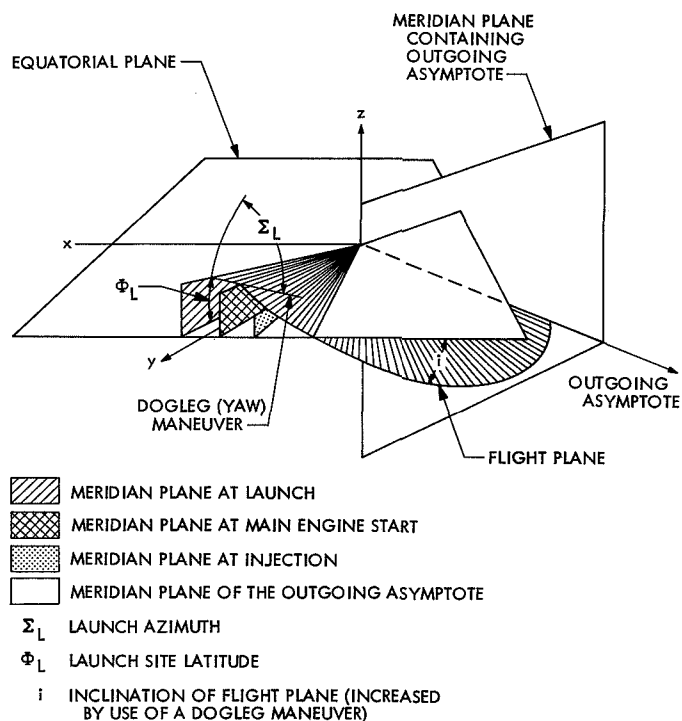


**Fig. 1. Dogleg maneuver to increase inclination**

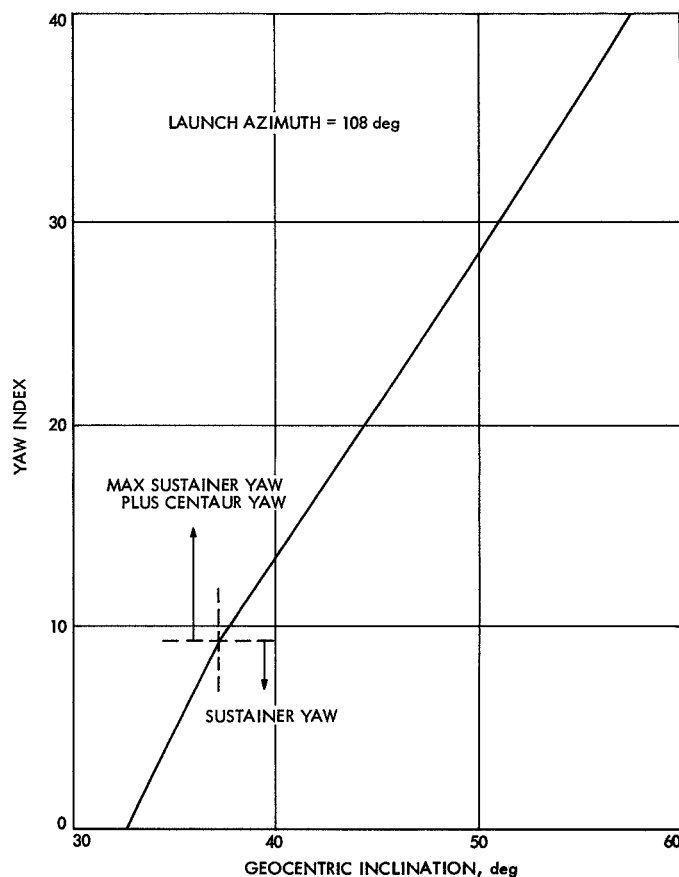


Fig. 2. Yaw index vs geocentric inclination

Immediately after *Centaur* MECO, the *Centaur* guidance system initiated a turning maneuver to bring the vehicle into alignment with the separation direction, which was primarily designed to point the spacecraft low-gain antenna toward the Earth. At the completion of this maneuver, separation occurred and the spacecraft was placed onto its Mars transfer trajectory, a type I transfer (i.e., the total heliocentric central transfer angle from the Earth at launch to Mars at encounter was less than 180 deg). The elements and injection condition of the transfer orbit at separation are shown in Table 3, including the Deep Space Station (DSS) used.

**1. Injection aiming point.** To satisfy various planetary quarantine constraints, it was necessary to aim the spacecraft at injection (postseparation) to a point further from the planet than the actual desired aiming point. The particular biasing direction chosen was dictated primarily by the desire to keep the midcourse velocity increment small, as well as to minimize the trajectory dispersions that would result from a larger-than-expected error in velocity increment. This bias was

then to be removed by the midcourse maneuver. The injection aiming point achieved by *Mariner VI* had the following coordinates:  $\mathbf{B} \cdot \mathbf{T} = 3,538$  km,  $\mathbf{B} \cdot \mathbf{R} = -13,089$  km,  $\text{TCA}^2 = 04:41:50$ , GMT July 31, 1969. The *Centaur* delivered *Mariner VI* to an aiming point 5600 km southwest of the specified aiming point, as shown in Fig. 3. The preferred aiming zone was selected by the scientific experimenters for a high-value science return. The midcourse maneuver was performed on March 1 at 00:54:44 GMT ( $L + 95$  h 25 min) and changed the velocity vector by 3.146 m/s. The scan platform unlatch was performed on March 6 at 19:11:38 GMT ( $M + 120$  h 18 min) and changed the velocity vector by 10.5 mm/s.

The *Mariners VI* and *VII* injection and midcourse aiming points are shown in aiming-plane views in Fig. 3. The aiming plane is perpendicular to the approach hyperbolic trajectory asymptote relative to Mars. The unit vector  $\mathbf{T}$  is parallel to the ecliptic plane, and the unit vector  $\mathbf{R}$  lies in the southern ecliptic hemisphere. The points which are plotted correspond to those points where the trajectory would have passed if not deflected by the gravitational field of Mars.

**2. Orbit estimation.** The primary tracking support was provided by DSSs 12 (Echo, Goldstone, Calif.), 41 (Woomera, Australia), and 51 (Johannesburg, South Africa), and Manned Space Flight Network (MSFN) station 75 (Ascension Island). However, the very first orbit used only seven data points, taken by Antigua station between MECO and separation. It was, therefore, biased, showing a miss distance in the  $\mathbf{B}$ -plane of 103,670 km. The characteristics of this and 33 other orbit calculations are given in Table 3.

The first estimate of the spacecraft orbit after separation was completed at  $L + 2$  h 25 min and was based on approximately 1 h of DSS 51 angular and two-way doppler data. When this solution was mapped forward to target, the  $\mathbf{B}$ -plane estimates indicated that the solution was very close to the nominal premaneuver aiming point ( $\mathbf{B} \cdot \mathbf{R} = -13,300$  km,  $\mathbf{B} \cdot \mathbf{T} = 17,100$  km,  $\text{TCA} = 05:01:32$  GMT and that the correction required to achieve the nominal postmaneuver aiming point was well within the midcourse-correction capability. This was verified by the second initial-condition evaluation (ICEV) and third preliminary evaluation (PREL) orbit computations completed at  $L + 5$  h and  $L + 11$  h, respectively.

<sup>2</sup>TCA = time of closest approach.

**Table 3. Results of premaneuver orbit computations for Mariner VI**

Orbit <sup>a</sup>	B, km	B • R, km	B • T, km	TCA, <sup>b</sup> GMT	Time of last data point, GMT		Stations used in orbit	Data types used <sup>c</sup>	Parameters estimated
					Date	Time			
ETR	103669.74	43657.477	94014.989	15:43:01.509	Feb 25	01:42:06	Antigua	Range, az, el	State vector
PROR-X	24777.882	-14636.396	19992.982	04:11:56.727		03:50:02	DSS 51	CC3, HA, dec	
ICEV-Y	13948.287	-13575.227	-3204.3617	04:52:40.721		03:32:00	DSS 51	CC3	State vector
ICEV-X	13816.627	-12999.501	4681.0404	04:38:32.189		05:59:00	DSS 51	RU, CC3	
PREL-X	13584.248	-13122.211	3512.7392	04:40:32.790		08:10:32	DSS 51	CC3	State vector
PREL-XB	12751.511	-12698.872	1157.4472	04:45:46.506		08:52:32	Ascension, DSS 51	RU, CC3	
PREL-XC	14386.036	-12522.663	7091.0269	04:34:05.708		09:17:32	Ascension, DSS 51	CC3	State vector
PREL-XE	13639.018	-12981.023	4185.1942	04:39:20.199		09:17:32	Station 5	RU, CC3	
DACO-YA	12995.738	-12879.224	1736.3124	04:44:36.425		15:06:32	Ascension, DSSs 51, 12	CC3	State vector
DACO-YB	13224.917	-12916.457	2839.6431	04:42:19.224		21:00:32	Ascension, DSSs 12, 41, 51	CC3	
DACO-YC	13239.561	-12915.764	2410.1594	04:42:10.773		22:03:32	Ascension, DSSs 41, 51	CC3	State vector
DACO-YD	13360.799	-12976.379	3181.9094	04:41:26.213	Feb 25	23:28:32	DSSs 41, 12, 51	CC3	
DACO-YE	13540.218	-13044.163	3531.4355	04:40:20.088	Feb 26	00:24:02	DSSs 41, 12, 51	RU	State vector
DACO-YF	13377.026	-12985.474	3212.8273	04:41:20.742	Feb 26	03:05:02	DSSs 41, 51, 12	RU, CC3	
NOMA-XA	13411.275	-12980.636	3371.2605	04:41:05.511	Feb 26	17:11:32	DSSs 51, 12, 41	CC3	State vector
NOMA-XD	13434.670	-13024.689	3293.6037	04:41:08.229	Feb 27	00:07:32	DSSs 41, 51, 12	CC3	
NOMA-XE	13413.430	-12988.397	3349.8718	04:41:06.928		00:07:32	DSSs 41, 51, 12	CC3	State vector
NOMA-XF	13336.354	-12899.804	3384.2877	04:41:03.594		00:07:32	DSSs 41, 51, 12	CC3	
NOMA-XH <sup>d</sup>	13486.224	-12806.334	4228.0090	04:38:27.560		01:31:32	DSSs 41, 51, 12	RU, CC3	State vector
NOMA-XI <sup>d</sup>	13478.042	-12839.830	4098.3379	04:38:53.035		02:57:32	DSSs 41, 51, 12	CC3	
NOMA-XJ <sup>d</sup>	13472.616	-12977.150	3620.0775	04:39:57.906		02:57:32	DSSs 41, 51, 12	CC3	State vector
NOMA-XK <sup>d</sup>	13488.059	-12871.664	4030.8833	04:39:30.227		02:57:32	DSSs 41, 51, 12	RU, CC3	
NOMA-2XA <sup>d</sup>	13413.097	-12896.523	3686.5803	04:40:06.322		16:22:32	DSSs 41, 51, 12	CC3	State vector
NOMA-2XB <sup>d</sup>	13432.471	-12918.651	3679.6365	04:40:04.921		16:22:32	DSSs 41, 51, 12	CC3	
NOMA-2XC <sup>d</sup>	13427.490	-12903.507	3714.4307	04:40:01.803		21:44:32	DSSs 41, 51, 12	CC3	State vector
NOMA-2XH <sup>d</sup>	13437.303	-12907.753	3735.1078	04:39:58.599		21:44:32	DSSs 41, 51	CC3	
NOMA-2XI <sup>d</sup>	13439.148	-12936.403	3641.4497	04:40:05.702		21:44:32	DSSs 41, 51, 12	CC3	State vector
NOMA-2XJ <sup>d</sup>	13415.121	-12909.190	3649.4222	04:40:10.654		21:18:32	DSSs 41, 51, 12	CC3	
NOMA-2XK <sup>d</sup>	13407.024	-12909.075	3619.9528	04:40:14.379	Feb 27	23:45:32	DSSs 41, 51, 12	RU, CC3	State vector
NOMA-2XL <sup>d</sup>	13435.518	-12930.540	3648.8711	04:40:09.659	Feb 28	02:25:32	DSSs 41, 51, 12	CC3	
LAPM-XC <sup>d</sup>	13430.326	-12934.428	3615.8279	04:40:13.618		20:37:32	DSSs 41, 51, 12	CC3	State vector
LAPM-XD <sup>d</sup>	13402.332	-12912.415	3590.5486	04:40:18.363		22:00:32	DSSs 41, 51, 12	RU, CC3	
LAPM-XE <sup>d</sup>	13427.237	-12933.272	3608.4884	04:40:15.082		22:00:32	DSSs 41, 51, 12	CC3	State vector
LAPM-XF <sup>d</sup>	13428.050	-12929.883	3623.6262	04:40:12.042	Feb 28	22:38:32	DSSs 41, 51, 12	CC3	

<sup>a</sup>Epochs on Feb 25 were 01:40:40.645 GMT for orbits ETR, PROR-X ICEV-X and PREL-XB; 01:39:00.000 GMT for orbits NOMA-XD, NOMA XJ, NOMA-XK, NOMA-2XB, NOMA-2XI, NOMA-2XJ, NOMA-2XL, LAPM-XC, LAPM-XE, and LAPM-XF; and 02:33:00.000 GMT for the others.

<sup>b</sup>TCA = time of closest approach.

<sup>c</sup>CC3 is two-way doppler (the same as coherent-counted three-way doppler with receiver and transmitter at same station); RU is Mark 1A ranging.

<sup>d</sup>Change of reflectivity coefficient and mass of spacecraft from 0.23998 and 384.1932, respectively, to 0.34423 and 385.69458.

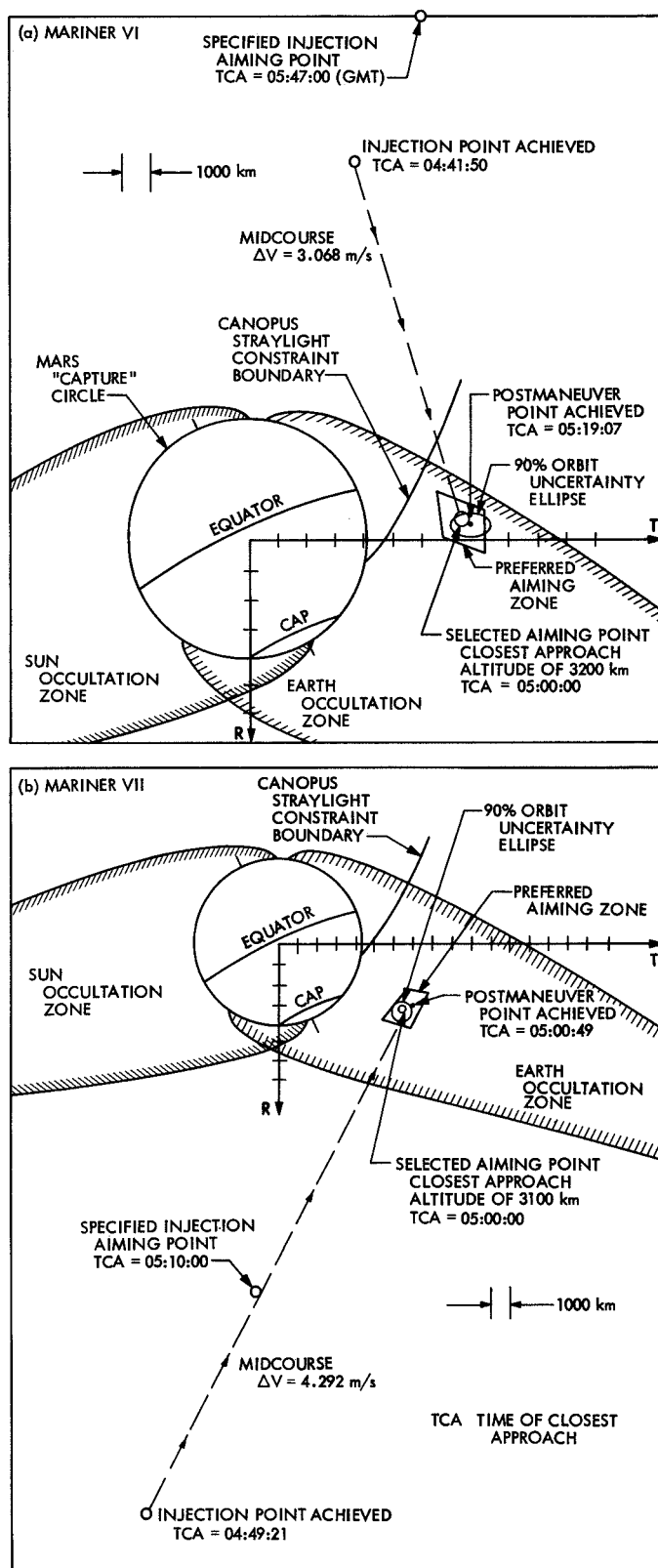


**Fig. 3. Mariners VI and VII injection and midcourse aiming points shown in an aiming-plane view**

During the second orbit computation period, a comparison was made between solutions with and without angular (HA, dec) data. One orbit was computed using DSS 51 angular and doppler data in the least-squares fit. The other orbit was computed using only DSS 51 two-way doppler data in the fit. The comparison showed a magnitude difference in the **B** vector of 10,830 km. Since it is known that angular data are biased, the sole purpose of using angular data is to hold the orbit until enough doppler data are obtained to converge independently to a reasonable solution.

During the data consistency (DACO) computation period from  $L + 14$  h to  $L + 27$  h, seven orbital solutions were obtained using various combinations of DSSs 41, 51, and 12, and MSFN station 75 data for consistency between stations. The solutions obtained from these computations indicated that the DSSs 41, 51, and 12 data were consistent. However, the MSFN station 75 data appeared to be biased (this bias is probably due to the inaccuracy of the surveyed station location). Since only one hour of tracking data was obtained from MSFN station 75, it was decided not to use these data in any later orbit computations.

During the DACO computation period, orbit solutions were also computed using doppler data only, ranging data only, and doppler plus ranging data. These three solutions are in fairly good agreement considering the amount of tracking data available. The comparison between the three solutions is as follows:

Parameter	Doppler only	Range only	Doppler and range
<b>B</b> , km	13361.13	13540.22	13377.03
<b>B · R</b> , km	-12983.65	-13044.16	-12985.47
<b>B · T</b> , km	3153.51	3631.4355	3212.83
TCA, GMT	04:41:27.83	04:40:20.09	04:41:20.74

The nominal maneuver (NOMA) orbit computation time block started at approximately  $L + 40$  h. The NOMA-2XK (second series, computing-string X, eleventh run) orbit solution was used for midcourse maneuver computation. The following amount of data was used in the computation:

DSS	Doppler	Ranging
41	23½ h	23½ h
51	27 h	15½ h
12	3 h	3 h

The orbit estimated only the state vector and, when this solution was mapped to target, it indicated the following results:

$$\begin{aligned} \mathbf{B} &= 13407.02 \text{ km} \\ \mathbf{B} \cdot \mathbf{R} &= -12909.08 \text{ km} \\ \mathbf{B} \cdot \mathbf{T} &= 3619.95 \text{ km} \\ \text{TCA} &= 04:40:14.38 \text{ GMT} \end{aligned}$$

Examining the observed minus computed residual plots of the NOMA-2XK solution, the data fit appears to be reasonably good. However, the data fit also indicates some small perturbation was not accounted for. Estimating for station locations, solar pressure in the Sun-probe direction, Earth ephemeris elements, and changing the values of the index of refraction for the tracking stations did not improve the data fit. An orbit

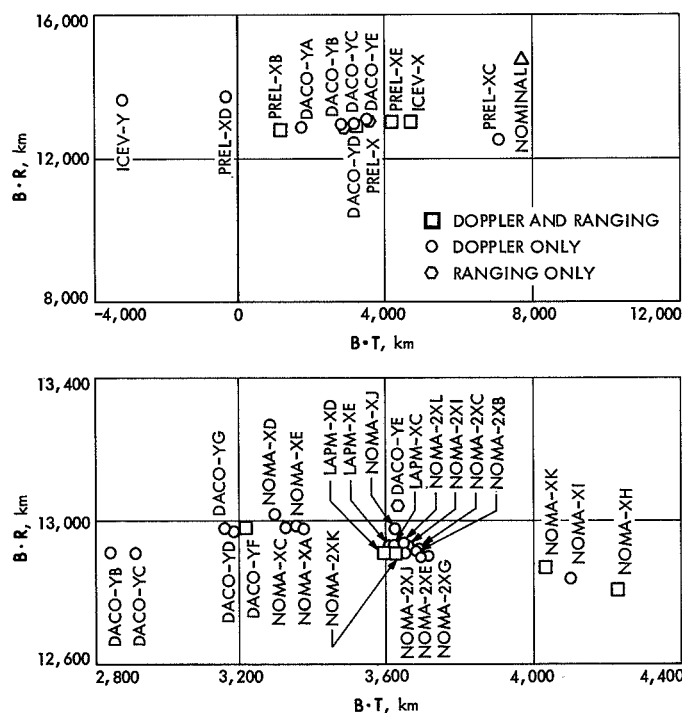


Fig. 4. Mariner VI premaneuver B-plane estimates

solution estimating the gravitational constant of the Earth along with the state vector did improve the data fit but it changed the gravitational constant by an unrealistic amount ( $7 \text{ km}^3/\text{s}^2$ ). It was suspected and later confirmed that the perturbation was due to an acceleration caused by the solar pressure in the tangential direction. Since the single-precision orbit determination program (SPODP) was unable to estimate the solar pressure in the tangential direction nor the gas leaks and the double-precision orbit determination program (DPODP) had not yet been certified, it was decided to use the NOMA-2XK solution for maneuver computation.

During this time, a similar orbit solution to NOMA-2XI was computed by the DPODP. The solution estimated the state vector by using the doppler data only. The ranging data were not used because the program that converts the SPODP data tape to a DPODP data tape handled the ranging data incorrectly. The comparison of these solutions is as follows:

Parameter	SPODP	DPODP	$\Delta$ SPODP-DPODP
$\mathbf{B}$ , km	13439	13425	14
$\mathbf{B} \cdot \mathbf{R}$ , km	-12936	-12929	-7
$\mathbf{B} \cdot \mathbf{T}$ , km	3641	3617	24
TCA, GMT	04:40:05.7	04:40:14.2	-8.5

The last premaneuver (LAPM) orbit computation time block was between maneuver minus 10 h ( $M - 10 \text{ h}$ ) and  $M - 1 \text{ h}$ . The orbits computed during this time block indicated solutions very close to the NOMA-2XK solution, which was used for maneuver computation. Therefore, the midcourse maneuver was performed on the NOMA-2XK solution.

The convergence of the orbit for B-plane values is shown in Fig. 4; the convergence for time of closest approach is shown in Fig. 5.

#### B. Mariner VII Launch

After Mariner VII was launched on a direct ascent trajectory and had entered the shadow of the Earth, the launch azimuth was 102.88 deg and no yaw maneuver was required.



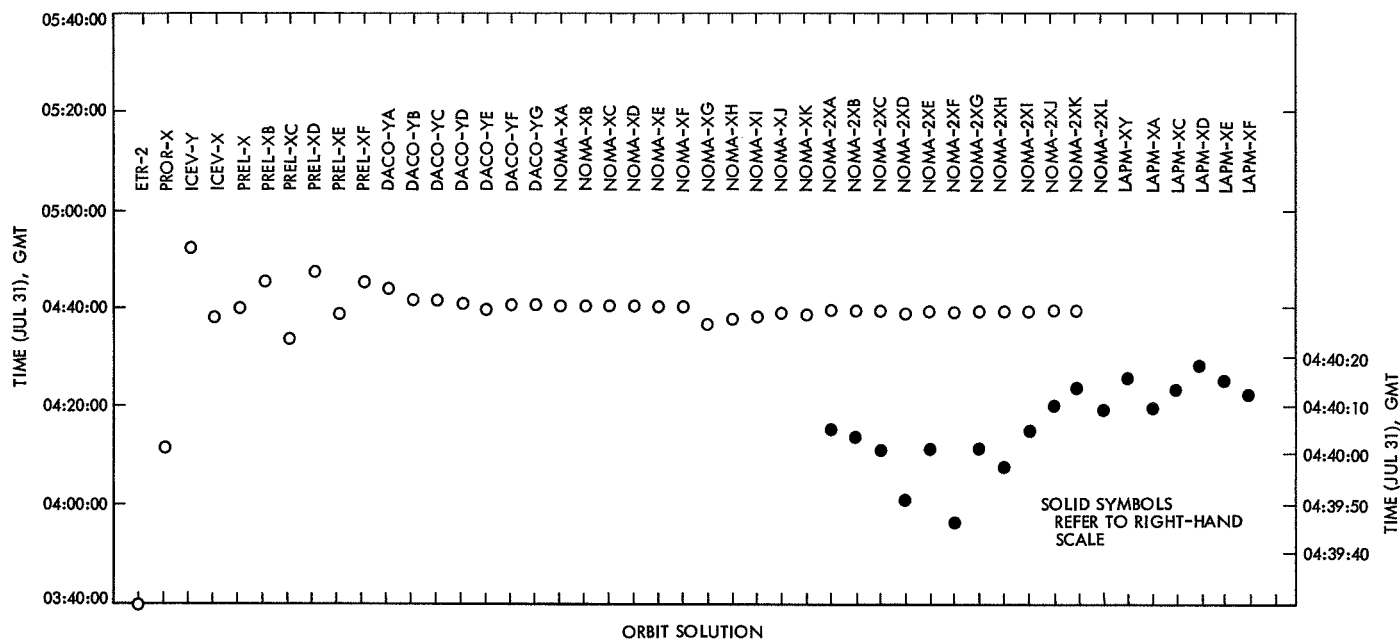


Fig. 5. Mariner VI premaneuver estimates of time of closest approach

1. *Characteristics of the phase.* The *Mariner VII* near-Earth phase was essentially similar to that of *Mariner VI*, with a few exceptions. First, there was no external reason for performing the maneuver and scan-unlatch early, so there was more time to obtain a satisfactory estimate of the premaneuver trajectory. Second, suspected problems in the *Mariner VII* central computer and sequencer (CC&S) immediately after launch gave rise to a ground-command moratorium, which, in turn, meant: (1) no ranging during the first five days of flight, and (2) the Canopus sensor remained locked on the star Vega, which it had acquired initially, until April 1, causing the nonradial component of solar pressure to be about 180 deg from the expected vector during this period (see Part 3 Spacecraft System Performance). These factors tended to neutralize the advantage of extra time. The achieved injection aiming point for *Mariner VII* proved to be:

$$\begin{aligned} B &= 30074 \text{ km} \\ B \cdot T &= -6758 \text{ km} \\ B \cdot R &= 29305 \text{ km} \\ TCA &= 04:49:21 \text{ GMT on August 5} \end{aligned}$$

This was well within the capability of the spacecraft propulsion subsystem to bring it to the desired aim point.

2. *Premaneuver orbit estimation.* The primary tracking support was provided by DSSs 12, 41, 51, and 62 (Cebreros, Spain). Tracking data were also provided by DSS 14 (Mars, Goldstone, Calif.) and MSFN station 75.

The convergence process for the inflight orbits and the time of closest approach are shown in Figs. 6 and 7, respectively.

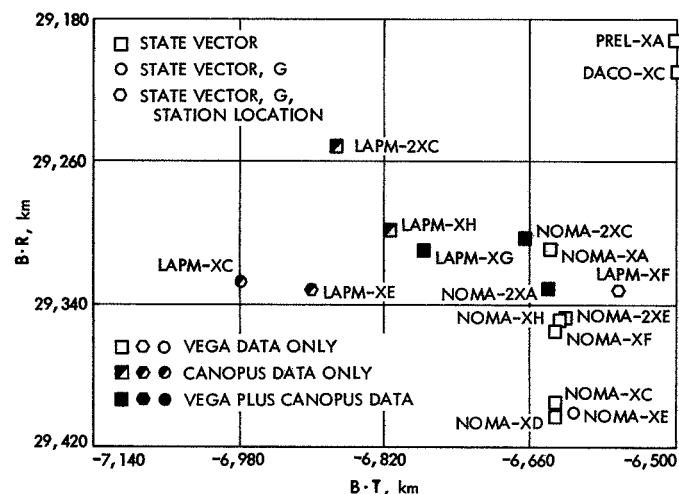


Fig. 6. Mariner VII premaneuver B-plane estimates

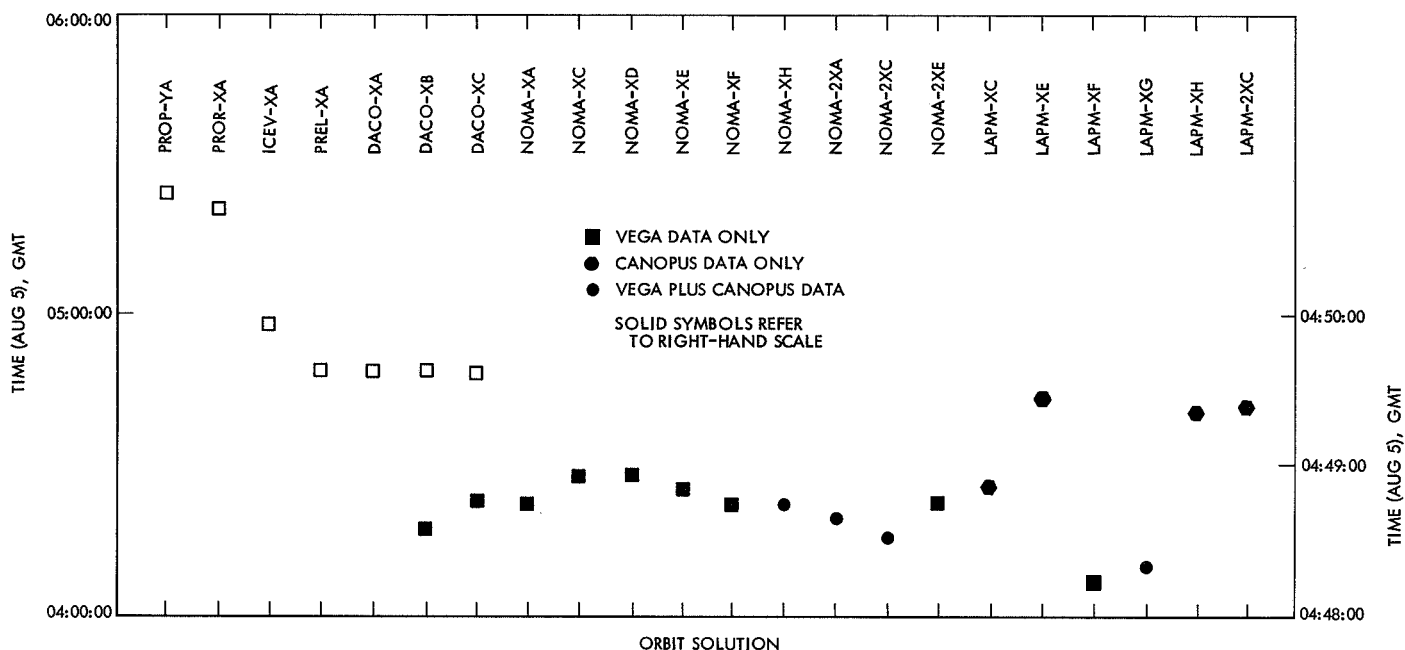


Fig. 7. Mariner VII premaneuver estimates of time of closest approach

The activity of estimating the orbit prior to the maneuver was essentially similar to that of *Mariner VI*. The NOMA-XF orbit, computed at approximately  $L + 3\frac{1}{2}$  days, with doppler data only (26 h from DSS 41, 14 h from DSS 62, and  $8\frac{1}{2}$  h from DSS 12), indicated the following results:

$$\begin{aligned} B &= 30095 \text{ km} \\ B \cdot R &= 29355 \text{ km} \\ B \cdot T &= 6632 \text{ km} \\ \text{TCA} &= 04:48:45.623 \text{ GMT on August 5} \end{aligned}$$

The effect of the roll-control lock on the star Vega during the first four days of flight is shown in the following orbit solutions using, respectively, Vega-position data (orbit NOMA-2XE), Canopus data (orbit LAPM-XH), and a combination (orbit LAPM-XG):

Parameter	Vega	Canopus	Combined
B, km	30085	30093	30082
B · R, km	29348	29297	29309
B · T, km	−6622	−6874	−6777
TCA, GMT	04:48:45	04:49:23	04:48:22

These solutions were calculated in single precision (SPODP). The corresponding DPODP orbits (for the first two cases only) are as follows:

Vega data block (state only)	Canopus data block (state only)
B = 30083 km	B = 30100 km
B · R = 29327 km	B · R = 29291 km
B · T = −6701 km	B · T = −6931 km
TCA = 04:48:01 GMT	TCA = 04:49:09 GMT

When the three components of solar pressure were estimated in the DPODP process (this capability was provided only later in SPODP), the solutions were:

Vega data block (state + 3 G)	Canopus data block (state + 3 G)
B = 30085 km	B = 30056 km
B · R = 29322 km	B · R = 29260 km
B · T = −6732 km	B · T = −6869 km
TCA = 04:48:10 GMT	TCA = 04:49:14 GMT

The Canopus-data solutions were preferred, because they used the latest block of tracking data. However,

because the data block began five days after injection, it covered a relatively shorter arc than desired, and the solution was still moving very slightly when the last premaneuver orbit was calculated.

The LAPM-XG (last premaneuver, computer string X, first series, seventh run) orbit was used for maneuver calculation. Ranging data were not used in the solution because of an apparent inconsistency between doppler and range results:

Parameter	Doppler only	Range only	Doppler and range
<b>B</b> , km	30100	30688	30800
<b>B • R</b> , km	29291	29815	29922
<b>B • T</b> , km	−6932	−7268	−7302
TCA, GMT	04:49:09	04:48:39	04:48:47

Table 4 gives characteristics of 24 solutions calculated during the *Mariner VII* premaneuver phase.

**Table 4. Results of premaneuver orbit computations for *Mariner VII***

Orbit	B, km	B • R, km	B • T, km	TCA, GMT	Time of last data point, GMT		Stations used in orbit	Data types used	Parameters estimated
					Date	Time			
ETR	42046.92	21938.25	−35869.99	07:39:43.09	Mar 27	22:35:24	Antigua	Range, az, el	State vector
PROR-YA	28079.11	27601.8	5155.28	05:23:46.41	Mar 28	00:02:02	DSS 51	HA, dec, CC3	
PROR-XA	27254.76	26740.687	5268.56	05:20:47.39		00:43:32	DSSs 51, 62	CC3, C3	State vector
ICEV-XA	22239.54	21978.57	3397.00	04:57:48.28		03:18:02	DSS 51	CC3	
PREL-XA	29914.58	29191.05	−6539.45	04:48:42.88		16:33:32	DSSs 41, 51, 12		State vector and G
DACO-XA	29839.32	29121.08	−6507.54	04:48:35.55		18:03:32	DSSs 41, 51		
DACO-XB	29634.21	28957.30	−6297.73	04:48:34.81		11:11:32	DSSs 51, 12		State vector
DACO-XC	29927.47	29209.59	−6515.59	04:48:45.84	Mar 28	18:03:32	DSSs 41, 12		
NOMA-XA	30051.32	29309.22	−6637.11	04:48:44.81	Mar 29	17:49:32	DSSs 41, 51, 62, 12		State vector
NOMA-XC	30134.81	29395.97	−6632.03	04:48:55.18		19:46:32	DSSs 41, 51, 62		
NOMA-XD	30141.56	29403.11	−6631.05	04:48:55.61		19:46:32	DSSs 41, 62, 12		State vector
NOMA-XE	30136.03	29401.19	−6614.41	04:48:50.43	Mar 29	19:46:32	DSSs 41, 62, 12		
NOMA-XF	30094.82	29355.08	−6631.55	04:48:45.62	Mar 31	17:33:32	DSSs 41, 62, 13		State vector
NOMA-XH	30087.18	29349.31	−6622.44	04:48:45.59	Apr 1	17:59:02	DSSs 41, 62, 12, 14		
NOMA-2XA	30074.31	29331.94	−6640.88	04:48:40.57	Apr 2	17:18:02			State vector
NOMA-2XC	30052.56	29303.49	−6667.99	04:48:33.38	Apr 3	18:00:02			
NOMA-2XE	30085.27	29347.56	−6621.52	04:48:45.49	Apr 1	16:24:32			State vector, G, and station location
LAPM-XC	30146.31	29327.55	−6978.16	04:48:52.55	Apr 4	18:02:02		CC3	
LAPM-XD	24343.02	21965.52	−10492.78	04:23:23.21	Apr 4	18:02:02		RU, CC3	State vector, G, and station location
LAPM-XE	30132.42	29331.74	−6900.10	04:49:28.22	Apr 6	19:00:02		CC3	
LAPM-XF	30057.32	29332.10	−6562.83	04:48:15.22	Apr 1	16:24:32			State vector
LAPM-XG	30082.44	29309.03	−6777.44	04:48:22.01	Apr 6	10:03:02			
LAPM-XH	30092.89	29297.17	−6814.41	04:49:22.63	Apr 7	19:01:02			State vector
LAPM-2XC	30047.91	29251.12	−6873.80	04:49:24.73	Apr 8	10:37:02	DSSs 41, 62, 12, 14	CC3	

### III. Midcourse Maneuver

Midcourse correction maneuvers to the *Mariners VI* and *VII* trajectories were required to achieve the encounter-parameter accuracy necessary to satisfy the objectives of the scientific experiments to be performed. These maneuvers were accomplished by means of small changes in the spacecraft velocity vector; this caused the trajectories to be slightly perturbed from the nominal trajectories while retaining the desired end conditions.

#### A. Maneuver Implementation

After the desired postmaneuver aiming point had been selected by the principal investigators, and orbit determination personnel had determined a best estimate of the trajectory, the required velocity correction was computed by use of a linear search scheme with the integrating trajectory program SPACE. The required pitch and roll turns to align the motor thrust axis along the negative velocity direction were computed, and the number of central computer and sequencer (CC&S) pulses required to implement these turns was determined as a function of the spacecraft temperature. The duration of the burn could be controlled only to the nearest 0.05 s. To eliminate the effects of this resolution error as much as possible, a modified velocity-correction vector was determined, with a burn duration that was an integer multiple of 0.05 s, the same spatial miss as before, and a slightly altered time of arrival. This was done because the arrival time is generally a less critical parameter than is the spatial miss. Also, a bias was included in selection of the maneuver aiming point to account for the small velocity increment that would be caused by unlatching the scan platform at a later time on the trajectory.

After the three maneuver parameters (pitch turn, roll turn, and burn duration) had been computed, the appropriate commands were stored in the CC&S, and the maneuver was executed.

#### B. Inflight Results

The accuracy requirements for both *Mariners VI* and *VII* were satisfied with only one midcourse maneuver for each spacecraft. The maneuver for *Mariner VI* was computed on February 28, 1969, based on the best estimate of the orbit at that time. It was determined that no constraints were violated, and motor ignition occurred at 00:54:44 GMT on March 1, 1969. The midcourse maneuver for *Mariner VII* proved to be more complex.

The standard maneuver, with the star Canopus as the roll position reference, would have required a pitch turn of 69.5 deg, which would have caused a battery-share condition (tilting the solar panels by this amount). Maneuver computations were made by use of the stars Vega and Sirius for the roll reference. A similar problem to that with Canopus existed if Vega were used, but a very attractive maneuver resulted from use of Sirius. Consequently, on April 7, 1969, the command was sent to acquire Sirius; the final maneuver calculations were then made, and motor ignition occurred at 20:22:09 GMT on April 8.

Table 5 lists the actual maneuver parameters that were calculated, the commanded maneuvers (which differed from those calculated because of quantization of the commands), and estimates of the actual maneuvers performed. Statistics on the maneuvers are also given. The encounter parameters resulting from the injections and the maneuvers are listed in Table 6. Table 7 indicates the sensitivity of the maneuver parameters to the time of maneuver execution. Figure 8 is a **B**-plane diagram of the Mars capture radius, with actual and desired injection aiming points. The cone and clock angles of the Earth and Sun during the midcourse turns for each spacecraft are given in Figs. 9 and 10. Figure 11 shows the 1-m/s capability ellipses at the

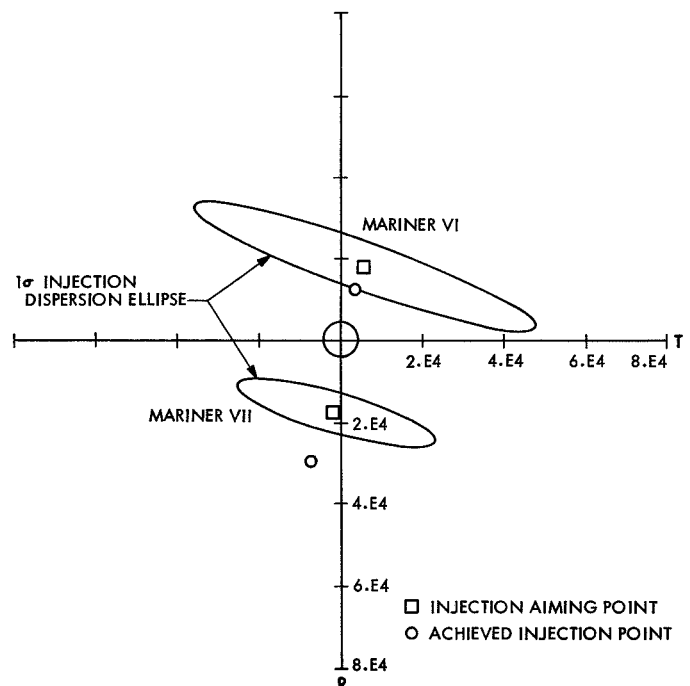


Fig. 8. Plot of injection dispersions and aiming points

**Table 5. Mariners VI and VII maneuver parameters and statistics**

Parameter	Mariner VI			Mariner VII		
	PT, <sup>a</sup> deg	RT, <sup>b</sup> deg	$\Delta V$ , <sup>c</sup> m/s	PT, deg	RT, deg	$\Delta V$ , m/s
Computed value	-23.33	78.68	3.0679	-35.64	-12.83	4.2920
Commanded value	-23.44	78.72	3.0679	-35.58	-12.84	4.2920
Time interval, s	130.0	454.0	5.350	193.0	71.0	7.600
Best estimate of actual value	-24.11	77.97	3.1456	-36.25	-12.65	4.2879
Estimated error	-0.67	-0.76	0.0777	-0.67	0.19	-0.0041
A priori standard deviation	0.400	0.378	0.038	0.384	0.352	0.054
Error in standard deviations	1.68	2.01	2.04	1.74	0.54	0.076
Standard deviation in estimate of actual value	0.23	0.03	0.008	0.077	0.185	0.015

<sup>a</sup>PT = pitch turn.  
<sup>b</sup>RT = roll turn.  
<sup>c</sup> $\Delta V$  = change in velocity.

**Table 6. Desired and actual encounter parameters and statistics**

Parameter	Mariner VI		Mariner VII	
	Desired	Actual	Desired	Actual
Injection				
B • R, km	-17,900	-13,077	18,109	29,324
B • T, km	5,920	3,684	-1,324	-6,840
TCA <sup>a</sup> (Jul 31)	05:46:39	04:41:26	—	—
(Aug 5)	—	—	05:10:18	04:49:13
MCR, <sup>b</sup> m/s	—	2.075	—	1.936
Midcourse				
B • R, km	-643	-410	3,439	3,537
B • T, km	7,400	7,786	6,520	6,669
TCA (Jul 31)	05:17:26	05:18:44	—	—
(Aug 5)	—	—	05:01:02	05:00:11
Miss in number of standard deviations	—	0.29	—	0.25

<sup>a</sup>TCA = time of closest approach, GMT (1969).  
<sup>b</sup>MCR = midcourse correction requirement to achieve injection aim point.

time of the maneuver for each spacecraft, along with actual and desired injection aiming points and desired postmaneuver aiming points.

These two maneuvers represent the most accurate maneuvers ever made with a *Mariner* class spacecraft. As shown in Table 6, the differences between the desired and actual results (compared to *Mariner V*, the *Mariner Venus 1967* mission) were:

Spacecraft	$\Delta B$ , km	$\Delta TCA$ , s
<i>Mariner VI</i>	450	78
<i>Mariner VII</i>	178	-51
<i>Mariner V</i>	3290	-1565

The final encounter parameters were subsequently changed by the perturbations that affected both spacecraft. Even with the effects of these perturbations taken into account, the encounter trajectories were very close to those desired.

**Table 7. Sensitivity of maneuver parameters to maneuver time**

Date (1969)	Maneuver time (GMT)	$\Delta V$ , m/s	PT, deg	RT, deg
<b>Mariner VI<sup>a</sup></b>				
Feb 28	00:50	3.122	-23.65	78.66
Mar 1	00:50	3.073	-23.49	78.38
Mar 2	00:50	3.032	-23.31	78.11
Mar 7	00:50	2.874	-22.12	76.88
<b>Mariner VII<sup>a</sup></b>				
Apr 2	20:30	4.332	-40.32	-13.75
Apr 5	20:30	4.300	-38.46	-13.32
Apr 8	20:30	4.282	-36.64	-13.02
Apr 12	20:30	4.273	-34.24	-12.79

<sup>a</sup>Mariner VI turns are based on a Canopus roll reference; Mariner VII turns are based on a Sirius roll reference.

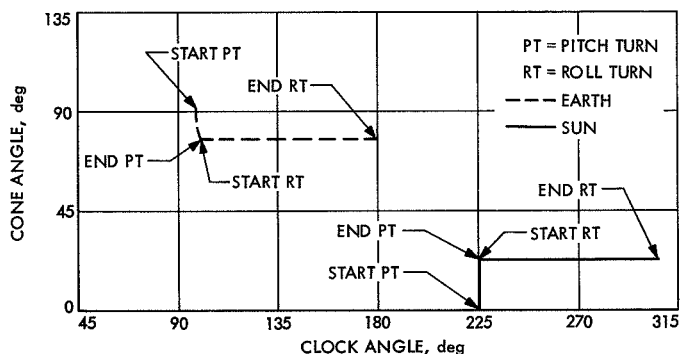


**Fig. 9. Cone and clock angles of the Sun and Earth for Mariner VI during maneuver turns**

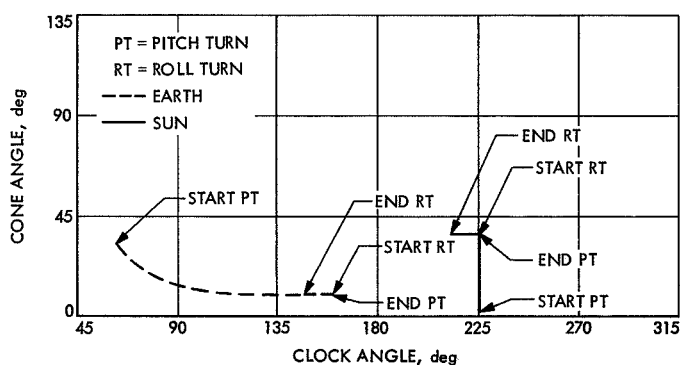


**Fig. 10. Cone and clock angles of the Sun and Earth for Mariner VII during maneuver turns**

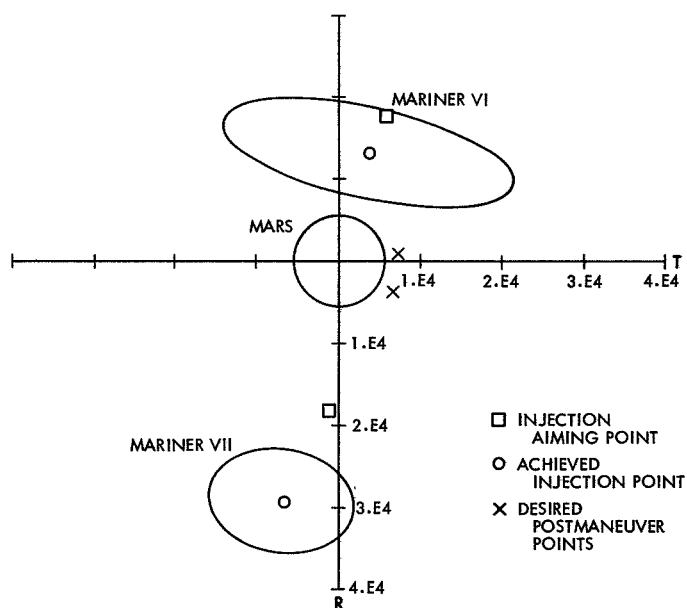


**Fig. 11. Plot of 1-m/s capability ellipses and aiming points**

The actual postmaneuver values quoted are exclusive of the effects of the scan-platform unlatch. Although the nominal arrival times for *Mariners VI* and *VII* were 05:18 and 05:05, respectively, the desired times shown in Table 6 for the midcourse maneuver are those determined to lead to zero resolution error, as discussed below. The midcourse correction requirement (MCR) was to null the injection error at the time of the maneuver; i.e., to alter the trajectory so that it would pass through the desired injection aiming point.

#### IV. Heliocentric Phase

This phase was characterized by the very low sensitivity of the spacecraft velocity profile to its position in space. Under these conditions, the orbit determination process took several weeks to converge to as good an estimate as had been attained at the time the maneuver was performed. Because of requirements to track other spacecraft, it was not possible to schedule continuous tracking coverage during this period, which further delayed the time at which good orbit estimates became available.

Initial results were used to determine whether or not a second maneuver would be necessary. In both cases, the maneuvers placed the spacecraft on sufficiently accurate trajectories so that all mission requirements were satisfied.

After a significant amount of tracking data had been accumulated, the results were used to plan detailed encounter sequences, which would be modified based on the tracking data accumulated during the encounter phase.

##### A. Mariner VI

The spacecraft, after leaving the vicinity of the Earth, proceeded on an approximately elliptical trajectory about the Sun until it approached the vicinity of Mars. Figure 12 shows the heliocentric orbit.

The midcourse maneuver had occurred 4 days after launch; the scan platform was unlatched less than 6 days after the maneuver. The perturbation caused by scan unlatch had been estimated and allowed for in the maneuver, but the actual profile of the unlatching departed somewhat from that predicted, and the short interval between nongravitational-force events did not allow for adequate convergence of the postmaneuver orbit calculation before the additional perturbation.

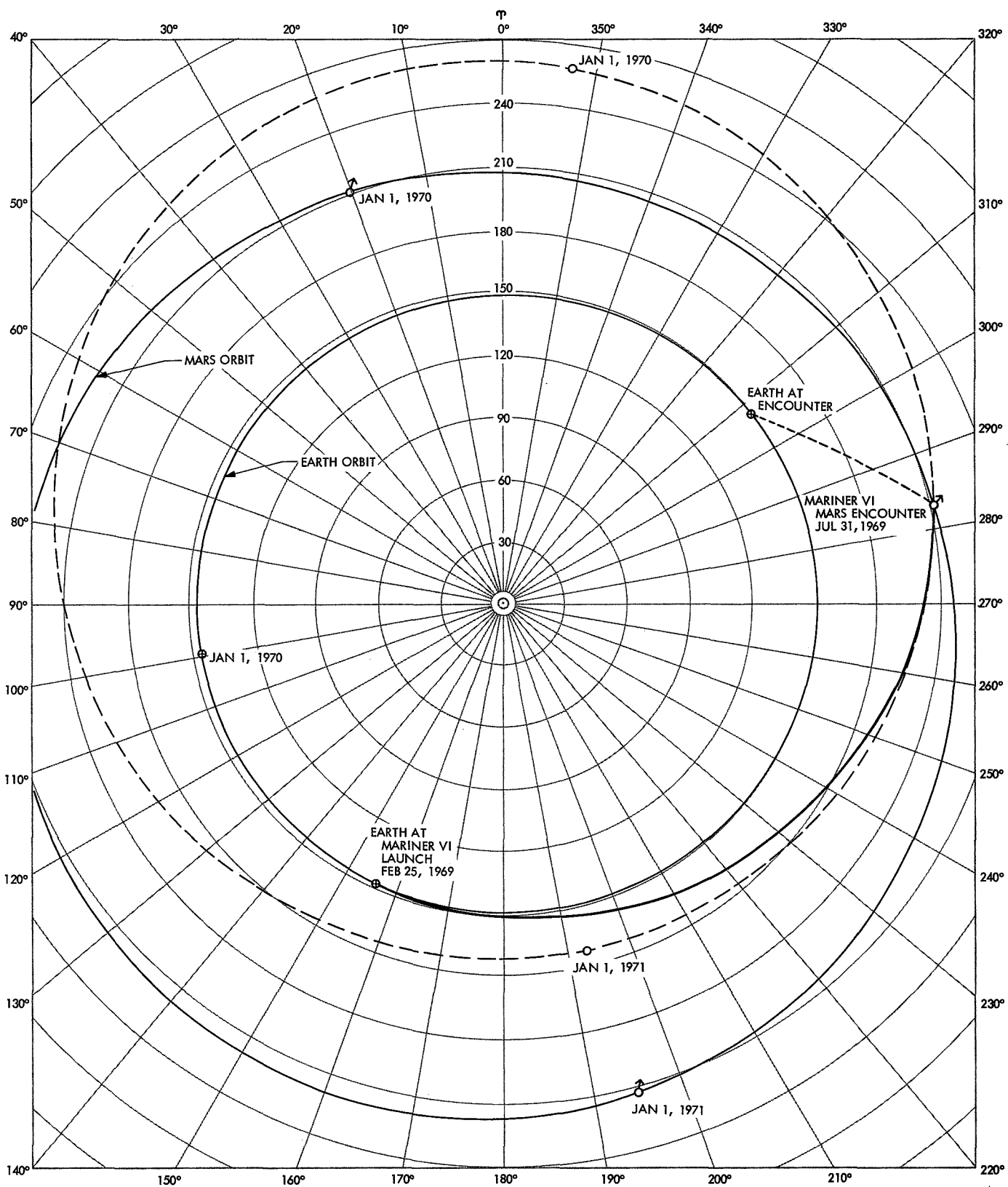


Fig. 12. Heliocentric orbit of *Mariner VI*

**1. Magellanic Cloud perturbation.** A small anomaly occurred during the heliocentric phase on about April 20, 1969. The cone angle of Canopus changes during this phase so that Canopus slips out of the field of view of the Canopus tracker if the cone angle of the tracker is not updated. During the update period, around 22:30 GMT on April 20, the Canopus cone angle was anomalously switched to the incorrect position. The subsequent loss of Canopus and the many roll-jet actuations while it was attempted to acquire the brightest spot in the Large Magellanic Cloud resulted in a 2-mm/s change in radial velocity. The aiming point at Mars changed slightly, by only 50 km in the **B**-plane, and 12 s in arrival time.

**2. Orbit determination.** The primary tracking support during this period was provided by DSSs 12, 41, and 51. Tracking data were also provided by DSSs 14, 62, and 42. Continuous tracking coverage was provided until 10 days after the maneuver. Thereafter, the tracking coverage was intermittent, and averaged about 45 h/wk. At  $E - 9$  days, continuous tracking coverage was again provided, and continued until  $E + 6$  days.

The first orbit computation showed a large offset from the maneuver aiming point, which was discovered to be caused by a timing error in the tracking data. A new calculation was performed, whose results (compared with the aiming point) are as follows:

Orbit POST 1	Maneuver aiming point (MAP)	POST 1 — MAP
$\mathbf{B} \cdot \mathbf{R} = -460$ km	$\mathbf{B} \cdot \mathbf{R} = -643$ km	$\Delta \mathbf{B} \cdot \mathbf{R} = 183$ km
$\mathbf{B} \cdot \mathbf{T} = 7779$ km	$\mathbf{B} \cdot \mathbf{T} = 7452$ km	$\Delta \mathbf{B} \cdot \mathbf{T} = 327$ km
TCA = 05:17:28 GMT	TCA = 05:17:50 GMT	$\Delta \text{TCA} = -22$ s

This orbit was based on about 20 h of doppler and range data. At this point, the doppler-only and range-and-doppler solutions were in agreement. With additional data, these solutions began to diverge; 7 days after the maneuver, the disparity was as follows:

Doppler only	Doppler and range
$\mathbf{B} = 7649$ km	$\mathbf{B} = 7410$ km
$\mathbf{B} \cdot \mathbf{R} = -384$ km	$\mathbf{B} \cdot \mathbf{R} = -412$ km
$\mathbf{B} \cdot \mathbf{T} = 7639$ km	$\mathbf{B} \cdot \mathbf{T} = 7398$ km
TCA = 05:18:03.493 GMT	TCA = 05:18:17.123 GMT

At this point, the scan unlatch perturbed the orbit. This precluded further calculation making use of additional accumulated data, which were expected to bring the solutions together. The best estimate of the orbit between maneuver and scan unlatch, expressed in target conditions, is:

$$\begin{aligned}\mathbf{B} &= 7745 \text{ km} \\ \mathbf{B} \cdot \mathbf{R} &= -436 \text{ km} \\ \mathbf{B} \cdot \mathbf{T} &= 7733 \text{ km} \\ \text{TCA} &= 05:19:09 \text{ GMT}\end{aligned}$$

The maneuver evaluation, based on tracking data, gives the comparison shown in Table 8 in terms of velocity increment.

**Table 8. Mariner VI maneuver evaluation in terms of velocity increment**

Parameter	$\Delta DX$ , m/s	$\Delta DY$ , m/s	$\Delta DZ$ , m/s	$\Delta V$ , m/s
OD estimate <sup>a</sup>	-0.57525	2.3608	-1.9977	3.1456
Commanded maneuver <sup>b</sup>	-0.54672	2.3031	-1.9516	3.0679
Maneuver error <sup>c</sup>	-0.02853	0.0577	-0.0461	0.0777

<sup>a</sup>OD estimate = current best postmaneuver estimate minus current best premaneuver estimate mapped to postmaneuver epoch.  
<sup>b</sup>Commanded maneuver = midcourse velocity increment computed by maneuver group based on NOMA 2XK orbit.  
<sup>c</sup>Maneuver error = OD estimate minus commanded maneuver.

Expressed in terms of changes to target conditions, the maneuver evaluation is as shown in Table 9.

**Table 9. Mariner VI maneuver evaluation in terms of target condition changes**

Parameter	$\Delta \mathbf{B} \cdot \mathbf{R}$ , km	$\Delta \mathbf{B} \cdot \mathbf{T}$ , km	$\Delta \text{TCA}$ , s
OD error <sup>a</sup>	-168	64	72
Maneuver error <sup>b</sup>	401	270	-18
Overall error <sup>c</sup>	233	334	54

<sup>a</sup>OD error = Current best premaneuver estimate minus orbit used for maneuver computation.  
<sup>b</sup>Maneuver error = overall error minus OD error.  
<sup>c</sup>Overall error = current best postmaneuver estimate minus maneuver aiming point.



After the scan platform was unlatched and (within a few days) continuous tracking ended, the orbit solutions converged very slowly. A solution restrained by *a priori* statistics was more than 1250 km (in the **B**-plane) and 2 min (in arrival time) from one in which the data were fitted without *a priori* restraint when only 5 days of intermittent tracking data were available. With 18 days of intermittent tracking data, this difference had fallen to less than 450 km and 40 s; after 43 days, the solutions had converged. The effect of scan unlatch, by comparison of the best estimates of the orbit before and after its occurrence (at common epoch), was calculated to be 0.0105 m/s; the uncertainty in the velocity components is as large as that in the difference components. The best estimate of the post-unlatch orbit, expressed as target conditions, is:

$$\mathbf{B} = 7638 \text{ km}$$

$$\mathbf{B} \cdot \mathbf{R} = -437 \text{ km}$$

$$\mathbf{B} \cdot \mathbf{T} = 7626 \text{ km}$$

$$\text{TCA} = 05:19:02 \text{ GMT}$$

During the spacecraft Canopus-tracker cone-angle anomaly (see Spacecraft System Performance in Part 3), the attitude-control gas jets were fired many times to move the field of view of the Canopus tracker to the Large Magellanic cloud. Because of a slight imbalance in the roll-control jets, a net impulse was imparted to the spacecraft, resulting in a small perturbation of the orbit. The total doppler change shown by the doppler residuals was 0.03 Hz. Therefore, the previous tracking data were invalidated for cumulative orbit-determination purposes, as had been the case after the maneuver and scan-unlatch events.

With approximately 2 months of intermittent tracking data, the following solutions were obtained:

Parameter	Solution A	Solution B	Solution C
<b>B</b> , km	7550	7616	7628
<b>B</b> • <b>R</b> , km	−511	−418	−367
<b>B</b> • <b>T</b> , km	7533	7064	7619
TCA, GMT	05:19:13.114	05:19:08.376	05:19:05.539

Solution A was computed using only doppler data, and estimated only the state vector. Solution B was also computed using only doppler data, and estimated the state vector and the three components of solar pressure and station locations. Solution C was computed using doppler and planetary ranging data, and estimated the same parameters as those of solution B. The orbit solutions at *E* − 5 days are listed in Table 10.

The four solutions agreed quite well. However, much more confidence was placed in the time of closest approach that was computed by use of doppler and range data.

The numerical results of the pre-unlatch, post-unlatch, and post-Magellanic orbit computations are presented in Table 11. Figures 13–15 show the **B**-plane estimates of the orbits computed during the pre-unlatch, post-unlatch, and post-Magellanic periods. Figures 16–18 show the time of closest approach of the pre-unlatch, post-unlatch, and post-Magellanic orbits.

**Table 10. Orbit solutions at *E* − 5 days**

Orbit	Type of data	Parameters estimated	<b>B</b> , km	<b>B</b> • <b>R</b> , km	<b>B</b> • <b>T</b> , km	TCA, GMT
3 POST 49	Doppler	State vector; three components of solar pressure	7586	−302	7580	05:18:53.889
3 POST 89	Doppler	State vector; three components of solar pressure; station location	7599	−359	7591	05:18:54.147
3 POST 91	Doppler and range	State vector; three components of solar pressure	7575	−320	7568	05:19:03.754
3 POST 47	Doppler and range	State vector; three components of solar pressure; station location	7587	−402	7577	05:19:02.441

**Table 11. Results of pre-unlatch, post-unlatch, and post-Magellanic orbit computations for Mariner VI**

Orbit	B, km	B • R, km	B • T, km	TCA, GMT	Time of last data point, GMT		Deep Space Stations used in orbit	Data types used <sup>a</sup>	Parameters estimated <sup>b</sup>
					Date	Time			
POST 1	7793.0214	-460.19057	7779.4223	05:17:27.575	Mar 1	21:54:02	41, 51, 12	RU, CC3	State vector
POST 2	7801.5570	-452.76303	7788.4078	05:17:28.080	Mar 1	21:43:32		CC3	
POST 3	7831.6724	-448.18057	7818.8376	05:17:25.818	Mar 2	01:14:32		RU, CC3	
POST 4	7519.9435	-314.07063	7513.2819	05:18:23.792	Mar 2	14:56:32		RU, CC3	
POST 5	7498.8235	-367.30898	7589.9407	05:18:06.153	Mar 2	19:44:32		CC3	
POST 6	7520.8736	-341.91268	7513.0975	05:18:19.516	Mar 3	15:26:32		CC3	
POST 7	7421.5097	-338.52906	7413.7848	05:18:29.219	Mar 3	15:26:32		RU, CC3	
POST 8	7433.1472	-346.04453	7425.0875	05:18:26.429	Mar 3	22:10:32		CC3	
POST 9	7852.3048	-371.35706	7843.5185	04:17:45.335	Mar 4	00:54:32			
POST 10	7876.3022	-370.36533	7867.5896	05:17:42.795		00:54:32			
POST 11	7816.4545	-358.72908	7808.2183	05:17:51.893		18:56:32		CC3	State vector State vector and G State vector
POST 12	7431.2828	-392.38301	7420.9160	05:18:18.262		19:51:32		RU, CC3	
POST 13	7807.0068	-360.90796	7798.6602	05:17:52.380		21:15:32		CC3	
POST 14	7542.1301	-381.79101	7532.4603	05:18:19.830		21:15:32		CC3	
POST 15	7721.3483	-351.07192	7713.3629	05:18:03.304	Mar 4	18:30:32		CC3	
POST 16	7383.5481	-388.59577	7373.3149	05:18:24.069	Mar 5	19:40:32		RU, CC3	
POST 17	7409.1778	-383.41172	7399.2503	05:18:22.650	Mar 4	22:26:32		RU, CC3	
POST 18	7392.6953	-388.20316	7382.4956	05:18:23.214	Mar 5	22:24:32	41, 51, 12	RU, CC3	
POST 19	7648.6165	-384.31128	7638.9550	05:18:03.493	Mar 4	18:32:32	41, 51, 13	CC3	
POST 20	7397.2372	-417.82706	7385.4274	05:18:17.192	Mar 6	18:39:32	41, 51, 12	RU, CC3	
POST 21	7409.6218	-411.67594	7398.1763	05:18:17.123	Mar 6	18:54:02	41, 51, 12	RU, CC3	State vector State vector and G State vector and station location State vector State vector State vector State vector, G, and station location State vector State vector and G State vector
2 POST 4	7651.1004	-357.15901	7642.7595	05:17:44.949	Mar 10	09:29:32	41, 51	CC3	
2 POST 11	7718.8713	-393.71728	7708.8235	05:17:30.490	Mar 11	15:28:32	41, 51, 12		
2 POST 13	7150.8454	-476.80965	7134.9311	05:18:39.625	Mar 12	17:45:32			
2 POST 14	7203.0341	-472.11011	7187.5452	05:18:17.842	Mar 12	17:45:32			
2 POST 15	7251.9190	-473.42394	7236.4490	05:18:13.023	Mar 12	17:45:32			
2 POST 18	8025.9455	-352.70477	7998.1720	05:17:04.945	Mar 13	19:38:32			
2 POST 19	7255.1697	-413.63569	7243.3686	05:18:19.010	Mar 16	08:58:32			
2 POST 21	7159.5740	-451.59686	7145.3171	05:18:34.135	Mar 17	19:35:02	41, 51, 12	CC3	
2 POST 23	7020.7920	-451.77824	7006.2411	05:18:37.722	Mar 19	16:54:02	41, 51, 12, 14	PRU, CC3	
2 POST 24	7409.7139	-411.02479	7398.3049	05:18:01.708	Mar 19	08:41:02		CC3	State vector State vector and G State vector State vector
2 POST 28	7535.1354	-413.10636	7523.7996	05:17:58.681	Mar 20	18:30:02			
2 POST 29	7545.1992	-397.43958	7534.7242	05:17:50.533	Mar 20	18:30:02	41, 51, 12, 14		
2 POST 32	7600.23	-391.81	7590.13	05:17:45.228	Mar 24	17:56:02	42, 41, 51, 12, 14	CC3	

<sup>a</sup>PRU indicates planetary range units.

<sup>b</sup>KM is the mass of the Moon multiplied by the gravitational constant. MM is the Mars-to-Sun mass ratio.

Table 11 (contd)

Orbit	B, km	B • R, km	B • T, km	TCA, GMT	Time of last data point, GMT		Deep Space Stations used in orbit	Data types used	Parameters estimated
					Date	Time			
2 POST 38	8099.24	−340.94	8092.06	05:16:57.464	Mar 25	07:54:02	42, 41, 51, 12, 14	CC3	State vector
2 POST 40	7957.13	−354.67	7949.22	05:17:10.601	Mar 29	14:14:02	↓	↓	
2 POST 41	7754.1692	−360.57140	7745.7813	05:17:31.125	Apr 3	12:36:02	↓	↓	
2 POST 42	7688.0597	−370.29846	7679.1366	05:17:37.123	Apr 7	10:54:02	42, 41, 51, 12, 14	↓	
2 POST 43	7681.3892	−369.87816	7672.4785	05:17:37.862	Apr 9	13:12:02	14, 12, 51, 41	↓	
2 POST 44	7626.0869	−377.70226	7616.7277	05:17:44.069	Apr 18	21:31:02	42, 41, 51, 62, 12, 14	CC3	
2 POST 48	7415.5997	−540.24786	7395.8932	05:17:58.148	Apr 18	21:31:02	42, 41, 51, 62, 12, 14	CC3, PRU	
2 POST 50	7605.9919	−378.02251	7596.5918	05:17:46.462	Apr 23	17:35:02	42, 41, 51, 62, 12, 14	CC3	
2 POST 55	7583.8298	−368.51970	7574.8705	05:17:50.382	Apr 30	14:02:02	42, 41, 51, 62	↓	
3 POST 2	7517.1291	−477.36714	7501.9564	05:19:01.457	Jun 2	02:16:12	41, 51, 62, 12	↓	State vector
3 POST 3	7552.1426	−428.35860	7539.9844	05:19:04.285	Jun 2	02:16:12	41, 51, 62	↓	State vector, solar pressure, and station location
3 POST 5	7535.5111	−459.40841	7521.4936	05:19:07.358	Jun 16	22:01:02	41, 51, 62, 12	↓	State vector
3 POST 6	7585.9066	−378.59128	7576.4530	05:19:07.910	Jun 16	22:01:02	↓	↓	State vector, solar pressure, and station location
3 POST 7	7543.2270	−476.64540	7528.1526	05:19:11.255	Jun 23	00:49:02	↓	↓	State vector
3 POST 8	7606.2994	−377.447761	7597.0754	05:19:09.831	Jun 25	01:35:02	41, 51, 62, 12	↓	State vector, solar pressure, and station location
3 POST 9	7544.4506	−472.42847	7529.6442	05:19:12.699	Jun 30	07:33:02	42, 41, 51, 62, 12	↓	State vector
3 POST 10	7617.2135	−380.69839	7607.6940	05:19:09.592	Jun 30	07:53:02	42, 41, 51, 62, 12	↓	State vector, solar pressure, and station location
3 POST 16	7617.8870	−400.86622	7607.3323	05:19:08.174	Jul 7	14:12:02	42, 14, 12, 62, 51, 41, 72	↓	State vector
3 POST 17	7628.0903	−367.87485	7619.2142	05:19:05.517	Jul 7	14:12:02	42, 41, 62, 72, 51, 12, 14	↓	State vector, solar pressure, and station location
3 POST 19	7624.1379	−369.0434	7615.2008	05:19:07.907	Jul 14	07:49:02	41, 72, 51, 62, 12, 14	CC3	State vector, solar pressure, and station location
3 POST 22	7609.5196	−254.50233	7605.2623	05:19:06.992	Jul 14	07:49:02	41, 51, 62, 12, 14	CC3, PRU	State vector
3 POST 30	7471.3125	−491.26776	7455.1431	05:19:30.799	Jul 21	04:50:02	11, 41, 51, 62, 12, 14	CC3	State vector

Table 11 (contd)

Orbit	B, km	B • R, km	B • T, km	TCA, GMT	Time of last data point, GMT		Deep Space Stations used in orbit	Data types used	Parameters estimated
					Date	Time			
3 POST 31	7603.5634	—370.44968	7594.5336	05:19:02.151	Jul 21	04:50:02	41, 72, 51, 62, 12, 14	CC3	State vector, solar pressure, and station location
3 POST 32	7600.2911	—383.62063	7590.6032	05:19:03.640	Jul 21	04:50:02	↓	CC3, PRU	State vector, solar pressure, and station location
3 POST 37	7583.7563	—318.64433	7577.0590	05:19:00.631	Jul 23	16:00:02		CC3	State vector, KM, and solar pressure
3 POST 38	7579.3768	—321.75321	7572.5441	05:19:04.035	↓	16:00:02		CC3, PRU	State vector, KM, and solar pressure
3 POST 39	7593.1372	—381.63736	7583.5402	05:19:01.713		16:00:02	41, 72, 51, 62, 12, 14	CC3	State vector, KM, solar pressure, and station location
3 POST 46	7474.4644	—346.66963	7466.4204	05:18:56.876	Jul 23	06:31:32	14	PRU	State vector
3 POST 47	7587.2651	—401.9796	7576.6089	05:19:02.441	Jul 26	06:21:02	41, 72, 51, 62, 12, 14	CC3, PRU	State vector, KM, solar pressure, and station location
3 POST 48	7592.8269	—385.52853	7583.0326	05:18:59.990	↓	06:21:02	41, 72, 51, 62, 12, 14	CC3	State vector, KM, solar pressure, and station location
3 POST 49	7586.4945	—302.46619	7580.4625	05:18:53.889		06:21:02	41, 51, 62, 12, 14	CC3	State vector, KM, and solar pressure
3 POST 89	7599.913	—358.82755	7591.4371	05:18:54.147		02:30:02	41, 72, 51, 62, 12, 14	CC3	State vector, MM, solar pressure, and station location
3 POST 91	7574.7801	—320.2213	7568.0079	05:19:03.754	Jul 26	02:30:02	41, 72, 51, 62, 12, 14	CC3, PRU	State vector, MM, and solar pressure

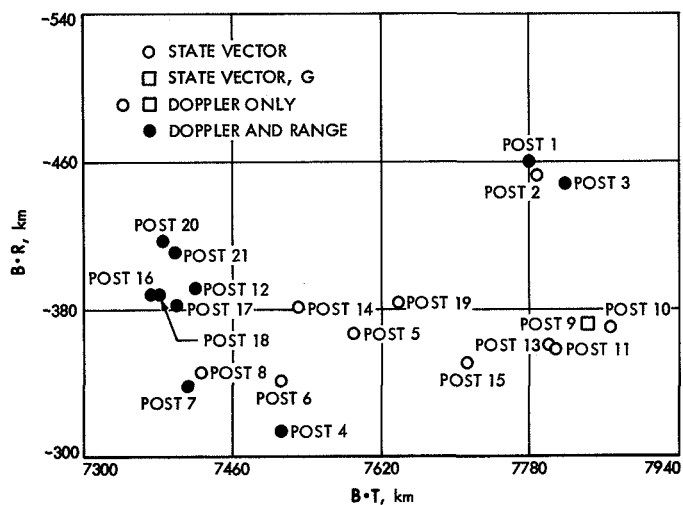


Fig. 13. Mariner VI pre-unlatch B-plane estimates

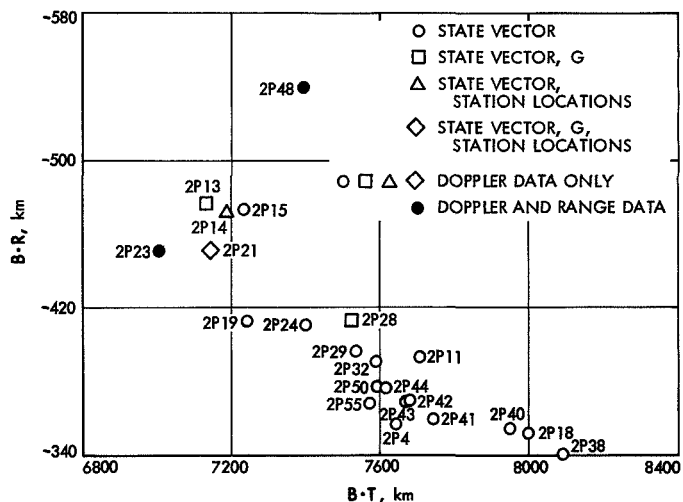


Fig. 14. Mariner VI post-unlatch B-plane estimates

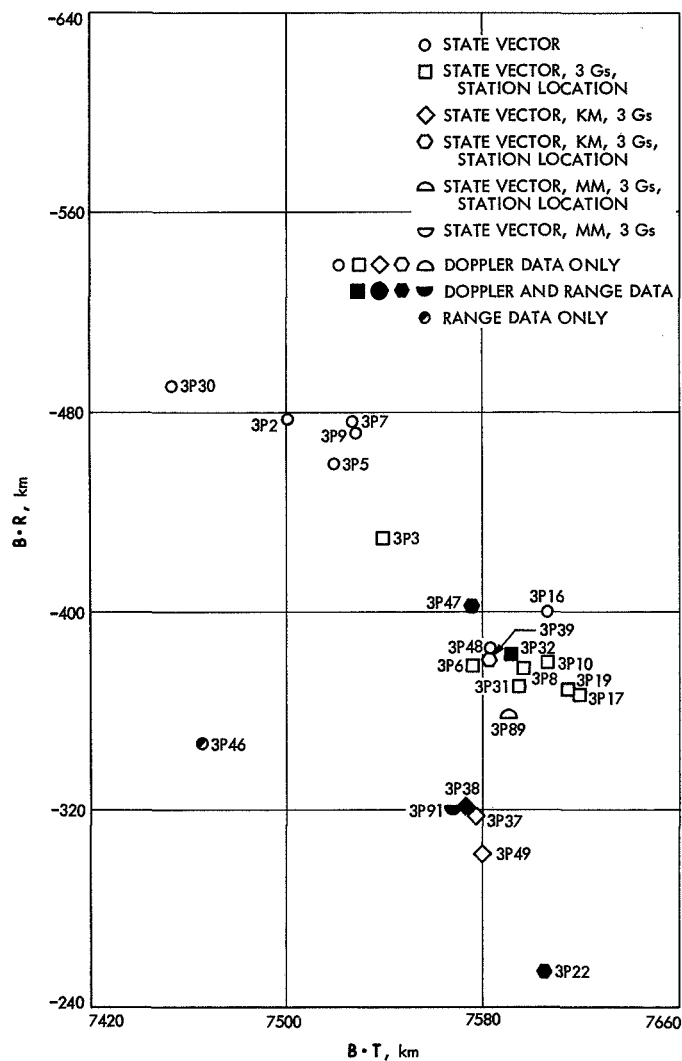
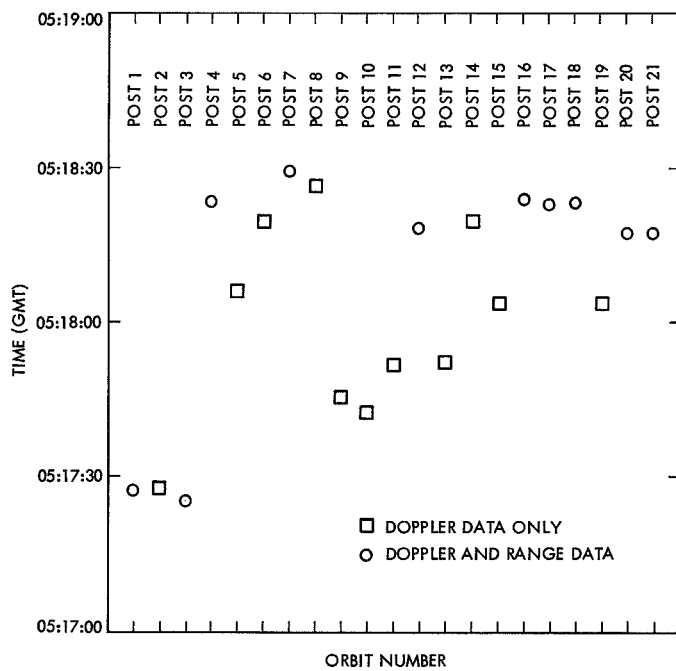
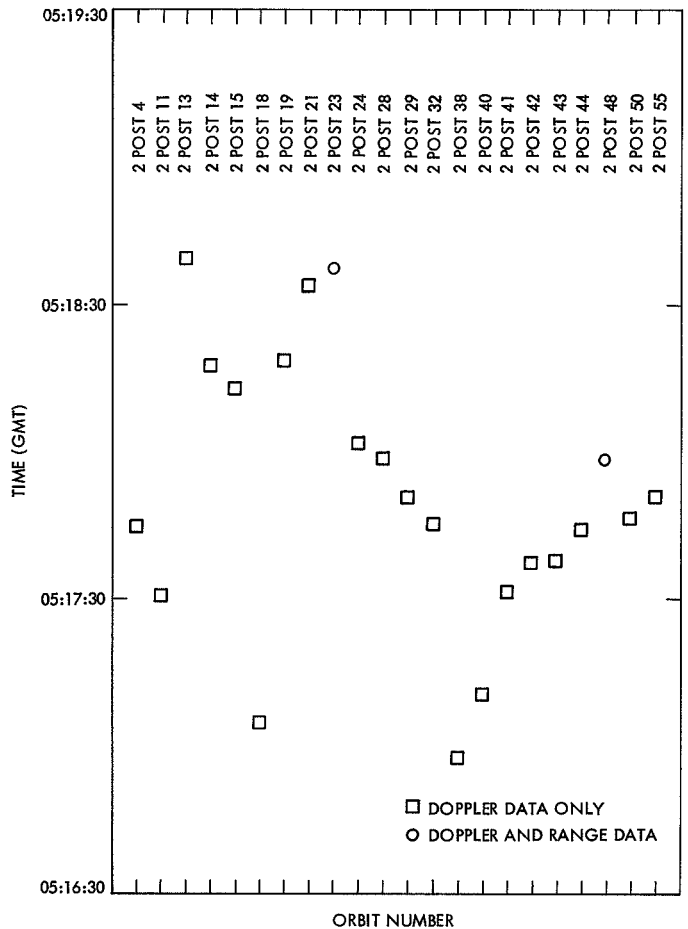


Fig. 15. Mariner VI post-Magellanic B-plane estimates



**Fig. 16. Mariner VI pre-unlatch estimates of time of closest approach, July 31, 1969**



**Fig. 17. Mariner VI post-unlatch estimates of time of closest approach, July 31, 1969**

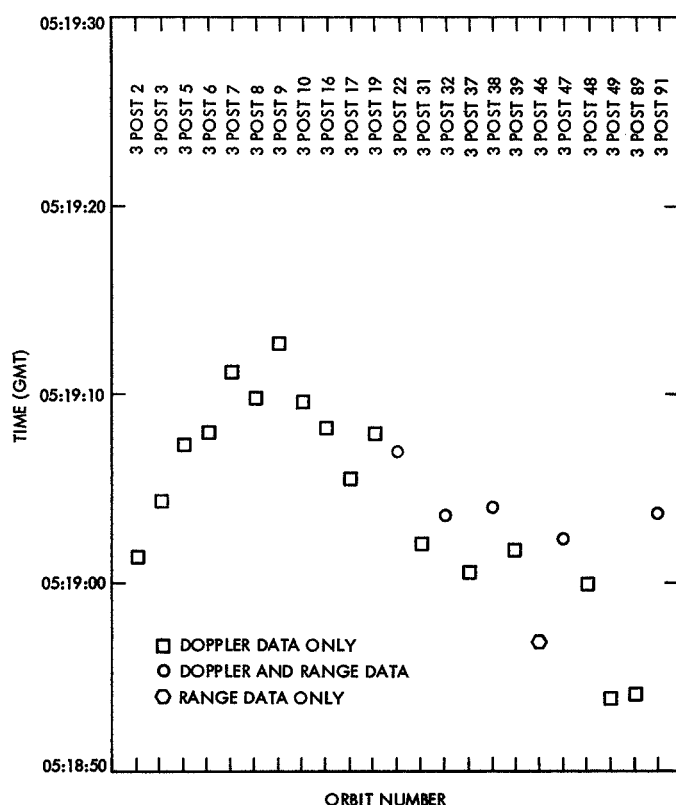


Fig. 18. Mariner VI post-Magellanic estimates of time of closest approach, July 31, 1969

## B. Mariner VII

After the midcourse maneuver (April 8, 1969), the Mariner VII spacecraft continued (cruise mode) in a heliocentric orbit (Fig. 19). Near-Earth ranging continued for about 2 wk, and terminated several days earlier than expected (see Spacecraft System Performance in Part 3 of this volume). Planetary ranging was started on June 20, on an experimental basis, and regular ranging passes began on July 8. The scan platform was unlatched on May 8, in the middle of the no-ranging period, changing the velocity vector by 0.0108 m/s.

**1. Spacecraft major anomaly.** Near the end of the heliocentric cruise period for Mariner VII (and during the late far-encounter of Mariner VI, which therefore dominated the tracking schedule), the spacecraft suffered a major anomaly, which is described fully under Spacecraft System Performance. The radio signal was first lost at approximately 22:11 GMT on July 30, and roll reacquisition occurred at approximately 11:35 on July 31. One effect of the anomaly, inferred to take the form of venting the battery electrolyte to space, changed the

spacecraft velocity by  $-7.67$  cm/s in the Earth-radial direction. No nongravitational acceleration was observed in the doppler data before the first loss of signal; it was estimated to have lasted about 2 h (into a 7-h telemetry and tracking blackout). After the signal had been reacquired, a second telemetry blackout occurred; at that time, a second period of acceleration began. One-way doppler data were received throughout this period, but were not usable for precise analysis. The second acceleration continued on a diminishing scale for several days. The total effect was estimated to be 39.2 cm/s, with an upper bound of 90 cm/s and a lower bound of the Earth-radial component.

**2. Orbit determination.** The primary tracking support during this period was provided by DSSs 12, 41, 51, and 62. Tracking data were also provided by DSSs 14 and 42.

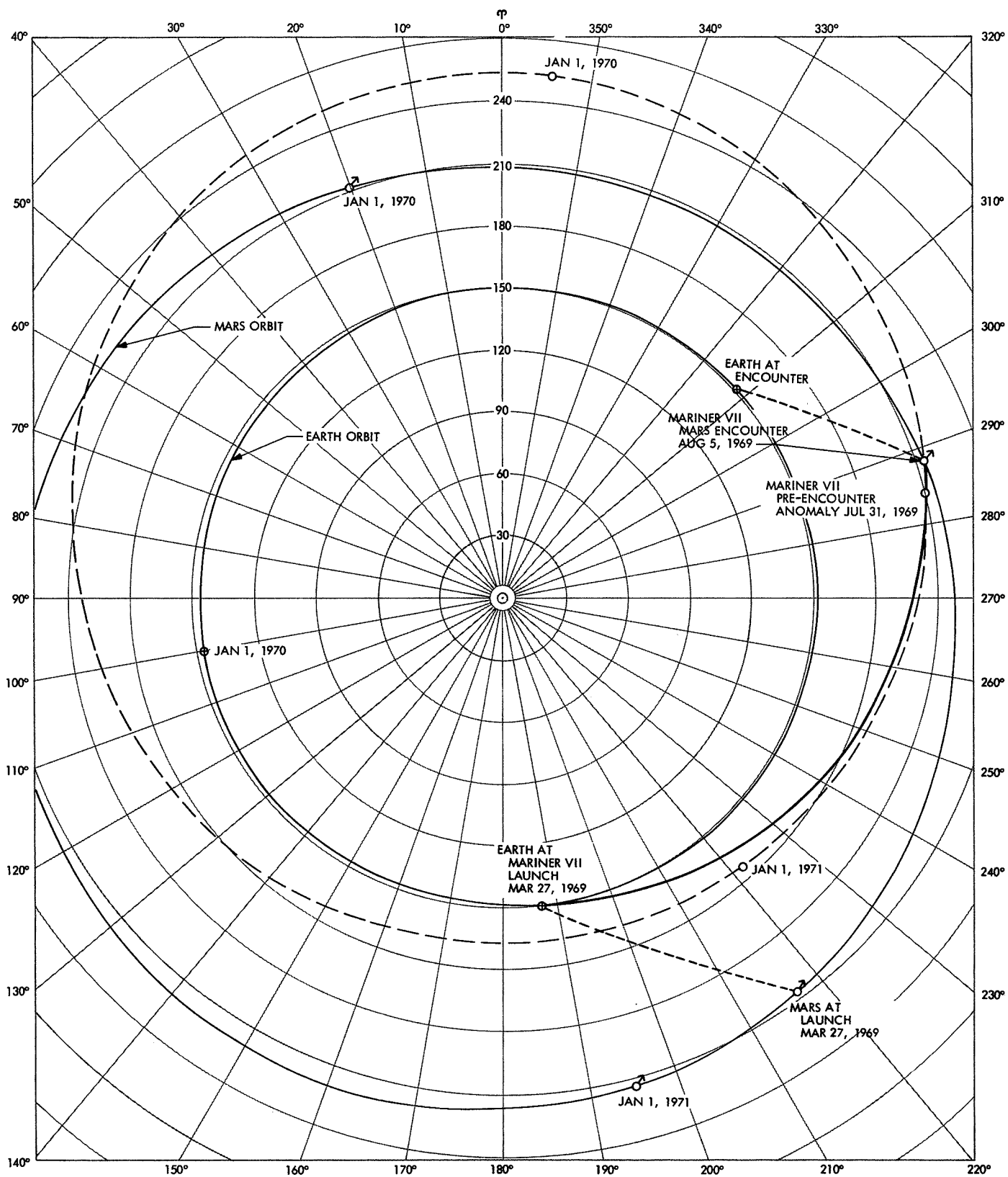
With about 2 days of tracking data after the maneuver, orbit solutions were computed by use of doppler and range data. These orbits estimated only the state vector; when these solutions were mapped to the target, they showed the comparison with the maneuver aiming point listed in Table 12.

Table 12. Comparison of orbit solutions (POST 4 and POST 5)

Orbit POST 4 (doppler only)	Orbit POST 5 (doppler and RU)	Maneuver aiming point
B•R = 2959 km B•T = 6684 km TCA = 05:00:59.333 GMT	B•R = 3540 km B•T = 6409 km TCA = 04:58:55.716 GMT	B•R = 3440 km B•T = 6528 km TCA = 05:01:09 GMT

With 7 days of data, the following solutions were computed:

Parameter	Doppler only	Doppler and RU	Doppler and RU and PRU
B • R, km	3427	4136	3566
B • T, km	6522	6094	6421
TCA, GMT	04:59:54.409	04:59:24.316	04:59:14.300



**Fig. 19. Heliocentric orbit of Mariner VII**



The range RU is the data from the Mark IA ranging system for near-Earth tracking. The range PRU is the data from the planetary ranging system for tracking at greater distances. The doppler and range PRU solution was not computed during premaneuver operations.

The preliminary evaluation of the midcourse maneuver based on Deep Space Station tracking data was made by use of the current best estimate of the premidcourse orbit; the state vector of this orbit was mapped to an epoch after the midcourse maneuver. This mapped forward state vector was differenced with the state vector of the current best estimate of the pre-unlatch orbit at the same epoch. The results of this comparison are given in Table 13.

**Table 13. Mariner VII maneuver evaluation in terms of velocity increment**

Parameter	$\Delta DX,$ m/s	$\Delta DY,$ m/s	$\Delta DZ,$ m/s	$\Delta V,$ m/s
OD estimate <sup>a</sup>	-1.7121	-0.6049	3.8844	4.2879
Commanded maneuver <sup>b</sup>	-1.6996	-0.57226	3.8994	4.2920
Maneuver error <sup>c</sup>	-0.0125	-0.0326	-0.0150	-0.0041
<sup>a</sup> OD estimate = current best postmaneuver estimate minus current best premaneuver estimate mapped to postmaneuver epoch.				
<sup>b</sup> Commanded maneuver = midcourse velocity increment computed by maneuver group based on LAPM-XG orbit.				
<sup>c</sup> Maneuver error = OD estimate minus commanded maneuver.				

The effect of these errors, when mapped to the target, are listed in Table 14.

**Table 14. Effect of errors mapped to target**

Parameter	$\Delta B \cdot R,$ km	$\Delta B \cdot T,$ km	$\Delta TCA, s$
OD error <sup>a</sup>	15	-63	51
Maneuver error <sup>b</sup>	82	204	-109
Overall error <sup>c</sup>	97	141	-58
<sup>a</sup> OD error = current best premaneuver estimate minus orbit used for maneuver computation.			
<sup>b</sup> Maneuver error = overall error minus OD error.			
<sup>c</sup> Overall error = current best postmaneuver estimate minus maneuver aiming point.			

When the scan platform was unlatched at 19:18 GMT on May 8, the inflight pre-unlatch orbit (POST 30) solution indicated the following results:

$$B = 7553 \text{ km}$$

$$B \cdot R = 3536 \text{ km}$$

$$B \cdot T = 6674 \text{ km}$$

$$TCA = 05:00:21.538 \text{ GMT}$$

This solution was computed by estimation of the state vector, solar-pressure coefficient along the Sun-spacecraft direction, and station locations. The current best estimate of the pre-unlatch orbit is as follows:

$$B = 7549 \text{ km}$$

$$B \cdot R = 3537 \text{ km}$$

$$B \cdot T = 6669 \text{ km}$$

$$TCA = 05:00:11.324 \text{ GMT}$$

This solution estimated the state vector, gravitational constant of the Moon, and solar-pressure coefficients by use of doppler and range PRU data.

With about 5 days of intermittent tracking data, the post-unlatch orbit solution was as follows:

$$B = 7412 \text{ km}$$

$$B \cdot R = 3724 \text{ km}$$

$$B \cdot T = 6409 \text{ km}$$

$$TCA = 04:59:29.766 \text{ GMT}$$

This orbit solution estimated only the state vector, and use was made of doppler data only. No ranging data were taken until June 27, at which time the ranging system was tested for a very short time. Several days of testing culminated with normal ranging data starting on July 8.

The effect of scan unlatch was evaluated by comparison of the current best estimates of pre- and post-unlatch orbits. Uncertainties in the velocity components were nearly as large as the differences observed, but the value

of  $\Delta V = 0.0108$  m/s was indicated; or, in terms of target conditions,

$$\Delta \mathbf{B} \cdot \mathbf{R} = -6 \text{ km}$$

$$\Delta \mathbf{B} \cdot \mathbf{T} = -37 \text{ km}$$

$$\Delta \text{TCA} = 25.302 \text{ s}$$

where  $\Delta$  is the post-unlatch orbit minus the pre-unlatch orbit.

At approximately  $E - 5$  days, the following orbit solutions were computed:

Parameter	2 POST 39 (doppler and PRU)	2 POST 44 (doppler only)
$\mathbf{B}$ , km	7544	7502
$\mathbf{B} \cdot \mathbf{R}$ , km	3545	3513
$\mathbf{B} \cdot \mathbf{T}$ , km	6659	6629
TCA, GMT	05:00:38.075	05:00:39.942

The 2 POST 39 orbit solution estimated the state vector, the gravitational constant of the Moon, and the solar-pressure coefficients. The 2 POST 44 orbit solution

estimated the same parameters plus the station-location parameters. These two orbit solutions agreed quite well.

The current best estimate of the post-unlatch orbit is as follows:

$$\mathbf{B} = 7522 \text{ km}$$

$$\mathbf{B} \cdot \mathbf{R} = 3531 \text{ km}$$

$$\mathbf{B} \cdot \mathbf{T} = 6642 \text{ km}$$

$$\text{TCA} = 05:00:36.626 \text{ GMT}$$

This solution was computed by use of the doppler and range PRU data and by estimation of the state vector, the solar-pressure coefficients, and the gravitational constant of the Moon. Because the effects of the pre-encounter anomaly on the flight path continued through encounter, and could not be entirely isolated before encounter, these effects are discussed in Section V, Encounter Phase.

The numerical results of the postmidcourse and post-unlatch orbit computations are presented in Table 15. Figures 20 and 21 show the  $\mathbf{B}$ -plane estimates of the postmidcourse and post-unlatch inflight orbits. Figures 22 and 23 show the TCA of the postmidcourse and post-unlatch inflight orbits.

**Table 15. Results of postmidcourse and post-unlatch orbit computations for Mariner VII**

Orbit	$\mathbf{B}$ , km	$\mathbf{B} \cdot \mathbf{R}$ , km	$\mathbf{B} \cdot \mathbf{T}$ , km	TCA, GMT	Time of last data point, GMT		Deep Space Stations used in orbit	Data types used	Parameters estimated
					Date	Time			
POST 1	7586.4872	3392.5023	6785.6991	05:00:42.476	Apr 9	00:30:32	41, 62	CC3	State vector
POST 4	7309.2714	2958.5062	6683.7628	05:00:59.333	Apr 10	16:45:32	41, 62, 12	CC3	
POST 5	7278.5541	3449.6747	6409.1412	04:58:55.716	Apr 10	16:45:32	↓	RU, CC3	
POST 7	7270.9879	3360.9996	6447.5535	04:58:50.859	Apr 11	16:49:32	↓	RU, CC3	
POST 8	7345.9110	3411.5881	6505.6492	04:59:48.385	Apr 11	18:16:32	↓	CC3	
POST 11	7359.4929	3415.7120	6518.8225	04:59:55.759	Apr 14	19:52:02	41, 62, 12	CC3	
POST 13	7362.4530	4136.4199	6093.6275	04:59:24.316	Apr 15	20:36:02	41, 62, 14	RU, CC3	
POST 14	7367.6791	3426.3727	6522.3727	04:59:54.409	↓	↓	41, 62, 12, 14	CC3	
POST 15	7344.9639	3565.9663	6421.2441	04:59:14.300	↓	↓	↓	PRU, RU, CC3	
POST 17	7027.2827	3502.7279	6092.0930	04:58:06.300	Apr 15	20:36:02	↓	RU, PRU	State vector
POST 21	7384.4751	3404.3237	6552.9419	04:59:38.997	Apr 23	00:33:02	41, 62, 12, 14	CC3	State vector, G, and station location

Table 15 (contd)

Orbit	B, km	B • R, km	B • T, km	TCA, GMT	Time of last data point, GMT		Deep Space Stations used in orbit	Data types used	Parameters estimated
					Date	Time			
POST 22	7337.5640	3445.0600	6478.5341	04:59:09.190	Apr 23	00:33:02	41, 62, 12, 14	PRU, CC3, RU	State vector
POST 25	7412.1574	3429.2021	6571.1986	04:59:57.734	Apr 29	11:26:02	42, 41, 62, 12, 14	CC3	State vector
POST 26	7415.7140	3440.0118	6569.5618	04:59:57.210	May 5	01:06:12	42, 41, 62, 12, 13		State vector
POST 27	7560.4195	3525.3227	6688.1902	05:00:17.826	May 5	01:01:62	41, 62, 12, 14		State vector, solar pressure, and station location
POST 30	7553.1920	3536.2973	6674.2270	05:00:21.538	May 8	13:53:02	62, 12, 41, 14		State vector, solar pressure, and station location
POST 31	7461.9857	3480.8462	6600.374	05:00:11.553	May 8	18:53:02	41, 62, 12		State vector
2 POST 2	7412.3244	3724.4544	6408.6654	04:59:29.766	May 12	23:09:02	41, 51, 62, 12		
2 POST 3	7494.5804	3515.0269	6619.1630	05:00:32.155	May 26	23:47:02	41, 51, 62, 12		
2 POST 4	7538.6452	3600.3692	6623.3303	05:00:35.020	May 31	23:47:02	41, 51, 62, 12		State vector
2 POST 5	7556.9090	3552.6944	6669.7250	05:00:42.611	Jun 2	00:26:02	41, 51, 62, 12, 14		State vector, solar pressure, and station location
2 POST 8	7542.2323	3574.8431	6641.2169	05:00:38.514	Jun 5	00:26:02	41, 51, 62, 12, 14		State vector
2 POST 13	7535.0961	3489.7965	6678.2470	05:00:44.466	Jun 16	12:22:02	41, 51, 62, 12		State vector
2 POST 14	7553.4587	3522.860	6681.631	05:00:44.658	Jun 16	12:22:02	41, 51, 62, 12		State vector, solar pressure, and station location
2 POST 16	7542.6396	3536.126	6662.3736	05:00:43.749	Jun 23	01:19:02	11, 41, 51, 62, 12, 14		State vector
2 POST 17	7549.9826	3553.5243	6661.434	05:00:43.530	Jun 23	01:19:02	41, 51, 62, 12, 14		State vector, solar pressure, and station location
2 POST 20	7539.0735	3498.3012	6678.2865	05:00:45.672	Jun 30	11:51:02	41, 12, 14, 51, 62	CC3	State vector, solar pressure, and station location
2 POST 21	7590.0065	3592.0584	6686.2032	05:00:39.336	Jun 30	11:51:02	62, 14, 51, 41, 12	CC3, PRU	State vector, solar pressure, and station location
2 POST 24	7515.2819	3459.6721	6671.5909	05:00:47.856	Jul 7	10:49:01	62, 14, 51, 41, 12	CC3	State vector
2 POST 25	7513.8685	3414.9761	6692.9930	05:00:47.628	Jul 7	10:49:02	41, 14, 11, 12, 51	CC3	State vector, solar pressure, and station location
2 POST 27	7545.9401	3505.9699	6682.0196	05:00:46.297	Jul 14	21:50:02	41, 51, 62, 12, 14	CC3	State vector, solar pressure, and station location

Table 15 (contd)

Orbit	B, km	B • R, km	B • T, km	TCA, GMT	Time of last data point, GMT		Deep Space Stations used in orbit	Data types used	Parameters estimated
					Date	Time			
2 POST 28	7580.6531	3537.6862	6704.5561	05:00:40.331	Jul 14	21:50:02	41, 51, 62, 12, 14	CC3, PRU	State vector, solar pressure, and station location
2 POST 32	7586.855	3736.4204	6602.9938	05:00:47.604	↓	↓		CC3	State vector
2 POST 33	7652.719	3902.4348	6582.9405	05:00:41.642	Jul 14	21:50:02		CC3, PRU	State vector
2 POST 34	7556.4342	3542.9296	6674.3799	05:00:43.212	Jul 21	07:12:02		CC3	State vector, solar pressure, and station location
2 POST 35	7575.3661	3566.1848	6683.4494	05:00:40.089	Jul 21	07:12:02		CC3, PRU	State vector, solar pressure, and station location
2 POST 39	7544.2336	3545.2972	6659.3035	05:00:38.075	Jul 22	20:55:02		CC3, PRU	State vector, KM, and solar pressure
2 POST 40	7553.7557	3544.1185	6670.7155	05:00:38.745	Jul 22	20:55:02		CC3, PRU	State vector, KM, solar pressure, and station location
2 POST 41	7526.2818	3498.2350	6663.8778	05:00:42.278	Jul 22	20:55:02		CC3	State vector, KM, solar pressure, and station location
2 POST 42	7502.3278	3512.8554	6629.0849	05:00:39.942	Jul 26	07:15:02	41, 72, 51, 62, 14, 12	CC3	State vector, KM, solar pressure, and station location

### C. Ionospheric Calibration

The precision of spacecraft tracking required and practiced in *Mariner* Mars 1969 tracking and orbit determination included the consideration of error sources that had previously been negligible. One such source was the effect on the signal of charged particles along the tracking ray path, particularly in the ionosphere of the Earth. This was calibrated during July 1969, at the end of the cruise phase and during encounter.

As described in Ref. 1, the charged particles along the ray path of the radio signal transmitted to and received from a spacecraft have various effects upon the signal. Among these effects are absorption, refraction, scintillation, polarization rotation, phase-path length decrease, and group path delay. For orbit determination, the two effects of concern are phase-path decrease and group path delay.

The charged particles in the interplanetary space plasma and in the ionosphere of the Earth decrease the phase-path length between the spacecraft and the track-

ing station. As the number of charged particles in the terrestrial ionosphere changes, the phase-path effect also changes, corrupting the observed doppler because the change in phase-path effect cannot be distinguished from doppler. Similarly, the group path delay corrupts ranging data that are dependent upon the group velocity of the signal.

Ideally, calibration of the spacecraft signal should be performed from measurements made along the ray path of the signal. Although experiments with ranging of *Mariner VII* indicate that the charged-particle effect can be measured by comparing counted doppler to differenced range, the *Mariner* Mars 1969 orbit determination activities relied upon outside measurements of the terrestrial ionosphere to calibrate tracking data. These outside sources are Faraday rotation data made by monitoring of geostationary satellites and ionosonde data made by vertical soundings of the ionosphere.

The procedures described in Ref. 1 were used to process the ionospheric measurements. These were obtained from the Faraday rotation polarimeters at the

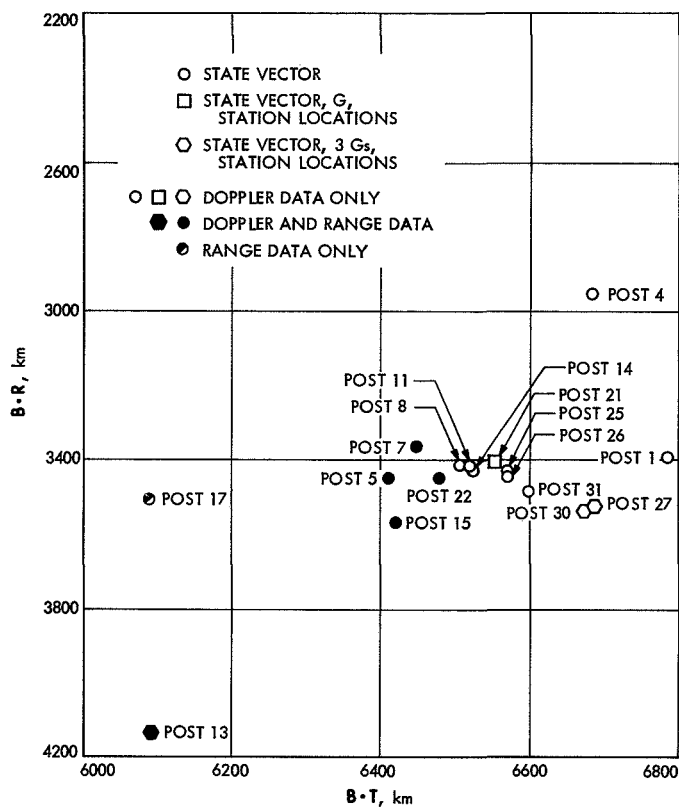


Fig. 20. Mariner VII postmidcourse B-plane estimates

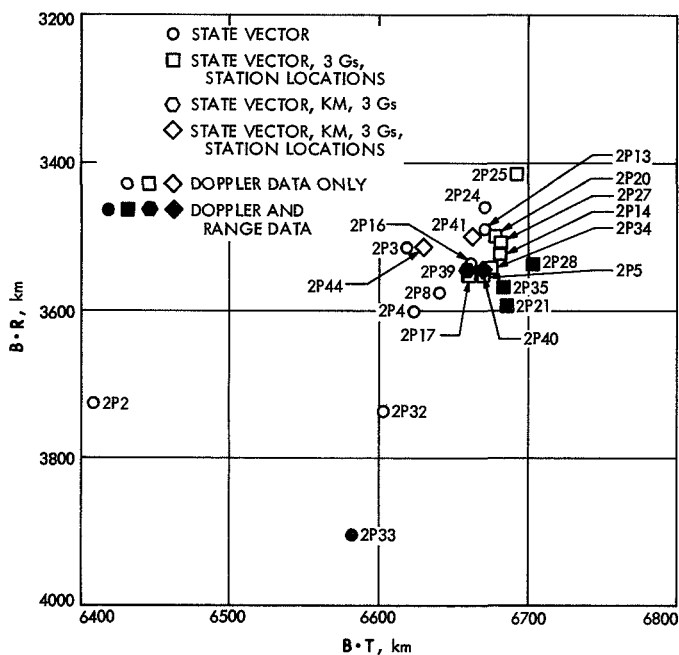


Fig. 21. Mariner VII post-unlatch B-plane estimates

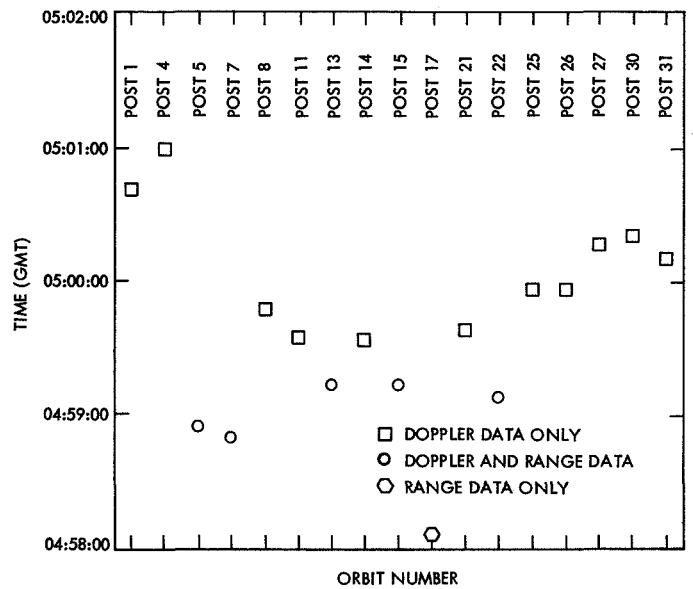


Fig. 22. Mariner VII postmidcourse estimates of time of closest approach, August 5, 1969

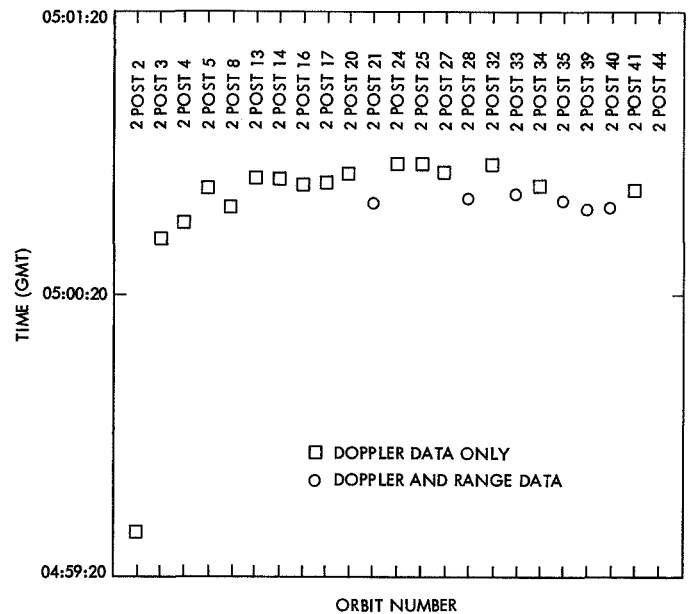


Fig. 23. Mariner VII post-unlatch estimates of time of closest approach, August 5, 1969

Venus site, at Goldstone, and at the University of New England, Armidale, Australia; others were obtained from ionosonde vertical sounding stations at Tortosa, Spain; Mount Stromlo, Australia; Woomera, Australia; and Johannesburg, South Africa. These measurements were converted to total electron content and mapped to the *Mariner* spacecraft ray path; range and doppler corrections were then computed and applied to *Mariners VI* and *VII* radio tracking data. The resulting calibrations are listed in Table 16.

**Table 16. Changes in orbital parameters caused by ionospheric effect**

Spacecraft	$\Delta \mathbf{B} \cdot \mathbf{R}$ , km	$\Delta \mathbf{B} \cdot \mathbf{T}$ , km
<i>Mariner VI</i>	-53	48
<i>Mariner VII</i>	-40	20

The  $\mathbf{B} \cdot \mathbf{T}$  parameter is the component of the  $\mathbf{B}$  vector (a vector from the center of the planet to the aiming point) in the ecliptic plane, and  $\mathbf{B} \cdot \mathbf{R}$  is the component perpendicular to  $\mathbf{B} \cdot \mathbf{T}$ .

The ionospheric effect was considerably lower than had been anticipated, as 1969 was a year of high ionospheric concentrations caused by solar flare activity. However, during the period when the calibration was performed (July 1 to August 5, 1969), the ionosphere was relatively inactive. This low activity was particularly noticeable in the southern hemisphere, where the total columnar electron ionospheric content was typically less than half of the content in the northern hemisphere. Because of the southerly declination of the *Mariner VI* and *VII* spacecraft, most of the radio tracking data were obtained from stations in the southern hemisphere. Consequently, the smaller effect of the southern ionosphere outweighed the effect in the northern ionosphere, and reduced the magnitude of the calibration for the entire network.

## V. Encounter Phase

This phase was characterized by an increasing sensitivity of the spacecraft velocity profile to its position relative to Mars. Because of the high approach speeds, only the last few hours of pre-encounter data could be used to significantly increase the accuracy of the orbital estimates. So that the use of tracking data could be

maximized, final pre-encounter orbits were computed with tracking data obtained up to approximately  $E - 4$  h. These final orbits were then used as the basis for positioning the scan platform to point the scientific instruments. Postencounter tracking data, being very sensitive to the exact geometry near Mars closest approach, were then processed to accurately determine the actual orbits.

The dual encounter, already complex operationally because of the short interval between the targeted times of arrival, was complicated further by the *Mariner VII* pre-encounter anomaly that is described above and in Spacecraft System Performance in Part 3 of this volume. Since the orbit determination phenomena of this event and the *Mariner VII* encounter proved to be closely related, they are discussed together in the paragraphs that follow.

### A. *Mariner VI*

When the spacecraft approached the vicinity of Mars, approximately  $2 \times 10^6$  km from the planet, the orbit could be approximated by a hyperbolic trajectory with respect to Mars (Fig. 24).

**1. Encounter requirements.** Far-encounter instrument pointing was not dependent upon trajectory updates; the planet was acquired and tracked by the far-encounter planet sensor (FEPS). However, repeated updates of the flyby trajectory parameters were necessary for near-encounter pointing and timing, in consultation with the principal investigators, to determine the regions of Mars to be viewed by the instruments (see Vol. III of this report). A plot of the spacecraft cone and clock angles of Mars during this phase is given in Fig. 25.

**2. Orbit determination.** The basic encounter strategy was that orbit solutions would be computed for a long data arc and a short data arc. The long data arc had a data span from the attempted Magellanic cloud acquisition (May 3) to the latest data point. The short data arc had a data span from  $E - 5$  days to the latest data point. The parameter set to be estimated for the short data arc included the state vector and the mass ratio of Mars to Sun; the long-data-arc parameter set included the state vector, mass ratio of Mars to the Sun, and the solar pressure coefficients.

The primary tracking support was provided by DSSs 41, 62, and 12. Tracking data were also provided by DSSs 14 and 51.

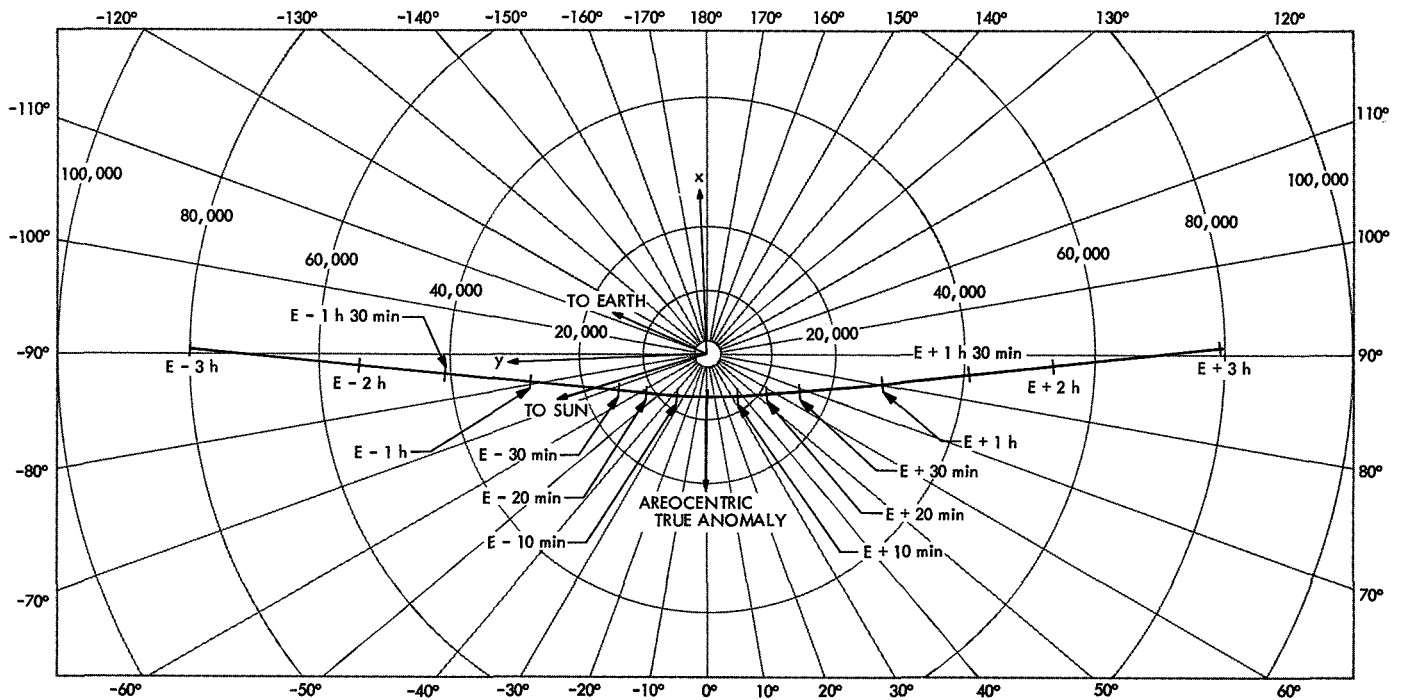


**Fig. 24. Mariner VI areocentric trajectory**

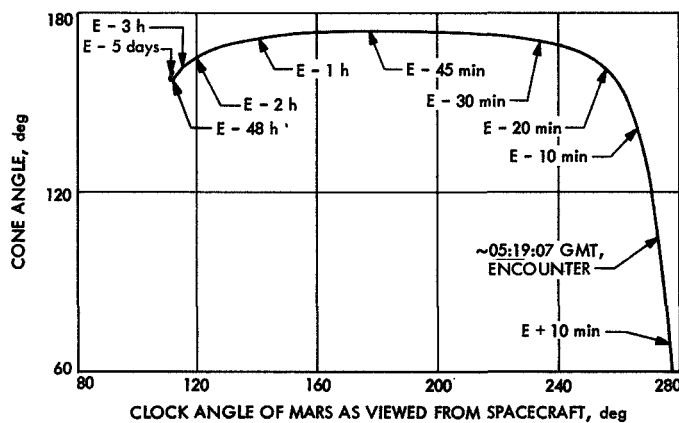


**Fig. 25. Mariner VI cone vs clock angle at encounter**

At  $E - 61$  h, the best available TCA was needed for the spacecraft platform update. The reason for the importance of this update was that the TV shutter mechanism was energized, and would not be adjusted again. At this time, the DPODP encounter operations team recommended the following value for the TCA: 05:19:05.412 GMT on July 31, 1969.

The DPODP and SPODP long-data-arc orbit solutions at  $E - 5$  days are presented in Tables 17 and 18.

With the TCA and the  $E - 5$  days orbit solutions of SPODP and DPODP, the following orbit solution was recommended by the orbit determination group to the Mariner Mars 1969 project at  $E - 61$  h:

$$\mathbf{B} \cdot \mathbf{R} = -339 \text{ km}$$

$$\mathbf{B} \cdot \mathbf{T} = 7560 \text{ km}$$

$$\text{TCA} = 05:19:05 \text{ GMT}$$

A problem that occurred during early encounter operations was the change of phase from heliocentric phase to target center (areocentric) phase. During this change of phase, the data appeared to be noisy and biased. Orbits were computed without consideration of the data obtained during change of phase. However, the confidence on the long-data-arc orbit solutions was somewhat lessened. Therefore, after this time, efforts by the SPODP were concentrated on the short data arc, which had a data span with an epoch located after the change of phase. The DPODP had a similar phasing problem. The phasing problem did not affect the DPODP long-data-arc orbit solutions, but it did perturb the DPODP short-data-arc orbit solutions until the phasing was moved out of the data span.

**Table 17. Long-data-arc orbit solutions for DPODP at  $E - 5$  days**

Orbit	B, km	B • R, km	B • T, km	TCA, GMT	Data type used	Parameters estimated
CM1	7565	—331	7557	05:19:11.263	Doppler	State vector, solar pressure coefficients
CM3	7572	—383	7562	05:19:11.592	Doppler	State vector, solar pressure coefficients, station location
CM2	7594	—290	7589	05:19:06.893	Doppler and range	State vector, solar pressure coefficients
CM4	7591	—329	7584	05:19:05.698	Doppler and range	State vector, solar pressure coefficients, station location

**Table 18. Long-data-arc orbit solutions for SPODP at  $E - 5$  days**

Orbit	B, km	B • R, km	B • T, km	TCA, GMT	Data type used	Parameters estimated
3 POST 49	7586	—302	7580	05:18:53.889	Doppler	State vector, solar pressure coefficients
3 POST 89	7599	—359	7591	05:18:54.147	Doppler	State vector, solar pressure coefficients, station location
3 POST 91	7575	—320	7568	05:19:03.754	Doppler and range	State vector, solar pressure coefficients
3 POST 47	7587	—402	7577	05:19:02.441	Doppler and range	State vector, solar pressure coefficients, station location

At approximately  $E - 1$  day, short-data-arc orbit solutions were computed (Table 19).

At approximately  $E - 3$  h, the SPODP and DPODP short-data-arc orbit solutions were computed and are presented in Table 20.

A DPODP orbit solution that applied ionospheric corrections to the tracking data was computed shortly before this time, with the following result:

$$\mathbf{B} \cdot \mathbf{R} = -387 \text{ km}$$

$$\mathbf{B} \cdot \mathbf{T} = 7615 \text{ km}$$

$$\text{TCA} = 05:19:06.2 \text{ GMT}$$

From these inputs (the short-data-arc and long-data-arc orbit solutions), the orbit determination group recommended the following orbit to the *Mariner* Mars 1969 project for the final spacecraft platform update:

$$\mathbf{B} \cdot \mathbf{R} = -380 \text{ km}$$

$$\mathbf{B} \cdot \mathbf{T} = 7580 \text{ km}$$

$$\text{TCA} = 05:19:06 \text{ GMT}$$

The  $1\sigma$  dispersion ellipse associated with this orbit was 100 by 40 km with the semimajor axis approximately parallel to the  $R$ -axis in the  $\mathbf{B}$ -plane. When the platform pointing angles were rounded off to achievable values, the orbit that was actually used for the final platform update was as follows:

$$\mathbf{B} \cdot \mathbf{R} = -350 \text{ km}$$

$$\mathbf{B} \cdot \mathbf{T} = 7560 \text{ km}$$

$$\text{TCA} = 05:19:05 \text{ GMT}$$

An orbit solution was computed with doppler data up to the time of infrared spectrometer (IRS) gas venting and by an estimation of the state vector, mass ratio of Mars to the Sun, and station locations. The data span of this solution was from  $E - 5$  days 2 h to  $E - 40$  min. When this solution was mapped to target, it indicated the following results:

$$\mathbf{B} = 7605 \text{ km}$$

$$\mathbf{B} \cdot \mathbf{R} = -364 \text{ km}$$

$$\mathbf{B} \cdot \mathbf{T} = 7596 \text{ km}$$

$$\text{TCA} = 05:19:07.118 \text{ GMT}$$



**Table 19. Short-data-arc orbit solutions for SPODP and DPODP at  $E - 1$  day**

Orbit	B, km	B • R, km	B • T, km	TCA, GMT	Data type used	Parameters estimated
3 POST 106	7482	—373	7473	05:19:13.381	Doppler	State vector
3 POST 109	7497	—404	7487	05:19:12.131	Doppler	State vector, station location
3 POST 105	7598	—429	7586	05:19:01.688	Doppler and range	State vector
3 POST 107	7613	—398	7602	05:19:03.396	Doppler and range	State vector, station location

**Table 20. Short-data-arc orbit solutions for SPODP and DPODP at  $E - 3$  h**

Orbit programs	B • R, km	B • T, km	TCA, GMT	Data type used	Parameters estimated
SPODP	—364	7463	05:19:09.476	Doppler	State vector, mass ratio of Mars to Sun
SPODP	—371	7585	05:19:07.272	Doppler	State vector, mass ratio of Mars to Sun, station location
DPODP	—385	7475	05:19:08.81	Doppler	State vector, gravitational constant of Mars
DPODP	—298	7579	05:19:06.3	Doppler and range	State vector, gravitational constant of Mars

With approximately 14 days of postencounter data added, orbit solutions were computed with pre- and postencounter data. The solutions are presented below:

Doppler only	Doppler and range
B = 7602 km B • R = —331 km B • T = 7595 km TCA = 05:19:06.783 GMT	B = 7603 km B • R = —336 km B • T = 7595 km TCA = 05:19:06.908 GMT

The solution called POST ENC 28 was computed with doppler data only. The solution called POST ENC 26, computed with doppler and range data on August 14, was designated the best estimate as of that date.

Because of the abnormality that occurred during IRS gas venting and because gas venting was still observed at  $E + 4$  days, the  $3\sigma$  dispersion ellipse associated with the current best estimate was assessed as 50 km circular.

The numerical results of the encounter orbit computations are presented in Table 21. Figure 26 shows the B-plane estimates of the orbits computed during encounter. Figure 27 shows the TCA of the encounter orbits.

**Table 21. Results of encounter orbit computations for Mariner VI**

Orbit	B, km	B • R, km	B • T, km	TCA, GMT	Time of last data point, GMT		Stations used in orbit	Data types used	Parameters estimated
					Date	Time			
3 POST 53	7574.2687	—466.98688	7559.8590	05:18:59.660	Jul 27	15:03:02	DSSs 41, 51, 62, 12, 14	CC3, PRU	State vector, KM, solar pressure, station location
3 POST 54	7583.3042	—309.40463	7576.9895	05:18:50.040		15:03:02		CC3	State vector, KM, solar pressure
3 POST 55	7584.7068	—366.35194	7575.8535	05:18:54.566		15:03:02		CC3	State vector, KM, solar pressure, station location
3 POST 64	7580.1992	—434.60336	7567.7298	05:19:01.082		15:03:02		CC3, PRU	State vector, KM, solar pressure, station location
3 POST 66	7591.4688	—378.99110	7582.0028	05:19:00.736	Jul 27	15:03:02	DSSs 41, 51, 62, 12, 14	CC3	State vector, KM, solar pressure, station location

Table 21 (contd)

Orbit	B, km	B • R, km	B • T, km	TCA, GMT	Time of last data point, GMT		Stations used in orbit	Data types used	Parameters estimated
					Date	Time			
3 POST 67	7588.6468	—315.74644	7582.0750	05:18:52.905	Jul 27	15:03:02	DSSs 41, 51, 62, 12, 14	CC3	State vector, KM, solar pressure
3 POST 69	7575.3787	—405.03638	7564.5425	05:19:01.409	Jul 27	15:03:02	DSSs 51, 62, 12, 14	CC3, PRU	State vector
3 POST 85	7550.4154	—346.01244	7542.4828	05:19:00.398	Jul 28	20:59:02	DSSs 41, 51, 62, 12, 14	CC3, PRU	State vector, KM, solar pressure
3 POST 86	7582.9349	—351.65693	7574.7762	05:19:01.000		20:59:02		CC3, PRU	State vector
3 POST 87	7565.8782	—446.76131	7552.6758	05:18:59.654		20:59:02		CC3, PRU	State vector, KM, solar pressure, station location
3 POST 88	7406.6729	—402.70448	7395.7167	05:19:58.255		20:59:02		CC3	State vector
3 POST 90	7590.3538	—309.14269	7584.0557	05:18:53.049	Jul 28	02:30:02	DSSs 41, 62, 12, 14	CC3	State vector, MM, solar pressure
3 POST 92	7578.0047	—407.11572	7567.0610	05:19:01.227	Jul 29	17:50:02	DSSs 41, 51, 62, 12, 14	CC3, PRU	State vector
3 POST 93	7432.5854	—353.84335	7424.1573	05:19:25.164		17:50:02		CC3	State vector
3 POST 94	7586.4957	—414.20109	7575.180	05:19:01.547		17:50:02		CC3, PRU	State vector, station location
3 POST 95	7460.5489	—386.05775	7450.5533	05:19:22.785		17:50:02		CC3	State vector, station location
3 POST 96	7564.0199	—345.93851	7556.1047	05:18:41.033		17:50:02		CC3	State vector, MM, solar pressure, station location
3 POST 97	7570.8595	—331.182087	7563.584	05:18:32.722	Jul 29	17:50:02		CC3	State vector, MM, solar pressure
3 POST 105	7597.7125	—428.56446	7585.6156	05:19:01.688	Jul 30	01:06:02		CC3, PRU	State vector
3 POST 106	7482.9207	—373.06805	7472.9207	05:19:13.381		01:06:02		CC3	State vector
3 POST 107	7612.6347	—398.4893	7602.1976	05:19:03.396		01:06:02		CC3	State vector, station location
3 POST 108	7616.9150	—413.17172	7605.7005	05:19:03.253		01:06:02		CC3, PRU	State vector, MM, station location
3 POST 109	7497.4719	—403.87088	7486.5860	05:19:12.131		01:06:02		CC3	State vector, station location
3 POST 110	7551.0103	—347.61898	7543.0043	05:19:01.417		01:06:02		CC3, PRU	State vector, KM, solar pressure
ENC 1	7656.9162	—337.28006	7649.4839	05:19:07.664		15:17:02		CC3, PRU	State vector, MM
ENC 2	7494.8485	—371.36799	7485.6421	05:19:10.551		15:17:02		CC3	State vector, MM, station location
ENC 3	7616.1762	—289.02332	7610.6901	05:19:06.452		15:17:02		CC3, PRU	State vector, MM, station location
ENC 4	7465.4401	—372.70959	7456.1304	05:19:11.298		15:17:02		CC3	State vector, MM
ENC 14	7603.2390	—261.92297	7598.7259	05:19:06.400		18:09:02		CC3, PRU	State vector, MM, station location
ENC 15	7530.5783	—374.79631	7521.2456	05:19:09.126		18:09:02		CC3	State vector, MM, station location
ENC 17	7627.6784	—315.56244	7621.1479	05:19:06.552		21:55:02		CC3, PRU	State vector, MM
ENC 18	7594.4701	—248.91543	7590.8901	05:19:06.200		21:55:02		CC3, PRU	State vector, MM, station location
ENC 19	7467.7610	—380.160	7458.0782	05:19:09.609	Jul 30	21:55:02	DSSs 41, 51, 62, 12, 14	CC3	State vector, MM

Table 21 (contd)

Orbit	B, km	B • R, km	B • T, km	TCA, GMT	Time of last data point, GMT		Stations used in orbit	Data types used	Parameters estimated
					Date	Time			
ENC 20	7559.3544	-323.65788	7552.4221	05:19:07.683	Jul 30	21:55:02	DSSs 41, 51, 62, 12, 14	CC3	State vector, MM, solar pressure, station location
ENC 21	7539.5023	-389.53211	7529.4328	05:19:08.689	Jul 30	21:55:02	DSSs 41, 51, 62, 12, 14	CC3	State vector, MM, station location
ENC 26	7471.989	-363.78475	7463.1278	05:19:09.476	Jul 31	01:01:50	DSSs 41, 51, 62, 12, 14	CC3	State vector, MM
ENC 28	7569.1796	-373.1961	7559.9737	05:19:07.359	Jul 31	01:05:02	DSSs 41, 62, 12, 14	CC3	State vector, MM, station location
ENC 29	7565.739	-346.90921	7557.7813	05:19:07.673	Jul 30	22:56:32	DSSs 41, 51, 62, 12, 14	CC3	State vector, MM
ENC 30	7584.8663	-339.77107	7577.2522	05:19:07.094	Jul 30	23:44:02	DSSs 51, 62, 12, 14	CC3	State vector, MM, station location
ENC 31	7594.0646	-371.27483	7584.9833	05:19:07.272	Jul 31	01:52:32	DSSs 41, 51, 62, 12, 14	CC3	State vector, MM, station location

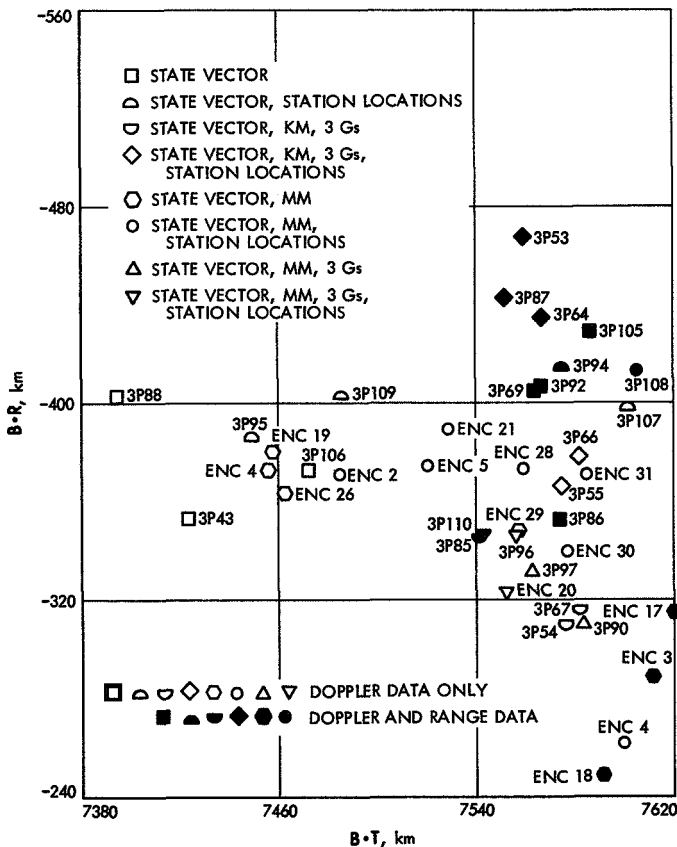


Fig. 26. Mariner VI encounter B-plane estimates

### B. Mariner VII

The *Mariner VII* encounter differed from that of *Mariner VI* in a number of significant aspects. The first of these was the *Mariner VII* pre-encounter anomaly, described in Section IV of Part 1 and in Spacecraft System Performance in Part 3 of this volume. In the course of this event, which began about 5 days and 7 h before closest approach to Mars, the spacecraft orbit was perturbed slightly (Fig. 28) by a nongravitational acceleration that persisted at a much diminished rate for several days,<sup>3</sup> and minor damage occurred to spacecraft engineering subsystems which necessitated extraordinary operational procedures before the encounter was satisfactorily carried out. The second difference was that the far-encounter sequence was begun on schedule, a day earlier relative to closest approach. The third difference was that, on the basis of data gathered by *Mariner VI*, the principal investigators requested changes in the near-encounter planetary coverage, which were programmed during the latter part of far-encounter.

**1. Encounter events.** The areocentric *Mariner VII* trajectory is shown in Fig. 29 and the cone and clock angles of Mars are given in Fig. 30. With the differences

<sup>3</sup>Although reduced from  $36 \times 10^{-10} \text{ km/s}^2$  at 06:50 to  $14 \times 10^{-11} \text{ km/s}^2$  in the Earth-radial direction by 22:00 GMT, July 31.

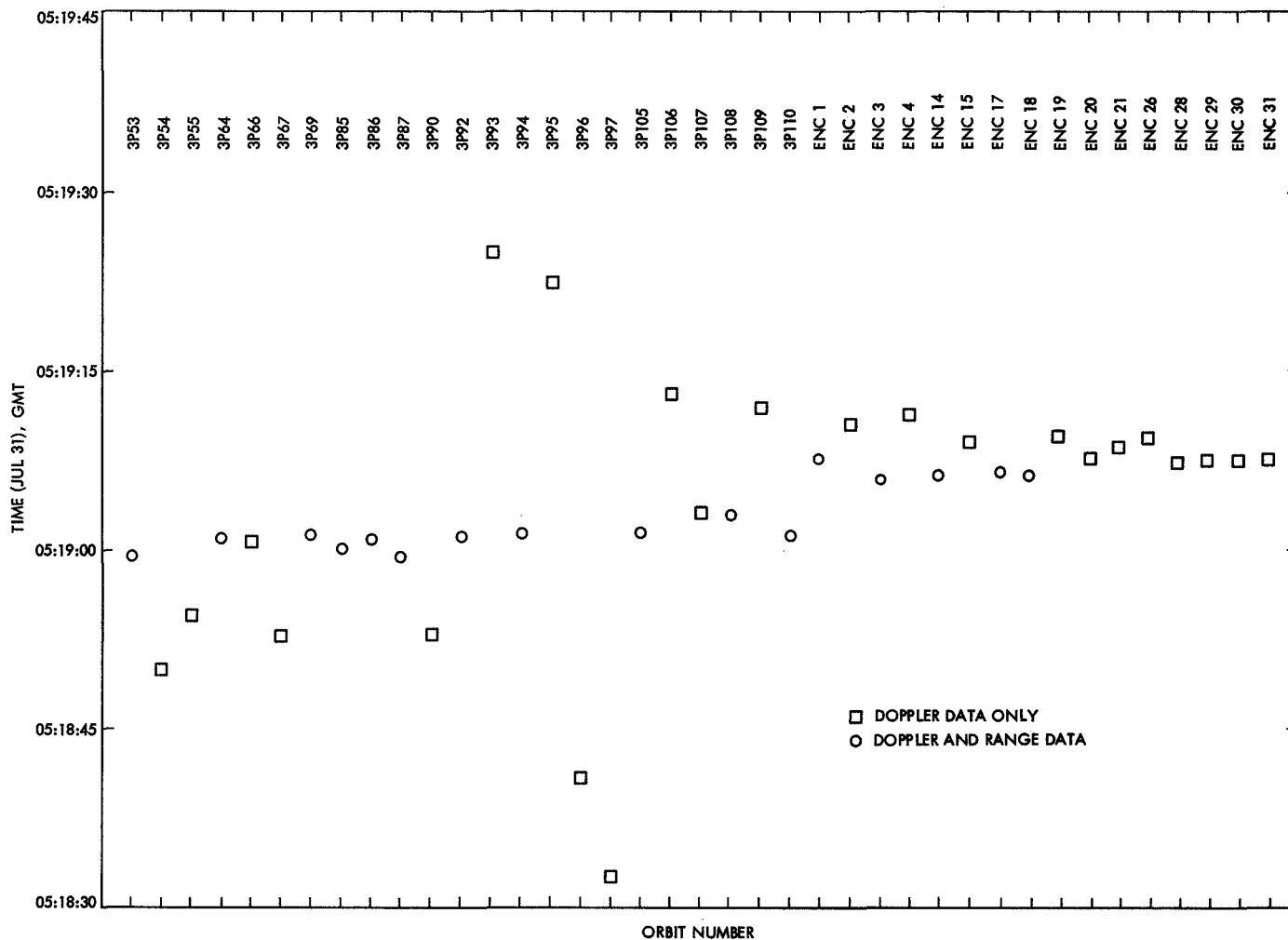


Fig. 27. Mariner VI encounter estimates of time of closest approach

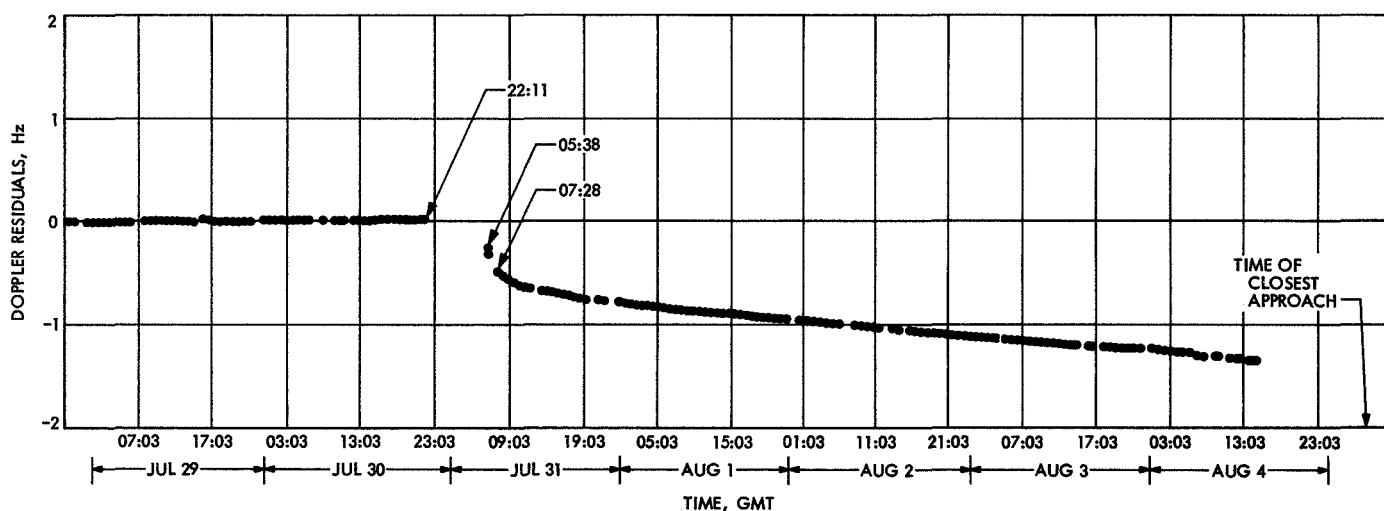


Fig. 28. Doppler residuals vs time near Mariner VII pre-encounter anomaly

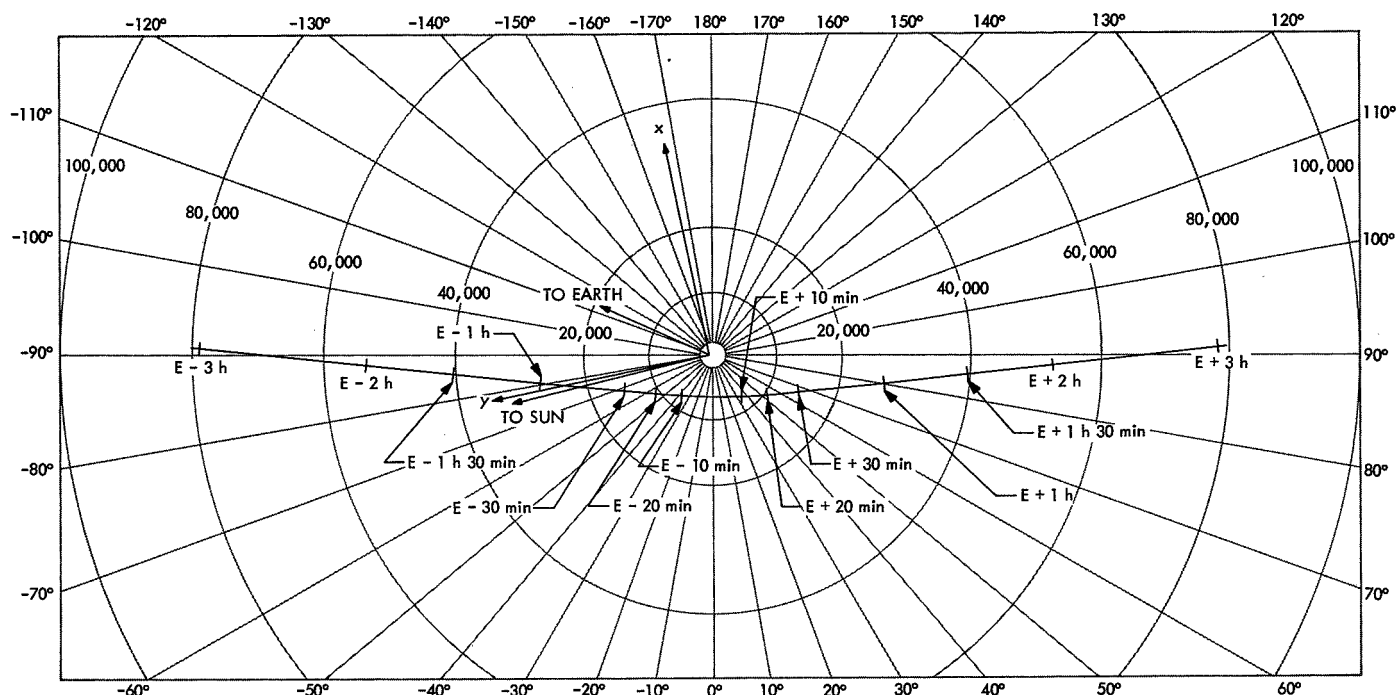


Fig. 29. Mariner VII areocentric trajectory

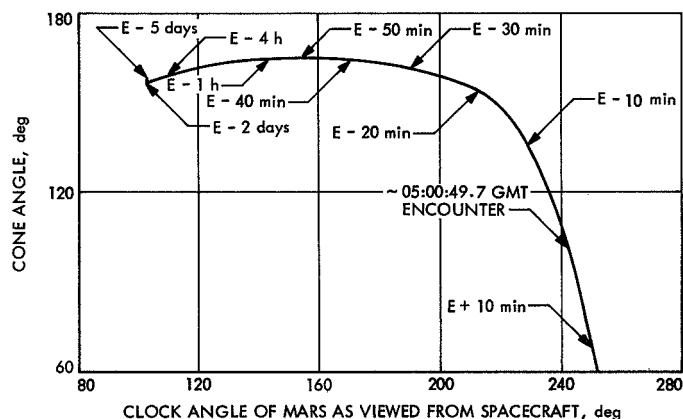


Fig. 30. Mariner VII cone vs clock angle at encounter

noted, the *Mariner VII* encounter sequence was similar to that of *Mariner VI*, and it was successfully completed.

**2. Orbit determination.** The primary tracking support was provided by DSSs 14, 41, 51, and 62. Tracking data were also provided by DSS 11.

The first orbit after the pre-encounter anomaly was computed with approximately 1 day of doppler data.

The epoch of this orbit was at 22:00 GMT, July 31. The solution indicated a change of 600 to 700 km in  $\mathbf{B} \cdot \mathbf{R}$  and a change of 260 to 270 km in  $\mathbf{B} \cdot \mathbf{T}$ . However, with only 1 day of data, the uncertainties of this solution were larger than the indicated differences. Previous studies indicated that the short-data-arc solutions would not be tied down until the near-target data (hours before encounter) were used in the orbit solution.

As more orbit solutions were computed with more data added, the solutions indicated that the spacecraft still had a small acceleration. With the knowledge that there was a small acceleration acting on the spacecraft, the strategies were:

- (1) To model the small acceleration in the orbit computation.
- (2) To keep the data arc used in computing the orbit solution as short as possible to minimize the model error.

In the SPDP, this small acceleration could be modeled by the solar pressure model, or the attitude control jet model. Both of these models were tried and the two solutions were quite similar. The solutions computed

with data (doppler and range) up to  $E - 9$  h are given below:

Solar pressure model	Attitude control model
$\mathbf{B} = 7713$ km	$\mathbf{B} = 7687$ km
$\mathbf{B} \cdot \mathbf{R} = 3927$ km	$\mathbf{B} \cdot \mathbf{R} = 3896$ km
$\mathbf{B} \cdot \mathbf{T} = 6638$ km	$\mathbf{B} \cdot \mathbf{T} = 6626$ km
TCA = 05:00:49.680 GMT	TCA = 05:00:48.368 GMT

At approximately  $E - 3$  h, orbit solutions were computed with doppler and range data that had a data span from  $E - 2$  days 5 h to  $E - 4$  h. The solutions are presented below:

Parameter	Solution E23	Solution E26	Solution E27
$\mathbf{B}$ , km	7692	7578	7535
$\mathbf{B} \cdot \mathbf{R}$ , km	3769	3829	3811
$\mathbf{B} \cdot \mathbf{T}$ , km	6705	6540	6500
TCA, GMT	05:00:49.774	05:00:52.788	05:00:53.520

Solution E23 estimated the state vector, mass ratio of Mars to Sun, attitude control jets, and station location, and it used doppler and range data in the solution. Solution E26 estimated the same parameters as E23, but it used only doppler in the orbit solution. Solution E27 used only doppler data and estimated only the state vector.

The orbit solutions obtained prior to  $E - 6$  h were concentrated in the range of 3850 to 3920 in  $\mathbf{B} \cdot \mathbf{R}$ . As more near-target data were added, up to  $E - 3$  h, there were 3 orbit solutions that moved past 3800 to approximately 3769.

At approximately  $E - 3$  h, two DPODP estimates of the spacecraft orbit were presented:

Solution A	Solution B
$\mathbf{B} \cdot \mathbf{R} = 3450$ km	$\mathbf{B} \cdot \mathbf{R} = 3780$ km
$\mathbf{B} \cdot \mathbf{T} = 6800$ km	$\mathbf{B} \cdot \mathbf{T} = 6640$ km
TCA = 05:00:47.7 GMT	TCA = 05:00:49.7 GMT

Solution B was computed with the short data arc and an estimate of the state vector, solar pressure coefficients, and the mass of Mars. Solution A used a longer data arc than solution B and attempted to model a motor burn through the pre-encounter anomaly.

It was decided to use the short data arc. After consideration of solution B and the SPODP solutions, the following orbit solution was recommended to the *Mariner* Mars 1969 project for the final spacecraft platform update:

$$\begin{aligned}\mathbf{B} \cdot \mathbf{R} &= 3800 \text{ km} \\ \mathbf{B} \cdot \mathbf{T} &= 6670 \text{ km} \\ \text{TCA} &= 05:00:50 \text{ GMT}\end{aligned}$$

The  $1\sigma$  dispersion ellipse associated with this solution was 300 km circular.

It was decided to choose an orbit that, if in error, would minimize the effect of the orbit determination errors on science results. Therefore, it was recommended at the  $E - 3$  h meeting to use  $\mathbf{B} \cdot \mathbf{R} = 3700$  km,  $\mathbf{B} \cdot \mathbf{T} = 6700$  km, and to "round" the platform clock angle to the larger achievable value. The actual orbit that was used for the final spacecraft platform update was:

$$\begin{aligned}\mathbf{B} \cdot \mathbf{R} &= 3650 \text{ km} \\ \mathbf{B} \cdot \mathbf{T} &= 6725 \text{ km} \\ \text{TCA} &= 05:00:47 \text{ GMT}\end{aligned}$$

An orbit solution was computed with doppler data up to the time of IRS gas venting and estimating the state vector, mass ratio of Mars to Sun, attitude control jets, and station location. The data span of this solution was from  $E - 2$  days 5 h to approximately  $E - 50$  min. When this solution was mapped to target, it indicated the following results:

$$\begin{aligned}\mathbf{B} &= 7639 \text{ km} \\ \mathbf{B} \cdot \mathbf{R} &= 3764 \text{ km} \\ \mathbf{B} \cdot \mathbf{T} &= 6647 \text{ km} \\ \text{TCA} &= 05:00:49.691 \text{ GMT}\end{aligned}$$

With approximately 3 days of postencounter data added, orbit solutions were computed with pre- and

postencounter data (doppler only). The solutions are presented below:

Parameter	Solution 1	Solution 2	Solution 3
<b>B</b> , km	7632	7632	7622
<b>B • R</b> , km	3630	3631	3628
<b>B • T</b> , km	6714	6713	6703
TCA, GMT	05:00:50.037	05:00:49.984	05:00:49.997

Solution 1 estimated only the state vector. Solution 2 estimated the state vector, mass ratio of Mars to the Sun, and the solar pressure coefficients. Solution 3 estimated the same parameters as solution 2 except the solar pressure coefficients were replaced by the attitude control jets.

By the use of range data with the doppler data, the orbit computation showed the following results:

$$\mathbf{B} = 7644 \text{ km}$$

$$\mathbf{B} \cdot \mathbf{R} = 3623 \text{ km}$$

$$\mathbf{B} \cdot \mathbf{T} = 6731 \text{ km}$$

$$\text{TCA} = 05:00:48.754 \text{ GMT}$$

The results are quite similar to solution 2 even though the data fit was not as good. Orbit solutions were also computed with pre-encounter data and approximately 9 days of postencounter data. These solutions further confirm solution 2.

Because of the abnormality that occurred before encounter and the IRS gas venting, the  $3\sigma$  dispersion ellipse associated with solution 2 was assessed to be 50 km circular.

The numerical results of the encounter orbit computations are presented in Table 22. Figure 31 shows the **B**-plane estimates of the orbits computed during encounter. Figure 32 shows the time of closest approach of the encounter orbits.

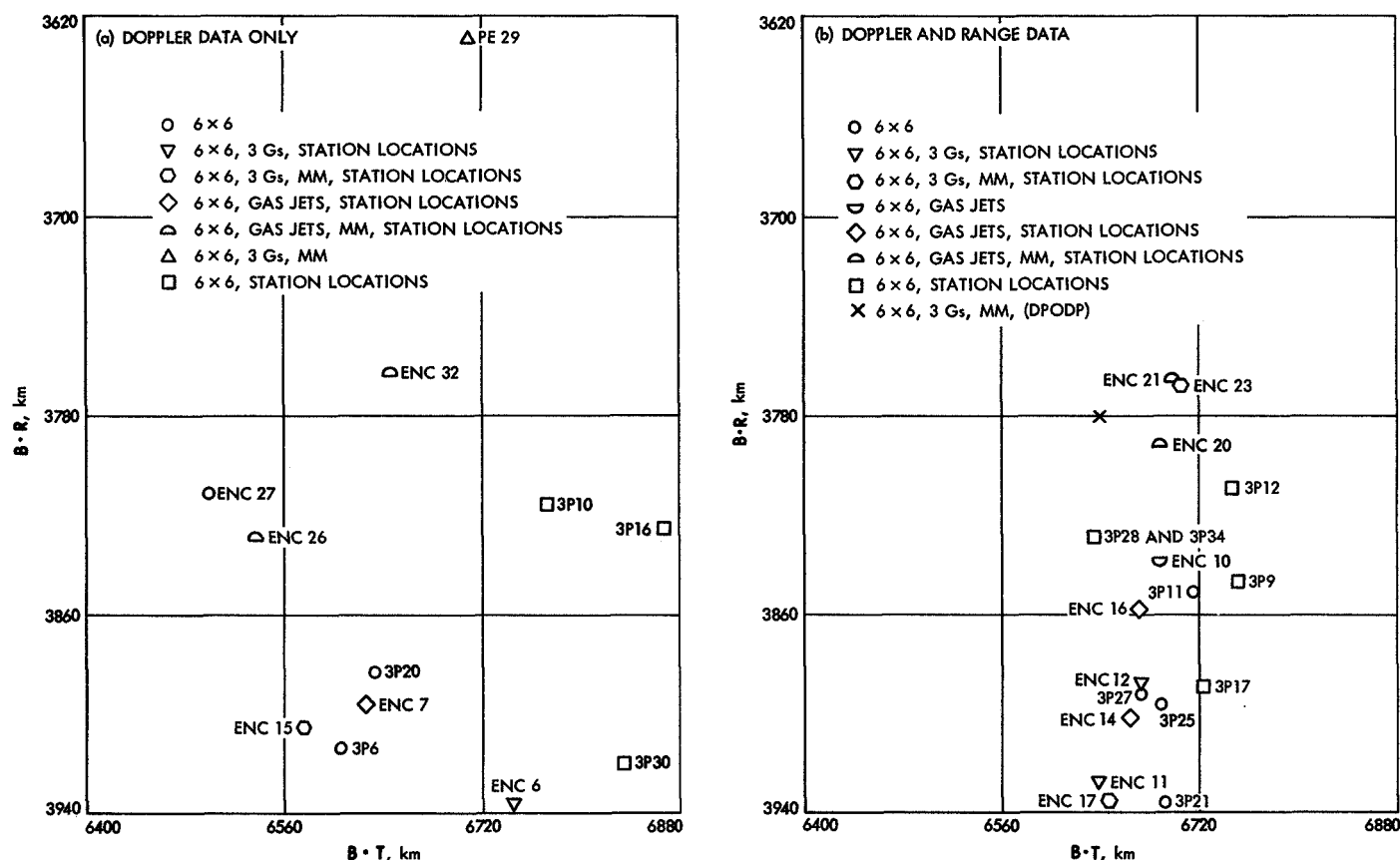
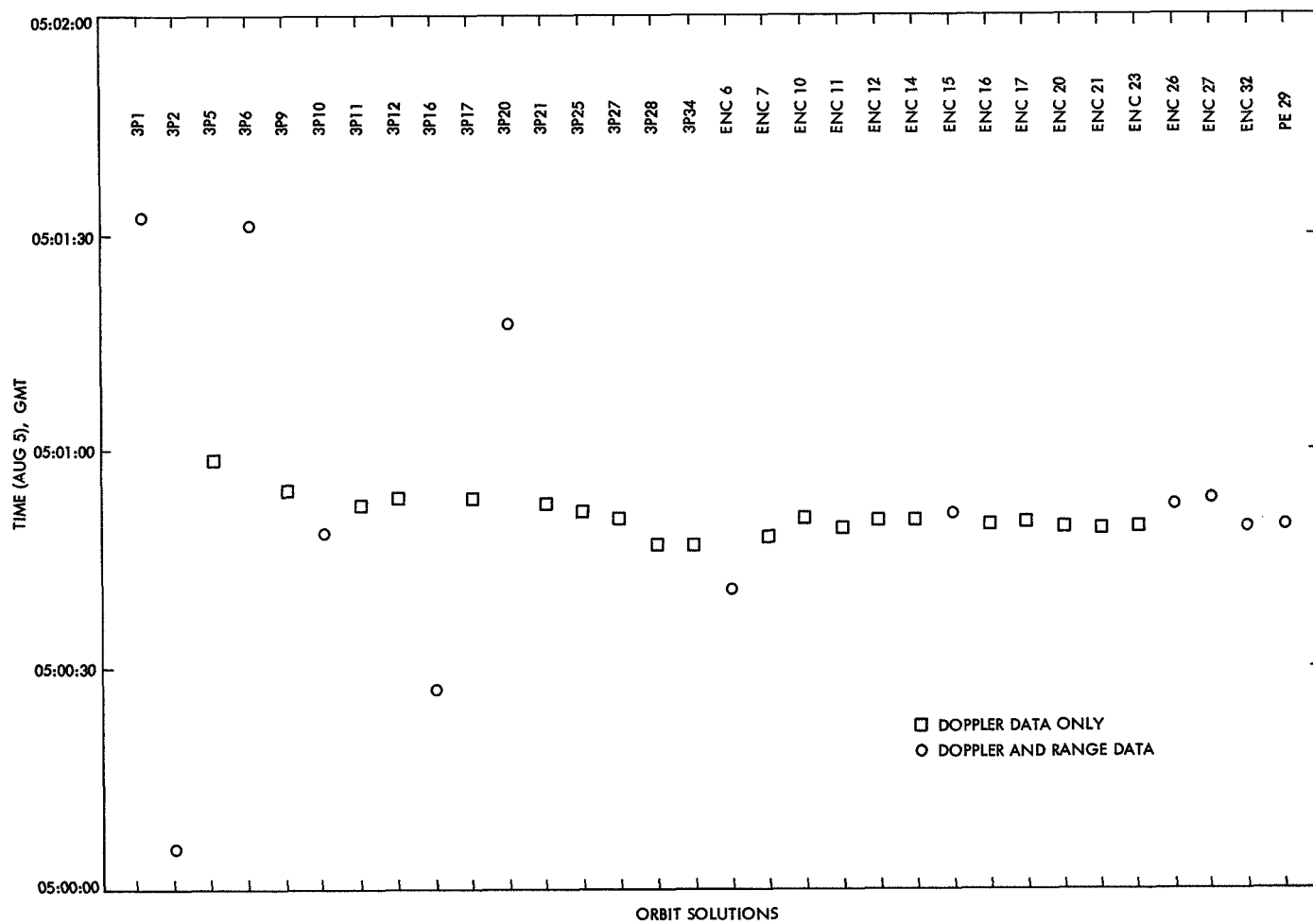


Fig. 31. Mariner VII encounter B-plane estimates



**Fig. 32. Mariner VII encounter estimates of time of closest approach**



**Table 22. Results of encounter orbit computations for Mariner VII**

Orbit	B, km	B • R, km	B • T, km	TCA, GMT	Time of last data point, GMT		Stations used in orbit	Data types used	Parameters estimated
					Date	Time			
3 POST 1	7326.4719	3620.5259	6369.3784	05:01:32.229	Aug 1	00:15:02	DSS 11	CC3	State vector
3 POST 2	8124.5777	4191.0274	6960.1759	05:00:05.735	Aug 1	20:23:32	DSSs 11, 41, 51	CC3	State vector
3 POST 5	7870.9892	4084.6202	6728.1684	05:00:58.731	Aug 2	03:49:32	DSSs 11, 41, 51, 62, 14	CC3, PRU	State vector
3 POST 6	7678.0366	3913.6062	6605.7499	05:01:31.245		03:49:32		CC3	State vector
3 POST 9	7772.4686	3847.7373	6753.2349	05:00:54.495		03:49:32		CC3, PRU	State vector, station location
3 POST 10	7774.2539	3816.4406	6773.0203	05:00:48.350		15:34:32		CC3	State vector, station location
3 POST 11	7742.3102	3851.1216	6716.5038	05:00:52.412		15:34:32		CC3, PRU	State vector
3 POST 12	7749.6709	3809.7215	6748.5863	05:00:53.305		15:34:32		CC3, PRU	State vector, station location
3 POST 16	7861.1400	3826.4310	6867.0186	05:00:27.276		20:32:32	DSSs 11, 41, 51, 62, 14	CC3	State vector, station location
3 POST 17	7767.0004	3888.9461	6723.2725	05:00:53.617		20:32:32	DSSs 41, 51, 62, 14	CC3, PRU	State vector, station location
3 POST 20	7688.2803	3883.0558	6635.6260	05:01:17.622		20:32:32		CC3	State vector
3 POST 21	7763.2170	3936.3765	6691.2241	05:00:52.937	Aug 2	20:32:32		CC3, PRU	State vector
3 POST 25	7742.0462	3986.6265	6689.9608	05:00:51.930	Aug 3	15:37:32		CC3, PRU	State vector
3 POST 27	7726.3851	3981.8348	6674.6271	05:00:50.943		15:17:02		CC3, PRU	State vector
3 POST 28	7662.7104	3829.3290	6637.2911	05:00:47.258		15:17:02	DSSs 41, 51, 62, 14	CC3, PRU	State vector, station location
3 POST 30	7885.4538	3930.3092	6836.1574	04:59:43.946		21:02:32	DSSs 41, 52, 14	CC3	State vector, station location
3 POST 34	7662.7104	3829.3290	6637.2711	05:00:47.258	Aug 3	15:17:02	DSSs 41, 51, 62, 14	CC3, PRU	State vector, station location
ENC 6	7810.9285	3935.8620	6746.8207	05:00:41.033	Aug 4	15:19:02	DSSs 41, 62, 14	CC3	State vector, solar pressure, station location
ENC 7	7686.7592	3896.2547	6626.1197	05:00:48.368	Aug 4	15:19:02	DSSs 41, 62, 14	CC3, PRU	State vector, gas jets, station location
ENC 10	7716.8320	3839.0414	6694.1208	05:00:50.872	Aug 4	20:19:02	DSSs 41, 62, 14	CC3, PRU	State vector, gas jets
ENC 11	7712.7685	3926.9575	6638.2078	05:00:49.680	Aug 3	16:07:02		CC3, PRU	State vector, solar pressure, station location
ENC 12	7722.9194	3887.3479	6673.2308	05:00:50.666	Aug 4	20:19:02		CC3, PRU	State vector, solar pressure, station location
ENC 14	7722.8371	3901.9613	6664.6012	05:00:50.729		20:19:02		CC3, PRU	State vector, gas jets, station location
ENC 15	7650.3105	3906.3579	6577.8124	05:00:51.538		22:53:02		CC3	State vector, MM, solar pressure, station location
ENC 16	7707.6027	3857.9457	6672.580	05:00:50.106		22:53:02		CC3, PRU	State vector, gas jets, station location
ENC 17	7724.6774	3936.4614	6646.4209	05:00:50.359	Aug 4	22:53:02	DSSs 41, 62, 14	CC3, PRU	State vector, MM, solar pressure, station location

Table 22 (contd)

Orbit	B, km	B • R, km	B • T, km	TCA, GMT	Time of last data point, GMT		Stations used in orbit	Data types used	Parameters estimated
					Date	Time			
ENC 20	7688.1067	3792.2613	6687.7301	05:00:49.590	Aug 4	22:53:02	DSSs 41, 62, 14 ↓	CC3, PRU	State vector, MM, gas jets, station location
ENC 21	7686.7158	3766.4942	6700.6806	05:00:49.552	Aug 4	22:53:02		CC3, PRU	State vector, MM, gas jets, station location
ENC 23	7692.1020	3768.9396	6705.4848	05:00:49.774	Aug 5	01:12:02		CC3, PRU	State vector, MM, gas jets, station location
ENC 26	7578.1699	3829.0213	6539.6675	05:00:52.788		01:12:02		CC3	State vector, MM, gas jets, station location
ENC 27	7535.1539	3811.3938	6500.1401	05:00:53.520		01:12:02		CC3	State vector
ENC 32	7638.5430	3763.5883	6647.0099	05:00:49.691	Aug 5	04:14:57	DSSs 41, 62, 14 ↓	CC3	State vector, MM, gas jets, station location
POST ENC 29	7631.764	3630.9142	6712.6954	05:00:49.984	Aug 8	18:47:02		CC3	State vector, MM, solar pressure

### C. Trajectory Estimates From Spacecraft-Based Optical Data

In addition to radio tracking data, optical data acquired by the spacecraft were used to estimate target parameters for the two flights. This process was similar in some respects to that anticipated from the optical approach guidance subsystem designed early in the project but not flown on the mission. The results provide an interesting comparison to those obtained from radio tracking data.

During the Mars encounter phase, the TV camera and the FEPS were used to measure the direction of the optical center of Mars relative to the spacecraft. This direction, correlated with scan platform position and spacecraft limit cycle position was expressed as a pair of angles (cone and clock angle) relative to the spacecraft celestial attitude references.

Procedures were developed so that TV and FEPS data taken up to  $E - 20$  h would be processed to have orbital estimates available to FPAC by  $E - 12$  h. Additional data taken subsequent to  $E - 20$  h were to be processed after encounter. For *Mariner VI*, 24 far-encounter TV pictures taken between  $E - 46$  h and  $E - 31$  h, and FEPS error signals measured between  $E - 49$  h and  $E - 20$  h were used. For *Mariner VII*, 53 far-encounter TV pictures taken between  $E - 67$  h and  $E - 22$  h, and FEPS error signals (assumed to be zero

mean) between  $E - 68$  h and  $E - 20$  h were used. (Subsequent to the *Mariner VII* pre-encounter anomaly at  $E - 127$  h, telemetry measurements of FEPS error signals, coarse cone and clock angle, and fine cone angle positions were lost. Therefore, only fine clock angle position data were available. The clock angle of Mars was reconstructed, but the cone angle of Mars was not used.)

The *Mariner VI* orbital estimates that were made with FEPS error signals showed large systematic errors, which indicated that preflight FEPS calibrations had changed. After recalibration, which was done by correlating FEPS error signals at the times that TV pictures were taken, the data still proved erratic, indicating that surface features of Mars may have affected the center of brightness that the FEPS tracked. Because of these erratic FEPS data, only TV data were used in arriving at the results given here for both *Mariners VI* and *VII*.

The estimates of encounter parameters listed in Table 23 show a comparison between two sets of optical tracking solutions and the best postencounter solution based on radio tracking data. The initial conditions shown in the tables were used in obtaining the solution based on optical tracking data. They are estimates of the orbital parameters based on radio tracking data that used short data arcs and "loose" *a priori* statistics and are considerably different from the best orbital estimates available. This was deliberately done so that estimates

**Table 23. Encounter orbital estimates**

Parameter	Initial conditions	Optical data <sup>a</sup>	Optical data <sup>b</sup>	Postencounter radio data
<b>Mariner VI</b>				
B • R, km	—14	—368	—327	—336
B • T, km	7485	7473	7469	7596
TCA, GMT <sup>c</sup>	05:19:06	05:18:57	05:19:00	05:19:06.9
<b>Mariner VII</b>				
B • R, km	3795	3597	3599	3631
B • T, km	6746	6744	6788	6731
TCA, GMT	05:00:53	05:00:50	05:00:52	05:00:50.0
<sup>a</sup> Batch processing program solution. <sup>b</sup> Sequential estimate program solution. <sup>c</sup> Times of closest approach refer to Jul 31 for <i>Mariner VI</i> and Aug 5 for <i>Mariner VII</i> .				

based on optical tracking data could move to a solution. The two optical tracking solutions were computed with different programs developed in parallel. One program was a batch processor that used weighted least squares; the other used a Kalman filter and made sequential estimates. Table 24 lists the statistics associated with the estimates presented in Table 23.

**Table 24. Statistics of orbital estimates**

Parameter	Initial conditions	Optical data <sup>a</sup>	Optical data <sup>b</sup>	Postencounter radio data
<b>Mariner VI</b>				
SMAA, km <sup>c</sup>	361	159	173	10
SMIA, km <sup>d</sup>	79	73	74	10
$\theta$ , deg <sup>e</sup>	75	74	74	—
$\sigma_{TCA}$ , s	6	6	6	0.5
<b>Mariner VII</b>				
SMAA, km	360	217	223	15
SMIA, km	182	141	151	15
$\theta$ , deg	74	45	40	—
$\sigma_{TCA}$ , s	60	13	13	0.5
<sup>a</sup> Batch processing program solution. <sup>b</sup> Sequential estimate program solution. <sup>c</sup> SMAA indicates semimajor axis of the 1 $\sigma$ uncertainty ellipse. <sup>d</sup> SMIA indicates semiminor axis of the 1 $\sigma$ uncertainty ellipse. <sup>e</sup> $\theta$ indicates the orientation of the 1 $\sigma$ uncertainty ellipse, measured counterclockwise from T to the SMAA.				

## VI. Postencounter Trajectory Characteristics

### A. Postencounter Status

After successfully completing close encounters with Mars, the two *Mariner* spacecraft had gained energy so that they were in solar orbits with perihelion distances significantly greater than the Earth aphelion distance. Though not primarily designed as Mars swingby missions, the trajectories were fairly efficient in this respect. If Mars had been a massless planet, and an impulsive maneuver had changed the pre-encounter orbits into the resulting postencounter orbits, the velocity requirements would have been 1.584 km/s for *Mariner VI*, and 1.446 km/s for *Mariner VII*.

Table 25 summarizes the postencounter trajectory parameters. Notice that both orbits had periods of approximately 1.75 yr, and that solar conjunctions occurred 9.5 days apart at the end of April and beginning of

**Table 25. Mariner trajectory parameters<sup>a</sup>**

Parameter	<i>Mariner VI</i>	<i>Mariner VII</i>
Semimajor axis, 10 <sup>6</sup> km	216.57	210.43
Seminor axis, 10 <sup>6</sup> km	211.68	205.93
Period, days	636.24	609.35
Longitude of ascending node, deg	342.64	347.13
Argument of periapsis, deg	203.54	173.08
Eccentricity	0.2113	0.2056
Inclination, deg	1.78	1.82
Time of aphelion, GMT	Feb 3, 1970 13:20	Jan 1, 1970 09:10
Aphelion distance, 10 <sup>6</sup> km	262.35	253.70
Time of solar conjunction, GMT	Apr 30, 1970 01:20	May 9, 1970 13:50
Distance from Sun at conjunction, 10 <sup>6</sup> km	251.13	236.32
Distance from Earth at conjunction, 10 <sup>6</sup> km	401.96	387.07
Sun—Earth—probe angle at conjunction, deg	0.95	1.79
Earth—Sun—probe angle at conjunction, deg	178.48	177.06
Earth—probe—Sun angle at conjunction, deg	0.57	1.16
Time of perihelion, GMT	Dec 18, 1970 16:10	Nov 20, 1970 01:20
Perihelion distance, 10 <sup>6</sup> km	170.80	167.16
<sup>a</sup> Based on osculating conic at conjunction.		

May, 1970. During the time of near-solar conjunction, it was possible to perform an extremely sensitive test of general relativity theory by measuring the effect of the Sun mass on the radio signals being transmitted from the spacecraft.

### B. Heliocentric Orbits of Mariner VI and Mariner VII

Figures 33 and 34 show the celestial latitude and longitude of the two spacecraft for a period of several years

following launch. The heliocentric ranges of the spacecraft are given in Fig. 35.

Figures 36 and 37 show the cone and clock angles of the Earth from the spacecraft, and Fig. 38 gives the Earth-to-spacecraft range. Figure 39 shows the motion in cone angle of Canopus as the spacecraft travels in orbit, and Fig. 40 shows the variation in Mars-to-spacecraft range.

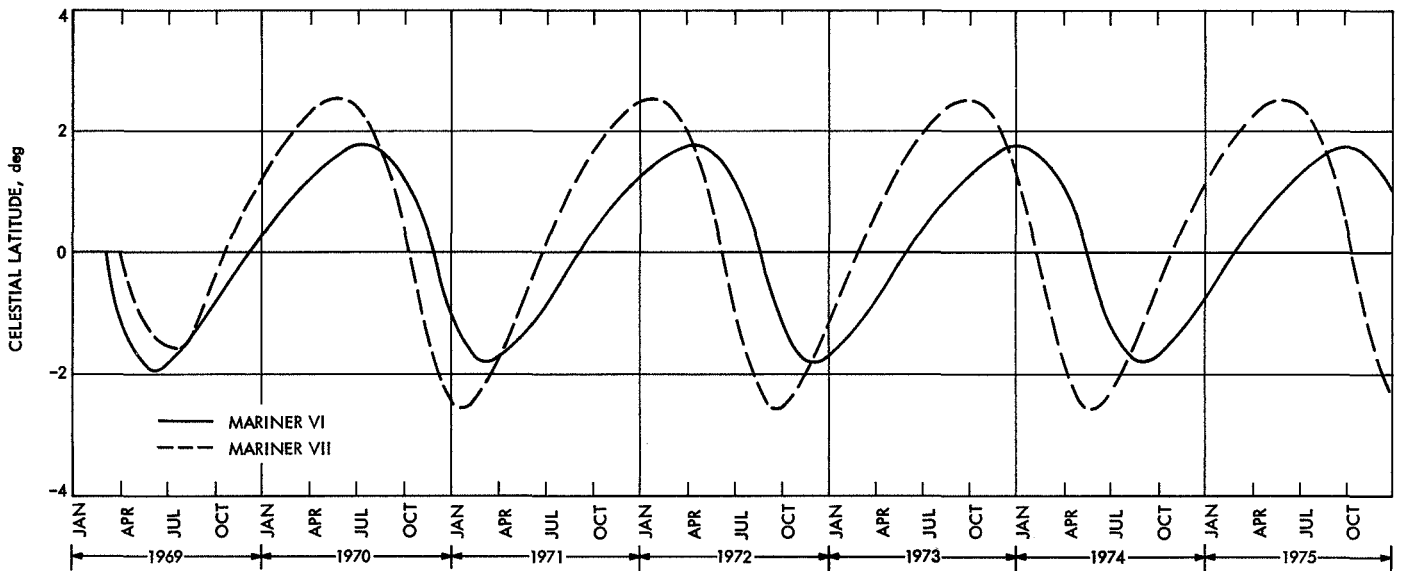


Fig. 33. Mariners VI and VII celestial latitude for period 1969–1975

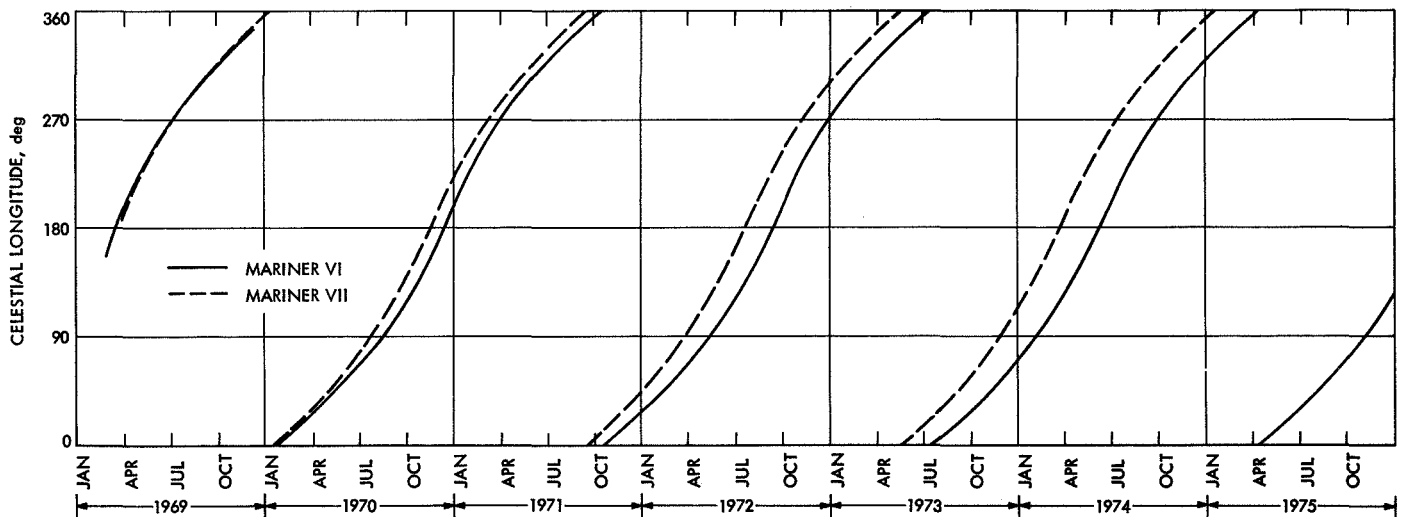
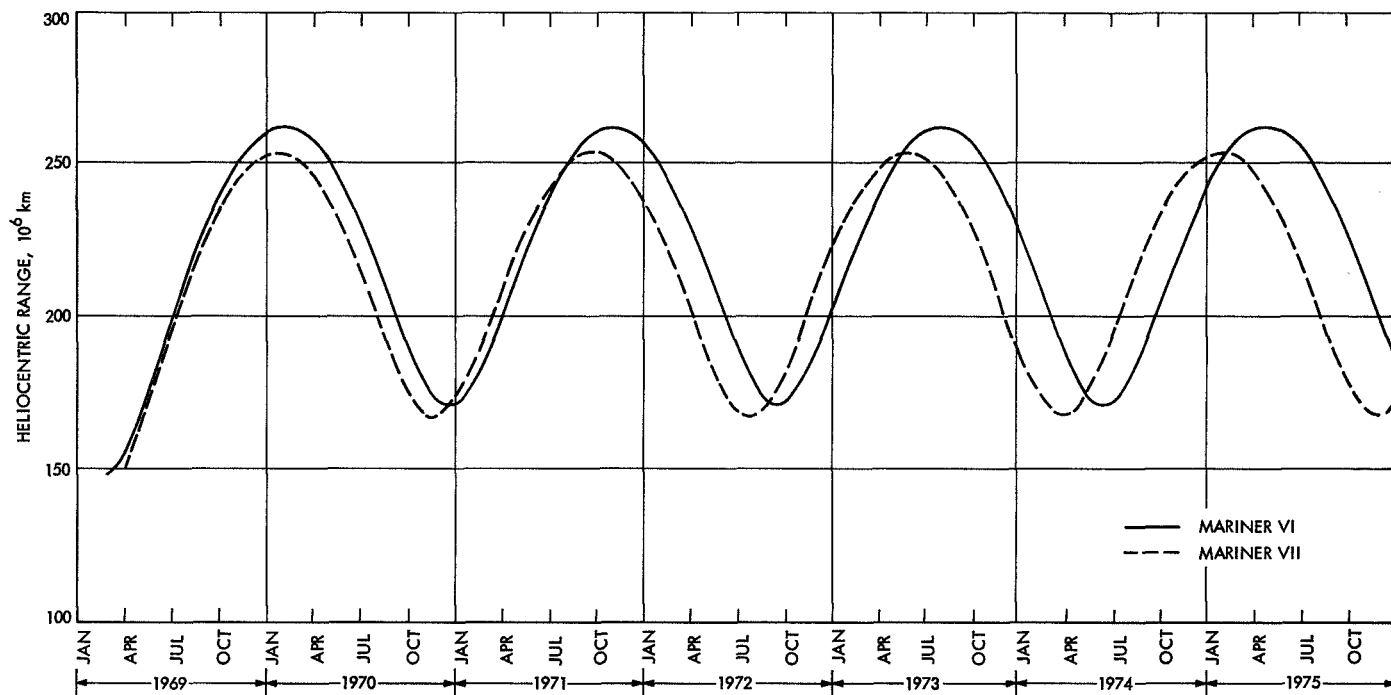
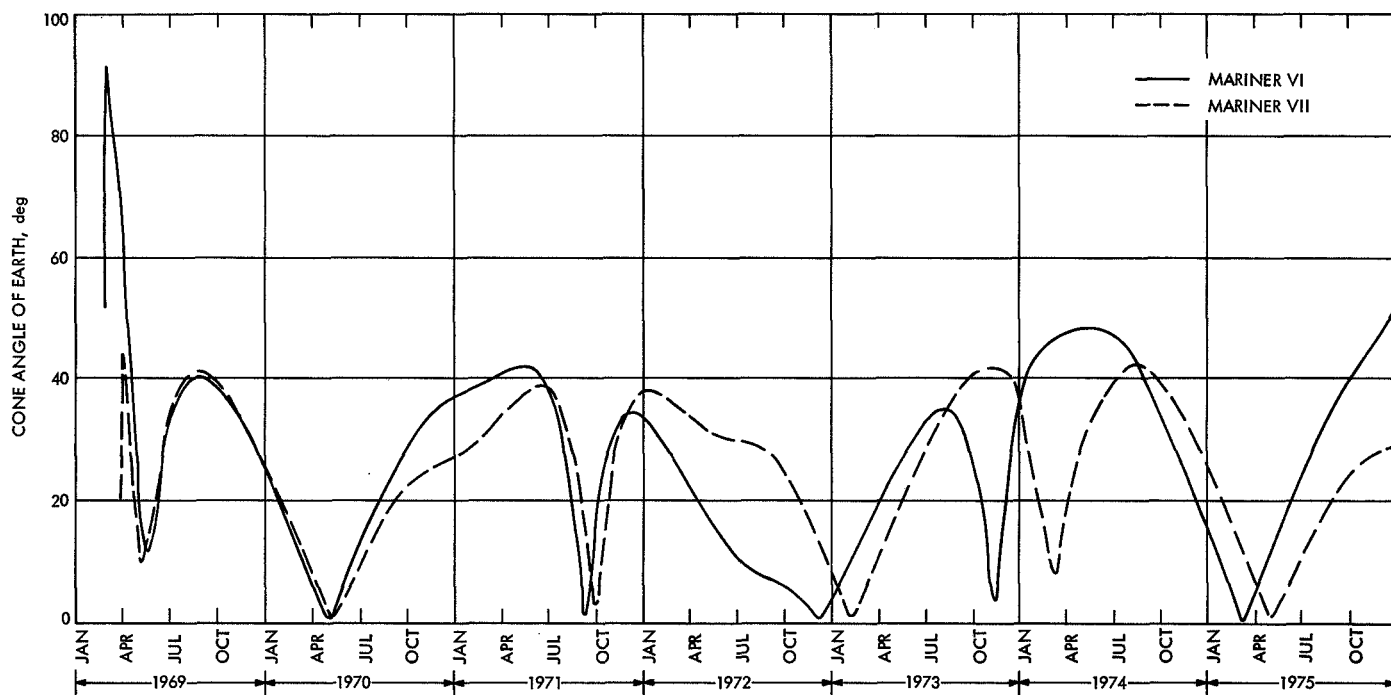


Fig. 34. Mariners VI and VII celestial longitude for period 1969–1975



**Fig. 35. Mariners VI and VII heliocentric range for period 1969–1975**



**Fig. 36. Mariners VI and VII cone angle of Earth for period 1969–1975**

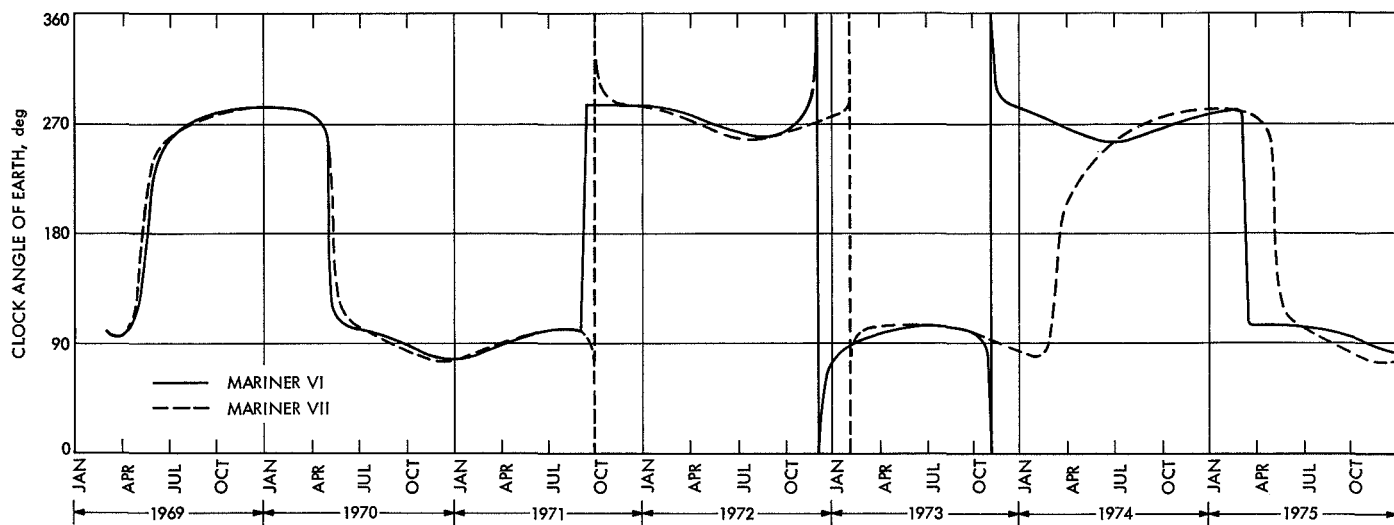


**Fig. 37. Mariners VI and VII clock angle of Earth for period 1969–1975**

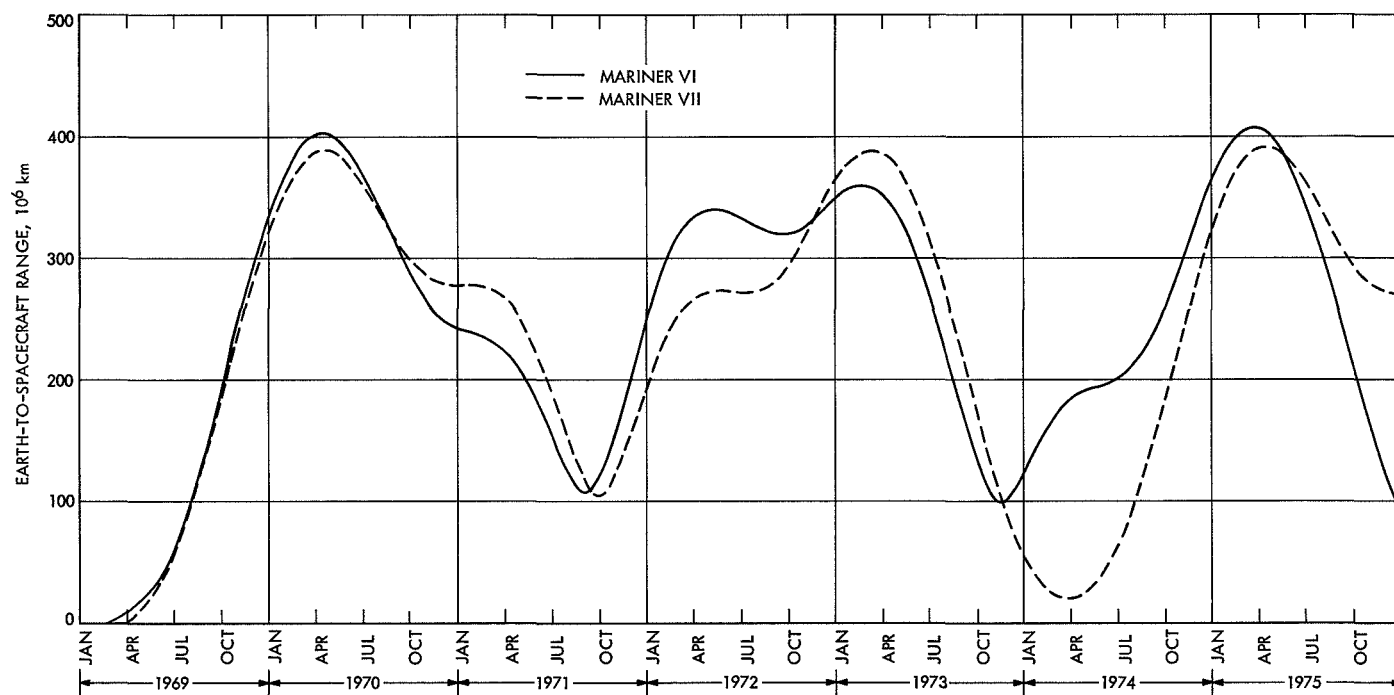


**Fig. 38. Mariners VI and VII Earth-to-spacecraft range for period 1969–1975**

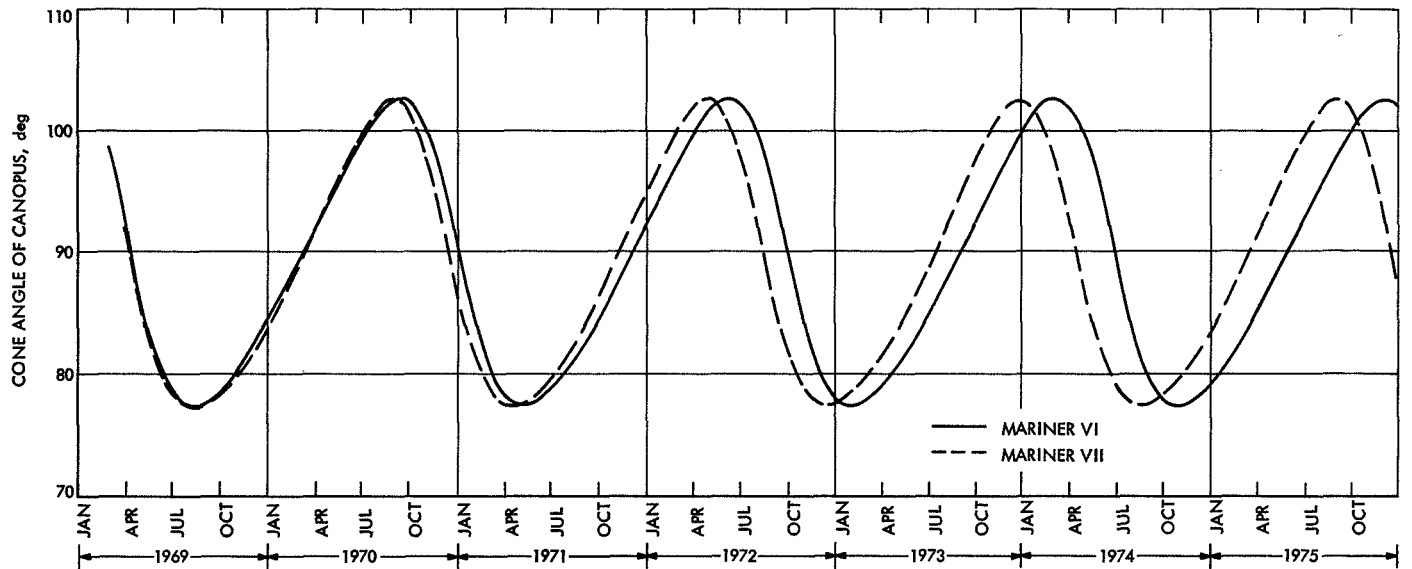


**Fig. 39. Mariners VI and VII cone angle of Canopus for period 1969–1975**

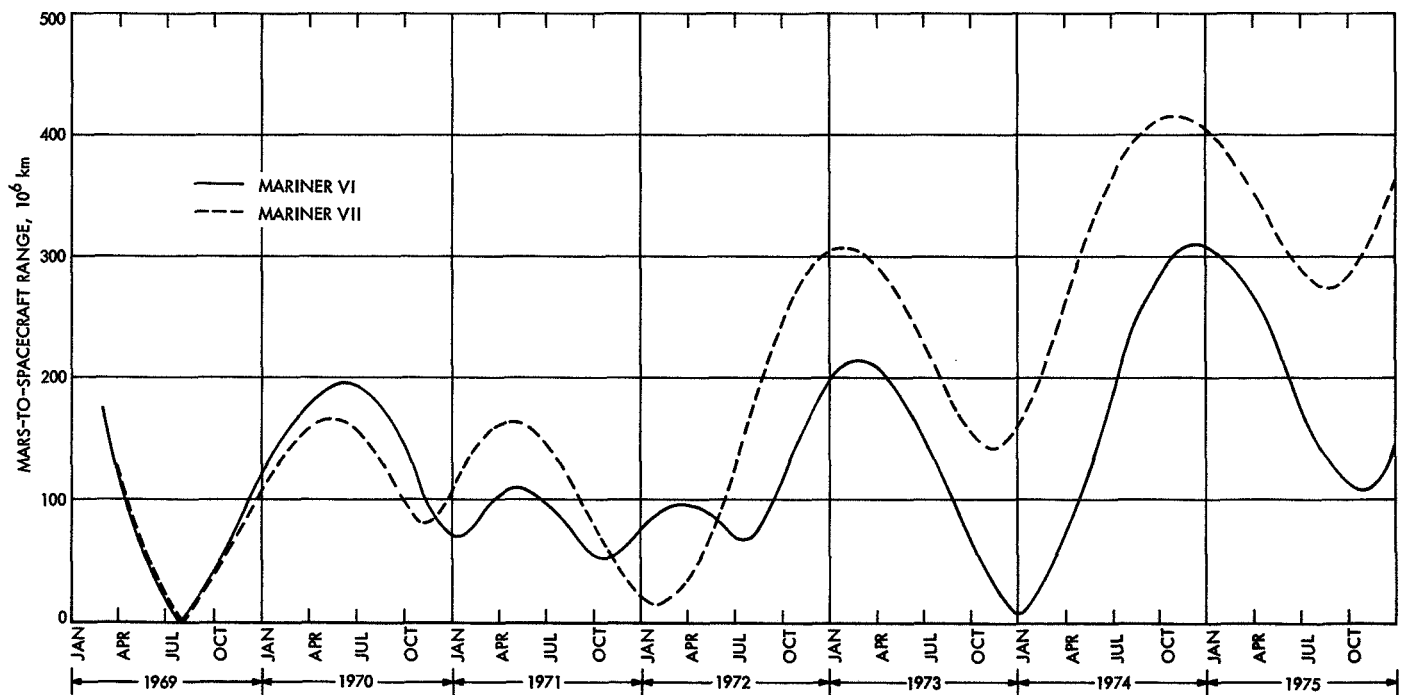


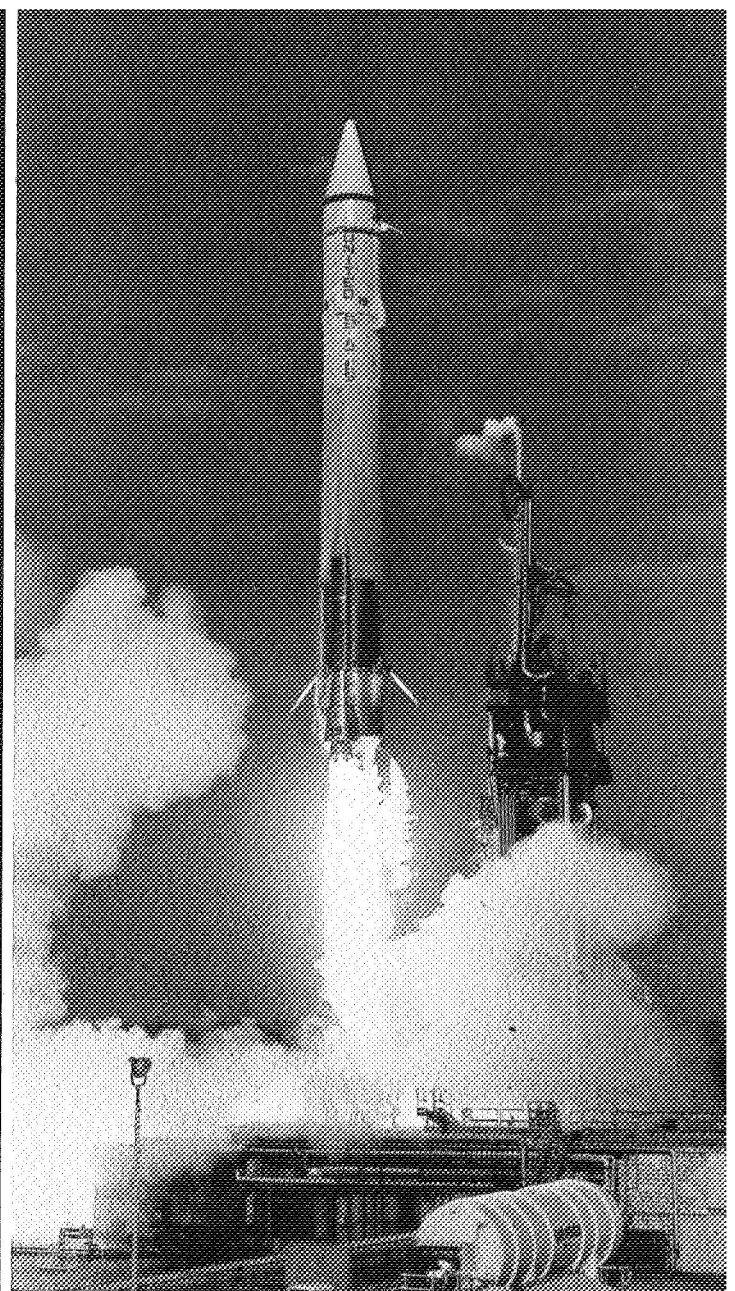
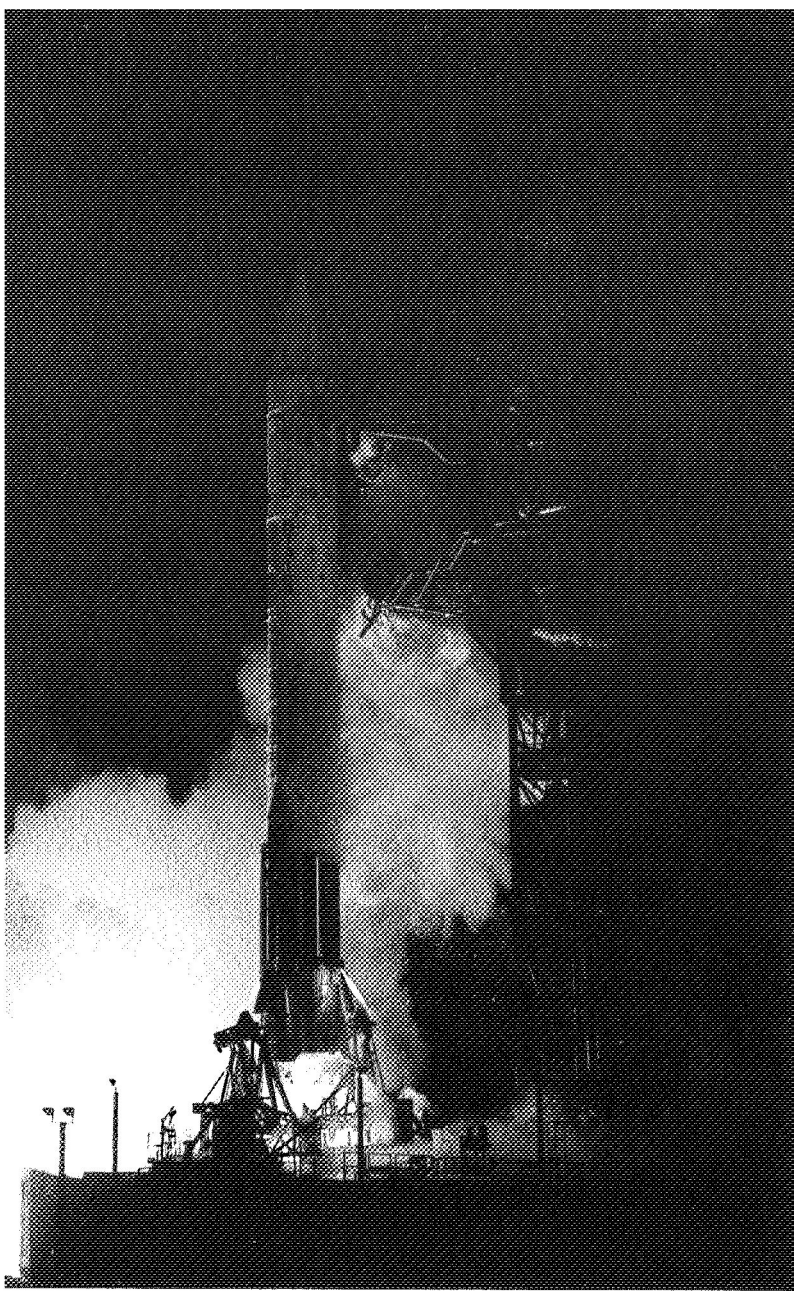
**Fig. 40. Mariners VI and VII Mars-to-spacecraft range for period 1969–1975**

## Reference

1. Ondrasik, V., and Mulhall, B. D., "Estimation of the Ionospheric Effect on the Apparent Location of a Tracking Station," in *The Deep Space Network*, Space Programs Summary 37-57, Vol. II, pp. 29-42. Jet Propulsion Laboratory, Pasadena, Calif., May 31, 1969.







## Part 2. Launch Phase Performance



## Mission Considerations

The excess launch capability provided by the *Atlas/Centaur* vehicle was to be used to provide an extended launch window as described under Mission Design, Analysis, and Engineering in Part 1 of Volume I of this *Mariner Mars 1969* project report. A 45-day launch period (February 23–April 8) and a related 18-day Mars arrival period (July 29–August 15) were established, with preferred arrival dates (July 29 and August 5) selected by the principal investigators.

Firing tables and other launch calculations were prepared on the basis of the first spacecraft being launched February 24 or later, and the second March 24 or later. This planning was intended to provide optimum recovery time in case the first launch and early flight revealed the need for hardware changes in the second vehicle or spacecraft, while preserving an adequate period for the second launch. Plans were established to provide for emergency extension of the launch period by as much as 38 days, with arrival dates also extended. The daily launch window was reduced to 1 h, on the basis of launch-on-time history of the vehicle and to limit the number of targeting calculations required.

Tracking and telemetry requirements for launch vehicle and spacecraft coverage were established by the project, and were met by elements of the Air Force Eastern Test Range (AFETR), Manned Space Flight Network (MSFN), and Deep Space Network (DSN). The implementation was less difficult than on many prior projects because the direct-ascent trajectory placed

most of the critical events relatively close to the launch site, where the downrange facilities are concentrated. A typical Earth-track of the *Mariner VI* launch phase is illustrated in Fig. 1 to show the relationship of sites, events, and coverage.

*Mariner VI* was counted down and launched on February 25, 15 minutes into the launch window. Critical early-flight operations conducted in the next several days provided no reason to make changes in vehicle or spacecraft equipment for *Mariner VII*, but certain spacecraft subsystem questions required a delay of three days in the second launch, which was conducted on March 27, 47 min into the launch window.

The most southerly flight azimuth permitted by AFETR Range Safety is 108 deg true. After initiating its flight on 108 deg, the AC-20 vehicle (*Mariner VI*) successfully performed two programmed southeast “dog-leg” or yaw maneuvers to skirt the safety zones around the Bahama and Leeward Islands and reach the desired 133-deg effective flight azimuth for February 25, 1969 (GMT). The AC-19 vehicle (*Mariner VII*) was launched at 102.79 deg true into a planar trajectory, and yaw maneuvers were unnecessary.

Near-Earth tracking and telemetry support by the AFETR and MSFN and launch-phase support by DSN elements were satisfactory. Launch-phase tracking and telemetry coverage for *Mariners VI* and *VII* is shown in Table 1.

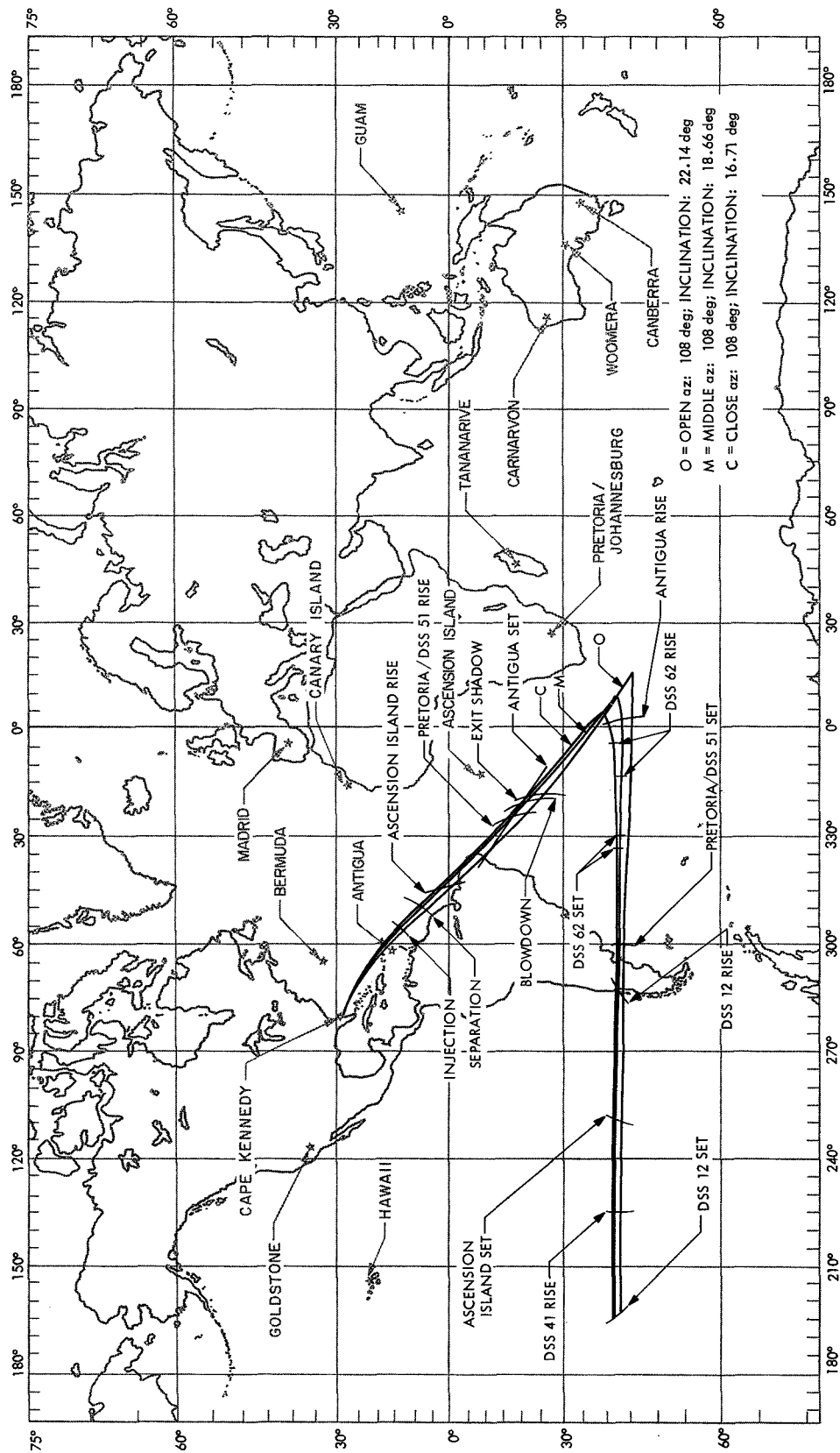


**Fig. 1. Earth tracks for Mariner Mars 1969 (launch date: February 25; arrival date: July 31)**

**Table 1. Launch-phase tracking and telemetry coverage**

Station	Coverage, s from launch		Station	Coverage, s from launch	
	Mariner VI	Mariner VII		Mariner VI	Mariner VII
Vehicle tracking			Vehicle telemetry		
AFETR radar station			Mainland (TEL-4)	0-559	0-540
1.16	0-562	0-350	Grand Bahama Island	30-705	50-625
0.18 <sup>a</sup>	—	15-539	Bermuda	238-750	235-836
19.18	14-545	14-530	Antigua	374-1596	342-1444
3.18	92-597	—	Ascension Island	905-5120	881-6386
3.13	97-390 <sup>b</sup>	92-571	Spacecraft tracking and telemetry		
7.18	200-904	200-775	Coverage, GMT		
91.18	390-1114	380-1093	DSS 71	Prelaunch-01:38	16:57-22:29
40.48 <sup>c</sup>	682-1073	—	MSFN Ascension Island	01:45-12:53	22:37-09:24
12.18	1076-5405 <sup>b</sup>	1025-5513 <sup>b</sup>	DSS 51	01:52-09:27	22:45-06:00
12.16	1125-4198	1068-5134	DSS 62	—	22:41-02:00
<sup>a</sup> Skin track to 263 s. <sup>b</sup> One or more dropouts of varying lengths occurred during these intervals. <sup>c</sup> Skin track only.					

# Launch Operations

## I. Introduction

The decisions to proceed with preparations for the *Mariners VI* and *VII* launches were made during launch readiness reviews at the AFETR on February 3-4 and March 20, 1969. After performance of the space vehicle composite readiness test, four days before the scheduled opening of the launch window, a systematic procedure was followed to establish and verify a launch-ready condition of the vehicle that culminated in the launch countdown. Although unscheduled holds occurred during each countdown, both *Mariners VI* and *VII* were launched within the scheduled launch window on the first launch attempt.

## II. Countdown and Launch

The launch countdown integrated the operations of the *Atlas/Centaur*/spacecraft systems into a common operation and established the launch readiness of the combined space launch system. The spacecraft status checks paralleled the *Atlas/Centaur* launch preparations from a separate control console in the blockhouse until approximately nine minutes prior to launch. At this time a GO signal was transmitted to the *Atlas/Centaur* test conductor's console indicating the spacecraft readiness

for launch. An automatic sequence of launch vehicle operations was initiated by the test conductor at approximately  $T - 10$  s. A typical spacecraft launch countdown is illustrated in Fig. 1. Preplanned holds were incorporated into the countdown at  $T - 90$  min for a 60-min duration and at  $T - 10$  min for a 10-min duration for the purpose of increasing the launch-on-time capability.

### A. *Mariner VI* Launch

The *Mariner VI* launch countdown began on February 24 at a countdown time of  $T - 500$  min. The spacecraft joined the launch vehicle countdown at  $T - 210$  min, following the end of the radio frequency silence period. During preparation for the launch vehicle guidance autopilot test, a *Centaur* guidance system anomaly was observed in which the W gyroscope drift rate appeared to increase significantly. Investigation of the problem revealed that the anomaly resulted from an erroneous gyro-torquing signal. The problem was resolved during a hold at  $T - 80$  min that used up the 10 min of holding time scheduled for the built-in hold at  $T - 10$  min and 15 min 2 s of the planned 60-min launch window. The countdown was resumed and proceeded smoothly through liftoff. The spacecraft was launched in accordance with launch plan 2531-2 (Table 1).

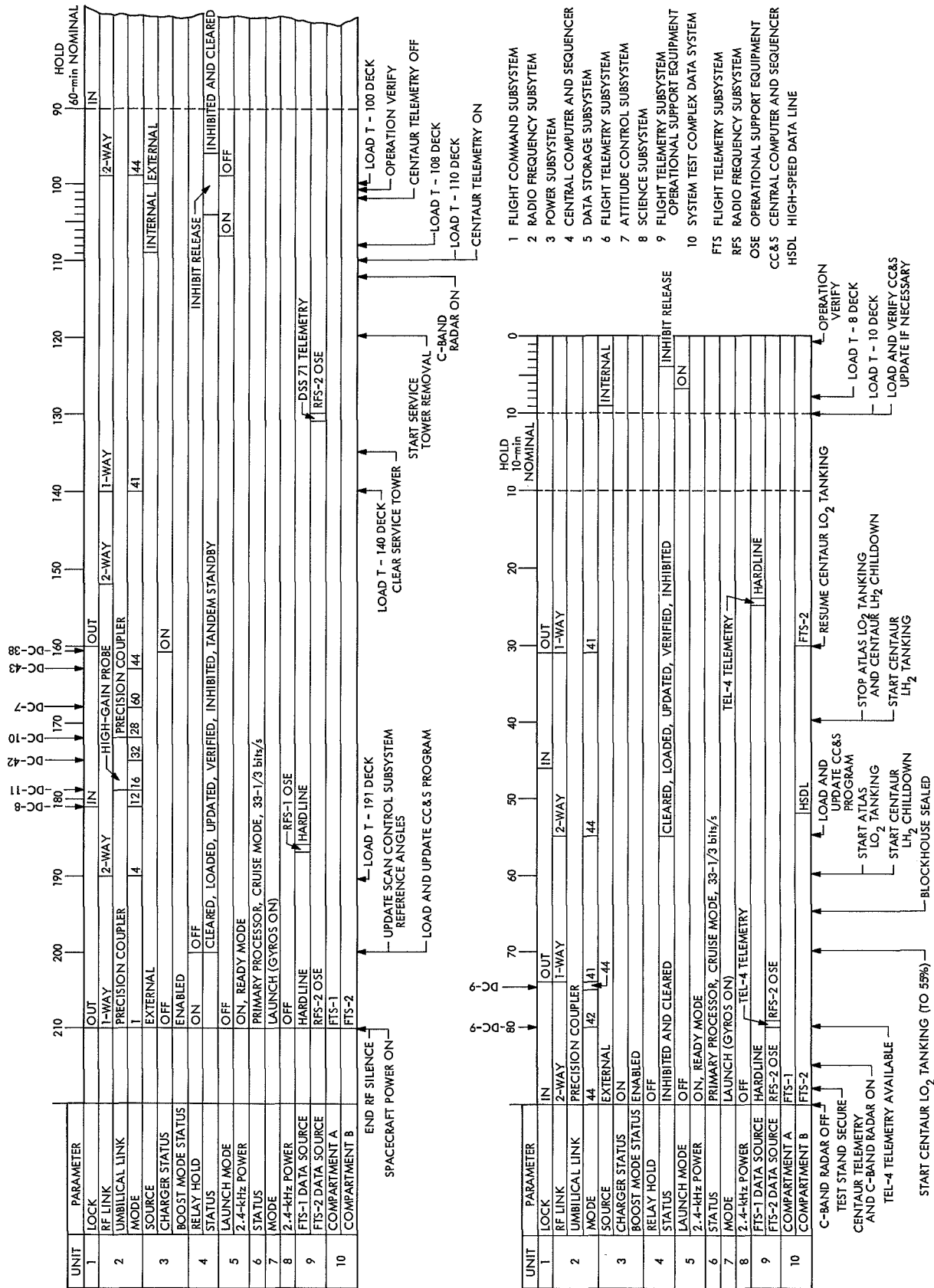




**Table 1. Mariner Mars 1969 launch plans**

Item	Mariner VI	Mariner VII
Launch vehicle designation	AC-20	AC-19
Spacecraft designation	M69-3	M69-2
Launch plan	2531-2	27810-2
Launch date, GMT	Feb 25	Mar 27
Launch window, GMT	00:54-01:54	21:35-22:35
Arrival date, GMT	Jul 31	Aug 5
Mars pass	Equatorial	South polar
Central computer and sequencer tape	L-0031	L-0810
Update position	2	2
Far-encounter clock angle, deg	111	102
Far-encounter cone angle, deg	158	157
Near-encounter clock angle, deg	264	227
Near-encounter cone angle, deg	130	127

All spacecraft and launch vehicle systems performed satisfactorily throughout the powered phases of flight, and the spacecraft was accurately injected into a Mars transfer trajectory. During powered flight, *Atlas* booster engine cutoff (BECO) occurred about 5 s early because of early actuation of the autopilot backup staging accelerometer. No significant vehicle performance was lost because the sustainer engine continued to burn to liquid oxygen depletion (about 20 s longer than planned). The *Centaur* engine burned about 7 s longer than planned without adversely affecting the flight. Damage to launch complex 36B was moderate. The powered flight sequence of events and launch vehicle performance are described under Launch Vehicle Performance in this part of Volume II.

Weather conditions were good throughout the launch countdown. During the launch vehicle propellant-tanking phase, the anemometer indicated surface winds had exceeded the launch criteria; however, launch vehicle rate gyroscope data indicated that the launch vehicle was in a safe configuration at all times, and countdown

operations proceeded. At liftoff, surface winds were 8 knots from an azimuth of 350 deg. The surface temperature was 50.9°F, with a relative humidity of 82%, and a dewpoint of 46°F. Sea-level atmospheric pressure was 30.03 in. Hg. There was 3/10 cloud cover at 1500-ft altitude. Visibility at liftoff was 10 mi.

#### **B. Mariner VII Launch**

The *Mariner VII* launch countdown began on March 27 at a countdown time of  $T - 500$  min. The spacecraft joined the launch vehicle countdown at  $T - 210$  min, following completion of the radio frequency silence period. The countdown proceeded very smoothly until about  $T - 7$  min when the *Centaur* guidance optical acquisition signal in the ground support equipment became intermittent, which prevented closed loop (automatic) azimuth alignment of the guidance inertial platform. The countdown continued down to  $T - 56$  s while guidance personnel attempted unsuccessfully to resolve the problem. The count was halted at this point to confirm the configuration, then recycled to  $T - 10$  min and held for 38 min. During this time, the inertial platform was satisfactorily aligned using the computer-controlled launch set to torque the platform in conjunction with meter measurements of drift. The count was resumed at  $T - 10$  min and continued through liftoff. The launch was 47 min and 1.198 s into the planned 60-min launch window. There were no spacecraft anomalies during the countdown. The spacecraft was launched in accordance with launch plan 27810-2 (Table 1).

All spacecraft and launch vehicle systems performed satisfactorily throughout the powered phases of flight. The *Centaur* engine burned about 9 s longer than planned without adversely affecting the mission. Damage to launch complex 36A was moderate.

Weather conditions were good throughout the launch countdown. At liftoff, surface winds were 2 knots from an azimuth of 90 deg. The surface temperature was 60.8°F, with a relative humidity of 37% and a dewpoint of 34°F. Sea-level atmospheric pressure was 30.14 in. Hg. Visibility was 10 mi with 8/10 cirrus cloud cover.

## Launch Vehicle Performance

### I. Vehicle

Properties and characteristics of the SLV-3C *Atlas/Centaur* vehicles that launched *Mariners VI* and *VII* are described under Launch Vehicle in Part 3 of Volume I of this report, and they are summarized in

Table 1. Launch vehicle characteristics

Item	Stage		
	<i>Atlas</i> booster	<i>Atlas</i> sustainer	<i>Centaur</i>
Engine	Rocketdyne up-rated MA-5 system; two gimballed thrust chambers	MA-5; one gimballed sustainer; two gimballed verniers	Pratt & Whitney RL 10A3-3; two gimballed; 14 H <sub>2</sub> O <sub>2</sub> control thrusters
Thrust	168,000 lb each at sea-level conditions	Sustainer: 58,000 lb; verniers: 670 lb each at sea-level conditions	15,000 lb each at vacuum conditions
Propellant	RP-1/LO <sub>2</sub>	RP-1/LO <sub>2</sub>	LH <sub>2</sub> /LO <sub>2</sub>
Construction	Engines, frame, and aerodynamic skirt	Thinwall pressurized main propellant tanks, external conduits	Thinwall pressurized tanks with external insulation
Guidance	<i>Atlas</i> autopilot, 5.7-g staging sensor	<i>Centaur</i> guidance	Honeywell inertial guidance with navigation computer

Table 1. Physical characteristics of the combined space vehicle (*Atlas* booster and sustainer, *Centaur*, and payload) included an overall length of 117 ft, a basic diameter of 10 ft, and a weight at liftoff of about 323,000 lb.

The AC-19 vehicle had originally been designated for the *Mariner VI* launch (with spacecraft M69-3) on February 24; however, while on the launch pad 10 days before launch with the spacecraft aboard, the *Atlas* stage (then 5402C) suffered a loss of tank pressure that resulted in partial collapse of the LO<sub>2</sub> tank. The spacecraft suffered no damage, and the *Centaur* sustained only paint abrasion that was repairable on the spot; however, *Atlas* vehicle 5402C suffered substantial tank-skin damage and was replaced. The AC-19 then became the launch vehicle for *Mariner VII*, which included spacecraft M69-2. Both vehicles met their originally scheduled launch-readiness dates.

### II. Sequence of Events

The nominal flight sequence for the *Atlas/Centaur* that begins with the ignition of the *Atlas* engines continues through direct ascent to spacecraft injection and terminates with the deflection of the *Centaur* vehicle from the Mars trajectory. The sequence is shown in Fig. 1. Predicted and actual event times are shown in Table 2, and the phases of the launch sequence are discussed in the paragraphs that follow.

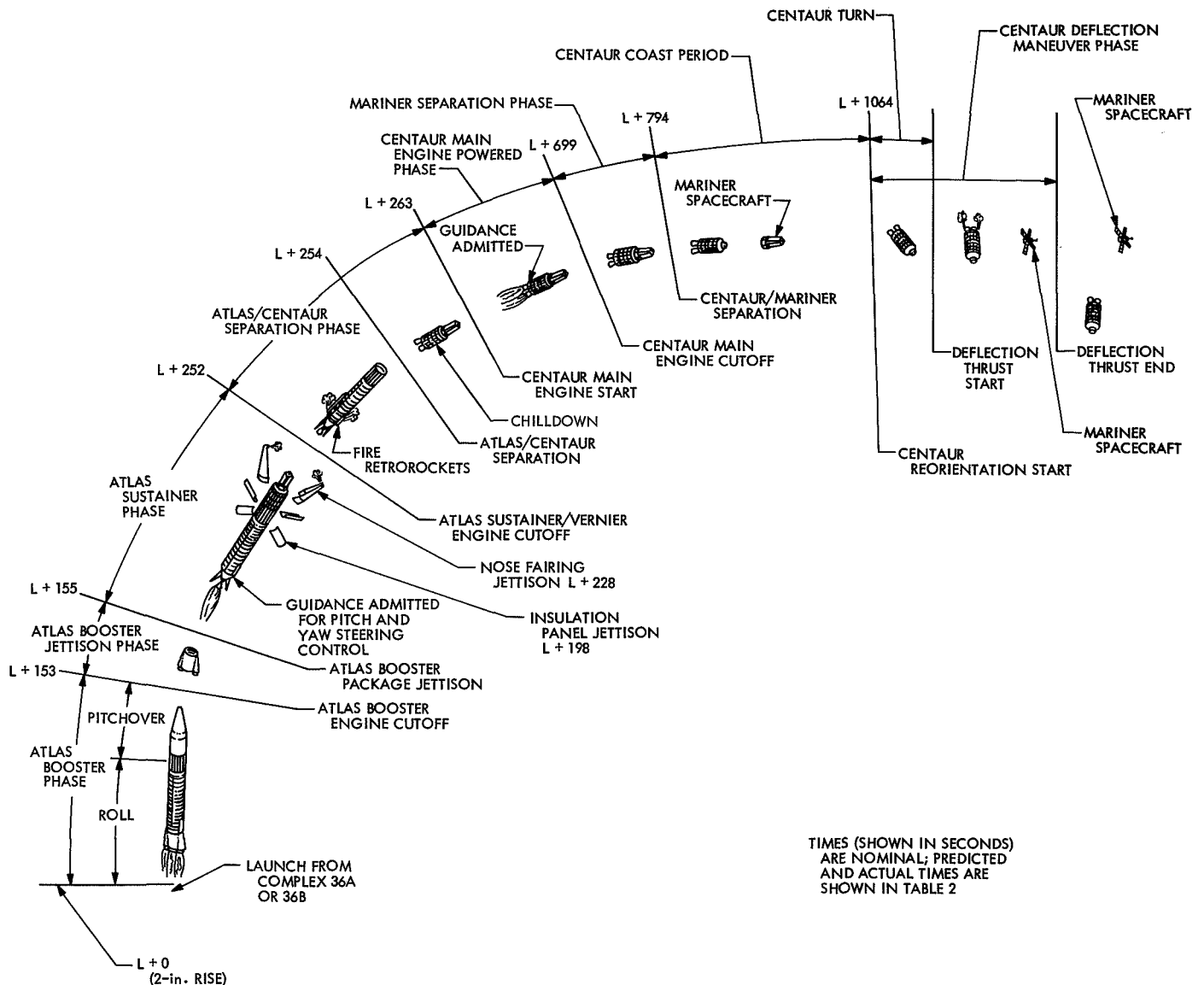


Fig. 1. Atlas/Centaur nominal flight sequence

### A. Atlas Booster Phase of Flight

Hypergolic ignition of all five *Atlas* engines occurred simultaneously approximately 2 s prior to liftoff. When all engines reached nearly full thrust, the launcher mechanism began a controlled release of the vehicle. At 2 s after liftoff (liftoff defined as 2-in. vertical motion), the vehicle began a 13-s programmed roll from the fixed launcher azimuth (105.0 deg for launch complex 36A and 115.0 deg for launch complex 36B) to the desired flight azimuth. At  $L + 15$  s, the roll program was completed and the vehicle began a programmed pitch, bending the flight path over to maximize booster performance. The pitch program continued until BECO.

The pitch program included supplemental pitch and yaw programs for windshear relief. During this period, the vehicle was controlled by the *Atlas* autopilot; the booster engines were gimballed for pitch, yaw, and roll control; the vernier engines were active for roll control only; and the sustainer engine was centered.

At approximately 152 s, BECO was initiated by a signal from *Centaur* guidance when vehicle acceleration reached a nominal value of 5.7 g. At approximately 3 s after BECO, with the sustainer engine locked in a null position, the booster section was jettisoned by release of pneumatically operated latches.

Table 2. Powered flight events

Event	Mark No.	Predicted <sup>a</sup> time from launch, s		Actual time from launch, s	
		AC-20	AC-19	AC-20	AC-19
Liftoff		0.0	0.0	0.0	0.0
Atlas booster engine cutoff	1	152.05	152.53	147.16	150.37
Atlas booster package jettison	2	155.15	153.47	150.12	153.45
Insulation panel jettison	3	197.05	195.37	191.72	195.12
Nose fairing jettison	4	234.05	232.37	228.44	231.90
Atlas sustainer/vernier engine cutoff	5	252.29	253.14	270.85	254.99
Atlas/Centaur separation (fire retrorockets)	6	254.29	256.99	272.87	256.98
Centaur main engine start	7	263.79	264.64	282.34	266.46
Centaur main engine cutoff	8	699.59	701.51	725.50	712.21
Centaur/Mariner separation	9	794.59	807.21	820.58	807.28
Centaur reorientation start	10	1064.59	1078.30	1091.20	1078.75
Centaur blowdown start <sup>b</sup>	11	1549.59	1562.21	1575.60	1562.35

<sup>a</sup>Nominal times were taken directly from the best preflight nominal and do not include allowance for actual flight events or programmer subroutine times.  
<sup>b</sup>Last programmed event. End blowdown and power changeover were not programmed for these flights.

## B. Atlas Sustainer Phase of Flight

At BECO + 8 s, *Centaur* guidance was admitted for pitch and yaw steering control during the sustainer flight phase. For the AC-20 flight, the first of two yaw steering commands to meet range safety restrictions was also initiated by *Centaur* guidance at this time. During this phase, the sustainer engine gimbals were unlocked and the engine was gimballed for pitch and yaw control while the vernier engines provided roll control as commanded by the *Atlas* autopilot. At BECO + 45 s, the two insulation panels on the *Centaur* cryogenic tanks were cut into four sections by firing a chain of linear shaped charges. The sections rotated outward under the effects of vehicle acceleration to about 46 deg where they were released from the hinges and cleared the vehicle. This event was timed to occur at an altitude at which the aerodynamic heating rate was rapidly decreasing, approximately 50 nmi. At BECO + 82 s, squibs were fired to unlatch the clamshell nose fairing, which was jettisoned about 1 s later by nitrogen gas thruster jets activated by pyrotechnic valves. Nose fairing jettison was timed to occur when the aerodynamic heating of the spacecraft was such that excessive temperatures would not result, but while the vehicle was still under acceleration.

Other programmed events that occurred during the sustainer phase of flight were: (1) unlocking of the *Centaur* hydrogen-tank vent valve to relieve hydrogen

boil-off pressure, (2) starting of *Centaur* boost pumps prior to *Centaur* engine start, and (3) locking of the *Centaur* oxidizer-tank vent valve followed by pressurization of the tank. The vehicle continued its ascent under sustainer and vernier engine thrust. Sustainer and vernier engine cutoff (SECO and VECO) occurred as a result of oxidizer depletion at approximately 252 s of flight. At SECO, the *Centaur* hydrogen-tank vent valve was locked and pressurization of the tank took place.

Separation of the *Atlas* from the *Centaur* occurred 2 s after SECO by the firing of shaped charges at the forward end of the interstage adapter. This was followed by ignition of the eight retrorockets, located at the aft end of the *Atlas* tank section, which backed the *Atlas* and the interstage adapter away from the *Centaur*.

## C. Centaur Main Engine Power Phase

Chilldown of the *Centaur* propulsion system was initiated 8 s before ignition of the *Centaur* main engines. Main engine start (MES) was commanded 11½ s after SECO. *Centaur* guidance was reenabled 4 s after *Centaur* MES to provide steering commands. For AC-20, these commands included those necessary to accomplish the second of two yaw maneuvers necessary to reach the desired flight azimuth after skirting the range safety zones. Main engine cutoff (MECO) was commanded by guidance at approximately 11 min 42 s when sufficient impulse had been delivered for injection into the transfer

trajectory. At MECO, the *Centaur* hydrogen peroxide engines were enabled for attitude control.

After MECO and before spacecraft separation, the vehicle was oriented to a predetermined separation vector. At MECO + 95 s, the *Centaur* programmer signaled the *Centaur* pyrotechnic firing relay to provide the firing current to the spacecraft separation mechanism. The V-band was released, and the spacecraft was separated from the launch vehicle by three spring assemblies, imparting a forward velocity of 2 ft/s to the spacecraft relative to the *Centaur*.

#### D. *Centaur* Deflection Maneuver Phase of Flight

Following spacecraft separation, the *Centaur* vehicle coasted under attitude stabilization for a period of 270 s (MECO + 365 s). At MECO + 365 s, the *Centaur* was commanded to reorient to a predetermined deflection vector, which was about 90 deg with respect to the flight path. At MECO + 460 s, deflection thrust was initiated; this consisted of firing two 50-lb hydrogen peroxide engines for 40 s, followed by the firing of the two 3½-lb hydrogen peroxide engines for 350 s. On completion of the hydrogen peroxide engine firing at MECO + 850 s, the launch vehicle was approximately 10,700 ft away from the spacecraft and beyond possible exhaust-plume contamination. At this time, the *Centaur* propellant cool-down valves were opened and the residual propellants in the tanks were allowed to blow down to depletion. This blowdown operation provided additional deflection thrust to the vehicle, further perturbing its orbit and guaranteeing that the *Centaur* vehicle would not impact the target planet. The *Centaur* programmer was commanded to stop at approximately MECO + 1850 s. The closest approach to Mars by the *Centaur* tank was computed to be approximately 637,019 km for AC-19. Although not computed, the expected AC-20 *Centaur* closest approach was approximately the same.

Additional computed data relative to spacecraft/*Centaur* separation are as follows:

Time from spacecraft injection	Separation distance, km
5 h	592.7
10 h	1,629.6
15 h	2,587.3
5 days	24,474.0

Additional data on the *Centaur*/Mars trajectory for AC-19 are shown in Table 3. (*Centaur* flight telemetry and DSN tracking data were used to compute the data given in these tables. The *Centaur* state vectors at approximately 175 s after start of blowdown, derived from the telemetry, were used. Since the amount of additional energy resulting from the remaining blowdown is unknown, the values given are approximate.)

**Table 3. *Centaur* (AC-19) conic data relative to Mars**

Parameter	Value
Epoch (Aug 3), h	15.732
Semimajor axis, km	818.9
Eccentricity	778.875
Inclination, deg	19.9
Longitude of ascending node, deg	255.6
Argument of perifocus, deg	278.8
Radius of closest approach, km	637,019.0
Vis-viva energy, km/s <sup>2</sup>	52.3
<i>Centaur</i> closest approach to Mars, km	637,019

### III. Vehicle Performance

The performance of the *Atlas*/*Centaur* AC-20 and AC-19 vehicles was completely satisfactory, providing very accurate injection of *Mariners VII* and *VI* into their prescribed Mars transfer trajectories.

#### A. Guidance and Flight Control

Autopilot performance was satisfactory throughout both flights; programmed events were properly initiated, and vehicle stability was controlled. Vehicle disturbances were at or below expected levels and similar to previous SLV-3C flights. During the *Atlas* phases of the flights, the vehicles were easily controlled after *Atlas* autopilot activation at 42-in. motion. Vehicle stability was also satisfactorily maintained during the *Centaur* phases of the flights.

Analysis of the AC-20 telemetry data revealed *Atlas* BECO occurred 5 s earlier than expected. Investigation of the early engine cutoff indicated that the autopilot backup staging accelerometer had prematurely activated at 143.96 s at an acceleration of 5.02 g, rather than at the designed setting of  $5.9 \pm 0.2$  g; BECO occurred 3.1 s

later when the accelerometer output was enabled by the flight control programmer. Actual BECO occurred at 147.05 s; expected BECO time was 152.05 s. The premature BECO preempted the normal cutoff mode, and the guidance discrete was not generated. The guidance system switched into the sustainer phase as a function of sensing booster thrust decay. As a result of the 5-s premature BECO, the sustainer engine cutoff was extended 18.6 s past the expected flight time, to deplete the additional unexpended propellants.

The guidance systems performed well for both flights, injecting both spacecraft into near-perfect trajectories to Mars. Accuracy of the injection was indicated by the midcourse correction requirement, 10 days after injection, obtained from JPL tracking data. The correction requirements needed to intersect the targeted point were as shown in Table 4.

**Table 4. Midcourse correction requirements, AC-19 and AC-20**

Parameter	AC-20	AC-19
Actual miss only, m/s	0.90	1.87
Preflight-computed miss only ( $3\sigma$ ), m/s	8.5	7.6
Actual miss plus time of flight, <sup>a</sup> m/s	2.18	2.01
Preflight-computed miss plus time of flight ( $3\sigma$ ), m/s	9.7	9.1
Uncorrected target miss, km	5,368	12,746
<sup>a</sup> Three-sigma requirement = 13.5 m/s.		

Analysis of the flight telemetry data indicated satisfactory performance of the *Centaur* flight control system for both flights. Vehicle stability was satisfactorily maintained during all desired controlled flight periods, which included the *Centaur* powered phase, the spacecraft preseparation alignment and separation sequences, and the retromaneuver/blowdown periods. *Centaur* residual angular rates just prior to spacecraft separation were less than 0.05 deg/s in each axis for AC-20 and less than 0.08 deg/s for AC-19, both well within the specified allowable of 0.5 deg/s in any axis. Data through approximately 2200 s for each flight indicated both vehicles were still under control at that time.

Guidance sensor data were used in the guidance reconstructed trajectory program to reconstruct the flight trajectory. The program flight trajectory vs the JPL tracking indicated that the guidance position and ve-

locity vectors at spacecraft separation were within the  $3\sigma$  estimates for guidance hardware errors. The orbital parameters at injection indicated close agreement with the nominal. Table 5 shows engineering nominal values vs program flight (guidance) and JPL tracking data at spacecraft separation.

## B. Propulsion and Propellant Utilization

For both flights, *Atlas* propulsion system performance was satisfactory. Engine thrust levels were near expected values throughout the flights. On AC-20, BECO was commanded 5 s early, as previously mentioned, resulting in a longer-than-planned sustainer phase.

Performance of the *Atlas* propellant utilization systems was also satisfactory.

The *Centaur* propulsion systems performed satisfactorily throughout all phases of both flights. Telemetered information indicated satisfactory operation of the main engines, the propellant feed systems, and the hydrogen peroxide systems. The main engine burn durations were both slightly longer than predicted: 7.4 s for AC-20 and 8.8 s for AC-19. This phenomenon had occurred on most of the previous *Centaur* flights, and is not considered detrimental to performance.

Operation of the *Centaur* propellant utilization systems was satisfactory throughout powered flight.

## C. Pneumatic, Hydraulic, and Electrical Power Systems

Operation of the *Atlas* pneumatic system, including the programmed tank pressurization and pneumatic control functions, was properly accomplished throughout the flights. The *Centaur* propellant tanks were maintained at satisfactory pressure levels during all phases of the flights, with expected occurrences of "burp" pressurizations and hydrogen tank ventings. The "burp" pressurization is a technique whereby the *Centaur* propellant tank pressures are suddenly increased to provide a better net positive suction head to the engines as a part of the prestart cycle. The  $\text{LO}_2$  tank is "burped" (a rise of approximately 10 psi in 2 s) at the time of *Atlas* BECO and the  $\text{LH}_2$  tank is "burped" (a rise of approximately 2 psi in 1 s) at the time of *Atlas* SECO. On the AC-20 flight, because of the premature BECO and the consequent extended sustainer engine burn, the length of time for which the  $\text{LO}_2$  tank remained at the elevated pressure was 24 s longer than expected.

Table 5. Injection orbital parameters for AC-19 and AC-20

Trajectory measurement	Altitude, <sup>a</sup> km	Perigee altitude, <sup>a</sup> km	Inclination, deg	Eccentricity	Energy, km <sup>2</sup> /s <sup>2</sup>	Angular momentum, km <sup>2</sup> /s
<b>AC-19</b>						
Nominal (engineering)	720.81	111.05	30.983	1.274817	16.88072	76,707.615
JPL tracking	704.08	110.61	31.012	1.274801	16.88085	76,704.781
Guidance (GRT <sup>b</sup> )	705.16	110.73	30.997	1.274891	16.88605	76,706.961
<b>AC-20</b>						
Nominal (engineering)	781.78	90.93	43.369	1.181519	11.1846	75,001.553
JPL tracking	719.76	90.93	43.363	1.181634	11.1913	75,004.619
Guidance (GRT <sup>b</sup> )	720.28	91.03	43.365	1.181525	11.1847	75,002.204

<sup>a</sup>Referenced from a mean equatorial radius.  
<sup>b</sup>GRT = guidance reconstructed trajectory program.

Telemetry data through more than 2200 s for each of the flights indicated satisfactory performance of the *Atlas* and *Centaur* hydraulic systems.

The *Atlas* and *Centaur* electrical systems satisfactorily supplied ac and dc power to the vehicles throughout the flights. One unexpected dc-current demand was observed during both flights. At spacecraft separation, following the initial current spike at squib firing, the current began to increase rapidly. Following this increase, the thermal relays, which protect against short circuit damage or excessive current demands, began to open. The plot shown in Fig. 2 is typical of the current demand experienced on both flights. Similar transients were also discovered on reexamination of AC-16 flight data.

#### D. Telemetry, Tracking, and Range Safety Command

The *Atlas* and *Centaur* instrumentation and telemetry systems functioned well on both vehicles, and there were very few measurement anomalies. A total of 106 *Atlas* and 158 *Centaur* measurements were telemetered on each flight. Continuous *Atlas/Centaur* data (with the usual short dropout at booster jettison) were obtained until well beyond spacecraft separation (2250 s for AC-20 and 2230 s for AC-19).

The *Centaur* C-band tracking beacon operation was not completely satisfactory for either flight. Evaluation of the systems can only be made on the basis of received tracking data and station operator logs, since the airborne system is not instrumented. The AC-20 received signal

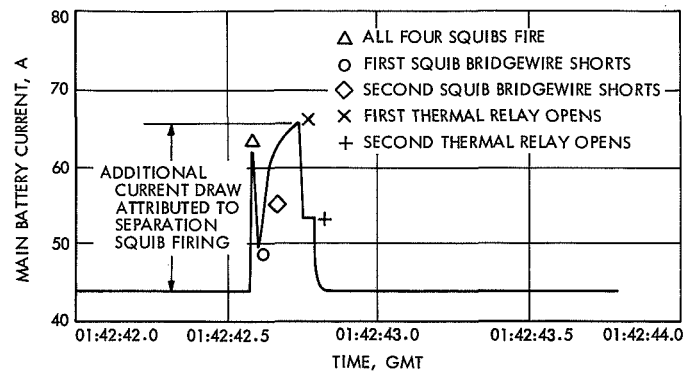


Fig. 2. *Centaur* (AC-20) main battery current at spacecraft separation

strength indicated normal operation of the C-band system until 691 s. At that time, the received signal strength became very erratic with subsequent occasional excursions to the noise threshold. The AC-19 received signal strength was observed to decrease at 759 s and subsequently the signal level was lower than expected at all stations. The signal decreases of these two flights appear to be similar to a step decrease observed on the AC-6 flight; an investigation at that time concluded there was a partial failure in the beacon itself. Final track was lost on AC-20 by Pretoria station at 5425 s, and on AC-19 by Ascension station at 5513 s.

Analysis of flight data indicated satisfactory operation of the *Atlas* and *Centaur* range safety command systems for both AC-20 and AC-19. At 746 s for AC-20 and 717 s for AC-19, the RF disable command was sent by the

Antigua transmitter, removing vehicle power from the range safety command system and terminating system operation.

#### E. Vehicle Loads and Environment

Vehicle loads and thermal environments were within expected ranges throughout both flights. Maximum axial accelerations at selected times are shown in Table 6. The 6-Hz longitudinal liftoff oscillations were normal, reaching maximums (peak to peak) at 0.52 g at 0.6 s for AC-20 and 0.62 g at 0.5 s for AC-19. In either case, the oscillations were essentially damped out by 25 s.

**Table 6. Peak axial accelerations**

Time	Acceleration, g	
	AC-20	AC-19
BECO	5.35	5.71
Sustainer phase	1.93	1.90
MECO	5.99	5.61–5.68

For each flight, the three high-frequency accelerometers located on the forward adapter and on the spacecraft to monitor the inflight vibration environment provided satisfactory data, indicating expected steady-state vibration levels. The vibration environment experienced by the spacecraft is discussed under Spacecraft Dynamic Environment, also in Part 2 of this volume. During the launch sequence and immediately following BECO and staging, two of the high-frequency measurements exhibited data bias level shifts on both flights; however, intelligence was recovered during these periods of instability.

The maximum steady-state vibrational levels experienced during the launch sequence reached 0.7–0.9 g rms for AC-19 and 0.9–1.1 g rms for AC-20. Predominant frequencies on all three accelerometer measurements were between 100 and 120 Hz and 220 and 300 Hz for AC-19 and AC-20, respectively. The pressure environment within the spacecraft compartment decreased to essentially zero psia by 130 s into each flight. For AC-20, the ambient temperature in the spacecraft compartment was 66°F at liftoff, decreasing to the lower intelligence band limit (60°F) by 46 s as a result of gas expansion within the nose fairing as the vehicle ascended. The AC-19 liftoff temperature was 63°F, decreasing to the lower intelligence band limit by 42 s.

#### F. Separation and Retromaneuver Systems for Both Flights

All vehicle separation systems functioned normally. Booster section jettison occurred as planned; resulting vehicle rates and high-frequency accelerometer data were comparable to those of previous flights.

Satisfactory insulation panel jettison was confirmed by normal transient effects on vehicle rates, axial acceleration, vibration, etc. The time of 35-deg rotation, derived from the breakwire instrumentation, was approximately 193 s, which is consistent with times determined on previous flights.

Normal separation of the nose fairing was verified by indications of a 3-deg rotation from disconnect wires which are incorporated in the pullaway electrical connectors of each fairing half. The spacecraft compartment pressure remained at zero throughout nose fairing jettison, with no pressure surge at thruster bottle discharge.

*Atlas/Centaur* separation occurred as planned. Displacement data obtained with respect to time is in close agreement with expected values and indicates successful *Atlas* retrorocket operation. There was no indication of contact between stages when the *Atlas* cleared the *Centaur* in either flight.

Spacecraft separation occurred successfully in both cases. The magnitude of the *Centaur* rates following separation also indicates a smooth, well-controlled separation.

All phases of the *Centaur* retromaneuver were executed as planned for both flights. Following spacecraft separation, both *Centaur* vehicles remained aligned to the pre-separation vector for approximately 271 s; only the attitude control motors remained on so as to increase the separation distance before beginning the turning maneuver to reach the retrovector. The turning maneuver required about 59 s, and was complete about 36 s prior to the start of the lateral thrust phase. Thrusting by the *Centaur* vernier engines increased the lateral separation from the spacecraft to insure that propellant blowdown through the main engines would not contaminate the spacecraft. Propellant blowdown (retrothrust) began about 755 s after spacecraft separation when the separation distance had increased to about 10,000 ft. The programmer was stopped 54 s after the start of blowdown, and the vehicles remained in the blowdown configuration until main battery depletion.



# Spacecraft Dynamic Environment

## I. Summary of Flight Dynamic Environment

This summary includes: (1) a brief description of dynamic environment encountered by each spacecraft during the launch phase, and (2) the pertinent information relevant to separation plane environments as compared to ground test results. Flight data indicated, in general, that the launch environment was well covered by the system-level ground tests.

### A. Random Vibration Environment

Accelerometer locations and characteristics used to obtain the separation-plane environmental data are shown in Fig. 1 and Tables 1 and 2. Figures 2 and 3 show the acceleration power spectral density analysis in  $\frac{1}{3}$ -octave

band resolution for the separation plane flight acceleration during liftoff; in addition, the figures show the acceleration power spectral density materializing during ground tests at the same measurement location.

The data indicate that ground test levels at the measurement location were well above the flight environment in the higher frequency range (above about 70 Hz). Below 70 Hz, however, the flight environment appears to have exceeded the ground test exposure. The higher flight level in the lower frequency range is believed to have been caused by total launch vehicle response to the external liftoff acoustic field in which the bulk of the low-frequency content was transmitted to the spacecraft mechanically through the adapter.

Table 1. High-frequency accelerometer characteristics

Centaur measurement No.	Location		Measurement range, g	Frequency response, kHz	Direction or sensitivity
	Structure	Quad			
CY124O	JPL spacecraft adapter	I	$\pm 30$	2	z-axis
CY125O	Forward end of spacecraft bus structure	I	$\pm 20$	2	z-axis
CY126O	Spacecraft scan platform	IV	$\pm 20$	2	z-axis

Table 2. Low-frequency accelerometer characteristics

Centaur measurement No.	Location		Measurement range, g	Resonant frequency, Hz	Direction or sensitivity
	From x-axis, deg	Quad			
CA677A	315	IV	-2 to +8	250	Longitudinal
CA678A	135	II	-2 to +8	250	Longitudinal
CA679A	45	I	-2 to +8	250	Longitudinal
CA680A	225	III	$\pm 1$	100	Tangential
CA681A	135	II	$\pm 1$	100	Tangential
CA682A	315	IV	$\pm 1$	100	Tangential

Other sources of low-frequency energy are attributed to the existence of low-frequency transients affected by the latch release during liftoff; nevertheless, the liftoff transient environment is well covered by the low-frequency system sinusoidal vibration tests. The transient low-frequency content of the acceleration time history was not separable when performing stationary random vibration power spectrum density analyses.

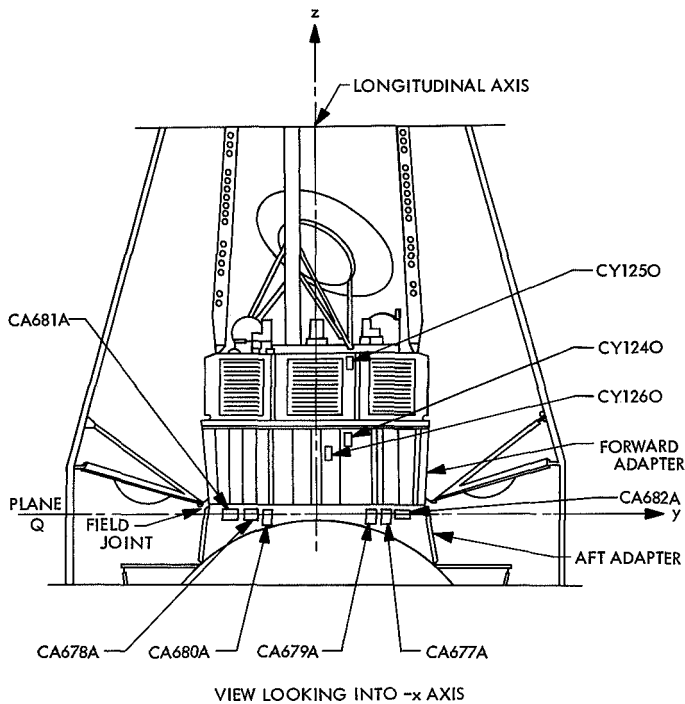


Fig. 1. Accelerometer locations

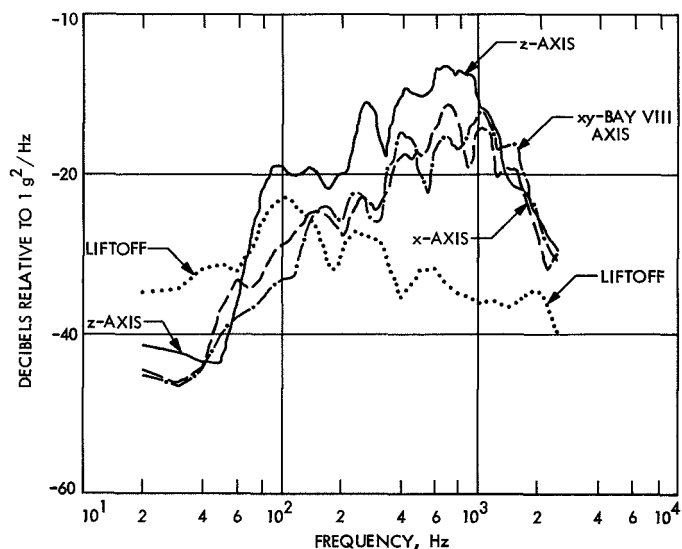


Fig. 2. Mariner VI random vibration flight response during liftoff vs system ground test response

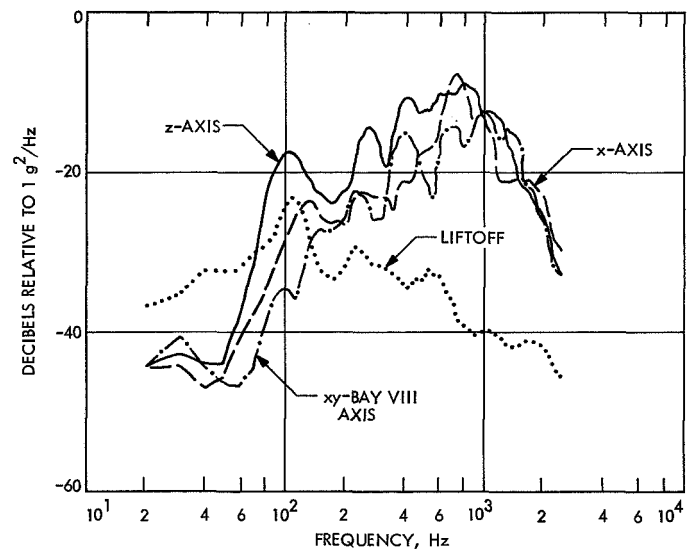


Fig. 3. Mariner VII random vibration flight response during liftoff vs system ground test response

## B. Transient Dynamic Environments

Figures 4 and 5 show the shock spectra of the acceleration measurements made during the events of insulation panel jettison, shroud separation, and *Atlas/Centaur* separation at the adapter flight measurement location. In comparison to the flight environment, and within the limitations of shock spectra analysis for assessment of severity of transient environments, the ground test shock spectrum equivalent is given. The shock spectra are given for 2.5% damping ratio in all instances. Data

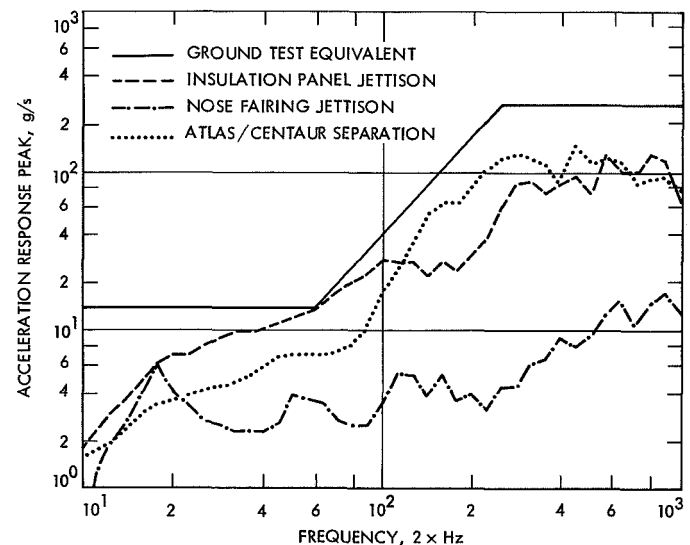
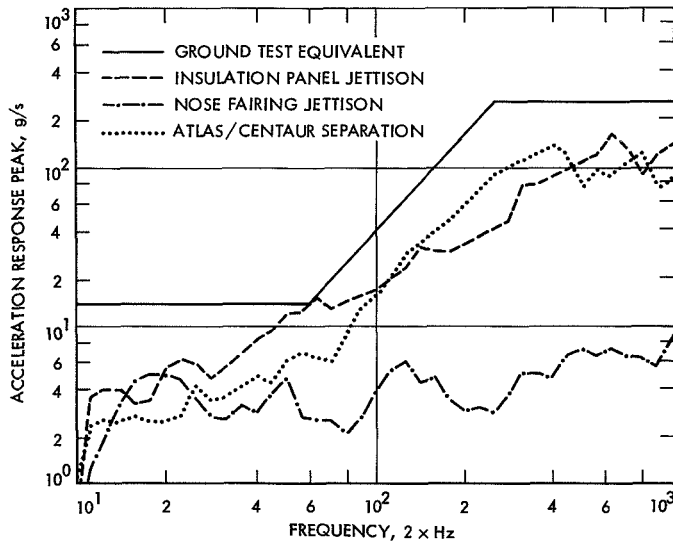


Fig. 4. Mariner VI shock spectra of acceleration measurements during flight events vs ground test equivalent



**Fig. 5. Mariner VII shock spectra of acceleration measurements during flight events vs ground test equivalent**

presented indicate, in general, that test levels were adequate, although slightly conservative in the range from 400 to 2000 Hz.

### C. Flight Anomalies

The most conspicuous flight anomaly indicated by the flight data was the presence of square waves in the time histories of the acceleration measurements at the top of the spacecraft bus and the scan platform. The anomaly was repeated consistently on both flights. A significant effort was made to investigate the anomaly; however, the investigation was closed without result because of the lack of sufficient data.

## II. Mariners VI and VII Low-Frequency Flight Acceleration Measurement

To determine the flight base motion of *Mariners VI* and *VII*, six accelerometers were used on each spacecraft to measure via telemetry the low-frequency (0–100 Hz) response time history at the aft *Centaur*/spacecraft adapter from liftoff to spacecraft separation. The accelerometers were located on the periphery of the adapter in a plane *Q* perpendicular to the longitudinal *z*-axis, 3 in. below the field joint on a radius of 28.15 in. from the *z*-axis (Fig. 6 and Table 2). To determine the motion of plane *Q*, three tangential accelerometers approximately 90 deg apart and three longitudinal accelerometers, also approximately 90 deg apart, were used. The main objective of the measurement was to deter-

mine the three linear accelerations  $\ddot{X}_0$ ,  $\ddot{Y}_0$ , and  $\ddot{Z}_0$ , of the center 0 of plane *Q* and the three rotational accelerations  $\ddot{\theta}_x$ ,  $\ddot{\theta}_y$ , and  $\ddot{\theta}_z$ , about the *x*, *y*, and *z* coordinates through center 0 (Fig. 7) from the six linear accelerations measured by the three tangential accelerometers and the three longitudinal accelerometers.

The purpose of the measurement was twofold: (1) to provide data to be used to determine the vibration specifications of future spacecraft, and (2) to provide an input to a computer program in an effort to define the loads that caused the measured acceleration vs forces. These loads can then be used to predict the response of future spacecraft that use the same booster or second stage.

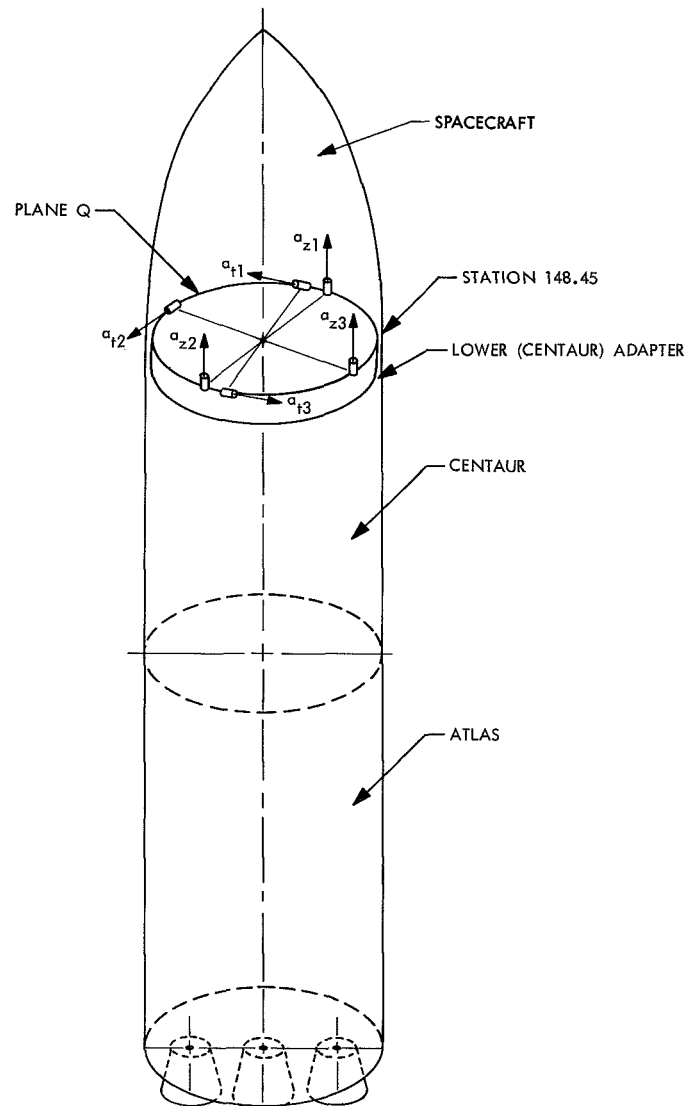


**Fig. 6. Low-frequency accelerometer measurements**

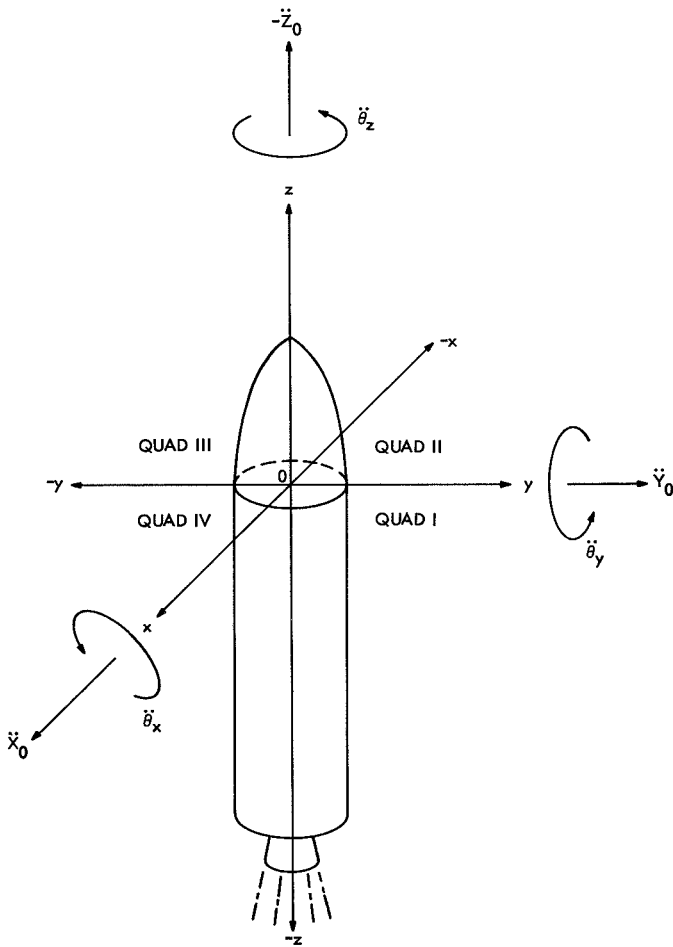


Fig. 7. Low-frequency acceleration coordinate system

#### A. Accelerometers

The transducers used to measure the six components of acceleration were Systron Donner servo accelerometers model 4310. Those accelerometers were electrically damped and the nominal sensitivities were  $\pm 1$  g full scale for the tangential accelerometers, and  $-2$  to  $+8$  g full scale for the longitudinal accelerometers. The resonant frequency was nominally 100 Hz for the  $\pm 1$ -g type and 250 Hz for the other type. The accelerometers were mounted on rigid plastic blocks. The electrical outputs of the accelerometers were connected directly to the telemetry inputs.

#### B. Equations of Motion

Term  $a_{t1}$ ,  $a_{t2}$ , and  $a_{t3}$  the three tangential accelerations and  $a_{z1}$ ,  $a_{z2}$ , and  $a_{z3}$  the three longitudinal accelerations.

Assuming the six linearity degrees of freedom  $\ddot{X}_0$ ,  $\ddot{Y}_0$ ,  $\ddot{Z}_0$ ,  $\ddot{\theta}_x$ ,  $\ddot{\theta}_y$ , and  $\ddot{\theta}_z$  of plane Q are related to the  $a_t$  and  $a_z$  expressions by:

$$\ddot{X}_0 = 0.6527 (a_{t3} - a_{t2}) \quad (1)$$

$$\ddot{Y}_0 = 0.7779 (a_{t1} - a_{t2}) \quad (2)$$

$$\ddot{Z}_0 = 0.5 (a_{z1} - a_{z2}) \quad (3)$$

$$\ddot{\theta}_x = 0.02507 a_{z1} + 0.00162 a_{z2} - 0.02669 a_{z3} \quad (4)$$

$$\ddot{\theta}_y = -0.00162 a_{z1} + 0.02507 a_{z2} - 0.02345 a_{z3} \quad (5)$$

$$\ddot{\theta}_z = 0.017762 (a_{t1} + a_{t3}) \quad (6)$$

#### C. Accelerometer Reading Correction

To recover the desired time histories in accordance with Eqs. (1-6), proper amplitude and phase relationships between the measured values of the  $a_t$  and  $a_z$  expressions had to be maintained. Two causes of amplitude and phase errors existed in the measurement of expressions  $a_t$  and  $a_z$  (i.e., the telemetry playback discriminator filters and the accelerometer roll-offs). Concerning the first source of error, special discriminators were used in the playback of the telemetry tape that gave a phase coherence of better than one degree between channels for a frequency range from 0 to 100 Hz. For the second source of error, correcting circuits were built with analog operational amplifiers to correct for amplitude and phase. Fig. 8 shows the playback arrangement.

#### D. Data

Two telemetry tapes were recorded during the powered phases of flight for both *Mariners VI* and *VII*. The first tape, identified as "TEL-4," was recorded at the Cape Kennedy station and contained all the events from time of liftoff to about 9 min into the flight when loss of signal occurred. The second tape, identified as "Antigua," was recorded downrange at the Antigua

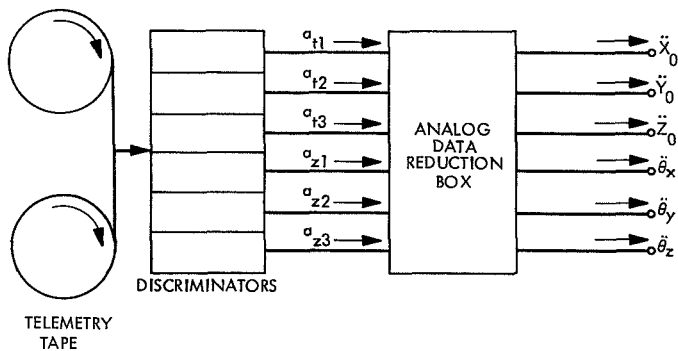


**Fig. 8. Playback arrangement for flight data**

station and contained events from about 9 min into the flight to the end of the powered phase.

The taped tangential and longitudinal acceleration measurements were converted to the desired linear and rotational accelerations through the playback process

described earlier. The resulting traces of acceleration measurements, covering the times of significant events, are shown in Figs. 9 and 10 for *Mariners VI* and *VII*, respectively.

It should be noted that insulation panel jettison and *Atlas/Centaur* separation are particularly strong events and, therefore, some saturation of the signals occurred during these times.

A 12-mode model of the *Mariner* Mars 1969 spacecraft was simulated on an analog computer. The configuration was equivalent to the spacecraft during launch and system-level forced-vibration testing. The mathematical model was subjected to transient-type flight loading obtained from the system described earlier and sinusoidal vibration test levels. The spacecraft response from the different loading conditions was compared with results from the model. In general, the dynamic response resulting from test loading was higher.

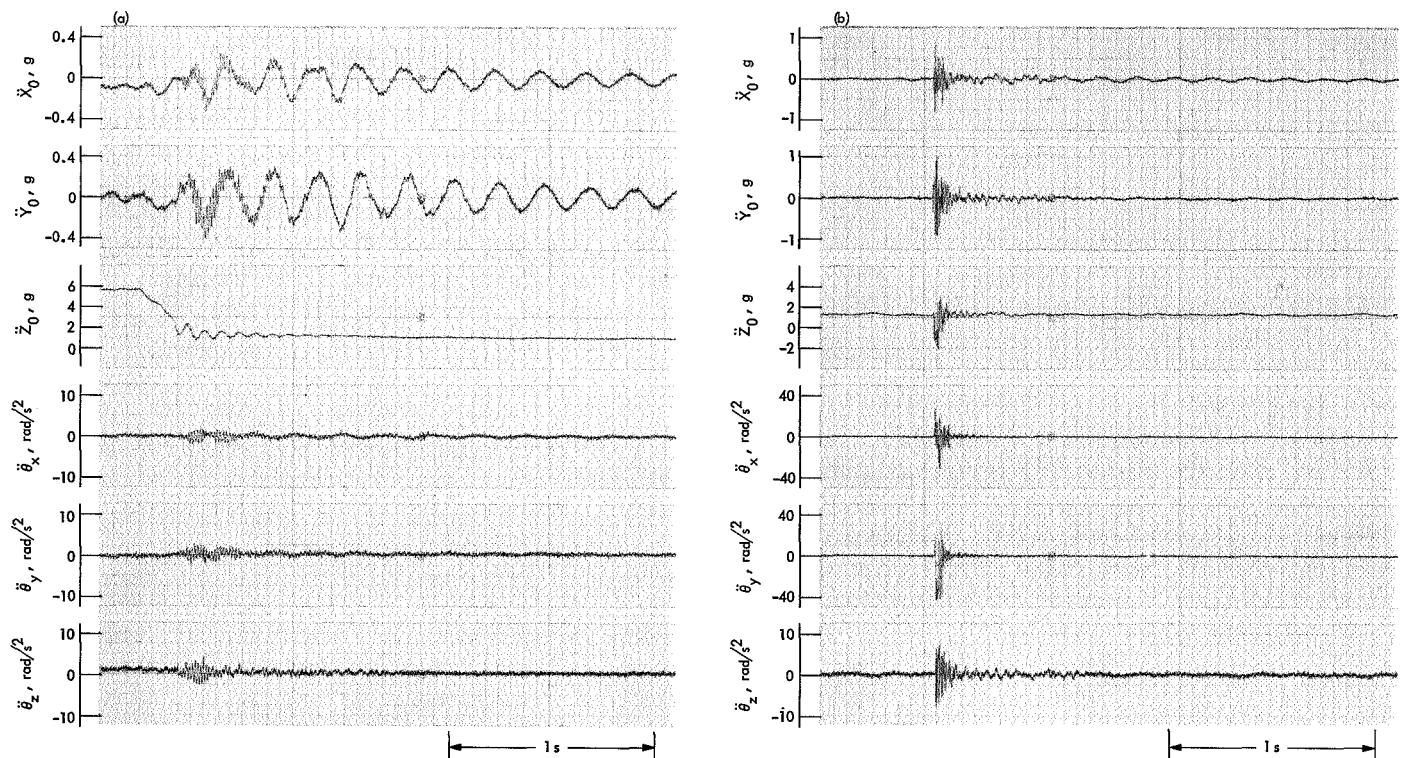


**Fig. 9. Mariner VI (AC-20) acceleration measurements: (a) *Atlas* BECO, (b) insulation panel jettison, (c) nose fairing jettison, (d) *Atlas/Centaur* separation, and (e) *Centaur* MECO**

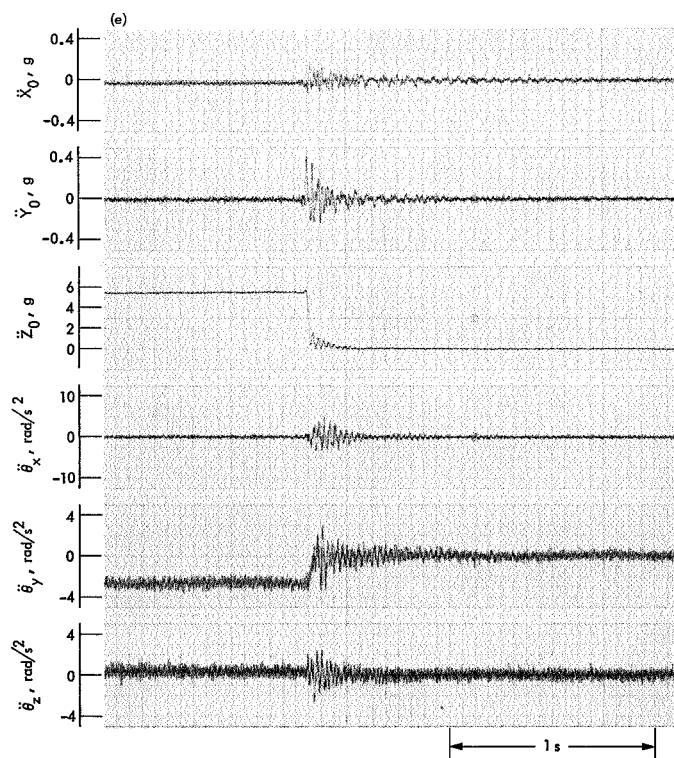
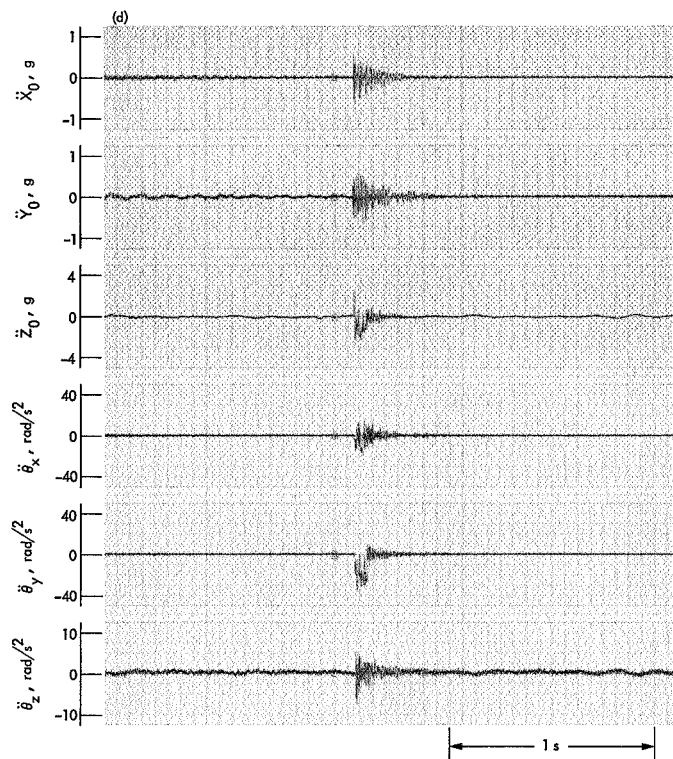
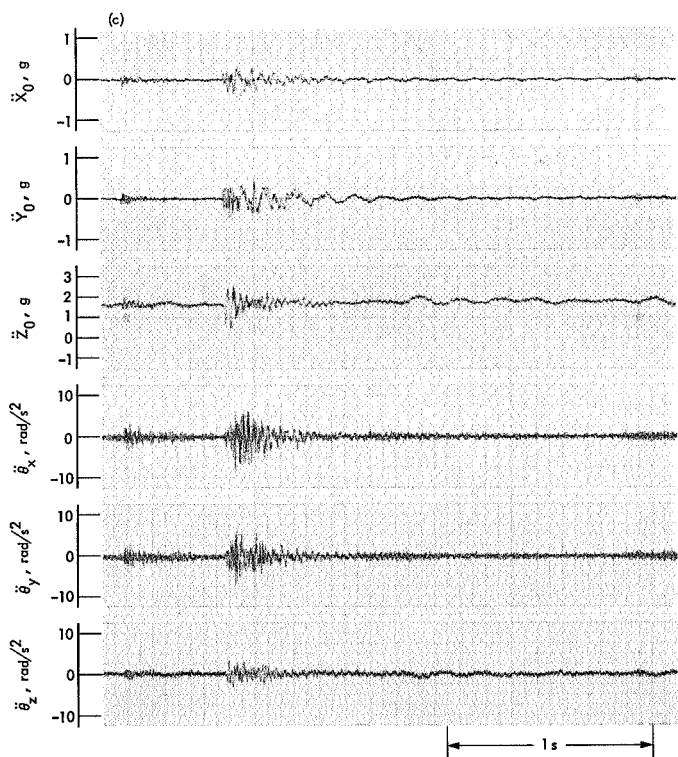
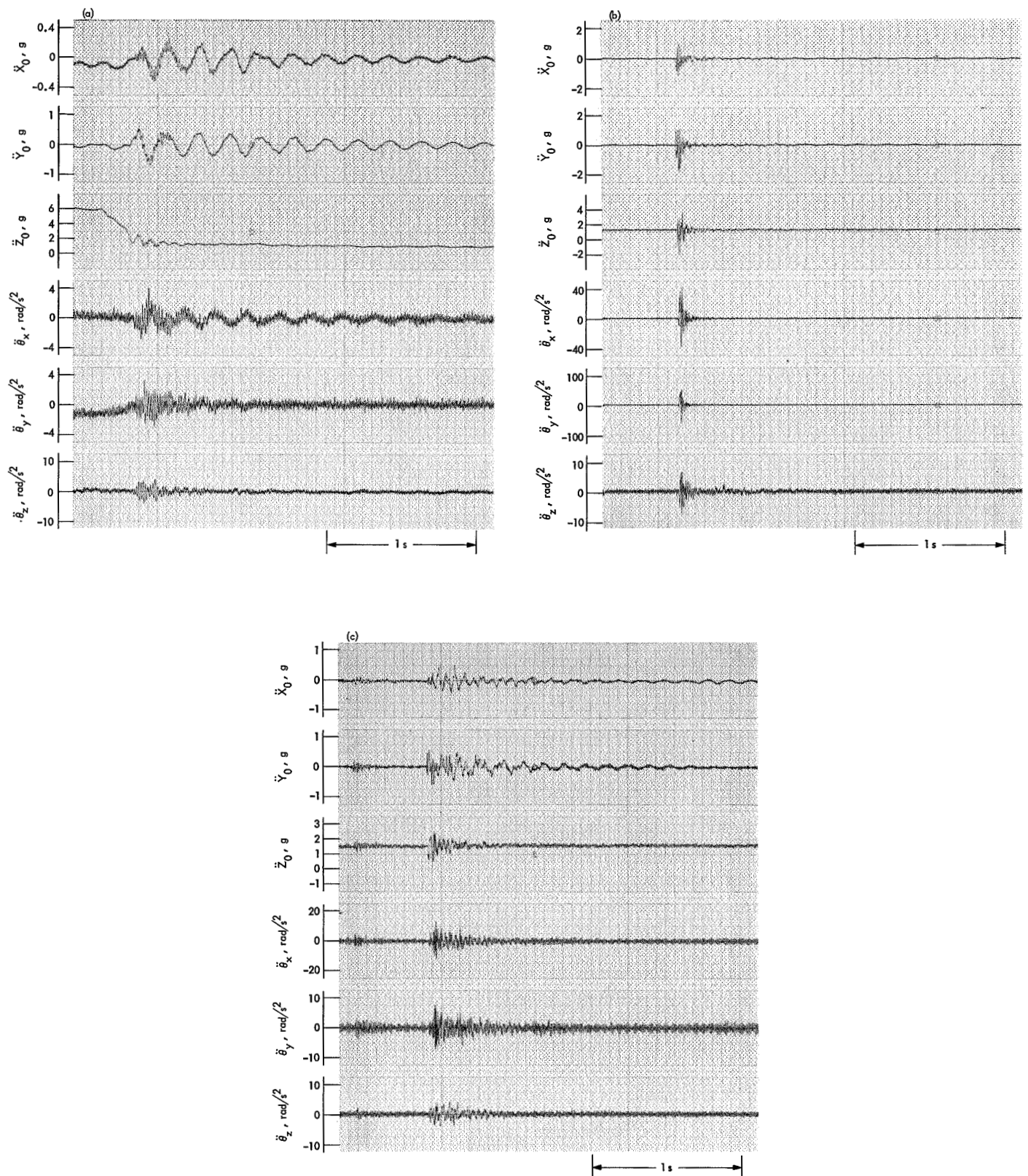


Fig. 9 (contd)



**Fig. 10. Mariner VII (AC-19) acceleration measurements: (a) Atlas BECO, (b) insulation panel jettison, (c) nose fairing jettison, (d) Atlas/Centaur separation, and (e) Centaur MECO**



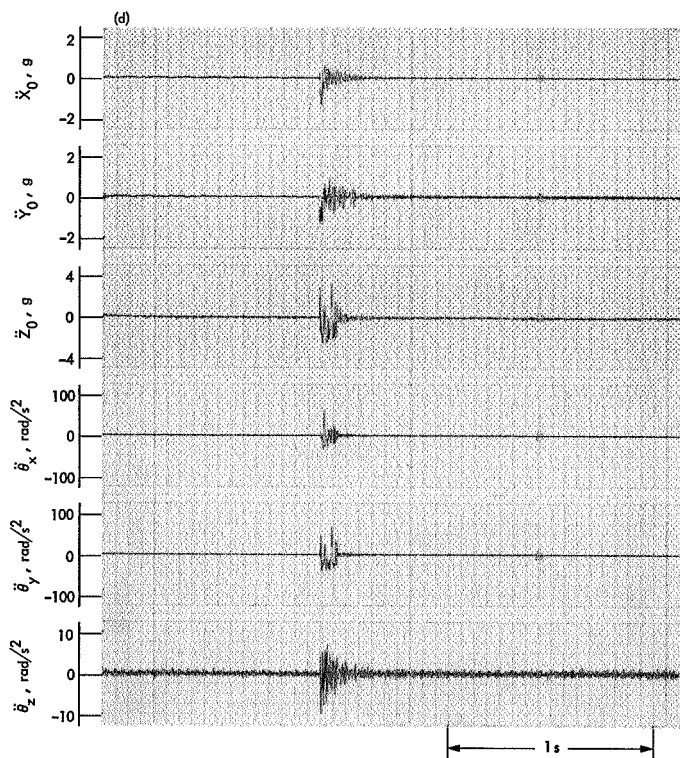
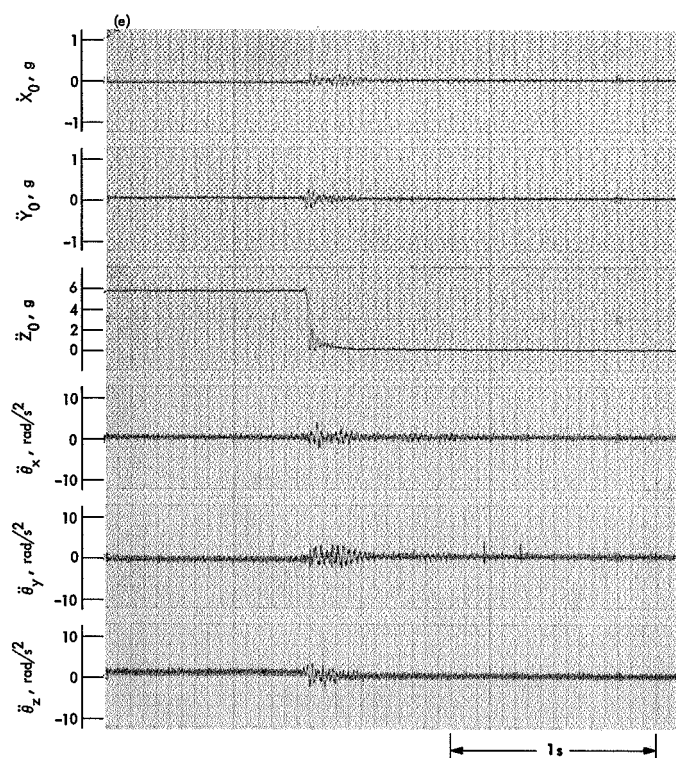


Fig. 10 (contd)









### Part 3. Space Flight Performance



## Spacecraft System Performance

Flight operations were conducted on an essentially continuous basis throughout the *Mariner* Mars 1969 mission for both spacecraft (*Mariners VI* and *VII*). Thus, the performance of each spacecraft is discussed herein in terms of the more significant phases and events, including nonstandard operations; i.e., deviations from expected performance are described chronologically for both *Mariners VI* and *VII*. The discussion includes the launches, trajectory-correction maneuvers, cruise periods, cloud mapping, far- and near-encounters, playback phases, the *Mariner VII* pre-encounter anomaly, and postencounter exercises.

### I. *Mariner VI* Launch

The spacecraft countdown for *Mariner VI* proceeded normally and smoothly on February 25, 1969, to liftoff at 01:29:02.013 GMT. (Unless otherwise noted, all times are given in GMT.) The prelaunch spacecraft events occurred on schedule as follows: (1) data storage subsystem in launch mode at  $T - 00:06:50$  (01:22:10), (2) central computer and sequencer (CC&S) inhibit release at  $T - 00:04:00$  (01:25:00), and (3) CC&S operation verify at  $T - 00:01:00$  (01:28:00). The spacecraft performed normally during the powered-flight phase (see Part 2, Spacecraft Dynamic Environment, for a discussion of the dynamic environment). Spacecraft/*Centaur* separation occurred at 01:42:43 ( $L + 00:13:41$ ).

At separation, the following spacecraft events took place as expected: (1) pyrotechnics subsystem armed, (2) attitude control subsystem turned on, (3) CC&S relay hold off, (4) data storage subsystem in launch terminate mode, and (5) temperature control flux monitor (TCFM) temperature set.

At 01:43:02 ( $L + 00:14:00$ ), the first in an unexpected series of step changes in the low-gain antenna drive occurred; the drive dropped from 44 to 40 in data number (DN). These step changes, each amounting to approximately 0.4 dBmW, were observed again at approximately  $L + 2$ ,  $L + 61$ ,  $L + 63$ , and  $L + 71$  h. The final step change (upward 0.4 dBmW) left the low-gain antenna drive within its prelaunch predicted range.

At 01:45:46 ( $L + 00:16:44$ ), a digital end of tape (DEOT) was observed in the data storage subsystem, which turned off the digital tape recorder (DTR). The DTR made almost four tape passes while in the launch mode. At 01:51:48 ( $L + 00:32:46$ ), an analog end of tape (AEOT) occurred, which turned off the analog tape recorder (ATR). This single AEOT occurred 1 min 37 s later than predicted; this was considered normal, however, because the running time depended upon servo-controlled tape speed, which was determined by the data recorded on the tape. The ATR had made approximately  $\frac{3}{4}$  of a tape pass while in the launch mode. The data

storage subsystem power was turned off on time by the L3 event from the CC&S at 03:24:57 ( $L + 01:56:00$ ).

Approximately at separation + 4 min (01:46:41), the solar panel deployment squibs were fired, and the solar panels were fully deployed 4 s later. The spacecraft emerged from the shadow of the Earth at 01:55:12 ( $L + 00:26:10$ ), and immediately went into a Sun-search maneuver, *Mariner VI* acquired the Sun at 01:58:35 ( $L + 00:29:33$ ). During the launch period, 9 A-h of charge were used from the battery, leaving its state of charge at 82% at the time of Sun acquisition by the solar panels. Battery charging brought the battery up to full charge by the time of the trajectory-correction maneuver, and the battery charger was commanded off at approximately  $L + 97$  h.

As indicated above, the attitude control subsystem had been turned on at *Centaur*/spacecraft separation; however, the Canopus tracker remained off (as designed). At 05:25:01 ( $L + 03:56:00$ ), the CC&S turned on the Canopus tracker. The spacecraft then went into a roll search, which terminated 17 min 19 s later with the acquisition of a star. A good star map was obtained during the roll search, confirming Canopus as the star acquired. Thus, at 05:42:20 ( $L + 04:13:18$ ), the spacecraft was attitude-stabilized, with the Sun and Canopus as reference objects and limit cycles nominal; this completed the launch phase for attitude control.

The CC&S performed normally during the launch phase; all event times occurred as predicted within the uncertainties caused by data sampling.

The radio frequency subsystem (RFS) operated normally during the launch phase, with the following exceptions:

- (1) As noted earlier, several step changes in the low-gain antenna drive occurred, which left the drive within its predicted range at  $L + 3$  days. Operation continued at a stable point thereafter. This problem with fluctuating power levels could have been caused by either an impedance discontinuity in the connectors or RF cabling internal to the RFS, causing reflected power back into the traveling-wave tube amplifier (TWTA) assembly, or by varying conditions within the TWTA producing variable output power.
- (2) With the ranging transponder on, and no uplink, the best-lock frequency, as indicated by the space-

craft static phase error (SPE) and verified by acquisition tests performed by the Deep Space Network (DSN), deviated from the nominal by approximately 7 kHz at S-band frequency.

- (3) There was one occurrence of the RFS being acquired in "false lock" at  $L + 18$  h with the ranging channel on. The false lock was expected with a high probability under the condition of strong uplink signal, which existed in this instance.

The explanation for RFS problems (2) and (3) was that, with the ranging channel energized in the transponder, a spurious feedback path was produced. Intensive analysis and testing of the RFS before launch could not locate the feedback path precisely. However, mission operations were conducted in such a manner as to prevent these problems from having any deleterious effect upon the flight.

## II. *Mariner VI* Trajectory-Correction Maneuver

The trajectory-correction maneuver for *Mariner VI* was initiated at 23:19:44 (Earth-observed time) on February 28, 1969, by a DC-27 ground command, and was successfully completed. Canopus acquisition was maintained until the inertial-control mode was established at the start of the pitch turn. Telemetry during the maneuver sequence verified that all turns were correct, and that the motor burn appeared to be normal.

At 02:00:00 on February 28, 1969, the flight-path analysis and command (FPAC) group communicated to the spacecraft performance analysis and command (SPAC) group the required maneuver parameters:

- (1) Pitch turn =  $-23.33$  deg.
- (2) Roll turn =  $78.68$  deg.
- (3) Motor burn duration =  $5.35$  s ( $\Delta V$  of  $3.06788$  m/s).

Because of the resolution of turns capable of being programmed by the CC&S, the actual maneuver parameters loaded into the CC&S were: 131-s pitch turn (equivalent to  $23.24$  deg), 453-s roll turn (equivalent to  $78.72$  deg), and motor burn duration of  $5.35$  s. The polarities of the pitch and roll turns were negative and positive, respectively.

The maneuver phase formally commenced at 20:00:00 on February 28, 1969, when the maneuver parameters

were sent to the spacecraft computer and to the fixed sequencer, and were verified. The spacecraft state at this time is shown in Table 1.

**Table 1. Mariner VI spacecraft state at midcourse**

Parameter <sup>a</sup>	State
Science power	Off
RFS lock status	In lock
TWTA mode	Low power
Power amplifier	2
Exciter	2
Transmitting antenna	Low gain
Ranging channel	On
Bit rate	33 1/3 bits/s
FTS mode	Cruise
FTS chain	A
Command lock status	In lock
Data storage power	Off
Power source	Solar array
Battery charger	On
Power chain	Main
Acquisition state	Sun and Canopus acquired
Gyros	Off
Canopus sensor cone position	2
Canopus sensor gate setting	1
Scan platform latch status	Latched
CC&S mode	Tandem standby
Propulsion pressure status	Normal

<sup>a</sup>RFS = radio frequency subsystem, TWTA = traveling-wave tube amplifier, FTS = flight telemetry subsystem, CC&S = central computer and sequencer.

Next, at 22:10:00, a DC-9 command was sent to the spacecraft to turn off the ranging channel, improving telecommunication performance by approximately 1 dB. The maneuver-enable command DC-14 was next transmitted at 22:20:00; this command was used to ensure that the attitude control and pyrotechnic subsystems were enabled to receive maneuver events from the CC&S. Finally, the maneuver start command DC-27 was transmitted at 23:18:39, which initiated a tandem maneuver that used outputs from both the computer and the fixed sequencer. The sequence of events during the maneuver is given in Part 1, Mission Summary.

The performance of the trajectory-correction maneuver was nominal, with a 3.068-m/s velocity change imparted to the spacecraft. *Mariner VI* had not pitched far enough off the Sun line to interrupt the solar power mode. During and after the motor burn, the Canopus sensor, which remained on (but not in the control loop) throughout the maneuver, detected brightness sources; these were

thought to be either dispersed rocket-exhaust gases or dust particles dislodged from the spacecraft.

The maneuver phase was concluded at 01:45:00 with the transmission of three CC-4 commands to the CC&S fixed sequencer; these commands contained minimum pitch, minimum motor burn, and infinite roll parameters. This precaution was taken to ensure that an inadvertent maneuver would not produce a motor burn.

### III. Mariner VI Scan-Platform Unlatch

Before the launch of *Mariner VI*, the scan platform had been locked in place in its stowed position (225 deg in clock, 96 deg in cone) by the latching mechanism that secured the scan platform to its supporting structure. The CC&S had also been programmed before launch to issue a C5 event to unlatch the scan platform at  $L + 34$  days (March 31, 1969), thus allowing time for a delayed maneuver. However, project management decided to unlatch the scan platform by ground command on March 6 ( $L + 9$  days) because a successful midcourse maneuver had already been accomplished and the need for a second maneuver was highly unlikely; furthermore, it was desired to verify the function and temperature effects of scan-platform unlatching well before the second *Mariner* launch (*Mariner VII*).

At 19:10:34 on March 6, the scan-unlatch command DC-45 was transmitted to the spacecraft; at 19:11:47, the command was confirmed in SPAC as having fired the pyrotechnics squib that opened the valve to cause the unlatch to begin. The scan-platform unlatching process took longer than expected. The platform latch gas pressure, sampled 15 s after the DC-45 command was received, was 701 psia instead of the expected 407 psia. As evidenced by a counter 4 event, the actual time of platform release was 249 s (4 min 9 s) after the DC-45 command, or 160 to 170 s longer than the prediction based on the actual latch pressure reading at DC-45 + 15 s. The anomaly was thought to be caused by clogging of the porous metal restrictor in the vent from pyrotechnics blowdown debris. Because the restrictor is a porous plug, it was believed that it could not have completely sealed itself.

Shortly after the DC-45 command was received by the spacecraft, the Canopus sensor detected bright particles in its field of view and the sensor lost Canopus lock. The spacecraft automatically went into roll search upon losing the star reference, and completed a 360-deg rotation

before regaining Canopus acquisition. This scan-unlatch/attitude control interaction was totally unexpected. Theories advanced have generally ascribed the interaction to a "dirty" spacecraft. The cause of the particles leaving the spacecraft and appearing in the Canopus sensor field of view was thought to be either pyrotechnics shock or a scouring of the lower thermal shield by scan latch gas-plume impingement. Whereas the loss of Canopus lock and the subsequent roll search during the scan-platform unlatching process was a surprise and an annoyance, a loss of Canopus lock caused by infrared spectrometer (IRS) cooldown just before near-encounter would have been catastrophic to the objectives of the mission. The dividends yielded by the scan-unlatching exercise were, therefore, a modification of the near-encounter strategy whereby the spacecraft would be placed on inertial hold (gyros on) shortly before the time of IRS cooldown. This method was successfully tried during the *Mariner VII* scan-platform unlatch, and proved to be the correct solution to a potentially disastrous problem.

Before unlatch, the scan-platform temperatures averaged 7.7°F higher than predicted, whereas the average bus temperature was 2°F lower than expected. It was later shown that this difference was caused by the thermal path provided between the latched platform and the bus because, after scan unlatch, the spacecraft temperatures had stabilized at their predicted levels; that is, the average bus temperature rose about 1.5°F and the platform temperatures fell about 6°F.

The impact of scan unlatching on the trajectory of *Mariner VI* to Mars was to perturb it slightly. The trajectory effect of unlatching the scan platform was to move the closest approach point about 100 mi closer to the planet.

#### IV. *Mariner VII* Launch

The prelaunch countdown for *Mariner VII* proceeded normally on March 27, 1969, until less than 1 min ( $L - 56$  s) before the scheduled launch, when the *Centaur* guidance acquisition could not be obtained. Launch was then held until the problem was resolved. The countdown was resumed at  $T - 10$  min, and liftoff occurred 47 min into the launch window. The prelaunch spacecraft events occurred on schedule as follows: (1) data storage subsystem in launch mode at  $T - 00:06:50$  (22:15:13), (2) CC&S inhibit release at  $T - 00:04:00$  (22:18:01), and (3) CC&S operation verify at  $T - 00:01:00$  (22:21:01).

Liftoff occurred at 22:22:01.198 on March 27, 1969, on a launch azimuth of 102.79 deg. *Mariner VII* injection appeared to be as accurate as had been that of *Mariner VI*. During the boost phase, the low-gain antenna drive was indicated at 3 dB lower than expected; however, at separation, it returned to its normal value. Spacecraft/*Centaur* separation occurred at 22:35:28 ( $L + 00:13:27$ ), and the following spacecraft events took place as expected: (1) pyrotechnic subsystem armed, (2) attitude control subsystem turned on, (3) CC&S relay hold off, (4) data storage subsystem in launch terminate mode, and (5) TCFM temperature set.

At separation, the CC&S appeared to go into the programmed readout mode, but the flight telemetry subsystem (FTS) did not transmit the memory data to the Earth, and remained in the engineering telemetry mode. The CC&S had responded to an electrical power transient that had caused unrequested readout of memory without the telemetry being set to receive the readout; this was evidenced by the number and frequency of event register 2 changes. It was believed that, at spacecraft/launch vehicle separation, an electrical transient caused flag 9 in the CC&S to be set, which then caused the readout. All readings returned to normal after the readout, and the CC&S subsequently issued the internal commands programmed on time. At 17:31:00 on April 1 ( $L + 5$  days), a coded command pair was transmitted to the spacecraft to check the remaining CC&S flags (1, 4, 5, and 7). At 17:48:18, just after the coded command pair was received, a DC-2 CC&S memory readout found that at least one flag was set. The CC&S performed normally during the launch phase of *Mariner VII* except for the unexpected internal-memory readout that occurred at spacecraft/launch vehicle separation.

At 22:35:48 ( $L + 00:13:47$ ), a DEOT was observed in the data storage subsystem, which turned off the DTR. The DTR had made more than three tape passes while in the launch mode. At 23:17:01 ( $L + 00:55:00$ ), an AEOT occurred on time, which turned off the ATR. The ATR had made about 1.4 complete tape passes while in the launch mode. Power to the data storage subsystem was turned off on time by the L3 event from the CC&S at 00:18:00 ( $L + 01:56:00$ ).

An unexpected power profile occurred when the launch vehicle separated from the spacecraft. The Canopus sensor Sun shutter closed, causing an additional 6.5 W of power demand. At the same time, the pitch and yaw gyros were in saturation, drawing an additional 2.4 W

of power. At the time of solar panel deployment, an unexpected 11-W power spike was observed; this was caused by the pitch gyro being in saturation and three sets of gas jets firing simultaneously. The solar panels were deployed at 22:39:22 ( $L + 00:17:22$ ), approximately 4 min after separation, and they were first illuminated by the Sun at 23:12:45 ( $L + 00:50:44$ ) when the spacecraft exited from the shadow of the Earth. The spacecraft acquired the Sun at 23:14:33 ( $L + 00:52:32$ ); the solar panels reached thermal equilibrium about 1.5 h later, with an array performance about 2% higher than expected.

The spacecraft battery had a full charge when *Mariner VII* was put on internal power during the count-down. The total power drawn from the battery was 10.6 A-h over a period of 60 min 12 s (through Sun acquisition). The spacecraft, which had been launched with its battery charger on, then began to charge the battery at the full rate of 650 mA. The battery charger, having brought the battery up to 95% of full charge, was commanded off by a DC-38 command at 18:46:34 on April 4 ( $L + 8$  days).

The gyros were on at launch, and the attitude control subsystem performed normally until just before separation, when the Canopus sensor shutter closed as the launch vehicle oriented the sensor toward the Sun. The shutter reopened after separation, and the Sun sensors came on as expected. The Canopus sensor was turned on by CC&S event L2 at 02:18:00 on March 28 ( $L + 03:56:00$ ); at 02:23:57 ( $L + 04:01:56$ ), an object identified as the star Vega was acquired. The acquisition of Vega rather than Canopus was attributed to a known warm-up characteristic of the Canopus sensor. Vega has an intensity 0.55 times that of Canopus, so it is equally probable that the sensor would not have locked onto Vega when it first came into its field of view. The DC-21 command to continue the roll search toward Canopus was not sent because of the conflicting inputs as to the identity of the acquired object, and a possible violation of the low-gate dropout level. The gyros went off 3 min after the acquisition of Vega at 02:26:57 ( $L + 04:04:56$ ), and limit-cycle activity became normal.

After considerable analysis by SPAC, project management decided that the star Canopus should be acquired as the second celestial reference (the Sun being the first) to replace Vega. Therefore, at 16:45:00 on April 1 ( $\sim L + 5$  days), a DC-21 ground command was trans-

mitted to the spacecraft. The command caused the Canopus sensor to break Vega lock and go into a roll search for Canopus. At 16:57:03, after a roll search of 10 min, Canopus was acquired by the sensor, and the gyros turned off 3 min later. Limit cycling continued normally thereafter.

The radio frequency subsystem behaved normally following spacecraft/launch vehicle separation. However, during the period between launch and separation, the low-gain antenna drive unexpectedly changed erratically, indicating RF output power fluctuations up to 3 dB. The spacecraft telemetry indicated an RF decrease of about 2.6 dB shortly after *Centaur* main engine start and an increase of 2.4 dB shortly after separation. The Antigua tracking station recorded a 3-dB increase in the received RF power at separation. At the same time, the base temperature of TWTA 2 (the power amplifier in use) rose 3°F, although it was expected that the TWTA base temperature would drop at this time. However, ground tests validated that, if approximately 5 W of lost RF output power were reflected back into the TWTA, the TWTA base temperature would rise about 3°F.

As a result of this RFS deviation, the spacecraft ranging channel was not turned on until April 1 ( $L + 5$  days) with a DC-9 command at 19:56:06. Ranging performance thereafter was normal. Automatic gain control (AGC) and SPE variation tests were made with ranging on and off and with the spacecraft receiver in and out of lock. No unexpected results occurred in this testing.

## V. *Mariner VII* Trajectory-Correction Maneuver

The trajectory-correction maneuver for *Mariner VII* was initiated at 18:52:38 (Earth-observed time) on April 8 by the DC-27 ground command, and was successfully completed. The star Sirius was used as the roll-reference object instead of Canopus, and the acquisition of Sirius by the sensor was maintained until the inertial-control mode was established at the start of the pitch turn. Telemetry during the maneuver sequence verified that all turns were correct, and that the motor burn appeared to be normal.

Early iterations of the maneuver by FPAC disclosed that the pitch angle off the Sun line was about 68 deg and the roll turn about -62 deg. The final iteration of maneuver turns on April 4 determined that a pitch turn



of 69.49 deg and a roll turn of  $-62.22$  deg were required. These parameters were based on use of the Sun and Canopus as reference objects at the start of the maneuver. However, these maneuver turns would have produced two conditions in the spacecraft having elements of risk:

- (1) Starting the maneuver from Canopus would have brought the field of view of the Canopus sensor close enough to the Sun during the turns to actuate the Sun shutter (as happened during the launch phase), thereby blocking off the sensor to protect it.
- (2) The large pitch angle off the Sun line would have reduced the power available from the solar array to a point at which it could not support the power demand, and would have required the use of the spacecraft battery in a share mode.

Although neither of these conditions per se was dangerous, they would have introduced undesirable risks too early in the mission. For example, if the Canopus Sun shutter were successfully actuated to close, but failed to reopen at the end of the maneuver, the Canopus sensor would have been rendered useless for the remainder of the mission. Such a failure would have meant the loss of the roll reference, necessitating that the gyros be kept on. Also, a new encounter strategy would have been needed to meet this degraded condition.

To preclude the risks associated with a maneuver off Canopus, project management decided to perform the required thrust-vector pointing with the star Sirius as the roll reference. The midcourse maneuver conference on April 7, 1969, ratified this decision, and FPAC proceeded to determine the final maneuver parameters required to achieve the selected *Mariner VII* aiming point at Mars with Sirius as the roll reference. At 02:00:00 on April 7, FPAC communicated to SPAC the required maneuver parameters, which were as follows:

- (1) Pitch turn =  $-35.64$  deg.
- (2) Roll turn =  $12.83$  deg.
- (3) Motor burn duration =  $7.6$  s ( $\Delta V$  of  $4.292$  m/s).

The maneuver phase formally commenced at 15:45:00 on April 8 with the transmission of the DC-21 command to the spacecraft (roll off Canopus and onto Sirius). At 15:46:25 (Earth-observed time), the DC-21 command was received; breaking Canopus lock, the spacecraft rolled for 1 min 45 s and acquired Sirius at 15:48:11. The gyros turned off 3 min later. The spacecraft state at this time is shown in Table 2.

**Table 2. *Mariner VII* spacecraft state at midcourse**

Parameter <sup>a</sup>	State
Science power	Off
RFS lock status	In lock
TWTA mode	Low power
Power amplifier	2
Exciter	1
Transmitting antenna	Low gain
Ranging channel	On
Bit rate	$33 \frac{1}{2}$ bits/s
FTS mode	Cruise
FTS chain	A
Command lock status	In lock
Data storage power	Off
Power source	Solar array
Battery charger	Off
Power chain	Main
Acquisition state	Sun and Sirius acquired
Gyros	Off
Canopus sensor cone position	3
Canopus sensor gate setting	1
Scan platform latch status	Latched
CC&S mode	Tandem standby
Propulsion pressure status	Normal

<sup>a</sup>RFS = radio frequency subsystem, TWTA = traveling-wave tube amplifier, FTS = flight telemetry subsystem, CC&S = central computer and sequencer.

At 16:30:00, the transmission of 20 coded commands commenced for the purpose of loading the CC&S memory with the maneuver parameters. After this transmission, a DC-2 command at 17:00:00 produced a CC&S memory readout. The readout indicated that all coded commands had loaded the spacecraft memory with the correct parameters. Next, the Y1 event (radio test cyclic) from the CC&S to the RFS was received at 17:18:21, which turned the ranging channel off. As with *Mariner VI*, it was desirable to have the ranging channel off to assure maximum telecommunications performance during the maneuver. The maneuver-enable command DC-14 was next transmitted, at 18:25:00, to ensure that the attitude control and pyrotechnics subsystems were enabled to receive maneuver commands from the CC&S. Finally, the first maneuver-start command DC-27 was transmitted at 18:51:14 to initiate a tandem maneuver.

The trajectory-correction maneuver was performed nominally, and a 4.297-m/s spacecraft velocity change resulted. As expected, the pitch turn did not place the power subsystem in a battery-share mode, nor did the maneuver permit the Canopus Sun shutter to come close enough to the Sun to be activated. The star Vega was acquired by the Canopus sensor, after the automatic

reacquisition signal and roll search were initiated, because it was the first acquirable object to come into the field of view of the sensor. After the maneuver, a DC-21 command was sent at 21:00:00 to roll the spacecraft off the star Vega. An 11-min roll search ensued, and Canopus was acquired at 21:12:35. The gyros turned off 3 min later, and *Mariner VII* went into its cruise phase on a Mars encounter trajectory. Three CC-4 commands were sent at 21:30:00 to load the CC&S fixed sequencer with minimum-pitch, minimum motor-burn, and maximum-roll parameters. The *Mariner VII* spacecraft condition and performance were exactly as expected throughout the trajectory-correction phase.

## VI. First Cruise Period, *Mariners VI and VII*

### A. *Mariner VI*

Because of the bright particles observed in the field of view of the Canopus sensor in conjunction with squib-firing events (e.g., the trajectory-correction maneuvers and the *Mariner VI* scan-platform unlatching), a sequence was designed to place the spacecraft on gyro control just before a squib-firing event at encounter. In this event, the IRS cryostat would be initiated shortly before the planet came into view of the science instruments. If the spacecraft were to lose Canopus and go into a roll search at that time, it would be catastrophic to the objectives of obtaining near-encounter TV pictures and science-instrument scans of the planet.

Consequently, an inertial encounter sequence contained in 28 coded commands was transmitted to *Mariner VI* commencing at 13:00:00 on April 18. This sequence was followed by DC-32 and DC-14 commands to place the spacecraft in the computer-only maneuver mode to enable an automatic inertial encounter sequence at the planet. A DC-2 command (CC&S memory readout) was transmitted at 14:15:00, and verified that the sequence was correctly entered into the CC&S.

Two quantitative commands were sent at 12:00:00 on April 18 to adjust the clock and cone near-encounter reference potentiometers on *Mariner VI*. These adjustments were necessary to accommodate the preprogrammed encounter sequences in the CC&S, and were based on the flyby parameters of the actual trajectory.

A number of anomalies occurred involving the RFS of *Mariner VI*: (1) On April 6, the RFS locked up to the command sideband in uplink. The lockup occurred

when the DSS 51 transmitter came on with command modulation on. Normal acquisition procedures were successful after both the command mode and the station transmitter were turned off. (2) A large fluctuation in local oscillator drive started at 03:37:01 on April 18. This fluctuation was on the order of 1.2 dB. Performance of the RFS was assessed as normal at the time, this surprise notwithstanding. The local oscillator drive stabilized again after April 26. (3) Short-term instability in the auxiliary oscillator of exciter 2 was noted at times during the period between April 9 and June 5. The cause of the instability has not been established; however, the total variation was actually very small, although it showed 8 DN total change in telemetry. While the RFS was locked to the command sideband, the flight command subsystem (FCS) indicated *in lock*. It was shown in ground testing that the spare spacecraft behaved similarly under the same unusual circumstances.

### B. *Mariner VII*

The first cruise period of *Mariner VII* was highlighted by the unlatching of the scan platform, a Canopus cone angle change, updating of the CC&S encounter program parameters, loading of the all-axis-inertial sequence at encounter, and the discovery of a degraded receiver. All elements of the spacecraft system worked together, with results well within the predictions of the analysts. All FCS commands were properly received by the various subsystems, as were the CC&S commands. The FTS faithfully responded to all inputs, including CC&S memory readouts. The only concern was with the performance of the receiver.

The *Mariner VII* RFS appeared to be degraded during this cruise period. No difficulties were experienced with the exciter or TWTA, but receiver performance was below the expected level.

After the daily Y1 event, the ranging channel was turned on each day from April 10 to 17, and then again from April 20 to 24. Between April 16 and 21, the ranging channel reached the Mark I ranging threshold at a time when a 9-dB margin should have existed. Subsequent measurements were continued with the spacecraft receiver ranging channel. Ranging remained off following the Y1 event on April 25.

On April 24 at 19:13, the spacecraft receiver lost phase lock with the uplink carrier for no apparent reason.

On April 25, the spacecraft receiver AGC varied  $\pm 1$  DN with ranging modulation applied. Also, when changing from full ranging code to clock code only, the AGC indicated a 1.2-dB (1-DN) increase in signal strength. These changes represented either a previously unknown characteristic of the ranging code or an unanticipated and previously unobserved characteristic of the receiver. On May 8, a test was conducted to look for AGC fluctuations with ranging and command modulation applied. Only one toggle of the AGC channel was seen.

## VII. *Mariner VI* Canopus Cone Angle Anomaly and Magellanic Cloud Mapping

On April 20, a C1 event was programmed for issuance by the CC&S in *Mariner VI* to step the Canopus cone angle (CCA) in the Canopus tracker. It was necessary to update the CCA periodically to prevent the star Canopus from passing out of the field of view of the tracker. The C1 command was issued on time from the CC&S, but the update circuits failed to respond correctly. Instead of advancing from position 3 to 4, as expected, the cone angle anomalously switched to position 2. The next reading of channel 108 (Canopus intensity) at 22:26:43.6 indicated black space instead of the normal Canopus-acquired value. The loss of Canopus from the field of view of the Canopus tracker caused the gyros to turn on, and a roll search was initiated. An anomaly conference was held immediately, and it was agreed that ground commands should be used to test the CCA update circuits further to determine whether CCA position 4 could be achieved. (The major events of this sequence are shown in Part 1, Mission Summary.) Three DC-17 commands were sent, and the cone angle was observed to step back and forth between positions 2 and 3. The commanding activity then terminated with the spacecraft attitude stabilized on the Sun and Canopus.

The failure to successfully step the CCA to position 4 after three DC-17 commands apparently meant that Canopus would not be visible in the CCA field of view after about May 5 (from position 3); therefore, it would not be available as a roll reference at encounter. An intensive study was initiated to identify possible alternate roll references and modes at Mars encounter. The study disclosed that several brightness peaks in the Large Magellanic Cloud (LMC) might be suitable roll references within view of the Canopus tracker from

CCA position 2 or 3 at encounter. Consequently, a test was devised to ascertain whether *Mariner VI* could indeed lock onto a roll reference in the LMC.

A 40-h gyro drift test, which established that the spacecraft drift rates were satisfactory, was completed on April 30. These data were desired to ascertain the expected gyro drift during the planned inertial mode for encounter.

The special test to find a roll reference for the Canopus tracker in the LMC was conducted on April 30. The spacecraft was rolled off Canopus, and completed a 360-deg roll search to produce a good star map. Next, the spacecraft CC&S was programmed for a maneuver that would turn the spacecraft through the LMC. A 124-s positive (cw) roll turn through the LMC revealed, in the Canopus intensity channel, three "brightness" peaks in the LMC. The Canopus brightness gate was then adjusted to allow the spacecraft to acquire any object bright enough to produce a roll-error signal. In a new roll search, the second brightness peak of the LMC was acquired by the Canopus tracker. However, the limit cycle in roll was very sporadic; at first it was thought that the LMC acquisition was an extended rather than a point source, of low intensity, causing the erratic, noisy, and gas-consuming roll limit cycle. The Canopus tracker lost lock on the LMC 5.5 h later, and went into a DC-15 roll search mode with the gyros off. In this mode, the ccw roll jets were continuously firing; after 30 s, however, the roll-inhibit timer was actuated and the jets were shut off, causing the spacecraft to "free-wheel" in the ccw direction.

A DC-19 command was sent at 00:15:00 on May 1 to terminate the DC-15 mode and turn the gyros on at 00:17:46. The spacecraft continued to roll within the rate deadband of  $-0.018$  deg/s and the Canopus tracker error signal went to the roll search bias, indicating the removal of the DC-15 mode. Next a DC-21 command was sent at 01:00:00 to remove the 30-s roll inhibit; the spacecraft then went into a roll search at 01:02:56. After a 3-min roll search, the Canopus tracker acquired the star Al Na'ir at 01:05:54, and the gyros turned off 3 min later. The Canopus tracker remained locked onto Al Na'ir for about 17 min; at 01:22:30, it lost lock and the spacecraft went into a roll search with gyros on. Canopus was acquired in a normal manner after a 4-min roll search at 01:26:37, and the gyros turned off 3 min later.

With the loss of the LMC and Al Na'ir by the Canopus tracker, all other plans to acquire the LMC at this time were abandoned. It was believed that the loss of lock on the LMC and Al Na'ir was caused by noise on the Canopus tracker roll-error channel, which resulted in both the disacquisition and the failure to reacquire on flyback and sweep. The roll-error signal (channel 114) was noticeably noisy on the LMC and Al Na'ir, but not at all noisy on Canopus.

A second attempt to obtain a lock on the LMC by the *Mariner VI* Canopus tracker was attempted on May 2 by use of a testing method different from that used in the first exercise.

A detailed map of the Large Magellanic Cloud was made by stepping the spacecraft across it in roll at the rate of one discrete step of 0.158 deg/min for 80 min. The stepping direction was then reversed, and the LMC was brought to the center of the field of view of the Canopus tracker, in an effort to acquire the brightest peak of the LMC. For details of this exercise, see Section III-B, Attitude Control Subsystem Performance, under Spacecraft Engineering Subsystem Performance, also in Part 3 of this volume.

Successful acquisition of the LMC was accomplished at 23:23:00 on May 2 in the DC-15 mode (that is, with the Canopus brightness gates overridden). However, the roll-error signal in channel 114 showed numerous noise spikes and "hash" during this acquisition—a condition that did not exist when the tracker was locked onto Canopus. The gyros were turned on in the rate mode by an M1 command at 00:48:02 on May 3 in the hope that this would quiet the noise in the roll-error channel, the derived-rate circuits in roll being removed when the gyros came on. The spacecraft was in an acceptable state at this point, and it was decided to keep the LMC acquired, although the roll error continued to be quite noisy.

Some 14 h later, the Canopus tracker lost acquisition of the LMC at 14:50:20, and the spacecraft went into a cw roll search. The cw direction of the roll search was opposite to the normal ccw direction for a roll search. The loss of acquisition was attributed to high voltage across the Canopus tracker image-dissector tube causing saturation of the roll-error demodulator (a condition known as "punch through"). The punch through condition resulted from the dim brightness source,

causing high voltage across the tube since the voltage is inversely related to the light source in the sensor field of view. Fortunately, the gyros were on, and rates exceeding the gyro rate deadband were prevented. After a 2-min roll search, the tracker acquired an unknown star at 14:52:19. Four more cw roll searches and acquisitions of unknown stars occurred over the next 2 h, all of these effects being caused by "punch through" in the Canopus tracker. Then the star Al Na'ir was acquired after a 40-s cw roll search at 16:57:09. The appearance of the roll-limit cycle on Al Na'ir was more regular than that on the LMC, but many noise spikes were evident, and it was apparent that the Canopus tracker was degrading with time. Accordingly, project management decided that the Canopus tracker should be turned off with a DC-20 command, but only after a final attempt to step the CCA to position 4.

Thus, the plan developed on May 3 was to send the following commands: a DC-18 to hold the spacecraft in roll under inertial control, but also a  $2\frac{1}{4}$ -deg step in roll would result because the gyros were already on; a DC-21 to cancel the step of DC-18 by a roll position step of  $-2\frac{1}{4}$  deg; up to nine DC-17s, if necessary, to step the CCA to position 4; and finally, if position 4 were not attained, a DC-20 to turn off the Canopus tracker.

The command sequence started at 22:30:00 on May 3 with the transmission of a DC-18 command, and the spacecraft apparently roll-stepped  $2\frac{1}{4}$  deg; the observed effect on the roll-error signal (channel 114) was to reduce it to 0 DN. Next the DC-21 command was sent at 22:40:00, which brought the roll-error signal back up to 53 DN and apparently roll-stepped the spacecraft  $-2\frac{1}{4}$  deg. Because the roll-error signal was noisy, it was difficult to perceive any difference in the magnitude of the roll steps. The CCA step command DC-17 was transmitted at 22:48:00. At 22:51:07, the Canopus intensity reading on channel 108 dropped from 79 to 90 DN on Al Na'ir, and the roll error went to 0 DN as the CCA position change barely kept Al Na'ir in the cone-angle field of view. The next reading of channel 309 at 22:52:03 indicated that the tracker had stepped to position 4. Thus, the problem of moving the CCA to position 4 (which started 13 days earlier on April 20) was finally solved. Normal Canopus acquisition followed shortly, but the gyros remained on because of the M1 in effect; when they were turned off on May 13, the gyros had been on continuously, in the rate mode, for about 261 h.

As described earlier, the failure of the CCA to step properly on April 20 provoked a great deal of analysis and effort in attempts to work around the failure. It was discovered that the Canopus tracker could not, for great lengths of time, track stars dimmer than 0.14 times Canopus. For future missions, it is recommended that a Canopus tracker be designed that can track weaker objects; it would be a good investment in reliability.

## VIII. Second Cruise Period, *Mariners VI and VII*

### A. *Mariner VI*

After the reestablishment of cruise-mode operations by the solution of the CCA stepping problem on May 3, *Mariner VI* entered a second interplanetary-cruise phase of the mission. This phase continued until the start of the calibration of the high-rate telemetry subsystem (HRTS) and the data storage subsystem on July 12, 1969. Included in this cruise phase were the occurrence of an anomaly and the execution of flight-operations sequences that modified the cruise configuration to some extent, as described in the paragraphs that follow.

1. **May 13.** Gyros were turned off after transmission of a DC-13 command to allow the spacecraft to use Canopus as a roll reference. The CC&S received two coded commands to reset flag 5 and a DC-32 command to place the CC&S in the computer-only mode for an inertial-at-encounter sequence.

2. **May 26.** A C1 event (CCA step) from the CC&S was issued (on time) at 21:28:09 to command the attitude control subsystem to update its CCA position from 4 to 5. However, instead the CCA anomalously went to position 3; the Canopus tracker then lost Canopus, the gyros came on, and the spacecraft went into a roll search. A strategy adopted for solving this problem was to transmit six DC-17 commands (the CCA step command) on the supposition that the previous stepping action of the CCA (May 3) placed the cone-angle logic in the descending sequence. However, a total of eight DC-17 commands were required to achieve CCA position 5.

After the first two DC-17 commands, which only toggled the cone angle between positions 3 and 4, the cone-angle logic behaved as if it were on the descending portion of the cone-angle update sequence. Six more DC-17 commands took the logic through the remaining positions on the descending sequence, and then up the ascending sequence to the desired position 5.

The sequence was as follows: 4 to 3, 3 to 4, 4 to 3, 3 to 2, 2 to 1, 1 to 2, 2 to 3, 3 to 4, and 4 to 5.

Failure-mode analysis of this failure (on April 20) and recovery (on May 3) indicated that two separate failure modes must have been responsible, although the faults could not be conclusively determined.

3. **June 5.** The CC&S received 122 coded commands to incorporate the N4-N1\* feature in the encounter sequence. This feature would enable the CC&S to send an N4 command to the scan control subsystem, followed by an N1\* command after near-encounter TV pictures 1 to 4 and 6 to 12 had been taken. The N4 command would cause the scan control subsystem to send an automatic aperture control (AAC) signal to the TV subsystem. (The AAC allows the TV subsystem to reset the exposure control on the cameras, alleviating the TV-inverted raster problem.) The N1\* command would follow the N4 command in about 150 ms; this would be long enough for the AAC function for TV, but not long enough to allow any appreciable slew of the scan platform (the N4 command causes the scan platform to slew to the final cone-angle position of 101 deg).

In addition, a QC-1-1 and a QC-3-1 command were transmitted to update the near-encounter cone- and clock-angle references by 1 deg each (to 128.87 and 263.83 deg, respectively) according to the wishes of the experimenters and the latest knowledge of the orbit. The philosophy of this update was that command capability may be lost at any time; therefore, the "best" angles should be maintained on the near-encounter reference potentiometers at all times.

4. **June 16.** The TWTA in the RFS was switched to the "high-power" mode (20 W) by a DC-42 command, and the CC&S received nine coded commands, to accomplish the following:

- (1) Delete the C2 event (to switch the FTS to 8½ bits/s), which was to occur on June 19. The switch to 8½ bits/s was made unnecessary by the higher downlink performance achieved by the TWTA in the high-power mode.
- (2) Delete the C6 event (to switch the FTS to 33½ bits/s), which was to occur on July 10. This event was unnecessary because the bit rate was to remain at 33½ bits/s.

- (3) Load in a P4 event (switch TWTA to low power) for occurrence on June 24. This event was programmed to ensure a fail-safe return in the RFS to TWTA low power if the TWTA high-power mode should produce anomalous behavior in the spacecraft.

**5. June 24.** The CC&S received 20 coded commands to change seven words in the CC&S memory. Six words were to change words 4 and 5 of the executive routine so that CC&S dumps could be taken over an hour scan point without losing events in the M1-M2, M4,  $\overline{M4}$ , reacquisition sequence. The seventh word deleted the P4 event (switch TWTA to low power) by replacing it with a dummy event.

**6. June 26.** The ranging transponder was turned on and off by two DC-9 commands to check its operation. The ranging transponder was then turned on by a DC-9 command and off by a Y1 (radio test cyclic) command to observe its effects.

**7. June 27.** The ranging transponder was turned on by a DC-9 command. Uplink was turned off, and no self-lock or SPE bias was seen in the data. No offset in the best-lock frequency was apparent. The spacecraft receiver threshold measured  $-153.5$  dBmW (nominal).

## **B. Mariner VII**

After the reestablishment of cruise-mode operations, the successful testing of the inertial-all-axis sequence at scan-platform unlatch (which provided a good test for IRS gas venting at encounter), and the updating of the CC&S for TV picture sequences at encounter, the spacecraft entered a second interplanetary-cruise phase of the mission. Included in this cruise phase were special tests and sequences and a major anomaly, as described in the paragraphs that follow.

**1. May 22.** A command threshold test was run because the early ranging threshold and AGC stability had caused doubt in the command channel performance. Results of the test indicated that the command threshold was about 7 dB lower than predicted.

**2. May 27.** The CC&S received 42 coded commands, which were to update the encounter parameters and provide for N4-N1\* events (as in *Mariner VI*), following TV pictures 1-12 at near-encounter, to alleviate the TV-inverted raster problem.

**3. May 29.** Receiver and command threshold tests were run again. Results indicated that the command threshold was still about 7 dB lower than predicted. The Canopus cone angle position was stepped normally from position 4 to 5 by a DC-17 ground command; the tracker was now in the final Canopus cone angle position for encounter.

**4. May 30.** Eleven coded commands were transmitted to the spacecraft to change the CC&S memory as follows:

- (1) Delete the C1 event (Canopus cone angle step) that was to occur on June 3. This event was no longer needed because the CCA had been stepped to its final position (5) on May 29.
- (2) Add a P3 event (TWTA to high power) for occurrence on June 9.
- (3) Change the time of the M1 event (gyros on) from  $E - 25$  to  $E - 56$  h. It was decided that a longer gyro warm-up period was needed for the inertial-hold sequence at near-encounter.

**5. June 3.** A receiver threshold test was run, and a threshold of  $-147.4$  dBmW was indicated (this was the same degradation from  $-152$  dBmW that had been seen earlier).

**6. June 5.** A test of the SPE and AGC stability of the receiver indicated normal operation. A downlink spectrum analysis was performed in which DSSs 12, 13, and 14 took part. A phase lock loop transfer function,  $H(S)$ , was measured as normal. However, these tests revealed little about the spacecraft degraded receiver threshold.

**7. June 9.** Five coded commands were sent to the spacecraft to modify the CC&S memory as follows: (1) Delete the P3 event due this date because a ground command was intended to be used instead; (2) add a P4 event (TWTA to low power) for occurrence on June 19 (this was a precautionary measure in case the TWTA high-power mode, soon to be initiated, caused the receiver to degrade further and cause command capability to be lost). The spacecraft RFS was switched to the TWTA high-power mode (20 W) by a DC-42 ground command; the switching to high power was accomplished normally, with no anomalies. A command threshold test run indicated that the degradation seen earlier was being removed by the TWTA high-power mode. Results indicated that the command threshold was within 1 dB of

the predicted level, and the receiver threshold had improved to nominal ( $-152.3$  dBmW).

**8. June 10–13.** Repeated receiver threshold and command threshold tests performed during this period indicated that the spacecraft receiver threshold was no longer degraded ( $-152$  dBmW) and the command threshold was nominal at  $-147$  dBmW.

**9. June 19.** Eight coded commands were sent to the spacecraft to change the CC&S memory as follows: (1) Delete the P4 event (TWTA to low power) because it was no longer needed as a fail-safe backup in case TWTA high power produced anomalies; (2) delete the C2 event (FTS to  $8\frac{1}{2}$  bits/s) and the C6 event (FTS to  $33\frac{1}{2}$  bits/s) because telecommunications performance would allow the bit rate to remain at  $33\frac{1}{2}$  bits/s throughout the mission.

**10. June 20–July 2.** The RFS continued to surprise operations analysts during this period, as it had in the past. The spacecraft receiver performance was more stable since the TWTA had been commanded to high power on June 9 and warmed up the RFS. Two threshold tests made during this period exhibited a receiver threshold of  $-151$  and  $-152$  dBmW, respectively, a very acceptable level of performance.

On June 20, the ranging channel was commanded on with a DC-9 ground command for the first time since April 25. Upon turn-on, the traveling-wave tube (TWT) helix current immediately increased from 6.81 to 7.66 mA. At the same time, the low-gain antenna drive decreased from 41.28 to 41.23 dBmW. Both of these changes were completely unexpected. When the ranging channel was commanded off by a DC-9 command, the measurements returned to normal preranging values.

After reevaluation of the RFS performance, it was decided to try ranging again. Accordingly, on June 23, a DC-9 command was sent, and the same telemetry indications appeared; this time, however, ranging was left on (to be turned off by the Y1 cyclic event). Ranging was turned on again on June 27, and DSS 14 reported the acquisition of good ranging data. The TWTA continued to perform well in the high-power mode.

**11. July 7.** An anomaly occurred in the CC&S that revealed a circuit failure. The CC&S was to have issued the C3 event to switch the RFS transmitter to the space-

craft high-gain antenna; a counter 2 event was observed at 19:22:40 (indicative of a computer event), but the RFS did not switch to the high-gain antenna. A CC&S memory readout was ordered by a DC-2 command, and received at 20:05:20; the readout indicated that the program had issued the event in question. A DC-11 (transmit high) ground command was then sent to the spacecraft, and, at 20:38:06, the RFS switched to the high-gain antenna.

With the observed failure of the C3 event to switch to the high-gain antenna, and the success of the DC-11 ground command to accomplish the switch, suspicion centered on the CC&S as the cause. Therefore, flight tests were conducted to test the relay drivers in the CC&S that issue events.

On July 9, a set of coded commands was sent to the CC&S, and the A3-D1 drivers were excited by a real-time CC&S command. This action set the timing of events relay ( $\overline{TE}$ ), which caused channel 220 to start counting. Another set of coded commands was then transmitted to excite the C1-D1 relay drivers to reset the timing of events relay. Channel 220 *did not stop* counting when the counter 2 event indicated that  $\overline{TE}$  should have been actuated. Because the C1 driver was also required for the CC&S C3 event that did not occur, the evidence strongly suggested that the C1 source driver or its associated logic had failed. Additional coded command transmissions to the spacecraft generated real-time CC&S commands to test the C3-D0, C3-D2, B3-D5, A1-D5, and B2-D7 drivers; resulting N11, N10, N1 (FTS), N1 (data storage subsystem), and F3 events confirmed those drivers to be working properly. This testing further isolated the C1 source driver as the problem.

The failure of the C1 source driver made the CC&S incapable of issuing the following events: N8 (stop ATR), N9 (stop DTR), C3 (transmit high), N6 (enable pyrotechnics for IRS cooldown), M3, M4, M5, and  $\overline{TE}$  (stop pitch and roll turns, stop timing of events), L1 (deploy solar panels), and L2 (Canopus tracker off). This failure had a serious impact on the planned encounter strategy, and immediate action on July 10 resulted in the transmission of 37 coded commands to accomplish the following:

- (1) To prevent a roll search if IRS cooldown were to occur (associated with another failure of the C1 source driver), the N6 (pyrotechnics) event was removed from the program.

- (2) To prevent an infinite pitch turn associated with the inertial sequence at encounter, the inertial sequence was disabled with a DC-13 command, and the CC&S was placed in the tandem standby mode with a DC-33 command.
- (3) The TV gate was set, the TV-AAC reset sequence was disabled, and a routine to test for flag 4 after narrow-angle acquisition was loaded into the CC&S to protect the encounter sequence as much as possible from any further relay-driver failures.
- (4) The CC&S fixed sequencer was loaded with minimum pitch and roll turns and an infinite motor burn in anticipation of using a sequencer-only maneuver mode in place of the computer-only maneuver mode for the inertial sequence at encounter.

A probable cause of the failure was believed to be a gold-aluminum intermetallic reaction producing corrosion in an integrated circuit block in the logic of the C1 source driver.

## IX. Data Storage Subsystem High-Rate Calibration, *Mariners VI and VII*

The high-rate telemetry subsystem was planned as an engineering experiment for the mission; instead, as the flights progressed, it became the prime method of returning science data for the strategy of the encounter sequence developed by the encounter planning team. Therefore, it became imperative that a verification be made of the predicted performance of the HRTS. By playback of a test picture (recorded on the ATR just before launch) over the HRTS, an evaluation could be made of the telecommunications link in the high-rate mode. As a result of evaluating the HRTS, the following test objectives were also planned to be met:

- (1) Generally assess data storage subsystem performance, including tape recorder pressures, ATR running time, playback amplifier gains, and some verification of data storage subsystem internal logic and power consumption.
- (2) Compare recorded test picture played back with same picture played back just before launch; also compare playback on each pass of test picture with other passes.
- (3) Erase and verify erasure of single test picture stored on ATR.

- (4) Utilize and evaluate real-time TV link between Goldstone and Space Flight Operations Facility.
- (5) Evaluate telecommunications link with spacecraft ranging channel on and DSS 14 in duplex-ultra-cone configuration (this would match encounter configuration as close as possible without turning science power on).
- (6) Verify some temperature-control performance, as infrared radiometer (IRR), bay V, and cone-actuator heaters were to be switched off when data storage subsystem was turned on.

The data storage subsystem high-rate calibration test was initiated on July 9 for *Mariner VII* and on July 12 for *Mariner VI*; each test is described in the paragraphs that follow.

### A. *Mariner VII*

The data storage subsystem power was turned on by a DC-47 ground command at 01:56:13 on July 9 for the first time since the launch phase. The pressures observed in both tape transports were as expected ( $> 1.4$  atm) and both tape recorders indicated they were on track 1. The test picture stored on the ATR (track 1) was played back to the Earth four times (all in the playback 2 mode) for the FTS and data storage subsystem. On July 15, the test picture on the ATR was erased and verified by a playback. The data storage subsystem responded correctly to the following commands: DC-23 (ATR track step), DC-3 (playback 1), DC-44 (playback 2), DC-39 (ATR erase), CC&S F3 (ATR erase), CC&S N1 (ready mode), and DC-1 (cruise mode). Tape running times were nominal, and compared almost exactly to ground-test predicted times. The subsystem was assessed as completely normal at the conclusion of the test on July 15, and the power to it was allowed to remain on until encounter.

The high-rate calibration sequence revealed that a gain shift in the ATR of approximately  $-10\%$  had occurred since just before launch, when the test picture had been played back. (See television subsystem discussion under Scientific Instrument Performance, also in Part 3 of this volume, for the impact of this shift on the TV pictures.) The following paragraphs contain a description of events of the *Mariner VII* data storage subsystem high-rate calibration test.

The test began on July 9 at 01:56:13 with the receipt by the spacecraft of a DC-47 (data storage subsystem



power on) command by the spacecraft. The data storage subsystem and the FTS were placed in the playback 1 mode by a DC-3 command, then in the playback 2 mode by a DC-44 command. The test picture was played back to the Earth at 16.2 kbits/s. All AEOTs occurred on time, and the test picture was played back to the Earth a total of four times. At 05:37:17, a DC-1 (cruise mode) command was received by the spacecraft. The ATR stopped playback; the data storage subsystem was placed in the ready mode on track 4; and the FTS was placed in the cruise data mode at 33½ bits/s.

At 00:44:00 on July 15, a DC-39 command placed the data storage subsystem in the ATR erase mode. The erasure was of the last few feet of tape because the DC-1 command on July 9 had placed the data storage subsystem in the ready mode just before the end of track 4. Various commands were sent to confirm that erasure and playback modes were operable in the spacecraft. At 03:49:01, a DC-39 command placed the data storage subsystem in the ATR erase mode, which ended at 03:49:56 when the AEOT was observed. The data storage subsystem was then in the ready mode (track 1) for both tape recorders. Power to the subsystem was left on for encounter.

The test objectives of the high-rate calibration were satisfactorily met, and the test demonstrated the capability of the real-time TV link, the telecommunications downlink with ranging on, the erasure function of the data storage subsystem, and the 16.2-kbits/s (playback 2) FTS mode.

## B. Mariner VI

The data storage subsystem power was applied at 02:01:57 on July 12; it was the first time subsystem power had been on since  $L + 2$  h on February 25. The subsystem transport pressures were normal ( $> 1.4$  atm), and the subsystem controller logic came up in the ready mode, as expected. Performance of the subsystem during the playback of the prerecorded picture on the ATR and during the subsequent erase sequence on July 15 was normal in all respects. The signal-to-noise ratio (SNR) in channel C (the high-rate channel) was 0.7 dB lower than predicted, but this was considered to be within tolerance.

The sequence for the data storage subsystem high-rate calibration was very similar to the *Mariner VII* sequence described earlier. The prerecorded test picture was played back four times on July 12, and then the DC-1 command

was timed to arrive at the spacecraft just after the ATR came up on track 1 (because of an AEOT during playback 2). The DC-1 command stopped playback in the subsystem at the start of ATR track 1, placed the subsystem in the ready mode, and switched the FTS from the playback 2 mode to the cruise mode.

On July 15, the ATR test picture was erased twice—first by a DC-39 ground command and then by a CC&S F3 command. The playback 2 mode in the FTS and data storage subsystem was then initiated, and the portion of ATR track 1 containing the prerecorded test picture was played back twice to verify the erasure. The playback 2 mode was then terminated by the issuance of a CC&S N1 event, which placed the subsystem in the ready mode and the FTS in the encounter 1 data mode. A DC-1 command then placed the FTS in the cruise mode. The exercise was concluded with the transmission of a DC-39 command that placed the subsystem in the ATR erase mode; this command was used to reposition the tape at the AEOT and to reset the track counter to 1. The AEOT, which occurred 3 min after the DC-39 command was received, placed the subsystem in the ready mode on track 1, where it remained for encounter.

## X. Mariner VI Far-Encounter

The far-encounter phase of the *Mariner VI* flight was extremely successful for both the spacecraft and ground systems. Because there were no discernible spacecraft problems at  $E - 3$  days, project management elected to perform the standard mission sequence, which required a large number of ground commands and the proper functioning of the HRTS. The programmable CC&S and the high-rate playback system performed exceptionally well, combining to yield 50 far-encounter pictures. There was, however, a minor anomalous condition in the scan control subsystem, in which it was discovered that apparent offsets in the calibrations of the scan clock and cone reference potentiometers necessitated last-minute corrections.

During the 2 wk before the initiation of its far-encounter phase, *Mariner VI* had undergone special testing and conditioning to ensure that the spacecraft would perform the encounter sequence (with a high probability of success) designed for the *standard* mission. It is appropriate to note here that the *conservative* mission, if chosen, would have required no high-rate telemetry and no command activity from the Earth because its sequence had been programmed into the CC&S before launch and

updates of its near-encounter scan-platform slews had been achieved with coded command loadings during the interplanetary cruise period.

Special testing became necessary because of the discovery of a failed CC&S relay source driver in *Mariner VII*. The *Mariner VI* relay drivers were tested on July 15 and 25, and no failures were discovered. All but one of the relay drivers to be used in the encounter phases were tested by observing normal CC&S outputs and by issuing certain events; this was accomplished by loading real-time CC&S commands (i.e., events that are issued on the first minute or second scan after they are loaded into memory). All events loaded into the CC&S were issued with the proper responses resulting. The one untested relay driver was to be verified at about  $E - 48$  h, when the first F2 (far TV picture) event was to be issued.

To condition the spacecraft battery for possible use during encounter, the 15-W battery test load was commanded on with a DC-50 ground command on July 23 at 07:18:15. The test load remained on for 10.5 h, during which time it was estimated that 158 W-h of charge were drained from the battery. The test load was commanded off at 17:49:41; 21 min later, the battery charger was turned on by a DC-38 command to restore the charge used by the test load.

The final preconditioning for encounter occurred on July 25, when updates were commanded in the CC&S and scan platform subsystem. The CC&S updates consisted of coded-command loadings to accomplish the following:

- (1) Modify the far-encounter F2 sequence so that two pictures could be taken of one of the Martian satellites (Phobos).
- (2) Change the Y1 event period from 24 to 3 h.
- (3) Change the time of the N6 data automation subsystem (DAS) event.
- (4) Change three postencounter cruise events.
- (5) Add the capability for a fifth scan-platform slew during near-encounter.
- (6) Change the slew magnitude values.

The scan control subsystem updates consisted of transmitting quantitative commands to step the scan clock and cone near-encounter reference potentiometers to

their final near-encounter positions (262 and 129 deg, respectively).

The far-encounter phase started on July 29 at 00:32:38 with the issuance by the CC&S of the M1 event, which turned on the spacecraft gyros. The gyros were energized at this time ( $\sim E - 53$  h) in the rate control mode to provide a long enough warm-up period ( $\sim 51$  h) so that spacecraft thermal conditions would be stable when the spacecraft was to go into the all-axis-inertial mode ( $E - 2$  h). The gyro turn-on appeared to be normal in all respects. The battery charger was switched off at 00:56:14 by ground command DC-38; it was estimated that the battery had achieved 97% of full charge at this time.

The next command sent (DC-25) was a time-critical command; its transmission time was determined from the requirement that a blue filter should be in place when the first TV-A camera picture was to be recorded of the planet limb at near-encounter. Consequently, the DC-25 command was transmitted at 01:16:23. Science and scan-platform power were turned on, the FTS was switched to the encounter 1 data mode, and the scan platform initiated its slew from the stowed position (225 deg in clock, 96 deg in cone) to the near-encounter reference position. After about 0.5 h of evaluation of the science and scan control subsystems in the encounter 1 data mode, a series of four commands (on approximately 0.5-h centers) was transmitted to verify that the scan platform would slew throughout the operating range of all modes intended for the encounter sequence.

Accordingly, a DC-28 command was sent to slew the platform to the far-encounter position and to place the data storage subsystem in the far-encounter wait state. The far-encounter planet sensor (FEPS) was energized upon receipt of the command; when the planet came into its field of view, control of the scan control subsystem was transferred to the closed-loop mode in which the scan platform tracked the planet from the error signal present in the FEPS. Next a DC-25 command was transmitted to slew the scan platform back to the near-encounter references and to place the data storage subsystem in the ready mode. A DC-41 command followed, which slewed the scan platform in cone to the fixed cone-angle reference position of 101 deg. Finally, a DC-25 command was sent to switch cone-angle control to the near-encounter reference, and the scan platform then slewed in cone back to the near-encounter position. This series of commands demonstrated that the scan platform was capable of operating in all of the modes

necessary for the standard mission; however, some deviations were noted. The data taken while the FEPS was tracking the planet indicated that the platform clock and cone position telemetry was reading 0.7 and 0.07 deg low, respectively. In addition, data taken while the scan control subsystem was in the near-encounter mode indicated that the cone reference potentiometer was 0.48 deg high. These observations led to the decision to adjust the telemetry readouts by the factors enumerated to obtain the true scan-platform position.

The next command (DC-44) was sent at 03:24:00 to switch the FTS data mode from encounter 1 (channel A at 66½ bits/s, channel B at 33½ bits/s) to encounter 2 (channel B at 33½ bits/s, channel C at 16.2 kbits/s). It was desired to be in the encounter 2 data mode to obtain ultraviolet spectrometer (UVS) and digital TV data during the slew to far-encounter position by the scan platform shortly thereafter.

The DC-28 command was transmitted next (at 03:44:00) to prepare the spacecraft for the first far-encounter picture-taking sequence. The data storage subsystem switched to the far-encounter wait state, from which it could record the pictures, and the scan platform commenced its slew to the far-encounter position. After a slew of 1 min 20 s, the planet-in-field-of-view (PIFOV) event was issued by the scan control subsystem, indicating that the FEPS was tracking the planet and that control of the scan platform position was transferred to the closed-loop mode.

After evaluation of the performance of the various subsystems for 1 h in the encounter 2 data mode, a DC-32 command to initiate the far-encounter 33-picture "C" sequence was sent. This command started a cycle-generator program in the CC&S that would issue 33 F2 commands to the DAS on 37-min centers, with the first F2 command occurring 37 min after receipt of the DC-32 command. Each F2 command ordered the DAS to take a TV-B camera (narrow-angle) picture; ATR start and stop signals to the data storage subsystem from the DAS recorded the picture on the ATR. These 33 F2 commands were chosen to ensure proper ATR tape position. The last picture (33) would not be fully recorded because, at AEOT = 4, the ATR is full, and the recording would stop. This would ensure that one fail-safe erase command (F3) would erase the entire tape. When the ATR is erased, all four tracks are erased simultaneously; the erasing starts at the position of the

erase heads and proceeds to the end-of-tape mark. The Earth-observed time of the DC-32 command was 04:55:47, indicating that the far-encounter C picture sequence was initiated in the CC&S. Telemetry indications showed that the first F2 command was issued on time 37 min later (at 05:32:40). The ATR start, which placed the data storage subsystem in the far-encounter record mode, and the ATR stop, which ended recording of the picture, were confirmed shortly thereafter. The process was repeated on 37-min centers over the next 19 h 44 min during which the 33 pictures were recorded on the spacecraft ATR (which takes TV data only).

Before completion of the C sequence recording, three commands were transmitted to the spacecraft: (1) a DC-46 command at 05:55:00 to deploy the transparent cover on the TV-A camera, (2) a DC-44 command at 08:25:00 from DSS 41 to switch the FTS from the encounter 2 to the encounter 1 data mode because the encounter 2 data mode is above threshold only over DSS 14, and (3) a DC-44 command at 22:24:00 from DSS 62 to switch the FTS to the encounter 2 data mode (this was done to maximize the amount of encounter 2 data received by DSS 14 by having the FTS in the encounter 2 data mode at station rise).

The C picture-recording sequence was concluded at 01:17:20 on July 30 by an AEOT = 4 signal, as expected. This terminated the recording of far-encounter picture 33 at 25 s into the picture (it takes 42.2 s to record a picture). Thus, more than half of picture 33 was recorded on the ATR.

Playback to the Earth of the 33 stored pictures was at 16.2 kbits/s over the HRTS. This mode was initiated on July 30 with the transmission of DC-3 and DC-44 commands on 1-min centers at 01:25:00; the DC-3 command placed the data storage subsystem and the FTS in the playback 1 mode, and the DC-44 command toggled them to the playback 2 mode. The playback was achieved during a 2 h 51 min period over DSS 14. While the 33 pictures were being played back, an update period occurred in which 14 coded commands were transmitted to the spacecraft to update the CC&S for near-encounter slewing and for the N8 (ATR stop), N9 (DTR stop), and P2 (playback start) events. The playback mode terminated at 04:28:05 (just 8 s after AEOT = 4 occurred) with the receipt of a DC-25 command, which switched the data storage subsystem to the ready mode and the FTS to the encounter 1 data mode, and initiated the slew of the scan platform to the near-encounter references.

Two erasures of the ATR were performed after the switching of the FTS to the encounter 2 data mode by a DC-44 command. The first erasure was ordered by a DC-39 command at 04:53:26, and the second erasure by a CC&S F3 command at 05:32:46. A DC-32 command was sent between the two ATR erasures to enable the CC&S for the far-encounter "B" sequence. If the DC-32 command had not been sent, the spacecraft would automatically have executed the conservative mission. This command was used to select the 17-picture B sequence by setting a flag in the CC&S so that, at the time of the F1 event (1 h 15 min later), the B sequence would be started.

The next commands received by the spacecraft (at 05:51:28, 05:52:27, and 05:54:29) were two DC-23 commands and a DC-9 command, respectively. The two DC-23 commands were used to step the ATR from track 1 to track 3 in preparation for the 17-picture sequence. It was desirable to record the 17 pictures on tracks 3 and 4 to achieve correct tape positioning because an AEOT = 4 would have terminated the record mode, ensuring that a single erase command (F3 or DC-39) would completely erase the entire tape. The DC-9 command turned on the ranging channel.

The B sequence was initiated on time (06:32:46 on July 30) with a telemetry indication of the F1 event from the CC&S. The F1 event started a cycle-generator program in the CC&S that would clock out 17 F2 events in the following manner: the first seven would occur on 64-min centers from the time of the F1 event, the eighth would occur 2 min after the seventh, and the last nine would occur on 56-min centers from the time of the eighth. In addition, the F1 event placed the data storage subsystem in the far-encounter wait state and initiated the slew of the scan platform to the far-encounter position. After an 83-s slew, the FEPS acquired the planet, and the scan platform once again was tracking Mars in preparation for the second far-encounter picture-taking sequence. The first F2 event of the B sequence occurred on time at 07:36:45, and the first picture was recorded on the data storage subsystem. Subsequent F2 events were issued at the expected times until the seventeenth F2 event at 22:26:50 completed the far-encounter B picture-recording sequence. Before the occurrence of the second F2 event, the spacecraft received a DC-44 command to switch the data mode from encounter 2 to encounter 1. The command was sent from DSS 41 soon after DSS 14 set to minimize loss of science data because only DSS 14 could receive encounter 2 data.

Shortly after the occurrence of the seventeenth F2 event, an N1 event (as programmed) was issued by the CC&S at 22:32:47. This placed the data storage subsystem in the ready mode, and initiated a slew of the scan platform from the far-encounter position (under FEPS control) to the near-encounter reference position. Two DC-23 commands and a DC-44 command then prepared the spacecraft for playback of the 17 stored far-encounter pictures. The two DC-23 commands stepped the ATR from track 1 to track 3, and the DC-44 command switched the FTS from the encounter 1 to the encounter 2 data mode.

Playback started 2 h later (01:02:32), on July 31, with the transmission of DC-3 and DC-44 commands on 1-min centers to place the FTS and data storage subsystem in the playback 2 mode. During the 1 h 25 min playback of the 17 far-encounter pictures, a final update of the CC&S for the near-encounter slewing parameters was performed. Fourteen coded commands were received by the spacecraft between 01:11:33 and 01:24:35, followed by two commanded CC&S memory readouts to verify that the coded commands were loaded correctly.

The far-encounter phase for *Mariner VI* concluded when the playback of the 17 pictures of the B sequence was terminated by a DC-25 command received at 02:27:56, which switched the FTS to the encounter 1 data mode and placed the data storage subsystem in the ready mode.

## **XI. *Mariner VI* Near-Encounter**

The near-encounter phase of *Mariner VI* saw nominal performance of the spacecraft system. The RFS and FCS performed in an excellent manner; the RFS had no recurrence of the self-lock problem noted earlier in the mission, and the auxiliary oscillator continued to be stable. The auxiliary oscillator frequency predicts used for acquiring the downlink signal upon exit from occultation were highly accurate. The FCS processed all commands transmitted to the spacecraft. Three data modes were used by the FTS: encounter 1, encounter 2, and playback 1. No anomalies occurred, and SNRs in all modes were within tolerance. The power subsystem supported the largest power demand of the mission without any battery sharing; that is, the solar panels supplied all the power required. The CC&S correctly issued all events programmed in its memory: M2, N6, N8, N9, P2, F3, N7, N1,  $\overline{M1}$ , Y1, N5, four scan-platform clock-angle

slews, one scan-platform cone-angle slew, and eleven N4-N1\* events.

The attitude control subsystem was switched to the all-axis-inertial mode at approximately  $E - 2$  h (after the gyros had been running in the rate control mode since about  $E - 53$  h). The all-axis-inertial mode was chosen as protection should bright particles, caused by the IRS cooldown event, cause the Canopus sensor to lose lock, and thereby produce an undesired roll search. At the time of IRS cooldown initiation, a single bright particle, whose brightness was 1.38 times that of Canopus, was seen in the telemetry data; however, it did not cause the Canopus sensor to flyback and sweep. Nevertheless the IRS cooldown was not normal. Evidence of normal  $H_2$  venting was seen in the attitude control limit cycle, but apparently the  $N_2$  cooldown was inhibited in some manner, for it "leaked" over a period of some 5 days. The pyrotechnic subsystem, responding correctly to commands, fired the IRS cooldown squibs at approximately  $E - 37$  min. No pyrotechnics events occurred at the time of NAMG-1 viewing of the planet or when the backup command arrived at the spacecraft, which indicated that the expended cooldown squibs had no bridgewires short-circuited to ground.

Encounter-phase temperatures approximated those taken during ground testing in the thermal-vacuum chamber with science power on. The TV-B camera vidicon temperature was  $3^\circ F$  lower than predicted; the TV-A camera vidicon was  $2^\circ F$  cooler. The IRS radiator plate worked very well, the temperature being  $10^\circ F$  lower than predicted.

The data storage subsystem performed nominally during near-encounter, with one exception. Portions of data on DTR tracks 1 and 2 were garbled, as evidenced by the data returned during the playback 1 mode from exit occultation until 12 h later. While being recorded, these same data were transmitted in parallel over the high-rate link (encounter 2 data mode, 16.2 kbits/s). These real-time digital data were then received with no anomalous indications during the near-encounter phase, so none of the original digital data was lost. Hence, the DTR data essentially formed a redundant data source for near-encounter. See Section II-D, Data Storage Subsystem Performance, under Spacecraft Engineering Subsystem Performance, for details of this anomaly.

The science subsystem (ultraviolet spectrometer, television, infrared spectrometer, and infrared radiometer)

performed nominally in the near-encounter phase, with the exceptions noted below. The cooldown system used for the channel 1 detector of the IRS failed. A particulate contaminant, perhaps generated in the launch environment plugged the cryostat (probably in the  $N_2$  orifice). The IRS channel 2 data were returned, and the channel was completely nominal, because its detector was cooled by a radiator plate that faced black space. An anomaly also occurred in the infrared radiometer (IRR) data: scan-platform slewing during near-encounter apparently generated noise that was seen in the IRR data.

The scan control subsystem performed nominally during the near-encounter phase. As noted earlier, the cone reference potentiometer calibration was 0.48 deg high; therefore, to obtain true platform cone position, 0.48 deg was subtracted from the telemetry indication. The scan platform responded properly to CC&S commands, and performed four slews in clock (one each after pictures 8, 13, 17, and 32) and one slew in cone (after picture 8). A feature of the near-encounter sequence discussed earlier was the issuance by the CC&S of 11 N4-N1\* events to the scan control subsystem (one N4-N1\* event after each of near-encounter pictures 1-4 and 6-12). This strategy was developed as a consequence of a problem uncovered after the launch of *Mariner VII*.

A spacecraft wiring error produced a TV-inverted raster, and this would result in adjusting the TV shutter in a manner to cause saturation of pictures during the automatic near-encounter picture-taking sequence. To alleviate this problem, it was decided to use the N4 command from the CC&S to the scan control subsystem. The N4 command transfers control of the scan platform cone angle from the near-encounter reference cone potentiometer to the *fixed* cone reference (101 deg nominal); as a result, a relay closure is output from the scan control to the TV subsystem to reset the shutter to its minimum exposure setting. This relay-closure function, labeled automatic aperture control (AAC), could then be programmed by means of an N4 command to occur before any near-encounter picture desired. However, the N4 command would also cause the scan platform to slew to its fixed cone position of 101 deg (if it was not already there), and thereby upset the planned slewing sequence. To prevent the scan platform from slewing when the N4 event occurred, it was decided to have the CC&S issue an N1\* command immediately after the N4 command. The N1\* command would transfer control of the scan platform position back to the near-encounter

reference potentiometers and reset the latching relay that issues the AAC. It was shown, in ground testing of the proof-test model spacecraft, that a spacing of as much as 150 ms between the N4 and N1\* commands would produce no change in the scan-platform position; it was apparently the inertia of the scan platform that prevented it from following a virtual step function change of such short duration.

Preparation of the spacecraft for the near-encounter sequence started at 02:28:55 on July 31 with receipt of the DC-25 command, which switched the data storage subsystem to the ready mode in anticipation of an erasure of the ATR, and switched the FTS to the encounter 1 data mode. Next the DC-44 command, received at 02:34:35 ( $E - 2$  h 44 min), placed the FTS in the high-rate data mode (encounter 2), in which it was to remain until occultation. Following this event, two erasures of the ATR were performed, the first initiated by a DC-39 command and the second by the CC&S F3 command. Simultaneous with the F3 command, the CC&S issued the M2 command, which placed the spacecraft in all-axis-inertial hold. As discussed earlier, the all-axis-inertial hold was desired to prevent a possible roll search caused by a potential loss of Canopus if bright particles were to come into the Canopus sensor field of view upon initiation of IRS cooldown.

A dummy event was next issued by the CC&S aboard the spacecraft at  $E - 51$  min, and was observed on the Earth at 04:32:49. This event placed the CC&S in the *seconds scan* mode so as to accurately time the numerous near-encounter events it was shortly to issue. After the dummy event, the spacecraft received (at Earth-observed time) a DC-26 command at 04:39:36, a DC-36 command at 04:40:35, another DC-36 command at 04:42:33, and an N6 command to pyrotechnics from the CC&S at 04:43:32. The purpose of the DC-26 command was to enable NAMG-1 (or DC-49) in the pyrotechnic subsystem; thus enabled, if either the planet came into the field of view of NAMG-1 or the DC-49 command were received, the pyrotechnic subsystem would fire the IRS cooldown squibs and start the IRS motor. However, the DC-26 command also enabled the near-encounter sequence mode in the DAS, thereby enabling NAMG-2.

At this point, the time was  $E - 44$  min, and the NAMG-2 signal was not to occur until about  $E - 14$  min;

therefore, it was prudent to prevent an erroneous NAMG-2 signal by disabling the near-encounter sequence mode in the DAS with a DC-36 command. Hence, the first DC-36 command was to disable NAMG-2 in the DAS (but not NAMG-1 in the pyrotechnic subsystem), and the second DC-36 command was a backup.

In addition, the DC-36 command ordered the TV-B camera to take a far-encounter picture. This was no problem, however, because the near-encounter sequence was to use only three of the four ATR tracks for 24 near-encounter pictures. Thus, the two DC-36 commands ordered the recording of two TV-B (narrow-angle) pictures of dark space on track 1 of the ATR, but ensured the disabling of NAMG-2. The N6 (pyrotechnics) event was a backup to the DC-26 command in enabling NAMG-1 (or DC-49) in the pyrotechnic subsystem.

The next series of events received by the spacecraft consisted of a DC-49 command at 04:47:14, a NAMG-1 at 04:49:13, and a DC-49 command at 04:51:18. As expected, the first DC-49 command fired the IRS cooldown squibs and started the IRS motor; however, the IRS cooldown was not successful, probably because of a plugged cryostat. The time of NAMG-1 was the expected time of receipt, and was not seen in the data because the first DC-49 command performed the IRS firing in the pyrotechnic subsystem. Furthermore, the second DC-49 command exhibited only the normal event-register responses; because neither the NAMG-1 nor the second DC-49 command produced pyrotechnics events in the event registers, it was concluded that the IRS cooldown squibs had no bridge-wires short-circuited to ground. This implied that the spent squibs had opened the firing circuit to ground, as expected.

The TV experimenters wished the TV picture that the CC&S counted as number 1 in the near-encounter slewing strategy to be a TV-A (wide-angle) picture taken with a blue filter; also, the picture was to contain the limb of the planet. The strategy adopted to assure this condition was to have NAMG-2 (which starts the near-encounter picture-taking sequence) enabled in the DAS by an N6 event just before the NAMG-2 expected time of triggering. Along with the timing of the DC-25 command at  $\sim E - 52$  h to place a blue filter at the proper time, this strategy would ensure that the correct picture would be counted as number 1.

The next two events observed were: (1) the CC&S N6 event to the DAS at 05:10:04, which enabled the near-encounter sequence logic in the DAS, and (2) the NAMG-2 PIFOV signal to the DAS, which initiated the near-encounter sequence at 05:10:10. The N6 event occurred on time, but the NAMG-2 occurred 12 s earlier than predicted; however, no problem was posed by this because the tolerance on that event was  $\pm 15$  s. Immediately upon receipt of the NAMG-2, the DAS issued the start encounter timer command to the CC&S, thereby initiating the CC&S near-encounter program and the ATR and DTR start commands to the data storage subsystem; this placed the subsystem in the near-encounter record (both) mode. The ATR then commenced to record TV data (from the position on track 1 where it had previously stopped), which were the outputs of the wide- and narrow-angle cameras shuttering alternately on 42.2-s centers. The two TV cameras took 26 pictures of the Martian surface, with the wide-angle picture overlapping and the narrow-angle picture centered successively in each region of overlap. The 26 TV pictures were recorded on tracks 1, 2, 3, and part of 4; pictures 1, 3, and 5 showed the limb of the planet.

The DTR started to record in digital form the data from the IRS, IRR, and UVS instruments plus every seventh picture element (pixel) from the TV pictures. However, these data were also transmitted in real-time to the Earth over the high-rate telemetry link (encounter 2 data mode at 16.2 kbits/s) before, during, and after the period of digital recording; this mode was the primary method of return of the near-encounter digital data.

The near-encounter sequence proceeded in an expected manner. Ground commands and CC&S commands were processed in the spacecraft nominally. Following the NAMG-2 signal, the first of nine backup DC-16 commands on 1-min centers arrived at 05:10:11 (Earth-observed time) to provide a backup to it; thus, if the NAMG-2 signal had failed or been late, the first DC-16 command would have started the near-encounter sequence in the same way.

The first of 11 N4-N1\* events issued by the CC&S to the scan control subsystem was received after picture 1 shuttered at 05:10:33. As noted earlier, this combination of commands had the net effect of resetting the AAC in the TV subsystem. The remaining 10 N4-N1\*

events were issued, as expected, following pictures 2-4 and 6-12.

The scan platform, upon which the TV cameras and science instruments were mounted, moved from one angle to another in four slews during near-encounter according to the CC&S computer-programmed sequence, thus covering areas that would not have been within range if the instruments had maintained a fixed angle during the swath of *Mariner VI* across the planet. In this way, the platform slewed to new positions after specific TV pictures had been taken, as shown in Table 3.

**Table 3. *Mariner VI* near-encounter scan-platform positions.**

Slew	After near-encounter picture	Clock position, deg		Cone position, deg	
		From	To	From	To
1	8	261.7	248.1	128.4	128.3
2	13	247.9	267.8	128.3	100.1
3	17	267.8	265.8	—	—
4	32	265.8	271.9	—	—

The slews in clock position were accomplished by the issuance of appropriate N3 commands on 1-s centers from the CC&S to the scan control subsystem, which produced about 1 deg of motion for each N3 command. Thus, the first clock slew resulted from 14 N3 commands (13.7 deg), the second clock slew from 20 N3 commands (19.7 deg), the third clock slew from two N3 commands (2 deg), and the fourth clock slew from six N3 commands (6.1 deg). The polarity of each slew was determined by programming the set or reset of the clock polarity relay in the CC&S before each slew for a negative or positive direction. The single slew in cone position (after picture 13) was achieved by the N4 command from the CC&S that initiated the slew of the scan platform to the final cone position of 100.1 deg from a fixed-reference source. To ensure that the scan platform would slew in cone, use was made of 20 N4 commands on 1-s centers after picture 13, two N4 commands on 1-s centers after picture 17, and six N4 commands on 1-s centers after picture 32, plus three DC-41 ground commands on 1-min centers (after the 20 N4 commands); however, the first N4 command at 05:19:01 was sufficient.

The ATR was stopped by the N8 command from the CC&S at 05:32:19, just after the spacecraft crossed the terminator to the night side of Mars, but the DTR continued to record digital science data for 2.5 min afterward to obtain measurements on the dark side of the planet. The ATR was stopped before the end of track 4 rather than have it continue recording until the end of track 4, at which time it would have automatically been stopped by the end-of-tape mark, for two cogent reasons:

- (1) After the terminator of the planet had been crossed, pictures of dark space having no scientific value would be recorded on the balance of ATR track 4.
- (2) Experience had shown that several minutes were needed after high-rate telemetry (16.2 kbits/s) was initially received on the Earth before the DSN equipment could lock up on the downlink to produce satisfactory data.

Next day it was planned to play back the TV pictures stored in the ATR to DSS 14 over the high-rate telemetry link; therefore, it was desirable to have the ATR initially commence its playback with data that were of no value because these data would be lost during the few minutes it took the DSN equipment to achieve good data output.

The DTR recorded data on all of its tracks until the DEOT = 4 signal (at the end of track 4) was seen at 05:34:46; this terminated the record mode. As a backup to stop the DTR, an N9 event from the CC&S was issued 9 s later to the data storage subsystem. As noted earlier, all science data recorded on the DTR were also transmitted to the Earth in real-time on the high-rate telemetry link.

Approximately 5 min after completion of recording, the spacecraft passed behind Mars at 05:39:52, and radio contact was lost for 20 min. The S-band occultation experiment was conducted as *Mariner VI* entered and exited the occultation zone. The spacecraft entered occultation in the two-way RF mode; that is, the up-link frequency transmitted from the Earth was coherently retransmitted to the Earth by the spacecraft RFS. Exit data were obtained in the one-way RF mode, in which the spacecraft transmitter derives its frequency from its on-board auxiliary oscillator (a crystal-controlled oscillator). During the entry and exit of the radio beam through the Martian atmosphere, the frequency and

amplitude of the signal received on the Earth were changed by effects of refraction on the propagation of the radio signal.

Three minutes after the spacecraft entered occultation, the CC&S was programmed to issue a P2 event to command the data storage subsystem and FTS to the playback 1 mode (270 bits/s). It is assumed that the event was issued on time because, at exit from occultation, the FTS and data storage subsystem were indeed in the playback 1 mode. The choice of this mode at that time was determined by two considerations: (1) It was discovered in ground testing of the proof-test model spacecraft that any large transient occurring in the spacecraft while the data storage subsystem was in the ready mode with science power on would result in spurious ATR start and stop signals from the DAS to the data storage subsystem. This situation would result in the destruction of all or part of the data stored in the subsystem. Therefore, placing the subsystem in the playback 1 mode would make it immune to such spurious signals, and thus neutralize that potential threat. (2) It was believed that a change of mode should be accomplished as soon as possible after *Mariner VI* entered occultation so that the spacecraft would have "settled out" any disturbances resulting from a change of mode by the time it exited; therefore, its state would be least disruptive to the occultation experiment.

The near-encounter phase was essentially complete when the spacecraft had exited from behind Mars at 05:59:42. The FTS was in the playback 1 mode at 270 bits/s, and the data storage subsystem was playing back science data stored in the DTR.

## XII. *Mariner VI* Playback

The playback phase of *Mariner VI* was initiated by the CC&S P2 command at the assumed time of 05:42:41 on July 31, which was during the 20-min period when the spacecraft was occulted from the Earth by the planet and no radio link was present. Upon exit of the spacecraft from occultation at 05:59:42, the radio link was restored, and the data confirmed that the FTS and the data storage subsystem were in the playback 1 mode at 270 bits/s.

The playback phase continued for about 24 h; it was then suspended so that *Mariner VII* encounter



operations could begin. The *Mariner VI* playback phase resumed on August 7, and continued until it was terminated on August 11. During the playback phase the data storage subsystem was exercised in the following modes:

- (1) Two playbacks of the stored near-encounter science data on the DTR in the playback 1 mode at 270 bits/s.
- (2) Six playbacks of the near-encounter pictures stored on the ATR in the playback 2 mode at 16.2 kbits/s (over the high-rate telemetry link).
- (3) Two analog-to-digital transfers of data from the ATR to the DTR, followed by playbacks of the DTR in the playback 1 mode at 270 bits/s.

At this point, it is appropriate to review the playback modes that the spacecraft could employ during the mission.

In the playback 1 mode, the DTR plays back its stored data to the Earth through the FTS at 270 bits/s. After the playback 1 mode has been initiated, the DTR is constrained by the data storage subsystem logic to play back its four tracks twice unless it is interrupted by commands that place it in another mode. However, if it is interrupted by other commands, the next time the playback 1 mode is restored, the DTR will play back from the point at which it was stopped when it terminated the playback 1 mode. The constraint of playing back the four tracks of the DTR twice is satisfied when nine end-of-tape marks are counted in the data storage subsystem logic. Upon completion of two playbacks of the DTR, the subsystem automatically enters the analog-to-digital transfer mode in which the ATR plays back data through an analog-to-digital converter (A/DC) to the DTR until the DTR is filled (as evidenced by four end-of-tape signals). Then the playback 1 mode is automatically started, and the DTR plays back its recorded data. The process of analog-to-digital transfer and DTR playback would then continue indefinitely. Thus, the playback 1 mode is essentially a DTR playback at 270 bits/s.

In the playback 2 mode, the ATR plays back recorded TV data in analog format into an A/DC. The output of the A/DC is a bit stream with a data rate of 16.2 kbits/s. These digital data are then returned to the Earth through the FTS over the high-rate telemetry link. The only Deep Space Station capable of receiving the high-rate telemetry is DSS 14, with its 210-ft-diam

antenna. To enter the playback 2 mode, a DC-44 command is required, and the data storage subsystem must be in the playback 1 mode when the DC-44 command is used. To exit from the playback 2 mode, another DC-44 command is required to place the data storage subsystem in the playback 1 mode. Thus, the playback 2 mode is essentially an ATR playback at 16.2 kbits/s.

The data storage subsystem performed nominally in the playback phase, with the following exceptions: (1) During the playback of track 1 of the DTR (at 270 bits/s), an excessive number of bit errors were present, causing the ground equipment to drop lock repeatedly and resulting in the loss of digital data stored on that track. However, because those data were transmitted in real-time (in parallel) over the high-rate telemetry link, all near-encounter digital science data were returned to the Earth. The cause of the problem was believed to be a degraded tape-to-head interface caused by debris buildup on the face of the playback head. (2) During the playback of the eight near-encounter pictures stored on ATR track 1 in the playback 2 mode (16.2 kbits/s), it was found that the ATR had experienced a 46% reduction in gain compared to the level of gain observed before launch. Fortunately, this did not cause the loss of any data, but the first eight pictures of the near-encounter sequence were degraded. It was believed that this problem had a cause similar to that of the DTR; i.e., a piece of debris lodged on the face of the playback head.

A description of the activities performed during the playback phase of *Mariner VI* is contained in the paragraphs that follow.

The DTR continued to play back its stored science data at 270 bits/s for approximately 18.5 h, during which time three tracks and 20 min into the fourth track were played back. Meanwhile, three events took place to properly return the spacecraft to a modified cruise mode: (1) A DC-48 ground command was received at 07:10:36 on July 31 to precondition the spacecraft for science power turn-off by positioning the TV camera shutters (which had been shuttering alternately on 42.2-s centers since the DC-25 command turned science power on at  $E - 53$  h) to the closed position and by positioning the IRR mirror to the calibrate (stowed) position. (2) An  $\overline{M1}$  event was issued by the CC&S to the attitude control subsystem at 09:32:51, which

removed the all-axis-inertial mode and aligned the spacecraft with the Sun and Canopus. The gyros turned off 3 min later. (3) An N5 command was issued by the CC&S at 12:32:50, which turned off power to the science instruments and the scan platform.

After initially entering the playback 1 mode, the data storage subsystem was constrained by its logic to play back the DTR data twice (unless interrupted by appropriate commands) before it would automatically enter the analog-to-digital transfer state. Because DSS 14, with its 210-ft-diam antenna, was the only Deep Space Station capable of receiving high-rate data (16.2 kbits/s), it was necessary to wait until the spacecraft was again in its view. Thus, at 00:37:43 on August 1, a DC-44 command was received by the spacecraft, which interrupted the DTR playback of its data on track 4 and switched the data storage subsystem and FTS to the playback 2 mode (16.2 kbits/s) over DSS 14. In this mode, the 26 near-encounter pictures contained in the ATR were played back at 16.2 kbits/s over the high-rate telemetry link to the Earth. Thus, it would take only 2 h 50 min to play back the four tracks of the ATR. After playing back the 26 near-encounter pictures once, the data storage subsystem automatically played them back a second time.

During this double playback of the ATR data, three ground commands were transmitted to the spacecraft on August 1:

- (1) A DC-13 command was received at 02:46:43 to ground the motor-burn-start capacitors in the pyrotechnic subsystem, to disconnect the attitude control subsystem from the CC&S maneuver relays, and to switch the CC&S to the nontandem standby mode.
- (2) A DC-33 command was received by the spacecraft at 02:56:44 to switch the CC&S to the tandem standby mode.
- (3) A DC-9 command was received by the spacecraft at 04:41:44 to turn on the ranging channel in the RFS.

Upon completion of two playbacks of the 26 near-encounter pictures stored in the ATR, it was necessary to suspend the playback phase of *Mariner VI* so that mission operations personnel could start the activities associated with the upcoming *Mariner VII* encounter. Therefore, at 05:51:45 on August 1, a DC-1 command

was received that switched the FTS to the cruise data mode and placed the data storage subsystem in the ready state, thus suspending the playback phase of *Mariner VI*.

The spacecraft continued to cruise in this mode, while *Mariner VII* was undergoing its encounter and post-encounter phases, until August 7, when a DC-3 command was received at 16:17:38, which switched the FTS and data storage subsystem to the playback 1 mode. The DTR then resumed playing back its data from the point on track 4 at which it had been stopped on August 1 (00:37:43) when the data storage subsystem had been switched to the playback 2 mode by a DC-44 ground command. The spacecraft remained in the playback 1 mode for the next 7 h. During this period, 23 coded commands were transmitted to modify the CC&S memory as follows:

- (1) Change the occurrence of Y1 events from 3- to 24-h intervals.
- (2) Modify the remaining cruise event times.
- (3) Remove the all-axis-inertial instruction from the executive subroutine.

A CC&S memory readout was commanded by a DC-2 command at 23:17:43 to verify that the coded commands were accepted properly. Finally, a DC-9 command was received at 23:22:41 to turn on the ranging channel in the RFS.

The DTR was on track 1 during the second playback of its data when a DC-44 command was received at 23:30:00, switching the spacecraft to the playback 2 mode. At this time, DSS 14 was in view of the spacecraft and the high-rate telemetry could, therefore, be received. The playback 2 mode was maintained for about 5.5 h, during which a third and fourth playback of the near-encounter pictures stored in the ATR were accomplished. Upon completion of the fourth playback of ATR data, a DC-44 command was received at 05:10:45 on August 8, which switched the spacecraft back to the playback 1 mode. The DTR then resumed playback from the point on track 1 at which it was halted 5.5 h earlier. The data storage subsystem remained in the playback 1 mode for approximately the next 18 h, during which tracks 1, 2, 3, and part of 4 in the DTR were played back. Then, at 23:14:57 on August 8, a DC-44 command was received that switched the spacecraft from the playback 1 to the playback 2 mode.

After switching from DTR playback (playback mode 1) to ATR playback (playback mode 2), the spacecraft commenced the fifth playback of the 26 near-encounter pictures stored in the ATR over the high-rate telemetry link (DSS 14); this was followed by a sixth playback. The high-rate playback of the data continued for 5 h 41 min, through a fifth and sixth playback, when a DC-44 command was received at 04:55:52 on August 9, which switched the spacecraft to the playback 1 mode. At this point, the DTR resumed its playback of stored near-

encounter data, continuing until 16:17 on August 9, when the data storage subsystem logic had counted nine DEOTs, thus signifying completion of the double playback of the four tracks of the DTR. The analog-to-digital transfer mode then immediately started. In this mode, the ATR played back its data through an A/DC, whose output was recorded on the DTR. The four tracks of the DTR were filled at 16:41:26 on August 9, as indicated by a DEOT = 4 signal. The data storage subsystem then automatically switched to the playback 1 mode; the DTR played back this digitized conversion of the ATR pictures at 270 bits/s for about 24 h 41 min. When all four tracks of the DTR had completed the playback at 17:21:00 on August 10, as evidenced by a DEOT = 4 signal, the data storage subsystem then switched to the analog-to-digital transfer mode. The DTR again recorded digitized data from the ATR in this mode until 17:45, when the four tracks were filled. Another DTR playback immediately ensued, and continued until 18:33:18 on August 11, when a DC-1 command terminated the playback and placed the spacecraft in the cruise mode.

Although two analog-to-digital transfers were accomplished, the playback of some near-encounter pictures was only a test to determine the adequacy of this mode. The primary return of near-encounter pictures was achieved by the six playbacks of those data in the playback 2 mode. Table 4 lists the modes employed in the playback phase of *Mariner VI* and the stimulus used to initiate or terminate each mode.

### XIII. *Mariner VII* Pre-Encounter Anomaly

On July 30 and 31, 1969, the *Mariner VII* spacecraft experienced a number of major anomalies that have become known collectively as the *Mariner VII pre-encounter anomaly*. This sequence of anomalous events was initiated by a loss of signal (LOS) from the spacecraft, reported by DSS 51 (Johannesburg) at about 22:11 on July 30, and was concluded some 13.5 h later with the reacquisition of the spacecraft roll reference at 11:35 on July 31, as reported by DSS 41 (Woomera). The anomalies began 5 days before the *Mariner VII* encounter and only 7 h before the *Mariner VI* encounter.

Although the *Mariner VII* anomaly had profound effects on the subsequent far- and near-encounter operations, the actual sequence executed and the science return obtained from the *Mariner VII* encounter were actually more desirable than those originally planned. It

**Table 4. *Mariner VI* playback phase**

Mode	Stimulus	Earth-observed time (GMT)	
		Time	Date
Start playback 1	P2 (CC&S) <sup>a</sup>	05:42:41	Jul 31
End playback 1 and start playback 2	DC-44 (FCS) <sup>b</sup>	00:37:43	Aug 1
End playback 2 and return to cruise mode	DC-1 (FCS)	05:51:45	Aug 1
End cruise mode and start playback 1	DC-3 (FCS)	16:17:38	Aug 7
End playback 1 and start playback 2	DC-44 (FCS)	23:30:00	Aug 7
End playback 2 and start playback 1	DC-44 (FCS)	05:10:45	Aug 8
End playback 1 and start playback 2	DC-44 (FCS)	23:14:57	Aug 8
End playback 2 and start playback 1	DC-44 (FCS)	04:55:52	Aug 9
End playback 1 and start A/D <sup>c</sup> transfer	Counter = 9 (data storage subsystem)	16:17:00	Aug 9
End A/D transfer and start playback 1	DEOT <sup>d</sup> = 4 (data storage subsystem)	16:41:26	Aug 9
End playback 1 and start A/D transfer	DEOT = 4 (data storage subsystem)	17:21:00	Aug 10
End A/D transfer and start playback 1	DEOT = 4 (data storage subsystem)	17:45:00	Aug 10
End playback 1 and return to cruise mode	DC-1 (FCS)	18:33:18	Aug 11

<sup>a</sup>CC&S = central computer and sequencer.  
<sup>b</sup>FCS = flight command subsystem.  
<sup>c</sup>A/D = analog-to-digital.  
<sup>d</sup>DEOT = digital end of tape.

is, therefore, appropriate to separate the description of the *Mariner VII* anomaly from the encounter phases of the spacecraft. The investigation, analyses, and conclusions with respect to this event were carried out by a failure review board instituted 2 wk after its occurrence. A documentation of the findings of the failure review board has been published,\* and the discussion presented herein is abstracted from that report.

The spacecraft state was in a normal cruise mode, with the following three exceptions:

- (1) The data storage subsystem was on and in the ready mode because a subsystem calibration had been performed 2 wk earlier, and it was then decided that the subsystem should remain on through encounter.
- (2) The RFS was in the TWT high-power mode (20 W) instead of the planned low-power mode (10 W) to support the high engineering telemetry data rate of 33½ bits/s.
- (3) The battery charger was on, as it had been for the previous 5 days, to replace charge drained from the battery to condition it properly for the encounter phase of the mission.

An abridged chronology of events is presented in Table 5. For convenience, this table may be divided into five segments, which are indicated by numbers in circles. The first segment encompasses the interval of time associated with an unexpected battery charge current profile, which was the first indication of anomalous spacecraft behavior, near the time of the *Mariner VII* pre-encounter anomaly. This profile started on July 26 (4 days before the anomaly), and continued (with numerous intervals of battery charger current fluctuations) through July 31 (13 h after the start of the anomaly).

The second segment of time in Table 5 is associated with the spacecraft LOS for a period of approximately 7 h (this segment of time will be referred to as the *first LOS*). The first LOS was reported by DSS 51, which was configured for a normal cruise track of *Mariner VII*. The signal was lost during a relatively inactive portion of the pass corresponding to the latter half of the scheduled track. Upon receipt of the report of the LOS, DSSs 11, 62, and 42 were called up to assist in the search for the spacecraft. Real-time analysis of the data showed the following:

- (1) The LOS was associated with the spacecraft and was not a malfunction of the tracking station.
- (2) The FTS was experiencing anomalous behavior.
- (3) Evidence existed to support the possibility of power transients on the spacecraft.
- (4) The nature of the downlink signal strength profile immediately before the LOS and the "weak periodic signals" reported by DSSs 11 and 42 implied a loss of either the Sun or roll references (or both).

The immediate concern was the possibility that the spacecraft had lost Sun acquisition and was being sustained, either partially or wholly, by the battery. The capacity of the battery was estimated to be approximately 5 h (if the spacecraft load was being supported solely by the battery). A recommendation was made to the project manager to transmit a DC-10 command (switch spacecraft-transmitted signal from high-gain to low-gain antenna) from DSS 11 as soon as possible. The intent of the DC-10 command was to reacquire the signal from the spacecraft if the attitude references had been lost, and to take appropriate corrective action before depletion of the battery should the battery be supporting the spacecraft electrical load. An element of risk associated with the proposed command exercise was the fact that DSS 11 (the only tracking station within view of the spacecraft and not committed to the *Mariner VI* encounter) had not been command-qualified. A separate SPAC-mission control-DSN interface network was established to preclude the possibility of interference with the *Mariner VI* encounter. After a successful test of network procedures on the new network, approval was given by the project manager to transmit 20 DC-10 commands to the *Mariner VII* spacecraft.

The first DC-10 command was transmitted by DSS 11 on July 31 at 05:10:00, with 19 additional DC-10 commands scheduled on 1-min centers. The round-trip light time to the spacecraft was 10 min 18 s; thus, the first expected time of the observed effects of the DC-10 command on the Earth was at 05:21:15. Tracking in three-way, DSS 42 reported a signal from *Mariner VII* at 05:21:15, with a signal level corresponding to that expected from the low-gain antenna. After confirmation of a nominal spacecraft signal, DSS 11 was requested to terminate transmission of the remaining DC-10 commands. A total of 12 DC-10 commands were transmitted to and received by the spacecraft.

---

\*Gottlieb, T., JPL informal report, Apr. 15, 1970.

Analysis of the spacecraft data revealed that *Mariner VII* had experienced a drastic change of state, but that it was Sun-acquired and not dependent on the battery.

At approximately 06:00 (about 45 min after the *Mariner VI* encounter), the SPAC team transferred its attention to the *Mariner VII* anomaly, and a more comprehensive effort to determine the exact nature of the anomaly was initiated.

The third segment of time in Table 5 is associated with a second LOS, which started at 06:33:49 (approximately 72 min after the reacquisition of the signal with DC-10 commands) and continued for about 70 min. This LOS was characterized by the presence of the main spacecraft carrier at the expected signal level and frequency, but with the absence of telemetry data modulation on the data subcarrier. The second LOS terminated abruptly and spontaneously at 07:43, when the data reappeared and showed another change in spacecraft state.

Because one of the effects associated with the first LOS was a component failure in the FTS, which in turn affected the ability to interpret the spacecraft status, a DC-6 command (switch FTS redundant elements) was transmitted to the spacecraft in an effort to alleviate the situation. The DC-6 command was received by the spacecraft, and the FTS switched to the redundant elements. The command, however, did not correct the problem, which indicated that the failure was not in the primary elements.

The fourth segment in Table 5 is associated with the reacquisition of the roll reference of the spacecraft. During the first LOS, the attitude control subsystem had lost roll reference (Canopus) and, upon reacquisition of the signal, was found to be in a free-roll state (the roll axis of the spacecraft was not under Canopus star tracker control; it was free to drift in angular position, the only controlling factor being gyro angular-rate limiting). Because the Canopus star tracker was found to be in a roll-search mode, it was deduced that the 30-s roll search inhibit logic had been set. To reinstate roll search to acquire Canopus, a DC-21 (roll search) command was transmitted to the spacecraft at 09:45:00. The spacecraft responded normally to the command, and an object was acquired at 10:02:01.

Because both Canopus and Jupiter were acquirable at this time, and the initial roll position of the Canopus

star tracker was unknown, there was no assurance that the object acquired was Canopus (the telemetry channel containing the tracker intensity was inoperative); therefore, another DC-21 command was transmitted at 10:17:00. After a second roll search, the spacecraft acquired an object at 10:34:21. From the duration of the roll search, it was determined that the second object acquired was Jupiter, and a third DC-21 command was transmitted at 10:40 with the intent of acquiring Canopus. An object, believed at the time to be Canopus, was acquired at 11:07:57. To increase the spacecraft telemetry signal strength, and to reestablish a normal cruise mode, a DC-11 (transmit via high-gain antenna) command was transmitted to the spacecraft at 11:20:00. Upon receipt of this command, the downlink signal from the spacecraft disappeared unexpectedly, and spontaneously reappeared at 11:35:19. At the end of the third LOS, the telemetry showed the gyros to be on and the spacecraft to be in the final phase of a roll-search mode.

In retrospect, it was found that the roll-reference object acquired at 11:07:57 was not Canopus and, as a consequence, the boresight of the high-gain antenna was not pointing to the Earth. Thus, when the DC-11 command was transmitted, the signal from the spacecraft was lost. Careful examination of the spacecraft telemetry data revealed that the object believed to be Canopus was actually an unknown object (at a clock angle of  $\sim 338$  deg) that was not present during the first roll search and was diminishing in brightness from the time it was acquired. It is believed that, sometime after the receipt of the DC-11 command, the object diminished in brightness sufficiently to violate the Canopus star tracker low-gate logic, and automatically initiated a roll search that finally culminated (at  $\sim 11:35$ ) in the reappearance of the spacecraft telemetry signal. Thus, the third LOS was a normal and expectable consequence of transferring the spacecraft transmitter to the high-gain antenna when the spacecraft was not Canopus-oriented in roll.

The fifth and final segment of time in Table 5 is associated with a special test performed on the spacecraft to determine the state of the battery, battery charger, and battery test load. The test was performed in an attempt to explain one of the trajectory perturbations noted after the second LOS. The doppler residual profile revealed that the spacecraft was experiencing an exponentially decaying force as a function of time (with a time constant of  $\sim 20$  h). Before the *Mariner VII* encounter, it was believed that the IRS gas containers were the most likely source of this force on the spacecraft.

**Table 5. Mariner VII pre-encounter anomaly—abridged sequence of events**

Time (GMT)	Event
Jul 26 14:12	Start of unexpected battery charger current fluctuations (continued through Jul 31)
Jul 30 22:10:58.66	Start of FTS <sup>a</sup> anomalous behavior
22:11:08	Spacecraft signal strength began gradually to decrease from -140 dBmW
22:11:48	Spacecraft signal strength leveled off at -162 dBmW
22:12:59	DSS 51 receiver went out of lock
Jul 31 03:51:00	DSS 11 picked up a weak periodic signal, but could not lock up
04:40:00	DSS 42 picked up a weak periodic signal, but could not lock up
05:10:00	DSS 11 transmitted first of 12 DC-10 commands (transmit low)
05:21:15	DSS 42 acquired three-way lock at a signal strength of -161.5 dBmW
05:25:21	DSS 41 TCP <sup>b</sup> in lock (engineering data showed numerous changes in spacecraft status)
06:28:19	Two-way station transfer from DSS 11 to DSS 41
06:33:49	DSS 14 and DSS 41 receivers went out of lock during station transfer
06:34	DSS 14 receiver regained lock, but there were no data on DAS <sup>c</sup>
07:43:18	DSS 41 TCP in lock (engineering data showed numerous changes in spacecraft status)
09:11:15	DC-6 command (switch FTS redundant elements) transmitted
09:45:00	DC-21 command (roll search) transmitted
10:02:01	Canopus acquired
10:17:00	DC-21 command transmitted
10:34:21	Jupiter acquired
10:40:00	DC-21 command transmitted
11:07:57	Unknown object acquired
11:20:00	DC-11 command (transmit high) transmitted
11:31:19	DSS 41 receiver went out of lock
11:35:19	DSS 41 TCP in lock (showed roll search)
11:38:01	Gyros off (Canopus acquired)

① = battery charge duration.      ③ = second LOS.  
 ② = first loss of signal (LOS).      ④ = third LOS.

**Table 5 (contd)**

Time (GMT)	Event
Aug 1 06:50:00	DC-38 command (battery charger off) transmitted
Aug 12 23:30:00 to Aug 13 03:13:08	Battery, battery charger, and battery test load were tested. Battery charger and test load were found to be operating; battery was found to have failed
⑤ = battery test.	

After a normal IRS cooldown at encounter, however, the only remaining source of the unexpected force on the spacecraft was the battery.

After a number of commands had been sent to the spacecraft on August 12 and 13 (13 days after the start of the anomaly) to turn on the battery charger and test load, it was concluded that the test load and battery charger were operating normally, but that the battery was open-circuited.

In the course of the investigation that followed the occurrence of the *Mariner VII* pre-encounter anomaly, it was determined that the spacecraft experienced a series of anomalies that resulted in the following general observed effects:

- (1) Four days before the anomaly, the battery began to fail while in the process of being recharged.
- (2) The anomaly was characterized by the complete loss of spacecraft telemetry on three separate occasions over a period of approximately 13 h.
- (3) The spacecraft trajectory was perturbed by approximately 130 km in the **R • T** plane as a consequence of the anomaly.
- (4) Of the 97 *Mariner VII* engineering telemetry channels, 20 were permanently disabled.
- (5) The battery failed.
- (6) The spacecraft temporarily lost its roll reference.
- (7) Of the 19 subsystems aboard the spacecraft, nine experienced various effects of what appeared to be major electrical transients on the spacecraft.

Although the evidence is inconclusive, it strongly implies that the most probable cause of the anomaly is structural failure of the spacecraft battery.

The failure sequence of events is believed to be as follows:

- (1) One of the 18 cells in the battery failed by short-circuiting its positive and negative plates.
- (2) In a manner unknown at present, the failed cell produced high internal pressures and propagated the failure to other cells in the battery.
- (3) The internal pressure, having reached a sufficiently high level, caused the outer case of the battery to rupture and allowed the fluid content of the battery to escape.
- (4) The fluid escaping from the battery pressurized the inside of the spacecraft bus to a level sufficiently high to induce a corona effect or arcing in the Canopus star tracker (one of the components of the attitude control subsystem).
- (5) This arcing was responsible for the observed electrical transients and the associated telemetry failure.
- (6) The gas escaping from the inside of the spacecraft bus, through the openings in the thermal blanket, caused the observed perturbation in the spacecraft trajectory.

#### **XIV. Mariner VII Far-Encounter**

The far-encounter phase of *Mariner VII* was extremely successful, notwithstanding the near-catastrophic anomaly that the spacecraft suffered on July 30 and 31, 1969. A total of 93 far-encounter TV pictures were returned in three sets of 34, 34, and 25 pictures, respectively, during the period starting at  $E - 67.5$  h and ending 2.5 h before closest approach. Thus, the primary objective of the *Mariner VII* far-encounter phase of returning narrow-angle TV-B camera pictures was eminently achieved.

Because of the effects of the pre-encounter anomaly on the engineering telemetry, a comprehensive investigation of spacecraft status and capabilities was held to determine whether any limitation or degradation in spacecraft performance was evident that would prevent the execution of the planned far-encounter sequence. Analysis of spacecraft status was hampered by the loss

of 20 telemetry channels that provided the following engineering data:

- (1) Pitch gyro rate/pitch Sun sensor fine position (channel 105).
- (2) Yaw gyro rate/yaw Sun sensor fine position (channel 106).
- (3) Roll gyro rate (channel 107).
- (4) Canopus intensity (channel 108).
- (5) Scan clock coarse position (channel 200).
- (6) Scan cone coarse position (channel 201).
- (7) Inverter output voltage (channel 203).
- (8) Inverter output current (channel 204).
- (9) 400-Hz inverter input current (channel 205).
- (10) Battery voltage (channel 206).
- (11) Scan cone reference angle/cone fine position (channel 207).
- (12) FEPS cross cone error signal (channel 208).
- (13) FEPS cone error signal (channel 209).
- (14) Power sequencer and logic (PS&L) raw current to RFS and heaters (channel 300).
- (15) TWT 2 anode voltage and indicator (channel 302).
- (16) TCFM guard temperature (channel 305).
- (17) Exciter supply voltage and indicator (channel 306).
- (18) Adaptive gate setting (channel 307).
- (19) TWT helix current (channel 308).
- (20) Canopus cone angle position (channel 309).

The most serious consequence of the above loss of telemetry was the inability to determine scan-platform cone position because of the failed channels 201 and 207. Such an inability would have inhibited the performance of the planned near-encounter sequence, which required scan-platform slews in cone position (as well as clock) from a *known* initial position. However, a method was found to overcome this handicap. It involved the use of the TV-B camera (narrow-angle field of view) and the planet Mars.

The plan evolved was to track the planet with the scan control subsystem in the far-encounter mode under FEPS control to determine whether the science and scan con-

trol subsystems were working correctly. Then quantitative commands were used to place the near-encounter reference potentiometers at the assumed far-encounter position of the scan platform. The scan control subsystem was then commanded to the near-encounter mode, and the scan platform moved slightly (from closed-loop to open-loop tracking) to the far-encounter position dictated by the near-encounter reference potentiometers. The high-rate telemetry mode was then commanded on (encounter 2), which produced digital real-time TV pictures of the planet through the TV-B camera.

The receipt of these pictures on the real-time TV display in the mission operations area showed Mars to be about 7 deg in cone angle and about 1 deg in clock angle offcenter of the field of view. It then became a matter of sending quantitative commands to center the planet in the TV-B camera field of view to establish the reference position. A TV-B picture was then recorded on the tape recorder in the near-encounter mode, followed by another TV-B picture recorded in the far-encounter mode. These two recorded pictures were then transmitted to the Earth over the high-rate telemetry link for comparison and refinement of the measurement of cone position. The number of quantitative commands to slew the near-encounter reference potentiometers back to the desired near-encounter initial position was then deduced, and the commands were sent. The cone angle stored in the near-encounter reference cone potentiometer was then determined, and it was merely required to keep track of commands to the near-encounter cone potentiometer to determine the current cone angle of the scan platform.

It is appropriate to note that a more ambitious far-encounter sequence, involving three sets of TV pictures, was planned for *Mariner VII* in the expectation of a successful two-set sequence from *Mariner VI*. Because the FEPS sensor had been verified in ground testing as operable from  $E - 76$  h, and the *Mariner VI* far-encounter sequence proved to be completely successful, the decision to implement a three-set sequence for *Mariner VII*, starting at about  $E - 68$  h, could be made with a high degree of confidence.

Thus, upon completion of the analysis of spacecraft status, including necessary spacecraft preconditioning and the successful determination of the scan-platform cone position, it was decided by project management to commit the spacecraft to the planned far-encounter sequence. However, the sequence was to be modified

somewhat to permit the first set of far-encounter TV pictures to fit the time available. Therefore, coded commands were loaded into the CC&S at 08:00 on August 2 to change the "D" far-encounter picture sequence intervals from 36- to 27-min centers. A DC-28 command received at 08:46:43 placed the scan control and data storage subsystems in the far-encounter mode. The scan platform then slewed to the far-encounter position, from which the FEPS signal (PIFOV) placed the scan control subsystem in the closed-loop planet-tracking mode. A DC-13 and a DC-32 command followed at 08:51:35 and 09:11:36, respectively, which initiated the 34-picture D far-encounter recording sequence. The first picture of this sequence was recorded at 09:38 on August 2 by an F2 event from the CC&S.

The process continued for the next 15 h, with an F2 event being issued by the CC&S every 27 min to command the recording of a TV-B picture on the ATR. The thirty-fourth F2 event, at 00:28:39 on August 3, triggered the recording of the last TV picture in this sequence; the recording was terminated at 10 s into the picture by an AEOT = 4 signal in the data storage subsystem, signifying that the fourth ATR track was full. A DC-3 and a DC-44 command placed the FTS and the data storage subsystem in the playback 2 mode 0.5 h later, and the playback of the stored TV pictures commenced over the high-rate telemetry link.

Some 4 min before the last TV picture of the D sequence was recorded, a DC-14 command was received, which connected the CC&S to the attitude control subsystem. Then, at 01:21:43, an M1 command was issued by the CC&S (as a result of a coded command loading), which turned the gyros on. At this point, the time was  $E - 51.5$  h, and (as with *Mariner VI*) the thermal conditions at near-encounter were desired to be stable when an inertial roll-control condition was to be used. Thus, a long enough warm-up period ( $\sim 48$  h) of the gyros in the rate control mode would provide stable thermal conditions when the spacecraft was to go on roll inertial control at  $E - 3$  h.

Playback of the D sequence of TV pictures stored on the four ATR tracks over the high-rate telemetry link at 16.2 kbits/s was completed in 2 h 53 min when a DC-25 command arrived at 03:59:55. This command was timed to arrive just after the fourth end-of-tape mark (AEOT = 4) occurred in the data storage subsystem. The command switched the data storage subsystem to the ready mode and the FTS to the encounter 1 data mode, and



the scan platform slewed to the near-encounter position.

An error in the design of the sequence was discovered shortly afterward, when an attempt to erase the ATR by a DC-39 command with the data storage subsystem in the far-encounter mode (as a result of a DC-28 command sent 14 min earlier) was not successful. This error apparently was not found earlier because this particular segment of the far-encounter phase had not been practiced, either in mission operations or in the Spacecraft Assembly Facility (SAF) with the proof-test model spacecraft. However, sufficient time remained to recover from the faux pas before the second set of far-encounter pictures was to be recorded. Accordingly, a DC-25 command was immediately transmitted to place the data storage subsystem in the ready mode, and was followed 2 min later by two DC-39 commands on 8-min centers, which erased the ATR twice and positioned the tape at track 1. The spacecraft was then ready to commence the recording of the C sequence of 34 TV pictures.

A DC-28 command received at 05:12:43 placed the scan control and data storage subsystems in the far-encounter mode, and caused the scan platform to slew to the far-encounter position, from which the FEPS signal (PIFOV) placed the scan control subsystem in the planet-tracking mode. A DC-32 command received at 05:28:41 initiated the C sequence cycle in the CC&S, and the first picture of the second 34-picture set was recorded 36 min later, at 06:05, by an F2 command from the CC&S. To record the balance of TV pictures in this second far-encounter set of 34, F2 commands were issued on 36-min centers over the next 19 h. The last picture of the C sequence was recorded and terminated 10 s into the picture by the fourth end-of-tape mark (AEOT = 4) at 01:53 on August 4.

Playback of the second 34-picture set commenced 0.5 h later with the receipt of DC-3 and DC-44 commands, which placed the FTS and data storage subsystem in the playback 2 mode. Taking almost 3 h, the playback of the stored 34 pictures was accomplished over the high-rate telemetry link to the 210-ft-diam antenna at DSS 14.

During the playback period, an update of the CC&S program was achieved with the transmission of 60 coded commands. This update changed the near-encounter slewing program from three to four slews, modified the

upcoming B far-encounter picture sequence timing, and changed several CC&S events that were to occur just before near-encounter to be compatible with the modified B sequence timing. The playback period ended with the receipt of a DC-25 command at 05:18:55 on August 4; the data storage subsystem switched to the ready mode, the FTS switched to the encounter 1 data mode, and the scan platform slewed to the near-encounter position.

Two erasures of the ATR were accomplished by transmission of two DC-39 commands on 8-min centers. These were followed at 05:46:51 by the receipt of a DC-28 command, which placed the spacecraft in the far-encounter mode preparatory to commencing the recording of the third and last far-encounter set of TV pictures. A DC-32 and a DC-23 command then enabled the far-encounter picture sequence generator in the CC&S and stepped the ATR track to 2, respectively. At 08:11:55, the CC&S issued the first F2 event of the 25-picture B sequence to command the recording on ATR track 2 of a TV-B picture. Proceeding for approximately 16 h, the CC&S issued F2 events on 47-min centers for the first 20 pictures, and on 12-min centers for the last five pictures. At 00:05:42 on August 5, the twenty-fifth and last picture of the B sequence completed its recording on ATR track 4, as indicated by an AEOT = 4 signal at 38 s into the picture.

A DC-23 command to step the ATR track from 1 to 2, and DC-3 and DC-44 commands to begin playback of the 25 stored pictures, were next received on the Earth. Playback over the high-rate telemetry link continued for 2 h 10 min, during which the far-encounter TV-B pictures recorded on ATR tracks 2, 3, and 4 were retrieved.

During the playback period, a final update of the near-encounter slew sequence in the CC&S was stored in memory by the transmission of six coded commands. Also, the final adjustment in the near-encounter scan-platform initial position (cone) was commanded with a QC-2-1 command. Finally, the spacecraft was placed on roll inertial hold with the transmission of DC-18, DC-21, and DC-13 commands.

The far-encounter phase of *Mariner VII* was concluded when the playback of the 25 pictures of the B sequence was terminated by a CC&S N1 command received at 02:24:52 on August 5, which switched the FTS to the encounter 1 data mode and placed the data storage subsystem in the ready mode.

## XV. *Mariner VII* Near-Encounter

The performance of the *Mariner VII* spacecraft during its near-encounter phase was outstanding, notwithstanding the known deficiencies (20 disabled telemetry channels and a failed battery); in fact, it exceeded the corresponding performance of *Mariner VI*. The IRS cooldown during this encounter was successful; moreover, the total *Mariner VII* science data return surpassed that of *Mariner VI*. Four scan-platform slews were accomplished during the picture-taking sequence, during which seven more TV pictures were obtained than had been acquired during the flyby of *Mariner VI* (33 vs 26). Thus, in the *Mariner VII* near-encounter, as it actually occurred, all of the instruments received more data than had originally been planned. The IRS, UVS, and IRR received increased polar coverage, and obtained additional atmospheric data.

Soon after the start of the *Mariner VII* far-encounter on August 2, the science investigators had completed a preliminary analysis of the *Mariner VI* science return. Their conclusions resulted in a request to project management for a longer near-encounter picture sequence, with an extended viewing period over the south polar cap and a sweep back over the planet (after the series of TV pictures was finished) for the other scanning instruments. However, the additional science data obtained on the lighted side of Mars would fill the DTR before passage over the dark side had been completed. Hence, much of the dark-side science data would have to be received by the high-rate telemetry mode without DTR backup; however, because *Mariner VI* had already demonstrated the effectiveness of the high-rate telemetry mode, this would not prove to be a problem.

Thus, for the first time in the history of interplanetary space exploration, the observations from one spacecraft (*Mariner VI*) in flight would provide the basis for formulating a new strategy for obtaining data from a second spacecraft (*Mariner VII*) in flight. Inasmuch as the *Mariner VI* encounter was successful, and the *Mariner VII* spacecraft was providing satisfactory performance despite its known deficiencies, project management readily approved the request of the science experimenters, and authorized the necessary command sequence for implementing the new near-encounter strategy.

Accordingly, on August 4, 80 coded commands were transmitted to *Mariner VII* to completely restructure the CC&S memory for the newly designed near-encounter sequence. This reprogramming capability of a computer-

ized CC&S clearly demonstrated the great flexibility that the CC&S could provide for mission planners in implementing alternate options of obtaining data from a spacecraft in flight.

Preparation of the spacecraft for the near-encounter sequence started on August 5 with the transmission of three commands (DC-44, DC-39, and DC-46) to place the FTS in the encounter 2 data mode, erase the ATR, and deploy the TV-A camera cover; these commands were received and acted upon properly by the spacecraft. Next, the CC&S N1\* command to the scan control and power subsystems placed the former in the near-encounter mode and slewed the scan platform to the near-encounter position. After this, a DC-26 command to enable NAMG-1 in the pyrotechnic subsystem and NAMG-2 in the DAS was received, followed by a CC&S F3 event to initiate a second erase of the ATR and to position its tape at track 1. During the 6 min 10 s erase period, backup DC-39 and DC-26 commands were received; in addition, a DC-36 command to disable NAMG-2 and reset the DAS near-encounter flip-flop (to prevent premature triggering of the near-encounter CC&S sequence) was received. When the DC-36 command was received by *Mariner VII*, no TV-B picture could be recorded in the data storage subsystem because it was in the erase mode, whereas the *Mariner VI* subsystem had been in the ready mode and thus able to record a TV-B picture.

After a QC-3-2 command had been sent for a final update of the initial scan-platform position, the first of a pair of DC-49 commands on 4-min centers was transmitted at 04:08:40 on August 5. The receipt of the first DC-49 command at 04:20:39 ( $E - 45$  min) showed that the IRS cooldown squibs had fired and that the IRS motor had started. In contrast to *Mariner VI*, the IRS cooldown on *Mariner VII* was successful, and, within 15 min after receipt of the command, the mission operations team could report that the IRS cooldown was normal.

Some 24 min after initiation of IRS cooldown, the CC&S N6 command to the DAS was issued, which enabled NAMG-2 and placed the DAS in the near-encounter mode. The near-encounter sequence could now be started at any time upon the receipt of a DC-16 or NAMG-2 command. As it turned out, the DC-16 command came first; its transmission time was selected to be coincident with the predicted time of NAMG-2. Thus, the near-encounter sequence was initiated with the receipt of the DC-16 command at 04:45:42, which placed

the data storage subsystem in the near-encounter both (ATR and DTR recording) mode and triggered the DAS to issue the start encounter timer command to the CC&S, thereby starting the CC&S near-encounter program. The ATR then commenced to record TV data at the beginning of track 1, these being the output of the wide- and narrow-angle TV cameras shuttering alternately on 42.2-s centers. The two TV cameras took 33 pictures of the Martian surface, filling all four tracks of the ATR. The actual occurrence of the NAMG-2 signal was 42 s later than predicted; however, the DC-16 command initiated the near-encounter sequence, and NAMG-2 actually became a backup. The first three near-encounter pictures included the limb of the planet.

The DTR recorded digital science data, and filled its four tracks in about 24 min; a DEOT = 4 signal then terminated the DTR recording. As was the case with *Mariner VI*, these data were transmitted in real-time over the high-rate telemetry link at 16.2 kbits/s to the Earth before, during, and after the period of digital recording. Thus, the high-rate telemetry mode was also the primary method of returning near-encounter digital science data, and the DTR became in fact a backup.

To avoid the TV problem of obtaining saturated pictures during the near-encounter sequence (because of a spacecraft wiring error), the same strategy used for *Mariner VI* was adopted for *Mariner VII*. It involved having the CC&S issue N4-N1\* events to the scan control subsystem after pictures 1-19 and N1\*-N4 events after pictures 20-22. Thus, the AAC reset the TV shutter to its minimum-exposure setting, and prevented saturation of TV pictures 2-23. The N1\*-N4 events after pictures 20-22 were used because the scan platform was already at its fixed cone-angle reference position (100.2 deg), and thus produced the same results as would an N4-N1\* event.

The scan platform moved from one angle to another in four slews during the near-encounter sequence in response to the CC&S computer-programmed commands. As a result, the area covered by the instruments favored the south polar region of the planet in accordance with the desires of the science investigators. The platform slewed to new positions after specific TV pictures, as listed in Table 6.

The data storage subsystem performed nominally during the near-encounter sequence. As expected, the DTR was stopped from recording at the end of

**Table 6. *Mariner VII* near-encounter scan-platform positions**

Slew	After near-encounter picture	Clock position, deg		Cone position, deg	
		From	To	From	To
1	9	217.5	250.8	135.7	144.7
2	20	250.8	233.7	144.7	100.2
3	27	233.7	228.8	—	—
4	37	228.8	249.8	—	—

its fourth track by a DEOT = 4 signal (05:10:04) and the ATR was stopped from recording by an AEOT = 4 signal (05:10:25) at the end of its fourth track. In each case, the CC&S (as evidenced by appropriate event-register changes) showed that an N9 and N8 event were issued to back up the DEOT = 4 and AEOT = 4 signals, respectively; because of the known C1 source driver failure in the CC&S, however, these events were inhibited from leaving the CC&S.

The last segment of science data, returned after both tape recorders had stopped, lasted for about 9 min, during which the real-time encounter 2 data mode (with no backup data storage subsystem function), providing science data at 16.2 kbits/s, was obtained.

At 05:19:35, some 19 min after closest approach, the spacecraft entered occultation, and radio contact was lost. The S-band radio beam was cut by the Martian surface at 58 deg south latitude; at the moment of occultation, the spacecraft was about 9050 km from the limb of the planet. Two minutes after *Mariner VII* entered occultation, the CC&S was to issue a P2 event to command the data storage subsystem and FTS to the playback 1 mode. The rationale for going into this mode at that time was exactly the same as that for *Mariner VI*.

The *Mariner VII* occultation experiment was conducted in precisely the same way as it had been for *Mariner VI*; i.e., entry data were in the two-way mode and exit data were in the one-way mode.

The near-encounter phase was completed when the spacecraft emerged from behind Mars (about 30 min after entry), at 38 deg north latitude and at a distance of about 20,000 km from the limb of the planet, at 05:49:12. The FTS was in the playback 1 mode at 270

bits/s, and the data storage subsystem was playing back science data stored on the DTR.

## XVI. Mariner VII Playback

The playback phase of *Mariner VII* saw nominal performance in all respects for the spacecraft system. Six playbacks of the 33 near-encounter pictures stored on the ATR were accomplished over the high-rate telemetry link at 16.2 kbits/s by use of the 210-ft-diam antenna at DSS 14. The near-encounter science data stored on the DTR were played back twice at 270 bits/s. Finally, one analog-to-digital transfer was achieved in which a segment of analog TV data stored on the ATR was transferred to the four tracks of the DTR and played back in digital form at 270 bits/s.

It is appropriate to note the reversal of roles of the playback 2 and playback 1 modes. At the outset of the mission, the playback 2 (and encounter 2) mode was considered an experiment because the use of the 16.2-kbits/s rate depended on the 210-ft-diam antenna at DSS 14, and also on a complex array of digital computers on the Earth. These computers provided bit-synchronization and reconstruction of the data that

had been block-encoded on the spacecraft, converting them back to a serial bit stream of 16.2 kbits/s and recording it on magnetic tapes. As it turned out for both *Mariners VI* and *VII*, the chain of equipment functioned perfectly; therefore, the playback 2 mode was actually used as the prime method of recovering the near-encounter pictures. The playback 1 mode became an experiment inasmuch as only one analog-to-digital transfer was attempted (just to check that it worked). Hence, the enormous capability of the high-rate telemetry mode had demonstrated that it was ready for more than merely an experimental role.

The playback phase of *Mariner VII* was started at the assumed time of 05:21:43 on August 5, 1969 (during the 30-min occultation period) by a CC&S P2 event, which switched the FTS and data storage subsystem to the playback 1 mode. The playback phase continued for 5 days (except for a 22.5-h hiatus on August 9), which was ended at 05:25:04 on August 10 by a DC-1 command that switched the FTS to the cruise mode and the data storage subsystem to the ready mode. Table 7 lists the modes used and the stimuli used to change them during the playback phase. The turn-off of science and scan control subsystem power, the removal of roll-axis inertial hold

Table 7. *Mariner VII* playback phase

Mode	Stimulus	Earth-observed time (GMT)		Mode	Stimulus	Earth-observed time (GMT)	
		Time	Date			Time	Date
Start playback 1	P2 (CC&S <sup>a</sup> )	05:21:43	Aug 5	End playback 2 and start playback 1	DC-44 (FCS)	05:15:53	Aug 7
End playback 1 and enter ready mode	DC-1 (FCS <sup>b</sup> )	06:29:02	Aug 5	End playback 1 and start A/D <sup>c</sup> transfer	Counter = 9 (data storage subsystem)	00:13:42	Aug 8
End ready mode and start playback 1	DC-3 (FCS)	06:33:01	Aug 5	End A/D transfer and start playback 1	DEOT <sup>d</sup> = 4	00:38:12	Aug 8
End playback 1 and enter ready mode	DC-1 (FCS)	00:14:16	Aug 6	End playback 1 and enter ready mode	DC-1 (FCS)	01:02:15	Aug 9
End ready mode and enter playback 1	DC-3 (FCS)	00:28:58	↓ Aug 6	End ready mode and enter playback 1	DC-3 (FCS)	23:32:41	Aug 9
End playback 1 and start playback 2	DC-44 (FCS)	00:29:57		End playback 1 and start playback 2	DC-44 (FCS)	23:33:44	Aug 9
End playback 2 and start playback 1	DC-44 (FCS)	06:11:09		End playback 2 and enter ready mode	DC-1 (FCS)	05:25:04	Aug 10
End playback 1 and start playback 2	DC-44 (FCS)	23:29:59					

<sup>a</sup>CC&S = central computer and sequencer.

<sup>b</sup>FCS = flight command subsystem.

<sup>c</sup>A/D = analog-to-digital.

<sup>d</sup>DEOT = digital end of tape.

and reacquisition of Canopus, and the updating of the CC&S for certain postencounter events were also undertaken during this phase, and carried out in a normal manner.

## XVII. Postencounter Science Exercises, *Mariners VI and VII*

After the playback phase was completed, a series of postencounter science exercises were executed with the two spacecraft. These exercises became essentially a "bonus" dividend of the *Mariner* Mars 1969 mission since they were possible because: (1) the primary mission ended several weeks early (owing to the high-rate telemetry capability) and (2) the telecommunications link was able to support the high-rate telemetry for an extended period. Dates and descriptions of the postencounter science exercises are shown in Table 8.

**Table 8. Postencounter science exercises**

Date	Exercise
<b><i>Mariner VI</i></b>	
Aug 11-12	UVS <sup>a</sup> scan of portion of southern celestial hemisphere
Aug 12-13	UVS scan of portion of northern celestial hemisphere
Aug 13-14	TCFM calibration
Aug 14	UVS and infrared radiometer scan of portion of northern celestial hemisphere
Sep 8-9	Photography of stars Vega, Altair, and Alpheratz
Oct 8-9	UVS scan of comet 69B
<b><i>Mariner VII</i></b>	
Sep 10-11	Photography of stars Vega, Altair, and Alpheratz
Sep 22-23	UVS scan of Milky Way
<sup>a</sup> UVS = ultraviolet spectrometer.	

### A. *Mariner VI*

**1. First exercise.** The objective of this first *Mariner VI* postencounter science exercise was to acquire ultraviolet spectrometer (UVS) data by scanning the UVS instrument through a portion of the southern celestial hemisphere; the data were to be returned to the Earth in real-time during the scan. This objective was accomplished basically by maneuvering the spacecraft off the Sun line to an orientation that would allow the scan platform to step through the segment of the hemisphere of interest, while simultaneously retaining the high-gain antenna telecommunications link with the Earth. The reason for the maneuver was to be able to point the scan

platform at the desired position. The maneuver parameters were chosen so that antenna pointing was also accomplished.

The spacecraft would be reoriented with a roll-pitch-roll maneuver, under CC&S control, that would result in pointing the high-gain antenna at the Earth. The 16.2-kbits/s HRTS link could then be used to transmit UVS data in real-time, thus removing any need for recording and playback. Next, the scan platform would be stepped in position (cone and clock) under CC&S control of the scan reference potentiometers from the stored CC&S scanning program. Thus, the hemisphere would be scanned by the UVS in segments resulting from steps of the scan platform produced by CC&S commands to the cone and clock reference potentiometers.

The exercise started at 18:30 GMT on August 11, 1969 with the transmission of 183 coded commands, to load into the CC&S memory a spacecraft maneuver program and a scan platform scanning program. The test continued, after completion of the coded command loading and a CC&S memory readout, with the transmission of commands DC-13, -14, and -32 at 00:01, 00:05, and 00:10, respectively, on August 12, to place the CC&S in the computer-only maneuver mode, to enable the interface between CC&S and attitude control, and to start the CC&S computer sequence, respectively.

Upon receipt of the DC-32 command, the CC&S issued command M1 to the attitude control subsystem, turning on the gyros for the start of a one-hour gyro warm-up period. During the warm-up, a test of the battery was performed so that its state could be determined prior to pitching the spacecraft off its Sun line. The test verified that the battery was in an operative state and thus could support an expected battery-share mode. In addition, quantitative commands were transmitted to update the cone and clock reference potentiometers to an initial position from which the scan platform would move during the exercise.

At the conclusion of the one-hour gyro warm-up period, the CC&S issued commands M2, M4, and  $\bar{M}4$  for a zero pitch turn; these commands were followed one minute later by commands M3 and M5, which initiated the first roll turn of 126 deg. Forty-five seconds after completion of the first roll turn, the pitch turn was initiated by command M4 from the CC&S to the attitude control subsystem. The pitch turn required 456 s to complete and was -81.3 deg. The spacecraft experienced its first battery-share condition during the flight

when it had been off the Sun at  $-36.7$  deg into the pitch turn. At the point the battery share started, the battery voltage dropped from 33.5 to 27.5 V and its discharge current was 3.5 A. The second roll turn started 45 s after completion of the pitch turn with the issuance of commands M3 and M5 by the CC&S; the turn was completed 196 s later, after a spacecraft roll of 34 deg.

The maneuver of the spacecraft had been completely nominal with the high-gain antenna pointed at the Earth and the scan platform now in the range of slew for the region of interest of the sky. Therefore, the next command DC-25 turned on scan control and science subsystems power, and the platform slewed to the position stored on the reference potentiometers: 101 deg in cone and 212 deg in clock.

Next, a DC-44 command turned on the HRTS and a DC-32 command started the scan sequence. The platform was slewed through four sectors of the hemisphere by CC&S commands. This scanning process was accomplished by the issuance of 122 N3 (clock slew) steps, 817 N10 (positive cone) steps and 768 N11 (negative cone) steps. The clock and cone ranges covered for each sector are described in Section III-C under Spacecraft Engineering Subsystem Performance. Operation of the scan control and science subsystems ended with receipt of the DC-1 command at 04:03:24 on August 12.

Another first for the *Mariner VI* flight was a programmed unwind (from the CC&S) of the original maneuver turns to reacquire the Sun and Canopus. The unwind turns commanded by the CC&S were: first roll turn,  $-34$  deg; pitch turn, 81.3 deg; and, second roll turn,  $-123$  deg.

During the pitch unwind turn, the power subsystem came out of battery share at a pitch angle of approximately  $-22$  deg. The share mode had existed for 2 h 35 min, during which time it was estimated that 800 W-h were drained from the battery. The CC&S issued command M1, the reacquire command, coincident with the end of the last unwind turn, and the spacecraft then rolled to Canopus through 3.64 deg. The gyros then turned off automatically 3 min later. The exercise ended with the transmission of command DC-38 to turn on the battery charger so that the charge in the battery that had been taken to support the spacecraft loads during the battery-share mode could be restored. The spacecraft performed in an outstanding fashion during this first postencounter exercise.

**2. Second exercise.** The second *Mariner VI* postencounter exercise, conducted on August 12–13, had as its objective the mapping of a segment of the northern celestial hemisphere by the UVS instrument. This objective was accomplished in the same manner as in the first exercise with the exception that the spacecraft was not required to be maneuvered; that is, it remained oriented to the Sun and Canopus.

The exercise commenced at 21:58 on August 12 with the transmission of the first of 25 coded commands to modify the CC&S program. The necessary quantitative commands were then sent to initialize the platform position at 110 deg in cone. Then commands DC-25, -44, and -32, transmitted at 22:50, 22:53, and 22:56, respectively, turned on scan control and science subsystems power, turned on the HRTS (16.2 kbits/s) and initiated the computer-controlled scan sequence, respectively. Two sectors of the northern celestial hemisphere were mapped in cone and clock angles.

The scanning activity took approximately  $6\frac{1}{4}$  h, during which time the CC&S issued 5667 commands, consisting of 184 N3 (clock step), 2737 N10 (positive cone step), and 2746 N11 (negative cone step) commands. The exercise concluded with the receipt of command DC-1, at 05:23:33 on August 13, which turned off scan control and science subsystems power. The performance of the spacecraft in this second postencounter exercise was, again, outstanding.

**3. Third exercise.** The third *Mariner VI* postencounter exercise was executed to obtain a calibration of the TCFM instrument. To accomplish this objective, it was required to pitch the spacecraft off the Sun line so that the instrument pointed toward black space.

The exercise started at 19:30 on August 13 with the transmission of the first of 129 coded commands to load into the CC&S memory a spacecraft maneuver program. Upon completion of the coded command loading, a CC&S memory readout was commanded, and, at 22:35, the memory was verified as correct. Next, commands DC-13, -14, and -32 were transmitted to initiate the maneuver sequence. Upon receipt of command DC-32, the CC&S issued command M1 to the attitude control subsystem to turn on the gyros. After a 31-min warm-up period, the CC&S issued the necessary commands to reorient the spacecraft. The commanded turns were a  $-45$ -deg roll followed by a 95-deg pitch. Since the downlink transmission was over the spacecraft low-gain antenna, all turns were seen in the data. The power

subsystem entered a battery-share condition at 39 deg into the pitch turn, and, by the end of the pitch turn, the solar panels were completely occulted from the Sun, resulting in the battery supplying the full spacecraft loads.

The TCFM was now pitched 95 deg off the Sun line, looking into dark space, and a 30-min period of data gathering ensued. At 00:06:23 on August 14, the CC&S issued command M4 to unwind the pitch turn, signaling the end of the TCFM calibration. The spacecraft pitched -95.1 deg (i.e., back toward Sun line) under inertial control. During the pitch turn unwind, the power subsystem came out of battery share at 19.3 deg off the Sun line. It was estimated the battery had provided 168 W-h of power during the 41 min the battery was supplying power.

Thus, the exercise was completely nominal, all subsystems performed as expected, and a successful TCFM calibration was obtained.

**4. Fourth exercise.** The fourth *Mariner VI* postencounter exercise, conducted on August 14, had as its objective the mapping of a segment of the northern celestial hemisphere not covered in the second exercise by the UVS and IRR instruments. The scheme for achieving this objective was much the same as in the earlier exercise (i.e., orient the spacecraft such that the platform could be slewed through the area of interest and the high-gain antenna would be pointed at the Earth).

The exercise started at 00:16 on August 14 by CC&S commands M3 and M5 to unwind the roll turn of the TCFM exercise, plus a needed additional roll increment for this experiment. Therefore, a 63.3-deg roll turn was commanded, followed by a 44.3-deg pitch turn and a second roll turn of -74 deg. The spacecraft was now oriented with the antenna pointed at the Earth and the scan platform in range for slewing through the desired segment of the northern celestial hemisphere. During the TCFM exercise, the necessary quantitative commands to the cone and clock reference potentiometers for initial scan platform position had been transmitted; when command DC-25 was transmitted at 00:26 to turn on science and scan control subsystems power, it was observed in the data at 00:39:40 and the platform slewed to its initial position of 119.5 deg in cone and 301.6 deg in clock. After a DC-44 command was sent to turn on HRTS at 16.2 kbits/s, a DC-32 command was transmitted to start the CC&S automatic scanning sequence. The scan platform slewed through the remaining uncovered

sectors of the hemisphere in clock and cone in response to CC&S commands.

Upon completion of these scans, another scan was undertaken for the IRR instrument alone. This scan was in clock position only, from an initial position of 151 deg to the end at 92 deg. The slewing was done in 1-deg steps on 2-min centers. The total number of CC&S commands to accomplish the scanning steps of this exercise was 840, consisting of 211 N3, 327 N10, and 302 N11 commands. A DC-1 command to turn off scan control and science power was received at 04:23:40 on August 14. Now it was necessary for the spacecraft to reacquire its celestial references; accordingly, 5 coded commands were sent to produce the following unwind turns: first roll turn, 74 deg; pitch turn, -44.35 deg; and second roll turn, -18.28 deg.

The spacecraft then reacquired the Sun and Canopus immediately after the completion of the unwind maneuver at 05:02:10. The power subsystem had been in a battery-share condition from 00:26:24 (when the spacecraft was pitched over at the start of the exercise) until 04:57:20 (when the spacecraft unwind pitch turn toward the Sun took place, near the end of the exercise), an elapsed time of 4 h 31 min. It was estimated the battery had started with a capacity of 970 W-h and 877 W-h had been used to support the spacecraft loads, a 93% depth of discharge.

Thus, the performance of the spacecraft in this exercise was outstanding. It had gone through six separate turns under inertial control, entered share mode, accommodated a large amount of scan activity, and returned the science data in real-time over the HRTS.

**5. Fifth exercise.** The fifth *Mariner VI* postencounter science exercise, conducted on September 8-9, had as its objective the determination of the threshold of the narrow-angle TV camera (TV-B) by taking pictures of several stars in the two extreme gain states of the TV subsystem.

During the far-encounter sequence, an attempt was made to take two pictures close together at a time when Phobos would be coming into view from around the back of the planet. Postencounter analysis had not been able to detect the satellite, so an inflight exercise was scheduled to determine, if possible, if the television camera was sensitive enough to detect Phobos, and to attempt to determine a threshold for the camera. The stars Vega ( $\alpha$ -Lyrae, visual magnitude 0.04), Altair ( $\alpha$ -Aquilae, visual

magnitude 0.77), and Alpheratz ( $\alpha$ -Andromedae, visual magnitude 2.15) were selected as the best three objects to view. All three of them are spectral type A stars, providing a fair match of spectral response so that the major difference in television camera response would be due to the relative brightness of the stars.

By slewing the scan platform to each star and recording on the ATR four pictures in one gain state (low = 000), in a pattern successively for each of the three stars, then repeating the recording in the reverse pattern but with TV in the other gain state (high = 111) under CC&S control, 24 pictures would be so recorded on the ATR. Then the high-gain antenna would be pointed at the Earth by reorienting the spacecraft and the stored TV pictures would be played back in the high-rate mode (16.2 kbits/s) downlink over the antenna.

The exercise started at 15:19 on September 8 with the transmission of the first of 279 coded commands to the CC&S, to load into its memory a picture-taking, scanning, and maneuver program. The coded command loading extended over a period of 6 h, and then a commanded CC&S readout verified that the memory was loaded correctly. Following the readout, quantitative commands were sent to set the cone and clock reference potentiometers at the initial position for the exercise. Then command DC-47, received at 22:12:53, turned on the data storage subsystem; this was followed at 22:17:53 with the receipt of command DC-25 to turn on scan control and science subsystems power, and the platform slewed to the initial references. However, the initial position had been miscalculated slightly and two more quantitative commands were sent to place the platform at the correct initial position of 115.3 deg in cone and 174.6 deg in clock, the position of the star Vega.

Now the ATR was erased twice by ground command (DC-39) to remove the near-encounter pictures, which had been stored there since encounter. Next, a DC-44 command turned on the high-rate telemetry subsystem and a DC-23 command stepped the ATR to track 2, since it was necessary to record the 24 pictures on tracks 2, 3, and 4. Command DC-14 was transmitted at 22:39 to enable CC&S control to the attitude control subsystem for the upcoming maneuver, and a DC-32 command was sent at 22:44 to start the CC&S picture-taking and slew sequence.

One second after the receipt of command DC-32 at 23:01:57, the gyros came on in response to command

M1 from CC&S for an almost 2-h warm-up period for the upcoming maneuver. The CC&S then began issuing the picture-taking and slewing commands. With the TV in the low-gain state (000), the CC&S issued command F2 for the recording of a TV-B picture; then it issued command N10 for a 1-deg platform step in cone; this was followed by: (1) another picture, (2) a 1-deg clock step, (3) another picture, (4) a  $-1$  deg cone step, (5) a fourth picture, and (6) a  $-1$  deg clock step. Thus, four pictures were recorded bracketing the star Vega. Next the CC&S issued the N3 (cw) and N10 commands necessary to slew the scan platform to the star Altair; the picture-taking sequence used at Vega was then repeated at Altair, resulting in the recording of four TV-B pictures of Altair in the low-gain state. Then the commands to slew to the star Alpheratz were issued; N3 (cw) and N11 commands were required, but the CC&S actually issued N3 (ccw) commands, slewing the platform 69 steps in the *wrong* clock direction. The picture-taking sequence at this location was repeated before anything could be done. The reason for the incorrect slew was that the final N3 (ccw) command pulse in the Altair sequence was not followed by a polarity reset before the slew to Alpheratz began. However, analysis disclosed that the absence of the polarity reset was the result of a human error in programming and, therefore, not a spacecraft problem.

The rest of the CC&S program was checked and found to be correct; accordingly, it was decided to send quantitative commands to slew the platform to Alpheratz and complete the exercise in recognition of the fact that pictures of Alpheratz in the low-gain state would not be taken. Command DC-16 was transmitted at 23:44 to produce narrow-angle acquisition and place the TV in the high-gain state (111); this was followed by seven QC-3-18 commands starting at 00:07 on September 9. A QC-3-12 command at 00:16 completed the corrective quantitative command sequence, and command DC-32 at 00:20 started the second part of the CC&S program. The picture-taking sequences at Alpheratz, Altair, and Vega in the high-gain state were uneventful; the pattern of four pictures bracketing each star with TV in the high-gain state was completely nominal, and, therefore, 12 more pictures were recorded on the ATR, completing the 24-picture sequence. A DC-48 command at 01:12:34 and a DC-1 command at 01:20 turned off scan control and science subsystems power.

The next part of the exercise was the execution of the maneuver to optimally point the high-gain antenna at the Earth. The maneuver was initiated by a DC-32



command that commanded the CC&S to start the maneuver sequence. The appropriate CC&S commands were issued, resulting in spacecraft pitch and roll turns of  $-1.43$  and  $-3.65$  deg, respectively.

With the antenna pointed at the Earth, commands DC-23, -3, and -44 were received, positioning the ATR at track 2 and placing the data storage and flight telemetry subsystems in the 16.2-kbits/s playback mode. The playback of the 24 pictures stored on tracks 2, 3, and 4 continued over the HRTS for about  $2\frac{1}{2}$  h.

Playback was concluded just before 04:24:44 when the CC&S issued the unwind roll turn command. This was followed by the unwind pitch turn. Since the roll unwind would not be large enough to allow Canopus to enter the field of view of the tracker, two DC-18 commands were sent to step the spacecraft  $2.25$  deg in roll while inertial hold was maintained. Command DC-19 was then sent to reset command DC-18 so that the star could be acquired in the normal manner. Commands to turn off the data storage subsystem, place the CC&S in tandem standby, and turn off the HRTS placed the spacecraft in a cruise mode to conclude the exercise.

On the whole, this exercise was satisfactory, and the spacecraft performed nominally in all respects. The error in programming the CC&S that triggered the clock slew in the opposite direction for going to the star Alpheratz was unfortunate. However, the real-time analysis and prompt reaction to the problem enabled mission operations personnel to obtain all high-gain-state photographs of the three stars and low-gain-state photographs of two of the stars.

**6. Sixth exercise.** The sixth and last postencounter science exercise on *Mariner VI* had as its objective the scanning of the comet 69B by the UVS instrument. The plan was to maneuver the spacecraft such that the high-gain antenna would be optimally pointed at the Earth so that real-time high-rate science data at 16.2 kbits/s would be received on the ground. Then the scan platform would be commanded to step in increments of 1 deg in cone by ground command to sweep across the track of the comet. The platform would remain at each step for 5 min to collect UVS data before being commanded to the next step.

The exercise started at 22:45 on October 8 with the transmission of the first of 51 coded commands to load the CC&S with a maneuver program. Coded command loading was completed at 23:49, and a commanded

CC&S memory readout verified that the loading was correct. At 00:30 on October 9, a DC-13 command was sent to place the CC&S in the nontandem standby mode for the computer-only maneuver that was to follow. Shortly before the DC-14 command (to enable CC&S actuators to the attitude control subsystem) was to be transmitted, the ground station lost lock with the spacecraft. Command DC-14 was transmitted at 00:43, a second DC-14 at 00:51, and a DC-32 command at 00:55; this sequence was followed by three quantitative commands to initialize the platform position. However, after a round trip light time of 23 min, telemetry indications showed that the DC-13 command was accepted; however, neither of the two DC-14 commands, nor the DC-32 command, nor any of the three quantitative commands was accepted because of an out-of-lock uplink condition. The ground transmitter was then turned off; after 2 min, it was turned on, and a tuning procedure followed to ensure uplink lock. The commands were retransmitted on 3-min centers and the spacecraft received them successfully. One second after the DC-32 command was received, the gyros came on, at 01:57:24, for the start of a 1-h warm-up period. Command DC-47 was transmitted next to turn on the data storage subsystem; although the subsystem was not to be used, the procedure was followed to minimize the science-power-on transient that was to follow. Next, the DC-25 command turned on scan control and science subsystems power at 02:52:26, and the platform slewed to the initial position of 203 deg in clock and 108.5 deg in cone. At 02:57:25, two counter 2 events signaled that the CC&S had issued commands M2, M4, and  $\overline{M4}$ , starting the maneuver sequence. The first spacecraft turn was a positive roll turn of 37.19 deg; this was followed by a pitch turn of  $-16.75$  deg and a second roll turn of  $-25.72$  deg.

When the DC-25 command was received, it was noted that the power subsystem momentarily went into battery share. The subsystem had boosted itself out of share by 02:52:31, but, during the pitch turn, shading on the panel by the low-gain antenna again forced the subsystem into battery share; this time the boost out of share was inhibited because the Sun gate was reset by the greater-than-6-deg pitch turn off the Sun line. The power subsystem stayed in share for the duration of the time the spacecraft was pitched off the Sun (about  $1\frac{1}{2}$  h).

After the last maneuver turn was completed and while UVS science data at 16.2 kbits/s were being received, five QC-2-1 commands sent on 5-min centers caused the platform to step in a 1-deg cone increment for each

command, thus sweeping through the track of the comet. The final platform position after these steps was 203 deg in clock and 103.5 deg in cone.

A DC-1 command, sent at 04:15, turned off the scan control and science subsystems, and a DC-13 command, at 04:19, commanded Sun reacquisition, which concluded the exercise. Again, all subsystems in this test performed in a normal manner. Although the momentary battery share at science subsystem power turn-on (command DC-25) was not expected, analysis indicated that the increasing heliocentric distance to the spacecraft was such that the solar array was receiving less luminance and, therefore, had less power-generating capability. Thus, a valuable data point was provided for assessing future (after October 9) solar array capacity.

## **B. Mariner VII**

**1. First exercise.** The first *Mariner VII* postencounter science exercise, performed on September 10–11, had the same objective as the fifth exercise on *Mariner VI* (i.e., the determination of the threshold of the narrow-angle TV camera (TV-B) by taking pictures, in the two extreme gain states, of several stars). The stars Vega, Altair, and Alpheratz were used in the same manner as in the earlier *Mariner VI* exercise. The procedure was as follows:

- (1) The spacecraft was initialized with the scan platform pointing at the star Vega and the TV in the low-gain state.
- (2) The program loaded in the CC&S memory commanded: (a) a TV-B picture be recorded on the ATR, (b) a positive 1-deg cone step, (c) a second picture, (d) a positive 1-deg clock step, (e) a third picture, (f) a negative 1-deg cone step, (g) a fourth picture, and (h) a negative 1-deg clock step.
- (3) The CC&S commanded a slew to the star Altair where the picture-taking sequence was repeated.
- (4) The CC&S commanded a slew to the last star Alpheratz, and the four-picture sequence followed.

Thus, at this point, 12 pictures were recorded with TV in the low-gain state.

The second part of the exercise was initiated by ground command DC-16, which triggered narrow-angle acquisition in the DAS, resulting in placing TV in the high-gain state. Then a DC-32 command started the

same CC&S-controlled picture-taking sequence described earlier, with the exception that the direction of scan platform slews was reversed; the sequence started at Alpheratz and ended at Vega. Thus, 12 more pictures were recorded on the ATR, but with TV in the high-gain state.

The 24 pictures stored on tracks 2, 3, and 4 of the ATR were then played back over the high-gain antenna in the high-rate mode (playback 2 at 16.2 kbits/s) over a 2½-h period. Just before starting the playback, the antenna was optimally pointed at the Earth in roll by the transmission of two DC-21 commands.

The playback was uneventful and nominal; upon its completion, commands were sent to: (1) turn off the HRTS, (2) reacquire Canopus, (3) turn off data storage subsystem, and (4) reestablish cruise mode. This completed the exercise.

**2. Second exercise.** The second and last postencounter science exercise on *Mariner VII* was conducted on September 22–23, 1969. Its objective was to return high-rate science data (UVS) from points in the Milky Way. Neither maneuvering of the spacecraft nor CC&S commanding was required. Therefore, the plan was to:

- (1) Send quantitative commands to initialize the scan platform cone and clock potentiometers and turn on scan control and science subsystems power so that the UVS would be slewed to the initial point in the Milky Way.
- (2) Turn on the HRTS and take UVS data for 25 min at the first point.
- (3) Send quantitative commands to slew the platform to the second point where UVS data would be collected for another 25 min.

This process would be repeated until the 13 designated points in the Milky Way were mapped by the UVS.

The exercise started at 20:10 on September 22 with the transmission of the first eight quantitative commands to initialize the scan platform potentiometers. These commands, a DC-25 (to turn on scan control and science subsystems power) and a DC-44 (to turn on HRTS), were sent from DSS 62 (85-ft antenna). When the HRTS was turned on, DSS 14 (210-ft antenna) was already in view of the spacecraft and that station began to process

the received 16.2-kbits/s science data. Deep Space Station 14 remained in an ultra-cone, listen-only configuration for the entire exercise because this mode improved downlink telecommunications performance by 1.5 dB. The remaining commands were transmitted from DSS 12 (85-ft antenna), which maintained two-way lock with the spacecraft. In accordance with the plan, quantitative commands were sent to step the platform to each suc-

ceeding point in the galaxy, with a 25-min period of UVS data collecting at each point.

The exercise was concluded with the transmission of command DC-1 at 05:25 on September 23 to turn off scan control and science subsystems power and the HRTS. The spacecraft performed in a nominal and expected manner throughout this 7-h exercise.

# Spacecraft Engineering Subsystem Performance

## I. Telecommunications Link

### A. Comparison of Measured Communications Link Performance to Predicted Values

The comparison of measured performance values for each of the communications links during launch, cruise, and encounter to that predicted was of prime concern to the telecommunications analyst. Results of these daily comparisons were utilized as a figure of merit for the combined spacecraft-to-ground station operations, and they provided the degree of confidence necessary for sequence planning throughout the mission. Lack of correlation pinpointed problem areas and, therefore, immediate investigation and correction were possible. No attempt will be made to describe each of the operational anomalies identified or sequence changes made as a result of these comparisons but, rather, the overall individual link performances will be presented in the following general format:

- (1) Direct comparisons displaying actual measured vs predicted values.
- (2) Histograms showing the number of times the difference between actual and predicted values fell within 0.25-dB increments.
- (3) Composite performance cumulative plots showing the number of cases where the difference between the actual and predicted values is within some deviation from the predicted value.

1. *Uplink carrier channel.* The major parameters involved in determining the uplink carrier level, as

received at the input terminal of the radio frequency subsystem (RFS), are the ground transmitter effective radiated power level, space loss, receiving antenna gain, polarization loss, and receive circuit losses. The final values for nontime-varying quantities used in the predicts program were:

Ground transmitter power level = 70.00 dBm

Transmit antenna gain = 51.80 dB

Transmit antenna ellipticity = 1.00 dB

Receiving circuit loss = -0.11 dB

Space loss is a time-varying quantity dependent upon probe-to-earth range. Receiving antenna gain is also a time-varying quantity dependent upon the spacecraft clock and cone angles. These quantities are computed by the communications predicts program (CP2M) utilizing the spacecraft trajectory tape.

Figures 1 and 2 show the uplink signal level comparisons for *Mariners VI* and *VII* from February 25 to August 8 during coverage by DSS 41; it is obvious that there is close correlation to the expected values. The abrupt changes are due to various mode changes, such as command modulation being applied to the carrier, and special threshold tests that were conducted periodically. The measured level appears to remain constant for several days and then it drops in a step function manner. This drop is due to the resolution of the telemetry system which, at -125 dBm, is approximately 1.1 dB per data number. Figure 3 contains the histogram plots

of the DSS 41 data for *Mariners VI* and *VII*. The associated cumulative plots are shown in Fig. 4; for both spacecraft, received level comparisons are biased somewhat positively. Perhaps a better measure of overall performance is shown in Fig. 5, wherein the cumulative composite performance of DSSs 12, 41, 51, and 62 are displayed. These graphs show a slight negative bias. The overall performance is certainly well within the expected tolerances and indicates that the preflight spacecraft calibrations used for the final predicts were accurate to within 1 dB.

**2. Downlink-received carrier level.** The downlink-received carrier level is determined primarily by the spacecraft modulation index, transmitter power level,

antenna gain, space loss, and the receiving antenna gain. The final values for nontime-varying quantities used in the communications predicts program are shown in Table 1.

**Table 1. Final values used in predicts program**

Parameter	<i>Mariner VI</i>	<i>Mariner VII</i>
Transmitter power output, dBm		
Low-power mode	40.90	40.50
High-power mode	43.70	43.00
Circuit losses, dB		
To low-gain antenna	-1.60	-1.40
To high-gain antenna	-1.40	-1.40
Receiving antenna gain, dB		
DSSs 12, 41, 51, and 62	53.30	53.30
DSS 14	61.50	61.50
Receiving antenna ellipticity, dB		
DSSs 12, 41, 51, and 62	0.4	0.4
DSS 14	0.2	0.2
Modulation index, deg		
Cruise mode	42.99	41.70
High-rate telemetry	65.10	65.67

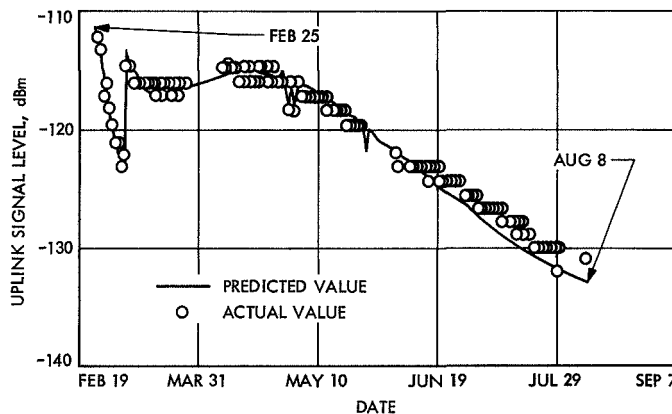


**Fig. 1. Uplink signal level between DSS 41 and Mariner VI**

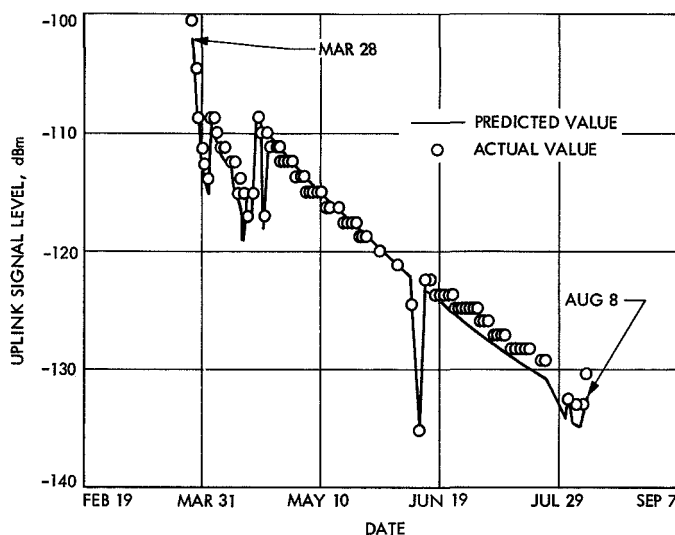


**Fig. 2. Uplink signal level between DSS 41 and Mariner VII**

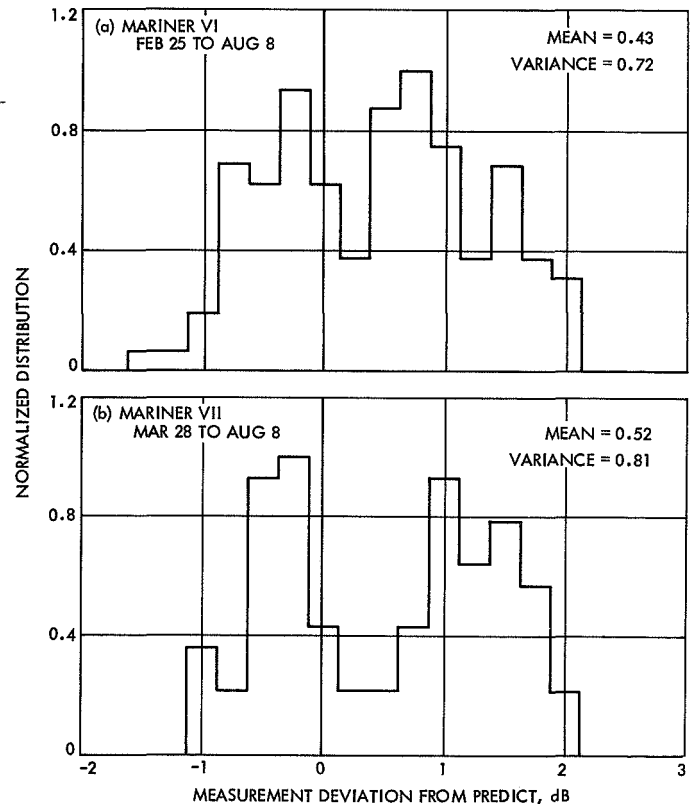


**Fig. 3. Uplink signal level measurement vs distribution of predictions for Mariners VI and VII**

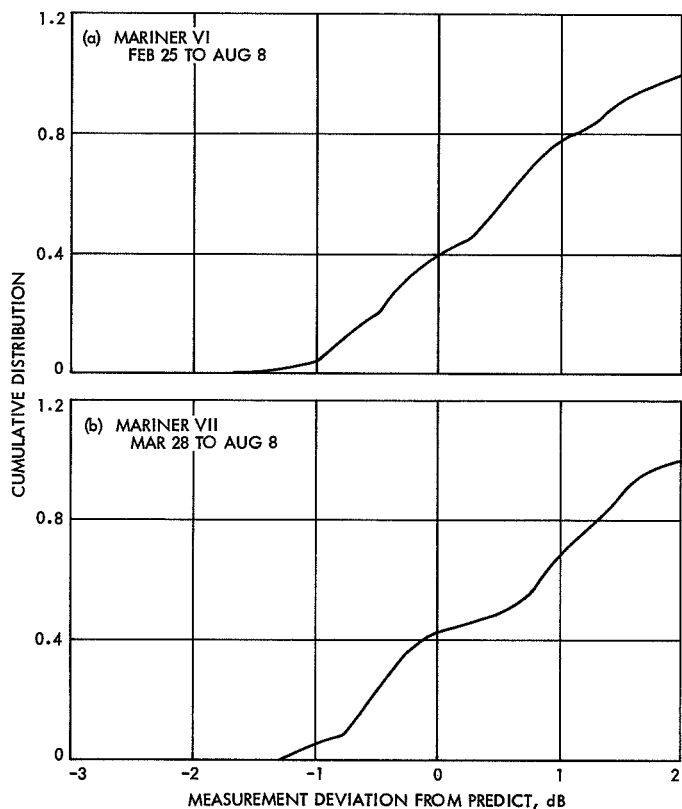


**Fig. 4. Uplink signal level measurements vs cumulative distribution of predictions for *Mariners VI and VII***

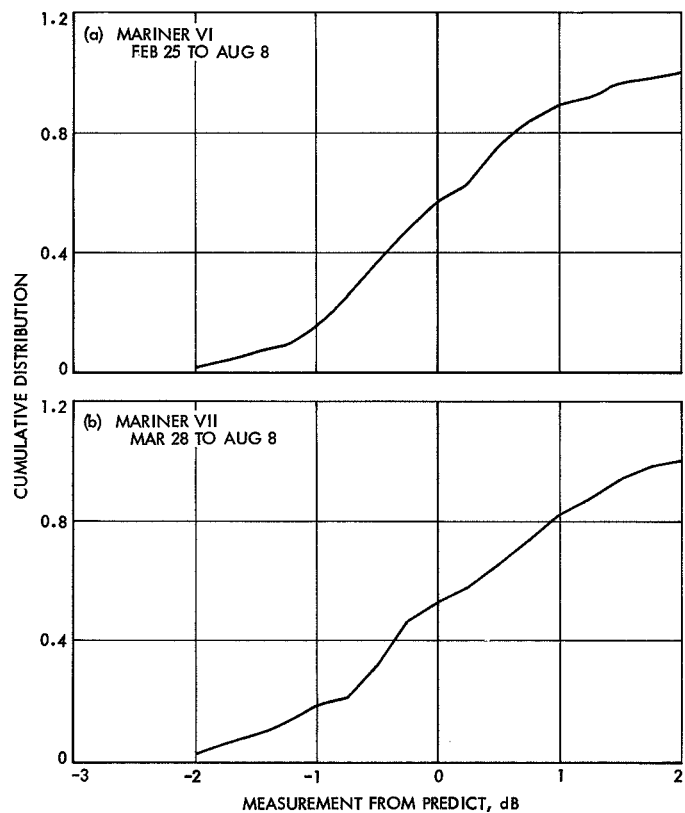


**Fig. 5. Uplink signal level measurements (DDSs 12, 41, 51, and 62) vs cumulative distribution of predictions for *Mariners VI and VII***

Figures 6 and 7 show the direct comparison of received signal level to predicted value for DSS 41. Figure 8 contains the histogram plots of these data. Figure 9 shows the cumulative distribution for DSS 41, and the composite cumulative performance distribution for DSSs 12, 41, 51, and 62 is shown in Fig. 10. Examination of these data reveals a definite negative bias for both spacecraft for the single station comparison and the all-station composite performance. One possible explanation for this biasing is an increase in modulation index that would cause a lower carrier level as will be seen in the signal-

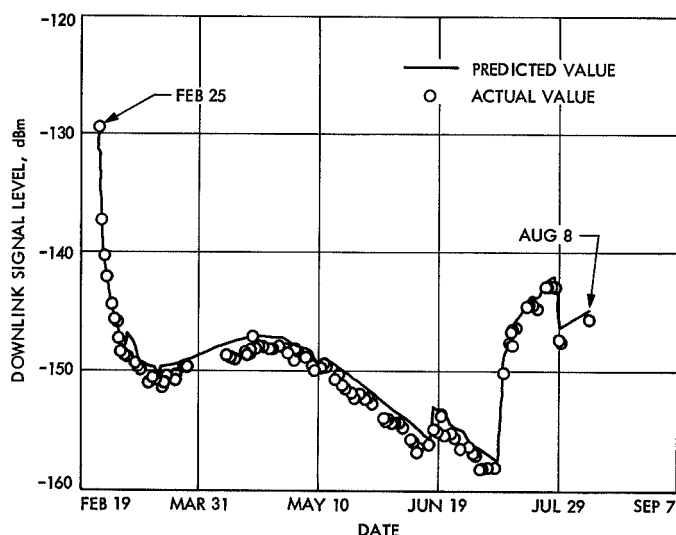


**Fig. 6. Downlink signal level between DSS 41 and Mariner VI**

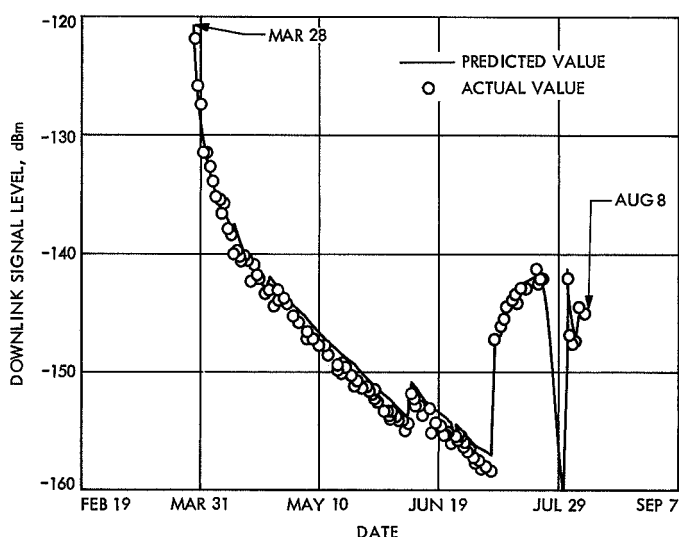


**Fig. 7. Downlink signal level between DSS 41 and Mariner VII**

to-noise ratio (SNR) comparison. This increase appears to be the case for *Mariner VII*; however, *Mariner VI* does not show a similar increase in data power. The large number of variables and tolerances involved in arriving at the received carrier level estimate prevents any logical approach to resolution of the slight biases observed, at least on a post mission analysis basis. For future missions, this type of statistical analysis will be performed in real-time, which will provide an opportunity for the identification of systematic discrepancies.

The received carrier levels were well within expected tolerances and, therefore, enabled the downlink carrier tracking function to perform in a nominal manner.

**3. Cruise telemetry signal-to-noise ratio.** From launch to encounter, both spacecraft were operated in the cruise telemetry mode at a data rate of 33½ bits/s. To evaluate channel performance, the ground station telemetry command processor (TCP) computed the mean and variance of the data bits and thus it provided an extremely accurate measure of the received data power to noise spectral density ratio on a real-time basis.

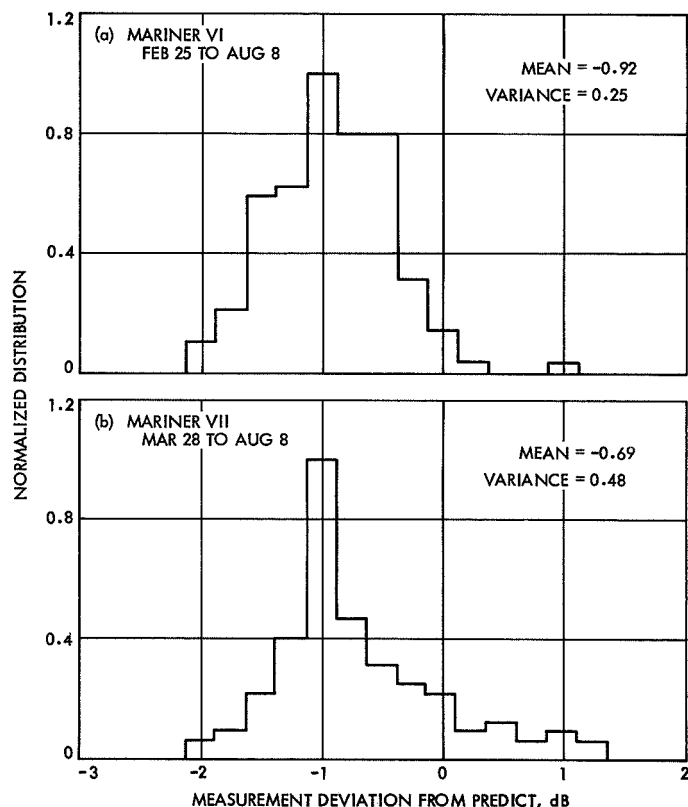


**Fig. 8. Downlink signal level measurements vs distribution of predictions for Mariners VI and VII**

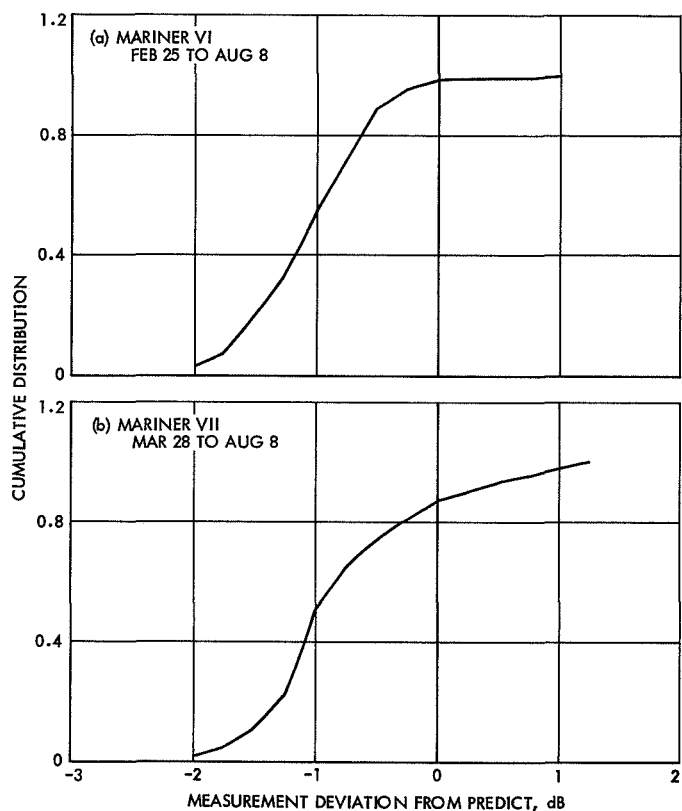


**Fig. 9. Downlink signal level measurements (DSS 41) vs cumulative distribution of predictions for *Mariners VI and VII***

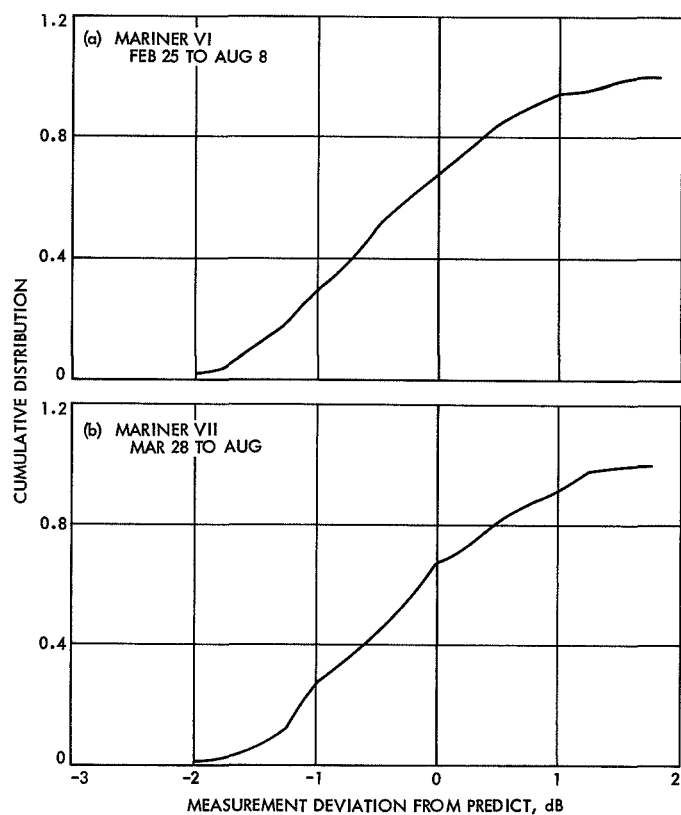


**Fig. 10. Downlink signal level measurements (DSSs 12, 41, 51, and 62) vs cumulative distribution of predictions for *Mariners VI and VII***



The received data power is primarily a function of modulation index, transmitter power level, space loss, receiving antenna gain, and losses through the receiver and subcarrier demodulation assembly due to noisy phase references. The station noise spectral density is primarily determined by the maser noise temperature and antenna elevation angle. The latter is a time-varying quantity dependent upon the flight-path geometry. The relationship of telemetry SNR to bit error rate is shown in Fig. 11. The design threshold point for the channel was 5.2 dB, which corresponds to a bit error rate of  $5 \times 10^{-3}$ .

Figures 12 and 13 show the single station direct comparison of SNR to predicted values for *Mariners VI* and *VII*. The histograms of these data are shown in Fig. 14 with the associated cumulative plots in Fig. 15. Composite station performance SNR is shown in Fig. 16. The *Mariner VI* data are in excellent agreement with expected values and show only a slight negative bias. *Mariner VII* data display a definite positive bias that, as stated previously, is believed to be due to a slightly higher modulation index than that assumed by the predicts program.

The received SNR throughout the mission was nominal and allowed receipt of high quality engineering data.

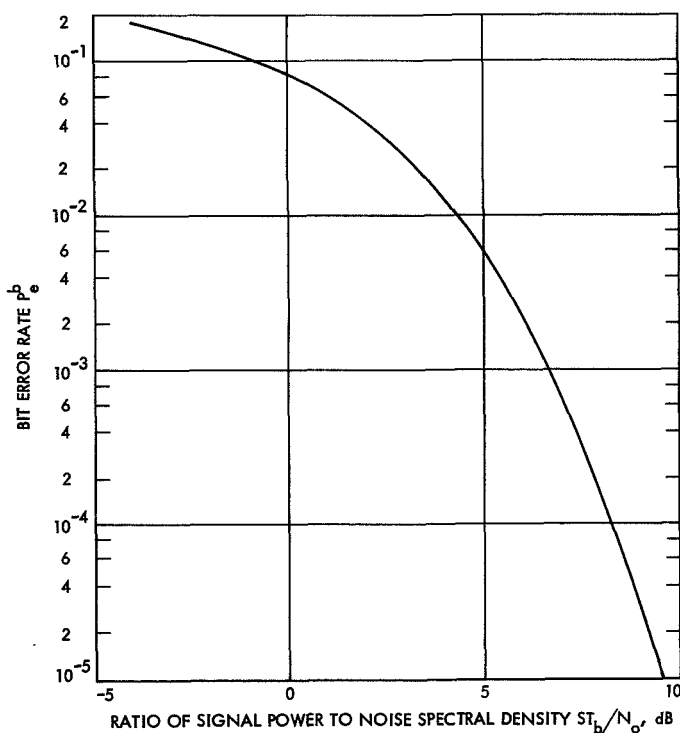


Fig. 11. Uncoded coherent bit error probability

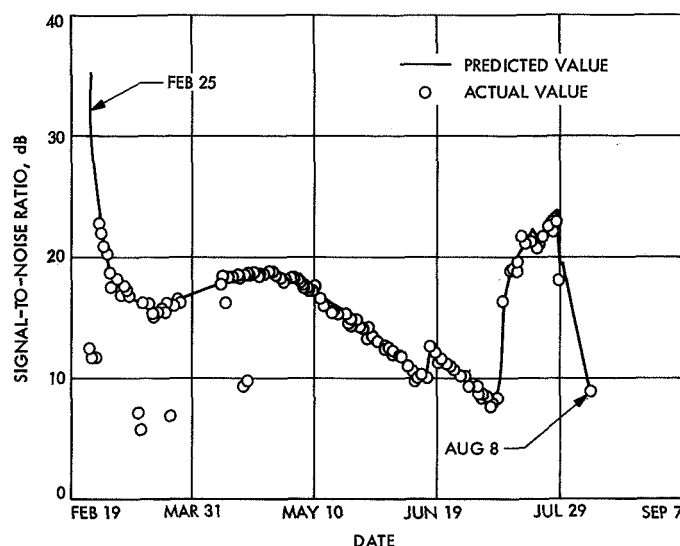


Fig. 12. Signal-to-noise ratio between DSS 41 and *Mariner VI*

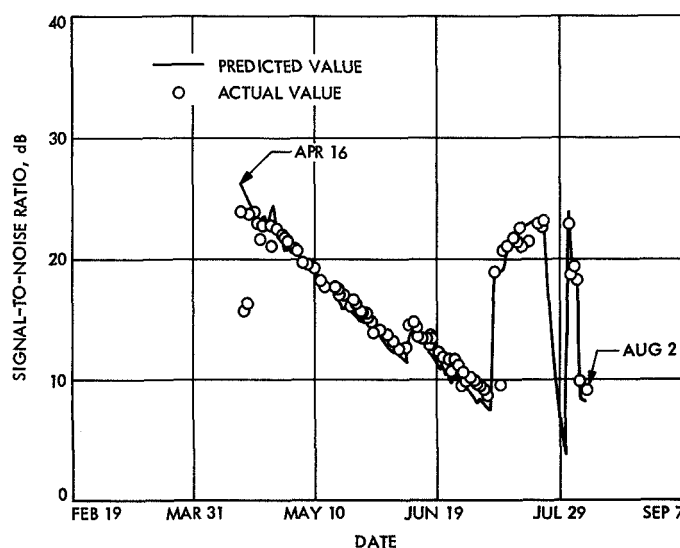
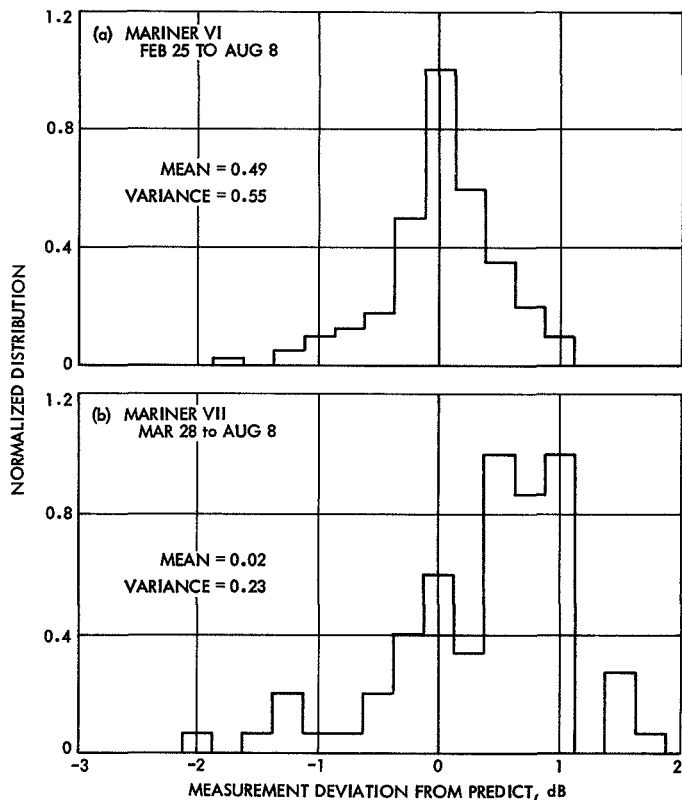
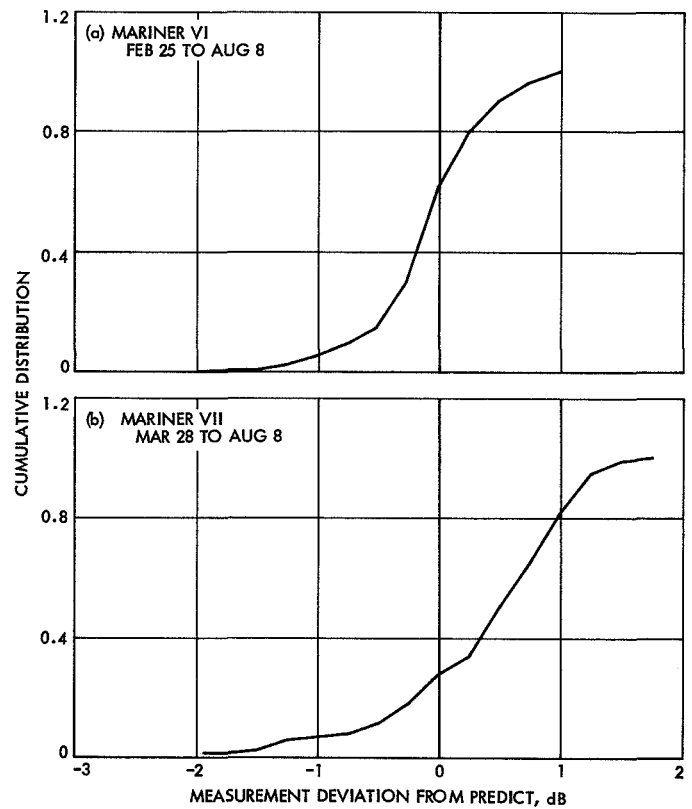


Fig. 13. Signal-to-noise ratio between DSS 41 and *Mariner VII*

**4. High-rate telemetry signal-to-noise ratio.** The high-rate telemetry (HRT) subsystem, operating at 16.2 kbits/s, provided the capability to return photographs and scientific information in near real-time. This subsystem, the first of its type to be flown on a planetary mission, was classed as an experiment to be used as a backup for the 270-bits/s prime playback link. Operational test, prior to encounter, verified that the high-rate link was performing well within design specifications; therefore, this link was used for the prime data return during encounter for both spacecraft. Since the HRT subsystem uses block coding



**Fig. 14. Signal-to-noise ratio measurements vs distribution of predictions for Mariners VI and VII**



**Fig. 15. Signal-to-noise ratio measurements (DSS 41) vs cumulative distribution of predictions for Mariners VI and VII**

techniques, its performance is evaluated in terms of word error rate for which one word length is 6 bits. Figure 17 shows the relationships of word error rate and bit error rate vs ratio of signal power to noise spectral density. Design threshold point was  $P_e^w = 1 \times 10^{-2}$ , corresponding to a value of 3.0 dB.

*Mariners VI and VII* encounter operations began on July 29 and ended on August 7. The comparison of predict vs measured SNR values are shown in Fig. 18–20, with associated histogram data shown in Fig. 21. A slight positive bias is evident on the *Mariner VII* data and again is believed to be due to a somewhat higher modulation index.

The HRT subsystem performed well within design specifications and, as a result of the real-time assessment capability afforded by the HRT, allowed a significant increase in photographic data return.

**5. Command link performance.** Approximately 1800 commands were transmitted to the *Mariner VI* and *VII*

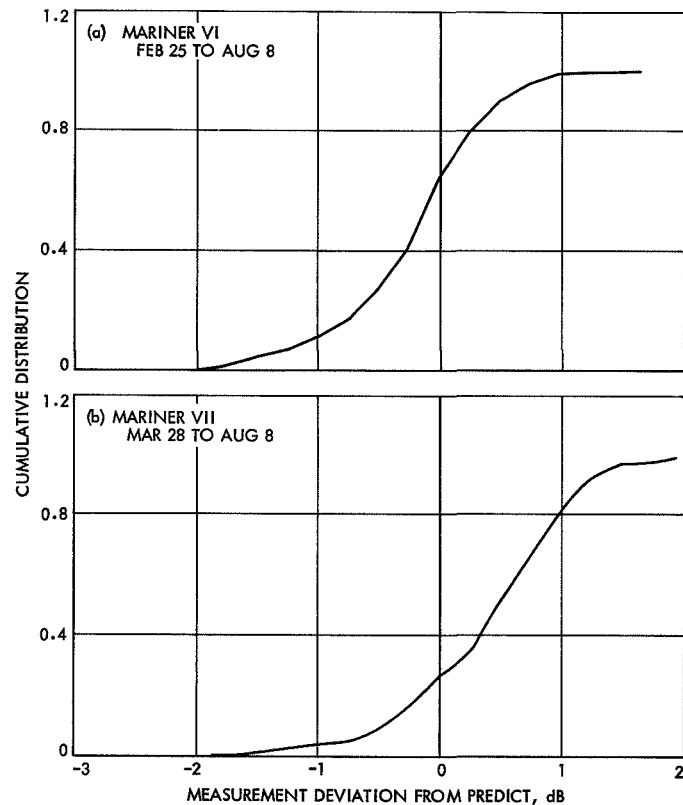


**Fig. 16. Signal-to-noise ratio measurements (DSSs 12, 41, 51, and 62) vs cumulative distribution of predictions for *Mariners VI* and *VII***

spacecraft from launch through encounter. All commands were received and processed without error and, therefore, demonstrated nominal performance of the command link. The measured values of the command composite SNR at the input to the flight command subsystem (FCS) are not telemetered; therefore, a quantitative analysis of link performance is not possible.

## B. Telecommunications System Group SPAC Function

The functions of the systems group within the spacecraft performance analysis and command (SPAC) operations were as follows:

- (1) Verify normal operation of spacecraft telecommunications subsystems.
- (2) Generate predicts and monitor actual vs measured performance.
- (3) Serve as the Telecommunications Division spacecraft representative to the SPAC team.
- (4) Coordinate spacecraft-tracking station activities.

The functions listed above are closely related to those performed by the systems group during the prelaunch

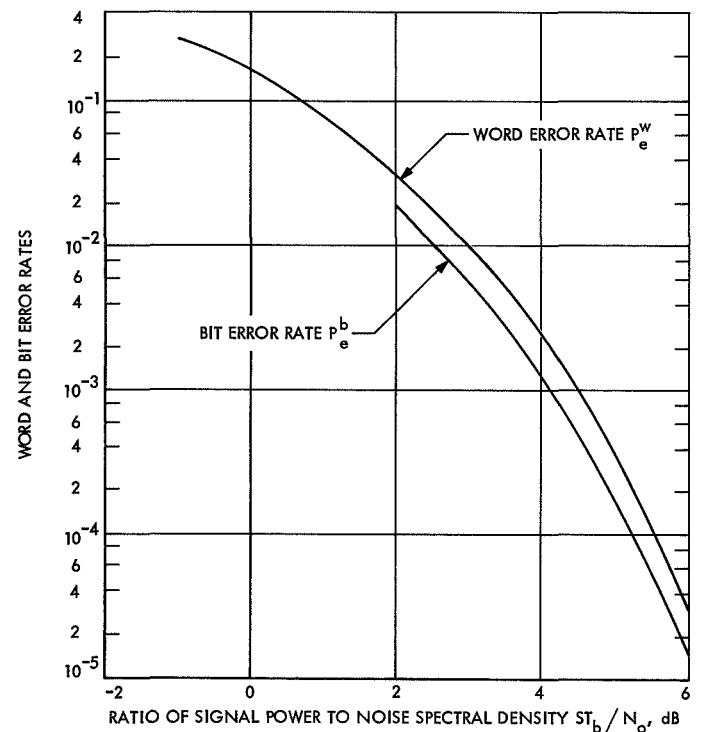


**Fig. 17. Word and bit error rates vs ratio of signal power to noise spectral density**

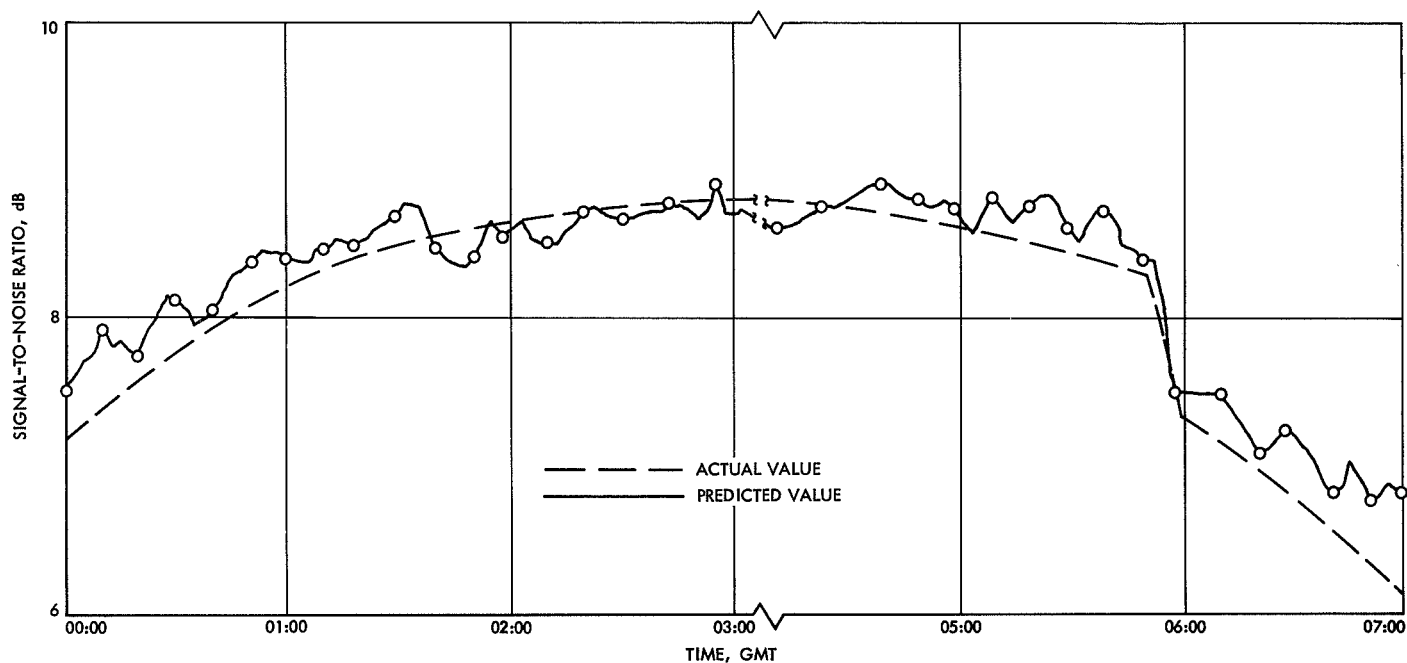


Fig. 18. High-rate margin measurements vs predictions for *Mariner VI*, July 29 and 30

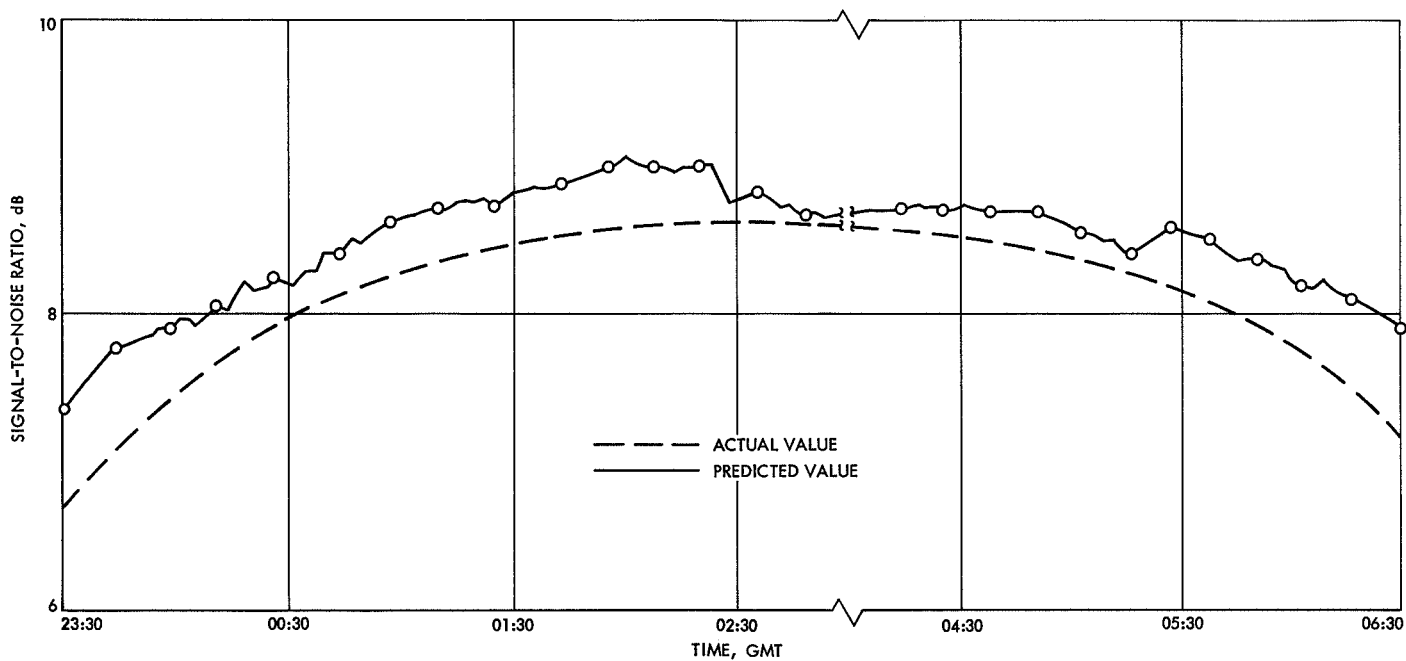


Fig. 19. High-rate margin measurements vs predictions for *Mariner VII*, August 3 and 4

design and testing phases; thus, an excellent basis exists for successful operations in the real-time postlaunch environment. To accomplish these objectives, two systems analysts were assigned for full-time support of the SPAC operations; the assignments began with the SPAC training exercises and extended through encounter of both spacecraft.

Two additional analysts were assigned to participate, on a part-time basis, to allow 24-hour coverage during critical mission phases and to provide support to the telecommunications analysis team (TCAT) on an as-required basis. Full-time programming support was maintained through encounter for running of the telecommunications performance prediction program (CP2M) and for special programming needed for problem oriented data processing.

Verification of the status of the four subsystems composing the spacecraft telecommunications system was the responsibility of the SPAC team members assigned to each of the subsystems. However, it was apparent that maintaining a full staff during noncritical periods was unnecessary unless abnormal operations were encountered. The telecommunications analyst generally monitored the subsystem status during each track and would notify a specialist only if questionable data were observed. Daily tabulations of all telemetry data were supplied by

the Space Flight Operations Facility (SFOF) data processing center RECORDS program for review by each analyst.

Of prime concern to the telecommunications analyst was the comparison of the communications link performance to that predicted by the CP2M program. This comparison required a detailed knowledge of both the spacecraft and ground station operating parameters. The results of these efforts are discussed in detail in succeeding paragraphs; however, in general, the results were in excellent agreement with that expected. The CP2M program served as an invaluable tool during real-time operations and allowed the analyst to provide exact communications link predicts upon which operational plans could be based.

Coordination of the spacecraft-tracking station activities was accomplished via an intercom network within the SFOF between the analyst and the track advisor located in the net operations control room. This communications network provided for informal bilateral flow of information between ground station and spacecraft operations teams concerning status, details of operational plan changes, and other information necessary for successful operations. This network allowed the prime operational networks to be used only for formal directions.

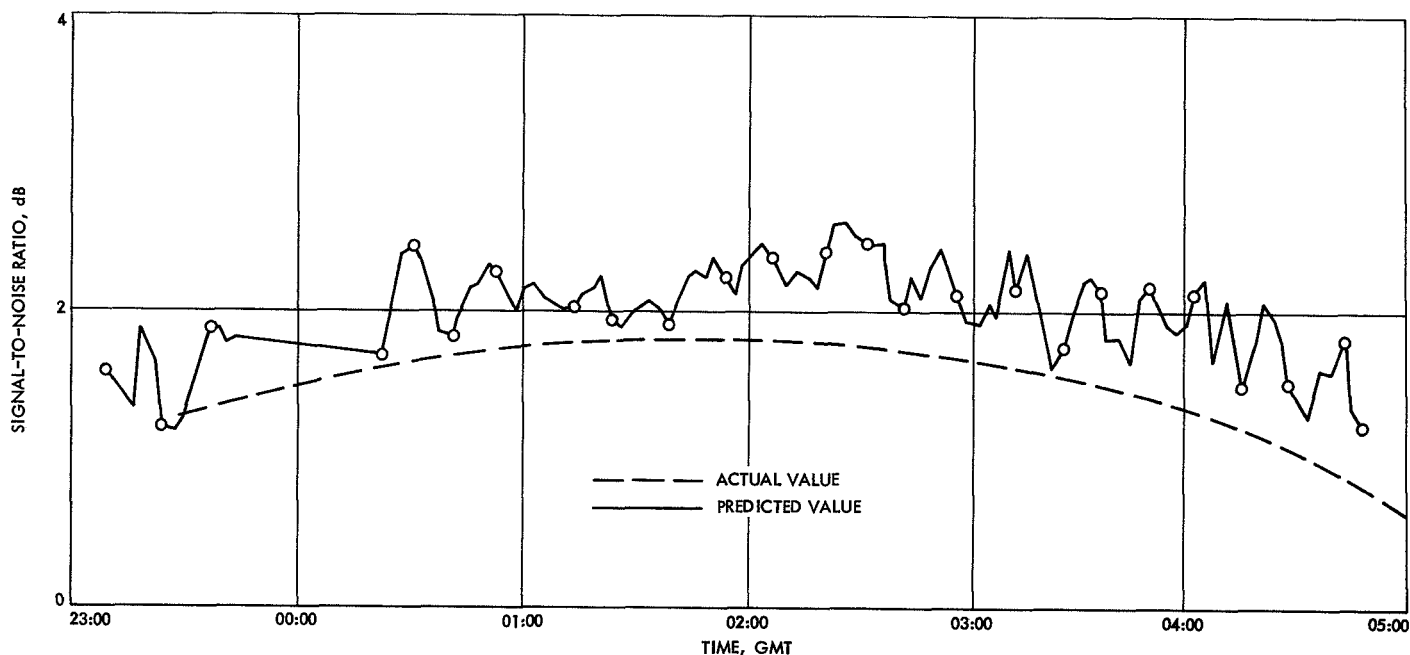
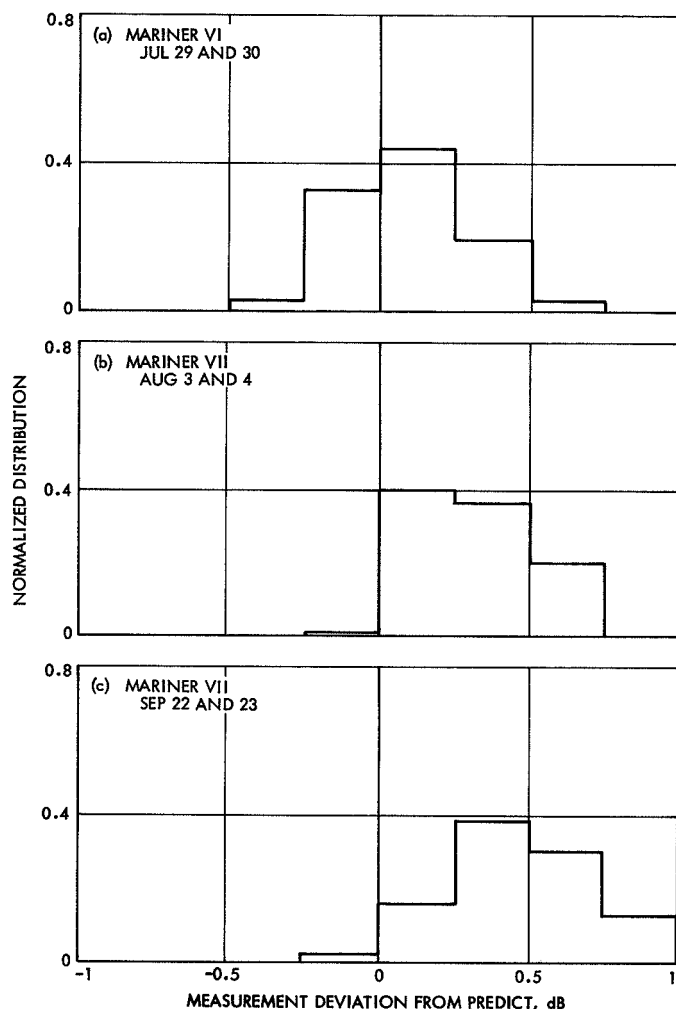


Fig. 20. High-rate margin measurements vs predictions for *Mariner VII*, September 22 and 23



**Fig. 21. Histogram of deviation of high-rate performance measurements from predictions**

Figure 22 depicts the data flow of the systems group assigned work area within the SPAC operations room. The TEL-1 and -2 positions were supplied with two teletypewriters which could select any of the processed spacecraft data formats. A video monitor provided a display of the ground station digital instrumentation subsystem output, which contained key status parameters in addition to received signal level and telemetry SNR. Two auxiliary teletypewriters were installed to enable real-time display of the HRT subsystem status and SNR. An external speaker was supplied to provide monitoring of the track control station voice command network.

### C. Telecommunications Analysis Software

Several computer programs were written to facilitate analysis of the telecommunications link performance.

The programs utilized for data analysis are briefly described in the following paragraphs.

**1. Performance prediction program.** The telecommunications performance prediction program generated estimates of earth-to-spacecraft and spacecraft-to-Earth telecommunications performance for the *Mariner Mars 1969* mission. The program calculates nominal signal levels, SNRs, and performance margins, as well as their favorable and adverse tolerances.

A block diagram of the CP2M program is shown in Fig. 23. Much of the input data is necessary for the execution of any link analysis. Geocentric and station-centered trajectory data can be entered from cards or from a tape generated by the JPL trajectory program. (The trajectory tape generated by the midcourse maneuver program can also be used.) Trajectory parameters are necessary for the calculation of uplink and downlink space loss, spacecraft receiving and transmitting antenna gains, doppler, and ground receiver noise temperature.

Certain spacecraft and ground tracking station parameters are entered directly into the program, since no computations are involved. These parameters include spacecraft transmitter power, receiver noise spectral density, Deep Space Station transmitting and receiving antenna gain and maximum ellipticity, zenith noise temperature, and uplink and downlink frequencies.

Spacecraft antenna patterns consisting of gain, gain tolerances, and ellipticity as a function of the angle from the antenna boresight axis may be inputted from cards or from a digital antenna pattern (DAP) tape. Before the gain for a particular point can be calculated, a transformation from spacecraft coordinates to antenna coordinates is necessary. The gain is then differenced with the peak antenna gain to find pointing loss. Tolerances are computed using gain tolerances and antenna boresight tolerances. Polarization loss is a function of both the spacecraft and station antenna ellipticities.

Other input data for CP2M may or may not be necessary, depending on the type of link analysis (telemetry, command, or ranging) being performed. For instance, the data defining the modulation and demodulation characteristics of the telemetry channel need to be loaded only when a telemetry analysis is executed; data giving the output SNR as a function of the input SNR in the ranging channel need to be loaded only for a ranging analysis.

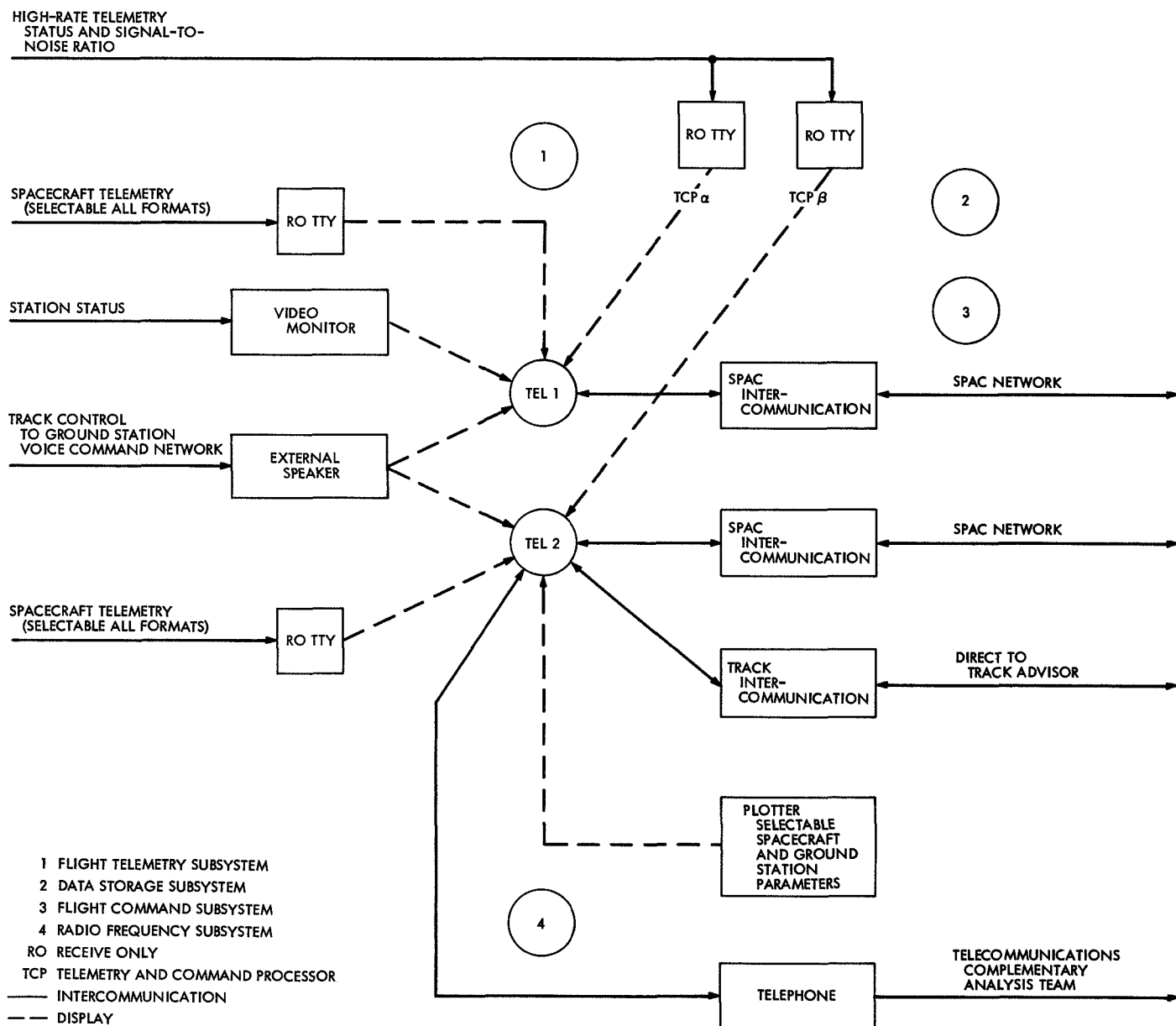
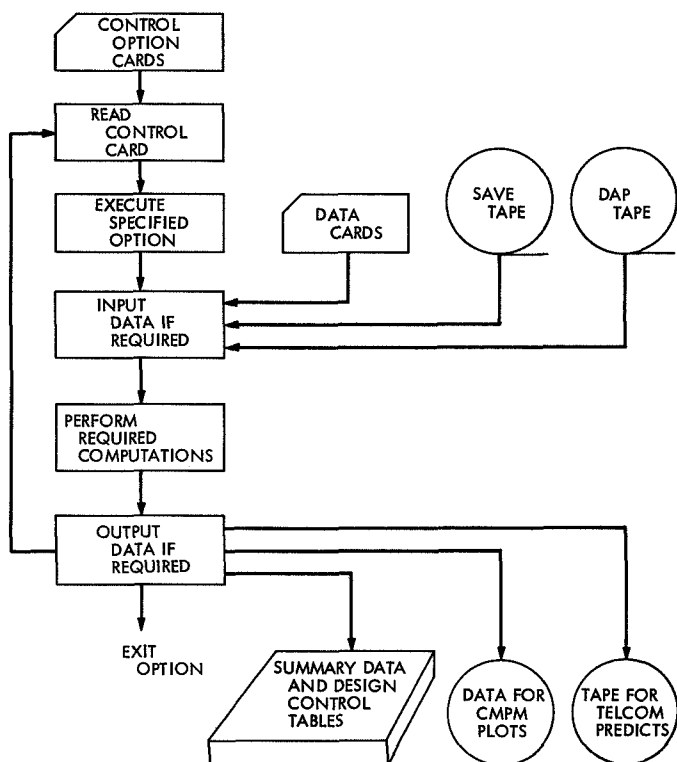


Fig. 22. Telecommunications SPAC area functional block diagram



**Fig. 23. Telecommunications performance prediction program CP2M block diagram**

The CP2M program may generate one or more of several types of output, according to options specified by the user. Summary tables (e.g., Table 2), usually printed out more often than the other output data, tabulate the parameters most often referred to in an operational environment. Design control tables, however, include each value used in describing a particular telecommunications link (e.g., Table 3).

Ranging signal level computations can be made for both the near-earth (Mark I) and the planetary ranging systems. Ranging channel performance is defined in terms of the received ranging power, which is a function of the uplink channel, the spacecraft, and the downlink channel characteristics. The combined performance parameters are shown in Table 4.

Other CP2M output includes a tape containing predicted signal levels and telemetry channel performance parameters for comparison with actual measurements; a predicts tape for use by ground tracking network; and station noise temperature tables vs time (on cards).

No method of plotting performance parameters was available in the 1969 version of CP2M. However, this has been implemented for future missions.

**2. Statistical data analysis program.** The statistical data analysis program (SDAP) is designed to take actual values of the downlink carrier, uplink carrier, and SNR for DSSs 12, 41, 51, and 62 and predicted values to make the three types of plots required. The downlink-carrier-level actual values are derived from track controller logs that contain hourly reports of the signal level. The uplink and SNR actual values are taken from the mission dependent tapes recovered via the SFOF RECORDS program. The predicted values are derived from communications prediction program CP2M. The production of plots is a five step procedure as shown by the flow chart of the program (Fig. 24).

First, the original data are separated into groups that depend on the station, the spacecraft, and downlink carrier, uplink carrier, or SNR; they are also divided according to predicted and actual data. Thus, the final result is groups of data for each station, each spacecraft, for each of downlink, uplink, and SNR, and for predicted or actual values as a function of time in the mission. After the data are separated, they are reformatted for the TYMSHARE system EASYPLOT plot routine.

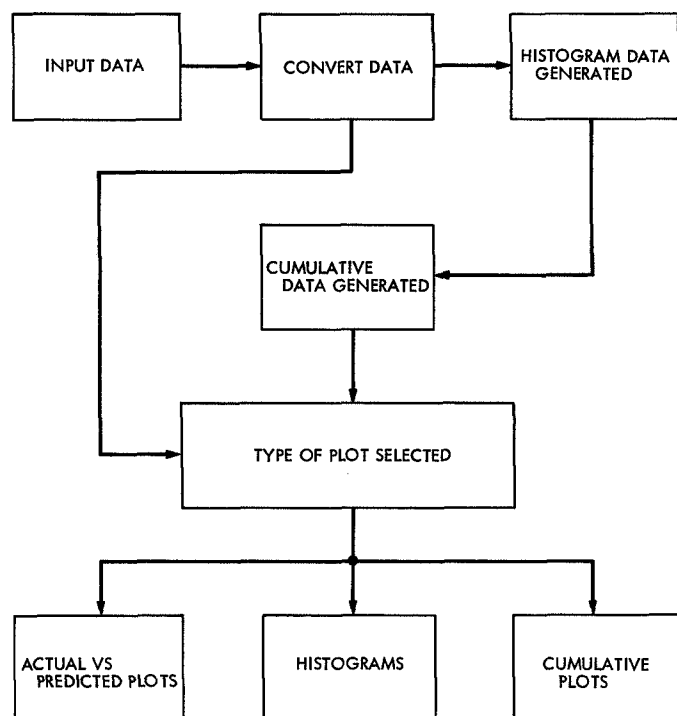


**Fig. 24. Plot production flow chart**



**Table 2. Summary for station-centered telemetry analysis<sup>a</sup>**

Trajectory data from DSS 12						
Parameter	Value	Parameter	Value	Parameter	Value	
Cone angle, deg	58.72	Clock angle, deg	98.40	Range, km	0.2191527E-6	
Azimuth, deg	185.01	Elevation, deg	17.73	Hour angle, deg	5.97	
Azimuth rate, deg	12.62	Elevation rate, deg/h	-0.90	Hour angle rate, deg/h	15.07	
Declination, deg	-36.93	Declination rate, deg/h	0.18	Range rate, deg/h	0.4095E-1	
Range acceleration, m/s <sup>2</sup>	0.01					
Parameter	Uplink			Downlink		
	Nominal value	Tolerance		Nominal value	Tolerance	
		Favorable	Adverse		Favorable	Adverse
Telemetry performance						
Channel 1 margin, dB	44.86	6.95	-5.65	—	—	—
Channel 2 margin, dB	—	—	—	38.84	6.95	-5.65
Tracking performance						
One-way margin, dB	68.14	6.41	-5.18	50.08	7.56	-5.23
Carrier level, dB	-84.53	4.71	-4.48	-119.48	5.86	-4.63
Two-way margin, dB	50.08	7.56	-5.23	—	—	—
Miscellaneous link data						
Antenna gain, dB	0.384	2.647	-2.664	-0.340	2.813	-2.832
Polarization loss, dB	-0.061	0.052	-0.052	-0.097	0.015	-0.015
Space loss, dB	-205.775	—	—	-206.488	—	—
Radio loss, dB	-0.000	-0.000	-0.000	-0.000	-0.000	-0.000
Doppler, <sup>b</sup> kHz	-28.905	—	—	-31.378	—	—
Ground received temperature, °K	66.686	-10.000	10.000	—	—	—
<sup>a</sup> Data obtained at L + 13 h on March 18, 1969; 11:33:57.491 GMT.						
<sup>b</sup> Two-way doppler = -62.799 kHz; doppler standard deviation = 0.430 Hz.						

Table 3. Design control table for station-centered telemetry and command analyses<sup>a</sup>

No.	Parameter	Uplink			Downlink		
		Nominal value	Tolerance		Nominal value	Tolerance	
			Favorable	Adverse		Favorable	Adverse
1	Total transmitter power, dBm (same power in watts)	70.000 10000.000	1.000 2589.252	-1.000 -2056.718	39.020 7.980	1.100 2.300	0.000 0.000
2	Transmitting circuit loss, dB	0.000	0.000	0.000	-2.130	0.370	-0.370
3	Transmitting antenna gain, dB	51.000	1.000	-0.500	7.250	1.500	-1.500
4	Transmitting antenna pointing loss, dB	0.000	0.000	-0.250	-7.590	1.313	-1.332
5	Space loss, dB	-205.775	0.000	0.000	-206.488	0.000	0.000
	Frequency, MHz (Range = 2.19153E-05 km)	2116.000	—	—	2297.000	—	—
6	Polarization loss, dB	-0.061	0.052	-0.052	-0.097	0.015	-0.015
7	Receiving antenna gain, dB	7.000	1.500	-1.500	53.000	1.000	-0.500
8	Receiving antenna pointing loss, dB	-6.616	1.147	-1.164	0.000	0.000	-0.250
9	Receiving circuit loss, dB	-0.080	0.010	-0.010	0.000	0.000	0.000
10	Net circuit loss, dB	-154.532	3.708	-3.477	-156.055	4.198	-3.967
11	Total received power, dBm	-84.532	4.708	-4.477	-117.035	5.298	-3.967
12	Receiver noise spectral density, dBm/Hz (Elevation = 17.734 deg)	-165.675	-0.700	0.700	-180.360	-0.706	0.607
	Zenith noise temperature, °K	—	—	—	55.000	-10.000	10.000
	Zenith noise spectral density, dBm/Hz	—	—	—	-181.196	-0.872	0.726
13	Carrier power/total power, dB	0.000 (-1.644)	0.000 (0.150)	0.000 (-0.550)	-2.440 (-6.360)	0.560 (1.460)	-0.660 (-1.820)
14	Received carrier power, dBm	-84.532 (-86.172)	4.708 (4.858)	-4.477 (-5.027)	-119.475 (-123.395)	5.858 (6.758)	-4.627 (-5.787)
15	Carrier threshold noise bandwidth, dB/Hz	13.000	-1.000	0.000	10.800	-1.000	0.000
Carrier tracking (one-way)							
16	Threshold signal-to-noise ratio in $2B_{LO}$ , dB	0.000	0.000	0.000	0.000	0.000	0.000
17	Threshold carrier power, dBm	-152.675	-1.700	0.700	-169.560	-1.706	0.607
18	Performance margin, dB	68.143 (66.503)	6.408 (6.558)	-5.177 (-5.727)	50.084 (46.164)	7.563 (8.463)	-5.234 (-6.394)
Carrier performance (data demodulation)							
16	Threshold signal-to-noise ratio in $2B_{LO}$ , dB	8.000	0.000	0.000	—	—	—
17	Threshold carrier power, dBm	-144.675	-1.700	0.700	—	—	—
18	Performance margin, dB	58.503	6.558	-5.727	—	—	—
Subcarrier performance							
19	Loss through receiver, dB	Data 1			Data 2		
		-0.000 (-0.102)	-0.000 (0.001)	-0.000 (-0.001)	-0.000 (-0.102)	-0.000 (0.001)	-0.000 (-0.001)
20	Subcarrier power/total power, dB	-3.660 (-10.200)	0.750 (1.000)	-0.880 (-0.500)	-3.660 (-7.200)	0.750 (1.000)	-0.880 (-0.500)

<sup>a</sup>Where only one value is given, it is the result obtained by both telemetry and command analyses. Where two values are given, the one in parentheses is the result obtained by command analysis and the other is the result of telemetry analysis.

Table 3 (contd)

No.	Parameter	Uplink			Downlink		
		Nominal value	Tolerance		Nominal value	Tolerance	
			Favorable	Adverse		Favorable	Adverse
Subcarrier performance (contd)							
		Data 1			Data 2		
21	Received subcarrier power, dBm	−120.695 (−94.834)	6.048 (5.709)	−4.847 (−4.977)	−120.695 (−91.834)	6.048 (5.709)	−4.847 (−4.977)
22	Bit or sync integration rate, dB/bits/s	9.208 (0.000)	0.000	0.000	15.229 (0.000)	0.000	0.000
23	Threshold, dB	5.600 (11.700)	−0.200 (−1.000)	0.200 (1.000)	5.600 (14.700)	−0.200 (−1.000)	0.200 (1.000)
24	Threshold subcarrier power, dBm	−165.552 (−153.975)	−0.906 (−1.700)	0.807 (1.700)	−159.531 (−150.975)	−0.906 (−1.700)	0.807 (1.700)
25	Performance margin, dB	44.856 (59.141)	6.953 (7.409)	−5.654 (−6.677)	38.835 (59.141)	6.953 (7.409)	−5.654 (−6.677)

Table 4. Design control table for station-centered ranging analysis

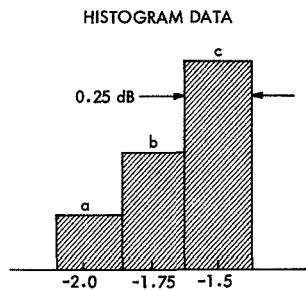
No.	Parameter	Uplink			Downlink		
		Nominal value	Tolerance		Nominal value	Tolerance	
			Favorable	Adverse		Favorable	Adverse
1	Total transmitter power, dBm (same power in watts)	70.000 10000.000	1.000 2589.252	-1.000 -2056.718	39.020 7.980	1.100 2.300	0.000 0.000
2	Transmitting circuit loss, dB	0.000	0.000	0.000	-2.130	0.370	-0.370
3	Transmitting antenna gain, dB	51.000	1.000	-0.500	7.250	1.500	-1.500
4	Transmitting antenna pointing loss, dB	0.000	0.000	-0.250	-7.590	1.313	-1.332
5	Space loss, dB Frequency, MHz (Range = 2.19153E-05 km)	-205.775 2116.000	0.000 —	0.000 —	-206.488 2297.000	0.000 —	0.000 —
6	Polarization loss, dB	-0.061	0.052	-0.052	-0.097	0.015	-0.015
7	Receiving antenna gain, dB	7.000	1.500	-1.500	53.000	1.000	-0.500
8	Receiving antenna pointing loss, dB	-6.616	1.147	-1.164	0.000	0.000	-0.250
9	Receiving circuit loss, dB	-0.080	0.010	-0.010	0.000	0.000	0.000
10	Net circuit loss, dB	-154.532	3.708	-3.477	-156.055	4.198	-3.967
11	Total received power, dBm	-84.532	4.708	-4.477	-117.035	5.298	-3.967
12	Receiver noise spectral density, dBm/Hz (Elevation = 17.734 deg)	-165.675	-0.700	0.700	-180.360	-0.706	0.607
	Zenith noise temperature, °K	—	—	—	55.000	-10.000	10.000
	Zenith noise spectral density, dBm/Hz	—	—	—	-181.196	-0.872	0.726
13	Carrier power/total power, dB	-9.000	0.000	-4.200	-5.010	1.120	-1.400
14	Received carrier power, dBm	-93.532	4.708	-8.677	-122.045	6.418	-5.367
15	Carrier threshold noise bandwidth, dB/Hz	13.000	-1.000	0.000	10.800	-1.000	0.000

Table 4 (contd)

No.	Parameter	Uplink			Downlink		
		Nominal value	Tolerance		Nominal value	Tolerance	
			Favorable	Adverse		Favorable	Adverse
Carrier tracking (one-way)							
16	Threshold signal-to-noise ratio in $2B_{LO}$ , dB	0.000	0.000	0.000	0.000	0.000	0.000
17	Threshold carrier power, dBm	−152.675	−1.700	0.700	−169.560	−1.706	0.607
18	Performance margin, dB	59.143	6.408	−9.377	47.514	8.123	−5.974
Carrier performance (data demodulation)							
19	Threshold signal-to-noise ratio in $2B_{LO}$ , dB	8.000	0.000	0.000	6.000	0.000	0.000
20	Threshold carrier power, dBm	−144.675	−1.700	0.700	−163.560	−1.706	0.607
21	Performance margin, dB	51.143	6.408	−9.377	41.514	8.123	−5.974
Turnaround channel							
22	Ranging power/total power, dB	−0.584	0.280	0.000	—	—	—
23	Ranging signal power, dBm	−85.116	4.988	−4.477	—	—	—
24	Ranging noise bandwidth, dB/Hz	61.760	−0.970	0.790	—	—	—
25	Ranging signal-to-noise ratio at the limiter	18.799	6.658	−5.967	—	—	—
26	Ranging power/channel output power, dB	−6.400	−0.000	−0.000	—	—	—
Demodulation and acquisition, planetary system							
27	Ranging power/total power, dB	—	—	—	−11.330	1.190	−1.540
28	Ranging signal suppression, dB	—	—	—	0.000	0.000	0.000
29	Ranging signal level, dBm	—	—	—	−134.765	6.488	−5.507
30	Required signal-to-noise ratio, dB (for 40-min acquisition)	—	—	—	3.610	0.000	0.000
31	Required ranging power, dBm	—	—	—	−176.750	−0.706	0.607
32	Performance margin, dB	—	—	—	41.984	7.193	−6.114

Next, the histogram data are generated by a comparison of the actual and predicted data, sorted into 0.25-dB increments of deviation from the predicted value, and then counted as to the number of times these deviations occur. Finally the data are normalized to 1 and reformatted to be compatible with the TYMSHARE EASYPLOT routine.

Then, the cumulative data are made from the histogram data. The number of times the deviation from the predicted value is equal to or greater than some integer multiple of 0.25 dB is counted. The data are normalized to 1 and formatted for the EASYPLOT plot routine. The following example will clarify the conversion from histogram data to cumulative data:



These data can be represented in the following manner:

$$a, -2.0$$

$$b, -1.75$$

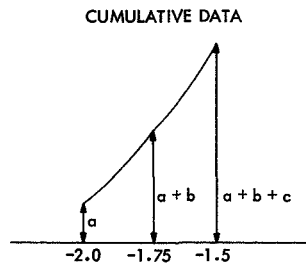
$$c, -1.5$$

where

$a$  = the number of times the actual value differs from the predicted value in the interval  $-1.875 \leq (\text{predict} - \text{actual}) \leq -1.625$

$b$  = the number of times for the interval  $-1.625 \leq (\text{predict} - \text{actual}) \leq -1.375$

$c$  = the number of times for the interval  $-1.375 \leq (\text{predict} - \text{actual}) \leq -1.125$



The cumulative data can be represented in the following manner:

$$a, -2.0$$

$$a + b, -1.75$$

$$a + b + c, -1.5$$

Since the data have been prepared for the plot routines, the next step is selection of the type of plot desired. When the choice is made, the program calls the appropriate data and plot routine.

The end results are actual vs predict plots, histograms, and cumulative plots.

*a. Actual vs predict plots as a function of time.* These plots show the predicted values of downlink carrier, uplink carrier, and SNR on the same graph as the actual, observed value for any time interval desired. At first glance, one is alarmed by the discontinuities in the plots, which are due to changes in the spacecraft state, such as ranging on or off, low/high power, low- and high-gain antenna, telemetry mode, etc. For this reason, it is recommended that most data analysis be restricted to the histograms and cumulative plots.

*b. Histograms.* The histograms show the number of times the difference between actual and predicted value fell in 0.25-dB increments of deviation from the predicted value. Actual values that deviate from the predicted value by more than  $\pm 2.5$  dB have been eliminated. In this way, the discontinuities mentioned above have been avoided. The histogram plots are normalized to 1.

*c. Cumulative plots.* The cumulative plots represent composite performance. They show the normalized number of times the difference between predicted and actual value is equal to or greater than some deviation from the predicted value. Increments of 0.25 dB are used, and actual values that deviate from predicted values by more than  $\pm 2.5$  dB have been eliminated.

**3. The limit cycling effects program.** The limit cycling effects program (LCEP) was written to calculate the results of spacecraft attitude on the high-gain antenna. Changes of attitude considered are changes due to the roll, pitch, and yaw of the craft. This calculation gives the predicted value of the gain of the high-gain antenna that can later be compared with the actual performance

The LCEP is designed to take values of the pitch, yaw, and roll of the spacecraft from the SFOF RECORDS program that outputs spacecraft telemetry channels in the form of time-tagged punch cards and calculates the high-gain antenna gain. The calculation is performed in four steps.

First, the values of pitch, yaw, and roll outputted by the SFOF RECORDS program in units of data number are converted to milliradians. The conversions are made by the following formulas. The coefficients B0, B1 . . . C0, C1 . . . D0, D1 . . . are derived from the spacecraft calibration data books.

where

PICH = value of pitch in milliradians

PIT = value of pitch in data number

where

YAW = value of yaw in milliradians

YAY = value of yaw in data number

where

COM = value of roll in milliradians

CAN = value of roll in data number

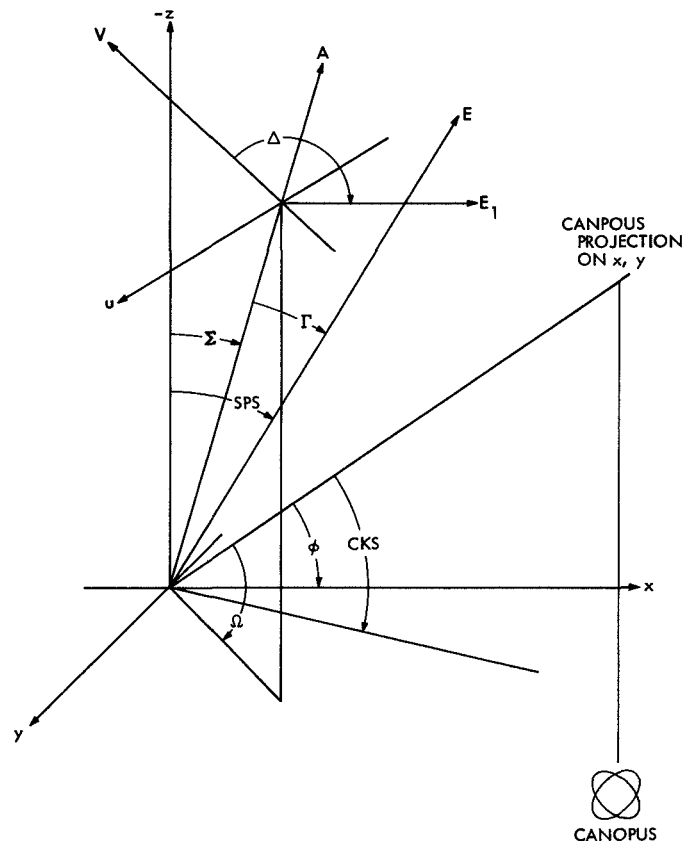
In the second step, the values of pitch, yaw, and roll are combined to give the antenna boresight cone and clock angles. Figure 25 is a diagram of the coordinates.

where

$$\Omega = \gamma + \text{COM}$$

 $\Sigma$  = antenna boresight cone angle $\Omega$  = antenna boresight clock angle $\alpha$  = antenna boresight cone angle nominal (no variation in spacecraft attitude)

$\gamma$  = antenna boresight clock angle nominal (no variation in spacecraft attitude)



- CKS SPACECRAFT REFERENCED CLOCK ANGLE
- SPS SPACECRAFT REFERENCED CONE ANGLE
  - $\Omega$  LOCATION OF THE ANTENNA BORESIGHT AXIS IN SPACECRAFT REFERENCED CLOCK ANGLE
  - $\Sigma$  LOCATION OF THE ANTENNA BORESIGHT AXIS IN SPACECRAFT REFERENCED CONE ANGLE
  - $\Delta$  ANTENNA REFERENCED CLOCK ANGLE
  - $\Gamma$  ANTENNA REFERENCED CONE ANGLE
  - $\phi$  LOCATION OF  $+x$  AXIS OF SPACECRAFT COORDINATE SYSTEM WITH RESPECT TO 0-deg SPACECRAFT CLOCK ANGLE
- E SPACECRAFT TO EARTH VECTOR
- $E_1$  PROJECTION OF SPACECRAFT TO EARTH VECTOR ON (U,V) PLANE
- A ANTENNA BORESIGHT VECTOR
- V VECTOR COINCIDENT WITH 0-deg CLOCK ANGLE IN ANTENNA COORDINATES
- ( $x, y, z$ ) SPACECRAFT COORDINATE SYSTEM
- ( $u$ ) ANTENNA COORDINATE

**Fig. 25. Spacecraft and high-gain antenna coordinate system**

Then the antenna boresight offset is calculated next with the formula

$$\cos \Gamma = \sin (\text{SPS}) \sin \Sigma \cos (\text{CKS} - \Omega) \\ + \cos (\text{SPS}) \cos \Sigma \quad 0 \text{ deg} \leq \Gamma \leq 180 \text{ deg}$$

where

SPS = spacecraft reference cone angle

CKS = spacecraft reference clock angle

$\Gamma$  = angle off-center antenna pattern, antenna boresight offset

Finally, the gain of the antenna is calculated from the antenna boresight offset angle. A curve fit to the high-gain antenna pattern is used.

$$G = E0 + (E1)(\Gamma) + E2(\Gamma)^2 + E3(\Gamma)^3 + E4(\Gamma)^4 \\ + E5(\Gamma)^5 + E6(\Gamma)^6 + E7(\Gamma)^7$$

where

$G$  = gain

$\Gamma$  = antenna boresight offset angle in degrees.

**4. Limit cycling effects program-PLOT.** This program is designed to reformat the data from LCEP to a form compatible with the TYMSHARE EASYPLOT plot routine. Plots are outputted for any time interval and include the variation in pitch, yaw, and roll (Canopus), the antenna boresight angle offset, the gain, and the difference of the gain from the nominal value (no variation in spacecraft attitude). Figure 26 is an example of plots output.

**5. Post mission analysis program.** The post mission analysis program (PMAP) collects the actual performance data from the mission dependent tapes (MDTs) over the time period requested; it reformats these data and produces an output tape for the plot and histogram program. The MDTs are generated by the IBM 7044

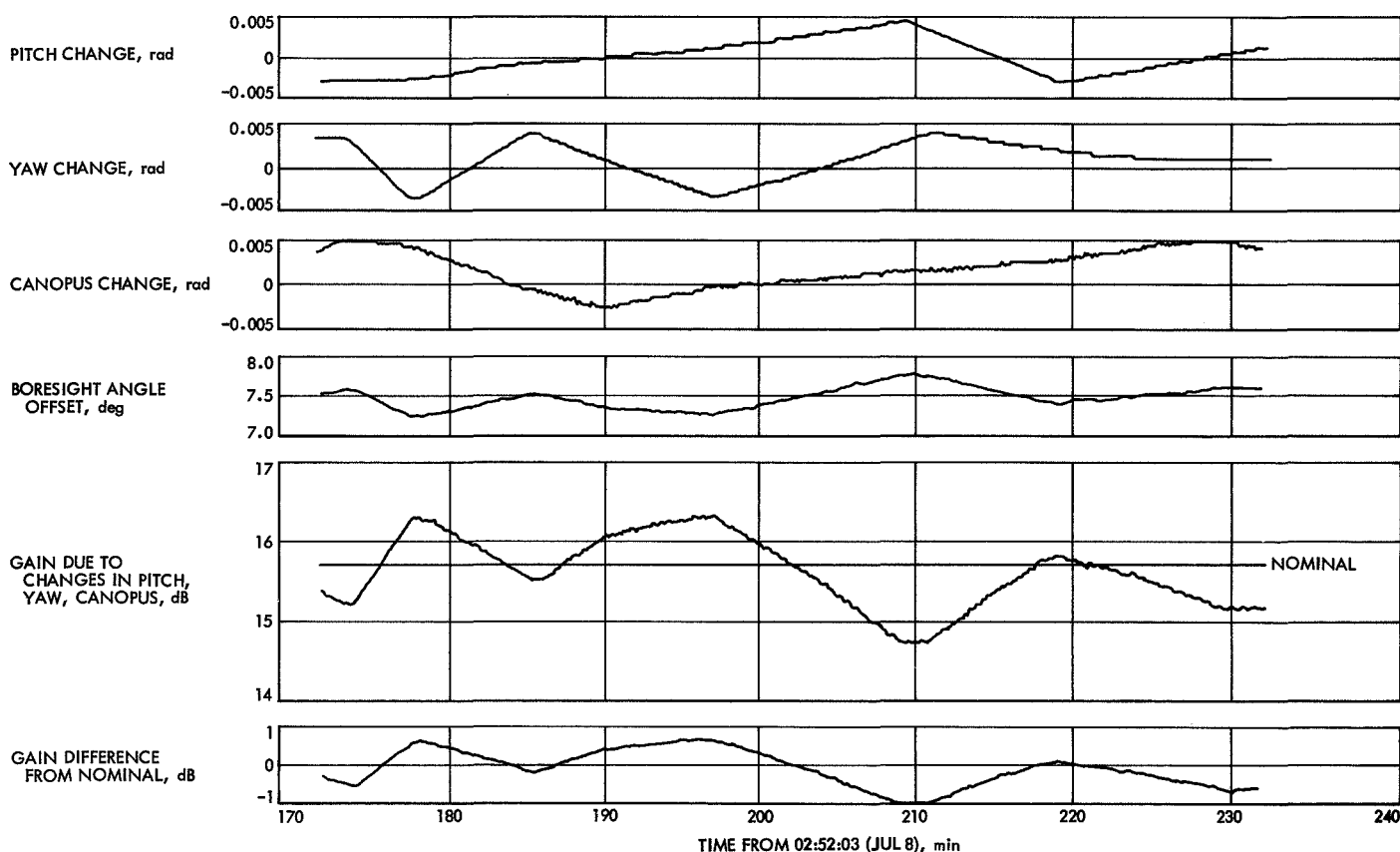


Fig. 26. Typical output of plotter showing high-gain antenna change for Mariner VII

Mariner Mars 1969 mission dependent program and are logs of time-tagged, frame-synchronized telemetry data.

When the spacecraft, Deep Space Station, GMT day, and zenith noise temperature are selected, all values for telemetry SNR, uplink and downlink carrier levels are calculated and stored. These calculations are as follows:

$$\text{Telemetry SNR} = 10 \cdot \log \left\{ \frac{1}{2} \left[ \left( \frac{N \cdot SQ}{XAB^{**2}} \right) - 1 \right]^{-1} \right\}$$

where

$N$  = sample size

$$SQ = \sum_{i=1}^N Xi^2, \text{ (from MDT)}$$

$$XAB = \sum_{i=1}^N |Xi|, \text{ (from MDT)}$$

$$\text{Uplink carrier level} = C_0 + C_1 \cdot X + C_2 \cdot X^2 + \dots + (C_5 \cdot X^5)$$

where

$C_i$  = coefficient of calibration curve for a particular spacecraft

$X$  = spacecraft AGC in data number, (from MDT)

$$\text{Downlink carrier level} = C_0 + C_1 \cdot X + C_2 \cdot X^2 + \dots + (C_5 \cdot X^5)$$

where

$C_i$  = coefficient for downlink carrier level calibration curves

$X = (LAGC/204.7) = \text{AGC in volts, (LAGC from MDT)}$

The trajectory tape is also scanned over the same period of time, and a table of ground station antenna elevation angles is read and stored. So-called "adjusted" telemetry SNR is then obtained by elimination of the degradation in ground station receiver noise spectral density due to the increase in system noise temperature at low elevation angles. Thus, degradation is expressed by the following relationship:

$$\text{Degradation} = 10 \cdot \frac{Tz + \Delta Te}{Tz + \Delta Tp}$$

where

$Tz$  = zenith noise temperature

$\Delta Te$  = temperature increase relative to zenith noise temperature at time  $T$

$\Delta Tp$  = temperature increase at time of peak elevation angle

Histogram data are compiled by subdivision of the range of a particular measurement into 0.25-dB intervals and by tabulation of the frequency of the values that fall within each of the subdivisions. These data are then compressed and shifted to produce a histogram of forty 0.25-dB cells, centered around the cell of highest frequency. The mean and variance of this grouped data are also calculated.

The results of all of these calculations are then printed on paper and written on the output tape for use with the plot and histogram program.

**6. Post mission analysis program—PLOT.** The post mission analysis program—PLOT is designed to read the tape made by the post mission analysis program and to produce time plots and histograms of the data mentioned earlier.

Each plot gives time along the  $x$ -axis with the values of SNR, uplink carrier level and downlink carrier level measured along the  $y$ -axis. The plots are then identified by station and spacecraft.

The histograms are drawn with the 0.25-dB intervals along the  $x$ -axis. The height of each cell is given as a percentage of the total and denoted along the  $y$ -axis. Also given with each histogram is the station, spacecraft, and GMT day along with the mean, variance, and total number of observations.

## II. Spacecraft Telecommunications Subsystems

The functions and relations of the four telecommunications subsystems (radio frequency, flight command, flight telemetry, and data storage subsystems) and the major elements within the subsystems are shown in Fig. 27.

### A. Radio Frequency Subsystem Performance

The radio frequency subsystem (RFS) receives uplink command and ranging signals transmitted by the Deep Space Instrumentation Facility (DSIF) and transmits telemetry and ranging signals to the DSIF. The RFS uses a high-gain antenna for transmitting during and after encounter, and a low-gain antenna to receive at all times and to transmit during cruise.



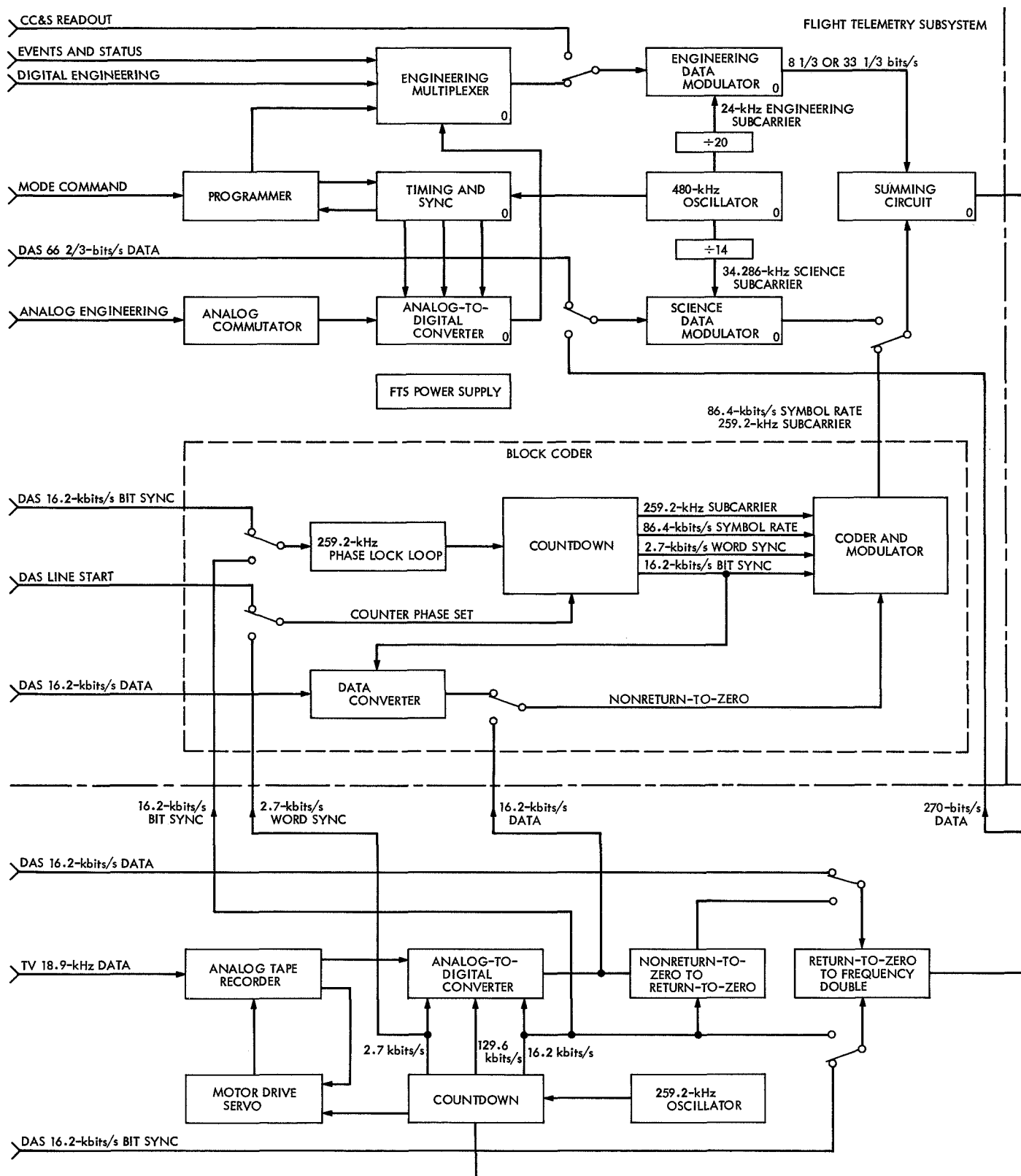


Fig. 27. Mariner Mars 1969 spacecraft telecommunications subsystems

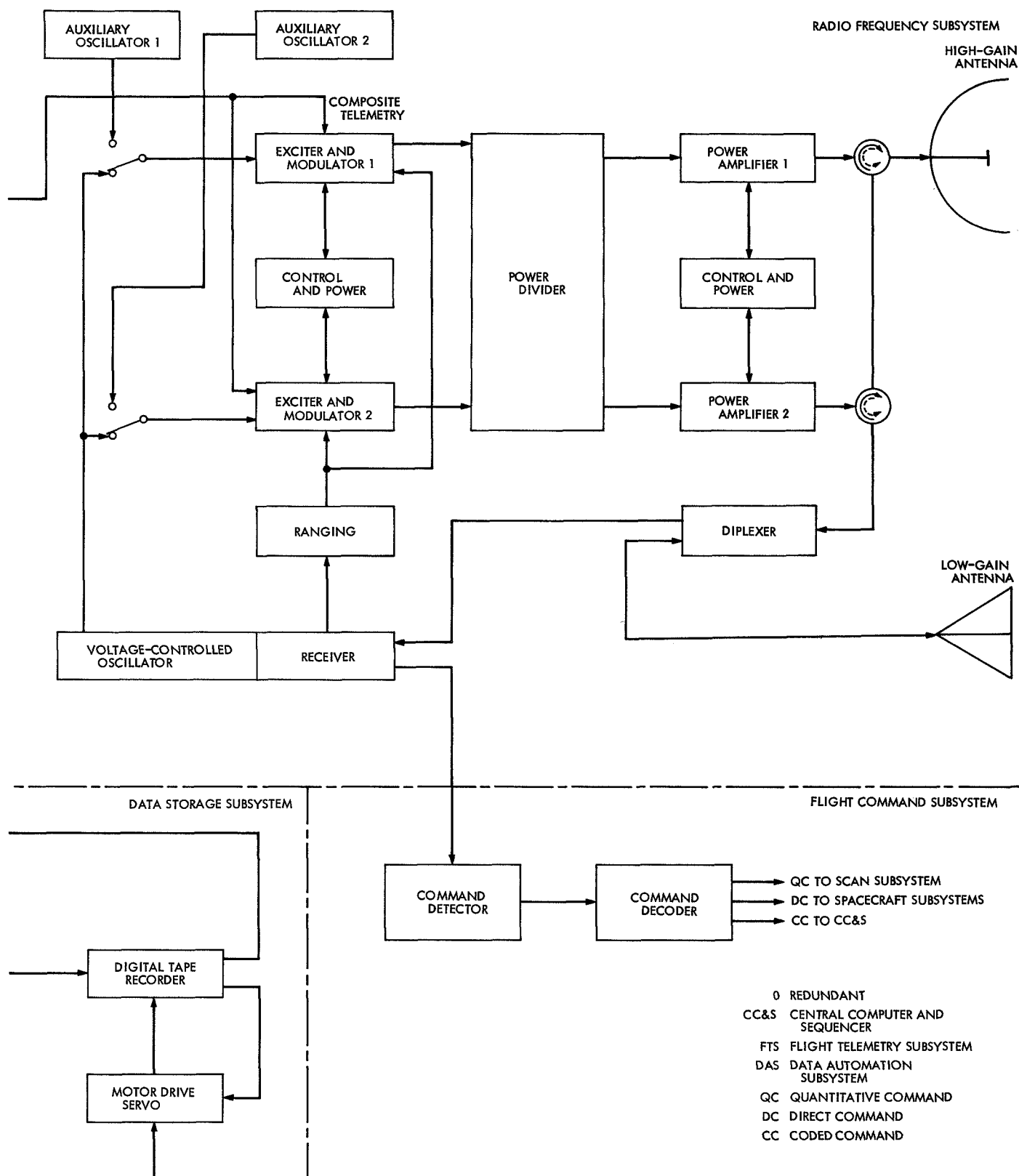


Fig. 27 (contd)

The radio frequency subsystems on both *Mariners VI* and *VII* performed well throughout the missions. Although there were a number of problems and anomalies, they did not prevent the RFS from fulfilling all mission requirements.

**1. Summary.** Before being included in the launch countdown at  $T - 210$  min, system test equipment, launch complex equipment, and communication links were checked and verified. This was followed by application of power to the spacecraft, placing it in the launch mode, and verifying all launch functions, including data sources and outputs. Radio frequency subsystem measurements were completed by  $T - 120$  min when removal of the launch pad service tower was initiated. Although it had no effect on the operation of the flight telemetry subsystem (FTS), tower removal caused small fluctuations of about 0.1 dB in output power indications for both *Mariners VI* and *VII*.

During countdown and launch, the RFS was transmitting in low power via the omnidirectional antenna to DSS 71, the checkout site at Air Force Eastern Test Range (AFETR), which remained in the one-way mode. After launch, spacecraft transmissions were received by various AFETR tracking stations (see Launch Operations in Part 2 of this volume). Some 25 min after launch, DSS 51 in Johannesburg acquired the signal, followed by two-way lock with the spacecraft radio. Although some anomalies were observed during this phase, tracking and telemetry data were received without interruption.

The RFS subsystems remained in the low-power, low-gain cruise mode until June. The ranging transponder was in operation in the near-Earth mode on *Mariner VI* from the day of launch until March 19; *Mariner VII* near-Earth ranging was not begun until April 1 and continued until April 25. The spacecraft transmitters were commanded into the high-power mode on June 9 (*Mariner VII*) and June 16 (*Mariner VI*), and the downlink signal was switched to the high-gain antenna for *Mariner VII* on July 7, and for *Mariner VI* on July 10. The ranging transponders resumed operation (with the R&D planetary distance ground equipment at DSS 14) on July 8 and 7, respectively. In this mode, transmitter at high power, receiving on the low-gain antenna and transmitting on the high-gain antenna, with the ranging transponder turned on for each DSS 14 pass, the spacecraft RFSs operated through encounter and playback.

**2. Antennas.** During both the *Mariners VI* and *VII* midcourse maneuvers, the spacecraft were in the receive

and transmit low-gain antenna mode. Therefore, any pitch, yaw, or roll maneuvers yielded true "free-space" antenna patterns of the low-gain antenna.

Predictions of the *Mariners VI* and *VII* low-gain antenna performance were made from full-scale spacecraft antenna pattern measurements performed on the JPL Mesa Spacecraft Antenna Range. Therefore, the data did not represent true free-space measurement conditions. To compensate for the known free-space error, a rigorous range analysis was performed to determine the magnitude of error so that a correction could be made. A 100% correction cannot be made because of the number of possible error sources. However, the correction error introduced into the *Mariner Mars 1969* antenna measurements was a magnitude of 4 dB less than what it was in earlier programs. The reduced error was attributed to a new approach in making the measurements and reducing the data.

Figures 28 and 29 show the predicted and actual low-gain antenna gain variations during the midcourse maneuvers of the *Mariner VI* and *VII* spacecraft. Figure 28 shows the gain variation of *Mariner VI* as a function of time from the beginning of the maneuver. At 0 s, the spacecraft broke lock with DSS 12 (began turn maneuver). The spacecraft continued to turn (change in cone angle) until 125 s. At this point, it stopped turning and began to roll (change in clock angle). It rolled from 125 until 1079 s and then stopped. The correlation be-

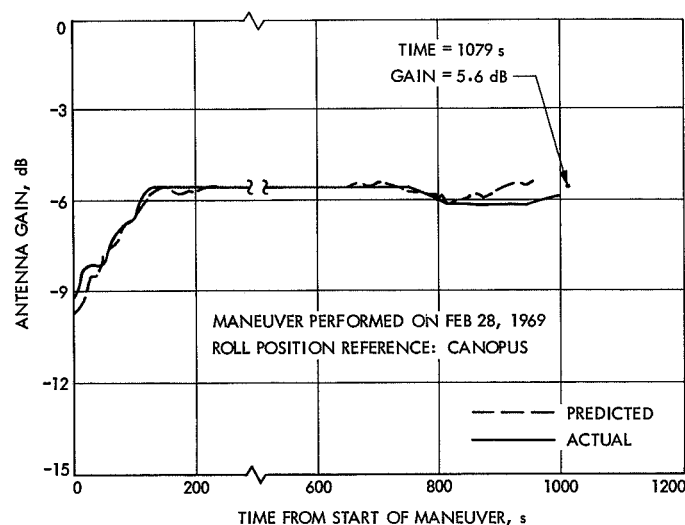


**Fig. 28. Gain variation of low-gain antenna during midcourse maneuver of *Mariner VI* (downlink)**

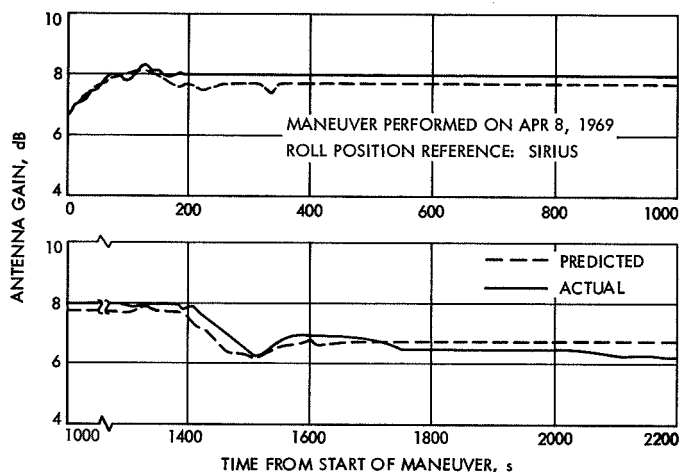


**Fig. 29. Gain variation of low-gain antenna during midcourse maneuver of *Mariner VII* (downlink)**

tween the predicted and actual gain variations was closer than that experienced on any other program.

Figure 29 shows the gain variation of the *Mariner VII* low-gain antenna as a function of time from the beginning of the maneuver. The spacecraft turned from 0 to 175 s, stopped, and then rolled from 175 until 1000 s and stopped. The spacecraft began to turn again at 1275 s, stopped at 1550 s, and rolled from 1550 to 2200 s. Here, again, the correlation between the predicted and actual gain variations was better than that achieved on any previous program.

**3. Transponder temperature effects.** During cruise, there was relatively little spacecraft activity. Radio frequency subsystem operating temperatures decreased rapidly during liftoff, then decreased gradually to temperatures about 10°F lower than at launch. About 110 days after launch, the RFS was commanded to the high-power mode and temperatures increased rapidly by about 13°F. Turning on the gyros also increased RFS temperatures by about 1–2°F. All of these fluctuations followed the predictions very closely and all temperatures remained well within the operating limits.

Radio frequency subsystem flight temperature histories for *Mariners VI* and *VII* were obtained by transducers located on the voltage-controlled oscillator (telemetry channel 404), traveling-wave tubes 1 and 2 (telemetry channels 418 and 433), and the auxiliary oscillator (telemetry channel 430).

Special tests were run on both RFSs to resolve some of the anomalies that occurred during the cruise phase.

The anomalies and special tests are described under Subsection B-1-d, which follows. The special tests included threshold sensitivity measurements, the effects of turning ranging on and off, attempted measurements of the receiver loop bandwidth, and analysis of the downlink spectrum.

During encounter, spacecraft temperatures vary as a result of changes in power requirements. Turning on the science subsystems and gyros results in a temperature rise in the RFS of about 2–4°F. This temperature rise causes slight changes in the telemetry calibrations and in the voltage-controlled oscillator (VCO) and auxiliary oscillator frequencies.

Accurate prediction of the downlink frequency upon spacecraft exit from occultation is essential to allow rapid acquisition by the ground station for support of the occultation experiment.

*Mariners VI* and *VII* both entered occultation in two-way lock and acquired one-way lock upon exit since best-lock frequency could not be predicted accurately enough (within about 100 Hz) to assure rapid acquisition of the preferred two-way lock. Predictions of best-lock frequency were believed to be within 500 Hz, and lock was obtained in a very few seconds several times during special tests made before encounter. However, temperatures varied during occultation, and confidence was not sufficient to guarantee a rapid enough lock-up. Therefore, the somewhat less accurate but more certain one-way data were used for the occultation experiment.

The RFS on each spacecraft functioned normally during playback, providing a 16.2-kbits/s data rate for the first time on a deep-space mission.

**4. *Mariner VI* problems and anomalies.** *Mariner VI* experienced a slightly greater than usual increase in automatic gain control (AGC) voltage when ranging was turned on during countdown. During launch, a drop of about 0.3 dB in output power occurred, followed by recovery. A false lock and some self locks occurred during cruise, as well as some temporary local oscillator and exciter drive level variations. There was also a period during which the downlink frequency was unstable, and the auxiliary oscillator frequency drifted upon transfer from two- to one-way track. A discussion of these problems and anomalies follows.

*a. Countdown anomaly.* The performance of *Mariner VI* RFS was normal during countdown in every respect

except one. The countdown procedure called for a DC-9 command to be sent at  $T - 80$  min and a second DC-9 command at  $T - 65$  min to verify ranging performance by turning ranging on for 15 min, and then off. When the first DC-9 command was received, ranging was turned on as expected and, at the same time, the telemetry indicated that the AGC voltage had increased by two data numbers, or about 2 dB. This general effect was well known. The effect, which is discussed later in this report in connection with the false-lock phenomenon, is caused by feedback from the video amplifier output stages through the +15-V line, modulating the VCO and creating sidebands that are multiplied and injected into the mixers. These sidebands correspond in frequency with the sidebands on the uplink signal and add to them, with the result that the carrier suppression of the received signal and the resultant AGC voltage are changed.

Previously, the change that occurred in AGC voltage was only one data number, so the effect during countdown appeared to be greater than usual. After some discussion, it was decided to proceed with the launch as planned. Calculations made later indicated that up to about 1.5 dB changes in AGC voltage could occur in this manner, depending upon the transfer characteristics of the feedback path and other factors. It seems probable that the effect barely exceeded one data number and that the AGC reading when the DC-9 command was sent was very close to the maximum in its data number range. No further occurrence of a two-data-number change in AGC voltage with ranging turned on or off was observed during the remainder of the mission.

*b. Launch anomaly.* The *Mariner VI* spacecraft was launched in the low-power (nominally 8-W transmitted) mode. An apparent drop of about 0.3 W in output power occurred during spacecraft separation about 13 min later. This output power change was indicated by the low-gain antenna drive telemetry channel; it was not confirmed by DSS 71. It is believed to have been caused by proximity effects of the solar panels reacting on the low-gain antenna. This was a night launch (01:29 GMT), and spacecraft temperatures decreased rapidly following liftoff, affecting the power monitor calibration. At  $L + 1$  h, the power output indication was close to its calculated value for the temperature at that time. At approximately  $L + 1$  h 54 min, the telemetry indicated a sudden output power drop of about 0.3 W. There was no spacecraft event at that time. Ground station AGC data confirmed the time and magnitude of the change. All other telemetry indications were normal. The power output remained at this level for more than 59 h, re-

covered to normal for 2 h, and dropped again to its lower value. About 16 h after the second drop, power output recovered fully and remained normal throughout the balance of the mission. During the low-power output period, both traveling-wave tube (TWT) base temperatures increased about 1°F, and, after recovery to full output power, both decreased to normal values. This was consistent with the power change of about 0.3 W, since the increased radiated power produces a decreased dissipated power within the RFS.

The nature of this problem is such that the fluctuating power levels could have been caused by either:

- (1) An impedance discontinuity in the connectors, RF cabling, or microwave components subsequent to the TWT output, causing reflected power back into the traveling-wave tube amplifier (TWTA) subassembly.
- (2) Varying conditions within the TWTA producing variable output powers.

Item (1) was investigated using the proof-test model spacecraft. A discontinuity with controlled reflection coefficient and phase was inserted at several points within the RFS. It was found that a voltage standing-wave ratio (VSWR) of about 2.0:1 established anywhere from the TWTA output up to, but not including, the low-gain antenna port produces telemetry channel 214 power steps similar to those observed on *Mariner VI*. Placing the discontinuity at the low-gain antenna port causes quite different symptoms and is not likely to be the source of trouble. Since both TWT temperatures varied with the channel 214 fluctuations, it is impossible to determine if the VSWR discontinuity was located such that the reflected power was dissipated in the on or off TWT.

Item (2) could also cause identical channel 214 symptoms to those verified for item (1). Changing gain conditions within the TWT would have had essentially the same effect on performance. Excess power not extracted by the wave would be intercepted at the collector of the TWT, causing temperature and power variations such as were observed. Researching pertinent test data from operations at JPL and AFETR provided some evidence of varying power levels in the past over about the same range of power output during thermal vacuum testing. This latter variation occurred at slightly lower temperatures. Since there is little data to analyze, the exact cause cannot be determined.

A somewhat similar variation in output power occurred on *Mariner VII* following launch.

c. *False lock.* On the first day after launch, DSS 41 attempted to acquire uplink lock with a signal level of  $-97$  dBm at the spacecraft. A false lock occurred, characterized by a static phase error (SPE) offset and transfer from the auxiliary oscillator to the VCO. Transmitter power was then reduced from 2 kW to 200 W and a new frequency prediction was used. A normal acquisition resulted. The ranging channel was on, and the false lock was typical of those seen during prelaunch tests.

False lock is caused by feedback of a beat frequency that is the difference between the uplink signal and the VCO frequency times 110.5 before phase lock is attained. This beat frequency is fed back from the video amplifier to the VCO via the +15-V power supply line. It frequency-modulates the VCO, producing sidebands at plus and minus the beat frequency. One of these sidebands mixes with the uplink signal in the first mixer, producing a signal near to the best-lock frequency. This latter signal passes through the crystal filter, producing an output from the phase and AGC detectors determined by phase relations around the feedback loop.

Since the phase conditions are determined partly by the transfer characteristics of a stray (uncontrolled) path, the result can be that the VCO is pushed off its best-lock frequency (producing an SPE offset) and/or AGC voltage is produced. Signal levels in excess of about  $-110$  dBm can cause false lock during uplink acquisition if they are offset more than about  $\pm 10$  kHz from best-lock frequency. Turning off the ranging channel, by means of a DC-9 or the cyclic Y1 command, breaks the path and allows normal uplink acquisition at considerably higher uplink signal levels.

d. *Self lock.* On the day after launch, it was also noted that the SPE stabilized at 5–10 kHz below its normal ( $\pm 1$  kHz) value. This occurred with no uplink signal and with ranging on. The following day, an SPE offset was noted in the presence of an uplink signal, but with the receiver out of lock (indicated by AGC voltage) and ranging on. This offset disappeared as soon as the uplink signal was turned off. Also, on the second day after launch, an SPE shift of about 4 kHz was noted when the first inflight Y1 command turned off ranging while the receiver was in one-way lock. On  $L + 23$  days, the receiver transferred from auxiliary oscillator to VCO

with no uplink signal. This also occurred with ranging on.

A test was run to learn as much as possible about the mechanism causing these anomalous effects and to determine their severity and any possible safeguards that could be applied. If a fairly strong self lock occurred, it appeared possible that it might persist and prevent further communication from the ground.

The results of the tests indicated that the effect occurred only with ranging on. It disappeared when a Y1 command turned ranging off. It was also demonstrated that uplink lock could be acquired during the self-lock condition at a signal strength of  $-135$  dBm at the spacecraft. Acquisition of uplink lock at lower signal levels was not attempted.

It was decided that extreme caution should be exercised in the use of ranging, and ranging was, accordingly, turned on only a few times during the rest of the flight. After transfer to high power, no further effects of the type described above were noted. Nevertheless, ranging was not turned on and Y1 cyclic commands were sent every 3 h during *Mariner VI* encounter as a precautionary measure.

The false lock and SPE offset effects that occurred with an uplink signal present were typical of the effects observed earlier when uplink acquisition was attempted with ranging on and at high uplink signal levels. The self lock required some source of a spurious signal, or of feedback of one of the coherent signals in the RFS, in addition to the false-lock condition. After considerable analysis and testing, it was concluded that a spurious signal generated in the RFS itself was the most probable cause of the anomaly. The probable source of the spurious signal appeared to be in the cascode circuits of the mixer–preamplifier. A parasitic oscillation was detected during the design phase and a minor circuit change was made to eliminate it. However, the expected elimination may not have been accomplished since a thorough test of the new circuit over the entire temperature range was not conducted because of schedule requirements.

A characteristic of this type of parasitic oscillation is that it may exist over a very narrow range of temperature and voltage conditions. It is generally unstable in frequency and has so much phase jitter the receiver

cannot phase lock onto it directly. However, the receiver can false-lock to it and it can produce any or all of the effects noted. The switch to high power about  $L + 100$  days raised the RFS temperature, and the spurious signal ceased or changed frequency and amplitude so that it no longer affected receiver performance noticeably.

A hypothesis was developed, based upon the existence of a parasitic oscillation at about one-fifth of the uplink best-lock frequency. This frequency was multiplied by 5 in the first mixer and looked like an uplink signal to the receiver. Its signal strength was just right to produce a weak self lock or an SPE offset, depending upon its frequency.

A test was run on the spare RFS to verify this hypothesis. A simulated parasitic signal was injected through the diplexer in an effort to avoid damage to a flight radio during disassembly. Each of the anomalous conditions was verified.

During the test phase, there were two similar occurrences of apparent uplink-signal acquisition when no signal was known to be present on the same RFS. It now appears these might have been self locks instead of being caused by external signals picked up over the air link, as suspected earlier. The first occurred during vibration testing and the second occurrence was at the AFETR. Four separate apparent acquisitions of uplink signal occurred. In both cases, the attempts to reproduce the anomaly were unsuccessful.

A threshold-degradation phenomenon experienced on *Mariner VII* and described later can be attributed to the same cause if the frequency of the signal resulting from the parasitic oscillation is either just inside or outside of the false-lock range. In these cases, the condition can cause blocking in the second IF (inside) or in the first IF (outside) and result in threshold degradation without AGC or SPE offsets. This also was verified during the tests on the spare RFS.

*e. Local oscillator drive variations.* The local oscillator drive telemetry (channel 422) had indicated erratic variations during test at JPL and at the AFETR. It was stable during countdown, launch, and the first 51 days after launch. From  $L + 52$  to  $+ 58$  days, the local oscillator drive varied erratically from its nominal value by  $+0.4$  to  $-1.0$  dB, returned to normal for about two days, then dropped about 0.7 dB and stabilized at that level. It remained stable, changing only according to its tempera-

ture characteristic following the switch to high power at  $L + 110$  days. At 19 days after the power switch, the local oscillator drive again became unstable, and during the following 20 days, it varied erratically from  $+0.5$  to  $-2.4$  dB above and below its normal value. It then stabilized at a value about 0.7 dB below its previous stable level.

The unstable operation of the oscillator was similar to that observed on the *Mariner Mars 1964* mission. It is believed to have been caused by variations in contacts between a tuning screw and its grounding fingers in the  $\times 3$  multiplier used in the  $\times 36$  multiplier output circuit. This variable grounding path changes the tuning of the circuit slightly. The effect of the slight detuning is large because the  $\times 3$  multiplier circuit was tuned into a flat resistive load on *Mariner VI*, and its mixer load has a reactive component that detunes the  $\times 3$  circuit so that it operates somewhat off its center frequency. At no time during the unstable periods was there any measurable effect upon the receiver threshold sensitivity or other performance parameter. The maximum degradation of receiver noise figure is estimated to be 0.5 dB at the lowest drive level. The problem was resolved on *Mariner VII* by changing the test and alignment procedure to permit retuning the  $\times 3$  output circuit after mating with the mixer. In addition, consideration should be given to redesigning the contact fingers for future programs.

*f. Exciter drive variations.* Some anomalous small variations in the telemetry indication of exciter drive to the TWT occurred starting at  $L + 74$  days. Exciter drive had been stable within a 0.03-dB range since launch, with only variations caused by the temperature sensitivity of the channel. On  $L + 74$  days, exciter drive telemetry (channel 210) indicated an increase in drive of about 0.05 dB. Drive continued to rise to a maximum of about 0.2 dB above normal, then returned to normal about a week later. After some minor fluctuations, it again rose by about 0.2 dB at 20 days after the first occurrence, remained at the higher level for a week, then gradually decreased to its normal value. There was no indication of any change in TWT helix current or output power at any time corresponding to the periods of increased drive.

The switch to high output power occurred a few days later, and exciter drive telemetry indications were normal for the higher temperatures prevailing during the balance of the mission.

Possible causes of this anomaly are as follows:

- (1) The exciter drive actually did increase slightly as indicated by channel 210 telemetry.
- (2) The sensitivity of channel 210 varied.
- (3) There was a change in VSWR between the exciter and the TWT input circuit.

The variation was small and could not be explained because of the lack of any other data. No similar effects were observed during any other phase of the program on any RFS or on *Mariner VII* during flight.

*g. Auxiliary oscillator drift.* A long-term frequency drift of the downlink signal was indicated by the doppler residuals each time that a switch from two-way to one-way tracking occurred. The drift was caused by a small temperature change in the vicinity of the crystal and oscillator circuit in the auxiliary oscillator module, coupled with the frequency characteristics (250 Hz/°F drift at S-band) of the oscillator over the mission temperature range. The effect was of about the same magnitude in both *Mariners VI* and *VII*.

The initial drift immediately after transfer was about 3 Hz in 1 min. The duration of the drift was about 1 h, corresponding to the thermal-time constant of this part of the RFS. To perform the occultation experiment adequately, rapid acquisition of the downlink signal upon exit from occultation was required. The accurate prediction of downlink frequency necessary to accomplish rapid acquisition was provided by calibrating the drift rate of the auxiliary oscillator.

*h. Short-term frequency instability.* From  $L + 54$  to  $+71$  days, the short-term frequency stability of the downlink signal was outside of specification limits in the one-way-lock mode. The specification limit is 0.459 Hz peak to peak in a 1-min interval at a  $\frac{1}{4}$ -s integration period at S-band. Frequency variations as indicated by doppler residuals were exceeding five times that limit. After day 71, the short-term frequency of the downlink signal remained normal.

Examination of the data and calculation of the modulation index required to produce an equivalent frequency modulation of the downlink signal indicated that the only place in the RFS where this amount of frequency modulation could occur was in the auxiliary oscillator. The possibility of noise on the AGC voltage

modulating the auxiliary oscillator via the transfer command line was experimentally investigated and rejected as a possible cause of the anomaly.

The remaining possible causes, none of which could definitely be assigned as the cause of the anomaly, were:

- (1) An intermittently unstable crystal. A similar effect had been observed in a similar oscillator; it occurred intermittently and disappeared when the crystal was replaced.
- (2) A faulty connection in the oscillator circuit. An unsoldered or fractured connection might have been stressed at the temperature involved so that noise resulted. Fractures of the connection to crystal elements have occurred.
- (3) A faulty component. It could probably be a tantalum capacitor that self-healed after some time.

*5. Mariner VI postencounter tests.* The *Mariner VI* self-lock and AGC offset anomaly could not be reproduced after the switch to high power as described earlier. This was attributed to the resulting temperature of about 14°F higher than that at which the anomaly occurred. After the major postencounter activities had been completed, tests were devised in an attempt to reproduce the anomalous performance. The temperature of the RFS was reduced (by a reduction in spacecraft power consumption) to the range in which the anomalies occurred and stabilized there with the radio in the same configuration as it had been during the anomalies. Arrangements were made to perform a spectrum analysis of the downlink signal with ranging on in an effort to learn something about any spurious oscillations in the RFS. Uplink lock was established and then broken several times because this had been the sequence of events when the anomaly had occurred. Despite this duplication of conditions, the anomaly could not be reproduced. At the distance to the spacecraft then prevailing, it was necessary to use the 210-ft antenna at DSS 14 for these tests; considerable manpower and other equipment were required. In view of the difficulty and cost of performing these experiments and the low probability of obtaining useful data, experiments were terminated in October 1969. The hypothesis contained in the description of the self-lock and AGC offset anomalies during the *Mariner VI* cruise phase offers an explanation of the mechanism by which the anomalies were produced; the failure to reproduce them after encounter is believed to have been caused by the unstable nature of the parasitic oscillation in the mixer-preamplifier.



Thorough analyses and tests of all circuits that could have contributed to the anomaly and the appropriate corrective action are recommended.

**6. Mariner VII problems and anomalies.** *Mariner VII* experienced a transmitter power output drop of about 3 dB soon after launch; recovery followed at *Centaur*/spacecraft separation. A threshold sensitivity degradation up to about 10 dB appeared intermittently and there were some minor variations of TWT helix current during cruise. About one week before encounter, the pre-encounter anomaly occurred, and some of the RFS telemetry channels were lost because of a failure in the FTS. The RFS was not damaged.

*a. Power output variations.* The *Mariner VII* power output during launch varied in a manner similar to that of *Mariner VI*. Since *Mariner VII* was launched about 3 h earlier, temperature changes after liftoff were smaller and less rapid and the effects on power monitor calibration were less.

The *Mariner VII* telemetry indicated an increasing transmitter power output at liftoff. The last telemetry reading at liftoff indicated a rise of about 0.1 dB above its previous stable value. It rose about 0.2 dB more just after liftoff, dropped 0.1 dB, and rose 0.2 dB at  $L + 3$  min, for a net increase of about 0.3 dB from prelaunch conditions. The power output indication then decreased to the level at launch for one data sample. The next sample occurred after nose fairing jettison (about  $L + 3$  min 50 s). This sample indicated a 3-dB drop in low-gain antenna drive power. Deep Space Station 71 (Cape Kennedy) dropped lock at that time and TEL-4 (Merritt Island) AGC indicated a sudden drop in output signal of about 25 dB. This large drop is believed to be unrelated to the 3-dB change. Merritt Island station also lost lock about 1 min later because of the low signal strength and low elevation angle of the spacecraft. Ground station and telemetry data indicated that power output remained low by about 3 dB until *Centaur*/spacecraft separation at about  $L + 13$  min; the Antigua station AGC showed a sharp upward rise of 3 dB at exactly that time, and the next telemetry sample indicated full recovery of low-gain antenna drive power. Throughout the balance of the mission, there were no recurrences of this anomalous condition. It was noted that, during the period of decreased output power, the temperature of the operating TWT increased by about 3°F, instead of continuing to decrease with ambient temperature as expected. All other telemetry readings (helix current, anode voltage, etc.) were normal during this period.

It was hypothesized that, since the operating TWT temperature increased, the power drop could have been caused by a change in voltage standing-wave ratio between the TWTA collector and the circulator switch in the RF switch assembly. (If the effect had occurred between the RF switch and antenna, the power not transmitted from the low-gain antenna would have been reflected through the circulating switch to the other tube, raising its temperature instead. An experiment confirmed that a VSWR of about 4.5:1 at any point between the TWT output and circulator switch would have the same effect as observed during launch.)

Since the anomalous 3-dB changes in output power occurred during the nose fairing jettison and spacecraft separation events, the accelerometer data during these times were reviewed. No shocks in excess of those nominally expected were observed. A review of vibration and pyrotechnic shock test data for both spacecraft failed to reveal any condition that could have caused the power level changes.

During the *Mariner VII* cruise phase, ground tests were run on the various RFS components and RFS configurations in an effort to further understand and verify the power drop anomaly. The tests performed were:

- (1) A test of TWT operation with a 4.5:1 output load VSWR resulted in a decrease in output power of 3.0 dB and an increase of 1.5°F in TWT temperature from that attained under normal operating conditions. The increase in TWT temperature was not as great as that observed on *Mariner VII*. However, the test was conducted at room pressure where increased convection cooling was present. Helix current and anode voltage were unchanged.
- (2) Proper TWT operation through critical pressure (sea level to  $1 \times 10^{-5}$  torr) was verified.
- (3) Tests were run on a coaxial cable of the type used in the RFS to determine if its failure modes might produce a high VSWR. The results indicated that to achieve a VSWR greater than 1.1:1 requires a nearly complete disconnection of the connector or nearly complete destruction of the cable.
- (4) The mechanical configurations of the TWT and all other circuit elements after the TWT were reviewed. The only element that can be identified as likely to have caused the anomaly is the center

conductor in the output connector of the TWT. The mechanical design of this part of the TWT is such that the threaded connection of the conductor can be loosened by mechanical shock, resulting in a power output variation.

The test described in item (1) verified that a high VSWR occurring between the TWT collector and RF switch input circuit was a probable cause of the power output anomaly, and item (4) indicates a probable means of producing the high VSWR.

*b. Threshold sensitivity degradation.* Intermittent degradation of the *Mariner VII* receiver threshold sensitivity occurred between  $L + 21$  and  $+ 102$  days. This condition could have existed before day 21 without being detected, since its effects were noticeable only at low uplink signal levels. On  $L + 102$  days, and thereafter, receiver performance was normal, and the anomalous condition did not recur. Attempts to induce the condition during special tests after encounter by establishing the same operating mode and temperature conditions were unsuccessful.

Thorough analytic investigation yielded no probable source of external noise or signal or other cause of the effect, and the anomaly could not logically be attributed to an internal component failure. It was determined, however, that a known design defect could cause this anomalous behavior. The design defect necessary to account for the threshold sensitivity degradation is a parasitic oscillation in one of the receiver modules. Such instabilities were known to have occurred during testing in eight different types of receiver modules. The most probable place for it to occur is in the mixer-preamplifier, where spurious signals of the frequency and level required to produce the anomaly were observed under critical conditions of temperature and supply voltage. A design correction was made in the mixer-preamplifier, but schedule requirements did not permit testing that was thorough enough to ensure that the flight radios were free of this defect.

An hypothesis was developed to explain the effect of a parasitic oscillation. It assumed a parasitic oscillation in the mixer-preamplifier at a frequency corresponding to one observed during vendor testing at about 404 MHz (one-fifth of the uplink signal frequency). This frequency when multiplied by 5 and mixed with the local oscillator injection frequency would produce a signal at a frequency near the IF. If the level of this signal is in a

certain range (corresponding roughly to that of the parasitic observed earlier), and its frequency is either outside the false-lock range or in the pass-band of the crystal filter, blocking of the desired signal can occur in either the first or the second IF. The anomalous performance described earlier will result.

The hypothesis was verified by testing with the spare RFS in the Spacecraft Assembly Facility. The spurious oscillation was simulated by injecting an S-band signal through the preselector—this to avoid disassembly and possible damage to the RFS. The threshold degradation effects were readily reproduced in this manner.

The same design defect that appears to have caused the *Mariner VII* threshold degradation could also, if it produced a frequency in the false-lock range of the receiver, have been the cause of the *Mariner VI* false-lock and SPE offset problems.

*c. Helix current variations.* Helix current varied when ranging was turned on or off on *Mariner VII*. This effect was noticed for the first time in flight at  $L + 95$  days. Similar, but generally smaller, variations had been noted earlier during tests on this RFS at JPL. With ranging on, increases in helix current from about 8 to more than 20% occurred between  $L + 95$  and  $+ 109$  days. Telemetry channel 308 (helix current) became disabled during the pre-encounter anomaly at  $L + 125$  days, preventing further observations.

Investigation indicated that the TWT helix current increased when TWT drive was amplitude-modulated; current increased with percentage modulation and modulation frequency. The source of the amplitude modulation was found to be the hybrid filter, which exhibited a nonlinear phase characteristic at the higher modulation frequencies. This was caused by its being tuned to a frequency in the center of the assigned S-band channels so that it could be used interchangeably in any RFS. Switching ranging on provided the high-frequency modulating signal.

These helix current variations had no measurable effect upon TWT performance. It appears that the downlink signal would be slightly degraded by the resulting distortion. Helix current variations can probably be corrected by tuning the hybrid filter to the downlink center frequency of the RFS on which it is to be used.

d. *Pre-encounter anomaly.* On July 30, 1969, a series of events known as the pre-encounter anomaly occurred on the *Mariner VII* spacecraft. These events and their effect upon other subsystems are discussed in some detail under Spacecraft System Performance, also in Part 3 of this volume. Only their effect upon RFS performance and the conclusions that can be drawn from the effect are discussed here.

First, telemetry performance was degraded, whereas downlink power was normal. Within 20 s of the time the anomaly occurred, it was apparent from ground station AGC that the spacecraft was rolling; downlink signal strength decreased, indicating the start of a near-normal roll search. The roll stopped at a point where the high-gain antenna pointing angle caused the downlink signal-to-noise ratio to be marginal, and downlink lock was soon lost by DSS 51 for the remainder of the pass. Apparently, the spacecraft stopped rolling since a normal roll search (with the spacecraft transmitting and locked on the Sun) would have caused the high-gain antenna beam to sweep the Earth every 24 min at a nominal roll rate. Deep Space Stations 51, 61, and 62 were all searching at this time, without acquiring a signal. Station 51 transferred uplink lock to DSS 11 with a frequency offset at the spacecraft receiver of about 3.2 kHz.

It is very likely that uplink lock was not lost at any time since automatic reacquisition at the prevailing offset is highly improbable. (It should be noted that the RFS receives on the low-gain antenna at all times.) A DC-10 command was sent, resulting in transfer to transmit on the low-gain antenna, and three-way lock was acquired almost immediately (DSSs 11 and 42 both acquired the signal) about 6 h after the initial events. The downlink signal level was normal for transmission over the low-gain antenna, but the telemetry data problems persisted.

All RFS temperatures remained constant (except for a period with gyros on, when they increased normally 1°F and decreased normally with gyros off) during the entire period, which further indicated normal RFS performance.

About 13 h after the initial event, a roll search apparently had been completed, and a DC-11 command was sent to transmit on the high-gain antenna. Ground AGC indicated that the high-gain antenna was not pointed toward the Earth when the DC-11 command was executed, and that a roll search was initiated and completed afterward.

The output voltages of the RFS power supplies are somewhat affected by power line (2.4-kHz) transients. Any transient on the +15-V power supply output will affect the VCO frequency. From data describing these effects, it was estimated that power line transients during the anomalous events did not exceed 20 ms in duration since spacecraft receiver lock was maintained throughout.

The net result of these events upon the RFS was a loss of telemetry data (through a failure in the FTS) on channels 308 (helix current), 306 (exciter voltage), 302 (anode 2 voltage), and channel 300 (dc current to TWTs). The RFS performance was otherwise unaffected, except for the effects of the spacecraft roll position upon the high-gain antenna pointing angle.

e. *Auxiliary oscillator drift.* The *Mariner VI* spacecraft exhibited an auxiliary oscillator frequency drift, following transfer from its VCO, similar to that described earlier for *Mariner VI*.

7. *Mariner VII postencounter tests.* The *Mariner VII* threshold degradation anomaly had appeared intermittently during cruise, as described earlier in this report. There was no degradation during the encounter phase. After encounter, attempts were made to reproduce the anomaly in a manner similar to that described previously for *Mariner VI* in this report. *Mariner VII* was operated in the same configuration and in the same temperature range in which the anomaly had occurred. The uplink signal strength was adjusted to the level at which threshold degradation had occurred, and arrangements were made to examine the downlink spectrum in case the anomaly was reproduced. The 210-ft antenna at Goldstone was also required for these tests. As in the case of *Mariner VI*, these attempts to reproduce the anomaly failed, and tests were terminated in October 1969 for reasons of economy.

8. *Recommendations for improvements.* Improvements in the design and test of the RFS are recommended in Volume I of this report. Additional recommendations, including suggested improvements for mission operations, are given herein.

a. *Telemetry channel improvements.* While the telemetry channels, as they were arranged and calibrated on the *Mariner Mars 1969* spacecraft, were generally adequate, the improvements suggested in the paragraphs that follow would considerably improve the accuracy and usefulness of some channels.

*Channel 111, receiver static phase error.* This channel is a measure of the VCO control voltage and it indicates the receiver VCO operating frequency when the receiver is in lock. For the present RFS design, the channel is adequate, although it uses only 85% of the full range available. A design change to use the full channel dynamic range would increase its resolution.

*Channel 115, automatic gain control.* This channel indicates the spacecraft-received signal level and whether the receiver is in or out of lock. As now mechanized, this channel provides signal level data from -70 dBm to threshold. Signal levels above -100 dBm are not experienced in flight and are considered less advantageous than the finer resolution that could be obtained if this range were reduced to -100 dBm to threshold. In addition, the zero- to 3-V channel is used over only a 2-V range as presently mechanized. By reducing the signal level range and utilizing the full channel capacity, a two-to-one improvement could be realized in resolution. Improvement of the calibration of this channel over the temperature range prevailing in flight would also permit more accurate signal level measurements and predictions for command performance.

*Channel 210, exciter drive.* This channel measures the RF output power of the exciter and, thus, the drive to the TWTA. The typical maximum resolution of this channel per data number is 0.03 dB and the minimum is 0.06 dB. This is finer resolution than is required; something on the order of 0.1 to 0.3 dB would be adequate and would increase the range of the channel. The channel also drifts one data number for each 1-2°F of temperature change. This channel was calibrated only at room temperature and at flight acceptance temperature limits. Its usefulness under varying temperature conditions could be greatly improved if data were taken during the spacecraft space simulation tests. The temperature stability of the channel could also be improved by redesign.

*Channel 213.* Channel 213 monitors the RF drive from the TWTA to the high-gain antenna. The approximate resolution of the channel is 0.1-0.3 dB per data number. The channel has the same temperature problem as channel 210.

*Channel 214.* Channel 214 monitors the RF drive from the TWTA to the low-gain antenna. The resolution is about the same as that of channel 213 and the channel

has the same temperature stability problem as channels 210 and 213.

*Channel 217, fine automatic gain control.* This channel indicates the receiver input signal level, as does channel 115, but its range was supposed to be from -130 dBm to threshold. The minimum received carrier predicted through the mission (i.e., to the end of postencounter operations) was -135 dBm. Actual mechanization of the channel resulted in a range of -140 dBm to threshold. At these levels, the channel is noisy and hard to read, as well as difficult to calibrate accurately. For this range and for the mission signal levels, this channel is useless and could be more effectively used by another spacecraft function.

*Channel 301.* Channel 301 is a status channel and indicates the TWTA power mode (high/low power) and the ranging channel on/off status. The ranging on/off status is required; however, six other telemetry channels give indications of high or low power as well as the received signal strength at the ground station. This channel is not too important as a power indicator, but, since it is an easily mechanized channel, it could be useful during a TWT failure.

*Channel 302.* Channel 302 indicates the second anode voltage of the TWTA. The voltage for each TWTA has a different center range so that the channel also indicates which TWT is on. The value of monitoring the second anode voltage is limited, but, since it is an indirect measurement of the regulated +20 Vdc of the TWTA, it is of some importance. The +20 Vdc is used to generate more critical tube voltages such as the helix voltage of about 1400 Vdc. A more important future use for this channel might be to monitor the TWTA cathode current or helix voltage.

*Channel 306.* This channel monitors the -25 Vdc supply of the exciter and also indicates which exciter is on by using a different voltage range for each exciter. The value of the channel is limited. The -25 Vdc is well regulated, and the exciter will work properly at voltages well above or below this level. Typically, if the exciter voltage failed, there would be no downlink signal to carry the telemetry information, and a command to switch to the other exciter would be initiated immediately, either automatically or from the ground. Therefore, it appears that this channel could be used more effectively for some other RFS or spacecraft function. The exciter voltage as well as selected voltages

from other RFS subassemblies could be put on digital status channels. One or two channels could effectively monitor many functions. They would be set up to change state when any voltage dropped to a level at which the performance of the subsystem would be questionable. Thus, for the redundant transmitter, the appropriate action by command could be taken to switch at the redundant element.

*Channel 308.* Channel 308 monitors the TWTA helix current. This is an important parameter of the TWTA because almost any change from nominal operation of the TWTA will be reflected in the helix current (or, more appropriately, in the beam interception current). However, the present resolution of the channel is about 0.15 mA per data number and this degree of resolution is not required. Certain TWT phenomena can cause normal current changes of a few tenths of a milli-ampere. Also, the present range does not extend to a point where increased helix current would begin to indicate a potential TWTA failure.

*Channel 404.* This channel monitors the receiver VCO temperature. This channel aids in the prediction of the temperature-variable best-lock frequency of the receiver. The resolution of this channel could be increased from 1°F to 0.2°F per data number. This would provide better measurement accuracy as well as better predictions of best-lock frequency.

*Channel 430.* Channel 430 monitors the auxiliary oscillator temperature. This channel aids in the prediction of the one-way tracking, temperature-variable downlink frequency. Increased resolution of the channel would allow more accurate calibrations as well as better predictions of the one-way frequency.

*b. Ranging measurements.* A test of Einstein's general theory of relativity will be performed in the extended mission. Precise calibration of the ranging-delay characteristics is required to support this experiment. The delay was measured on each flight radio at only three temperatures: room ambient and flight acceptance test limits. The ranging delay characteristic of the *Mariner* Mars 1964 transponder is known to vary rather erratically when measured in 10°C steps so that interpolations between widely spaced temperature points could produce large errors. Data at closely spaced temperature points were not taken on the *Mariner* Mars 1969 transponders, and, therefore, it is not known whether they behave in a like manner. Although these characteristics are believed

to be somewhat improved on the *Mariner* Mars 1969 transponders, calibration of ranging delay at five temperatures in the range during the mission is recommended. In addition, signal level effects should be measured in steps of 3 dB at about five levels centered on the level expected during the experiment. Measurement of signal level effects was made down to only -120 dBm prior to flight. The effects of doppler offsets and command modulation should also be calibrated.

*c. Spacecraft performance analysis and command group.* Sometimes valuable information can be obtained by the spacecraft performance analysis and command (SPAC) group during an anomaly (such as the *Mariner VII* pre-encounter anomaly) from ground station AGC data. Although ground station AGC data are available with samples each second at the DSIF from the two receivers usually in use, such data were not available at JPL for from one day to several months after the pre-encounter anomaly.

A two-channel recorder is recommended for presenting ground AGC data at the RFS station in SPAC on a real-time basis. A third channel could be added for time recording. The circuit should be continuously active so that suspected acquisitions during trouble periods can be observed by the RFS member of SPAC. During the *Mariner* Venus 1967 mission, ground station AGC data were provided at the RFS station and were quite satisfactory.

The present format of RFS data is generally adequate, but the spacecraft and Deep Space Station AGC data would be more conveniently usable if they were expressed in engineering units (dBm) instead of data numbers and volts. The continued use of data numbers for other data is recommended.

A printout of the one- and two-way doppler residuals data and of all telemetry channel signal-to-noise ratios should be available in the SPAC area. The addition of two teletype printers for this purpose is recommended.

Another SPAC problem is communication between the RFS analyst and the operator at the Deep Space Station, particularly when some information is to be transferred in either direction. The normal procedure is to transmit from the RFS analyst to the spacecraft bus chief, to the assistant flight operations manager, to track chief, to station operations manager, to station subsystem operator, with the reverse sequence for a reply. This

is not only time-consuming but also leads to errors and misunderstandings. An expedited procedure was used at times whereby the RFS analyst obtained permission to speak directly to the track chief and through him to the station. This facilitated such activities as two-way tracking acquisition and station transmitter power changes. Loudspeakers with volume controls were provided for each network so that all conversations could be monitored. An improvement could be effected by using only one speaker with a push button switch to select the desired network, such as track, bus, and DSIF.

*d. Deep Space Station transmitter power calibration.* During the mission, receiver problems on *Mariners VI* and *VII* AGC threshold, command bit error rates, and SPE curve tests were conducted. The procedure used for the SPE curves worked well. However, for the other two tests, reasonably predictable station signal levels were required. For these tests, the station transmitter power was reduced to a low received signal level at the spacecraft. The stations used several calibration methods with various accuracies and problems with techniques. Deep Space Station 12 used a bolometer calibration of the klystron output down to low but readable output levels and then attenuated the input to the klystron to obtain still lower output powers. This technique and uplink carrier suppression were the most accurate. For future missions, a standard technique such as that used by DSS 12 should be instituted. Once a technique and a procedure are established, errors such as those which occurred during the *Mariner Mars 1969* testing will be greatly reduced.

*e. Telecommunication analysis team.* The telecommunication analysis team (TCAT) serves as backup to SPAC during critical phases of the mission. The midcourse correction and encounter periods were the two most important in the *Mariner Mars 1969* flights. Performance and reference data and technical specialists are available in TCAT to solve problems. Generally, access to the TCAT area is restricted to those required to support the mission. However, during *Mariner Mars 1969* encounter periods, the TCAT area was opened to guests, with the result that it became overcrowded and extremely noisy. It was impossible for the TCAT members to function efficiently under these conditions. Therefore, it is recommended that access to the TCAT room be limited to necessary personnel during critical phases of future programs.

## B. Flight Command Subsystem Performance

The flight command subsystem (FCS) provides the following general functions:

- (1) Receives from the spacecraft radio subsystem the composite command signal containing the command word information and synchronization information.
- (2) Acquires phase coherence (lockup) with the synchronization information, which is a pseudo-random signal, and establishes a phase reference signal and bit synchronization signal.
- (3) Demodulates the command word information, which is a biphasemodulated sinusoidal subcarrier, using the phase reference established by the synchronization process, and detects and reconstructs the command word data bits.
- (4) Provides a detector lock signal indicating whether or not detector synchronization with the received signal has been established.
- (5) Decodes the command word data bits and provides discrete momentary switch closures to the proper spacecraft user subsystem.
- (6) Decodes the command word data bits and directs a serial binary bit word, representing coded command data and bit synchronization information, to the spacecraft central computer and sequencer (CC&S) subsystem.
- (7) Decodes the command word data bits and directs a serial, variable length pulse train to the scan control subsystem.

A block diagram of the FCS is shown in Fig. 30.

From launch through September 1, 1969, the flight control subsystems aboard both *Mariners VI* and *VII* operated normally. In the case of *Mariner VI*, a total of 1305 commands, consisting of 378 direct commands, 19 quantitative commands, and 908 coded commands were properly processed. The *Mariner VII* FCS successfully processed a total of 951 commands consisting of 261 direct commands, 38 quantitative commands, and 652 coded commands. The great number of coded commands transmitted indicates that the CC&S was updated many times. Whereas some of the direct commands were used as backup commands, many of the direct commands were used to change the mode of operation. Command DC-9 is a good example. Once every 24 h, the CC&S would turn the ranging system off. During the early part of the mission, each time this occurred a DC-9 was used to turn the ranging system back on.

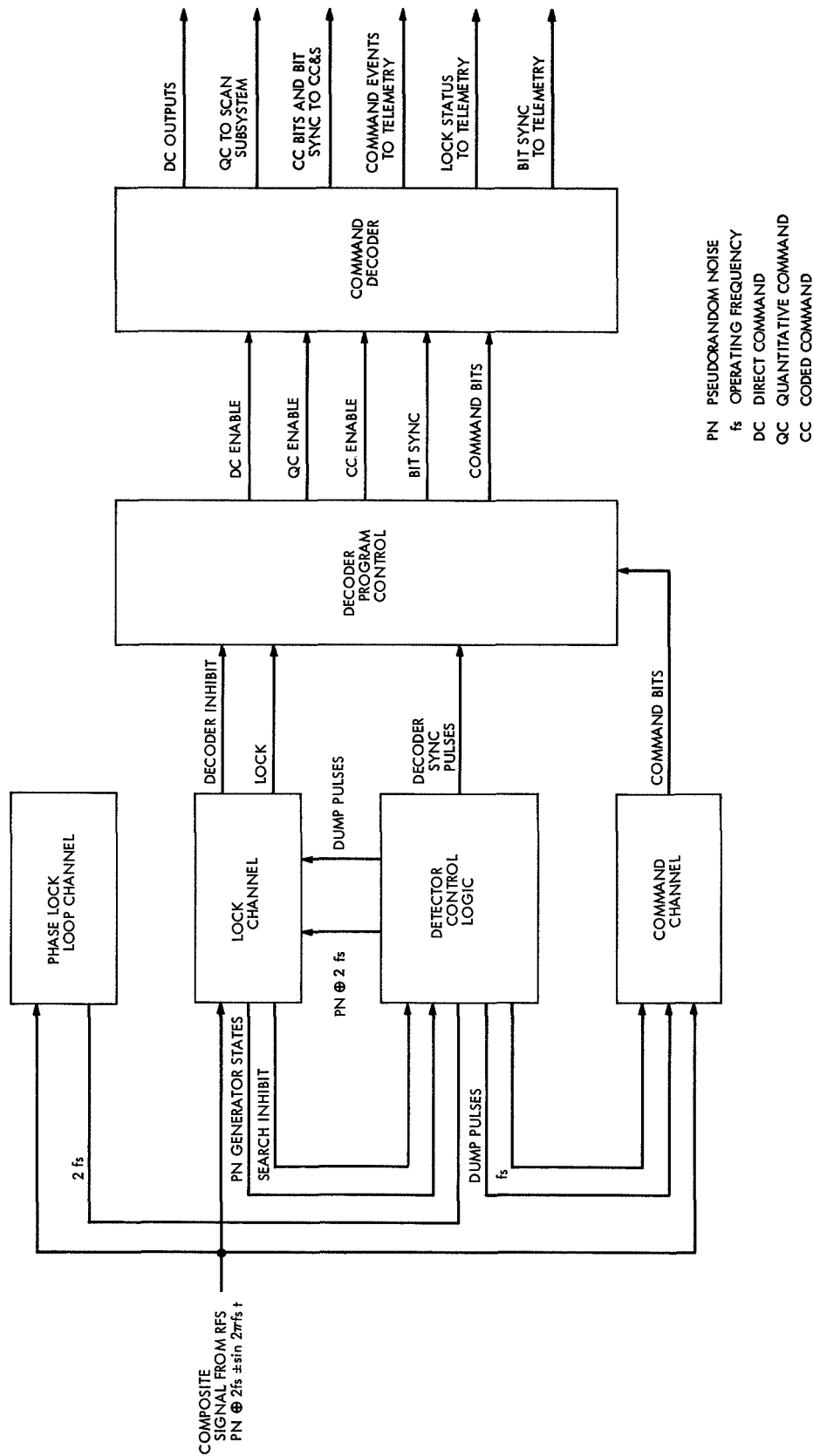


Fig. 30. Flight command subsystem block diagram

The performance of the VCO in the phase lock loop has been normal. The oscillator free-run frequency (the frequency when the command system is out of lock) has been within the maximum expected drift of  $\pm 0.05\%$  of its nominal frequency. Shortly after launch, the frequency offset of the *Mariner VI* VCO was  $+0.014\%$  and at 189 days into the mission the offset was  $+0.029\%$ . The *Mariner VII* VCO frequency offset at launch was  $+0.003\%$ , and at 150 days into the mission, the offset was  $+0.002\%$ .

Further evidence that the FCS performed normally is derived from the receiver/command performance tests conducted during the mission. For a power level of 2 dB below the command threshold level, both command systems operated as predicted. This was determined by counting the number of times the FCS showed an out-of-lock condition, calculating the probability of out of lock, and comparing this probability with a test-generated curve showing the probability of out of lock vs signal-to-noise ratio to the FCS. For both *Mariners VI* and *VII*, the observed signal-to-noise ratio to the FCS, as determined by the probability of out of lock, agreed to within 1 dB of the calculated level. The 1-dB discrepancy can be attributed to the test method and procedure that used nominal values of antenna temperature and receiver noise figure.

In all cases, the time for the FCS to acquire lock when command modulation was applied was less than or equal to the expected time; i.e., lock always occurred on the first attempt of correlation. However, the time required to reacquire lock after lock had been lost would occasionally require several seconds more than expected. This was attributed to the fact that the lock channel generates a one-in-lock indication because of noise. Each time a one-in-lock condition occurs, the time to lock is extended by 1 s. The expected probability of generating a one-in-lock indication because of noise was  $1.5 \times 10^{-2}$ , and the allowable range extended from  $1.12 \times 10^{-2}$  to  $1.83 \times 10^{-2}$ . The observed probability of a one-in-lock condition by using telemetry data yielded probabilities of  $1.4 \times 10^{-2}$  for *Mariner VI* and  $1.84 \times 10^{-2}$  for *Mariner VII*. Although the latter probability was slightly greater than the maximum expected, performance of the FCS was not degraded.

### C. Flight Telemetry Subsystem Performance

The conditioning, encoding, multiplexing, and subcarrier modulation of engineering data and the subcar-

rier modulation and block coding of scientific data are performed by the FTS. Approximately 90 measurements obtained by transducers and electrical pick-offs distributed throughout the spacecraft constitute the engineering telemetry data. Science data from the data automation subsystem (DAS) or the data storage subsystem include digitized TV picture data and outputs of the infrared and ultraviolet spectrometers and the infrared radiometer. The FTS provides an engineering channel during cruise, encounter, and playback, and either a medium-rate science channel or a high-rate, block-coded channel during encounter and playback.

The *Mariners VI* and *VII* flight telemetry subsystems were both launched with data processor A (the design incorporates redundant processors) at 33½-bits/s channel B data rate. Temperatures of both subsystems were 69°F after launch and slowly decreased to 65°F at  $L + 56$  days. The temperatures remained at 65°F throughout the remainder of the mission.

*Mariner VI* remained on data processor A at a 33½-bits/s data rate throughout the mission. All required telemetry functions were performed within the required specifications and no anomalies occurred through encounter.

The *Mariner VII* telemetry subsystem performed as well as that of *Mariner VI* from launch until 22:10:58 GMT on July 30 when a series of events occurred to the spacecraft. These events occurred during the near-encounter sequence. The data dropouts and other anomalies during this period are described at some length in terms of their effects on the various subsystems elsewhere in this volume. The next day, at 09:10:59 GMT, a DC-6 command to switch to redundant data processor B was sent and the FTS responded properly. It was determined from the data that the commutator switch for channel 104 (Fig. 31) was shorted and, therefore, the data on channels 103, 105, 106, 107, and 108 and analog data on subcommutator decks 200 and 300 were not valid. The digital data on these decks bypass the commutator, and analog-to-digital processing and were not affected. Data processor B functioned properly through encounter of *Mariner VII*.

The high-rate subcarrier (channel C at 259.2 kHz) was flown as an engineering experiment to obtain high-rate science and video data at Mars distances. On July 8, 1969, a high-rate telemetry channel calibration was run



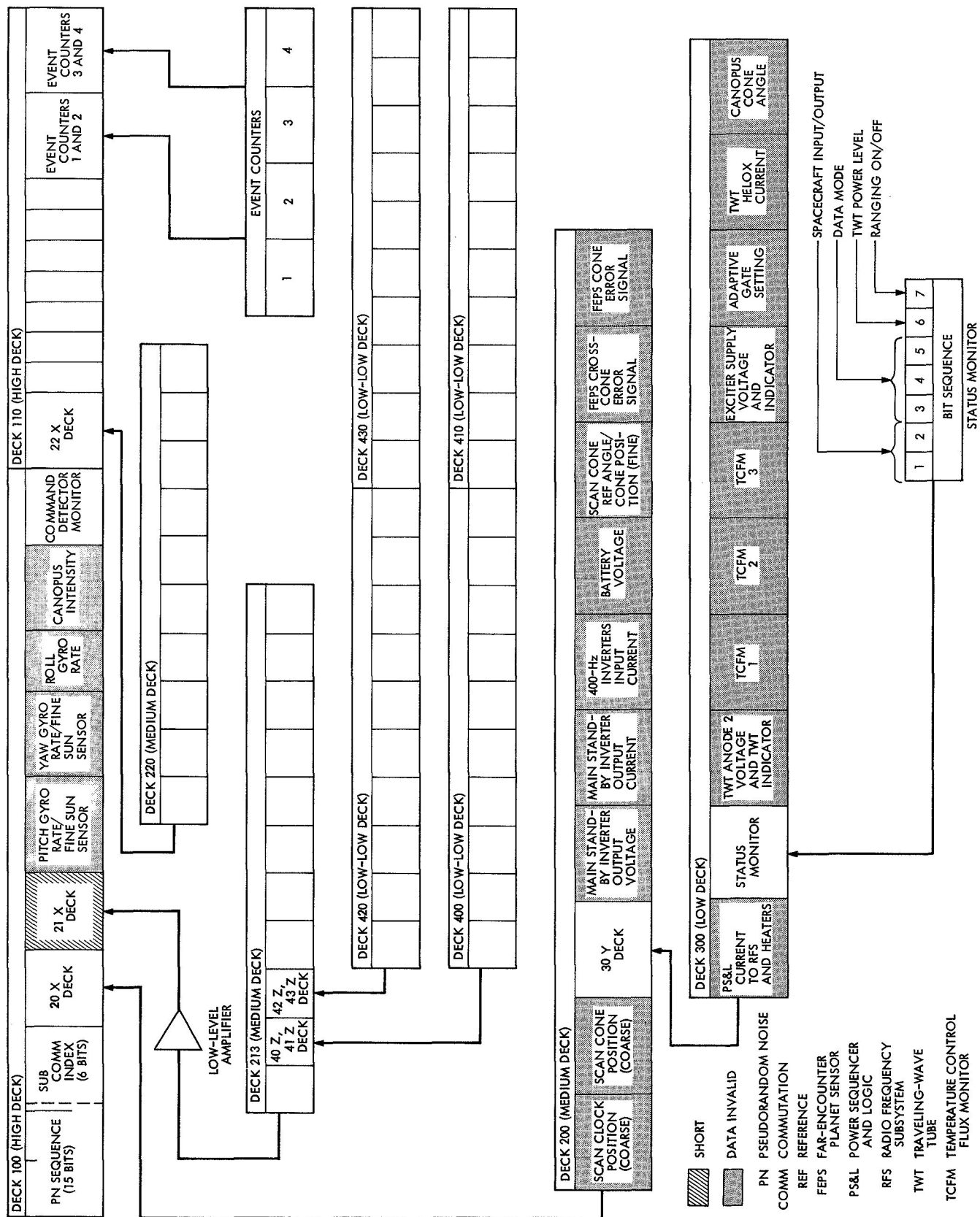


Fig. 31. Telemetry format showing effect of Mariner VII pre-encounter anomaly

with DSS 14 and *Mariner VII*. The *Mariner VI* calibration was run on July 11, 1969; the signal-to-noise ratio data obtained in this calibration were within  $\pm 0.5$  dB of the predicts.

During the encounter phases of *Mariners VI* and *VII*, the high-rate subcarrier C was used both for obtaining encounter data in real-time and for data storage subsystem high-rate playback (data rates on channel C are 16.2 kbits/s for both modes). Again, the channel C performance was within  $\pm 0.5$  dB of the predicted performance value. More details of the telecommunication link performance are given in Section I, which precedes this section.

At 01:00:00 GMT on August 18, another DC-6 command was transmitted to *Mariner VII* to toggle the telemetry subsystem back to data processor A for engineering evaluation of its condition. All data received from data processor A were good and the only anomaly remaining was the shorted commutator switch for channel 104 and its associated effects. The conclusion here is that the events of July 30 resulted in a noisy spacecraft electrical environment that induced the failure mode into commutator switch 104 but caused no other permanent damage to the FTS.

The data processors on both *Mariners VI* and *VII* were flown entirely at the 33 $\frac{1}{3}$ -bits/s engineering data rate because the subcarrier B signal-to-noise ratio never fell below +6 dB and acceptable bit error rates.

#### D. Data Storage Subsystem Performance

The data storage subsystem provides buffering between the high rate at which data are acquired by the TV and other scientific instruments and the lower rate at which these data can be returned to the Earth. A total of  $1.8 \times 10^8$  bits of data can be stored. The subsystem consists of a digital tape recorder and its electronics, an analog tape recorder and its electronics, an analog-to-digital converter, and control and power electronics.

The *Mariner Mars* 1969 subsystem differs from previous *Mariner* practice in that it uses two tape transports, one digital and one analog, rather than one digital machine. Each transport is similar to the earlier design except that four tracks are available instead of two, the packing density is higher, and the record and playback speeds are different.

In general, the data storage subsystems on both spacecraft performed well. However, the playback of the first eight near-encounter analog pictures from *Mariner VI* was degraded, and the digital tape recorder (DTR) track 1 playback of near-encounter data contained an excessive number of bit errors. A dropout problem was also experienced during playback of the *Mariner VII* analog tape recorder (ATR) track 4 near-encounter sequence. These problems are discussed in more detail in the paragraphs that follow.

If the high-rate telemetry system had not performed successfully, the bit error problem during the *Mariner VI* near-encounter sequence would have resulted in the loss of near-encounter digital data recorded on track 1 of the DTR. Utilization of the high-rate telemetry system essentially meant that the DTRs on both spacecraft were redundant equipment in that digital science data that were recorded on the DTRs during the encounter phase were simultaneously transmitted in real-time over the high-rate telemetry system.

Similarly, the ATRs were played back directly into the high-rate link, and the data were successfully recovered such that the analog-to-digital transfer mode was not used. This mode would have provided for the transfer of data from the ATR to the DTR for subsequent playback from the DTR at 270 bits/s.

The temperatures of the data storage subsystems on both *Mariners VI* and *VII* remained close to the predicted values throughout the mission. The internal pressure of the tape transport cases remained between the initial pressurization of 22 lb/in.<sup>2</sup> and the 20.6 lb/in.<sup>2</sup> telemetry threshold throughout both flights, indicating proper functioning of the pressure seals.

1. *Mariner VI*. During the launch countdown for *Mariner VI*, one TV calibration picture was recorded at the beginning of track 1 on the ATR in preparation for a performance test of the ATR during the cruise phase. The data storage subsystem was operated in the launch mode (ATR running at playback speed, DTR running at record speed). The subsystem performed normally during the launch phase; both tape transports stopped at the first end-of-tape following spacecraft separation. The subsystem remained in the ready mode until power was turned off at 03:24:57 GMT on February 25, 1969.

On July 11, 1969, the subsystem was turned on, and the calibration picture was played back from the ATR

four times. The subsystem performance was normal. On July 14, the ATR was erased to remove the calibration picture. The subsystem remained in the ready mode until far-encounter operations began.

The subsystem performed normally during the far-encounter portion of the encounter sequence. During the playback of the near-encounter picture sequence, it was found that the output amplitude from track 1 of the ATR had reduced to about 45% of the level that was observed prior to launch. This was noted by observing the digitized value of the "ones" in the pseudo-noise code that appears at the beginning of each TV picture line. During two successive playbacks of track 1 on the ATR, the averaged level of the "ones" was data number 28, whereas the level should have been 63.

This type of problem had never been observed before. Output signal amplitude changes of up to 10% had been noted during the test program, because of variations in the integrity of the tape-to-head interface in the ATR. The cause of this problem in flight was probably one of the following:

- (1) A piece of debris lodged on the face of the playback head.
- (2) Electronic degradation in the track 1 switching circuitry.
- (3) Electronic degradation in the track 1 record and/or playback amplifiers.
- (4) Debris lodged on the face of the record head.

It is felt that item (1) was the most probable cause of the problem. Fortunately, the problem did not cause the loss of any data, but did somewhat degrade the playback of the first eight pictures of the near-encounter sequence.

A second problem occurred during playback of the *Mariner VI* near-encounter digital data. The data on track 1 and part of track 2 on the DTR appeared to have sufficient bit errors such that the ground computer could not maintain lock on the data. A second playback of the same data verified that the problem remained. It is felt that the cause of this problem was undoubtedly similar to the cause of the problem on the ATR (i.e., a degraded tape-to-head interface caused by debris buildup on the face of the playback head). Fortunately, no data were lost because the same data were recovered via the high-rate telemetry link in real-time during near-encounter.

The near-encounter TV data on the ATR were played back six times, and the near-encounter data recorded on the DTR were played back twice. The ATR was erased and used to record additional TV data in support of the postencounter operations. At the completion of the postencounter operations, the number of tape passes accumulated on each flight tape transport is shown in Table 5. A total of 75 far- and near-encounter TV pictures were successfully recorded and played back on the ATR. Near-encounter digital data were recorded on the DTR and played back with the problems discussed earlier.

**Table 5. Data storage tape passes**

Mission phase	Mariner VI				Mariner VII			
	ATR		DTR		ATR		DTR	
	Record	Playback	Record	Playback	Record	Playback	Record	Playback
Prelaunch (to T - 24 h)	108.5	60.6	238.7	48.0	91.8	61.4	245.5	16.7
Launch (T - 24 h to end of launch)	0	0.9	5.3	0	0	1.8	5.8	0
High-rate calibration	1.5	3.5	0	0	1.5	3.5	0	0
Far-encounter	10.0	6.0	0	0	17.0	11.0	0	0
Near-encounter	4.0	24.0	4.0	8.0	4.0	24.0	4.0	8.0
Postencounter (through Sep 1, 1969)	3.0	1.0	0	0	0	0	0	0
Subtotals	127.0	96.0	248.0	56.0	114.3	101.7	255.3	24.7
Totals	223.0		304.0		216.0		280.0	

**2. Mariner VII.** As on *Mariner VI*, one TV calibration picture was recorded at the beginning of track 1 on the *Mariner VII* ATR during the launch countdown. The data storage subsystem was operated in the launch mode during launch, and performed nominally with both tape transports stopping at the first end-of-tape following spacecraft separation. The subsystem remained in the ready mode until the power was turned off at 00:18:00 GMT on March 27, 1969.

On July 8, 1969, the subsystem was turned on, and the calibration picture was played back from the ATR four times. Subsystem performance was normal. On July 14, the ATR was erased to remove the calibration picture. The subsystem remained in the ready mode until the time of the *Mariner VII* pre-encounter anomaly when, at 22:11:09 GMT on July 30, telemetry data indicated that the subsystem was turned off and back on again during the time of one medium-rate telemetry frame. Following this anomaly, the subsystem was exercised through various modes, and it was determined that subsystem performance had not been degraded.

The data storage subsystem performed normally during the complete encounter and playback sequences. The only noticeable change in performance was an apparent increase in the number of dropouts on track 4 of the ATR in the near-encounter playback sequence. The near-encounter TV data on the ATR were played back six times and the near-encounter DTR data were played back twice. The number of tape passes accumulated on each tape transport is shown in Table 5. A total of 128 far- and near-encounter pictures were successfully recorded and played back from the ATR. All near-encounter digital data were successfully recorded and played back from the DTR.

### III. Guidance and Control Subsystems

#### A. Central Computer and Sequencer Performance

The central computer and sequencer (CC&S) provides event timing and sequencing of all spacecraft functions that must be generated on a time-dependent basis. This sequencing is generated by a special purpose programmable computer with fixed sequencer redundancy in the maneuver mode. Timing and sequencing (with the exception of the fixed sequencer) is programmed into the CC&S prior to launch and can be modified during flight by coded commands. A simplified block diagram of the central computer and sequencer is shown in Fig. 32.

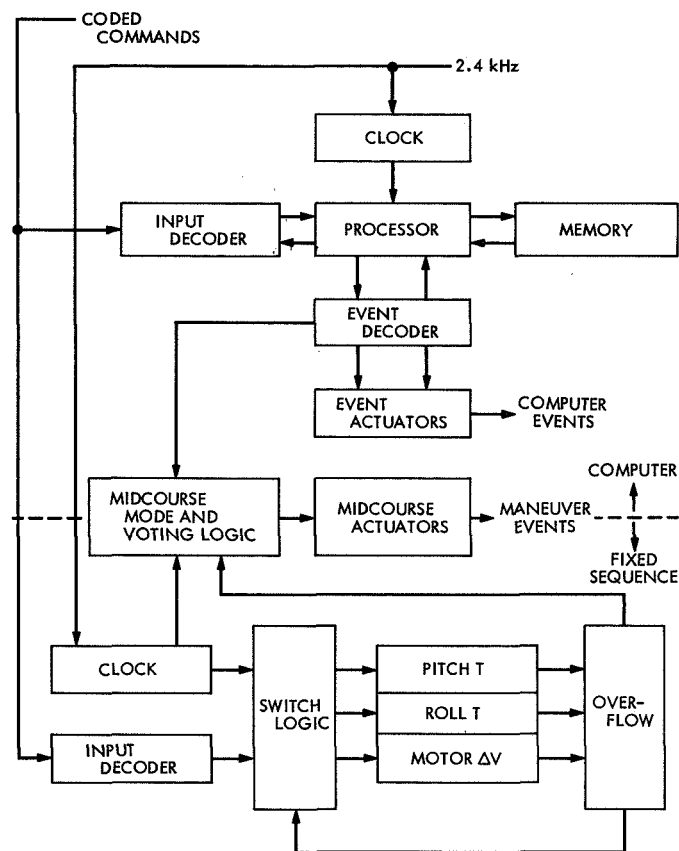


**Fig. 32. Central computer and sequencer simplified block diagram**

**Mariner VI.** There were no anomalies in the performance of the CC&S subsystem. All events occurred at the expected times. A total of 9001 spacecraft events were issued by the CC&S. Of these, 434 were in response to normal operation modes, 8257 resulted from special experiments, and 310 resulted from ground reprogramming to aid in trouble-shooting spacecraft problems. In all, a total of 907 coded commands and 176 direct commands were received by the CC&S. No errors occurred in the receipt of these commands.

The prime monitors of CC&S performance were event counters 2 (computer) and 4 (fixed sequencer) contained in telemetry channels 118 and 119, respectively. Table 6 summarizes these events and the performance modes in which they occurred. Of the 269 counter 4 events, 254 were sent as spacers between coded command pairs to the computer, event outputs accounted for 6, and sequencer receipt of 9 coded commands provided the balance. Of the counter 2 events, 3266 were associated with programming changes and verification and 8995 with spacecraft event actuations.

**Table 6. Counter 2 and 4 events for Mariner VI**

Mode	Counter	
	2	4
Launch events	4	6
Midcourse events	7	
Gyro drift calibration	3	
First maneuver to Magellanic cloud	5	
Second maneuver to Magellanic cloud	278	
Actuator matrix tests	12	263
Inertial at encounter	4	
Far-encounter (first set)	33	
Far-encounter (second set)	17	
Near-encounter	75	
Infrared and ultraviolet map of southern hemisphere	1,723	
Infrared and ultraviolet map of northern hemisphere	5,668	
Infrared, ultraviolet, and temperature control flux meter measurements of center of Milky Way	863	
Cruise events	16	
Y1 events	264	
Loading coded commands	322	
Memory dumps	2,967	
Totals	12,261	269

The command generation program was run 260 times throughout the mission. About two-thirds of these runs were in direct support of mission operations, whereas the other runs were used in support of the test program and in checking experimental programs.

*a. Launch events.* The inhibit was released on the *Mariner VI* at 01:25:00 on February 25. Three minutes later, the operation verify event was issued by the CC&S, which indicated that the CC&S clock was counting properly. One minute later the spacecraft was launched. The CC&S was enabled to send commands to other spacecraft subsystems when the spacecraft separated from the *Centaur*.

At 02:25:00, the CC&S issued backup commands to turn on the attitude control subsystem (L4) and to open the solar panels (L1). One hour after L4 and L1, the CC&S issued a command to the power subsystem (L3) to turn off power to the data storage subsystem. The final launch event occurred 2 h after L3 when the CC&S commanded turn-on of the Canopus tracker via the L2 event.

*b. Midcourse maneuver.* The CC&S was loaded for the first time on February 28 when the midcourse maneuver parameters were inserted. Twenty coded commands were sent, 14 of which (7 CC-1/2 commands<sup>1</sup>) went to the computer to change 7 computer words, and 6 CC-4 commands went to the fixed sequencer. Three of the latter were CC-4 spacers (a 1-s negative pitch turn) sent between the CC-1/2 commands to permit transmission of commands on 1-min centers. The last three CC-4 commands were the turn and burn values for the midcourse maneuver.

Of the seven words loaded into the computer memory, three were turn and burn durations, three were turn and burn start words, and one was the enable word for the computer subroutine.

The maneuver was a tandem maneuver controlled by the fixed sequencer, and checked by the computer. All event times and turn and burn durations were found to be correct when the maneuver was performed later that day. The maneuver consisted of a pitch turn of -131 s, a roll turn of +453 s, and the motor burn of 5.35 s (or 107 counts at 20 pulses/s).

Approximately 1 h after the maneuver was completed, the fixed sequencer was loaded with a precautionary sequence to minimize deleterious effects in case of an unexpected sequencer-only maneuver. A minimum pitch turn, infinitive negative roll turn, and minimum motor burn were set up in the fixed sequencer. If a sequencer-only maneuver were to start, the spacecraft would perform an insignificant pitch turn and then would begin rolling. The latter could then be stopped with a direct command. In this way, the solar panels would stay on the Sun, and the motor would not burn and, hence, the option of a future maneuver having a motor burn would be preserved.

*c. Cruise events.* On March 4, a DC-13 command was sent to the spacecraft to discharge the pyrotechnic capacitors. This command, however, put the CC&S in a nontandem standby status, which was not the desired nominal condition. A DC-33 command was sent to return the CC&S to the tandem standby state.

On March 23, the CC&S issued the first cruise event. The Canopus tracker was stepped to its next position by the C1 event. The second cruise event (C5), whose

<sup>1</sup>A CC-1/2 command consists of a CC-1 command followed by a CC-2 command. Each CC-1/2 pair changes a word in the CC&S memory.

purpose was to unlatch the scan platform, occurred on March 31. However, its purpose had already been accomplished by a direct command that had been issued earlier.

During the unlatch of the scan platform, Canopus lock was lost, presumably because of bright particles shot out by the explosive charges. To prevent a similar loss of lock during pyrotechnic events at encounter, a decision was made to load a subroutine to provide for inertial control of the spacecraft for that period. This subroutine was loaded into the CC&S memory on April 18. The coded commands consisted of 10 CC-1/2 commands and 8 CC-4 spacers.

The third cruise event took place on April 20 when the second C1 event of the mission occurred. The Canopus tracker was stepped in cone angle in the opposite direction to that expected. Several direct commands were sent in an attempt to reach the desired cone angle, but to no avail. This led to considerable CC&S activity for the next few days.

On April 28, the computer was loaded with eight words. Seven of these words constituted a sequence to provide for inertial hold so that gyro drift measurements could be made. This subroutine provided a gyro warm-up time of 24 h followed by a switch to all axes inertial to last for 18 h. This sequence was executed, but it was terminated by a DC-13 command after 17 h 16 min of inertial control. A DC-14 command was then sent to reenable the CC&S maneuver actuators. The eighth word that was loaded changed the sixth CC&S memory word, which contained the pseudorandom noise sequence used for synchronizing the data. This sequence was put in to make it easier to produce the machine language listing of the memory dump.

On April 30, a sequence was loaded into the computer requiring 11 computer words. This sequence provided for a roll to the calculated center of the Large Magellanic Cloud (LMC). The goal was to use the LMC as a substitute for Canopus because of the inability to step to position 4 in cone angle. The sequence was loaded, a memory dump taken and verified, and the maneuver was executed after a DC-32 command was sent to put the CC&S in a computer-only maneuver mode. The Canopus tracker locked onto the LMC, but only for a short period. Subsequently, other efforts were made to lock onto the LMC, as described below.

Later, on April 30, an update consisting of 17 words was sent to the computer. One word was used to clear flag flip-flop 5, which had been set by the DC-32 command. Two words were used to change the time for turning gyros on at encounter. Two words were used to change the time that the Y1 cyclic event would occur and to change the period for Y1 events from 23 to 24 h. Three words were sent to change three encounter slew magnitudes. One word was sent to update the value of one picture count word. Three words were sent to change the times of three encounter events, and five words were sent to update the cruise event chain. These words were all sent and verified by a DC-2 dump command. Proof that flag 5 had been reset was also established.

After lock was lost on the LMC, a decision was reached to make a second attempt to lock on. In this attempt, a subroutine was to be loaded into the computer that would cause the Canopus sensor to roll through the cloud and then back to the desired position. However, after only four and one-half computer words had been loaded, the transmission of commands was stopped because of excessive noise in the Canopus tracker. Since the transmission of coded commands had ceased after a CC-1 command had been sent, an attempt was made to load a CC-4 spacer into the fixed sequencer before the next hour scan to its normal state. This command was sent too late to achieve its purpose but other logic, not heretofore tested, accomplished the same purpose. No attempt was made to repeat this maneuver.

On May 2, four different sets of coded commands were loaded into the computer for a new attempt to lock onto the LMC. First, a roll maneuver was inserted to roll the Canopus sensor to the edge of the LMC. Eleven computer words were required for this maneuver. The words were loaded, and a memory dump was taken to verify the memory contents. The maneuver was then successfully executed.

A set of seven words was then loaded into the computer to enable a 900-ms roll turn each time a DC-32 command was received. Another dump was taken to verify the load. Eighty DC-32 commands were then sent on 1-min centers; each command caused the spacecraft to roll for approximately 900 ms. This roll swept the Canopus tracker through the LMC and provided a thorough plot of light intensity vs roll angle.

The third load of memory consisted of one word and its only effect was to reverse the polarity of the roll turn. A memory dump was taken to verify the proper loading of this word. Fifty-six DC-32 commands were then sent to roll the Canopus tracker back to the selected best position for lock-on. A direct command was then sent to condition the attitude control subsystem, which left the CC&S in a nontandem standby state.

The fourth set of coded commands was then sent to the computer. This set consisted of two computer words that provided for a gyros-on event (M1) and eliminated the entrance to the incremental roll subroutine upon receipt of another DC-32 command. A memory dump was not taken because of the fatigue of the participants and the confidence that had been established in the ability to load successfully. A DC-14 command was then sent to reconnect the CC&S to the attitude control subsystem, and a DC-32 command was sent to return the CC&S to a computer-only maneuver mode and to accomplish the other goals previously mentioned.

On May 13, after a DC-13 command was sent to turn off the gyros, a word was sent to the computer that would clear flag 5, if set. A DC-32 command was then sent to return the CC&S to a computer-only maneuver status. Flag 5 was thus set by the DC-32 command, but was immediately reset by the word in memory. A DC-14 command was sent to reconnect the CC&S to the attitude control subsystem. A memory dump was then taken to verify that flag 5 was reset.

A 43-word update of the CC&S memory was made on June 5. The changes can be summarized as follows:

- (1) Seven words to relocate the "inertial at encounter" subroutine, which was necessary to enable the addition of two new subroutines.
- (2) Five words to change the platform slew magnitudes.
- (3) Four words to modify the cruise event chain.
- (4) Ten words to provide a new subroutine for the N6 events to the pyrotechnic and data automation subsystems, which would be activated at near-encounter.
- (5) Fourteen words for a subroutine to provide automatic aperture control at near-encounter; in this subroutine, N4 (slew in cone to final position) and N1 (encounter phase) events are issued following each of the first  $n$  pictures to correct a discrepancy

by placement of the TV camera aperture at a more desirable setting.

- (6) One word to arm the executive to enable the optional far-encounter subroutine upon receipt of a DC-32 command.
- (7) One word to provide for negative cone polarity during the first near-encounter slew.
- (8) One word to change the time of the P1 and P2 events expected at the end of near-encounter.

A subsequent memory dump indicated that all words had been properly loaded.

On June 16, a three-word memory change was made. These words were used to (1) delete a C2 event expected on June 19, (2) add a P4 event for June 24, and (3) substitute a zero event for the C6 event that was to occur on July 10. A memory dump was taken to verify the loading.

A seven-word load was accomplished on June 24. Six of the seven words were inserted to interchange words 4 and 5 in the executive and all affected words so that memory dumps could be taken over hour scans. (Word 5 had contained the counting word for "inertial at encounter." Word 4 was the memory readout test word. If an hour scan were to occur during a memory dump, the countdown to the next "inertial at encounter" event would lose a beat and the event would be 1 h late.) The seventh word changed the P4 event on June 24 to a zero event. The memory contents were then checked and found valid by means of a memory dump. The "zero" cruise event time was not observed in the data since the spacecraft was not being tracked at the time, but subsequent data showed a counter 2 increase of one representing that event.

On July 10, two cruise events were observed. A C3 event caused the transmitter to switch to the high-gain antenna, and a zero event occurred 1 h later; both were on time.

*d. Actuator matrix tests.* Because of the failure of a source driver in the *Mariner VII* CC&S, a decision was made to test key actuator matrix functions in *Mariner VI*. The first of these tests was conducted on July 15 when four coded-direct commands were transmitted. (A coded-direct command consists of two CC-1/2 commands separated by a CC-4 spacer. The first CC-1/2 command contains a data word with a time value of

zero and the desired event address. The second CC-1/2 command contains a word that is placed in the executive, which decrements the data word in either minutes or seconds. After the second CC-1/2 command is loaded, the event is issued on the next appropriate scan, and the second word is automatically made a "no operation" instruction.)

One coded-direct command was used to test F3, one to test N1, one to test "timing of events," and one to test the reset of "timing of events." All events occurred as expected. A memory dump was then taken and verified.

Forty-four words were loaded into the CC&S memory on July 25. The first 16 words constituted 8 coded-direct commands that were used for further actuator matrix tests. The first two coded-direct commands generated two N11 events that caused two steps in platform negative cone angle. The third coded-direct command set the clock polarity negative while the fourth and fifth coded-direct commands caused N3 events that moved the platform two steps in negative clock. The sixth coded-direct command set the clock polarity positive, while the seventh and eighth coded-direct commands caused N3 events that moved the platform two steps in positive clock. The correct response of all coded-direct commands was confirmed by attitude control.

The remaining 28 words were loaded for the following purposes:

- (1) Eleven words to modify the far-encounter sequence so that pictures could be taken of the Mars satellite, Phobos.
- (2) Three words to change three postencounter cruise events.
- (3) Two words to change the Y1 period to 3 h.
- (4) Six words to add the capability for a fifth platform slew during near-encounter.
- (5) One word to change the time of the N6 event.
- (6) Five words to change the slew magnitude values.

Two memory dumps were then taken and verified; the reason for this is that if an error were found, no time would be lost in commanding a second dump.

*e. Far-encounter events.* On July 29, the gyros were turned on by the CC&S to begin their warm-up before

going to inertial mode for near-encounter. Later that day, a DC-32 command was sent to start the first of two sets of far-encounter pictures. The DC-32 command put the CC&S into the computer-only maneuver mode, as expected, and 33 photographs were commanded at 37-min intervals.

On July 30, at approximately  $E - 27$  h, a memory update of five words was made. Two platform slew magnitudes and the times of N8, N9, and P2 events were changed. The modifications were verified by means of two subsequent dumps.

An N1 cruise event to the data storage, flight telemetry, power, and scan control subsystems was confirmed later on July 30. After 1 h, an F3 cruise event was issued. A DC-32 command was then sent to enable the second set of optional far-encounter pictures. One hour after the F3 event, an F1 cruise event was issued, and the second optional far-encounter picture sequence was started. Seventeen photographs were commanded; the first seven commands were sent at 64-min intervals, the eighth command was sent 2 min after the seventh, and the last nine commands were sent at 56-min intervals. Shortly after the last of those pictures, another N1 cruise event was issued as expected.

*f. Near-encounter events.* The last update before near-encounter was made at approximately 4 h before closest approach. It was a minor update wherein 4 slew magnitudes and one picture count word were changed. Again, two memory dumps were taken to establish the integrity of the memory.

Early on July 31, at  $E - 2:51:33$ , an N1 cruise event was issued to the data storage, flight telemetry, power, and scan control subsystems. At  $E - 1:51:33$ , N7 and F3 cruise events were issued, and the "inertial at encounter" subroutine issued the commands required to put the spacecraft under inertial control. One hour later, the last cruise event before encounter occurred. This was a zero event, but at the same time, the N6 subroutine was enabled. At  $E - 00:40:51$ , the N6 (pyrotechnic subsystem) event was issued, and at  $E - 00:14:21$  the N6 (data automation subsystem) event occurred. With the latter, the near-encounter subroutine was enabled by the programmed insertion of an interrupt word into the executive that would respond to the setting of a flag by the narrow angle Mars gate. This flag was set at  $E - 00:14:12$ , and the near-encounter subroutine was initiated.



The near-encounter events pertaining to the CC&S then took place as follows:

- (1) The clock slew polarity at negative and the TV gate set so that pictures could be counted.
- (2) Four picture counts, each followed by N4 and N1\* events (N1\* is an N1 event to the power and scan control subsystems).
- (3) One picture count without N4 and N1\* events.
- (4) Three picture counts followed by N4 and N1\* events.
- (5) Fourteen slew steps in negative clock.
- (6) Four picture counts each followed by N4 and N1\* events.
- (7) One picture count without N4 and N1\* events.
- (8) Clock slew polarity set positive.
- (9) Twenty slew steps in positive clock with platform slewed to final cone angle.
- (10) Four picture counts.
- (11) Clock slew polarity set negative.
- (12) Two slew steps in negative clock.
- (13) Fourteen picture counts.
- (14) An N8 event.
- (15) One picture count.
- (16) Clock slew polarity set positive.
- (17) Six slews in positive clock.
- (18) An N9 event.
- (19) A P1-P2 event.
- (20) Reset of the TV gate at  $E + 00:18:19$ .

All these events took place as predicted.

Approximately four hours after closest approach, a reacquisition event was issued to terminate inertial control by the attitude control subsystem. Seven hours after closest approach, an N5 event was issued to terminate the playback of science data.

*g. Postencounter update.* On August 1, a DC-13 command was sent to disconnect the CC&S from the attitude control and pyrotechnic subsystems, and a DC-33 command was sent to return the CC&S to the tandem standby mode.

An update of eight words was made on August 7. In this update, two words were inserted to change the Y1 period back to 24 h, so that it would occur at approximately 17:30 each day. Four words were inserted to modify the cruise event chain, one word was changed to delete the "inertial at encounter" subroutine word from the executive, and one word was inserted to restore the memory readout test word to the executive. (The latter was erased during a programmed overlay during near-encounter.) A dump was then taken, and the memory contents were verified.

*h. Scans of southern and northern hemispheres and center of Milky Way.* On August 11, the largest single update was accomplished. Sixty-four words were loaded in preparation for ultraviolet and infrared scans of the southern celestial hemisphere. The memory was then verified by a dump. Then, early on August 12, a DC-13 command was transmitted to put the CC&S into the nontandem standby mode; a DC-14 command was sent to connect the CC&S to the attitude control subsystem, and a DC-32 command was sent to begin the sequence.

Under program control, the following events then occurred: (1) the platform clock slew polarity was set positive; (2) the gyros were turned on; (3) all-axes inertial mode was established; (4) a positive roll turn of 12 min 6 s was commanded; (5) a negative pitch turn of 9 min 36 s was executed; and (6) a positive roll turn of 3 min 16 s was accomplished.

A second and final DC-32 command was then transmitted. The sequence listed below then ensued under program control.

$$\begin{aligned}
 &7[2N3 + 14N10 + 2N3 + 14N11] + 9N10 \\
 &\quad + 2[2N3 + 20N10 + 2N3 + 20N11] + 6X + 10N10 \\
 &\quad + 14X + 2N3 + 30N10
 \end{aligned}$$

where

$$X = 2N3 + 30N10 + 2N3 + 30N11$$

and where

N3 = slew of one step in clock

N10 = positive slew of one step in cone

N11 = negative slew of one step in cone

All events were separated by 4-s intervals, except the N3 events, which were 1 s apart. In all, 122 N3, 817 N10, and 768 N11 events occurred.

After the platform slews, a reacquisition maneuver was conducted as follows: a negative roll turn of 3 min 16 s, a positive pitch turn of 7 min 37 s, and a negative roll turn of 11 min 50 s. The latter was ended with a reacquisition event that returned the CC&S to tandem standby mode and concluded the CC&S activities. All CC&S events had occurred as predicted.

The program for scanning the southern hemisphere was modified by a nine-word update on August 12 to permit ultraviolet and infrared scans of the northern celestial hemisphere. The entire memory was again verified by a dump.

The sequence required no spacecraft turns, only platform slews. These were initiated by a DC-32 command that set the computer relay and caused channel 420 to read 32. One second after receipt of the DC-32 command, the clock slew polarity was set positive and 4 s later the following event sequence then ensued:

$$22X + (2N3 + 55N10 + 2N3 + 64N11) + 23Y$$

where

$$X = (2N3 + 55N10 + 2N3 + 55N11)$$

and

$$Y = (2N3 + 64N10 + 2N3 + 64N11)$$

All events were separated by 4-s intervals, except the N3 event pairs, which were separated by 1 s.

From receipt of the DC-32 command to the last N11 event, over 6 h were required. Altogether, 184 N3, 2737 N10, and 2746 N11 events occurred.

On August 13, 45 words were loaded to permit spacecraft turns and platform slews to accomplish ultraviolet and infrared scans of the center of the Milky Way and temperature control flux monitor (TCFM) measurements. A memory dump was taken to verify correct loading.

Since spacecraft maneuvers were to be executed, it was necessary to send a DC-13 command to put the computer into the nontandem standby state, and a DC-14 command to connect the CC&S to the attitude control subsystem. A DC-32 command was then transmitted, which put the CC&S into the computer-only maneuver mode, and started the maneuver sequence. Events then took place under automatic control by

the computer, as follows: (1) gyros on, (2) all-axes inertial, (3) a negative roll turn of 4 min 19 s, (4) a positive pitch turn of 8 min 53 s, (5) a negative pitch turn of 8 min 53 s, (6) a positive roll turn of 6 min 4 s, (7) a positive pitch turn of 4 min 9 s, and (8) a negative roll turn of 7 min 6 s. At the end of the last turn the platform clock slew polarity was set negative.

A second DC-32 command was then sent to initiate the platform slewing sequence, which was to be followed automatically by a concluding reacquisition maneuver. The platform slews occurred as follows:

$$5X + 2N3 + 35N10 + 5N11 + 9Y$$

where

$$X = (2N3 + 35N10 + 2N3 + 35N11)$$

and

$$Y = (2N3 + 13N10 + 2N3 + 13N11)$$

In these slews, all events were separated by 4-s intervals, except the N3 event pairs, which were separated by 1 s.

After the platform slewing sequence, the slews then continued as follows: 5 N11 events at 1-s intervals; 91 N3 events at 1-s intervals; an N3 event after 1 s; after 1 s, 40 N3 events at 2-min intervals; after 14 s, a zero event; after 1 min 46 s, 21 N3 events at 2-min intervals. Two words were then loaded into the computer memory. One word deleted the P1 and P1-P2 events from the cruise chain, and left only one of three cruise events, a C2 event expected on August 27. The second word caused an early termination of the platform slews, and caused the immediate start of the reacquisition maneuver. The latter consisted of a positive roll turn of 7 min 6 s, a negative pitch turn of 4 min 9 s, and a negative roll turn of 1 min 45 s. The last turn was ended by a reacquisition event that caused the CC&S to assume the tandem standby state. A DC-13 command was then sent to discharge the pyrotechnic capacitors and the CC&S was thereby put in the nontandem standby mode. To return the CC&S to the tandem standby mode, a DC-33 command was transmitted.

Except for the Y1 events, the last event took place on August 27 when a C2 event caused the data rate to be switched from 33½ to 8½ bits/s.

**2. Mariner VII.** A total of 445 CC&S timed events were issued. In addition, a total of 653 coded commands

and 50 direct commands were received by the CC&S without error. The average clock error during the mission was 0.00070% slow. A total of 239 computer runs were made, two thirds of which were in direct support of operations; other computer runs were required for the many training tests that were conducted.

The prime monitors of CC&S performance are event counters 2 (computer) and 4 (fixed sequencer) contained in telemetry channels 118 and 119 respectively. Table 7 summarizes these events in accordance with the mode during which they occurred. Of the 4541 computer events, 595 represent discrete output events, 234 resulted from loading CC-1/2 command pairs; and 3712 resulted from executing 29 memory dumps. The 193 fixed sequencer events consisted in 7 midcourse events, 14 CC-4 commands for sequencer duration storage, 171 CC-4 commands used as spacers between CC-1/2 commands to the computer, and one anomalous event obtained when the fixed sequencer was loaded during a maneuver.

a. *Launch events.* The inhibit was released on *Mariner VII* at 22:18:01 on March 27. Three minutes later, the operation verify event was issued by the CC&S, indi-

cating that the CC&S clock was counting properly. One minute later the spacecraft was launched.

The spacecraft separated from the *Centaur* booster 17 min 27 s after launch. During and after the separation sequence, counter 2 events were seen to be accumulating. Of these events, 129 were seen and the rate of their accumulation was consistent with a CC&S dump having occurred. (The memory data were not seen on the ground because telemetry had not been changed from the engineering mode to the CC&S dump mode, as is done when a DC-2 command is sent). It was thus established that the flag 9 interrupt, which triggers the dump mode in the CC&S, had been somehow set by noise at separation.

At a CC&S time of 1 h (March 27 at 23:18:01) the CC&S issued backup commands to turn on the attitude control subsystem (L4) and to open the solar panels (L1). On March 28 at 00:18:01, the CC&S issued a command to the power subsystem to turn off power to the data storage subsystem. On March 28 at 02:18:01, the computer commanded turnon of the Canopus sensor via the L2 event.

However, there was still the possibility that when the unwanted dump took place, flags other than flag 9 could have been set (there are 8 other flags). The executive subroutine in the computer contained words that would have caused the reset of flags 2, 3, and 6 in a way that would leave no trace of their having been set. However, flags 1, 4, 5, 7, and 8 could have been set by noise and, if so, would remain set. It was decided to insert a word in the executive to test to see if any of these flags had been set. If, in a subsequent memory dump, the inserted word remained the same, then that would indicate that none of these flags had been set. But, if this word was changed, proof would have been obtained that one or more of the flags had been set.

The test word was sent to *Mariner VII* on April 1, and the memory dump taken later showed that at least one of the five remaining flags had been set. Insertion of this word also ensured that all flags had been reset; actually, this was the more important purpose of sending the word.

Later, on April 1, two coded commands were sent to the spacecraft to change word 6 in the computer memory. Word 6 contained a pseudorandom noise

**Table 7. Counter 2 and 4 events for *Mariner VII***

Mode	Counter	
	2	4
Launch events	4	
Midcourse events	7	7
Anomalous dump	129	
Inertial at scan platform unlatch	4	
Actuator matrix tests	21	
Anomalous event		1
Early turn-on of TV gate	1	
Turn on gyros prior to encounter	1	
Far-encounter (first set)	35	
Far-encounter (second set)	34	
Far-encounter (third set)	25	
Near-encounter	131	
Cruise events	17	
Y1 events	157	
Loading coded commands	234	185
Memory dumps	3712	
C7 events at end of dumps	29	
Totals	4541	193

sequence used for synchronizing memory dump data by the ground computer. This sequence was eliminated since it caused problems with the telemetry and command processor.

On April 3, a word was inserted in the computer memory to change the period for the Y1 cyclic events from 23 to 24 h so that they could be seen at the same time each day.

*b. Midcourse maneuver.* The memory words required for the midcourse maneuver were sent to the spacecraft on April 7. Twenty coded commands were sent, 14 of which (7 CC-1/2 commands) went to the computer to change 7 computer words and 6 CC-4 commands went to the fixed sequencer. The first three CC-4 commands were spacers (a 1-s negative pitch turn) sent between the CC-1/2 commands to permit transmission of coded commands on 1-min centers. The last three CC-4 commands were the turn and burn values for the midcourse maneuver. Of the seven words loaded into the computer memory, three were turn and burn durations, three were turn and burn start words, and one was the enable word for the computer subroutine.

The maneuver was a tandem maneuver controlled by the fixed sequencer and checked by the computer. It was unique in that it was executed from the star Sirius, rather than Canopus. All event times and turn and burn durations were found to be correct when the maneuver was performed later the same day. The maneuver consisted of a pitch turn of  $-193$  s, a roll turn of  $-71$  s, and a motor burn of 7.6 s (or 152 counts at 20 pulses/s).

Approximately 1 h after the maneuver was completed, the fixed sequencer was loaded with a precautionary sequence to minimize deleterious effects in case of an unexpected sequencer-only maneuver. A minimum negative pitch turn, infinite negative roll turn, and minimum motor burn were set up in the fixed sequencer. If a sequencer-only maneuver were to start, the spacecraft would perform an insignificant pitch turn and then would begin rolling. The latter could then be stopped with a direct command. In this way, the solar panels would stay on the Sun, and the motor would not burn and, hence, the option of a future maneuver having a motor burn would be preserved.

Subsequently, a DC-13 command was sent to the spacecraft to discharge the pyrotechnic capacitors. But this command put the CC&S in a nontandem standby status, which was not the desired nominal condition. A

DC-33 command was sent to return the CC&S to the tandem standby state.

*c. Cruise events.* On April 21, the first cruise event occurred. The Canopus tracker was stepped to its next position by the C1 event.

Two words were loaded into the computer memory on May 1 to delay the C5 event (unlatch scan platform) so that it would occur 1 wk later. When the scan platform was unlatched on *Mariner VI*, bright particles resulting from the pyrotechnic event caused the Canopus tracker to lose lock on Canopus and go into a roll search. It was desired to avoid this on *Mariner VII*, so the spacecraft was placed under inertial control during scan unlatch. But problems that required full attention on *Mariner VI* led to a delay in the scan unlatch exercise.

After the words were loaded to delay the C5 event, a memory dump was taken to verify proper loading; no problems were encountered.

On May 5, a block of commands changing seven words in the computer was sent to the spacecraft. The purpose of these commands was to provide for inertial control during the unlatching of the scan platform.

A DC-13 command was first sent to put the CC&S into the nontandem standby state. The commands were then loaded, and correct loading was verified by a memory dump. A DC-32 command was then sent to put the CC&S into the computer maneuver state, and a DC-14 command was sent to reconnect the CC&S to the attitude control subsystem.

Then, sequentially, the gyros were turned on, and the attitude control subsystem was commanded to go into an all-axes inertial state. When the latter occurred, two counter 2 events were received, as expected on adjacent lines on the teletypewriter. Since it was known that these events were approximately 200 ms apart, it was possible to fix the time of the "all-axes inertial" command at an Earth observed time of  $18:19:21.78 \pm 0.1$  s on May 8.

The C5 event (the second cruise event to be received) occurred when expected, and Canopus lock was not lost. As programmed, reacquisition subsequently took place. A DC-13 command was sent to put the CC&S into the nontandem standby state in anticipation of a DC-32 command on the following day.

A general update was made on May 9. Twenty words were inserted in the CC&S memory; seven of these words provided for inertial mode at near-encounter. Two words were inserted to change the number and interval of TV pictures in the first optional far-encounter. Six words had the purpose of changing three near-encounter slew magnitudes and the N8, N9, and P2 data words. Five words were loaded to change data words in the cruise chain.

An additional word was subsequently loaded to enable a test for determining whether flag 5 had been permanently set. Because of earlier operations, flag 5 should have been reset. The word was loaded and, in a memory dump that followed, it was found that the word had not changed, which proved that flag 5 had not been permanently set. A DC-32 command was then sent to put the CC&S in the computer-only maneuver mode, thereby setting flag 5. Another memory dump was taken in which it was found that the above word had changed; this fact confirmed that flag 5 had been reset.

A subroutine for automatically controlling the aperture of the TV camera during near-encounter was loaded on May 27. Included in this load was provision for N4 and N1 event pairs after the first twelve TV pictures at near-encounter. Fourteen words were required.

A word was also loaded to change the magnitude of one of the platform slews. A memory dump was taken to verify correct loading of all words.

On May 30, an update was made wherein four words were sent to add a P3 event and delete a C1 event from the cruise chain and to change the time for turning gyros on before near-encounter. Two memory dumps were taken. The first memory dump was verified only on the Honeywell computer. A second dump was taken to ensure that the words had been successfully inserted.

On June 9, two words were loaded to delete the P3 event expected on that day, and to add a P4 event to occur on June 19. A memory dump showed the loading to be correct.

Three words were sent to the CC&S on June 19. The P4 and C2 events expected later on June 19, and the C6 event expected on July 7, were all changed to zero events. Again, the proper loading of these words was verified by a memory dump. Later, the first two of the above zero events occurred at the expected times.

On July 7, a large spacecraft performance analysis and command (SPAC) crew was assembled to observe the switch to high-gain antenna as commanded by the CC&S C3 cruise event. A counter 2 event was observed at the expected time, but the switchover to the high-gain antenna did not take place. A direct command was sent to switch the antenna; this command was effective.

A memory dump was taken to see if the event address of the data word that had caused the counter 2 event were a C3 event. The result was affirmative. At this point the failure had been isolated to CC&S output circuitry and radio input circuitry. Shortly after the dump, a zero cruise event was observed, as expected.

A decision was made to proceed with a large update, which had already been planned for July 8. In this update, 52 words in the CC&S memory were changed. Two words were added to change the length of gyro warm-up time for "inertial at encounter;" seven words, to modify the cruise event chain; two words, to provide the capability of taking a fifth set of near-encounter pictures; seven words, to change the picture numbers and slew magnitudes at near-encounter; one word, to change the clock slew polarity for one near-encounter slew; four words, to change the automatic aperture control subroutine so that a selected number of N1\*-N4 event pairs would follow another selected number of N4-N1\* pairs; nine words, to provide a new subroutine for N6 and N7 events at near-encounter; three words, to change other near-encounter parameters; seven words, to modify the far-encounter program and parameters; nine words, to interchange words 4 and 5 in the executive so that dumps could be taken over hour scans; and one word, to change the Y1 time so that it would occur at a spacecraft time of 07:19:06 on August 5, just after near-encounter. A post-load memory dump showed all of the words to have been loaded correctly.

*d. Cause of C3 event failure.* In an effort to further isolate the cause of the C3 failure, a series of coded-direct commands were sent to the spacecraft on July 9. (A coded-direct command consists of two CC-1/2 commands separated by a CC-4 spacer. The first CC-1/2 command is a data word with zero in the time field. The second CC-1/2 command is a DSJ, DMJ, or DHJ, such that on the next appropriate scan, the event of the first word is issued.) Since issuance of the C3 event depended on operation of the C1 source driver in conjunction with the D0 sink driver, interest was centered upon other events requiring these drivers. To test the C1

source driver, one coded-direct command was loaded to turn on the timing-of-events relay. This was done, and telemetry channel 220 began to accumulate counts. A coded-direct command was then loaded to turn off the timing-of-events relay. The counter 2 event was received for this event, but channel 220 continued to accumulate counts. It thus appeared that the C1 source driver was not operating properly.

Two coded-direct commands were then loaded to test the N11 events by causing two steps of the scan platform in negative cone. The N11 event was verified by attitude control, which showed that the D0 sink driver had not failed. Two N10 events were then issued by means of coded-direct commands to return the platform to its original position and to test another matrix value.

A DC-13 command was sent to reset the timing-of-events relay, which terminated the accumulation of channel 220 counts. A DC-33 command was then transmitted to put the CC&S back into the tandem standby mode.

The loss of the C1 source driver eliminated the following computer events:  $\overline{TE}$ ,  $\overline{M3}$ ,  $\overline{M4}$ ,  $\overline{M5}$ , C3, L1, N6, N8, and N9. This loss deleted the possibility of performing computer controlled maneuvers and the "inertial at encounter" sequence. The latter, and N6 and C3 events could be replaced by ground commands. The L1 event would no longer be used, and the N8 and N9 commands were already backup commands.

Later on July 9, a computer word was loaded to change the N6 event to a zero event so that if the C1 source driver were repaired later, the unplanned restoration of the N6 event would not cause a catastrophe. Two dumps were taken to check the memory, since the first dump was verified only on the brush because of equipment failures, which invalidated the other means of verification.

Because of the loss of the C1 source driver, an emergency memory update was made on July 10. The "inertial at encounter" subroutine was deleted with one word. Since it was feared that other source drivers could be affected by a spreading contamination in an integrated circuit chip, other precautions were also taken. The automatic aperture control subroutine was disabled and other changes were made to the near-encounter program by a change of 10 words. A coded-direct command was used to turn on the TV gate. A memory dump showed satisfactory loading of these words.

*e. Event matrix tests and general updates.* On July 15, nine words were loaded into the CC&S memory. One coded-direct command was used to check event F3. A second coded-direct command was used to check event N1 to the data storage subsystem and the flight telemetry subsystem. Both events were observed to be effective. Two words were inserted to provide a reacquisition event at  $E + 4$  h by means of a countdown independent of any other events. In addition, three near-encounter data words were changed. Because of problems with a microwave link, three memory dumps were needed to prove memory integrity.

On July 26, 25 words were loaded into the CC&S memory. A coded-direct command was transmitted to set the scan platform clock to negative polarity. Two coded-direct commands were then transmitted sequentially to generate N3 events to move the scan platform two steps in clock. A coded-direct command was next sent to set the clock to positive polarity. Two more coded-direct commands were then sent to move the platform back two steps in clock. These operations were observed to have occurred in telemetry by the attitude control analyst.

At this time, a test was initiated to attempt to further pinpoint the portion of the C1 source driver circuitry that had failed. The CC&S was in a tandem standby maneuver mode with maneuver outputs disabled. The last three CC-4 spacers transmitted to the fixed sequencer were a minimum negative pitch turn, a positive 5-s roll turn, and a minimum burn. A DC-27 command was then sent to initiate a fixed sequencer maneuver, and a coded-direct command was sent (with a minimum negative pitch CC-4 spacer) to issue a reacquisition event so that it could be determined whether this would abort the maneuver. The plan went awry when an extra counter 4 event was received after the CC-4 spacer was loaded. The reacquisition counter 2 event was received and the maneuver was aborted, but due to the anomaly, a DC-13 command was sent as a precaution. Thus, the CC&S was put into the nontandem standby mode.

Later analysis and tests on the proof test model CC&S showed that one counter 4 event was caused by the CC-4 command that also turned on the pitch power switch, which caused a second counter 4 event. It was found that a clamp, included in the design to prevent loading of CC-4 commands during a maneuver, had not been wired properly into the CC&S subsystems. The conclusion was reached that if CC-4 commands were

not loaded during a fixed sequencer maneuver, the fixed sequencer would not exhibit anomalous behavior.

However, the anomaly mentioned earlier did cause the cessation of another test that had been planned for that day. A DC-27 command had already been sent to initiate a sequencer-only maneuver, which this time was to have been completed. But the maneuver was aborted by means of the DC-13 command before gyro warm-up was completed because of the lack of understanding concerning the cause of the extra counter 4 event.

A general memory update was then undertaken. Three words were inserted to modify the cruise chain. Four words were sent to change the N6 and N7 events. (The values were changed twice during the same update.) Three words were required to change platform slew magnitudes. One word was inserted in the executive to enable a test of the operability of flag 4 (the flag set each time a TV picture was taken). This test would await the turn-on of the science subsystem. Finally, three of the CC-4 spacers were used to establish the desired emergency roll and burn fixed sequencer values; i.e., minimum negative pitch, minimum negative roll, and infinite burn. A dump was then taken to verify the integrity of the memory.

*f. Two-step functions in telemetry data.* On July 30 and 31, at two different times, the data were suddenly lost while the spacecraft was being tracked, but later all data were regained. Each time the data returned, channel 420 had the same value as previously (23) but channel 220 and event counters 2 and 4 had changed from expected values. Before the first loss of data, these values were 126, 4, and 7, respectively. After the first loss of data, the readings were 63, 0, and 3, and after the second loss of data, the values were 20, 1, and 4. The only CC&S event that was expected during this period was a Y1 event on July 31.

The unexpected changes have been attributed to power transients and not to any malfunction of the CC&S (JPL Problem Failure Report 204653).

On July 31, when data were seen again after the second interruption, a Y1 event was received approximately 5 s earlier than expected. This is consistent with the power transient theory, because tests subsequently made on the proof test model CC&S showed that power transients exceeding -40% cause the clock to gain a few

seconds of count. Thereafter, CC&S events were all shifted to happen approximately 5 s earlier than they would have been expected to if no anomaly had occurred.

It was not known at this time whether the anomalies had modified the CC&S memory. Therefore, a memory dump was taken and a DC-30 command (CC&S inhibit) was held in readiness in case abnormal behavior should occur. The dump was successful, since no word had been changed by the transients. Also it is significant to note that the executive was enabled to respond to flags 4, 5, and 9. However, these flags were not set during the transients, because if they had been, it would have been apparent in the memory map.

Shortly after the dump was taken, a DC-33 command was transmitted to reenable the tolerance detector, which is disabled whenever a large power transient is received. Without the DC-33 command, an additional power transient could have inhibited CC&S scans. The DC-33 command also put the CC&S in the tandem standby mode.

On August 1, science power was turned on. At this time, since the TV gate had been enabled, the flag 4 flip-flop should have been set. A word had been inserted on July 27 into the executive subroutine to test for flag 4. When the CC&S memory was dumped, it was proved that flag 4 could be set and reset properly.

On August 2, more actuator matrix tests were performed. Coded-direct commands were transmitted to repeat the tests of positive and negative clock polarity, N3, N4, and N1 events. In all, six coded-direct commands were sent and all functions were proved operative. In addition, a memory update was made wherein two words were inserted to change the time of the N1 event expected after the first set of far-encounter pictures; one word was loaded to change the time between pictures in the first optional far-encounter set; one word was inserted to restore the automatic aperture control subroutine; and a word was inserted into the executive to test flag 6. The latter was done to determine whether the power transients had reset flag 6, which had been set by a DC-13 command before the transients occurred. In a subsequent memory dump, it was seen that the test word had not been modified, which showed that flag 6 must have been reset during the transient period.

*g. Far-encounter events.* Later on August 2, the first of three sets of far-encounter pictures was initiated when a DC-13 command and a DC-32 command were sent.

The DC-13 command put the CC&S into the nontandem standby mode, and the DC-32 command established the computer-only maneuver mode and started the picture-taking subroutine. Thirty-four photographs were taken at 27-min intervals as predicted.

On August 3, after the last of the photographs was taken, a small memory update was made. This update was preceded by a DC-14 command to connect the CC&S maneuver outputs to the attitude control subsystem. The update consisted of three words, of which the first was used to change the time between pictures for the second far-encounter picture set, and a coded-direct command was used to generate an M1 event to turn on the gyros in order to warm them up for near-encounter. The M1 event was confirmed by attitude control. In the memory dump that was taken next, it was found that word 98 was three counts greater than expected. Upon investigation, it was found that word 98 was a data word being counted down at the time to an N1 event that was to occur about 3 h later. The three words of the update (loaded on 1-min centers) were obviously loaded too close to the minute scan times and thus these inhibited the minute scans. (There was about a 30% possibility that this would occur.) A second dump was taken 10 min after the first (a procedure that had been instituted as part of encounter policy). This dump was identical to the first. About 3 h after the dump, the N1 event was received; it was 3 min late, as expected.

Later on August 3, a DC-32 command was transmitted to initiate the second set of far-encounter pictures. Thirty-four photographs were taken at 36-min intervals; the last picture was shot early on August 4.

On August 4, at approximately  $E - 26$  h, a 28-word change was made in the CC&S memory. The reasons for the changes are listed below:

- (1) One word to change a dummy event to an F3 event, provided a third optional far-encounter picture were selected.
- (2) One word to change the count of cruise events at which the N6-N7 subroutine would be enabled.
- (3) Three words to modify the cruise event chain.
- (4) Seven words to alter the far-encounter program to allow the taking of photographs of Phobos.
- (5) Two words to change the N6-N7 subroutine.
- (6) Five words to change the near-encounter slew magnitudes.

- (7) Four words to change the picture count numbers.
- (8) Two words to change the number of pictures before switching to and ending N1\*-N4 pairs.
- (9) Three words to change the N9, N8, and P2 data words.

Two dumps were taken and all changes were verified.

Shortly after the last dump, an N1 cruise event was observed, as expected. A DC-32 command was then sent to enable the third optional far-encounter picture set. After the F3 and F1 cruise events, the picture-taking sequence was initiated. Twenty-five pictures were taken; the first 20 were separated by 47-min intervals followed by five pictures at 12-min intervals. No anomalies were observed.

On August 5, at  $E - 4$  h, the final pre-encounter memory update was made; only two words were changed. One picture number data word was changed, and the other word was used to delete the requirement for a Mars gate sensor signal to enable the near-encounter subroutine; i.e., the flag 7 requirement was deleted. As preparation for a backup approach to achieve inertial mode at encounter, the fixed sequencer was loaded with minimum negative pitch, minimum negative roll, and infinite motor burn. (The latter was loaded so that the spent squibs could be used; thus, it would be a dummy burn whose purpose would be to prolong the inertial state.) Again, two dumps were successfully taken.

*h. Near-encounter events.* Early on August 5, a DC-13 command was sent as a safeguard to prevent any possible command to the pyrotechnic subsystem from the CC&S and to disconnect the CC&S reacquisition event expected after encounter. Subsequently, an N1 cruise event was issued at  $E - 2:41:23$ , an N1 event was issued at  $E - 1:41:23$ , and an F3 event was issued at  $E - 1:21:45$ . The latter was the last event in the far-encounter subroutine.

At  $E - 00:41:23$ , a dummy cruise event was issued and the near-encounter subroutine was initiated. The near-encounter events pertaining to the CC&S then took place as follows: N7 (remove TV covers); N6 (enable narrow angle Mars gate 2); clock slew polarity set positive; nine picture counts, each followed by N4 and N1\* events; 9 slew steps in positive clock and cone; 24 slew steps in positive clock; 10 picture counts, each followed by N4 and N1\* events; one picture count, followed by N1\* and N4 events; clock slew polarity set negative; 17 slews in negative clock



with platform slewed to final cone angle; 2 picture counts, each followed by N1\* and N4 events; 5 picture counts; 5 slews in negative clock; 8 picture counts; an N9 event<sup>2</sup>; an N8 event<sup>2</sup>; 2 picture counts; clock slew polarity set positive; 21 positive clock slews; a P1-P2 event; and the reset of the TV gate at  $E + 00:15:29$ . All these events took place as predicted.

Shortly after encounter, a DC-33 command was sent to put the CC&S into the tandem standby mode. At approximately  $E + 4$  h, the reacquisition event was issued, but it had no effect because the CC&S had earlier been disconnected from the attitude control subsystem. Two hours later, an N5 cruise event was issued.

*i. Postencounter update.* At approximately  $E + 17$  h, an update was made to the CC&S memory. Eight computer memory words were changed. Four words were used to change the cruise event chain, one word to eliminate the reacquisition count word from the executive, one word to change Y1 time, one word to remove the flag 4 test from the executive, and one word to restore the memory readout capability. The fixed sequencer was modified by establishing minimum negative pitch, infinite negative roll, and minimum burn in the maneuver registers. This returned the fixed sequencer to its status prior to near-encounter. The update was verified by means of a single memory dump.

Except for Y1 events, which occurred daily, only three more events were issued. These were a C2 event on August 20, a P1, P1-P2 event on August 25, and an additional P1-P2 event on August 25.

## B. Attitude Control Subsystem Performance

The attitude control subsystem (Fig. 33) provides three-axis position and rate orientation and stabilization for the spacecraft as soon as practical after injection into the interplanetary transfer orbit and maintains that orientation and stabilization during the interplanetary cruise period and the planetary encounter period, using the Sun and Canopus as position references.

*1. Flight performance.* Sufficient time elapsed between the events that happened on *Mariner VI* and those that happened on *Mariner VII* (5-30 days later) so that any lesson to be learned from an event on

*Mariner VI* could be, and was, applied to *Mariner VII*. The discussion of flight performance that follows will singly treat the performance of both spacecraft for each phase of the mission to more closely compare the performance of the two spacecraft and subsystems, and to illustrate the application of the lessons learned.

*a. Launch to Sun acquisition.* The launch of *Mariner VI* was uneventful, although the gyros were repeatedly saturated in what appeared to be a rough ride on the *Atlas* first-stage launch vehicle. Figure 34 shows plots of the gyro rates for the launch with the significant events noted. The spacecraft/*Centaur* separation transient was relatively mild; Fig. 35 illustrates the separation rates. The spacecraft was launched into the shadow of the Earth, from which it emerged at approximately 01:56:23 GMT (time is expressed as Greenwich Mean Time unless otherwise indicated). Sun acquisition was immediate and direct; the Sun gate event occurred at 01:58:37, and the last axis (yaw) passed through a null at 01:59:03. Integration of the gyro rates throughout the period from separation to Sun acquisition shows a net pitch movement of 13.8 deg to null the separation rates and the solar panel deployment, a maximum drift of 5.4 deg while in the shadow of the Earth, and a net movement of -25.6 deg. The corresponding values for the yaw axis are -10.7, -21.2, and -35.0 deg. (The roll axis is discussed separately.) The net pitch angle off the Sun of -6.4 deg, and the net yaw angle of 66.9 deg, place the cone angle of the  $-z$ -axis at 67.1 deg at separation, if maximum drifts are assumed to exist during the Earth shadow period.

The *Mariner VII* launch was similar to the *Mariner VI* launch in that the *Atlas* boost phase caused gyro saturation several times; Fig. 36 shows the *Mariner VII*/*Centaur* separation rates. *Mariner VII* was launched into the sunlight and immediately started acquiring the Sun; it turned through approximately a -25.7-deg pitch angle before it entered the shadow of the Earth at 22:40:59. During the time the spacecraft was in the shadow of the Earth, the angle drifted through was a maximum of -30.3 deg; when the spacecraft exited the shadow at 23:11:25 (as determined from the Sun sensor outputs), it turned through a 7.9-deg angle before acquiring the Sun in pitch. The corresponding yaw angles were -55.3, 15.7, and -38.7 deg. The total pitch angle of -48.1 deg and yaw angle of -78.3 deg placed the cone angle of the  $-z$ -axis at 82.2 deg. Sun acquisition occurred with a Sun gate event at 23:14:32, and the last axis null occurred at 23:15:00.

<sup>2</sup>Not effective because of the loss of C1 source driver, but counter 2 events were received.

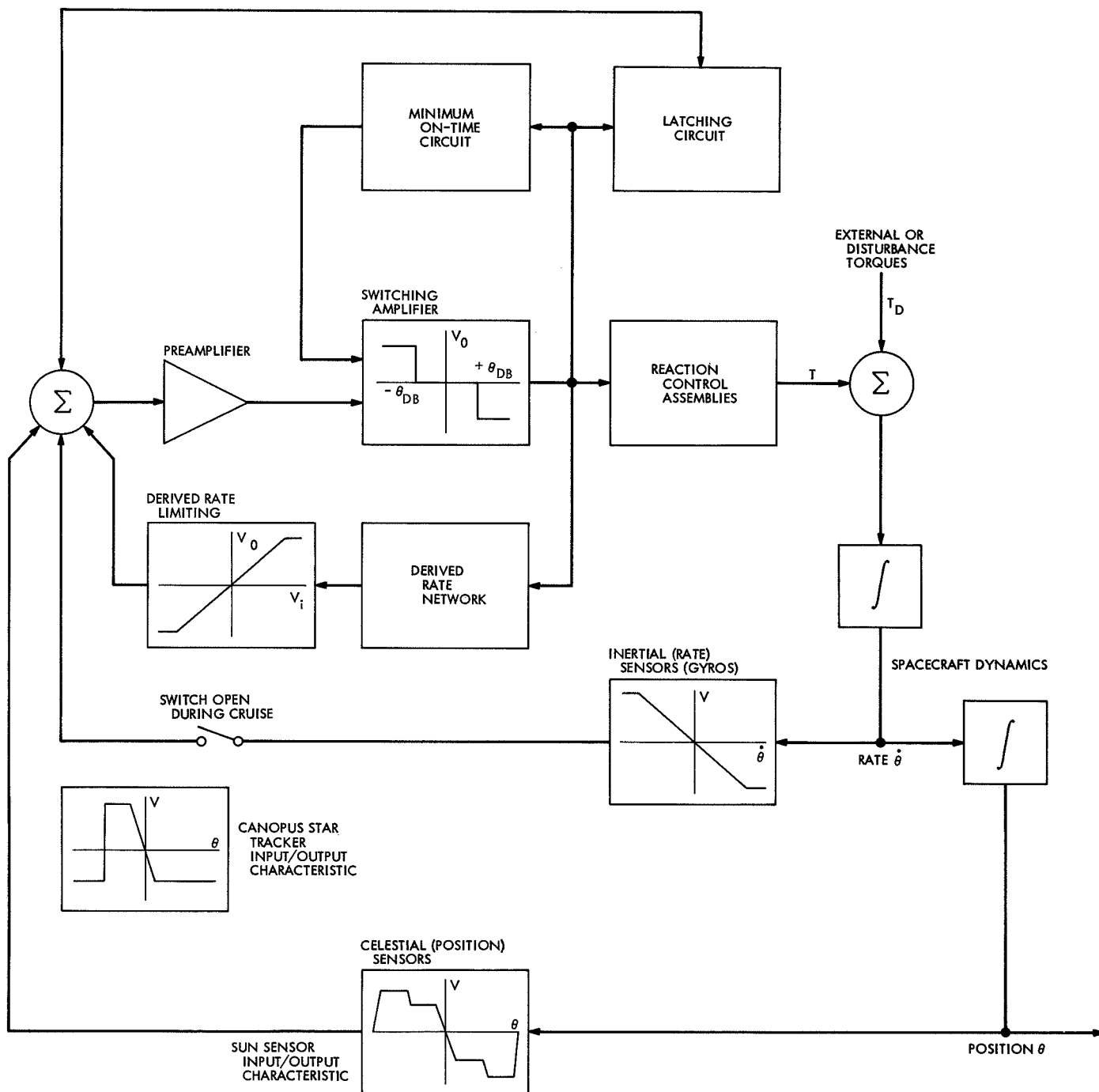


Fig. 33. Block diagram of attitude control subsystem

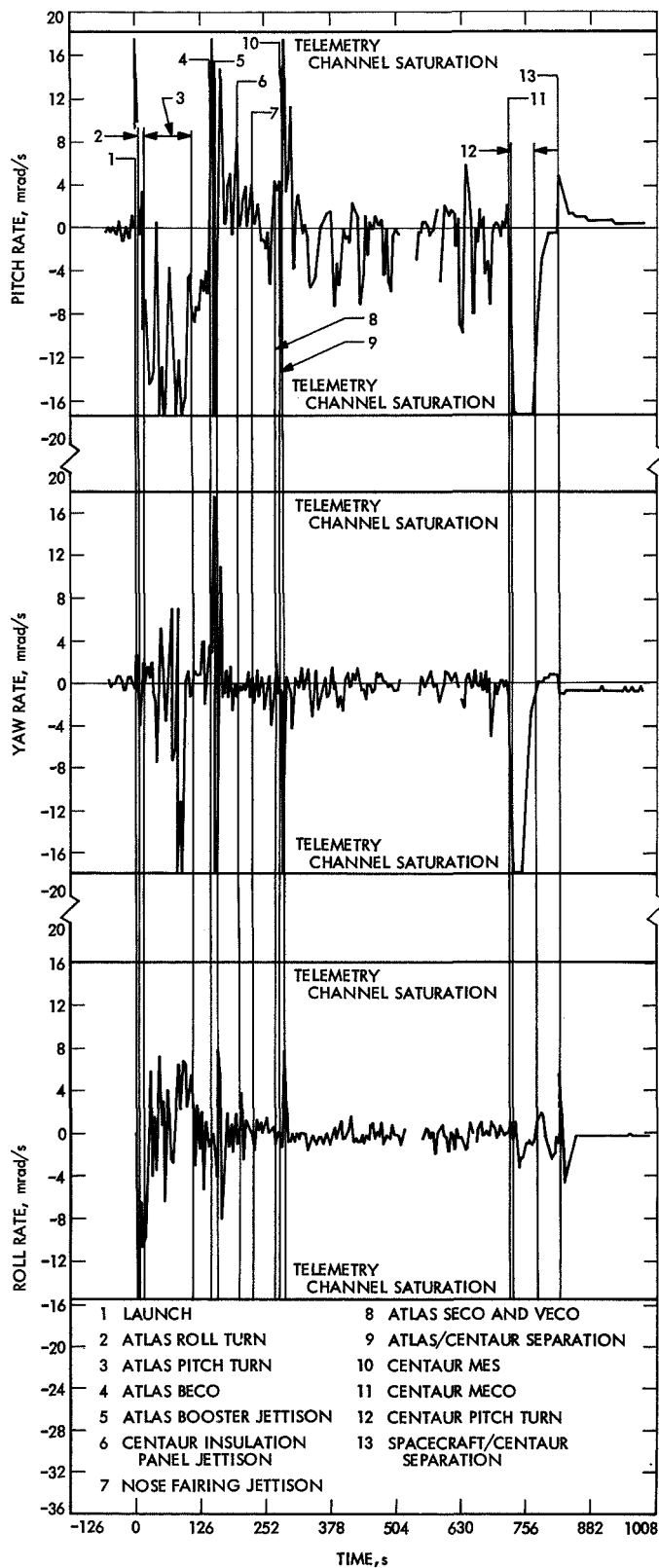


Fig. 34. Mariner VI pitch, yaw, and roll gyro activity, launch through separation

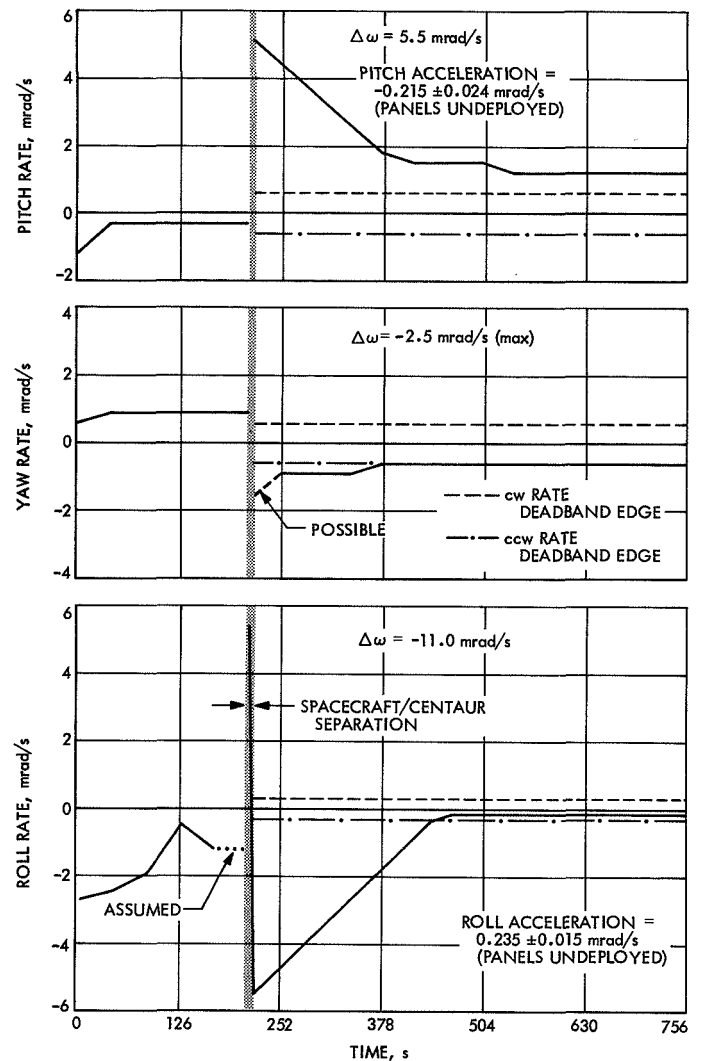


Fig. 35. Mariner VI spacecraft/Centaur separation rates

b. *Canopus acquisition.* For Mariner VI, the CC&S event L2 turned the Canopus star tracker power on at  $L + 4$  h. The telemetry indicated that the tracker cone angle position setting was C2 and the adaptive gate setting was G1, as expected. The tracker performed a flyback and sweep when power was turned on, and with no star in the field of view, the automatic roll search to acquisition was initiated. The roll search proceeded normally, at the expected rate of  $-3.8$  mrad/s, and Canopus was acquired at 05:42:07 when the tracker indicated a logic acquisition. Roll error signal null occurred at 05:42:46, and integration of the gyro rates indicated that the angle searched through was  $-222.5$  deg. The angle turned through at separation was approximately  $-2.7$  deg, and the angle drifted through, at the roll rate deadband edge, during the time between

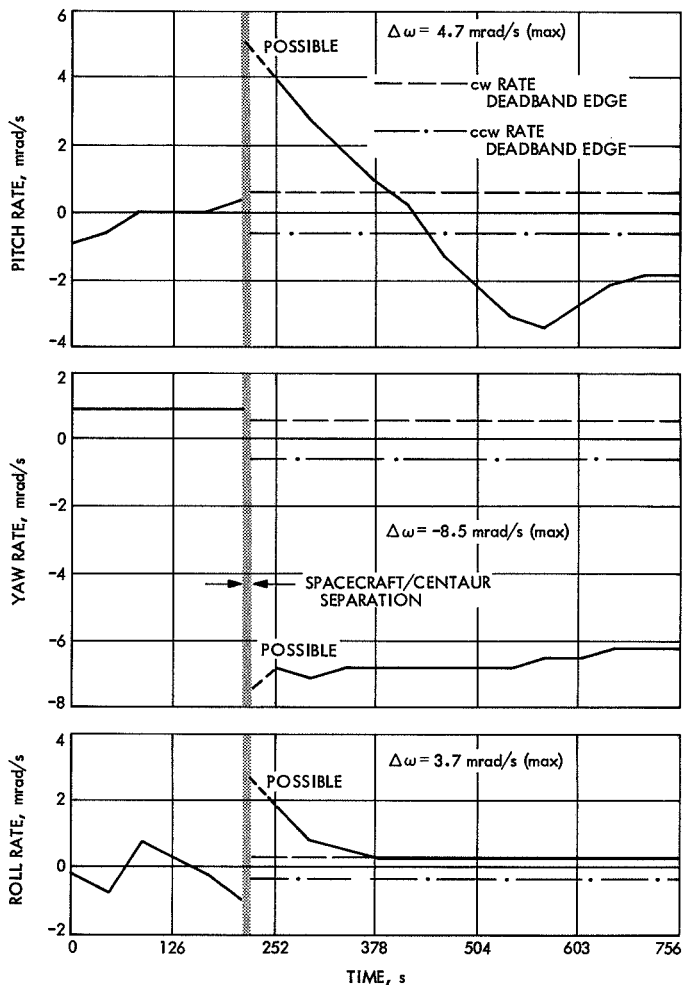


Fig. 36. Mariner VII spacecraft/Centaur separation rates

reduction of the separation rates and initiation of the roll search was as much as 120 deg over that period of 3 h 41 min. The initial position of the spacecraft at separation was then 105–345 deg clock angle. The gyros went off at 05:45:11, 3 min 4 s after the logic acquisition of the star.

The Mariner VII Canopus star tracker was turned on at  $L + 4$  h by CC&S event L2 on March 28. As expected, the telemetry indicated that the star tracker cone angle position was C3 and the adaptive gate setting was G1. This tracker had a warm-up characteristic, unlike other trackers. This characteristic is illustrated in Fig. 37; it was determined from data obtained on August 7, 1968. It was expected that a source dimmer than Canopus would appear brighter to the tracker than it was in actuality. Specifically, if the star Vega entered the field of view during the first half-hour of tracker operation, it

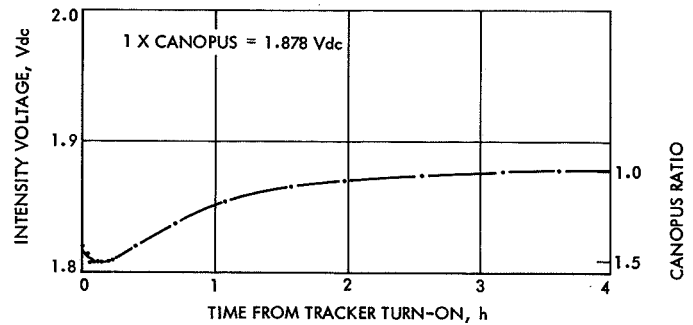
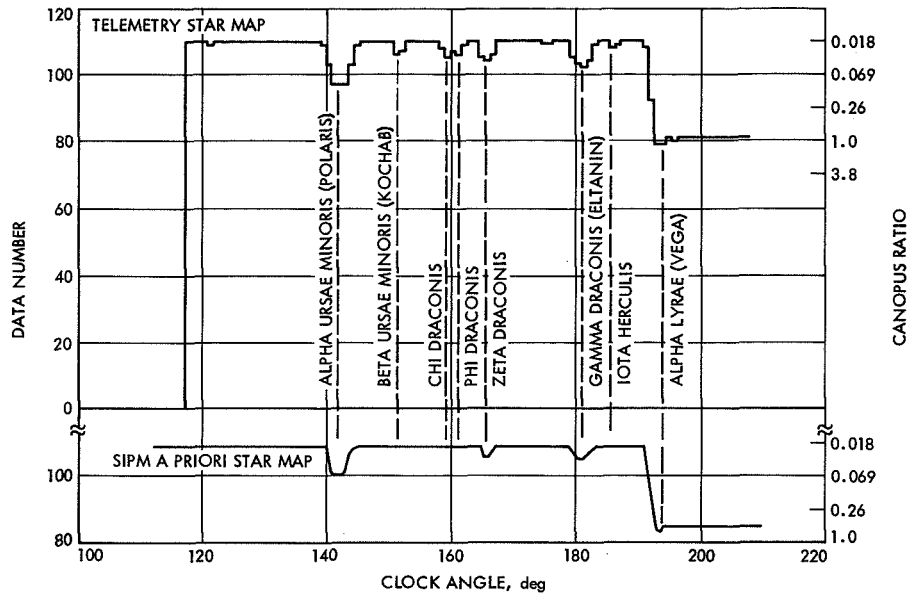


Fig. 37. Intensity-time characteristics of Canopus star tracker

would be expected to be acquired. At 02:23:56, a logic acquisition of Vega was indicated, and a roll error null was obtained at 02:24:45. The gyros went off at 02:26:56, exactly 3 min after the logic acquisition. Figure 38 is the star identification program for Mariner (SIPM) *a priori* star map for the initial roll search and the telemetered star map that shows the comparison and identification of the star acquired. It was decided at the time not to send the necessary ground command, DC-21, to override the star acquisition and continue the roll search to Canopus. There was no pressing need to acquire the star, and several events had happened during the launch that required immediate and further investigation. These events are described in Spacecraft System Performance, also in Part 3 of this volume. The warm-up characteristic of the tracker was observed while the spacecraft was Vega-acquired, and corresponded closely to that observed in ground test.

Canopus acquisition on Mariner VII was initiated at 16:45:00 on April 1, 1969, with the transmission of a DC-21 command. The gyros came on with the receipt of the command at the spacecraft at 16:46:09, and the roll search to Canopus was accomplished uneventfully. The star was acquired at 16:57:04, and the gyros went off at 17:00:02. The response to a  $1\times$  Canopus source was as predicted, and Fig. 39 shows the SIPM map for this roll search.

There are noticeably more stars identifiable from the telemetered star map than from the SIPM *a priori* star map. During the generation of SIPM for this new design of Canopus star tracker, the tests on the tracker that are used to create the model of the unit used in SIPM did not reveal the nature of the response of the tracker to dim and discrete light sources, such as the many minor stars. Additionally, there are only 423 stars available in the SIPM input table, and these stars only range



**Fig. 38. Initial Vega acquisition by Mariner VII**

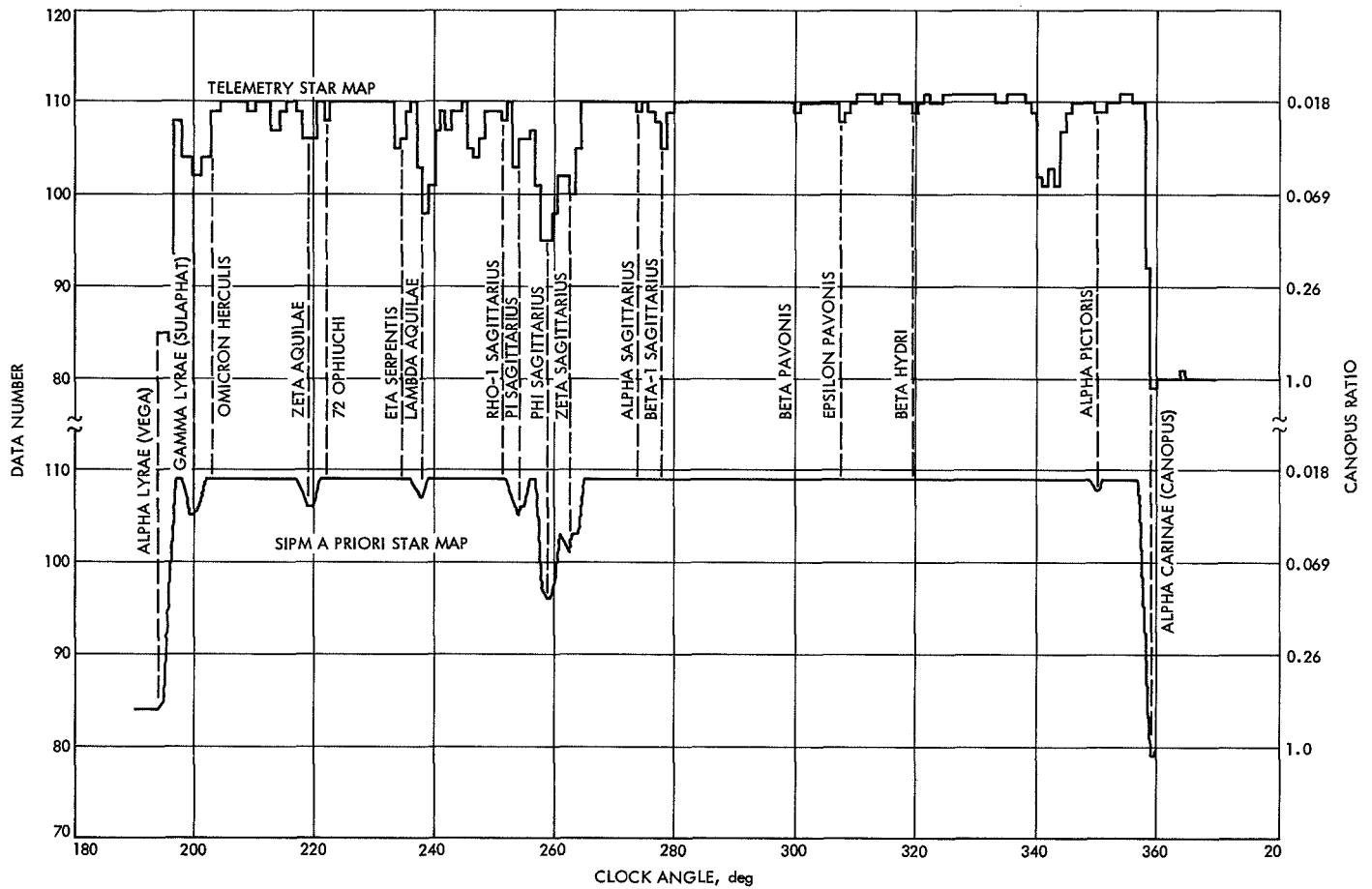


**Fig. 39. Initial Canopus acquisition by Mariner VII**

down to a Canopus ratio of 0.0108 in brightness. However, during the initial roll searches on both *Mariners VI* and *VII*, it became apparent that the tracker was capable of producing a response to very dim sources, and that it would be advantageous to increase the range of stars simulated in SIPM. Another characteristic of the tracker became evident when the object at 342-deg clock angle in Fig. 39 was identified as the Large Magellanic cloud (LMC), an external galaxy near the south ecliptic pole: the star tracker could respond to diffuse, bright sources as well as discrete objects. The basic SIPM catalog of stars was therefore supplemented with an additional star and object table of approximately 1100 entries and the necessary modifications made to the program to allow simulation of these objects.

c. *Midcourse maneuvers.* The *Mariner VI* midcourse maneuver was performed on February 28–March 1, 1969. Table 8 lists the required, commanded, and actual maneuver parameters (the required parameters are specified by the trajectory analysts; the commanded parameters reflect the capability of the spacecraft to achieve the desired parameters, and the actual parameters are the measure of spacecraft performance). The sequence of events is given in Mission Summary in Part 1 of this volume.

The *Mariner VII* maneuver was unique among *Mariner* maneuver sequences, in that the maneuver sequence was a roll–pitch–roll turn instead of the normal *Mariner* pitch–roll turn. The pitch–roll sequence offered several

disadvantages, including turning the low-gain antenna pattern away from the Earth (loss of communications: major constraint) and turning the Canopus tracker toward the Sun (energizing the tracker Sun shutter to cover the sensor: minor constraint). However, if the star Sirius could be used as a roll reference instead of Canopus, then a different set of turns could be used to orient the engine thrust vector in the desired direction with no violation of any constraints. The maneuver was carried out on this basis, and a DC-21 command to acquire Sirius was transmitted to the spacecraft. The spacecraft responded by starting the automatic roll acquisition override sequence. The star Sirius was acquired after a 36.1-deg roll, which corresponded to the initial maneuver roll turn. Table 8 also lists the pertinent maneuver parameters for *Mariner VII*.

The two maneuvers were similar in magnitude and result; these were the best maneuvers to date on a *Mariner* spacecraft, in terms of execution accuracy. Although data on the autopilot performance were limited to the gyro signals (the rate of telemetry information was one pitch, yaw, or roll gyro output sample every 4.2 s), the match of the telemetered data with a pre-maneuver, six-degree-of-freedom autopilot simulation was good enough to allow use of the simulation as an indicator of autopilot performance. In addition, extensive analysis of the autopilot resistor mix matrix had resulted in an improved method of determining the required resistor values, and the net result of these two major improvements in autopilot analysis and performance

**Table 8. Midcourse maneuver parameters for *Mariners VI* and *VII***

Parameter	<i>Mariner VI</i>			<i>Mariner VII</i>		
	Desired	Commanded	Actual	Desired	Commanded	Actual
Pitch turn magnitude, deg	−23.33	−23.35	−24.00 (1.85σ)	−35.64	−35.57	−36.31 (1.85σ)
Pitch turn duration, s		131			193	
Pitch turn rate, deg/s		0.17825	0.17819		0.18432	0.18432
Roll turn magnitude, deg	78.68	78.72	77.92 (2.1σ)	−12.83	−12.84	−12.65 (0.525σ)
Roll turn duration, s		453			71	
Roll turn rate, deg/s		0.17376	0.17369		0.18084	0.18081
Delta velocity, m/s	3.0679	3.0679	3.1456 (2.01σ)	4.2920	4.2920	4.2879 (0.076σ)
Engine burn time, s		5.350			7.60	

prediction were the maneuvers. It is calculated that, as an example, the total maneuver pointing error contributed by the autopilot was 0.57 deg for *Mariner VI* and 0.44 deg for *Mariner VII*. This error is reflected in Table 8 as equivalent errors in the pitch and roll turns. In addition, the redesign of the jet vanes for the *Mariner Mars 1969* thrust vector control assembly (TVCA) combined with the extensive testing of the TVCA and engine interaction provided a more accurate estimate and control of the drag and side forces generated by the vanes in the exhaust stream.

A previously unavailable tool for analysis of the maneuver turn polarity and duration, independent of the direct telemetry from the gyros, was the use of the Canopus star tracker intensity telemetry to confirm the correctness of the turns. Previous *Mariner* designs had turned off the Canopus star tracker during the maneuver as a consequence of the logic used in the system; however, for the *Mariner Mars 1969* design, the Canopus star tracker is normally never turned off. It was therefore possible to map the intensity response during the maneuver turns in the same manner that the roll to Canopus acquisition is mapped. The matching technique between the telemetered intensity information and the SIPM *a priori* map could then provide a confirmation of the turn direction and magnitude. This technique was used for both maneuvers; however, the confirmation of the turn magnitude is only approximate.

As mentioned, the Canopus star tracker, on previous missions, had been turned off during the maneuvers. This fact provided the basis for the only surprise of the *Mariner VI* maneuver: when the engine was ignited, the Canopus star tracker intensity response indicated that the objects up to nearly  $5\times$  Canopus brightness had entered the field of view. There were apparently three flyback and sweep sequences of the tracker acquisition logic (these sequences could also have been acquisitions and tracking of a particle, since the tracking function was not inhibited). There are two possible origins for these particles: (1) engine exhaust, and (2) "dust" particles accelerated off the spacecraft during the engine burn. Since the scanned field of view of the tracker in the biased position was approximately 95 deg from the engine centerline, and since the particles the tracker saw were particulate and not molecular in nature, the only things in the engine exhaust that the tracker could see were catalyst particles blown out at ignition. However, for these particles to enter the scanned field of view, they would have had to have a turning angle greater than

90 deg, which is unlikely. Therefore, the most probable origin for these particles is "dust" from the spacecraft. Since the spacecraft was being accelerated in such a manner that particles from the outer portion of the  $+y$  solar panel would pass directly across the trackers field of view, the second origin seems the most likely. Figure 40 shows, in part, the response of the tracker during the engine burns on both *Mariners VI* and *VII*. Note that the response lasted approximately 1 min.

*d. Scan platform unlatch and attitude control modes at encounter.* An extensive amount of analysis, centered about the scan unlatch process had preceded the launch of the spacecraft. The objectives of the analyses were: (1) to estimate the effects of the scan unlatch process with respect to the addition of an incremental velocity to the spacecraft, which would perturb the orbit after the midcourse maneuver had been performed, and (2) to estimate the effects of leakage within the unlatching mechanism that pressurized the spacecraft bus to a high enough pressure to cause an arc within the high voltage sections of the tracker. The tracker was not designed to be corona or arc proof; the image dissector used in the unit precluded such design, and protection against corona or arc was the reason the tracker was not turned on at launch until  $L + 4$  h, after the spacecraft bus had outgassed to less than  $10^{-4}$  torr. The analysis had shown that the scan unlatch mechanism would leak excessively during the scan unlatch process, and the valve crush gaskets were accordingly redesigned to alleviate the problem. The increase in spacecraft velocity attendant upon the release of the  $N_2$  gas at scan unlatch was estimated nominally at 10 mm/s, with a range of 3–13 mm/s. This value appeared to be an acceptable error in the midcourse maneuver targeting.

The scan unlatch on the *Mariner VI* spacecraft was commanded on March 6. The effect of the scan unlatch on the attitude control mode was at first similar to that of the midcourse maneuver. The tracker "saw" particles up to  $15\times$  Canopus brightness. Figure 40 shows the intensity response of the tracker. The tracker apparently did not go to a flyback and sweep, since the low gate was not violated and the high gate not enabled. Apparently, the tracker tracked these particles as they crossed the scanned field of view in a ccw direction, which caused the spacecraft to accelerate ccw for at least 21 s. There were eight samples of something other than Canopus (at 4.2 s between samples), and on the seventh sample the low gate was finally violated, which caused a flyback and sweep. Something near the intensity of Canopus was actually acquired near the cw edge of the total

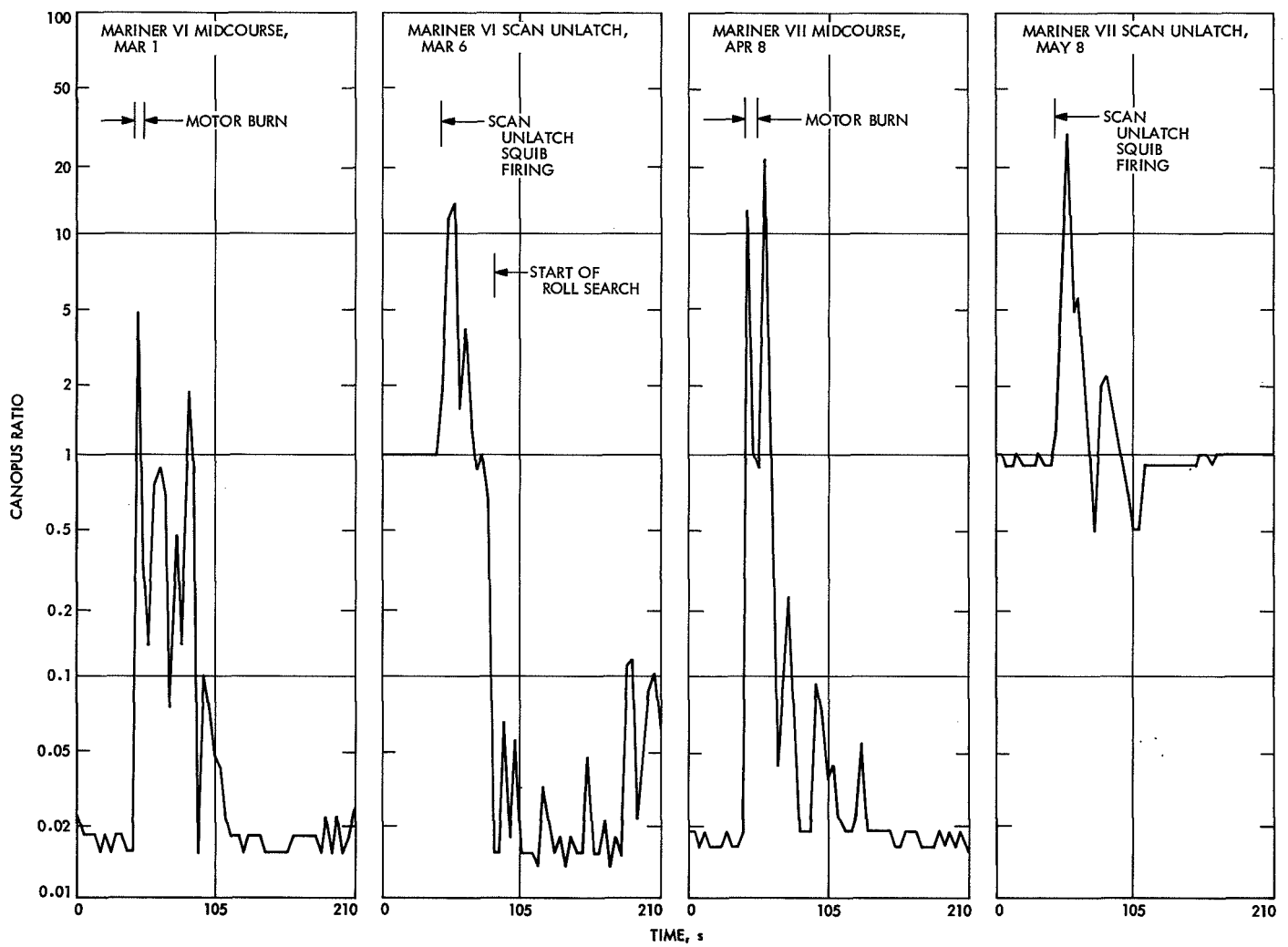


Fig. 40. Mariners VI and VII Canopus star tracker intensity responses for midcourse and scan unlatch events



field of view, but the accumulated ccw rate was too large and the acquisition was lost, and this initiated another flyback and sweep. Since nothing was acquired on this flyback and sweep, the automatic acquisition mode was initiated when the gyros were turned on and commenced a roll search. The roll search successfully acquired Canopus at 19:37:28, and the gyros turned off 3 min later.

The pitch and yaw limit cycle information clearly shows a positive pitch and a negative yaw torque during the time the latch was depressurizing and the spacecraft was accelerating ccw in roll. Since a ccw roll rate would result in an apparent negative pitch and positive yaw torque, the conclusion is inescapable: the torques evident were due to the escape of the latch gas. The direction of the pitch torque was that expected from a balanced exhaust tee; however, the presence of a yaw torque must be attributed to an unbalanced flow from the tee, or unsymmetrical impingement on the scan platform thermal blanket. This direction of gas flow would also produce a positive roll torque; a positive roll torque would then cause particles to be accelerated off the spacecraft, crossing the tracker field of view in a ccw direction. The greatest magnitude of torques evident were in the pitch and yaw directions, but the magnitude of pitch and yaw excursions were only +5 and -5.6 mrad, respectively, showing that the torques in roll were, of themselves, not enough to cause loss of Canopus acquisition. Loss of acquisition was entirely due to the tracking of the particles, and, as a result, the tracker caused the spacecraft to rotate far enough to remove Canopus from the field of view.

This unexpected loss of attitude control roll reference raised a serious question of procedure during the planetary encounter. Approximately 40 min before closest approach, the infrared spectrometer (IRS) was due to vent approximately 4 lb of nitrogen and 0.5 lb of helium gas to cool the cryostat to its operating temperature. It was apparent that if the miniscule amount of nitrogen released by the scan unlatch process could cause loss of Canopus acquisition by causing particles to enter the field of view of the tracker, then the amount and length of gas flow from the IRS cooldown would almost certainly have the same effect. A complete roll search lasts approximately 30 min; if reacquisition at encounter could be guaranteed, it would occur immediately before the science encounter sequence started. Obviously, such a risk was unacceptable, and so the alternate attitude control mode at encounter of all-axis inertial control, rather than the normal cruise control using the celestial position

references, was adopted. To test this mode, the necessary sequence was loaded into the CC&S, and the *Mariner VII* scan unlatch was performed with the attitude control under all-axis inertial control.

The scan unlatch command, C5, occurred at 19:19:24; Fig. 40 shows the tracker intensity response to the unlatch event. However, it appeared, from the tracker error signal, that these particles were moving cw with respect to the spacecraft, unlike the ccw particles of *Mariner VI*. The roll error signal was saturated in the cw direction for approximately 50 s, with one loss of acquisition after approximately 16 s followed by an immediate reacquisition. Since a high-gate violation was not observed after the low-gate violation, it is not likely that the gyros would have been commanded on, and it is entirely possible, had the spacecraft not been in the inertial mode, that the spacecraft would have accelerated cw in excess of 40 s and possibly as much as 50 s, until the second low-gate violation observed occurred. At that time, the gyros would have come on, and in an attempt to reduce the rate to within the rate deadband (or to go from the cw rate to the ccw roll search rate), the 30-s inhibit would have been energized, which would have shut off the roll channel control and required a DC-21 command to reset. In any case, Canopus acquisition would have been lost.

The CC&S  $\overline{M1}$  occurred at 20:19:22 and Sun and Canopus reacquisition were immediate. The gyros went off at 20:22:02, and the feasibility of using the all-axis inertial mode for the planetary encounter had been demonstrated. The sequence to place the attitude control subsystem in an inertial mode at encounter was loaded into the *Mariner VI* CC&S memory with coded commands on April 18, 1969. The sequence was enabled with a DC-32 command, and was completely automatic upon receipt of the command. The CC&S, at an appropriate time, would issue the M1 event; some time later, an M2, M4, and  $\overline{M4}$  event would be issued, and the reset of these commands would occur after the encounter was completed.

To demonstrate that the gyro drift in the all-axis inertial mode during the encounter period was acceptable, and to determine if the gyro drift characteristics had changed because of the launch environment, a gyro test was scheduled on *Mariner VI* starting on April 28, 1969. In addition, since the gyros dissipate a significant amount of electrical power in the form of heat, it was necessary to determine when in the encounter sequence the gyros were to be turned on to optimize the thermal

stabilization of the bus. A thermally stable spacecraft was important to the occultation experiment, since the radio was to enter occultation in the two-way (transponder) mode, and exit occultation in the one-way (auxiliary oscillator) mode, and the auxiliary oscillator was very sensitive to temperature changes at the extremes of frequency stability desired. After the gyros had been on for 24 h, they were placed in the all-axis inertial mode for another 17 h to perform a gyro drift test. The 17 h, although short for a drift measurement at the drift levels of the *Mariner* type gyros (typically 0.1 deg/h, maximum), was the maximum amount of time that a drift could be measured in the linear range of the celestial sensors if the drift rate was maximum. At the conclusion of the 17-h test, another test was performed on the spacecraft.

The gyro test was started with the loading of the CC&S memory with the required program on April 28. The CC&S memory was verified, and the maneuver sequence was started with a DC-32 command. The spacecraft gyros came on at 21:26:58 when the CC&S issued the M1 command; 24 h later, the CC&S issued the M2 command, at 21:26:57 on April 29. At 05:01:39 on April 30, the intensity telemetry indicated that the combined pitch and yaw gyro drift had effectively moved Canopus far enough in cone angle to make its apparent intensity less than the adaptive gate 1 dropout level.

Therefore, a DC-12 command (adaptive gate step), was transmitted to the spacecraft at 14:00:00 to step the adaptive gate to gate 2, so that Canopus acquisition would be maintained when the all-axis inertial mode drift test was terminated and optical control was restored. Command DC-13 was transmitted at 14:24:03 to optimize the time of the return to optical control for the Sun sensor telemetry. The drift test was moderately successful, as indicated by Fig. 41. The drift rates noted on the figure ( $-0.016$  deg/h pitch,  $-0.026$  deg/h yaw, and  $+0.071$  deg/h roll), suffer from the resolution of the telemetry and the limitation on the linear range of the telemetered sensor error signals, but are accurate to 10%. Another method of determining the roll gyro drift rate was to plot the extremes of the roll limit cycle as measured by the Canopus star tracker. As the spacecraft drifted in roll, the error signal increased; the slope of the increase was then the gyro drift rate. The roll gyro rate obtained in this manner is  $+0.066$  deg/h, which implies an error of 1.5 mrad as compared to the drift angle data shown in Fig. 40. After the drift test was complete and a preliminary analysis of

the thermal effects of the gyros on the radio had been made, an inertial-at-encounter sequence was loaded into the *Mariner VII* CC&S on May 9, 1969; it was enabled with the DC-32 command. The precaution of enabling the sequence was taken to prevent any loss of commanding capability from affecting the encounter sequence. These encounter maneuver sequences were updated periodically during the mission, as the encounter sequence of events became better defined.

*e. Canopus star tracker cone angle updates.* Since the roll reference star Canopus is not at the south ecliptic pole, the Sun-spacecraft-Canopus angle (the Canopus cone angle) changes with the spacecraft location in orbit. The field of view of the Canopus star tracker in the cone angle direction is from 11 to 12 deg, depending on the characteristics of the particular tracker. The seasonal variation in Canopus cone angle is approximately 32 deg; it is therefore necessary to gimbal the tracker cone angle field of view, and this is accomplished electronically within the tracker. There are five cone angle positions, covering the range of  $90 \pm 17$  deg. Figure 42 illustrates the cone angle coverage of the *Mariner VI* tracker, with the cone angle variation of the star shown. The CC&S command C1 to the tracker is used to change the cone angle position (CAP) to the next desired position. The cone angle positions are labeled C1 through C5, and C1 is the highest in angle. The scheduled cone angle update times for the spacecraft are shown in Table 9.

**Table 9. Scheduled Canopus cone angle updates for *Mariners VI* and *VII***

Change in cone angle position	<i>Mariner VI</i>	<i>Mariner VII</i>
C1 to C2	Launched in C2	Launched in C3
C2 to C3	22:25:00 GMT on Mar 29, 1969	Launched in C3
C3 to C4	22:25:00 GMT on Apr 20, 1969	01:20:00 GMT on Apr 21, 1969
C4 to C5	21:28:00 GMT on Jun 1, 1969	01:20:00 GMT on May 30, 1969

The first cone angle update was from position C2 to C3 on *Mariner VI*. The CC&S C1 command was observed at 22:25:53 on March 23, as expected. The tracker performance was entirely as expected for this update. The second update was also on *Mariner VI*, on April 20.

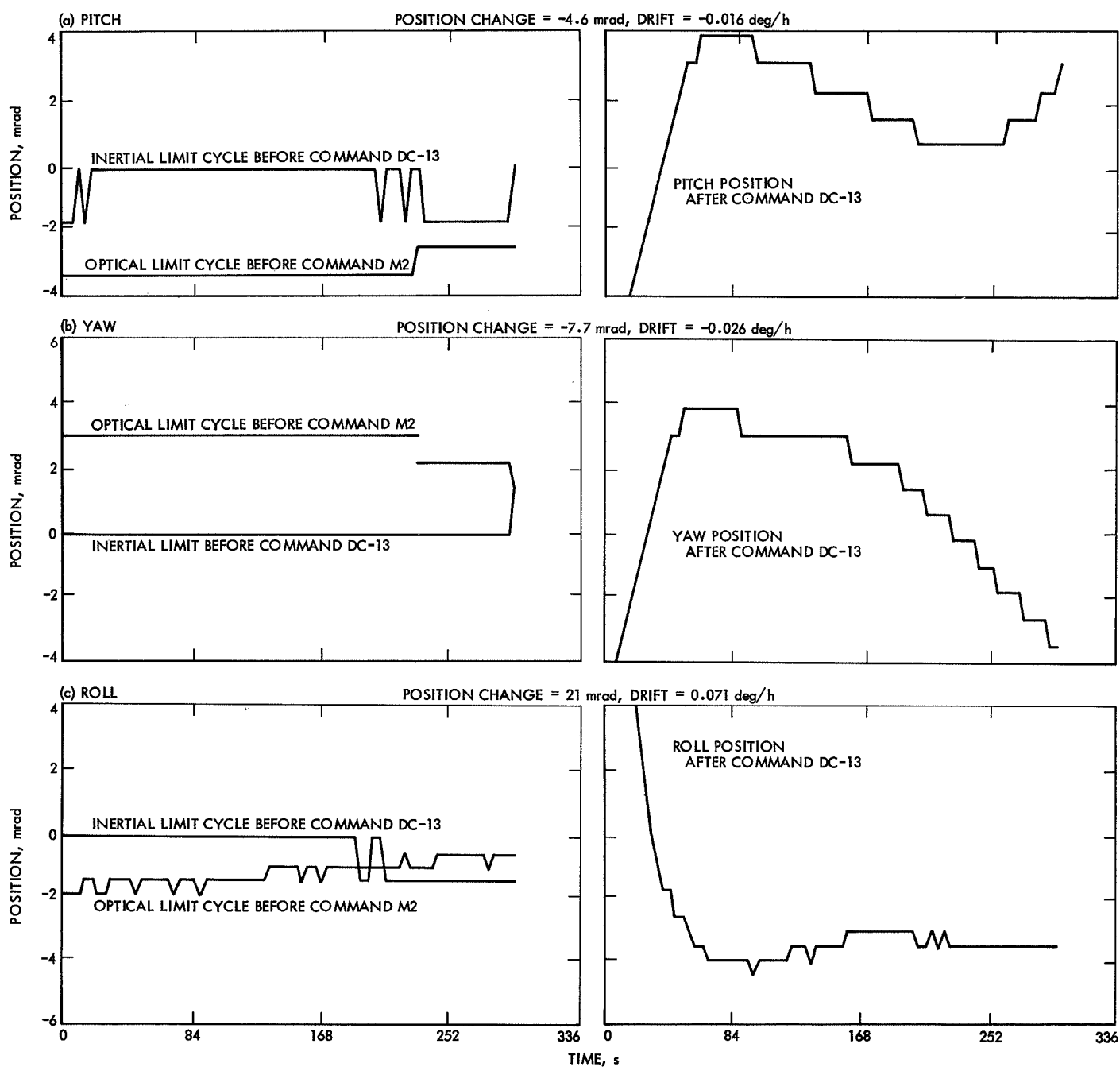
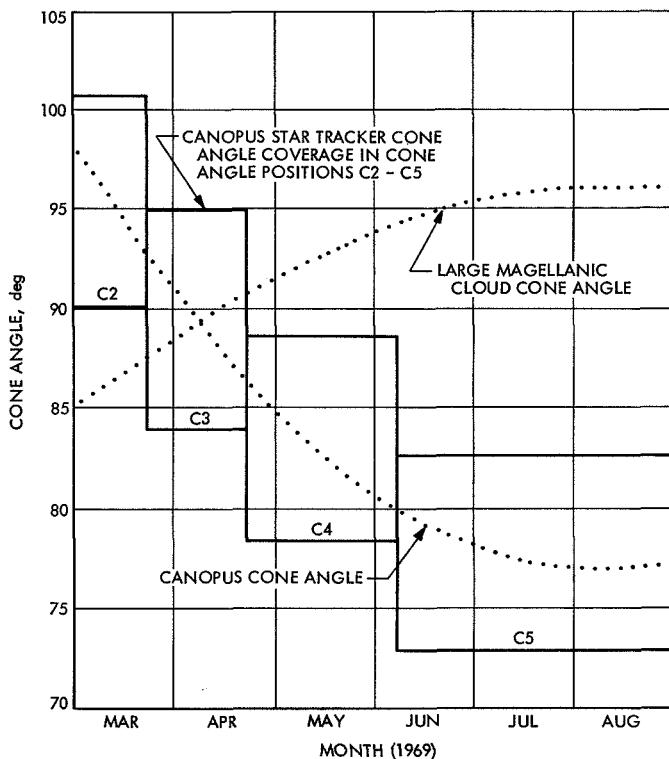


Fig. 41. Gyro drift rate for Mariner VI, April 29-30



**Fig. 42. Canopus cone angle, Large Magellanic Cloud cone angle, and Canopus star tracker cone angle coverage for Mariner VI**

The CC&S C1 command was observed at 22:26:42, and the immediate response was a drop in the telemetered intensity value, followed by a flyback and sweep, and then at 22:26:51 the spacecraft gyros came on, and a roll search was initiated. At 22:32:56, the cone angle position telemetry channel showed the CAP to be C2 instead of the commanded C4. Apparently, the CC&S C1 command had stepped the tracker to C2 instead of C4, with the result that loss of acquisition of the star occurred. A DC-17 command, the backup to the C1 command, was transmitted to the spacecraft at 00:00:00 on March 24, and the tracker responded by going to position C3, as expected. After the switch to position C3, Canopus was acquired by the tracker. A second DC-17 command, transmitted at 00:06:00, stepped the CAP back to position C2, and started another roll search. A third DC-17 command was transmitted at 00:15:00, and when it stepped the CAP back to position C3, it confirmed the supposition that the cone angle position was cycling between C2 and C3. The failure to step the position to C4 meant that Canopus would not be visible in the cone angle field of view after May 5, 1969, and therefore not available as a roll reference for encounter. Further, a CC&S command was

due on July 11 to transfer the radio transmitter to the high-gain antenna, and a roll reference would be needed for successful reception of the radio signal after that time.

Shortly after this step on *Mariner VI*, the CC&S on *Mariner VII* issued a C1 command at 01:18:44 on April 21. The step from position C3 to C4 on the *Mariner VII* tracker was normal and uneventful.

An immediate search for an alternate roll reference at encounter for *Mariner VI* was begun. The requirements were that an alternate reference be acquirable by the tracker, be usable as a roll reference, and be near 0 deg in clock angle at encounter. The most promising candidate was the Large Magellanic Cloud, mentioned before as an initially unidentified object during the first roll search to Canopus of *Mariner VII*. Figure 42 shows the cone angle variation of the Large Magellanic Cloud and Fig. 43 is an isophote-contour map of the cloud. There are three brightness peaks in the cloud; that labeled LMC-1 is the brightest. It was expected that LMC-1 would provide a suitable roll reference, and laboratory tests of the tracker with an LMC simulator were performed to verify that the tracker could acquire, null, and produce an acceptable limit cycle on the LMC. When the ground tests indicated that the concept of using the LMC was feasible, a test on *Mariner VI* was scheduled to demonstrate that feasibility.

Concurrently, an intensive study of the failure modes of the tracker cone angle position generator was in process. The cone angle generator is a three-stage, relay-driven binary counter that applies the output of a voltage divider from the  $\pm 120$ -V supply in the tracker to the image dissector cone angle deflection plates. Different values of voltage are applied to the deflection plates in accordance with the state of the binary counter. The counter stores the energy needed to change relay states on a capacitor, and the capacitor can only be charged if the relay contacts are made. If the command to transfer states does not last long enough for the capacitor to discharge enough energy to cause the relay to transfer, it is possible that the relay will only be partially transferred, and the set of contacts that are used to provide the charging voltage will not be made. In that event, no further transfer of the relay is possible by electrical means. There are several advantages to this type of circuit. In this particular application, fairly high voltages (up to 120 V) are switched, the circuit has a memory, it is insensitive to power transients, it consumes no power when a change is not being made, and it has a

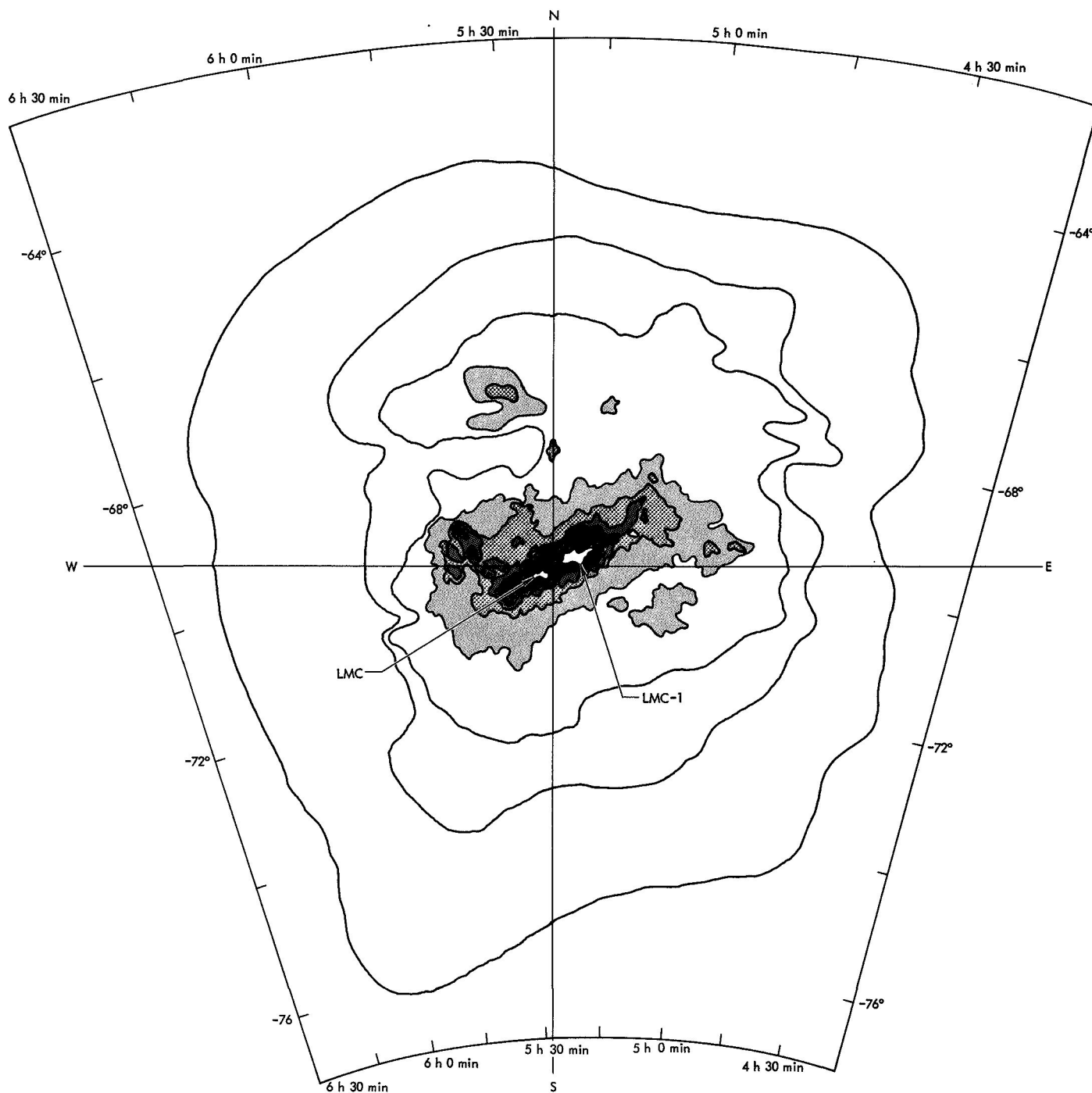


**Fig. 43. Isophote contours of Large Magellanic Cloud**

minimum component count. This circuit has been used with success on the previous *Mariner* flights with a Canopus tracker or sensor, although some trouble was experienced with incomplete transfers during ground tests. These problems were shown to be related to the quality and spacing of the command pulses from the test equipment; however, and there was no indication that there would be a problem in flight with the CAP generator. Table 10 shows the states of the CAP generator, and the progression of the positions.

**Table 10. Canopus star tracker cone angle position logic and voltage states**

Cone angle position	Binary counter states				Image dissector cone angle deflection voltage	
	Relays			Binary	Plate 1	Plate 2
	K1	K2	K3			
C2	0	0	0	0	50	0
C3	0	0	1	1	0	0
C4	0	1	0	2	50	100
C5	0	1	1	3	0	100
C4	1	0	0	4	-50	0
C3	1	0	1	5	0	0
C2	1	1	0	6	-50	-100
C1	1	1	1	7	0	-100

It appeared that the CAP cycling between positions C2 and C3 indicated that relay K2 in the CAP generator was failing to transfer, and that consequently position C4 was not obtainable.

The test on the spacecraft to demonstrate the feasibility of using LMC-1 as the roll reference for the rest of the mission would begin with the gyro drift test on April 28, 1969. At the conclusion of the gyro test, the spacecraft would be commanded to perform a roll search to obtain a star map, and then the spacecraft would be rolled to LMC-1 in the maneuver mode. The Large Magellanic Cloud would then be acquired with command DC-15, and the CC&S maneuver commands would be reset, leaving the spacecraft in a cruise mode with the gyros off and the LMC-1 acquired in roll.

After the successful conclusion of the gyro drift test on April 30, a DC-14 command was transmitted at 14:50:00 to enable CC&S control of the attitude control maneuver functions and a DC-21 command at 15:00:00

initiated the roll search. The search started with the gyros on command, at 15:02:58, and ended with the acquisition of Canopus at 15:27:25. The required coded commands to load the CC&S memory with the maneuver to roll to the LMC were transmitted next, and a DC-2 memory dump verified the load. A DC-32 command initiated the computer-only maneuver. It was transmitted at 17:00:00, and the gyros came on with the CC&S M1 event at 17:02:58. Fifteen minutes later, at 17:17:57, the CC&S issued the M2, M4 and  $\overline{M4}$  commands; the time was shortened between the gyros-on and the all-axis inertial mode commands because the gyros were already warmed up. At 17:25:55 the 124-s, 21.5-deg positive roll turn to the LMC began with CC&S command M5. Command  $\overline{M5}$  at 17:28:00 terminated the turn. Command DC-15 was sent at 17:55:00 to allow acquisition of the cloud, but no change in tracker intensity telemetry or roll position error signal was noted. A second DC-15 command was sent at 18:22:00 to ensure that the command was enabled to the tracker, and meanwhile a review of the acquisition geometry revealed that no change could really be expected. The LMC-1 was at approximately 342.4 deg in clock angle; after the 21.5-deg turn, the center of the scanned field of view in the biased position was 341.9 deg in clock angle, which means that even if LMC-1 had been acquired, the telemetry on the roll position error would still be saturated.

The CC&S commanded  $\overline{M1}$  at 18:28:00, and the spacecraft went into a short roll search upon the return to optical control. Integration of the gyro rates showed the search to be 4.7 deg, which indicated that the point acquired was approximately at 343.2 deg, about half-way between LMC-1 and LMC-2, the next brightest peak in the cloud. The gyros went off at 18:31:18, and the spacecraft was restored to the cruise state with a DC-13 command to CC&S to place the computer in the nontandem standby maneuver mode followed by: a coded command pair to reset a flag in the computer, a DC-32 command to enable the encounter maneuver sequence in the computer, and a DC-14 command to enable CC&S control of attitude control maneuver events. The scan control subsystem near-encounter clock angle reference potentiometer was adjusted for the new roll reference, and some necessary updating of event times in the computer was accomplished.

The spacecraft was in the cruise attitude control mode, with the Sun and LMC as references; however, the roll limit cycle on the LMC was very noisy, and it was initially assumed that the acquisition of the second brightness

peak (an extended, rather than point, source of low intensity), was causing the erratic, noisy, and gas-consuming limit cycle. Accordingly, a CC&S maneuver program featuring two roll turns, one to bring LMC-1 into the scanned field of view and the second to bring the center of the scanned field of view to the "boresight" of the tracker after the DC-15 command had been sent, was formulated. The plan was to load the program into the memory with coded commands, send command DC-19 to reacquire Canopus, and then execute the new maneuver. However, at 23:58:01, the roll error channel telemetry reading suddenly went to its negative limit, followed by a change to its positive limit, and the spacecraft went into the "DC-15 roll search" mode. This mode is the inputting of the tracker roll search voltage to the roll channel without a corresponding nulling gyro output signal, since the gyros are inhibited from turning on by the DC-15 command. The 30-s roll search inhibit logic was designed for just such a situation, however, and the roll position input was opened by the timer. Command DC-19, to reset command DC-15 and allow the gyros to turn on, was transmitted to the spacecraft, and at 00:17:46 on May 1 the gyros came on, damping the residual roll rate to the deadband level. Command DC-21, to reset the 30-s inhibit, was transmitted next, and at 01:02:45 the spacecraft commenced the roll search. One of the side effects of the DC-15 command is the removal of the adaptive gate stepping command inhibit; accordingly, all the time the DC-15 command was in effect, the adaptive gate had been stepping, and was then, in adaptive gate 3. Consequently, the star Al Na'ir was acquired at 01:05:54, at approximately 291 deg clock angle. Command DC-21 was transmitted at 01:20:00 to disacquire Al Na'ir and roll search to Canopus, but approximately 28 s before the flight command subsystem issued the command, acquisition of Al Na'ir was lost. The tracker performed a flyback and sweep, failed to regain acquisition, and initiated the roll search mode. Canopus was acquired in a normal manner at 01:26:37 and the gyros went off at 01:29:37. The roll error signal, when the tracker was acquired on Al Na'ir, was noisy in the same manner it was on the LMC, and it appears that acquisition was lost for the same reason: the roll error signal was very noisy for dim sources. It was decided that an attempt should be made to acquire the brightest peak of the LMC by stepping across the cloud in incremental roll steps, finding the brightest point in the cloud, and then rolling back to it and acquiring it with the tracker.

This sequence was started on May 2, 1969, with the transmission of 31 coded commands to load the sequence

parameters in the CC&S memory, followed by the DC-2 memory readout command. The DC-32 command started the maneuver sequence by commanding the CC&S to issue the M1 command at 15:33:04. After a 15-min gyro warm-up, the M2, M4,  $\bar{M}4$  series of commands was issued by the CC&S at 15:48:02. The 73-s, 12.70-deg roll turn started with CC&S command M5 at 15:53:03 and ended with command  $\bar{M}5$  at 15:55:16. The center of the scanned field of view of the tracker is  $-3.77$  deg from the geometrical center of the tracker, and with the roll turn starting at  $-0.16$  deg clock angle, the center of the scanned field of view was at 351.23 deg clock angle. Next, a block of 20 coded commands was loaded into the CC&S to give a 1-s positive roll turn each time a DC-32 command was sent to the spacecraft. After the load was verified with a DC-2 command, 80 DC-32 commands were transmitted to the spacecraft on 1-min centers, starting at 17:00:00 and ending at 18:19:00. Figure 44 illustrates the map of the LMC made by this technique. The LMC-1 and LMC-2 are clearly identifiable; LMC-3 (the third brightest peak) is not an outstanding, clearly identifiable point. A pair of coded commands was then loaded into the CC&S memory to reverse the direction of the roll, and 27 DC-32 commands rolled the spacecraft from the cw end of the initial mapping, at a clock angle of 338.63 deg for the center of the scanned field of view, to a clock angle of 342.9 deg for the center of the scanned field of view. The DC-15 command was then sent, at 20:15:00, and the tracker "acquired" LMC-1. The next step was to reduce the roll error signal to zero by rolling the spacecraft the required 3.77 deg to center the scanned field of view in the tracker field of view. A total of 29 DC-32 0.158-deg steps were required to null the roll error signal; this corresponded to a roll of 4.6 deg, to a spacecraft

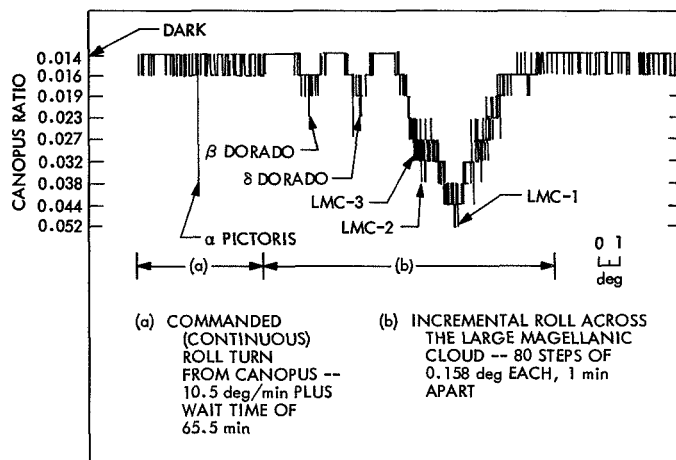


Fig. 44. Large Magellanic Cloud mapped by Mariner VI Canopus star tracker, May 2

clock angle of 343.3 deg. The apparent roll error null point of the LMC was not at LMC-1, but apparently 1.05 deg ccw of LMC-1 and 0.36 deg cw of LMC-2, at the point the tracker had acquired by itself on the previous attempt.

Command DC-13 was now sent to return to optical control, and, at 23:23:03, the Sun sensors came on for pitch and yaw control. The gyros went off at 23:26:08, and the spacecraft had once again acquired the Sun and LMC in the DC-15 command mode. The roll limit cycle did not appear to be significantly different from the previous acquisition attempt on April 30. It appeared that the low intensity source brightness was adversely affecting the operation of the tracker. The high voltage applied to the image dissector is inversely proportional to the source brightness, and at the higher voltages (about 1500 V) the "tube noise" is more pronounced. If the tube should "punch through" and go into heavy conduction, the roll error demodulator in the tracker would saturate. Since the preferred direction of saturation for the demodulator would produce a positive, saturated, roll error output voltage, it was decided that the gyros should be turned on with an M1 command from the CC&S. The reason for turning on the gyros was that if the image dissector should fail, producing the saturated, positive roll error signal, the spacecraft would accelerate in the positive direction, and the gyros would be needed for rate limiting. The 30-s roll inhibit is only operative in the negative direction; the April 30 operation on the LMC had ended with the set of the 30-s timer because the roll off the LMC had been in the ccw direction. At 00:30:00 on May 3, five coded commands were sent to the spacecraft to program the coded commands to issue an M1 command when a DC-14 and DC-32 command sequence was transmitted. The DC-32 command was transmitted at 00:45:00, and the gyros came on at 00:48:04. The spacecraft was then in an acceptable cruise state, with the gyros on in the rate mode.

The roll limit cycle continued to be noisy for the next few hours, with occasional noise bursts. Recovery from the noise bursts was normal, and the LMC remained acquired, but it was evident that the tracker was degrading, and could not be maintained in this mode for an extended period of time. Finally, at 14:50:20 on May 3, the roll error signal went to its positive limit and the spacecraft began a roll search in the anti-search direction. An unidentified star at approximately 314 deg in clock angle was acquired at 14:52:19. Acquisition on this star was maintained until 15:43:36, when a noise burst caused a 32-s cw roll search, followed by a ccw roll

search, during which acquisition of the star was lost and then regained. Similar occurrences were noted at 16:15:19 and 16:16:35. At 16:54:10, another noise burst caused another cw roll search of approximately 19 deg, to a clock angle of approximately 295 deg and, at 16:56:29, Al Na'ir was acquired once more, after an 8-deg roll search to 287 deg in clock angle.

The appearance of the roll limit cycle on Al Na'ir was more regular than that on the LMC, but many noise bursts were still evident, and it was clear that the Canopus star tracker would degrade to an unacceptable state if an attempt were made to continue the tracking of dim sources. Accordingly, the decision was made to turn off the tracker with a DC-20 command, to place the spacecraft roll axis in the inertial mode with a DC-18 command, and to use the roll-axis inertial mode of operation for roll position control for the rest of the mission. One more attempt was made to update the cone angle position before the tracker was turned off, however, by sending seven DC-17 commands on 7-min centers (the cone angle telemetry readout occurs every 7 min). The DC-18 command was transmitted at 22:30:00, and the 2.25-deg step that occurs when the DC-18 command is sent with the gyros on was evident in the roll error signal. A DC-21 command followed the DC-18 command, and the spacecraft, in the roll axis inertial mode, responded by stepping 2.25 deg ccw. Since the tracker was in the DC-15 command mode, there was no effect on the tracker from the DC-21 command. The first of the seven DC-17 commands was transmitted at 22:48:00, and at 22:51:07 the intensity reading dropped and the roll error went to the biased position, which indicated that acquisition on Al Na'ir had been lost for some reason. The cone angle telemetry readout occurred at 22:52:03, and indicated that the cone angle position had stepped to the C4 position with the first DC-17 command. The rest of the scheduled commands were summarily canceled, and a DC-12 command, to step to adaptive gate 1, and a DC-19 command, to reset the DC-15 and DC-18 commands and return to optical control, were transmitted at 23:10:00 and 23:20:00, respectively. A DC-21 command was not needed to start the roll search to Canopus, since the DC-12 command, in stepping the adaptive gate to gate 1, had caused a low-gate violation to occur when the DC-15 command was reset. The roll search to Canopus therefore started with the receipt of the DC-19 command at 23:23:07, and Canopus was acquired at 23:28:09. Since the CC&S M1 command was still in effect, the gyros did not go off with the acquisition, and some minor reprogramming of the CC&S was required to reset the M1 command



without inhibiting the encounter maneuver sequence. This reprogramming was accomplished 10 days later, on May 13, after 261 h 18 min 39 s of continuous gyro running time.

The roll limit cycle with Canopus as the roll reference had none of the noise characteristic with either the LMC or Al Na'ir as the roll reference. It was apparent that, with the relatively high source brightness presented by Canopus reducing the high voltage across the image dissector to the  $1\times$  Canopus level (about 1000 V), further degradation to the tracker would be halted. The reasons were not clear why the CAP failed to step to position C4 on April 20 (after two commands to step from position C3 to C4), and stepped to position C4 on May 3 after a "last ditch" type effort. The theory at the time was that relay K2 in the CAP generator binary counter was contaminated in a manner that prevented the logic contacts from mating, and the subsequent extensive maneuvering, rolling, and general level of activity on the spacecraft had in some manner dislodged the contaminant so that the final attempt was successful. The only step left was the step to position C5; since that did not involve the suspect relay, but the K3 relay, which transfers for every cone angle position step (and had been transferring for every step successfully), it appeared that there would be no further problem with the tracker CAP.

The next scheduled update of the tracker CAP was the *Mariner VI* step to position C5. On May 26, at 21:28:10, the CC&S issued the C1 command to the tracker, and the familiar flyback and sweep occurred, with the gyros coming on at 21:28:18 to start the roll search. The next reading of the cone angle position telemetry channel indicated the position to be C3 instead of C5. The immediate supposition was that the CAP was in the descending sequence (see Table 10 for the CAP sequence), and that six DC-17 commands would be required to sequence the CAP generator to position C5. Accordingly, a sequence of DC-17 commands on 7-min centers was begun at 22:51:00; it was interrupted with a DC-18 command at 23:28:00 to stop the roll search and inhibit the adaptive gate from stepping in the automatic mode. The sequence of cone angle positions obtained from the DC-17 command sequence is shown in Table 11; the eighth DC-17 command, transmitted at 23:47:00, resulted in a step to position C5, the desired CAP. To acquire Canopus, a DC-19 command was sent at 00:01:00 on May 27, and the roll search was restarted at 00:05:21, and it terminated with the acquisition of Canopus at

**Table 11. History of *Mariner VI* Canopus star tracker cone angle position**

Date	Command	Binary state/ actual cone angle position
Feb 25, 1969	Launch	0/C2
Mar 22	C1(1)	NA <sup>a</sup> /C3
Apr 20	C1(2)	NA/C2
Apr 21	DC-17	NA/C3
Apr 21	DC-17	NA/C2
Apr 21	DC-17	NA/C3
May 3	DC-17	NA/C4
May 26	C1(3)	NA/C3
	DC-17	4/C4
	DC-17	5/C3
	DC-17	6/C2
	DC-17	7/C1
	DC-17	0/C2
	DC-17	1/C3
	DC-17	2/C4
May 26	DC-17	3/C5
Nov 12	C1(4)	NA/C2
	DC-17	NA/NA
	DC-17	NA/C3
Nov 12, 1969	DC-17	NA/C4
Jan 8, 1970	DC-17	NA/C3

<sup>a</sup>NA = information not available.

00:11:13. The gyros went off at 00:14:18, and the spacecraft was back in the attitude control cruise mode, with the Sun and Canopus acquired.

The sequence of cone angle positions listed in Table 11 (up to and including the entries of May 26) was analyzed again for failure modes in the star tracker CAP generator. The possible failure modes that became apparent are:

- (1) Relay K2 may fail to transfer in two modes: either both sets of contacts fail to transfer, and the relay stays in the state it was before the transfer command was given (either the 0 or 1 state); or only the contacts switching the cone angle voltage fail to transfer; the relay itself transfers, but these contacts stay in the 0 or 1 state.
- (2) Relay K2 contacts are shorted together: the logic contacts that control the switching of the relay are shorted together so that the relay will not transfer out of the 1 state or out of the 0 state.

The failure in the cone angle circuitry is thus a generalized failure of relay K2 to transfer on command, either because the logic contacts are (intermittently) shorted together, or because the entire relay will not transfer. Furthermore, this failure is an intermittent type of failure, since the relay is required at times to stay in the 1 state, the 0 state, or to transfer normally. There are mechanisms that permit this type of behavior, such as a particulate contaminant in the relay operating mechanism, and this is the most likely type of failure.

The final tracker CAP update before the planetary encounter (the update to position C5 on *Mariner VII*), was accomplished on May 29, by the transmission of a DC-17 command to the spacecraft at 23:30:00. The step was uneventful in every respect. This update was accomplished early to free the memory space containing the C1 command in the CC&S for another use not related to the attitude control subsystem.

After the encounter, when the official *Mariner* Mars 1969 mission was over, periodic updates of the CAP were loaded into the CC&S memory on each spacecraft, since it was necessary to change the CAP with the seasonal variation of the Canopus cone angle. The *Mariner VII* memory was loaded on October 20, 1969 with a program that issued seven C1 commands at appropriate times through December 1970; a similar loading of the *Mariner VI* CC&S memory on October 31 created a C1 program that would issue seven C1 commands through January 10, 1971. The first of these commands was due on November 3, 1969 on *Mariner VII*. That command, and its consequences, are discussed separately in Subsection 2-e of this section. The *Mariner VI* commands, and their consequences, are listed in Table 11.

The first postencounter C1 update command was due at 01:42:30 on November 12, 1969. Since good telemetry could only be received by DSS 14 because of the spacecraft range from the Earth, the spacecraft was prepared for any eventuality when the C1 command occurred by the fact that it had been placed in the roll inertial control mode. A DC-18 command was transmitted from DSS 62 without verification of command system lockup at 18:35:00 on November 11. This command was followed by: (1) a DC-42 command to transfer the spacecraft radio transmitter to the high-gain antenna, and (2) five DC-21 commands to step the spacecraft 11.3 deg in clock angle to point the high-gain antenna at the Earth in clock angle. The C1 command was observed at 01:43:41 on November 12, and the next CAP telemetry reading indicated that the CAP had once again failed

to step properly. This time it stepped to position C2 instead of position C4. The flight telemetry subsystem was in the 8½-bits/s data rate, and therefore a DC-5 command was transmitted to switch to the 33½-bits/s rate to aid in the evaluation of the cone angle position telemetry. (A reading occurs every 28 min at 8½ bits/s, every 7 min at 33½ bits/s; with the round trip light time of approximately 40 min, not enough time was available in the tracking pass to cover all eventualities.) The DC-5 command was transmitted at 02:10:00, followed by two DC-17 commands at 02:18:00 and 02:20:00. The 2-min spacing of the DC-17 commands was a mistake, because when the first command was received, no change was noticed in the intensity telemetry or the roll error signal telemetry, and the second DC-17 command was received before a sample of the cone angle position telemetry occurred. Upon receipt of the second DC-17 command, the CAP stepped from whatever position it was in to position C3. It is apparent that the first DC-17 command was simply not received by the tracker, and, unfortunately, space was not left between the commands for further confirmation of the fact. A third DC-17 command was transmitted at 03:00:00, and the CAP stepped to the desired C4 position. It was decided that no further diagnostic work would be performed at that time. Canopus was reacquired when the spacecraft was stepped 20 deg cw with eight DC-18 commands, followed by a DC-19 command to return to optical control. Canopus was reacquired without incident, and the gyros went off at 04:44:15.

The last cone angle update (January 8, 1970) was accomplished in the same manner as that described for the first postencounter update. The spacecraft was placed in the DC-18 roll inertial control mode, and the cone angle position was updated with a DC-17 command. The use of the DC-17 command for updating was occasioned by the observation that every C1 command except the first had resulted in an anomalous stepping; in addition, the C1 command was not due until January 21, and it was desired that the CAP be updated early to allow time for resolving any problems that arose. This update was in the ascending order and, therefore, required three commands. When the first DC-17 command was transmitted, the CAP stepped to position C3. Since this was the desired CAP, no further commands were sent at this time, except for the DC-19 command that returned the spacecraft roll axis to optical control.

*f. Mariner VII pre-encounter anomaly.* The following paragraphs concern the effect of the *Mariner VII* pre-encounter anomaly on the attitude control subsystem.

When the spacecraft signal was first recovered, Canopus acquisition had been lost, and the 30-s roll inhibit logic had apparently been set because the Canopus star tracker was outputting the roll search voltage to the roll channel and the gyros were on, but the pitch and yaw limit cycles did not exhibit the behavior characteristic of a roll search.

The extent of the failure in the attitude control area of interest was the loss of all gyro telemetry, fine Sun sensor telemetry and tracker intensity response, adaptive gate setting, and cone angle position telemetry. In addition, most of the power subsystem telemetry that is helpful in analyzing the state and performance of the attitude control subsystem was lost. The only direct telemetry of attitude control subsystem functions that remained were the coarse Sun sensor telemetry channels, the tracker roll error signal, and reaction control assembly temperature and  $N_2$  pressure telemetry channels.

The next command sent was a DC-21 command, to attempt to reacquire Canopus. The only objects acquirable at that time in position C5, according to SIPM, were the planet Jupiter, at a clock angle of 91.2 deg, and Canopus. With no telemetry of the CAP, the first assumption was that no change had occurred to the cone angle position; with no telemetry of the intensity response, there was no immediate method of determining what object was acquired. The plan was, therefore, to: (1) acquire an object, (2) transmit a DC-21 command to start a new roll search, and (3) measure the time to acquire the next object. If that time corresponded to a 270-deg roll search at a search rate of approximately 4.0–4.3 mrad/s, then it would be assumed that the object acquired was Canopus, and the command to transfer back to the high-gain antenna would be sent. Reception of telemetry from the high-gain antenna would verify the acquisition of Canopus. If, however, the time to acquisition corresponded to the time required for a 90-deg search, then it would be assumed that the object acquired was Jupiter, and the DC-21 command would be sent to reacquire Canopus. If neither of these conditions were met, then it would be assumed that either the adaptive gate or the cone angle position had stepped, and an alternate plan would be worked out. In any event, a SIPM was available for any cone angle position, and the gate setting was included in the SIPM, so that a unique identification of CAP and adaptive gate setting could be determined from the roll search time between acquirable objects.

The first DC-21 command was sent at 09:45:00, and it resulted in a roll search, which confirmed the theory

that the 30-s roll search inhibit logic had been set. The search terminated after a calculated search angle of 71.2 deg. The second DC-21 command was transmitted to the spacecraft at 10:17:00, and the second roll search was terminated at 10:34:33, which indicated that an angle of 94.5 deg was searched through. Obviously, the second object acquired was Jupiter (which implied that the first object was Canopus), and so a third DC-21 command was sent at 10:40:00. This third roll search lasted until an acquisition occurred at 11:07:56, after an apparent roll search angle of 246.1 deg. At the time the third object was acquired, however, it was not apparent that the last search was approximately 34 deg short of Canopus. With the combination of circumstances that only two acquirable objects were listed in SIPM, and that there was no intensity telemetry, and finally that this spacecraft clock angle had already been searched through on the first search, it was concluded that this acquisition was Canopus, and the command to transfer to the high-gain antenna was sent at 11:20:00. The command was received at 11:31:19.38, and the spacecraft radio signal carrier was lost. At 11:35:11.24, one good line of data was restored, and the end of a roll search was indicated as the spacecraft acquired Canopus and the gyros went off.

The third, anomalous acquisition was unusual not only for the combination of circumstances noted previously, but also because some variation can still be noted as a function of object intensity, although the tracker intensity response channel is one of the telemetry channels affected by the pre-encounter anomaly. Every tenth line, during a 208/218/228 subcommutation frame, appears to have some proportion to the expected reading. Thus, during the roll searches to Canopus, Jupiter, and the final roll search, the telemetry channel reads one value when the expected reading is "dark," and it reads a slightly lower value when acquired on Canopus or Jupiter. For the third acquisition (of an object apparently at a clock angle of 337 deg), which had not been acquirable or had not been in the tracker field of view 1 h earlier, the intensity channel response was significantly different from that for the Canopus and Jupiter acquisitions. The reading at the initial acquisition was lower than that for the other acquisitions, which indicated that a brighter object was acquired. This reading subsequently increased in value, indicating that the brightness of the acquired object was decreasing. At the time the command to transfer to the high-gain antenna was received, the intensity reading was dimmer than that of either Canopus or Jupiter. It therefore seems likely that the object that was acquired at a clock angle of 337 deg was initially very

bright (but not greater than  $4\times$  Canopus, or a high-gate violation would have occurred). It then decreased in brightness to less than  $1\times$  Canopus, and probably to the point where a low-gate violation occurred, which initiated an automatic roll search, followed by the acquisition of Canopus. The source or nature of the acquired object is not understood. There is definitely no known celestial object at that time and place, not even one bright enough to be acquirable by the tracker. It is believed that this object is in some manner associated with the pre-encounter anomaly, but the nature of the association is not clear.

Further analysis of the available data indicated that the original loss of signal was due to a loss of Canopus acquisition; the decrease in signal strength corresponds to that expected if a roll search had been commanded. However, the roll search apparently ended after approximately 60 s of search. The cause of the roll search, and of the flight telemetry subsystem failure and the spacecraft power transients, is not evident. The best hypothesis at this time seems to be that the spacecraft battery essentially exploded, and that the outgassing of the electrolyte caused an arc in the tracker 700-V power supply, which in turn induced the flight telemetry subsystem failure and the various transients, as well as the loss of acquisition. In any event, the state of the spacecraft was that approximately 30% of the telemetry was unusable. There seemed to be no other permanent effects, and the only other apparent temporary effect was the stepping of the scan control subsystem reference potentiometers.

*g. Mariners VI and VII planetary encounters.* The *Mariner VI* encounter started on July 29, 1969 with the issuance of CC&S command M1 to turn on the gyros at 00:32:41 ( $E - 52$  h 46 min). The far-encounter phase of the mission was uneventful with respect to the attitude control subsystem, and at 03:32:51 on July 31 ( $E - 1$  h 46 min), the CC&S issued command M2, which placed the spacecraft in the all-axis inertial control mode. The IRS cooldown was enabled with one DC-26 command and two DC-36 commands. Command DC-49, to initiate the IRS cooldown, was transmitted at 04:35:41, with a backup DC-49 command at 04:39:41. At 04:47:16, IRS motor start was observed in the data, but no significant effect was noted in the attitude control subsystem. The magnitude and direction of torques expected from the  $N_2$  and  $H_2$  exhaust had been the subject of an extensive analysis, in a manner similar to the scan unlatch analysis. The effects predicted for the cooldown were a force in the  $z$ -direction and torques about the  $x$ - and  $y$ -axes. The nature of the torques depended

on the position of the scan platform, since the exhaust tube was attached to the platform and the impingement of the exhaust on the spacecraft was the major contributor to any disturbance to the attitude of the spacecraft that might result. Figures 45 and 46 show the magnitude of the forces and torques expected as a position of platform clock angle and the clock angles associated with the platform positions during the encounter. Figure 45 reflects data for a platform cone angle of 129 deg, and Fig. 46 reflects data for the fixed platform cone angle position of 101 deg. Analysis of the attitude control subsystem performance with a large applied torque resulted in Fig. 47, which shows the position error as a function of the applied torque.

For the *Mariner VI* spacecraft, the resolution of the limit cycle telemetry in the all-axis inertial mode was too coarse in both magnitude and time to provide either confirmation of the predictions or absolute torque levels. However, the initial reaction to the IRS cooldown was not nearly of the level predicted, and the science subsystem analysis reported that the IRS was not cooling down normally. Additionally, the torques exerted on the spacecraft lasted over a much longer period of time than expected, leading to the assumption that the  $N_2$  gas did not exhaust as planned, but exhausted at a smaller rate over a longer period of time. Table 12 compares the torques measured on the spacecraft as a function of time after the command to initiate IRS cooldown was received.

The *Mariner VI* encounter inertial mode of operation was terminated when the CC&S issued command  $\overline{M1}$ , at 09:32:52 ( $E + 4$  h 19 min 49 s). The observed disturbance in the roll axis when the IRS cooldown was commanded was not enough of a transient to cause a roll search, as had been feared. Only one sample of a brightness transient was observed in the tracker intensity response channel, and for the *Mariner VI* encounter, the insurance of the all-axis inertial mode was not required.

The *Mariner VII* encounter began in the same manner for the attitude control subsystem, with the issuance of CC&S command M1 at 01:21:44 on August 3, 1969. Previously, the first 34 pictures of the far-encounter sequence had been taken and were being played back. As with *Mariner VI*, the gyros were being turned on at  $E - 51$  h 39 min to allow the spacecraft bus to thermally stabilize for the occultation experiment. Since the computer maneuver commands could not be used for an inertial-at-encounter sequence, the plan was to send a DC-13 command at approximately  $E - 3$  h. This command would disable CC&S control of the attitude control

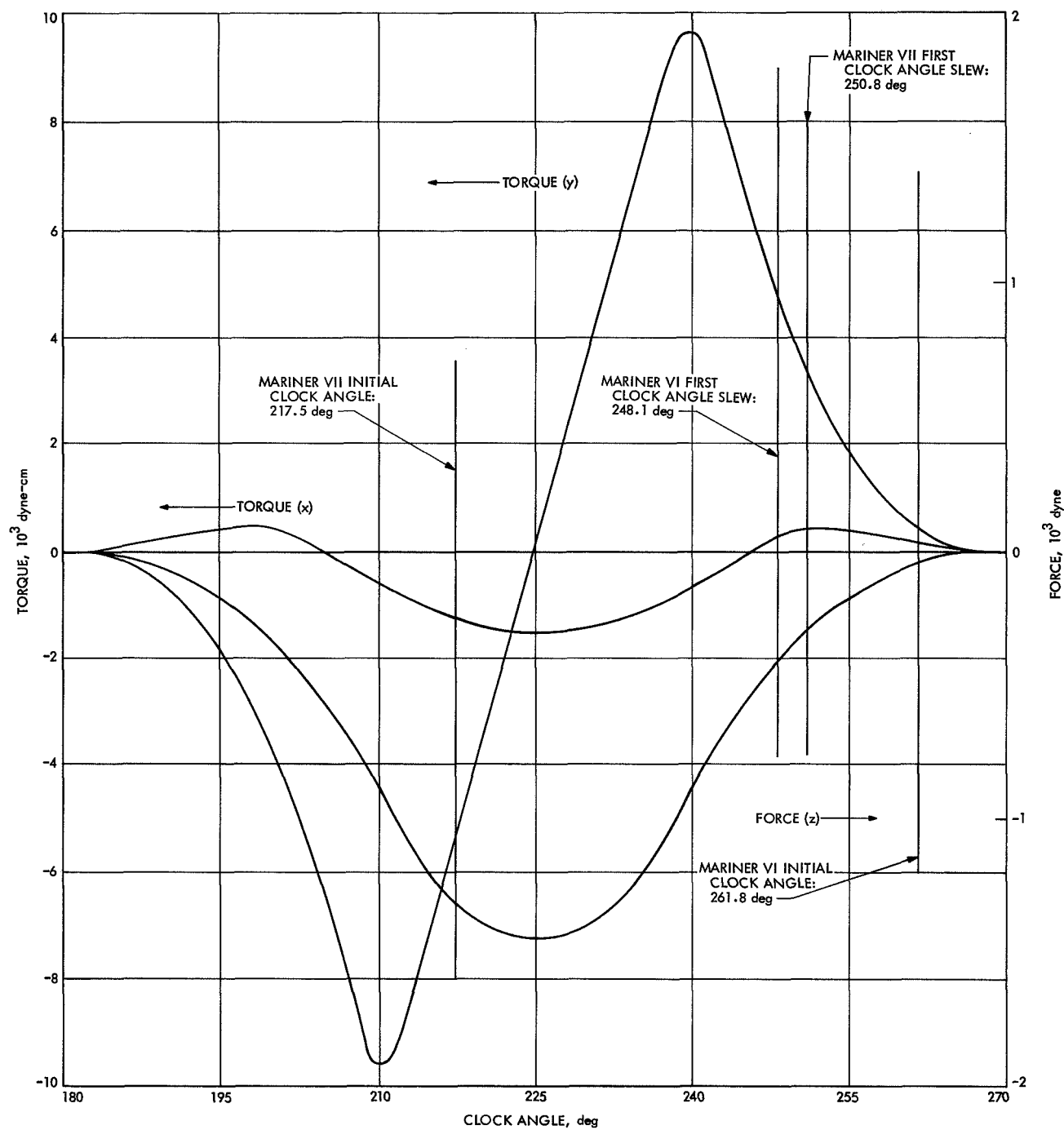


**Fig. 45. Mariner Mars 1969 IRS exhaust system impingement forces and torques for a scan platform cone angle position of 129 deg**

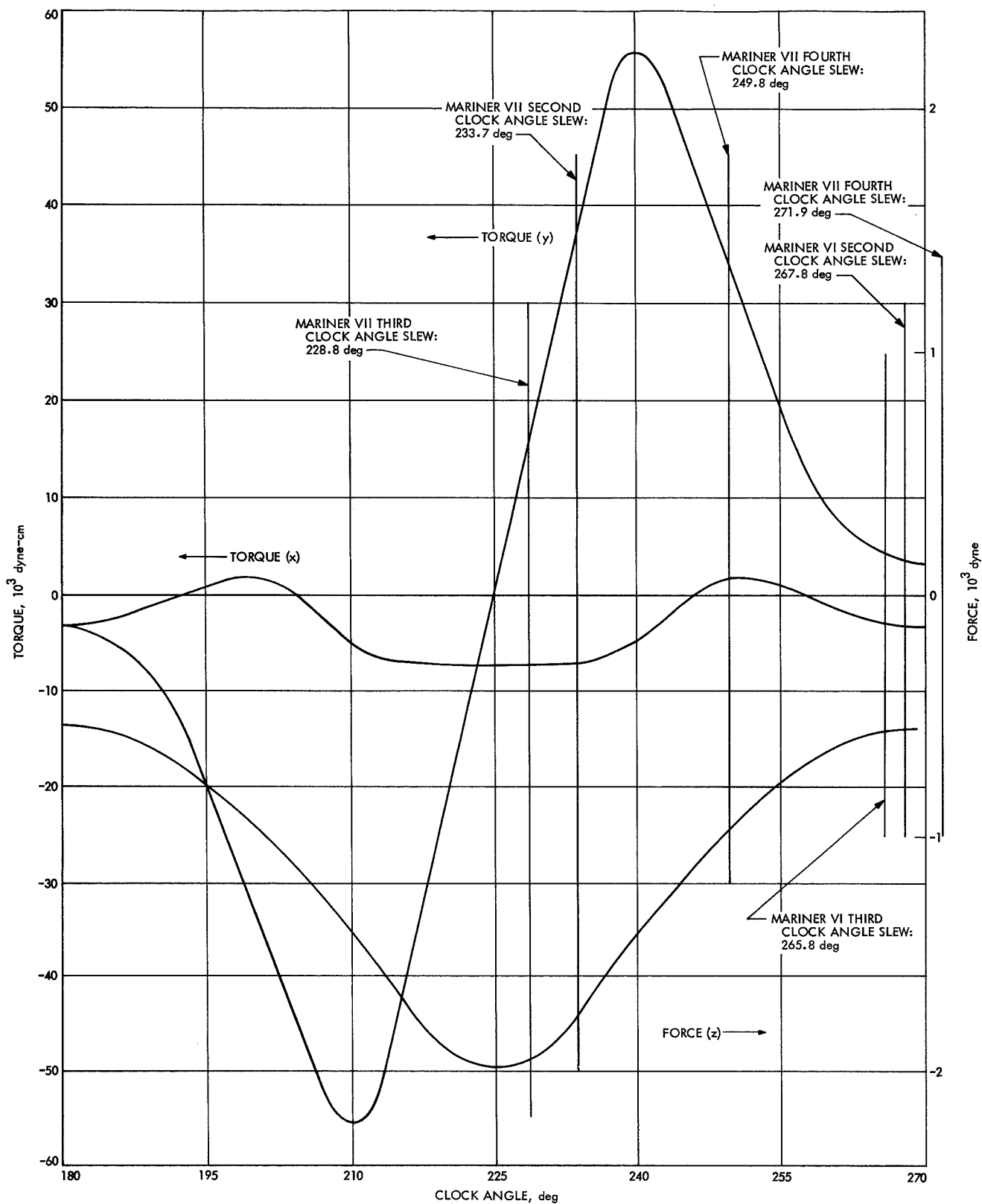


**Fig. 46. Mariner Mars 1969 IRS exhaust system impingement forces and torques for a scan platform cone angle position of 101 deg**

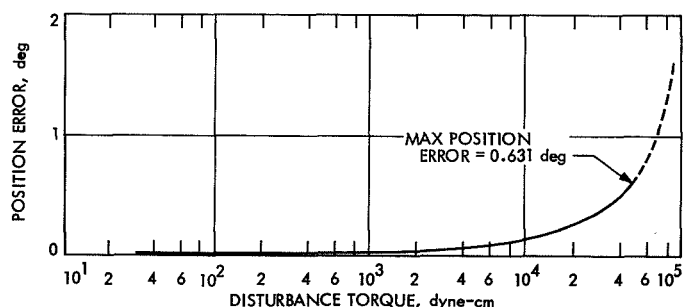


**Fig. 47. Maximum position error  $\theta_{\max}$  due to derived rate hangoff**

subsystem, and reset the M1 command, which would allow the gyros to turn off. A DC-18 command would then be sent to turn the gyros on in the roll axis inertial control mode, and the encounter would be accomplished in that mode. After the encounter, a DC-19 command would restore optical control of the roll axis. The reason for using the DC-13 command to turn off the gyros, and for turning off the gyros at all, was that that command sequence was the simplest available; the gyros were to be turned off before the DC-18 command was transmitted to avoid the 2.25-deg step that would occur if the DC-18 command were sent with the gyros on. If the DC-18 command were sent with the gyros on, a DC-21 command could be sent subsequently to step the spacecraft back by 2.25 deg, but there were two disadvantages to the DC-18/DC-21 command sequence. As demonstrated on July 26, the DC-21 command enables the

hard bias to the tracker and effectively removes the roll channel position telemetry; additionally, there would be no way to verify that the DC-21 command had been received and correctly interpreted by the spacecraft, since the gyro telemetry channels had been rendered useless by the pre-encounter anomaly. Further, the loss of the roll channel position telemetry was undesirable for several reasons. It was the only telemetry channel with information on spacecraft roll position, since the gyro channel was useless. It was the only channel that could provide information on the IRS cooldown effect on the spacecraft roll axis. No correction to the scan platform clock angle as a function of position in the limit cycle could be made without roll position telemetry. The only advantage of the DC-18/DC-21 command sequence was that the gyros did not have to be turned off and then turned back on; thus, power transients were avoided during a time of peak spacecraft power draw. This advantage was more apparent than real, however, since the gyros had already been turned on from a cold start with the M1 command.

The final plan adopted by the project was to use the DC-18/DC-21 command sequence, and at 01:49:00 on August 5, 1969, the DC-18 command was transmitted to the spacecraft; it was followed by the DC-21 command at 01:53:00, and the DC-13 command at 02:09:00. As expected, the roll position telemetry was driven to saturation when the DC-18 command was received, and it was not possible to verify the reaction of the subsystem to the DC-21 command. The DC-49 commands to start

**Table 12. External torques observed as a function of time after IRS cooldown**

Time after IRS cooldown	Mariner VI external torques			Mariner VII external torques		
	Pitch, dyne-cm	Yaw, dyne-cm	Roll, dyne-cm	Pitch, dyne-cm	Yaw, dyne-cm	Roll, dyne-cm
—1 h	—23 ±7	0	—30 ±4	—22	33	0
5 min	—1320	620	—716	20,500	3,200	—
10 min	—280	440	—470	—4,000	—460	—
15 min	—460	—	—335	—1,600	—12,000	—
20 min	—	—	—	—4,000	—21,000	—
25 min	—	—	—	—14,000	—21,000	—
35 min	—	—	—	—540 ±110	—290 ±150	—
45 min	—	—	—	—75,000	—210 ±180	—
50 min	—	—	—	—27,000	80 ±50	—
1 h	—	—	—	—230	50 ±25	—
2 h	—	—	—	—110 ±10	15,000	—
3 h	—	—	—	—10	2800 ±930	—
4 h	—	—	—	0	1,050 ±130	520 ±85

Table (12 (contd))

Time after IRS cooldown	Mariner VI external torques			Mariner VII external torques		
	Pitch, dyne-cm	Yaw, dyne-cm	Roll, dyne-cm	Pitch, dyne-cm	Yaw, dyne-cm	Roll, dyne-cm
5 h	$-120 \pm 20$	$92 \pm 6$	—	$7 \pm 1$	$1,150 \pm 270$	$420 \pm 42$
6 h	—	—	—	$16 \pm 3$	$640 \pm 80$	$260 \pm 20$
7 h	—	—	$-52 \pm 1$	—	$450 \pm 35$	$330 \pm 85$
9 h	—	—	—	—	$340 \pm 100$	$200 \pm 40$
10 h	$-123 \pm 8$	$61 \pm 6$	—	—	—	—
12 h	—	—	$-40 \pm 10$	$6 \pm 1$	$190 \pm 60$	$70 \pm 4$
14 h	$-125 \pm 22$	$77 \pm 3$	—	—	$170 \pm 55$	$50 \pm 10$
15 h	—	—	—	—	$100 \pm 15$	—
16 h	—	—	—	$6 \pm 1$	—	$40 \pm 5$
18 h	—	—	$-41 \pm 5$	$6 \pm 1$	$90 \pm 23$	—
19 h	$-131 \pm 13$	$90 \pm 13$	$-34$	—	—	—
23 h	$-155 \pm 17$	$92 \pm 6$	$-41 \pm 4$	—	—	—
29 h	$-178 \pm 21$	$100 \pm 5$	$-43 \pm 3$	—	—	—
35 h	$-95 \pm 2$	$49 \pm 4$	$-57 \pm 14$	—	—	—
42 h <sup>a</sup>	$-117 \pm 7$	$51 \pm 15$	$-26 \pm 11$	—	—	—
48 h	$-157 \pm 8$	$100 \pm 11$	$-50 \pm 10$	—	—	—
54 h	$-146 \pm 11$	$88 \pm 9$	$-43 \pm 3$	—	—	—
64 h	$-72 \pm 5$	$35 \pm 5$	$-32 \pm 1$	—	—	—
74 h	$-35 \pm 9$	5	$-46 \pm 4$	—	—	—
80 h	$-31 \pm 4$	0	$-31$	—	—	—

<sup>a</sup>After this time, the *Mariner VII* torques returned to cruise values that were different from the pre-encounter values only in pitch.

the IRS cooldown were transmitted at 04:08:40 and 04:12:40; IRS motor start was observed in the data at 04:20:39, and the reaction of the attitude control subsystem to the IRS cooldown cycle was immediate and apparent. Table 12 lists the torques apparent on *Mariner VII* as a function of time after the IRS cooldown. Comparison of the values and length of persistence of the torques on the two spacecraft illustrates the anomalous cooldown of the *Mariner VI* IRS gas system. Two DC-18 commands were transmitted to the spacecraft at 07:40:00 and 07:42:00, well after the encounter, to permit the tracker to acquire Canopus before the return to optical control. The DC-19 command, to return to optical control, was transmitted at 07:57:00; reacquisition was immediate and the gyros went off at 08:12:00; this event ended the *Mariner VII* encounter.

**2. Postencounter exercises involving the attitude control subsystem.** A number of postencounter exercises were performed with the two spacecraft for scientific observations and experiments.

*a. Mariner VI ultraviolet spectrometer subsystem scan of southern celestial hemisphere.* The first postencounter exercise on *Mariner VI* started on August 11 and ended on August 12, 1969. This exercise involved mapping of the southern celestial hemisphere with the ultraviolet spectrometer subsystem (UVS); it was controlled by the CC&S and was accomplished automatically. An initial maneuver turn sequence was required, since the region to be mapped was not in the cone and clock angle range of the scan platform. A maneuver turn sequence provided the opportunity to optimize the high-gain antenna pointing angle with respect to the Earth, and allowed the exercise to be conducted with the 16.2-kbits/s data rate, which eliminated the need to record the data and later play it back.

A turn sequence, which started with an M2, M4, and M4 series of commands, placed the spacecraft in the all-axis inertial control mode, and the first turn was a +126.19-deg roll turn (726 s) was required to place the spacecraft in the all-axis inertial mode. The following



turn was a  $-81.32$ -deg pitch turn (456 s), and the final turn was a  $+34.06$ -deg roll turn (196 s). After the scan platform slewing events, the unwinding of the turns was started by a  $-34.18$ -deg unwind (197 s), followed by the  $+81.32$ -deg pitch unwind (457 s), and the final  $-123.19$ -deg roll unwind (714 s). The reacquisition of the Sun was immediate, the roll search to Canopus lasted for 3.64 deg, and when the gyros went off, the attitude control portion of the exercise was ended.

*b. Mariner VI ultraviolet spectrometer subsystem scan of northern celestial hemisphere and temperature control flux monitor calibration.* The second and third postencounter exercises on *Mariner VI* were similar to the first; the northern celestial hemisphere and selected portions of the Milky Way were mapped by the UVS over a two-day period. In addition, the spacecraft was pitched 90 deg off the Sun line for a temperature control flux monitor (TCFM) calibration, and a slew across the Milky Way by the scan platform was performed for the infrared radiometer. The maneuver turn sequence that pitched the spacecraft off the Sun line for the TCFM calibration and the third part of the UVS exercise occurred on August 13–14, 1969.

*c. Mariners VI and VII TV threshold exercise.* The fourth postencounter exercise on *Mariner VI* and the first on *Mariner VII* were attempts to establish the threshold of the narrow-angle TV camera by taking pictures of three stars with visual magnitudes of approximately 0, +1, and +2 in the two extreme gain states of the TV subsystem. The attitude control subsystem was involved in this exercise only to the extent of reorienting the spacecraft so that 16.2-kbits/s playback of the recorded TV pictures with the high-gain antenna could be accomplished. The reorientation took the form of a pitch-roll maneuver turn sequence on *Mariner VI* and a roll-only turn on *Mariner VII*.

On September 9, 1969, after 2 h of gyro warm-up, the *Mariner VI* CC&S commanded a  $-1.43$ -deg pitch turn, followed by a  $-3.65$ -deg roll turn. The spacecraft stayed at this attitude until playback was complete, and the turns were then unwound. Two DC-18 commands then stepped the spacecraft  $+4.5$  deg in roll to allow the Canopus star tracker to reacquire Canopus without a complete roll search, and a DC-19 command returned the spacecraft to optical control. Two days later, on September 11, *Mariner VII* was rolled  $-4.5$  deg with a DC-18/DC-21 command sequence. After the playback was completed on *Mariner VII*, the spacecraft was rolled  $+9.0$  deg with four DC-18 commands and then it was

returned to optical control with a DC-19 command. Both sequences on both spacecraft were uneventful and routinely successful.

*d. Mariner VI scan of comet 69B by ultraviolet spectrometer subsystem.* Postencounter tests of the radio frequency subsystem (RFS) on both spacecraft involved turning on the gyros in the DC-18 mode for some time on both spacecraft (18 h 50 min on September 16 and 17 for *Mariner VII*; 54 h 10 min on October 1–4 for *Mariner VI*). The next major postencounter exercise on the spacecraft was a scan of the comet 69B by the *Mariner VI* UVS. The familiar roll-pitch-roll turn sequence was used to orient the spacecraft so that the high-gain antenna was pointing at the Earth and the area of the celestial sphere to be viewed was within the cone and clock angle limits of the scan platform. The turns were, in order,  $+37.19$  deg roll,  $-16.75$  deg pitch, and  $-25.72$  deg roll. Reacquisition of the Sun and Canopus was accomplished in the automatic mode, without unwinding of the turns. The turn sequence and reacquisition were again accomplished without incident.

*e. Mariner VII power chain switchover.* The first of the postencounter Canopus star tracker cone angle position updates was due on *Mariner VII* at 21:30:00, November 3, 1969. Previously, the CC&S memory on both spacecraft had been loaded with a program that issued C1 CAP updates at appropriate times. The *Mariner VII* CC&S issued the C1 command at 21:33:41, and the following events happened: the gyros came on and the spacecraft went into a roll search, the redundant elements of the power subsystem were switched in, and transients were seen by most spacecraft subsystems. What had apparently happened was that the CC&S C1 command had caused the Canopus star tracker to update the CAP from position C5 to some position other than the desired C4 position because of some failure in the CAP updating circuit. Since Canopus was not visible in any other position than C5 or C4, the tracker lost Canopus acquisition, performed a fly-back and sweep, and when no reacquisition occurred, initiated the roll search by turning on the gyros. The gyro turn-on transient apparently caused the power subsystem to go into the battery-share mode, but since the battery on *Mariner VII* was not capable of supporting any spacecraft load, the solar array attempted to supply the required current at some low voltage level that caused the failure sensor in the power subsystem to switch to the redundant power chain when the booster regulator went out of regulation. Apparently, by this time, the transient effect had vanished and the operation

of the power subsystem returned to nominal conditions, but on the standby chain. With the spacecraft in roll search, a DC-18 command was sent at 22:51:00 to place the roll axis in inertial hold. The spacecraft had completed at least two roll searches without acquiring anything, which indicated that if the Canopus star tracker was still working, it was in CAP C1, C2, or C3, since the star was acquirable in positions C4 and C5. Since no telemetry of either the roll search rate or the tracker intensity response was available, the roll position of the spacecraft was not known, and it was decided to search for the high-gain antenna pattern with the DC-18/DC-21, 2.25-deg step commands. Accordingly, after the DC-18 command was received by the spacecraft, a DC-11 command followed by five DC-21 commands were transmitted to the spacecraft. When the DC-11 command was received, the data continued to be received, which indicated that the spacecraft was within the limited range of the high-gain antenna beamwidth. A series of DC-18 and DC-21 commands established the roll position of the spacecraft with respect to the high-gain antenna.

Analysis of the spacecraft operating parameters failed to reveal the reason that the gyros on transient caused the power subsystem to go into the battery-share mode. There was apparently enough power margin supplied by the solar array to provide for the transient according to the telemetered spacecraft data, unless either the data were incorrect or the transient power-on characteristics of the gyro control assembly had changed significantly. In addition, the behavior of the tracker was not understood, and with no telemetry of the tracker intensity response of CAP, further analysis was not practical. It was, therefore, decided to turn the tracker off with a DC-20 command and leave the gyros on in the roll axis inertial mode to prevent any further gyros on transient from affecting the spacecraft adversely. The DC-20 command was sent at 18:10:00 on November 6, 1969, and, at 18:38:05, the roll position error channel and the power telemetry verified that the tracker had been turned off. Spacecraft roll position control was then being provided by the roll inertial control mode of operation; the roll gyro drift rate was approximately  $-0.02$  deg/h, which required one DC-18, 2.25-deg step as an update approximately every 5 days. These updates were sent periodically for the remainder of the tracking time.

**3. Flight performance of attitude control subsystem hardware.** Where measurable in flight, the flight performance of the hardware units comprising the attitude control subsystem is summarized in the following para-

graphs. Other parameters of interest are included, where applicable.

*a. Attitude control electronics.* The sizes of deadbands are established by a number of factors; however, it is appropriate to include them in this section of the report. Table 13 lists the parameters (the inertial values are calculated, since the accuracy of the inflight measurement is limited to approximately 2 mrad).

**Table 13. Deadband sizes for *Mariners VI* and *VII***

Deadband	Deadband size	
	<i>Mariner VI</i>	<i>Mariner VII</i>
Position, mrad		
Pitch	3.85, -3.71	3.91, -3.67
Yaw	3.66, -3.79	4.14, -3.89
Roll	4.79, -4.56	4.63, -5.31
Rate, mrad/s		
Pitch	0.60, -0.59	0.62, -0.61
Yaw	0.60, -0.59	0.59, -0.57
Roll	0.32, -0.32	0.33, -0.32
Inertial, mrad		
Pitch	3.14, -3.12	3.40, -3.00
Yaw	3.30, -3.20	3.10, -3.00
Roll	1.76, -1.76	1.76, -1.69

It should be noted that the derived rate networks were optimized for recovery from disturbance torques for the *Mariner* Mars 1969 design, instead of for minimization of noise effects on the switching amplifier. As a consequence, the "normal" characteristic of a valve firing only once at the edge of the deadband was modified to a "normal" one to two firings at the edge of the deadband. The derived rate characteristics are listed below:

Derived rates	Pitch and yaw	Roll
Charge time constant, s	9.9	10.6
Discharge time constant, s	19.8	21.2

*b. Gyro control assembly.* Total gyro running times, up to launch, through encounter, and as of 00:00:00 on January 1, 1970 are listed in Table 14.

**Table 14. Gyro running time for Mariners VI and VII**

Gyro control assembly	To launch, h	Through encounter, h	On Jan 1, 1970, h
Mariner VI	647.4	1033.6	1151.3
Mariner VII	603.2	691.8	1503.6

In addition, individual gyro running times should be added to these totals to obtain the total running time for each gyro, since the preassembly test times differ somewhat. The preassembly test times are listed in Table 15.

**Table 15. Running time for individual gyros**

Gyro	Running time, h	
	Mariner VI	Mariner VII
Pitch	750	605
Yaw	790	1075
Roll	930	910

c. *Reaction control assembly.* The gas weights at launch, through encounter, and at January 1, 1970 are listed in Table 16.

**Table 16. Gas weights for Mariners VI and VII**

Reaction control assembly	N <sub>2</sub> gas weight, lb		
	At launch	Through encounter	On Jan 1, 1970
Mariner VI			
+x, +y	2.86	2.30	1.64
-x, -y	2.87	2.41	1.77
Mariner VII			
+x, +y	2.79	2.53	2.08
-x, -y	2.75	2.44	1.90

The gas usage rates during cruise were those listed below:

Assembly	Mariner VI	Mariner VII
+x, +y	$4.22 \times 10^{-3}$ lb/day	$2.52 \times 10^{-3}$ lb/day
-x, -y	$3.58 \times 10^{-3}$ lb/day	$2.89 \times 10^{-3}$ lb/day

The several exercises on the spacecraft consumed an appreciable amount of the attitude control N<sub>2</sub> gas. Figures 48 and 49 are plots of the gas weight as a function of time, and illustrate the large gas usage for events, such as the planetary encounter.

4. *Conclusions.* The Mariner Mars 1969 attitude control subsystem was a direct descendent of the Mariner C subsystem used on Mariner IV; the only change of significance in the design of the subsystem was the redesign of the Canopus star tracker to incorporate logic functions that would permit automatic acquisition of Canopus and that would also compensate for significant changes in sensitivity or response of the image dissector. As such, the attitude control subsystem performed successfully, and the mission that was accomplished exceeded the minimum mission the subsystem was designed for by a substantial amount.

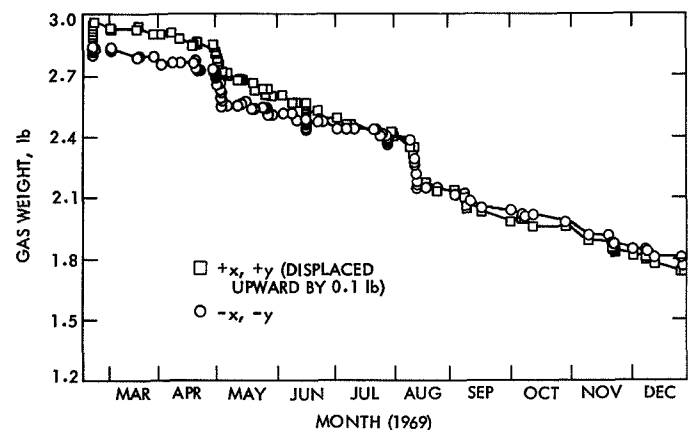


**Fig. 48. Mariner VI attitude control N<sub>2</sub> gas weight**

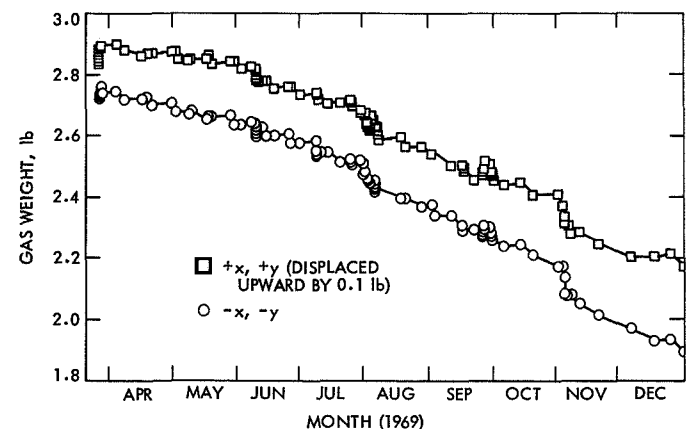


**Fig. 49. Mariner VII attitude control N<sub>2</sub> gas weight**

There were, however, certain areas wherein improvement in either design or fabrication would significantly improve spacecraft systems integration, operation, and reliability. The suggested improvements are as follows:

- (1) Several undesirable logic states of the attitude control subsystem were apparent before launch and some became apparent in flight. They should be eliminated through system or hardware design. These logic states are the following:
  - (a) There is no gyros-on event, and therefore no way to verify that Canopus acquisition was not lost and regained during a period when the spacecraft was not being tracked.
  - (b) The Sun gate event register indication is an AND function with CC&S M2.
  - (c) The DC-20 command turns off the Canopus star tracker and allows the gyros to turn off; this requires CC&S commands M1 or M2, or flight control subsystem (FCS) command DC-18 to turn the gyros back on for rate or position control of the roll axis.
  - (d) The DC-15 command allows the gyros to turn off without an acquisition signal from the tracker; this again requires CC&S commands M1 or M2, or FCS command DC-18 to turn them on for rate or position control of the roll axis.
  - (e) With CC&S command M2 (all-axis inertial control) or FCS command DC-18 (roll axis inertial control) commands in effect, the DC-21 command will enable the hard bias in the tracker, which causes the loss of any roll position telemetry from the tracker.
- (2) The cone angle position generator circuit in the Canopus star tracker is, in a circuit design sense, entirely adequate for its intended application. However, as evidenced by the failures and failure analyses, there appears to be a component problem in this circuit. (Adequate measures should be taken in component selection and procurement to eliminate future problems of the type postulated.)
- (3) The experience during the exercise involving the Large Magellanic cloud demonstrated the need for a bidirectional protection capability in the roll search inhibit logic. The opening of the roll position channel to the search voltage should exist whenever a continuous acceleration in either direction for more than 30 s is sensed.

- (4) Although the telemetry system is not designed for analysis of spacecraft performance, but rather for monitoring the state of the spacecraft and detecting gross deviations from expected performance, there is a continual demand for detailed analysis based on the telemetry data. The only improvement that can be made, given the current telemetry scheme, is to increase the data rate by data compression techniques and to increase the accuracy of the data by decreasing the resolution error. These techniques should be applied in the autopilot area as a minimum; the gyro and autopilot actuator telemetry should be switched to a mode during the midcourse maneuvers that greatly expands their resolution and increases the sample rate. Currently, there is no autopilot actuator telemetry for the *Mariner* Mars 1969 design; any change at all in that situation would improve the analysis capability.

### C. Scan Control Subsystem Performance

The scan control subsystem is a dual-channel, dual-mode servo control system that controls the two-axis pointing direction of the scan platform. The two modes are open-loop platform pointing and closed-loop planet tracking. A simplified block diagram of the subsystem is shown in Fig. 50. The subsystem is composed of the far-encounter planet sensor (FEPS), two scan control actuators, and the scan control electronics. The scan control electronics in turn is composed of three subassemblies: the mode control and logic, the power supply, and the servo amplifier and stepped motor subassemblies. Two narrow-angle Mars gates, although not functionally a part of the scan control subsystem, were designed, fabricated, and tested in conjunction with the subsystem.

**1. Calibration.** Ground calibration of the entire scan control subassembly before flight was intended to eliminate any necessity for an inflight calibration exercise. Although the scan actuator telemetry potentiometers were calibrated in the laboratory for each actuator individually and the reference potentiometers in the servo amplifier and stepper motor assembly were calibrated over their expected range of use, an end-to-end calibration was performed on each spacecraft before shipment to the AFETR. The calibration process was divided into two parts: measurement of the science instrument alignment with respect to the planetary platform mirror while the instruments were mounted on the spacecraft, and measurement of the scan control actuator (SCA) telemetry potentiometer readouts at various discrete positions of

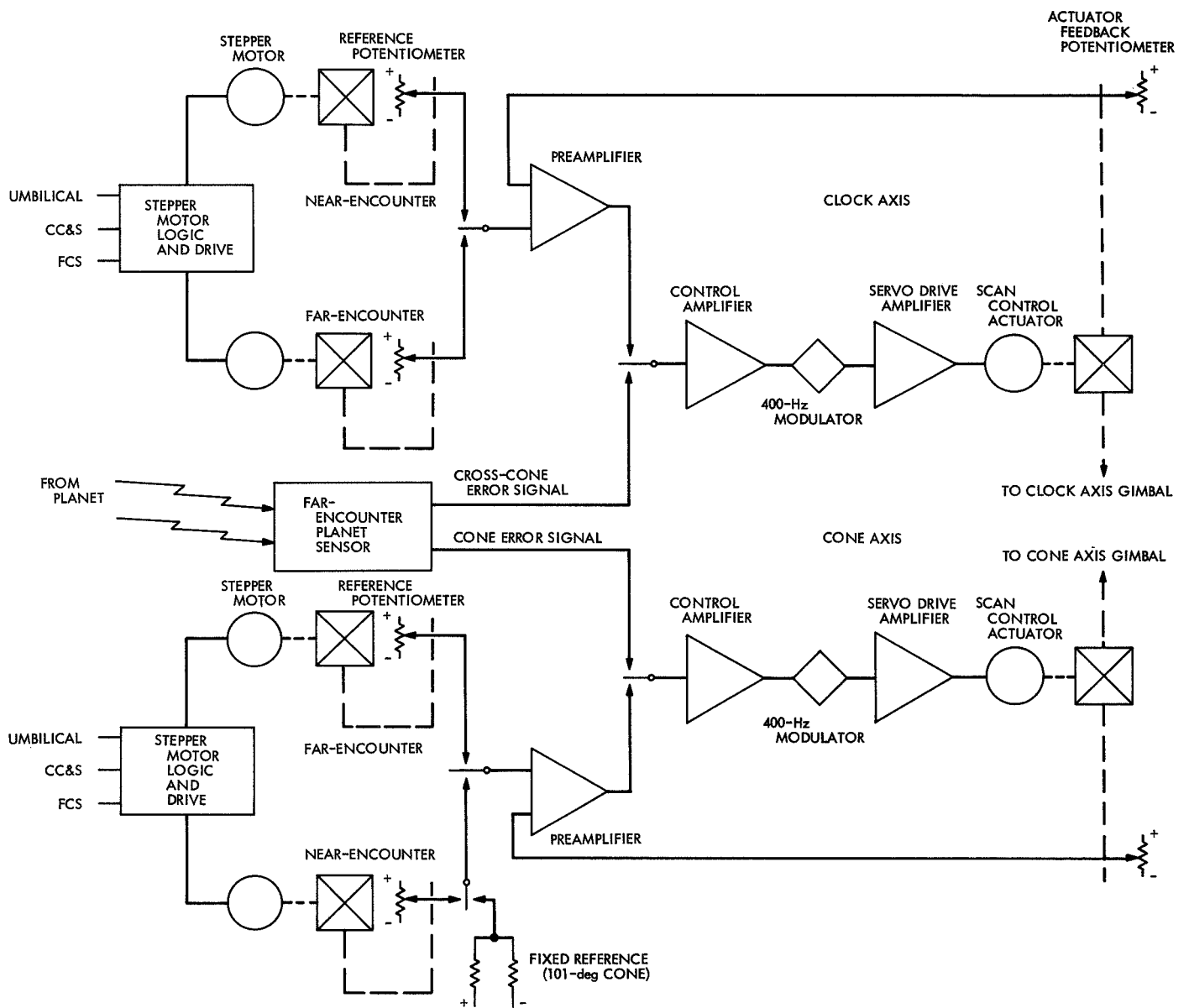


Fig. 50. Mariner Mars 1969 scan control subsystem block diagram

the scan platform. Certain supplementary tests, although not calibrations, showed that the FEPS would acquire a moving planet, the logic would switch from far-encounter reference potentiometer control to FEPS control, and that the entire scan control subsystem/platform combination would track a moving planet of various apparent angular diameters and brightnesses in a closed-loop fashion.

A basic problem in the system calibrations and tests was gravitational effects on the platform itself. The platform is a massive structure that weighs approximately 170 lb with all the instruments attached and 70 lb without the five science instruments. With the spacecraft level, the cone-axis SCA was unable to control the loaded platform, and, even with the platform unloaded, the distortion caused by platform weight was noticeable in the calibrations.

Other effects noticed were a "windup" in the platform journalled bearing that increased the apparent backlash

and the appearance of gear harmonic effects in the SCA telemetry potentiometer calibrations. Attempts were made to compensate for the bearing windup problem by: (1) applying an actuator torque in fixed direction at each point at which a calibration measurement was to be taken, and (2) reducing the raw data to a telemetry calibration curve that took into account the effects of gearing on the linearity of the actuator telemetry potentiometers. Figure 51 shows the telemetry block diagram. Because the rotation of the SCA output shaft is constrained to 218 deg by mechanical stops (the widest range of platform motion, in clock angle, is 215 deg), the coarse-position telemetry potentiometer is geared up by a factor of 1.6 to take maximum advantage of the 355-deg range of the potentiometer. The fine telemetry potentiometer provides a 50:1 resolution gain over the coarse potentiometer by virtue of its being geared up from the output shaft by 80:1. Thus, the platform position is determined to within  $\pm 0.017$  deg by the fine telemetry potentiometer in the ideal case.

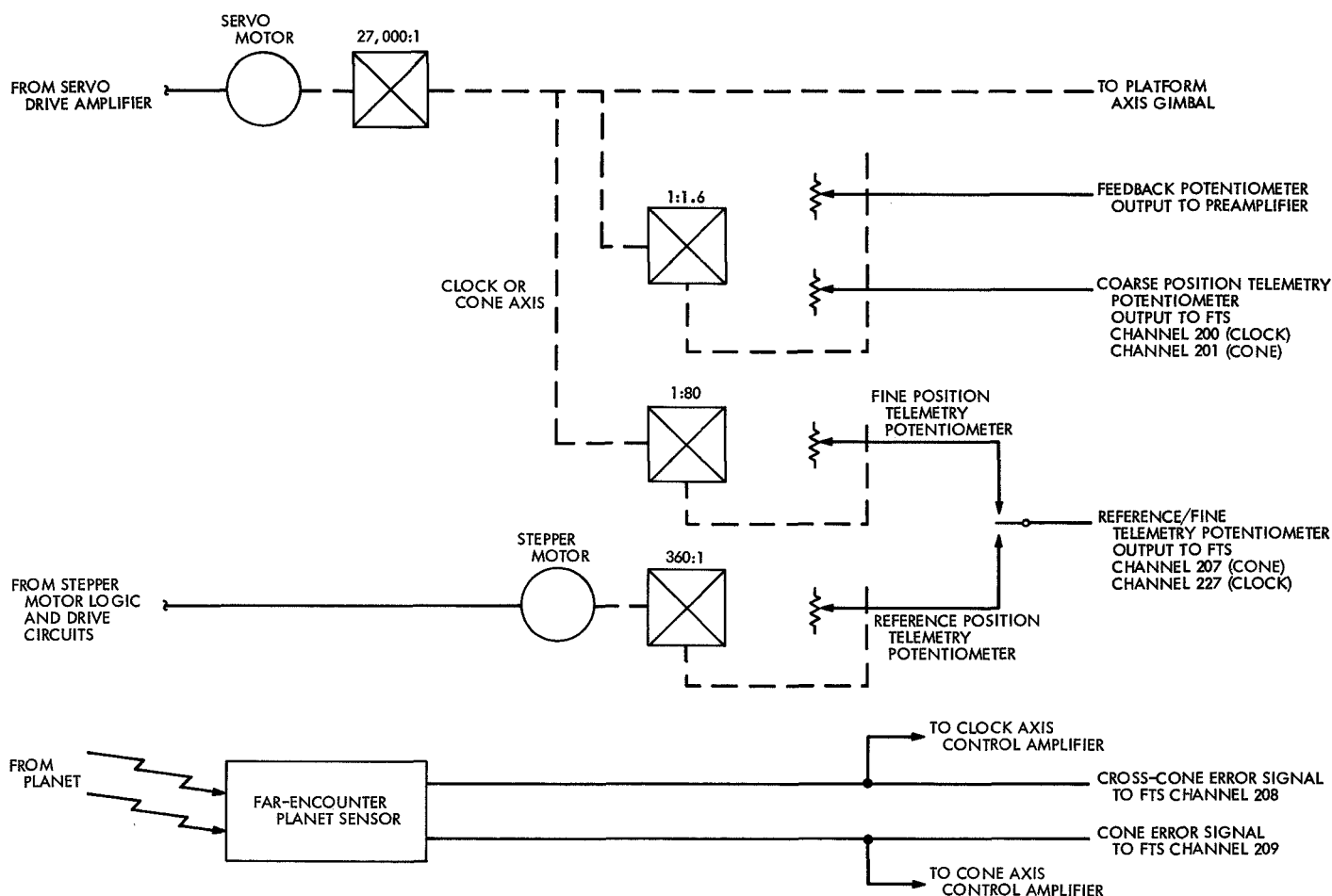


Fig. 51. Scan control subsystem telemetry block diagram

The final results of the calibration effort can be summarized for three types of scan platform pointing uncertainties as follows:

- (1) In the *a priori* platform pointing, far-encounter (planet-tracking) mode, the pointing uncertainty depends on the size of the planet, the illumination level of the planet at the FEPS, the FEPS scale factors and null offsets, and the scan control subsystem static response effects. Consequently, the pointing uncertainty varies with time in the mission. In general, the area in which the platform will point is an ellipse ranging from a major axis of 0.054 deg for a planet 1.1 deg in angular diameter to 0.82 deg for a 4-deg planet.
- (2) In the *a priori* platform pointing, near-encounter (open-loop) mode, the pointing uncertainty is a fixed quantity composed of the following error sources: (a) potentiometer calibration, 0.080 deg; (b) scan platform calibration, 0.123 deg; (c) scan control subsystem lag, 0.060 deg; and (d) attitude control limit cycles, 0.255 deg. The  $1\sigma$  total without the attitude control limit cycle effect is 0.16 deg, and the  $1\sigma$  total with the attitude control limit cycle effect is 0.30 deg.
- (3) The pointing uncertainty in given telemetry data depends on the accuracy of the sensor calibrations, with only the preflight calibrations. This uncertainty is composed of: (a) scan platform angle readout, 0.020 deg; (b) scan platform calibration, 0.123 deg; and (c) attitude control calibration, 0.051 deg. The  $1\sigma$  total rms error per axis is 0.134 deg.

## 2. Flight performance of the scan control subsystem.

The servo amplifier and SCA are not powered during the cruise portion of flight; however, the mode control and logic and the reference assembly portions of the subsystem are powered, so that updating of the stored near-encounter reference positions is possible. When the central computer and sequencer (CC&S) command N1 or command F1 (or flight control subsystem command DC-25 or command DC-28, which are, respectively, equivalent), is given, power is applied to the servo amplifier, and the SCA drives the scan platform to the position that the near- or far-encounter reference potentiometers dictate. If the command has been F1 (or DC-28), the far-encounter mode is selected by the scan logic, and the FEPS is also powered. When an object of sufficient brightness enters the FEPS field of view, control of the platform position is transferred to the FEPS.

Approximately three weeks in advance of launch, reference potentiometer settings were specified for any combination of the first 98 launch and arrival dates targeted and for each type of encounter (an equatorial or polar pass). If the launch and arrival dates and type of encounter are known, then the clock and cone angle of Mars at the initiation of the far-encounter and the near-encounter sequences may be specified. The reference potentiometers may then be updated on the pad, through the umbilical hardline connection, to the desired setting. For the near-encounter reference potentiometers, this setting is verified by the telemetry; the far-encounter setting is verified by reading the voltage ratio of a potentiometer ganged to the far-encounter reference potentiometer. Table 17 lists the launch settings of the two spacecraft.

**Table 17. Scan control subsystem reference potentiometer settings and updates during flight**

Reference potentiometer setting or update	Mariner VI			Mariner VII		
	Date (1969), GMT	Angle, deg		Date (1969), GMT	Angle, deg	
		Clock	Cone		Clock	Cone
Far-encounter launch setting	Feb 25	111.1	158.2	Mar 27	101.6	157.2
Near-encounter launch setting	Feb 25	263.8	129.9	Mar 27	226.6	126.7
Near-encounter update 1	Apr 18	262.8	127.9	May 9	222.6	125.7
Near-encounter update 2	Apr 30	265.9	127.9	Jul 8	223.6	125.7
Near-encounter update 3	May 3	262.8	127.9	Jul 26	224.6	124.7
Near-encounter update 4	Jun 5	263.8	128.9	Aug 3	221.5	125.7
Near-encounter update 5	Jul 25	261.8	128.9	Aug 3	215.4	136.7
Near-encounter update 6	—	—	—	Aug 4	215.4	135.7
Near-encounter update 7	—	—	—	Aug 5	217.4	135.7

As the spacecraft encounter parameters became more firmly established, and as the near-encounter philosophy evolved throughout the mission, the capability to update the position of the near-encounter reference potentiometers by ground command was exercised often. Updates of the near-encounter reference potentiometers on the two spacecraft are also shown in Table 17.

In addition, the near-encounter slewing sequence commanded by a program stored in the CC&S was updated during the mission. The function of this program was to change the reference potentiometer settings during the near-encounter sequence so that specific portions of the planet could be viewed by the scientific instruments at specific times during the sequence.

*a. Scan platform unlatch.* The scan platform is latched in place, in the stowed position at 225 and 96 deg clock and cone angles, respectively, during the launch and early phase of the mission. To minimize the effect of dynamic interactions between the platform and the rest of the bus during the midcourse motor firing, the platform is not unlatched until after the first midcourse maneuver.

The scan platform unlatch event was originally scheduled to occur on March 30, 1969 for *Mariner VI*. However, since this was after the scheduled launch of *Mariner VII*, it was decided to move the unlatch time up to March 6, so that if any problems became apparent with the *Mariner VI* unlatch, there would be a chance to take some corrective action on *Mariner VII*. Accordingly, the backup command to the CC&S platform unlatch command was transmitted to and received by the spacecraft on March 6.

There was an unexpected effect on the attitude control subsystem, which is discussed separately in Subsection B of this section, but the effect on the scan platform was nearly as expected. The unlatching process did take somewhat longer than expected (approximately 4 min), and there was no perceptible motion of the platform in cone angle. Telemetry channel 200, coarse platform clock angle position, had previously been toggling between two discrete values in approximately a 40:60 ratio; after the unlatch event, this ratio decreased to 6:94. Literal interpretation of the data indicated that the platform moved 0.60 deg in clock at the unlatch.

Because no specific problem had been discovered in the unlatching process itself, the second spacecraft,

*Mariner VII*, was launched with no modification to the latching mechanism. The *Mariner VII* scan unlatch event occurred as programmed, at 19:19:24 GMT on May 8, 1969 with the issuance of CC&S event C5. The actual unlatching of the platform occurred 2 min 27 s later, but this time there was no convenient toggling of a telemetry channel to give any measure of a movement of the platform. The telemetered values of the platform stowed position were as follows:

Spacecraft	Position, deg
<i>Mariner VI</i>	
Clock	225.25 (before unlatch) 225.85 (after unlatch)
Cone	95.26 $\pm 0.87$
<i>Mariner VII</i>	
Clock	225.40 $\pm 0.87$
Cone	95.50 $\pm 0.87$

*b. Encounter.* Since the two encounter sequences were significantly different, they will be discussed separately.

*Mariner VI.* The *Mariner VI* encounter began at 00:32:41 GMT on July 29, 1969 when the CC&S issued the M1 command to turn on the spacecraft gyros. An hour later, command DC-25 was transmitted to the spacecraft, and at 01:27:47 GMT, the  $+x$  solar panel current indicated the platform was slewing from the latched to the near-encounter reference position. The slew was clearly observable in the attitude control limit cycles, but did not provide as good an indicator of the start and stop times of the slew as had been hoped. The clock slew was from the stowed position of 225 deg to the reference position of 261.8 deg, a 36.8-deg slew. The cone slew was from the stowed position of 96 deg to the cone reference position of 128.9 deg, a 32.9-deg slew. The best resolution available from the telemetry indicated that the slew lasted  $23.9 \pm 0.5$  s, for an average clock slew rate of  $1.64 \pm 0.03$  deg/s and an average cone slew rate of  $1.38 \pm 0.03$  deg/s. These slew rates were somewhat higher than expected; an average slew rate of approximately 1.1 deg/s had been expected with the platform loading effects. However, the unloaded slew speed of the SCA was approximately 1.5 deg/s. It appeared, therefore, that the platform journal bearings were behaving somewhat better than expected.

After approximately a one-half-hour evaluation of the scan control and science subsystems, command DC-28



was transmitted to the spacecraft to place the affected subsystems in the far-encounter mode. At 02:05:18 GMT, the platform was observed to begin slewing to the far-encounter reference settings. The FEPS was powered upon receipt of the command, and, at 02:06:43 GMT, an indication that the sensor had acquired the planet was received when the planet-in-field-of-view event was recorded in flight telemetry subsystem (FTS) event register 2. The scan control subsystem in the closed-loop mode seemed to track the planet in an acceptable fashion; the maximum error signal noted at the time was approximately 0.02 deg, and the maximum platform excursion as the attitude control limit cycles were tracked out was 0.21 deg in cross-cone (0.59 deg in clock) and 0.28 deg in cone.

After a one-half-hour evaluation of the far-encounter mode of operation, the platform was returned to the near-encounter mode with a DC-25 command. A DC-41 command then tested the ability of the platform to slew to the fixed cone angle reference position, and another DC-25 command returned the cone axis to the near-encounter reference position. With the capability of the subsystem to operate in all its modes demonstrated, the platform was returned to the far-encounter mode with a DC-28 command to begin the far-encounter picture-taking sequence. The first sequence consisted of 33 pictures at 37-min intervals starting at 05:32:40 GMT on July 29. The recorded pictures were then played back over the 16.2 kbits/s link, and a DC-25 command was transmitted to the spacecraft to enable erasure of the tape recorder with a DC-39 command sequence. The scan control subsystem and platform were then returned to the far-encounter mode for the second far-encounter picture-taking sequence. Commanding in this mode was now automatic, by the CC&S, and the 17-picture second far-encounter sequence was initiated at 07:36:48 GMT on July 30.

The near-encounter sequence started at 22:23:00 GMT on July 30 with the transmission of a DC-25 command to return the spacecraft to the near-encounter mode again. This command was a backup to the automatic CC&S N1 command; the N1 command occurred at 22:32:51 GMT, and the DC-25 command was seen one round trip light time after it was transmitted, at 22:34:32 GMT. The recorded pictures were played back, and the tape recorder was erased. At 05:10:00 GMT on July 31, the science analysts reported that the TV was seeing the planet, and the near-encounter picture taking sequence started. Four platform clock angle slews

and one cone angle slew were programmed to occur after given pictures during the encounter. Table 18 lists the slew times, associated picture numbers, and platform angles; the tabulation includes neither attitude control limit cycle effects nor science instrument offsets.

**Table 18. Scan platform positions during near-encounter**

Slew	Picture No.	Earth-observed time, GMT		Platform position, deg	
		Date	Time	Clock	Cone
Mariner VI					
Initial	—	Jul 30	22:36:04	261.7	128.4
First	8	Jul 31	05:15:32	247.9	128.3
Second	13		05:19:01	267.8	100.1
Third	17		05:21:52	265.8	100.1
Fourth	32	Jul 31	05:32:26	271.9	100.1
Mariner VII					
Initial	—	Aug 5	03:52:43	217.5	135.7
First	9		04:51:42	250.8	144.7
Second	20		04:59:27	233.7	100.2
Third	27		05:04:23	228.8	100.2
Fourth	37	Aug 5	05:11:25	249.8	100.2

Table 19 shows a history of all slews other than the near-encounter slews. After encounter, at 12:32:50 GMT on July 31, the scan control subsystem was turned off with CC&S command N5.

When the scan control subsystem was initially turned on, on July 29, and slewed to the near-encounter reference position of 261.7 deg in clock and 128.4 deg in cone, the telemetry readout indicated that the actual platform angles were approximately 0.73 deg in clock and 0.69 deg in cone less than predicted. Within 16 min after reaching the near-encounter reference position, the clock angle telemetry showed an angular increase of 0.04 deg, and the cone angle telemetry similarly increased 0.07 deg. It was not (and is not) clear what the reason for the change was; it was never again noticed on *Mariner VI* in the near-encounter mode; however, a similar occurrence was noted on *Mariner VII*, also when the scan control subsystem was first turned on. The result was an apparent clock angle error of  $-0.69$  deg and a cone angle error of  $-0.62$  deg.

Table 19. Scan platform position history, excluding near-encounter sequences

Slew	Mode <sup>a</sup>	Earth-observed time from slew start, GMT		Position slewed to, deg		Cause of slew
		Date	Time	Clock	Cone	
Mariner VI						
0	Off	—	—	225.9	95.3	Stowed position
1	NE	Jul 29	01:27:42	261.7	128.4	DC-25 command
2	FE	↓	02:05:18	111.4	158.7	DC-28
3	NE		02:45:18	261.7	128.4	DC-25
4	NE		03:00:18	261.7	100.2	DC-41
5	NE		03:20:18	261.7	128.4	DC-25
6	FE	Jul 29	03:55:18	111.4	158.7	DC-28
7	NE	Jul 30	04:28:07	261.7	128.4	DC-25
8	FE	Jul 30	06:32:47	111.4	158.7	F1
9	NE	Jul 30	22:32:51	261.7	128.4	N1 command
Mariner VII						
0	Off	—	—	225.4	95.5	Stowed position
1	NE	Aug 1	22:24:01	224.6	120.7	DC-25 command
2	FE	Aug 2	00:21:32	102.9	158.0	DC-28
3	NE	↓	01:26:34	105.6	153.2	DC-25 <sup>b</sup>
4	NE		02:56:32	109.6	153.2	QC-3-4
5	NE		02:59:32	104.6	153.2	QC-4-5
6	NE		03:02:32	104.6	151.2	QC-2-1
7	NE		03:05:32	104.6	152.2	QC-1-1
8	NE		03:07:32	104.6	153.2	QC-1-1
9	NE		03:09:32	104.6	154.2	QC-1-1
10	NE		03:56:33	101.8	154.2	QC-4-3
11	NE		04:00:33	101.8	155.2	QC-1-1
12	NE		04:04:33	101.8	156.2	QC-1-1
13	NE		04:08:33	101.8	157.2	QC-1-1
14	NE		04:12:33	101.8	158.2	QC-1-1
15	FE		04:41:34	102.8	157.9	DC-28
16	NE		04:51:34	101.8	158.2	DC-25
17	NE		05:01:19	101.8	140.3	QC-2-18
18	NE		05:06:19	101.8	125.7	QC-2-15
19	NE		05:11:19	119.5	125.7	QC-3-18
20	NE		05:15:19	137.5	125.7	QC-3-18
21	NE		05:19:19	155.5	125.7	QC-3-18
22	NE		05:23:19	173.5	125.7	QC-3-18
23	NE		05:27:19	191.7	125.7	QC-3-18
24	NE		05:31:19	209.6	125.7	QC-3-18
25	NE		05:36:19	221.5	125.7	QC-3-12
26	FE	Aug 2	08:46:36	102.8	157.8	DC-28
27	NE	Aug 3	03:59:57	221.5	125.7	DC-25
28	FE	↓	04:20:44	102.8	157.5	DC-28
29	NE		04:54:46	221.5	125.7	DC-25
30	FE	Aug 3	05:12:45	102.8	157.5	DC-28 command

<sup>a</sup>NE = near-encounter, FE = far-encounter.

<sup>b</sup>Near-encounter/far-encounter mode.

<sup>a</sup>NE = near-encounter, FE = far-encounter.<sup>b</sup>Near-encounter/far-encounter mode.

Table 19 (contd)

Slew	Mode <sup>a</sup>	Earth-observed time from slew start, GMT		Position slewed to, deg		Cause of slew
		Date	Time	Clock	Cone	
Mariner VII (contd)						
31	NE	Aug 4	05:18:56	221.5	125.7	DC-25 command
32	FE	Aug 4	05:46:52	103.3	157.2	DC-28
33	NE	Aug 5	03:24:52	215.4	136.7	N1*
34	NE	Aug 5	03:52:43	217.4	136.7	QC-3-2 command

Since a great deal of care had been exercised in the calibration of the platforms pointing direction, the source of this error was not immediately apparent. When the platform was returned to the near-encounter position after the first excursion to the far-encounter position, the same type of error was noticed; this time, the values of the errors were  $-0.73$  in clock and  $-0.55$  deg in cone. When the platform was slewed to the fixed cone angle position with command DC-41, the cone angle error from the predicted value was  $0.07$  deg. Furthermore, in the far-encounter mode, when the platform position was corrected for FEPS error signals and attitude control motions and this corrected position was compared to the actual clock and cone angle of the planet, a similar  $-0.7$ -deg error in clock and  $-0.07$ -deg error in cone angle positions became apparent.

The final bit of evidence confirming what appeared to be systematic error in the calibrations was the results of the first few approach guidance runs, which showed that errors of approximately  $-0.6$  deg in clock and  $-0.11$  deg in cone angle were evident. The decision was made at that time to adjust the telemetry readout from the SCA by adding  $0.7$  deg to the telemetered clock angle and  $0.07$  deg to the cone angle to obtain the true platform position. An additional correction of  $-0.48$  deg was made to the cone angle reference potentiometer settings to correct the total telemetry error and to reconcile this total error with the error at the fixed cone angle position and with the approach guidance results. This assumes that a systematic error had been made in the extensive telemetry calibration procedure described previously; postencounter analysis of the prelaunch calibration data shows no such error, nor is it apparent where such an error could occur.

Several measures of the "open-loop" slewing speed of the scan control actuator/scan platform combination were

available during the transfers from the far- to near- and near- to far-encounter modes. Since the platform slews in both clock and cone simultaneously, a measure of the cone angle slew rate depended on determining from the power subsystem telemetry when the cone slew stopped (i.e., when the two-axis slew power became single-axis slew power). The measured clock slew rates varied from  $1.618$  to  $1.67$  deg/s; the average rate was  $1.63$  deg/s. In cone, the range of measured rates was from  $1.22$  to  $1.58$  deg/s, and the average value was  $1.44$  deg/s. The specifying of an average rate does not imply that the platform always slews at that rate, however; the platform rate at any one time may vary between the values given for the range of rates.

The far-encounter planet sensor performance was nominal. The planet was tracked, in the far-encounter mode, from as early as  $E - 51$  h 12 min to as late as  $E - 6$  h 41 min with acceptable results. The FEPS was originally designed for operation from  $E - 48$  h to  $E - 12$  h; tests in the laboratory verified that all the sensors would operate satisfactorily from  $E - 76$  h to  $E - 7.5$  h, although the specifications on null offset and scale factor could not be met for this extended range of operation.

A measurement of the size of the field of view was available during the slew from the near- to the far-encounter position by comparing the first two slews; the result was a half-angle of  $6.05$ – $6.85$  deg, which agrees well with the specified minimum of  $5$  deg.

*Mariner VII.* Although the *Mariner VII* pre-encounter anomaly is treated in detail elsewhere in this report, (see Spacecraft System Performance, also in Part 3 of this volume), a brief mention of its effects on the scan control subsystem is necessary to a discussion of the *Mariner VII* encounter.

The immediate effect on the scan control subsystem was the stepping of the near-encounter reference potentiometers and the loss of all telemetry except for the near-encounter clock reference position/platform fine clock angle position measurement (the other telemetry functions are depicted in Fig. 51). The tendency of the reference potentiometers to step with a power transient was well known and well documented; in fact, nearly every time the spacecraft was turned on during the ground test phase, the reference potentiometers would step. For a single power transient of the magnitude of turning on the system, the potentiometers would step one time; however, for the July 30 pre-encounter anomaly, the clock reference potentiometer stepped a total of four times. Since the cone reference potentiometer telemetry was no longer usable, it was not possible to tell how many times, if any, the cone reference potentiometer had stepped, or in what direction. Consequently, the platform cone angle was undeterminable by normal means.

Several independent approaches were made to the problem of compensating in some manner for the lack of knowledge of the cone angle position. The first of these was an attempt by the science investigators to design an encounter sequence that was relatively independent of the cone angle position of the platform so that the encounter could be carried out with the platform in its then-present position, whatever that was.

The second approach was to attempt to gain some information about the cone angle position of the platform from the telemetry in the face of the failure. The nature of the failure is described in the paragraph that follows.

The structure of the telemetry subsystem is such that there are 20 basic channels, sampled in succession at 0.21-s intervals (a telemetry bit rate of  $33\frac{1}{3}$  bits/s). Three of these channels contain subcommutated channels, some of which contain further subcommutations. The 20 basic channels are called the 100-level channels, (channels 100–119). The first level of subcommutation is the 200-level channels (channels 200–209, 210–219, and 220–229). Further subcommutations are designated the 300- and the 400-level channels. The mechanism of the failure seemed to be that the one 100-level channel that carried the 210-level channels was permanently turned “on” by the shorting of its field-effect transistor input switch. Further, this channel was fed by a low-level amplifier with an exceedingly low output impedance, so that

other channels on the same 100-level output line as this channel were effectively tied to it. For example, coarse clock angle position (channel 200) was slaved to FTS exciter drive (channel 210), and coarse cone angle position (channel 201) was slaved to the subcommutated channels 400–419 (these channels are subcommutated from channel 211). There were some exceptions, however, and one of these seemed to offer some hope of solution. Channel 207 (near-encounter cone reference position/platform fine cone angle position) appeared to be slaved to channel 217 (receiver automatic gain control fine measurement). Channel 217 was a digital channel, however, unlike the analog channel 207, and it was observed that the slaving was not absolute.

Accordingly, from 05:00 to 06:00 GMT on August 1, channel 217 was varied by changing the uplink signal strength in an effort to ascertain the effect on channel 207. In addition, a separate, special test was performed in the Spacecraft Assembly Facility on the proof test model spacecraft that had been maintained for flight support purposes, to determine the relationship of channels 207 and 217 in this failure mode. This test consisted of duplicating the failure and then varying channel 207 while holding channel 217 constant, and vice versa.

The third approach involved designing a spacecraft sequence that would allow a near-encounter picture of the planet to be taken with the platform at the far-encounter position. The platform would be stepped from the near- to the far-encounter reference position while remaining in the near-encounter mode, utilizing the capability to update the near-encounter reference potentiometers by ground command. The wide-angle television picture would be monitored in real-time, utilizing the 16.2-kbits/s high-rate data system. When the planet entered the field of view, the platform position would be adjusted to center the planet in the narrow-angle television field of view. A picture would then be taken, recorded on the tape recorder, and immediately played back through the high-rate data system. It would then be possible—knowing the time at which the picture was taken, the clock and cone angles of Mars at that time, the spacecraft position in the attitude control limit cycle at that time, and the narrow-angle television offset from the planetary platform mirror—to determine what the cone and clock angle setting of the platform was at the time of the picture. It would then be a simple matter to command the near-encounter reference potentiometers, at 1 deg/step, back to the desired

near-encounter reference position, and to proceed with the encounter as planned before the pre-encounter anomaly occurred.

The first two approaches described above proved fruitless. The planned near-encounter sequence, a polar pass of the spacecraft with heavy emphasis on instrument coverage of the Mars southern polar cap, was simply too dependent on cone angle for scientific return not to try to determine the platform cone angle in some manner. When the attempt to ascertain a relationship between channels 207 and 217 failed, it was decided to use the last approach, which was effectively a calibration of the scan control subsystem/scan platform using the television subsystem. The decision to use this method of determining the position of the near-encounter cone angle reference potentiometer was contingent upon the normal performance of the other subsystems, of course; up to that time, the science and scan control subsystems had not been turned on in flight, and any effects on them caused by the anomaly had not been evaluated. Accordingly, at 22:12:30 GMT on August 1, command DC-25 was transmitted to the spacecraft to turn on these subsystems. The command was received one round trip light time later, at 22:24:01 GMT, and the platform slewed from the stowed position to the near-encounter reference potentiometer setting. It was immediately noticed that the telemetered platform position was 0.63 deg lower than that predicted from the reference potentiometer setting, and this led to the conclusion that the *Mariner VII* scan control subsystem calibrations suffered from the same systematic error as those of *Mariner VI*. Once again, unfortunately, no cone angle telemetry was available to support this conclusion.

After approximately one and one-half hours of evaluation of subsystem performance, command DC-28 was transmitted to place the spacecraft in the far-encounter mode. Since it was not expected that Mars brightness would exceed the FEPS threshold, command DC-35 was transmitted shortly thereafter to enable FEPS control because the planet would be large enough and bright enough to provide error signals for the system. The DC-28 command was received at 00:21:33 GMT on August 2, and 69 s later, a planet-in-field-of-view event occurred without benefit of the DC-35 command. The planet brightness at this time was approximately 0.0017 ft-cd; the measured FEPS threshold is  $0.0033 \pm 0.0006$  ft-cd, with a simulator sized for an average planet angular diameter and brightness

over four preferred trajectories. Thus, the error in the transfer calibration of the FEPS was 40%, which is an acceptable error from the standpoint of the capability of simulating optical properties of the planet for the FEPS. The DC-35 command was received almost 4 min later, as expected, with no effect, also as expected. Once acquired, the subsystem was able to track the planet in a satisfactory manner, as the real-time digital video television pictures indicated.

Upon determining that all subsystems with the exception of the FTS seemed to be performing normally in both the far- and near-encounter modes, project management immediately made the decision to attempt the calibration of the cone angle reference potentiometer by the method outlined earlier. Accordingly, at 00:40:00 GMT the necessary commands to slew the near-encounter clock angle reference potentiometer  $-119$  deg were transmitted to the spacecraft; this was followed by the commands to slew the cone angle reference potentiometer  $+33$  deg and the DC-25 command that would return the scan control subsystem to the near-encounter mode. When the high-rate data system was turned back on by a DC-44 command after the DC-25 command, the planet was seen to be in the narrow-angle television camera field of view, approximately 7 deg below center in cone angle and 1-2 deg high in clock. Commands were sent to slew the reference potentiometer, and, thus, the platform, 4 deg up in clock; these were followed by a 5-deg negative movement to verify the directions in the real-time video being displayed. The cone angle verification consisted of a 1-deg negative cone angle movement, followed by a planned positive 6-deg movement. Only three of the six positive cone angle step commands were sent at that time, however, since the clock angle motion of the planet on the television monitor displaying the real-time digital television video appeared to be incorrect, in that the motion of the planet in clock (more properly cross-cone) appeared equal in magnitude to its motion in cone. Since the cone angle of the planet was at that time 158 deg, the cross-cone motion for a 1-deg clock motion should have been approximately 0.32 deg. After Polaroid pictures of the real-time television digital pictures were examined, it was realized that there was a certain amount of distortion in the television monitor, and that the subsystem and the planet were behaving normally. Accordingly, the commands to bring the planet into the center of the wide-angle television camera field of view were then transmitted: four 1-deg cone angle steps in the positive direction, and three

clock angle steps (approximately 1 deg in cross-cone) in the negative direction. Finally, command DC-36 was transmitted at 04:25:00 GMT to record the picture on the tape recorder. Five minutes later, a DC-28 command was transmitted to transfer to the far-encounter mode, and another DC-36 command 5 min later commanded another recording for comparison with the near-encounter mode picture. At the time the near-encounter mode picture (Fig. 52) was shuttered, the attitude control limit cycles had moved the spacecraft so that the planet had passed out of the narrow-angle television camera field of view and was just reentering. For comparison, the FEPS maintains the planet in the center of the television frame in Fig. 53, the far-encounter mode picture.

Analysis of the picture in Fig. 52 showed the platform position to be 101.65 deg in clock, 158.24 deg in cone; the net number of clock steps was -123 from the near-encounter reference position of 224.57 deg. The uncorrected telemetry readings of clock angle were 101.11 deg in the far-encounter/near-encounter mode and 223.89 deg at the near-encounter reference position. Thus, the 123 steps had moved the platform 122.92 deg by calibration or 122.78 deg by telemetry in clock angle. In addition, a Polaroid picture of a digital picture in the far-encounter/near-encounter mode was available; analysis of that picture showed the platform clock and cone angles to be 101.77 and 158.29 deg, respectively. The differences between the two measurements made from the pictures are comparable, since the measurements on the pictures are made in cross-cone and cone. The

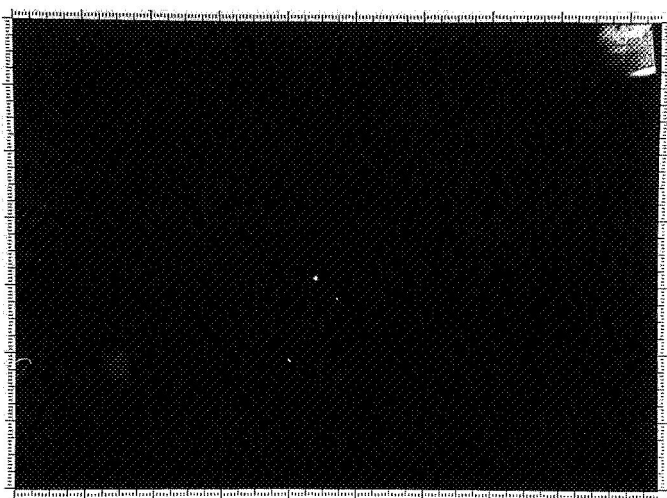


**Fig. 52. Recorded television picture used in recalibrating Mariner VII scan platform, near-encounter mode**



**Fig. 53. Recorded television picture used in recalibrating Mariner VII scan platform, far-encounter mode**

differences in planet position are then 0.045 deg in cross-cone and 0.05 deg in cone. With this confirmation that the clock angle of the platform could be scaled from the pictures and verified by telemetry, and that the commanded steps of the reference potentiometers were close enough to 1 deg/step to offer only small errors for a limited number of steps, a DC-25 command was sent to return to the near-encounter mode, and the necessary commands to step the cone reference potentiometer -33 deg and the clock reference potentiometer -120 deg to return to the desired near-encounter reference position. The cone angle of the platform was now known, and it was only necessary to keep track of the flight command subsystem (FCS) or CC&S commands to the cone angle potentiometer stepping motor to determine the cone angle of the platform.

After erasing the two recorded pictures from the tape recorder to verify that the erase function still worked, commands were sent to the CC&S to verify that the CC&S commands to the scan control subsystem still worked (i.e., that the platform would still slew in clock and cone, and to the fixed cone position, in response to CC&S commands). Although specific telemetry to verify the response to the cone angle slew commands was not available, other spacecraft responses were, and it was clear that the scan control subsystem was behaving normally. A series of commands was transmitted to the CC&S to change the timing between the far-encounter pictures to make up for the time used in the calibration exercise, and finally a DC-28 command was transmitted to and received by the spacecraft at 08:46:36 GMT on

August 2, and a planet-in-field-of-view event at 08:47:44 GMT enabled FEPS control of the platform. At 09:11:40 GMT, command DC-32 was received by the spacecraft, and the first 34-picture far-encounter sequence had begun.

After these pictures had been stored on the tape recorder, they were played back, once again over the 16.2-kbits/s data rate system. The spacecraft was then again placed in the near-encounter mode with a DC-25 command, transmitted at 03:48:13 GMT on August 3, and the tape recorder was erased. The far-encounter command DC-28 was then transmitted and was received at the spacecraft at 05:12:45 GMT; a planet-in-field-of-view event occurred at 05:13:48 GMT, and the second 34-picture far-encounter sequence began with the transmission of command DC-32 at 05:17:00 GMT. That sequence ended at 02:13 GMT the next day, August 4, when the command to play back those pictures was sent to the spacecraft. During the playback, a major alteration of the structure of the near-encounter was made by re-loading the CC&S memory to accommodate a 35-picture near-encounter sequence, with an extended viewing period over the southern polar cap, a sweep back onto the planet—after the television series was completed—for the benefit of the other instruments, and operation in the far-encounter mode, with the FEPS/platform combination tracking the planet, down to approximately  $E - 2$  h. This almost total revision of the planned near-encounter sequence was the result of the extremely successful *Mariner VI* encounter and the satisfactory performance to date of the *Mariner VII* subsystems, as well as the realization that the CC&S was much more versatile and usable than had previously been recognized.

After the playback was completed, the spacecraft was returned to the near-encounter mode with a DC-25 command, the tape recorder was once more erased, and a last DC-28 command, transmitted at 05:35:00 GMT on August 4, placed the spacecraft back in the far-encounter mode for the last far-encounter sequence. The FEPS acquired the planet at 05:47:54 GMT, and the last picture-taking recording sequence of 25 pictures started with the receipt of a DC-32 command, which had been transmitted at 05:40 GMT. In accordance with the new near-encounter strategy, two commands were sent to update the near-encounter clock and cone angle reference potentiometers, and once again the spacecraft settled down to the far-encounter picture-taking state.

This last sequence ended at 00:01:54 GMT on August 5, 1969, when playback of the recorded 25 pictures was commanded. During this playback, some of the encounter

timing parameters of the CC&S were changed by command, and the near-encounter cone angle reference potentiometer was again updated by command. Playback was finished by 02:14:00 GMT, when the series of commands necessary to erase the tape recorder was initiated; these commands were received at the spacecraft shortly after the CC&S had issued the complement of the N1\* command, a near-encounter command to only the FTS and the data storage subsystem, which left the scan control subsystem in the far-encounter mode, with the FEPS still tracking the planet.

The feasibility of tracking the planet with the FEPS/platform combination had been carefully examined before it was decided to commit the spacecraft to that mode of operation. Although this particular FEPS had been tested in the laboratory for operation as close in as  $E - 4.5$  h, it was clear that operation significantly beyond this time would saturate the signal processing electronics in the unit, which in turn would produce no signal output. The platform would then drift, or follow the attitude control limit cycles, until the FEPS field of view crossed the edge of the planet. At that time, the light level into the FEPS would be sufficiently reduced to bring the signal processing electronics into their linear range of operation, and an error signal would be produced, which would tend to drive the platform back toward the center of brightness of the portion of the planet in the FEPS field of view. It was apparent that the platform pointing direction would be toward an edge of the planet, but it was not apparent what that edge would be (i.e., whether that edge would be above or below the Martian equator, on the lit limb or on the terminator of the planet). As the spacecraft drew closer to the planet, it became apparent that the area about which the FEPS would center was going to be that part of the lit limb south of the Martian equator, close to the southern polar cap, which was the prime area of interest.

The far-encounter mode ended at 03:24:52 GMT, when the CC&S issued an N1\* command, and the scan platform slewed to the near-encounter references. The FEPS had tracked the planet successfully from as early as  $E - 76$  h 38 min to as late as  $E - 1$  h 36 min; the planet angular diameter over this time had varied from 0.20 to 9.5 deg and the planet brightness from 0.0017 to 4.5 ft-cd, indicating a tremendous dynamic range of satisfactory operation of the FEPS.

The final preparation of the scan control subsystem for the near-encounter sequence was the last updating of the near-encounter clock angle reference potentiom-



eter by command, at  $E - 1$  h 19 min, and at 04:45:56 GMT, the first near-encounter picture was taken. The *Mariner VII* near-encounter sequence for the scan control subsystem consisted of four programmed clock angle slews, two cone angle slews, and one cone angle slew to the fixed cone angle position. These slews were timed to occur after certain pictures (see Tables 18 and 19). The scan control subsystem was turned off after the encounter by command DC-1, transmitted at 06:17 GMT on August 5, 1969.

*c. Postencounter exercises.* A number of postencounter exercises of the two spacecraft were performed, involving the observation of various points of the celestial sphere with the ultraviolet spectrometer subsystem (UVS), television subsystem, and infrared radiometer (IRR).

*Mariner VI UVS scan of the southern celestial hemisphere.* The first postencounter exercise was a scan of certain portions of the southern celestial hemisphere by the UVS. It was necessary to reorient the spacecraft using a roll-pitch-roll maneuver turn sequence, since the region of the sky was that was of interest was out of the clock and cone angle range of the platform.

The maneuver sequence was started on August 12, and at 01:52:00 GMT, command DC-25 was transmitted to move the scan platform to the initial position of 212.1 deg in clock and 101.5 deg in cone. The clock and cone angles were stepped until the desired sector had been scanned; then a sufficient number of cone steps were given to transfer to the next sector, and the stepping sequence was restarted. The hemisphere was thus scanned in a 2-deg clock by 1-deg cone grid, with a 4-s wait at each point. The sectors covered were:

Sector	Coverage, deg
1	210-184 clock, 101-115 cone
2	182-176 clock, 110-130 cone
3	174-148 clock, 110-140 cone
4	146-90 clock, 120-150 cone

The motion of the platform was too fast to verify the cone angle positions (a given cone angle telemetry reading only appears every 42 s), but the clock angle performance of the platform appeared normal. It was possible to determine that the cone angle slews were in the right direction for a given clock angle.

The scan control subsystem operation was ended, when the platform reached approximately 91.2 deg in clock and 150.0 deg in cone, by the receipt of a DC-1 command.

*Mariner VI UVS scan of the northern celestial hemisphere, part I.* The second postencounter exercise on *Mariner VI* was similar to the first, in that a sector of the northern celestial hemisphere was mapped by the UVS using a CC&S-controlled programmed platform slew routine. The DC-25 command to turn on the scan control subsystem was transmitted at 22:50:00 GMT, and the DC-32 command to start the scanning program followed at 22:56:00 GMT. The sectors to be covered for this exercise were:

Sector	Coverage, deg
1	92-184 clock, 110-165 cone
2	186-274 clock, 101-165 cone

The platform was stopped at 273.7 deg in clock and 101.6 deg in cone by the receipt of a DC-1 command. Once again, the scan control subsystem performed normally, as expected, during the exercise.

*Mariner VI UVS scan of the northern celestial hemisphere, part II.* The August 12-13 sweeps through the sky by the scan platform did not completely cover that portion of the hemisphere desired. Accordingly, the third postencounter exercise was a combination of three separate experiments: (1) a 95-deg pitch off the Sun line for the temperature control flux monitor, (2) the completion of the UVS scans, and (3) an IRR scan. On August 14, a DC-25 command caused the platform to slew to an initial position of 301.6 deg in clock and 119.5 deg in cone. Command DC-32 was transmitted to the spacecraft, and the same scan slewing program used on August 12 caused the platform to sweep through the following sectors:

Sector	Coverage, deg
1	300-280 clock, 120-155 cone
2	278-244 clock, 150-163 cone

After the UVS scans were completed, a separate scan was performed for the IRR. This scan was in clock angle only, and was from an initial position of 151 to 91 deg in clock, in 1-deg steps on 2-min centers. The actual scan started at 151.7 deg in clock and 144.4 deg in cone



and ended at 92.2 deg in clock and 144.4 deg in cone. At the end of this slew, the scan control was turned off with a DC-1 command.

*Mariners VI and VII television threshold exercise.* The fourth postencounter exercise on *Mariner VI* and the first on *Mariner VII* were attempts to establish the threshold of the narrow-angle television camera by taking pictures of three stars, of visual magnitude approximately 0, +1, and +2, in the two extreme gain states of the television subsystem.

Table 20 lists the clock and cone angle positions of the stars and of the platform for the first picture in each series of four for both spacecraft. Attention is called to the resultant clock angle of *Mariner VI* for the first picture of Alpheratz; this is the result of an incorrect slew, due to an error in the CC&S program. No pictures for this star were obtained in the low-gain region. Since, in all cases except this one, the clock and cone angle positions of the platform for the low-gain state were within 0.03 deg of those for the high-gain state, only the low-gain state angles are noted. The clock angle for the high-gain state at Alpheratz for *Mariner VI* is noted in parentheses. All *Mariner VII* cone angles are calculated values, since there is no telemetry available for this function.

*Mariner VII viewing of 13 ultraviolet sources by the UVS.* On September 16, 1969, the second postencounter exercise on *Mariner VII* was conducted. This exercise

was an effort to duplicate some of the radio frequency subsystem problems apparent during the mission; the only consequence of this exercise to the scan control subsystem was that the subsystem was turned on from 05:35:00 GMT on September 16 until 00:50:00 GMT on September 17, 1969. The scan platform was not moved during this time; the subsystem was on only to dissipate power so as to warm up the bus.

The third postencounter exercise involved pointing the scan platform at 13 ultraviolet sources in the Milky Way for 25 min per source. The platform was commanded to each position by command updating of the near-encounter clock and cone reference potentiometers. Table 21 lists the desired clock and cone platform pointing angles, the actual platform clock and cone pointing angles, and the times the UVS started and stopped viewing each source. A procedural error made it necessary to return to one of the points to ensure adequate data at that point.

*Mariner VI scan of the comet 69B by the UVS.* The sixth and last postencounter science exercise on *Mariner VI* was the viewing of portions of the comet 69B by the UVS on October 9, 1969.

The roll-pitch-roll maneuver turn sequence that preceded the actual viewing sequence of the comet consisted of a +37.19-deg roll turn, a -16.75-deg pitch turn, and a final -25.72-deg roll turn. At that time, the scan platform had been already turned on, at its initial position of 203.1 deg in clock, 108.5 deg in cone. Five commands then caused five 1-deg decrements in the platform cone angle position at 5-min intervals, ending at a cone angle of 103.5 deg.

*Mariner VII power chain switchover.* On November 3, 1969, a C1 command was issued by the CC&S to the attitude control subsystem at 21:33:41 GMT. A C1 is a command to the Canopus star tracker to update the cone angle position of the tracker. When the command was received, the cone angle position evidently changed to some unknown position (the cone angle position telemetry channel was one of the channels lost permanently because of the pre-encounter anomaly), and the acquisition of Canopus was lost. The attitude control subsystem then initiated the automatic star acquisition sequence by turning on the spacecraft gyros and commencing a roll search. The power transient associated with the turning on of the gyros apparently caused a battery-share condition to exist in the power subsystem, and with the *Mariner VII* battery dead, the power subsystem failure

**Table 20. Star and scan platform positions for television pictures of three stars (September 10-11, 1969)**

Star and position	Mariner VI		Mariner VII	
	Position, deg		Position, deg	
	Star	Platform	Star	Platform
Vega				
Clock	174.56	174.6	174.17	174.0
Cone	115.28	115.4	115.26	115.6
Altair				
Clock	178.33	177.4	176.16	175.9
Cone	149.38	148.1	149.43	148.7
Alpheratz				
Clock	247.44	109.1 (245.7)	247.61	245.8
Cone	108.70	108.5	110.10	109.6

**Table 21. Ultraviolet sources viewed by the Mariner VII UVS (September 22–23, 1969)**

Source No.	UVS viewing time (start/stop)		Source position, deg		Platform position, deg	
	Date	Time	Clock	Cone	Clock	Cone
2	Sep 22	21:59:49/ 23:03:31	267.67	146.72	268.0	146.7
1	Sep 22	23:14:56/ 23:39:34	228.60	99.06	228.7	100.2
10	Sep 22/23	23:48:14/ 00:12:37	208.76	121.69	209.4	121.7
3	Sep 23	00:22:40/ 00:47:33	205.25	121.00	206.4	120.7
10		00:50:41/ 01:15:37	208.76	121.69	209.4	121.7
4		01:18:49/ 01:43:37	194.68	110.24	195.3	111.6
11		01:46:50/ 02:11:54	195.37	122.16	196.3	122.7
5		02:11:59/ 02:36:37	195.47	127.64	196.3	127.7
13		02:39:54/ 03:04:37	184.30	145.09	185.1	144.7
9		03:10:47/ 03:35:38	163.54	153.38	164.6	153.7
6		03:38:51/ 04:03:38	172.19	139.16	172.9	138.7
7		04:09:48/ 04:34:55	155.47	111.56	155.7	111.6
12		04:43:53/ 05:08:40	135.69	144.07	137.1	143.7
8	Sep 23	05:14:50/ 05:41:17	102.27	152.98	101.6	152.7

sensor caused a transfer to the redundant booster/regulator and 2.4-kHz inverter.

This power chain switchover produced the same results upon the scan control subsystem as that observed in all the commanded power chain switchovers during ground testing: the reference potentiometers stepped. The telemetry indication on the near-encounter clock angle reference potentiometer was that it stepped 1 deg negative, the opposite direction to the steps observed at the pre-encounter anomaly. The resolution of the telemetry prevents determining the exact number of steps, but previous power chain switchovers have produced only one step. However, with no cone angle telemetry, it is not possible to determine how many cone angle steps there were, or in what direction. Consequently, the platform cone angle is now (and forever, since there is no

planet with which to calibrate the platform cone angle position) indeterminate to within  $\pm 1$  deg.

### *3. Flight performance of the narrow-angle Mars gates.*

Two narrow-angle Mars gates (NAMGs) were mounted on each scan platform. The NAMG-1 was used for automatic initiation of the infrared spectrometer (IRS) cooldown, by sending a signal to the pyrotechnic subsystem when Mars entered the field of view. The time of cooldown initiation was preset to  $E - 35$  min by mounting the NAMG-1 at an offset angle of approximately 3.1 deg in cross-cone and 34.9 deg in cone. (The cross-cone angle is a function of the cone angle—the 3.1-deg number is actually in the platform  $L$ ,  $M$ ,  $N$  coordinate system—but cross-cone is a convenient visualization of the offset, although not technically accurate.) The NAMG-2 was boresighted with the narrow-angle television camera

and was used for automatic initiation of the near-encounter sequence by sending a signal to the data automation subsystem (DAS).

The NAMG is an electro-optical device that provides an output level change when the level of illumination on an object within the field of view exceeds some threshold value. For the *Mariner* Mars 1969 mission, this threshold was nominally set to 0.05 ft-cd, which was the equivalent of Mars subtending one-sixth of the  $1.5 \times 2.5$ -deg field of view. The original design specifications for both the NAMG and the scan platform specified mounting the instrument such that the limb of the planet would enter the field of view along the long side (the 2.5-deg dimension). However, the actual mounting of the sensor on the spacecraft was such that the planet would enter the field of view along the short dimension. This misorientation would cause one-sixth of the field of view to be filled earlier, as though the scan platform had been advanced one-sixth of a degree in cone angle, causing approximately a 6-s advancement in trigger time for each NAMG. Since the sequence was not this critical, it was decided not to change the orientation of the units.

Power is supplied to NAMG-1 when the pyrotechnic subsystem receives CC&S command N6 to pyrotechnic or FCS command DC-26; the output of NAMG-1 is also enabled at that time. The NAMG-2 is powered when the DAS receives CC&S command N1 or F1, or FCS command DC-25 or DC-28; however, the output of the NAMG-2 is not enabled until the DAS receives the CC&S N6 or FCS DC-26 command. No specific telemetry indication of either the NAMG-1 or NAMG-2 output is provided, but there is a status bit in the DAS data word format that indicates that NAMG-2 or its equivalent, command DC-16, has been received. Of course, the evidence that NAMG-1 has occurred is the IRS cooldown initiation, and the starting of the tape recorder shows that either NAMG-2 or its automatic backup, TV-PIV, has occurred.

Although the general time of the NAMG output signals is fixed for any given platform orientation, the exact time of NAMG-1 or NAMG-2 depends on several factors: the actual brightness of Mars, the actual threshold of the NAMG, and the actual pointing direction of the NAMG. The time of triggering was thus best depicted as a probability, whose probability density function closely approached a Gaussian distribution, with mean the nominal time of triggering and standard deviation approximately 4 s at the time it was due to trigger. However, for the

encounter sequence adopted for the two encounters, it was planned to send DC-49 and DC-16 commands as backups to NAMG-1 and NAMG-2, respectively, and, as it happened, the timing required for these backup commands would cause preemption of all the NAMG signals. This planned preemption of an automatic on-board function does not negate the value of that function, however; if, for some reason, there were some trouble in the ground command loop such that the command could not be received, then the NAMG would revert to the prime source for IRS cooldown initiation or near-encounter start.

At 12:28:47 GMT on July 30, 1969 (approximately  $E - 16$  h 50 min), the NAMG-2 status bit in the DAS data on *Mariner VI* changed to a 1, indicating that the NAMG-2 had seen the planet and triggered. Since the planet brightness at this time was 0.039 ft-cd, the NAMG-2 was boresighted with the FEPS, and the laboratory-measured NAMG-2 threshold was 0.034 ft-cd, the NAMG triggering was normal. At 22:32:51 GMT, as the scan platform slewed off the planet in response to a DC-25 command, the NAMG-2 status bit changed back to a zero, indicating that the NAMG was no longer viewing the planet. The NAMG-1 function was preempted by the DC-49 command as planned; command DC-49 was transmitted at 04:35:41 GMT. At 04:47:15.9  $\pm$  2.1 GMT, IRS motor start was observed in the data, indicating that the DC-49 command had triggered the IRS cooldown initiate. The first DC-16 command, to start the near-encounter sequence, was transmitted at 04:58:35 GMT. The transmission delay time of  $57 \pm 0.5$  s, plus the one-way light time of 5 min 18 s, meant that the command would be executed on the spacecraft at 05:04:50 spacecraft time; NAMG-2 was predicted to occur at 05:05:05 spacecraft time. The near-encounter sequence was initiated by a DC-16 command as planned, at 05:10:08 GMT.

The *Mariner VII* NAMGs behaved in much the same manner as the *Mariner VI* units. The NAMG-2 status bit in the DAS data changed state at 11:57:26 GMT on August 4, 1969, when the planet brightness exceeded the NAMG threshold, and disappeared at 03:24:59 GMT on August 5, when the platform was slewed off the planet in response to CC&S command N1\*. Command DC-49, to initiate the IRS cooldown sequence, was transmitted at 04:08:40 GMT, and IRS motor start was observed at 04:20:40 GMT as a consequence of the command. The DC-16 command was transmitted at 04:33:41 GMT, and the near-encounter sequence started, as predicted, with the receipt of the command, at 04:45:56 GMT.

**4. Conclusions and recommendations.** The *Mariner* Mars 1969 mission was the first to use a two-degree-of-freedom science instrument platform on an interplanetary spacecraft. The control and structural subsystems were new designs that represented conservative state-of-the-art design, with the emphasis on reliability and ease of integration with the existing basic *Mariner* spacecraft design. As such, the scan control subsystem/scan platform designs were an outstanding success, with enough design flexibility to withstand a severe accident to the spacecraft and, further, to successfully perform an encounter sequence based upon measured hardware performance instead of nominal or specified hardware performance. In addition, the flight performance of the subsystems themselves met or exceeded expectations; the only deficiency was the apparent bias in the telemetry calibrations. Nevertheless, there are facets of the scan control subsystem that are undesirable from spacecraft integration, reliability, or operations standpoints. Recommendations concerning these items are as follows:

- (1) The tendency of the reference potentiometers to step with a spacecraft power transient should be eliminated. Not only is this inconvenient during spacecraft testing (the potentiometers step each time spacecraft power is applied), but given the type of incidents that occurred on *Mariner VII*, the tendency to step presents operational problems that are surmountable only by exposing the spacecraft to a certain amount of further risk.
- (2) The scan control subsystem calibration procedure should be revised. The calibration procedure used for the *Mariner* Mars 1969 mission was the first attempt to accurately calibrate a two-axis scan platform, and the lessons learned will enable future efforts to be simpler and more accurate.
- (3) The location of the scan control subsystem telemetry channels in the telemetry format should be changed. The present format has the coarse platform position clock and cone readings grouped and the fine position readings grouped. The coarse and fine clock readings should be placed as close together as possible. The current format has the coarse and fine clock readings a minimum of 11.13 s apart (coarse and fine cone are a minimum of 16.8 s apart). The significance of this spacing is that there are 50 possible fine potentiometer readings; the coarse potentiometer reading at the time of the fine potentiometer reading must be known to determine the position of the platform, but the separation between the two means that the plat-

form could be 11.13 deg (at 1-deg/s) different in position at the time a fine potentiometer reading was taken than it was at the time the last coarse potentiometer reading was taken.

- (4) There should be a method of inhibiting the FEPS control of the platform. A FEPS failure that caused a saturated error signal output would cause the platform to drive into the appropriate mechanical stop, and the far-encounter mode would be unusable. A FEPS inhibit would permit far-encounter pictures to be taken in the same open loop manner as the near-encounter pictures were taken.
- (5) In conjunction with item (4), the far-encounter potentiometers should be made updatable in flight by ground or CC&S command, and telemetry of the potentiometer position should be made available.
- (6) Separate commands from the CC&S should be provided for the near-encounter clock angle reference potentiometer slew commands. The incorrect slew of the platform during the television threshold test on *Mariner VI* could not have happened if the commands were separate; the current mechanization is such that the positive and negative command are the same and only a polarity relay is set or reset to determine the slew direction.
- (7) The scan control subsystem should be able to be turned on separately from the data storage, data automation, and science subsystems. If this capability had been present on the *Mariner* Mars 1969 spacecraft, the idea of an inflight calibration, or at least a pre-encounter operational test of the scan control subsystem, might have been more feasible. The current mechanization of turning on all subsystems at once presents two disadvantages: a large power transient, and the unnecessary powering of other subsystems.

#### D. Power Subsystem Performance

The *Mariner* Mars 1969 power subsystem generates, stores, and conditions the electrical power required for the operation of the spacecraft and provides the switching functions to control power distribution to the various subsystems. A simplified block diagram of the power subsystem is shown in Fig. 54.

**1. Launch.** The *Mariner VI* power subsystem performed nominally as the spacecraft was launched at



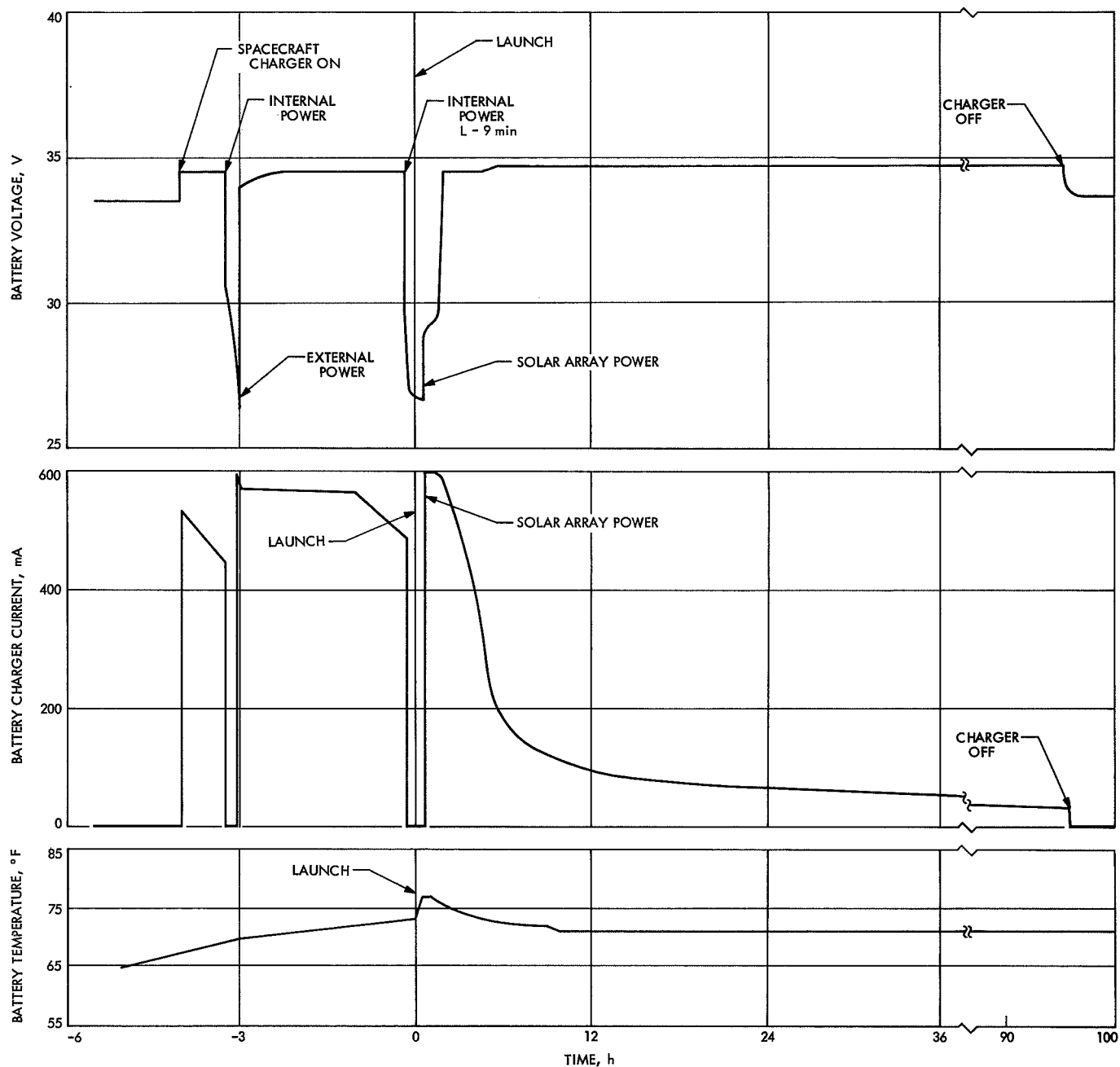


Fig. 55. Battery performance during *Mariner VI* launch

at  $L - 58$  s. The hold was caused by lack of radio frequency subsystem (RFS) confirmation of optical lock on the *Centaur* gyros. The second countdown on internal spacecraft power at  $L - 9$  min started at 22:12:58 and culminated in a successful liftoff at 22:22:01 GMT. The spacecraft was launched in daylight but entered the shadow of the Earth before acquiring the Sun. *Mariner VII* solar panels deployed at 22:39:22 GMT while the spacecraft was in the penumbra of the Earth, but no sunlight indication on the array was evident at the time. The spacecraft remained in the shadow of the Earth for about one-half hour and acquired the Sun about 2 min after emerging into sunlight.

It is notable that the open-circuit voltage solar array transducer, telemetry channel 423, apparently glimpsed sunlight at 22:28:48 GMT for one data sampling that is telemetered in 14-min intervals. Characteristics of the *Mariner Mars 1969* power subsystem telemetry are shown in Table 22. The open-circuit voltage sampling

occurred while the solar panels were still folded in launch configuration and the spacecraft was still attached to the *Centaur* vehicle.

The *Mariner VII* battery supported the spacecraft loads for nearly an hour during its launch sequence, including support during the two preliftoff countdowns. The total battery discharge during the *Mariner VII* launch was 10.6 A-h. An eight-day recharge period recharged the battery after returning 10.8 A-h before the battery charger was commanded off at 18:47 GMT on April 4. The *Mariner VII* battery performance during launch is shown in Fig. 56.

The steady-state power profiles of *Mariners VI* and *VII* deviated from estimated power levels based upon pre-launch spacecraft ground test data by less than the 3% telemetry error tolerance. Although the telemetry commutating systems of *Mariner Mars 1969* were not designed to reveal sudden power transients or surges,

Table 22. *Mariner Mars 1969* power subsystem telemetry

Telemetry channel	Telemetry function	Measurement range	Telemetry signal range (dc)	Nominal data number resolution
116	Power source logic output voltage	23–53 V	0–3 V	0.250 V
203 <sup>a</sup>	2.4-kHz inverter output voltage	40–60 V	0–3 V	0.155 V
204 <sup>a</sup>	2.4-kHz inverter output current	0–5 A	0–3 V	0.040 A
205 <sup>a</sup>	400-Hz inverter input current	0–1 A	0–3 V	0.008 A
206 <sup>a</sup>	Battery terminal voltage	23–40 V	0–3 V	0.130 V
215	Main 2.4-kHz inverter input current	0–5 A	0–3 V	0.040 A
216	Battery charger output current	0–1 A	0–3 V	0.008 A
221	Solar panel +x current	0–5 A	0–3 V	0.040 A
222	Solar panel –x current	0–5 A	0–3 V	0.040 A
223	Solar panel +y current	0–5 A	0–3 V	0.040 A
224	Solar panel –y current and booster converter status	0–5 A	0–3 V	0.040 A
225	Battery output current	0–15 A	0–3 V	0.120 A
226	Booster regulator input current	0–15 A	0–3 V	0.120 A
300 <sup>a</sup>	Radio frequency subsystem and dc heater current	0–5 A	0–3 V	0.040 A
405	Battery temperature	25–150°F	—	—
411	Case I temperature	3–130°F	—	—
419	+y solar panel outboard temperature	–40–160°F	—	—
423	Standard cell voltage	0–1 V	0–100 mV	0.80 mV
424	Standard cell current	0–100 mA	0–100 mV	0.80 mA
425	Radiation-resistant cell current	0–100 mA	0–100 mV	0.80 mA
434	Case VIII temperature	3–130°F	—	—
439	+y solar panel inboard temperature	–20–160°F	—	—

<sup>a</sup>Inoperative after *Mariner VII* pre-encounter anomaly.

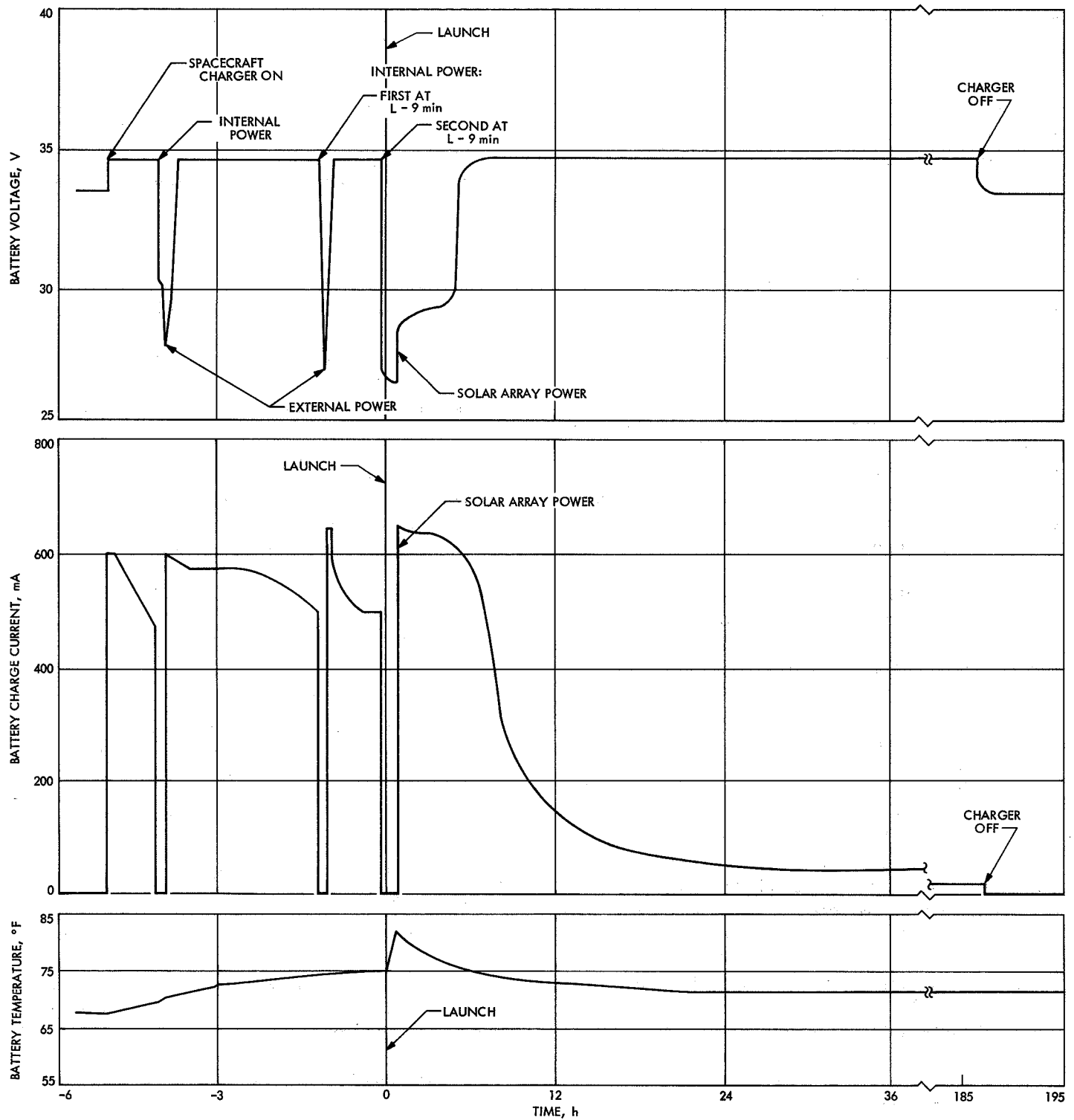


Fig. 56. Battery performance during Mariner VII launch



except by fortunate sampling of a given channel, unusual ac power surges were seen on *Mariner VII* after launch; none was noted for *Mariner VI*, however.

*Mariner VII* experienced unexpected ac power demands during a 7-min period after launch in an interval that included the orbit injection, spacecraft/*Centaur* separation, and solar panel deployment events. These data are shown in Fig. 57.

The initial power surge was noted at the orbit injection milestone of main engine cutoff, and attitude control data later indicated pitch and yaw gyros saturation. This operative mode required the gyros to draw an additional 1.2 W per unit. Another power surge on the 2.4-kHz bus at 22:34:34 GMT on March 27 demanded 8 W, and an investigation of the spacecraft attitude at this period revealed the Sun to be oriented into the Canopus star tracker. The power pulse is estimated to be that required by automatic Sun-shutter activation to prevent damage to the tracker. The indicated power difference between that required by the Sun shutter (6.5 W) and the indicated maximum power of the pulse (8 W) is probably the result of a decision point of telemetry channel 204, that of the 2.4-kHz inverter output current.

At separation, there is a net ac power loss of 8–10 W, as separation triggers the central computer and sequencer (CC&S) relay hold off (–14 W) and attitude control sensors on (+4 to 6 W). At separation, the 2.4-kHz bus settled to within one data number of expected power levels for two channel 204 data counts, or 8.4 s, after which another 12-W pulse appeared on the 2.4-kHz bus. This pulse occurred after the solar-panel deploy event, and later data investigation revealed that the attitude control jets on the solar panel outer edges fired and that the pitch gyro was near saturation. These events total 8 W and account for the major portion of the pulse. The balance of the pulse magnitude is not related to a spacecraft event, although it is possible that the 4-W balance is the result of a telemetry channel 204 decision point and that of a transient overshoot that was sampled by the commutator. The spacecraft power profile was nominal at the end of the 12-W pulse (22:40:08 GMT on March 27). The *Mariners VI* and *VII* launch parameters are compared in Table 23.

2. *Midcourse maneuver.* The midcourse maneuver for *Mariner VI* trajectory correction was performed on February 28, 1969. The array alone supported without difficulty the 267.3-W spacecraft load at the attitude required for the correct motor thrust.

**Table 23. *Mariners VI* and *VII* power subsystem launch performance comparison**

Parameter	<i>Mariner VI</i>	<i>Mariner VII</i>
Time spacecraft on battery power, min	36.8	59.8
Maximum battery discharge current, A	10.29	10.27
Total battery discharge before Sun acquisition, A-h	8.6	10.6
Minimum battery potential before Sun acquisition, V	26.68	26.68
Battery depth of discharge, %	16	20
Battery charge, h	96	187.5
Battery capacity returned, A-h	7.2	10.8
Minimum bus potential before Sun acquisition, V	25.83	25.84
Maximum near-Earth bus potential with array operating cold, V	46.98	46.76
Minimum array temperature in Earth shadows, °F	28 <sup>a</sup>	–118.1
After 24 h of postlaunch cruise:		
Primary bus potential, V	39.38	39.58
Battery potential, V	34.78	34.44
Total array output current, A	5.82	5.93
Spacecraft power demand at array, W (exclusive of battery charger)	235.7	241.4
Battery temperature, °F	70.4	72.4
Array temperature, °F	132	136
<sup>a</sup> Lowest data recorded; data loss prevented more accurate temperature reading.		

During the *Mariner VII* midcourse maneuver on April 8, 1969, the Canopus star tracker was locked onto Sirius, rather than Canopus, in an effort to:

- (1) Maintain the spacecraft on solar array power during the maneuver.
- (2) Prevent Sun shutter actuation on the Canopus star tracker.
- (3) Improve spacecraft attitude for communication.

3. *Pre-encounter.* *Mariners VI* and *VII* power subsystems pre-encounter performance is described in the paragraphs that follow.

a. *Battery conditioning.* The batteries of both spacecraft were preconditioned prior to encounter to enable the battery to provide energy on sudden demand with minimal potential decline. Many subsystems are turned on and others turned off after months in a cruise mode, and the possibility of a spacecraft electrical fault that

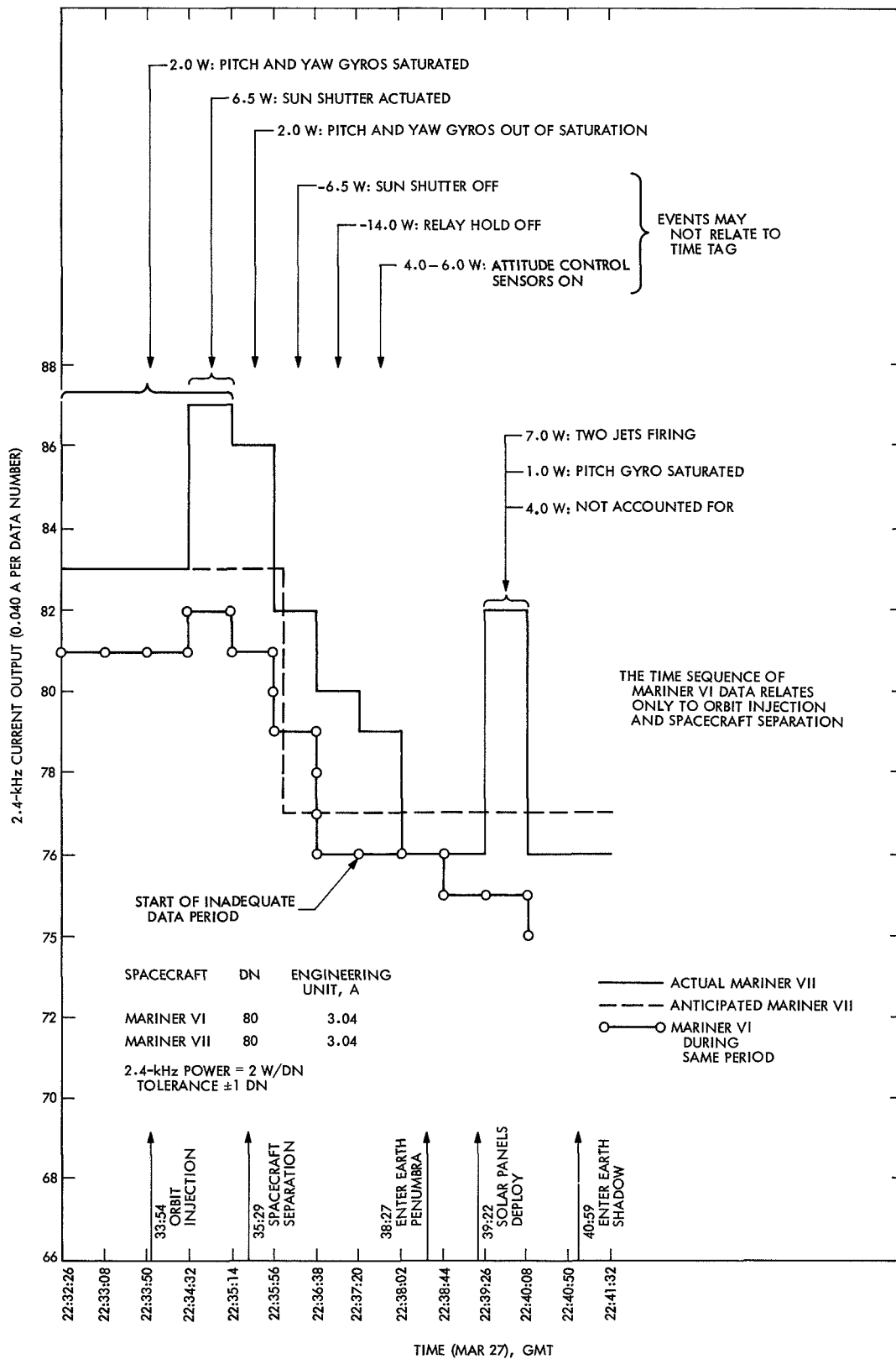


Fig. 57. Actual vs anticipated power demands of Mariner VII during launch with comparable Mariner VI data

causes battery share is greatest near encounter, particularly with the science-on command when several subsystems are switched. The purpose of battery conditioning is to minimize fault propagation to other parts of the spacecraft via the power subsystem. No battery discharge was expected with a nominal encounter sequence.

The conditioning cycle required the battery test load to discharge the battery for a short interval, followed by battery recharge. In this manner, the battery internal impedance was reduced to a level to permit battery discharge at worst-case rates if needed, without significant voltage drop. In one instance, after a long open-circuit stand during ground tests, the battery potential declined to 19.5 V for 40 ms upon the sudden application of a load. The booster regulator loses regulation when the potential of the dc power bus declines to 23 Vdc; it could precipitate a power chain transfer if the decreased bus potential lasts about 1.5 s. In a *Mariner Mars 1969* battery test that simulated long-term cruise conditions and subsequent preconditioning, a sudden application of an 11.8-A load dropped the battery potential to 26.5 V. This potential reflects as 25.5 V on the dc power bus after the potential drop of the battery blocking diode, a potential that is more than adequate to maintain the booster regulator in regulation.

Pre-encounter conditioning for the *Mariner VI* battery started at 07:18 GMT on July 23 as the 15-W battery test load began to discharge the battery. The battery discharged 5.9 A-h during a 10.5-h period, and then recharged for 127 h, returning 11.9 A-h to the battery. The discharge and charge modes were nominal.

The *Mariner VII* battery conditioning sequence started on July 25 when the 15-W battery test load was commanded on. The *Mariner VII* battery discharged for 14.5 h for a total capacity drain of 8.3 A-h; the discharge sequence was nominal. The battery recharge cycle that followed was anomalous in several respects, however.

On July 25, the battery charger was commanded on, and, after 14 h of charging, the magnitude of the recharge current rate remained significantly higher than typical, as shown in Fig. 58 after point 1. In addition, a series of unexpected charge current fluctuations occurred during the charge period. The battery charger current output is sensitive to battery terminal voltage changes; battery voltage fluctuations of 100 mV could cause the battery charger output to change from full

charge current rate, at 650 mA, to a 10 mA trickle charge rate. It is believed that a high-impedance short developed internal to the battery that occasionally cleared and occasionally intensified to cause minor battery voltage charges. As the battery potential varied, the battery charge rate fluctuated, as shown at points 2-8 in Fig. 58.

The battery temperature profile starting near point 3, at 71.4°F, unexpectedly rose to peak at 75.5°F before declining to nominal levels. The unexpected rise in battery temperature could have been caused by a battery internal short. The charge rate peak to 400 mA at point 4 appears associated with this temperature rise, and could have been the battery cell short intensifying. Further evidence of heating caused by a short at this time was the comparison of rates of temperature change of the battery and that of bay VIII, to which it is attached. Normally, temperatures of the battery and bay VIII rise as the battery charges, but bay VIII temperature changes lead that of the battery because of the operation of the battery charger. However, the battery appears as a heat source at this time, as its temperature leads that of bay VIII. It is believed that most of the capacity of a shorted cell depleted at this peak because a subsequent charge rate peak produced little temperature increase. The second peak, to 575 mA, occurred 10.5 h later at point 5, and it served only to delay a temperature decline that had already started. Also at this time, the battery temperature changes lag those of case VIII, as is normal in the battery-charge mode.

The charge rate tapered down after point 5 in a near-nominal manner for a period of 59.5 h, to the time of another anomaly, that of the pre-encounter loss of *Mariner VII* communication. Laboratory tests later revealed that the charge-rate decline starting at point 5 would have had the same nominal appearance if the battery had possessed a venting cell.

*b. Mariner VII pre-encounter anomaly.* The effects of the pre-encounter anomaly on *Mariner VII* power subsystem performance is discussed in the paragraphs that follow.

*First communication loss.* The first *Mariner VII* loss of signal (LOS), on July 30, 1969, was associated with the loss of the spacecraft roll reference lock on the star Canopus. The consequent automatic roll search for Canopus caused the high-gain antenna of the spacecraft

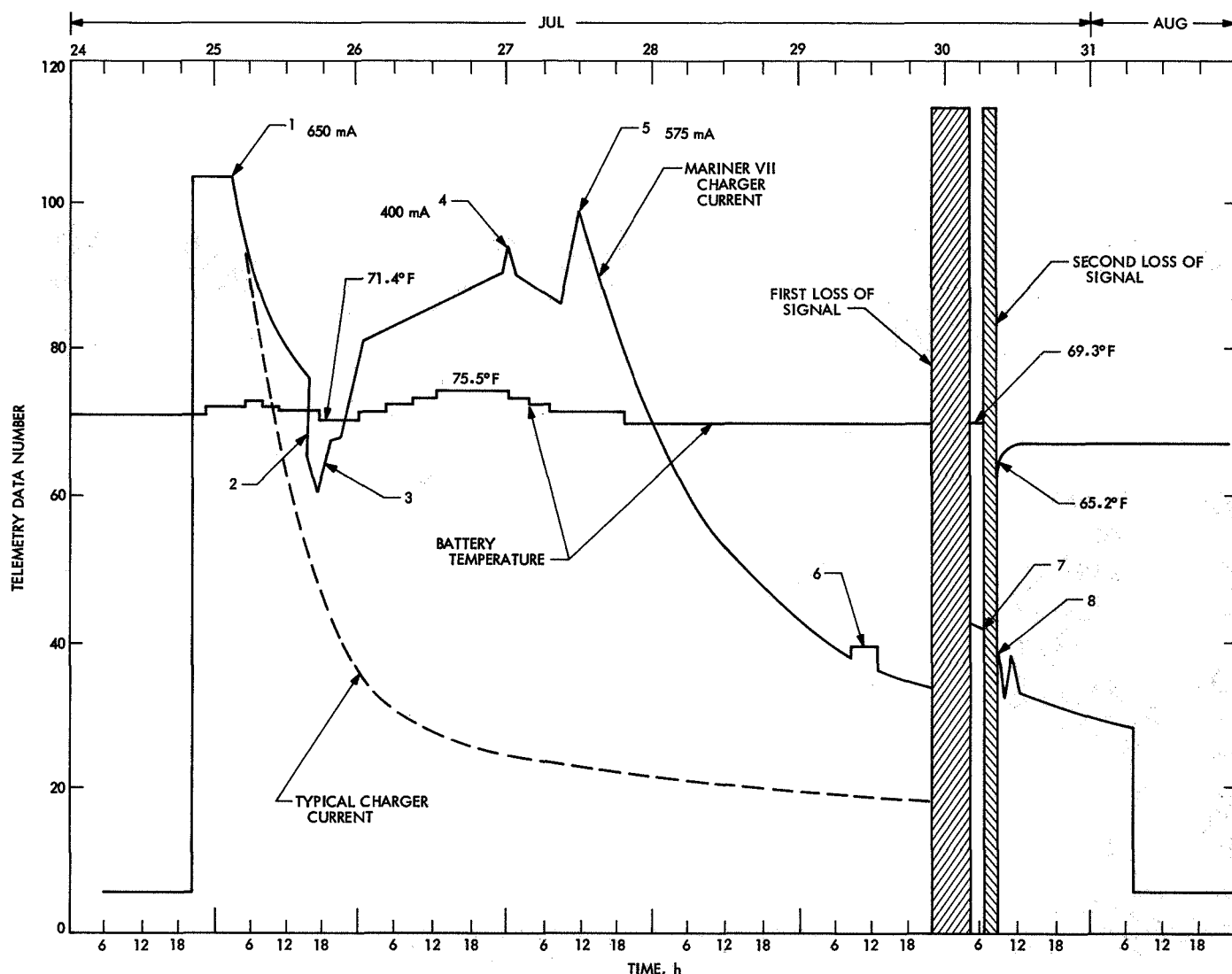


Fig. 58. Mariner VII battery pre-encounter conditioning anomalous charge sequence

to misdirect its signal as it pointed away from the Earth. It is believed that evaporation of vented battery electrolyte created an atmosphere that could have supported a corona or arc discharge to the spacecraft structure from a high-voltage source on the spacecraft. The battery is located within the thermal-blanket-enclosed cavity of the structure, which, despite vents, may have supported the minimum pressure of  $10^{-4}$  torr required to support an arc. The *Mariner* Mars 1969 battery was attached to the rear of the bay VIII electronics, and can be seen behind the empty bay in a photograph (Fig. 59) taken during the thermal control model test. Figure 60 is a view of the battery from above. Numbers designate thermistors. The battery case material is 100-mil-thick magnesium.

The spacecraft communication with the ground station was not immediately disrupted because of loss of two-way lock, but ceased in a manner to suggest high-gain antenna pointing error, about 2 min after the first transient indications. The radio is one of the two spacecraft subsystems having potentials higher than 50 V rms that could have arced to its own ground or to the structure, but two-way lock would have been lost immediately in this event.

However, arcing within the Canopus star tracker to its ground would have caused loss of the star acquisition and an automatic roll search to regain it. The RFS chassis are mounted in a manner to insure near zero impedance to the spacecraft structure. In this manner, an

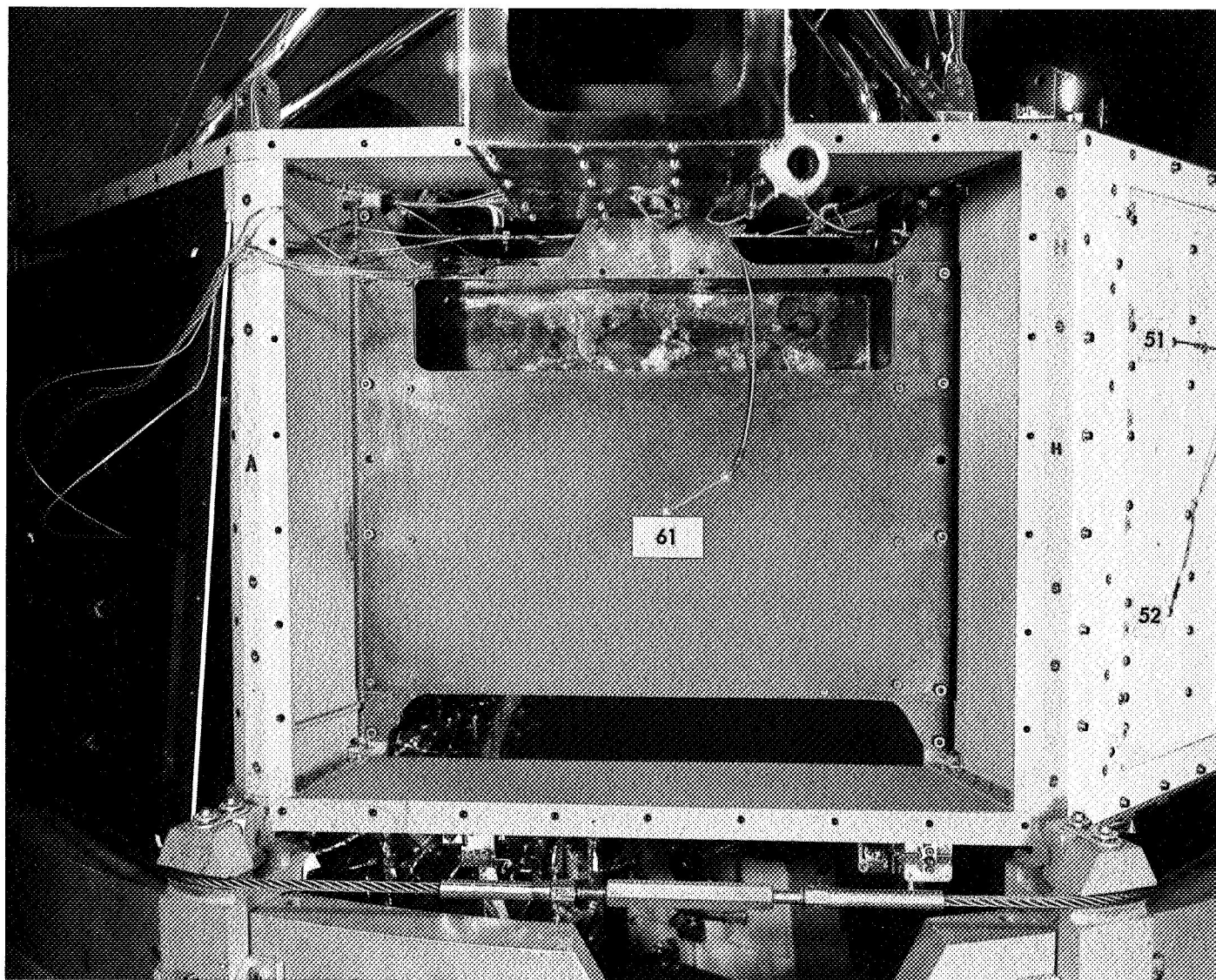


Fig. 59. Front view of battery mounted on bay VIII

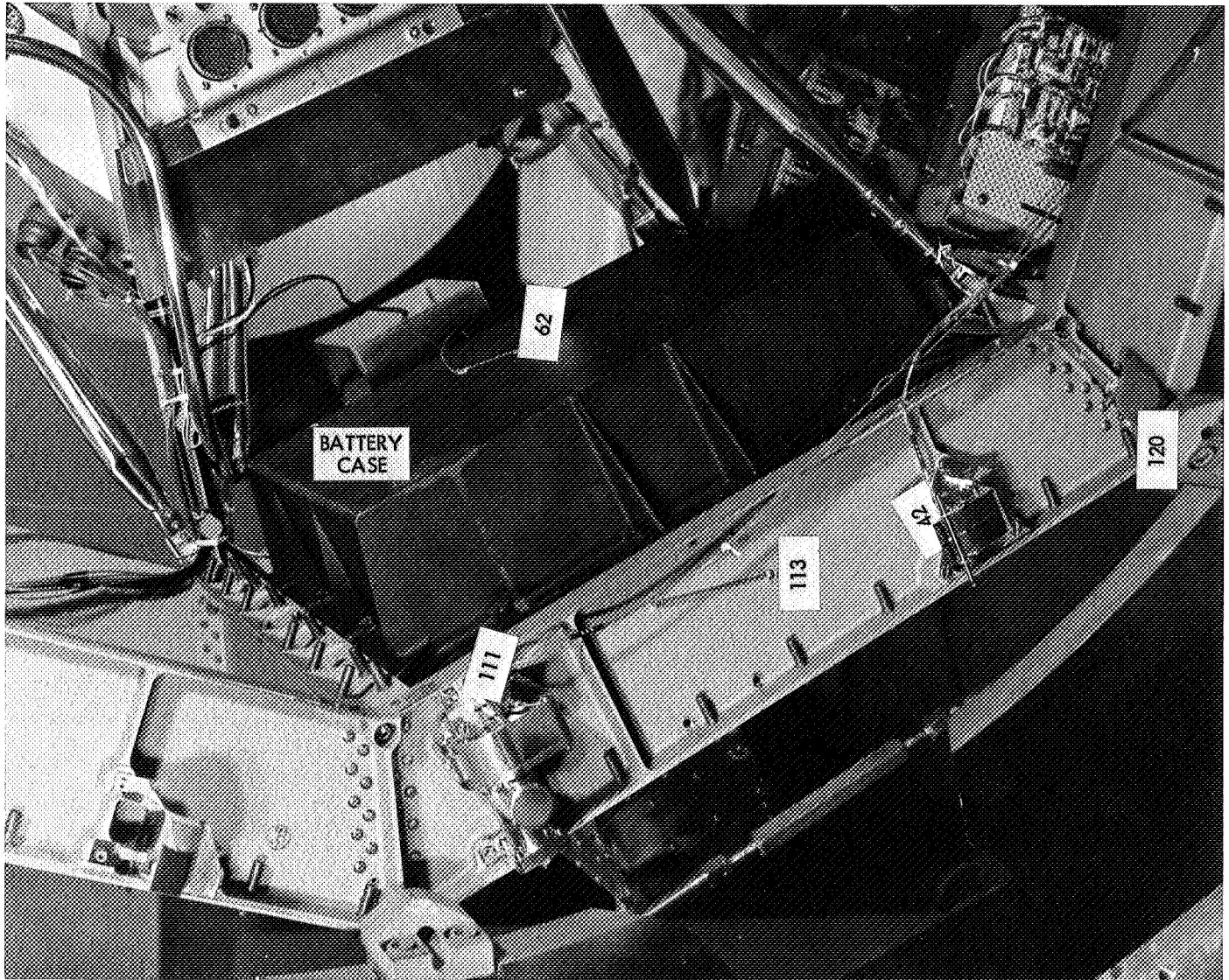


Fig. 60. Top view of battery mounted on bay VIII



arc or corona discharge from the RFS that followed a path to its own ground or to the structure would affect only the RFS in a closed loop. However, the 700-V supply line in the Canopus star tracker, discharging at high frequency to its ground cabling and having capacitance and inductance, could generate high frequency, high voltage, and current transients. The star tracker ground is connected to the attitude control ground where transients would also generate. Moreover, it would be expected that similar transients would occur on all of the subsystem returns associated with the radio grounding tree, except for radio, which is the sole subsystem at zero impedance with the structure. The electrical grounding network is shown in Fig. 61.

Restoration of engineering data after the first *Mariner VII* communication loss indicated this to be the case. The radio frequency subsystem, which is sensitive to power transients, remained unaffected and maintained two-way lock with a ground station despite reports of power transients at the time on each of the subsystems connected to its grounding network. The radio would lose lock if equivalent transients occurred directly on the 2.4-kHz power bus. All subsystems that were isolated from the structure were unaffected, as were all the science instruments associated with the data

acquisition grounding tree, since these were inoperative at the time.

*Telemetry loss.* After the first LOS of about 7 h, the spacecraft engineering data revealed five power subsystem telemetry channels were inoperative. These and other spacecraft telemetry channel failures enabled the problem to be traced to a failure in the spacecraft flight telemetry subsystem, possibly as a result of star tracker arcing. The *Mariner VII* power profile also changed, from a near-Mars cruise mode requiring 286 W at the solar array to that requiring 305 W at the array. The increased power level signaled that the gyros were operating.

*Second communication loss.* A second loss of spacecraft signal was experienced for a 70-min period starting at 06:34 GMT on July 31, after *Mariner VII* had regained data for about 72 min subsequent to the first communication loss. The second LOS is thought to have been associated with power transients that were generated in a manner similar to those that occurred at the first LOS, possibly after renewed battery venting. At this time, however, the radio frequency subsystem did lose lock, an event probably due to frequency change procedures related to the ground station transfer that

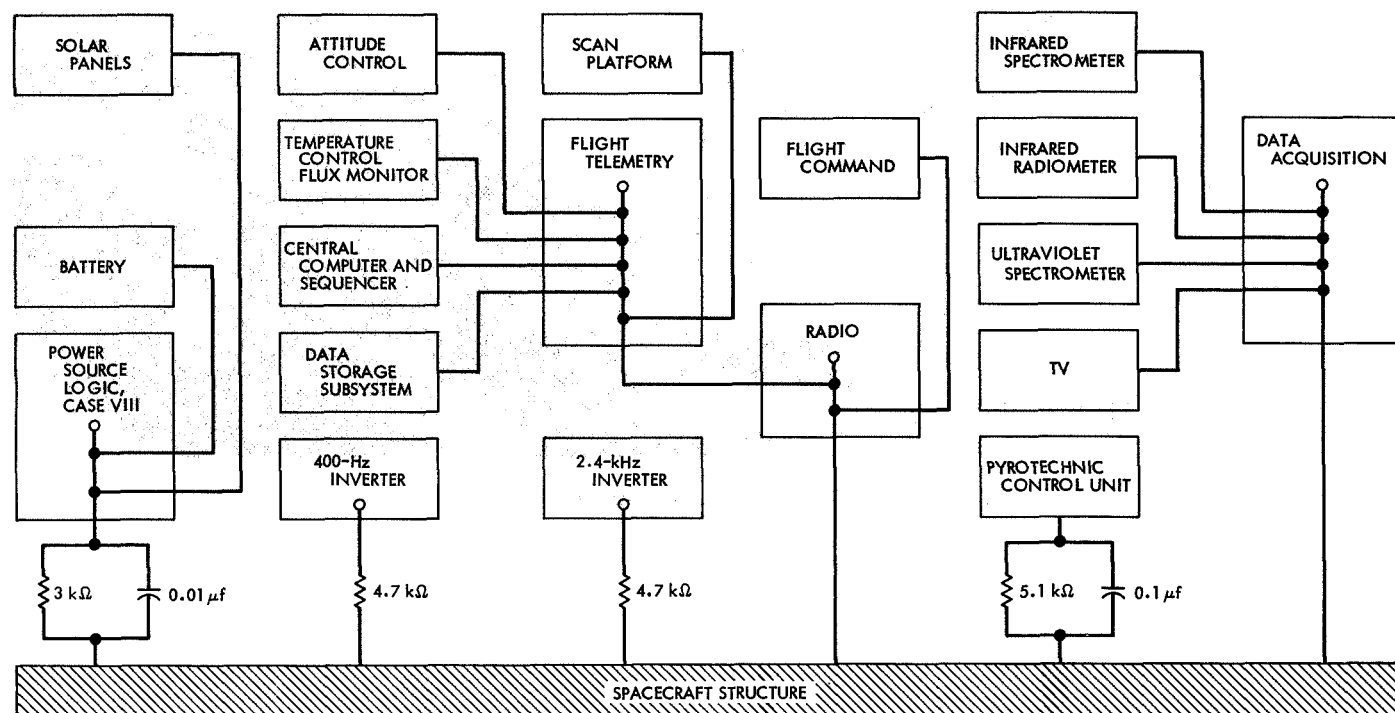


Fig. 61. *Mariner Mars 1969* electrical grounding network

was in process. It is believed loss of lock occurred during the short interval during the transfer when the spacecraft receiver operated off the center of its range and was more vulnerable to noise to which it is normally unaffected. The noise may have been generated by the arcing.

**Battery performance.** It is conceivable that the battery may have vented prior to the first LOS because of: (1) pressure that developed in a shorted cell, (2) pressure induced by battery overcharge during the battery pre-encounter conditioning sequence because of the effects of a shorted cell upon the charge rate, or (3) meteoroid damage. Battery venting is suggested by engineering data after the second LOS when the battery temperature transducer sensed unexpectedly low temperatures (see Fig. 58). The battery temperature was at 69.3°F before the second signal loss, and 65.2°F when the signal was restored. Telemetry again indicated nominal battery temperature (69.3°F) after a 2-h period. There is a possibility that the temperature transducer was cooled by electrolyte evaporation from the battery that may have vented. If the battery vented into the spacecraft bus, gas escaping through openings in the thermal blanket could have provided thrusts that contributed to spacecraft trajectory perturbations observed by doppler and ranging tracking.

**Power bus transients.** The spacecraft power profile was reviewed with respect to the power subsystem operating characteristics to determine a range of power transients that could have occurred directly at the 2.4-kHz power bus at the time of the anomaly. This is a range of transient power levels that, at its lower region, could cause the battery to share the spacecraft load with the array, and possibly cause the suspected shorted cell to reverse its potential and gas to the vent level. At the higher region of the range, the transient power surge would generate conditions that would precipitate automatic transfer to the power subsystem standby power chain.

The estimated *Mariner VII* solar array power-voltage performance characteristics at the time of the pre-encounter anomaly are shown in Fig. 62. Some of the estimated spacecraft operating modes are superimposed.

Power level A in Fig. 62 approximates the minimum spacecraft transient load at the solar array by the *Mariner VII* power subsystem on July 31, 1969 necessary to trigger a power chain transfer. A spacecraft load

at the array exceeding the 490-W magnitude for 1.5  $\pm$  0.5 s would have sufficiently stressed the conditioning electronics to generate power chain switchover trip parameters and caused the fail-sense circuit to transfer the power subsystem into the standby power chain. One *Mariner VII* power chain trip parameter is the operation of the booster regulator such as to cause its output potential to drift outside the range of 53.2–58.8 Vdc for the 1.5-s interval. Another is for the output frequency of the 2.4-kHz inverter to drift outside a 2250–2550 Hz range for the same interval. The transient load equivalent at the booster regulator output is 320–340 W; at the 2.4-kHz inverter output, the load equivalent is 288–306 W.

A transient total spacecraft load exceeding 517 W is estimated as necessary to have placed the *Mariner VII* power subsystem in a share mode (level B in Fig. 62) at the time of the pre-encounter anomaly. This power magnitude is the estimated 528-W maximum power point of the array at the time of the anomaly, less 2% for dc-power bus ripple power caused by booster regulator and traveling-wave tube converter operation. This is equivalent to 364 W at the booster regulator output and 323 W at the 2.4-kHz inverter output. If a share mode had occurred exceeding 1.5 s in duration under these conditions, it would have taken place with the power subsystem operating in the standby power chain, since trip parameters would have been exceeded.

Boost pulses occur automatically if a spacecraft load magnitude requires energy stored in the battery in addition to that provided by the solar array that is normally oriented to the Sun. Boost pulses (level C in Fig. 62) start about 5 s after the share condition is sensed; these are provided by the boost converter that is powered by the battery. These pulses would boost the array operating point out of a share condition at the time of the first anomaly if the spacecraft load did not exceed 425 W at the array with a minimum battery. This array load magnitude is equivalent to 282 W at the booster regulator output, and 254 W at the 2.4-kHz inverter output.

The battery nominal discharge voltage is about 27.5 V at a 5-A discharge rate. This potential reduces to 26.0 V if, at the time, a battery cell were shorted or possessed reduced capacity; if the cell were fully reversed, the potential would be about 23.7 V. However, if the battery potential were below 24.7 V for a sufficient interval at the time of share, the booster regulator lower voltage trip parameter would also have been exceeded,



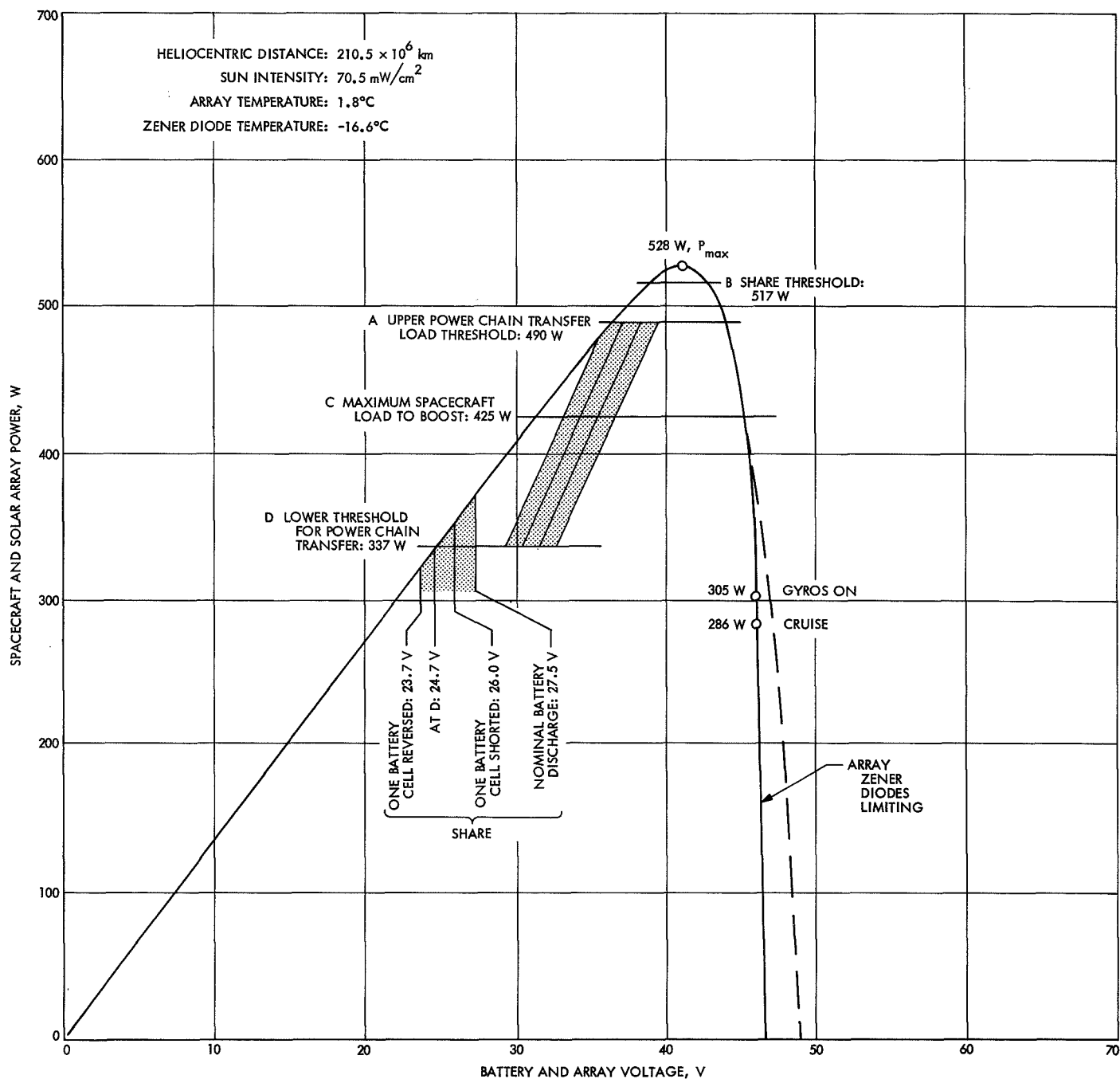


Fig. 62. Mariner VII power subsystem power-voltage characteristics at the time of pre-encounter anomaly

causing a power chain transfer (level *D* in Fig. 62). Since no transfer occurred, the battery potential minimum is 24.7 V which is shown to provide a minimum array output of 337 W on the array characteristics during a share condition. This battery potential level also indicates a cell could have been partially reversed, as much as 24.7–26.0 V (1.3 V), in a share condition, without causing a chain transfer.

Also as shown in Fig. 62, the cruise power level at the time of the anomaly at the array was 286 W (with 149 W at the booster regulator output and 134 W at the 2.4-kHz output).

Figure 63 shows the estimated current-voltage characteristics of the *Mariner VII* array at the time of the anomaly and some of the associated spacecraft load lines. The 286-W load line represents the cruise load at the array of *Mariner VII*, with high-power traveling-wave tube, before the anomaly. Gyros were on after the initial blackout when spacecraft communication was restored and the steady-state load at the array increased to 305 W.

Nominally, a transient load would have to be in excess of about 517–305 W (212 W at the array or 170 W at the 2.4-kHz power bus) to have caused the share mode shown at point A in Fig. 63. At share, the spacecraft load reduces from 305 to 289 W with gyros on because of reduced dc heater dissipation at the lower potential. If the transient load exceeded about 5 s in duration, there would have been boost pulses; if the transient load suddenly ceased, the operating point would spontaneously move back to the desirable operating point on the array at point B, since the array characteristics exceeded in power the operating point at A. The 517-W share threshold and 490-W power chain switchover threshold load lines are also drawn for reference in Fig. 63.

*Transient power magnitudes.* Accordingly, it appears that there could not have been a *Mariner VII* share mode that caused the battery to discharge for a lengthy period during the pre-encounter anomaly interval without causing a power chain transfer, since the array maximum capability was too large in magnitude. The total threshold spacecraft load at the array that would be required to cause share is 517 W without factors relating to uncertainty and 491 W with uncertainty. At the array, the minimum transient load would have had to exceed 491–305 W (186 W) to have caused share, and 490–305 W (185 W) to have caused transfer. This transient load is about 150 W at the 2.4-kHz bus. Transient loads

of greater magnitude could have existed for shorter periods than 1.5 s, the consequences of which may not have been telemetered, nor would they have caused power chain transfer, although they may have caused the battery to discharge for the short interval.

The *Mariner VII* battery charger was commanded off at 06:50 GMT on August 1, 1969. It was turned off earlier than anticipated because of the anomalous charge rates and the greater energy that the higher-than-expected rates returned to the battery. Battery charger operation was enabled for 156 h for the *Mariner VII* pre-encounter conditioning. The charger returned 25 A-h to the battery, exclusive of the capacity that may have been returned to the battery during the total 8.5-h interval when spacecraft communication was lacking.

**4. Encounter.** Because of a failure in the C1 driver circuit of the *Mariner VII* CC&S, the computer was incapable of switching the autopilot off automatically after a computer-controlled maneuver. The autopilot consequently was not used on *Mariner VII* during its near-Mars sequence. This is the only major deviation in the power profiles of the two spacecraft at encounter, other than sequence of events. The power profiles of *Mariners VI* and *VII* for the Mars encounter sequence are shown in Figs. 64 and 65, respectively. Actual power levels, based on prelaunch spacecraft data obtained during ground tests, deviated less than 1.5% from those estimated for the various operative modes shown. The largest steady-state load of the mission occurs at the nearest approach to the planet when the gyros, scan control motors, science instruments, and tape recorders are operating simultaneously. The *Mariner VI* highest steady-state level was 360 W; the comparable level for *Mariner VII* was 356 W. Picture-recording sequences on the analog tape recorder required an average steady-state power level of 5 W, and scan platform slews required an average of 4 W, in addition to the noted steady-state loads. Both encounter sequences were successfully supported by the power subsystems. Solar array flight data during the spacecraft cruise period indicated an estimated 44% array energy-conversion capability at Mars above the predicted spacecraft loads that permitted the TWT amplifier to operate in its high-power mode, an addition of 37 W at the array. Low-power amplifier operation had been planned with a minimum array at Mars.

**5. Postencounter.** The final *Mariner VII* battery test and other postencounter spacecraft events are discussed in the paragraphs that follow.

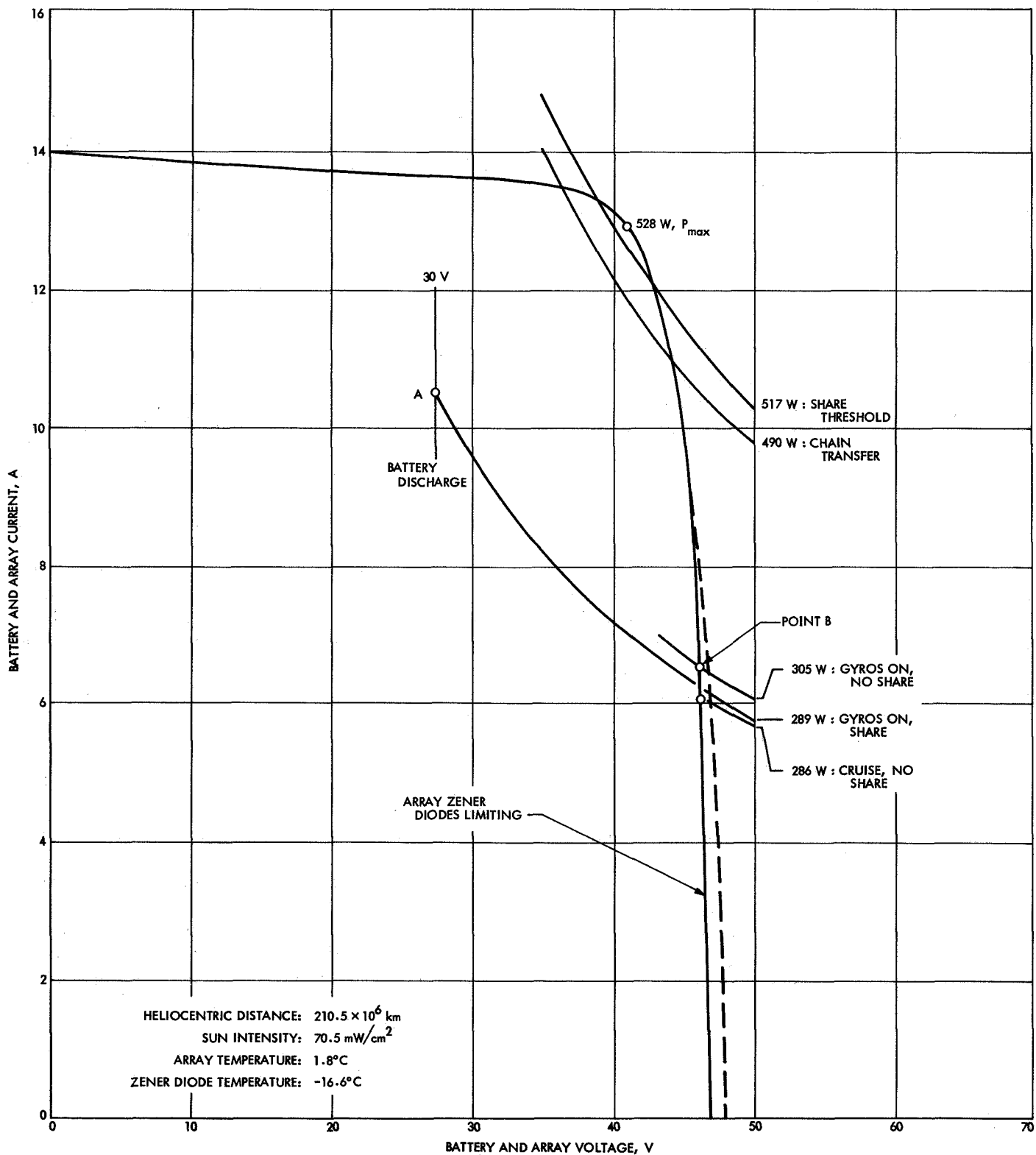


Fig. 63. Mariner VII power subsystem current-voltage characteristics at the time of pre-encounter anomaly

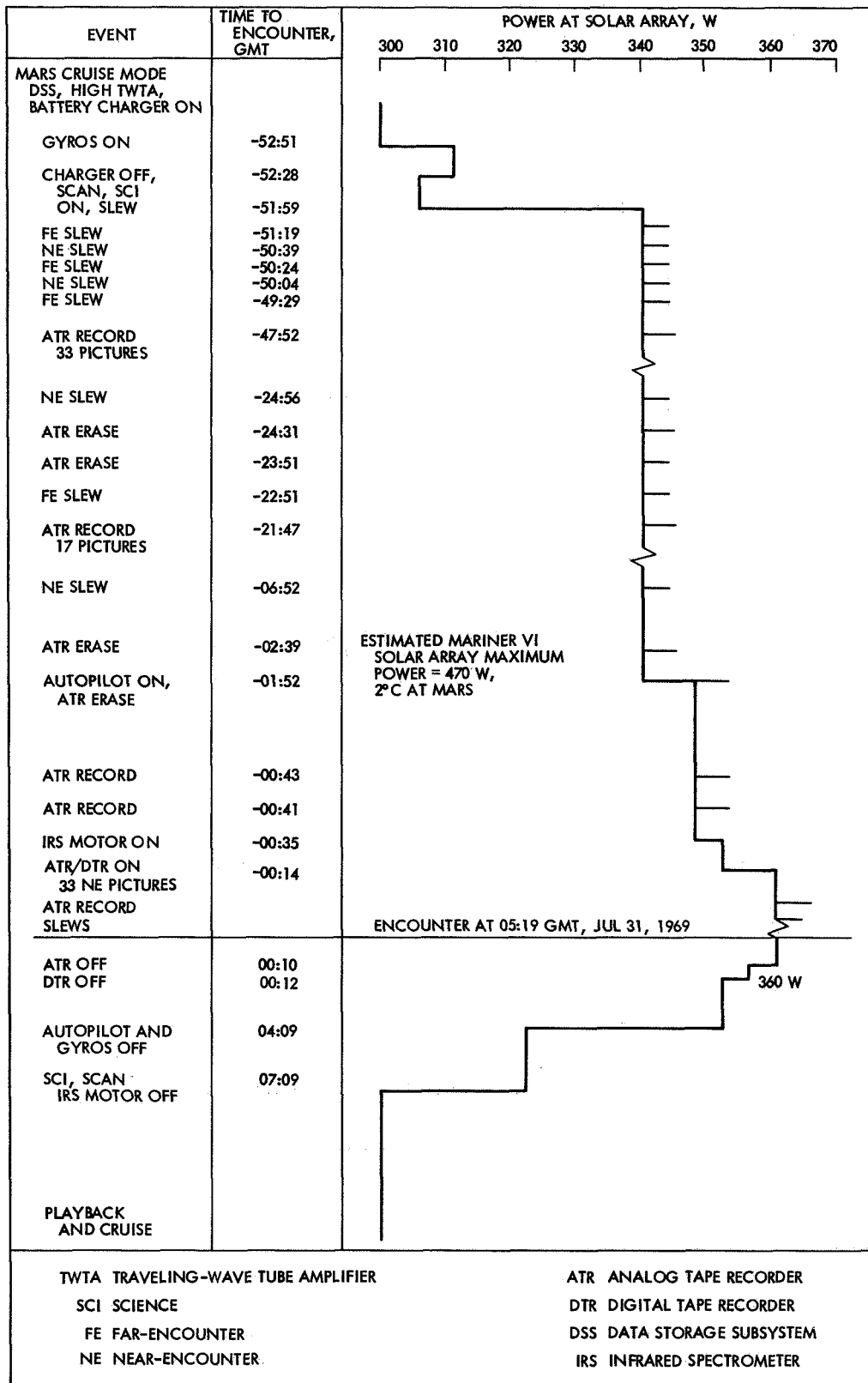


Fig. 64. Mariner VI encounter sequence power profile

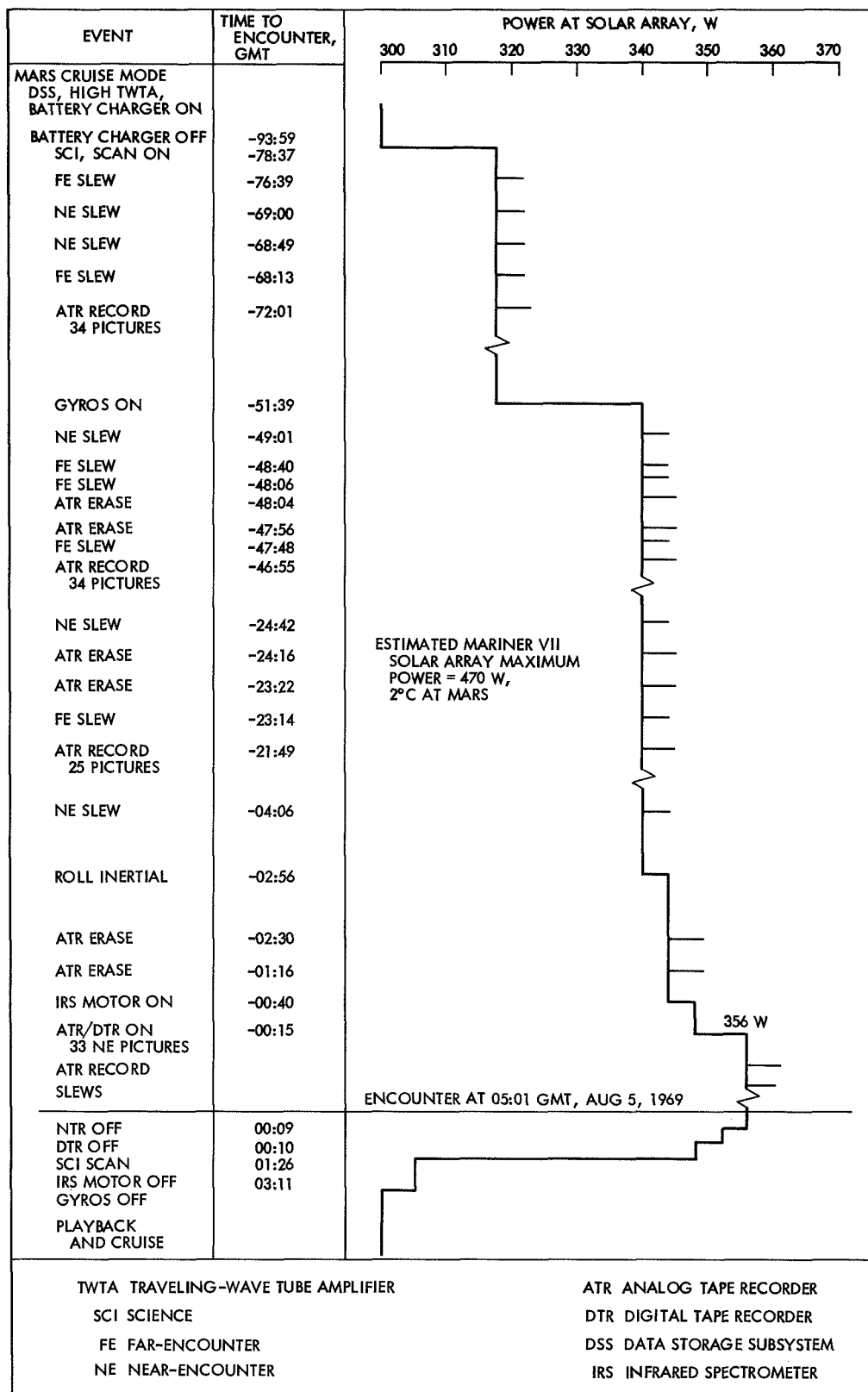


Fig. 65. Mariner VII encounter sequence power profile

a. *Final Mariner VII battery test.* On August 12-13, 1969, the status of the *Mariner VII* battery was determined by a series of tests with the battery charger and test load. The battery charger was commanded on, and the battery charge acceptance was unexpectedly low. This was shown by the initial charge rate that was lower than expected, and this rate declined to lower levels before charger turn-off. The battery test load was then commanded on, and the battery also provided lower-than-expected battery discharge current. The discharge current then dropped to a zero telemetry indication before the test load was turned off.

Circuit verification was made by simultaneously commanding on the battery charger and test load. In this mode, the battery charger is expected to limit at full-charge rate and the battery discharge current telemetry is expected to reach the magnitude a nominal battery would provide. Telemetry indications were as expected, which demonstrated nominal battery charger, test load, telemetry, and circuit operation. The *Mariner VII* battery appeared to have failed in a high-internal-impedance condition. Test results indicated that there was electrical continuity in the battery and that the circuit was not open, a condition that would have displayed zero charge and discharge currents immediately during the test modes.

The exact causes of silver-zinc battery failures are not always apparent from electrical data. At times, the causes are not completely defined after the failed unit is opened for inspection. The *Mariner VII* battery flight data indicate that the battery failed and they also suggest failure modes. A battery cell short is suggested as a failure mode during the charge cycle of the *Mariner VII* pre-encounter conditioning sequence. A battery cell that had vented and dried, causing high internal impedance, is suggested as a failure mode as the result of the postencounter *Mariner VII* battery test. *Mariner VII* data do not reveal the exact cause of the short or high impedance, nor have battery tests performed in the laboratory.

Possible causes of a shorted *Mariner Mars 1969* battery cell are as follows (it is not known which apply in the case of the *Mariner VII* battery):

- (1) Separator defects.
  - (a) Electrochemical. Separator lots are accepted on the basis of swatch tests. Actual separators that are cut from the material may contain small areas that vary because of manufacturing processes, or chemical content. Localized elec-

trochemical activity in these areas could cause higher silver penetration rates.

- (b) Mechanical. Structural weakness in the separator material about a battery cell pack stress point could result in an eventual plate short.
- (2) Zinc dendrite growth. On occasion zinc crystals (dendrites) may grow that pierce the separator material to short plates or grow over the separator top to cause the short.
- (3) Mechanical defect. Processes used in the battery manufacturing may have caused slight imperfections that resulted in damage. An imperfection such as a plate edge burr may have stressed the separator material or caused a small tear during the launch vibrational stresses.
- (4) Mechanical damage.
  - (a) The extra handling of *Mariner VII* to demate the spacecraft for hardware exchange could have also caused small battery damage.
  - (b) The battery could have been damaged by a meteoroid.
- (5) Defect or damage. The battery may have also vented because of unknown damage in handling or because of a mechanical defect; for example:
  - (a) A small, localized defect in the Cycloc mono-block container, such as a small crack that eventually leaked.
  - (b) A small defect in a battery cell seal that could have eventually leaked.

A number of laboratory tests have been conducted in an attempt to duplicate some assumed failure modes of the *Mariner VII* battery. However, duplication of all the observed performance anomalies of the battery has been unsuccessful. It has been impossible to recreate the exact space environmental conditions, such as zero gravity or the hard vacuum of space, in which the battery failure occurred. Events shown in level II of Fig. 66 serve to illustrate possible causes of increased pressure. There are no battery pressure data from the spacecraft. Some of the laboratory tests indicate there was no pressure increase because of a short or cell overcharge, but that it was possible to have had increased pressure if the battery containing a shorted cell discharged at a high rate and caused cell reversal.

Level I of the diagram in Fig. 66 places in perspective some of the sources of a cell short or high impedance

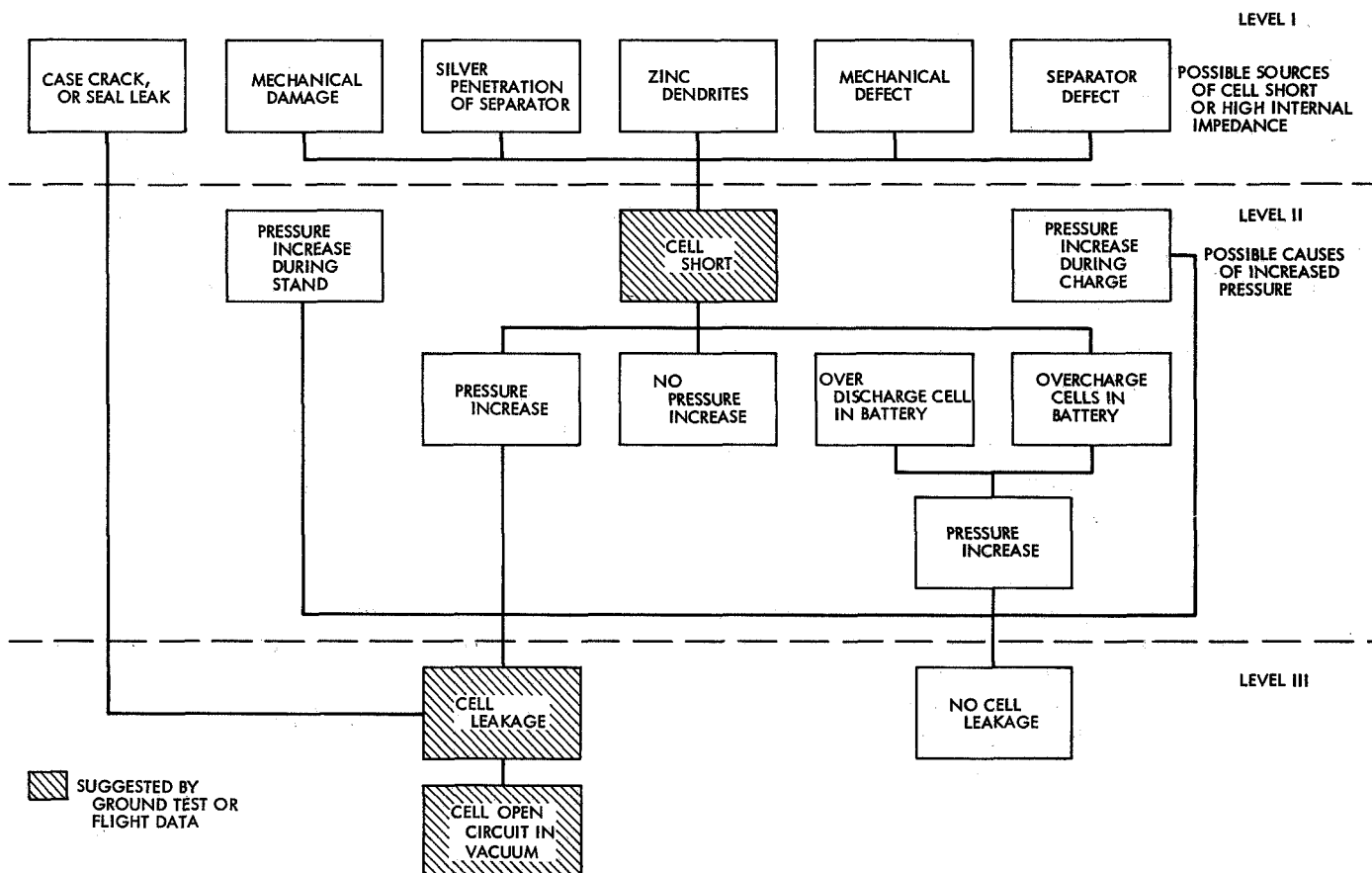


Fig. 66. Possible results of Mariner VI battery test (August 12, 1969)

that have been discussed. Level III summarizes interpretations that could be made of the results of August 12 tests of the spacecraft that utilized the battery test load and charger. Those blocks in the diagram marked by a shaded pattern note the battery events that are suggested by direct flight performance data or ground tests.

*b. Other spacecraft events.* Other spacecraft events during postencounter are discussed in the paragraphs that follow.

*Investigation of southern celestial hemisphere.* Adjustment of the attitude of the spacecraft for this investigation was required to properly orient the instruments mounted on the scan platform. This resulted in the solar array of Mariner VI operating 81.4 deg off the Sun vector. The solar array maximum power point with normal Sun orientation is estimated to have been 475 W, but the array would contribute less than 15 W after the necessary maneuver from the Sun. With the array as the prime power source, the spacecraft required 360 W at the array with science instruments, gyros, and autopilot on. There-

fore, battery power was required to support the spacecraft electrical power load at this attitude. Spacecraft loads reduce 18 W at the lower battery potential because of diminished dc heater dissipation. Of the resulting 342-W spacecraft load, the battery contributed 329 W and the array 13 W at the maximum off-Sun operation.

Before this operation mode was started, the battery status was examined with the use of the battery charger and 15-W test load in a procedure that was subsequently followed whenever battery operation was anticipated. The battery charger was first commanded on to note the battery performance in the charge mode, and, after the charger was turned off, the battery performance was noted during discharge with the 15-W test load. In this manner, the battery charge acceptance and retention could be inspected. Another inspection point was provided by examining the status of the battery charger relay and charger performance when the battery test sequence was started by toggling the charger on and off. Operation verification confirmed command capability to prevent battery drain by its test load if the test load

relay failed "on." The test load was sized to permit the battery charger to power it, and commanding the battery charger on while the test load was on prevented significant battery discharge. The battery test sequence prior to the southern celestial hemisphere scan and the nominal effect upon the battery voltage and the charge and discharge currents are shown in Fig. 67.

After the maneuver from the Sun, the battery initially supported the spacecraft load with 10.6 A, and the array contributed 0.5 A. The battery-array share mode continued for 26 min until the spacecraft science loads were commanded on and the battery discharge current increased to 12.4 A; the array contribution remained at 0.5 A. Figure 68 shows the battery discharge parameters during the investigation of the southern celestial hemisphere.

The spacecraft required battery support for more than 2.5 h during the investigation; the battery capacity drain was 797 W-h, for a 59% depth of discharge from an estimated 1350-W-h capacity. The battery charger was commanded on for a two-day period while the ultraviolet spectrometer scanned the northern celestial hemisphere of the galaxy. The scan sequence required only scan platform reorientation, whereas the solar array remained Sun-acquired. The battery recharge curve after the southern celestial hemisphere investigation is shown in Fig. 69. As the science instruments were turned on to

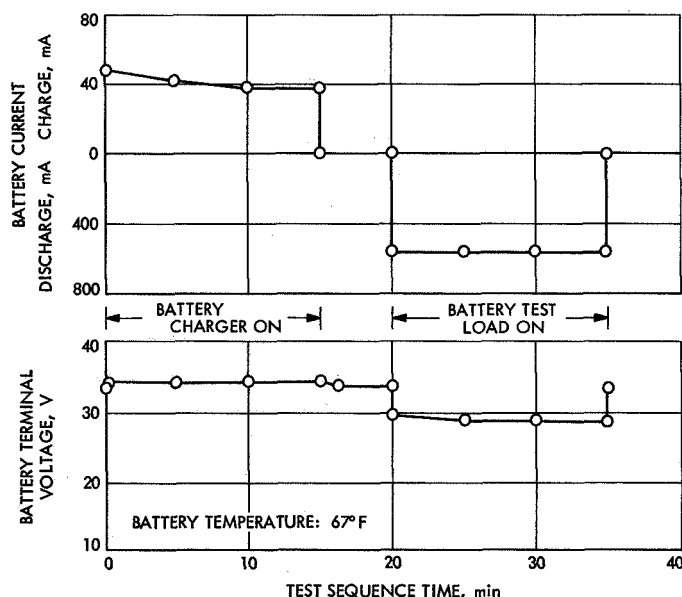


Fig. 67. Nominal Mariner Mars 1969 battery performance during self-test sequence

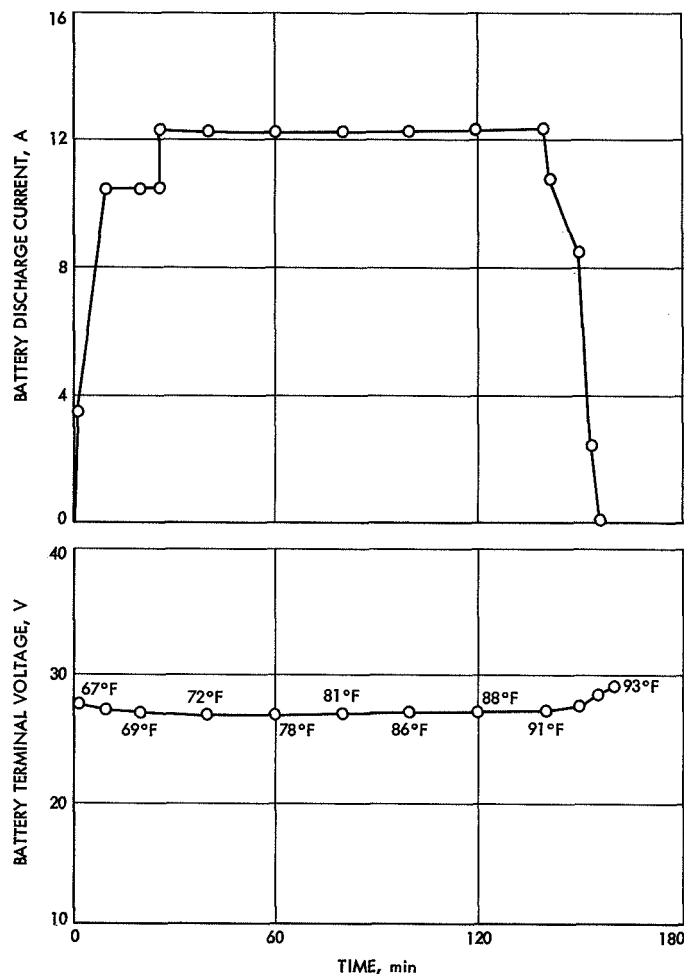


Fig. 68. Mariner VI battery performance in share during southern celestial hemisphere investigation

scan the northern celestial hemisphere, it was a normal function for the battery charger to switch off, as shown in the figure. Another ground command restored charger operation.

*Temperature control flux monitor calibration.* Another test, performed on August 13, required the Mariner VI solar array to be completely maneuvered from the Sun. In this manner, the temperature control flux monitor looked into deep space to enable the instrument to be zero calibrated. The battery supported the power requirements of Mariner VI for one-half hour at an 11.4-A discharge rate.

*Investigation of galaxy center.* A short time later, the spacecraft was oriented 38.2 deg from the Sun vector to enable the infrared radiometer to scan the central portion of the galaxial celestial sphere for 4 h. The battery discharged at rates of 2.3–6.0 A, depending upon modes



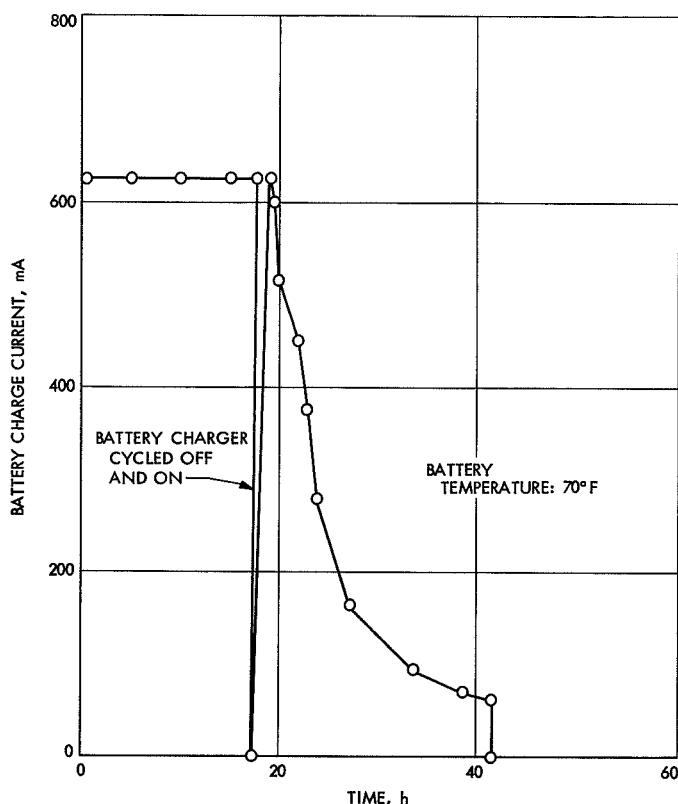


**Fig. 69. Mariner VI battery recharge curve after southern celestial hemisphere investigation**

of operation, as it shared the spacecraft electrical load with the solar array. Figure 70 shows battery performance on August 13 when the battery supplied 877 W-h for the experiments. The battery capacity at the start of the experiment was estimated at 970 W-h. The battery charger had returned 417 W-h of the 797 W-h used on August 11, and the net total depth of discharge was 93%.

The subsequent battery recharge over an interval of 16 days is shown in Fig. 71. The battery charger was commanded off at 22:30 GMT on August 29, at which time the battery was estimated to be 96.2% recharged. It had been estimated that 18 days would be required to fully recharge the battery, but the recharge period was limited because of constraints of available spacecraft tracking. However, data extrapolation indicates 99.4% recharge would have occurred in the 18-day charge interval, and there was continued predictable *Mariner VI* battery performance after 6 mo in space. The battery had been activated 11 mo prior to the start of the post-encounter experiments and had been previously subjected to six discharge-charge cycles that varied in depths of discharge from 4 to 20%.

*Unexpected share during comet 69B investigation.* Postencounter scientific investigation continued on October 8, 1969 when the *Mariner VI* ultraviolet spectrometer was used to scan the comet 69B tail. The event required the operation of spacecraft gyroscopes and scientific instruments as the array was oriented off the Sun line to view the comet. The power subsystem unexpectedly required the battery to supplement the energy supplied by the array to support the power drawn by the spacecraft when the science instruments were commanded on. This battery-sharing incident occurred when the array was still normal to the Sun vector. The battery again shared the spacecraft load with the array during the interval the ultraviolet spectrometer scanned the comet tail as the array was oriented from the Sun line.

The estimated *Mariner VI* solar array performance characteristics on October 8 with the array normal to the Sun are shown in Fig. 72. The spacecraft heliocentric distance was estimated at  $241.9 \times 10^6$  km, the array temperature at  $-15.9^\circ\text{C}$ , and the Sun intensity at  $53.40 \text{ mW/cm}^2$ . Array temperature evaluations are based on telemetered open-circuit voltage transducer data of the solar array (telemetry channel 423, Table 22) instead of the array temperature transducers located on the reverse surface of the solar panels. The open-circuit voltage transducers located on the Sun side of the array supplied data that enabled greater resolution of the array Sun surface temperature and provided array performance analyses of greater consistency.

The estimated maximum power point of the *Mariner VI* array on October 8 was 402 W (point A in Fig. 72). Point B was the operating point of the solar array-zener diode characteristics at 305 W with gyros operating. The zener diodes were limiting during this phase of the mission, and their average temperature on this date was estimated at  $-36.7^\circ\text{C}$ . The zeners are located on the spars at the rear of the solar panel.

Point C in Fig. 72 is the operating point off the array characteristics immediately after science instruments turned on (a 342.6-W steady-state load), causing a power subsystem share mode for 6–12 s. The minimum spacecraft load necessary to have precipitated a share condition is 394 W, about 2% less than the maximum array power due to dc power bus ripple power. Therefore, a power transient of more than 50 W occurred when the instruments and platform motors started to operate; this sudden power demand caused the array operating point to dip to the battery discharge potential. Results of analysis

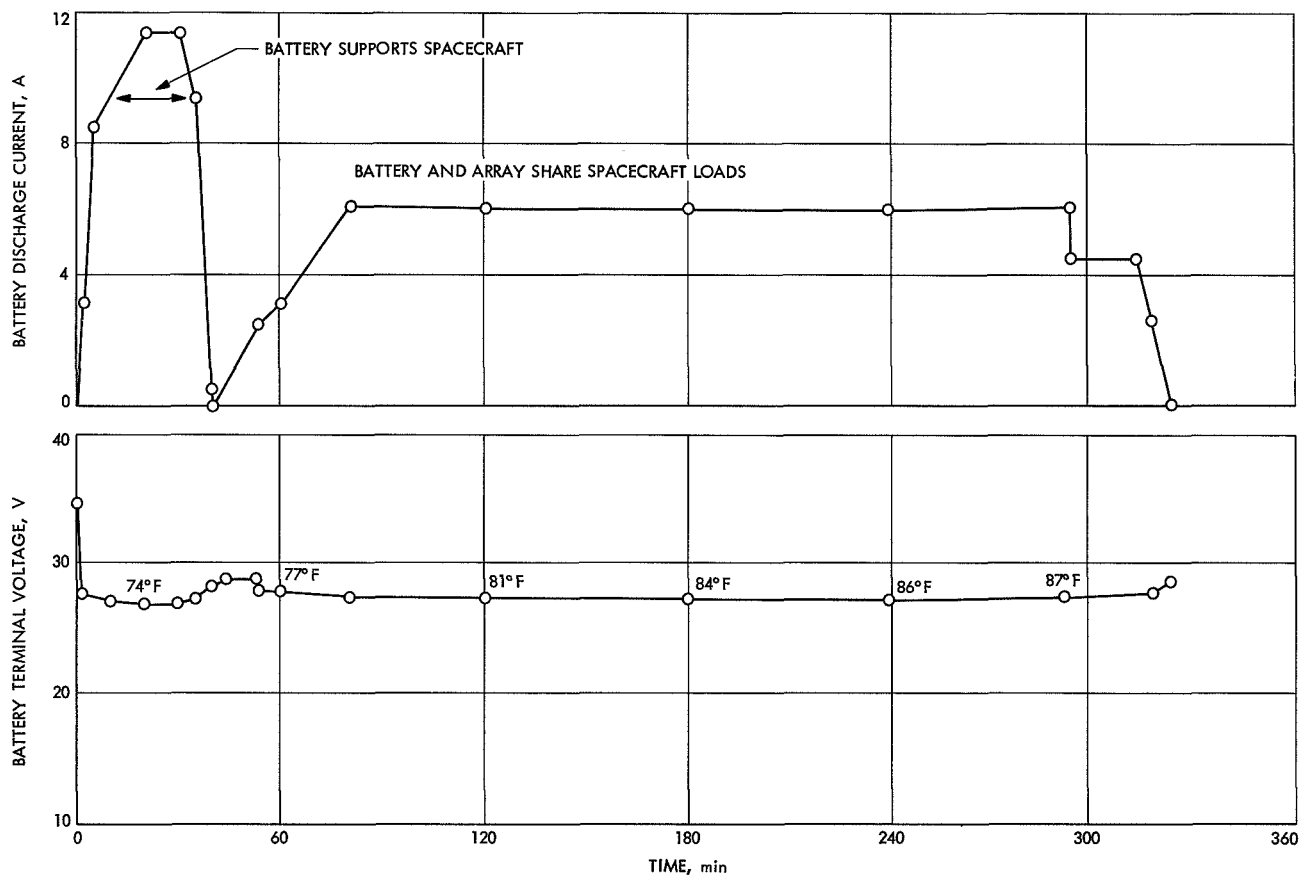


**Fig. 70. Mariner VI battery performance during 93 % depth of discharge**

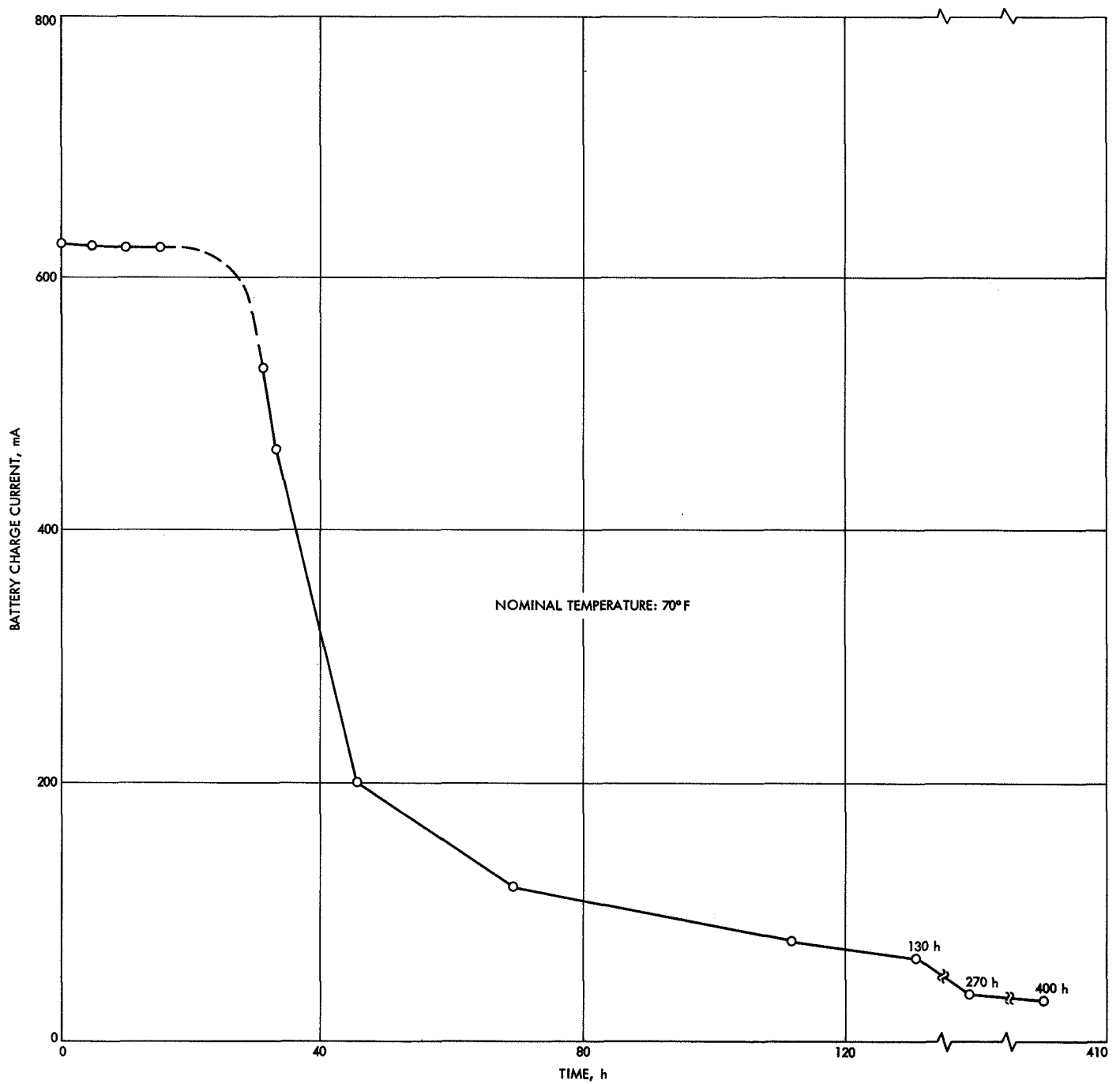
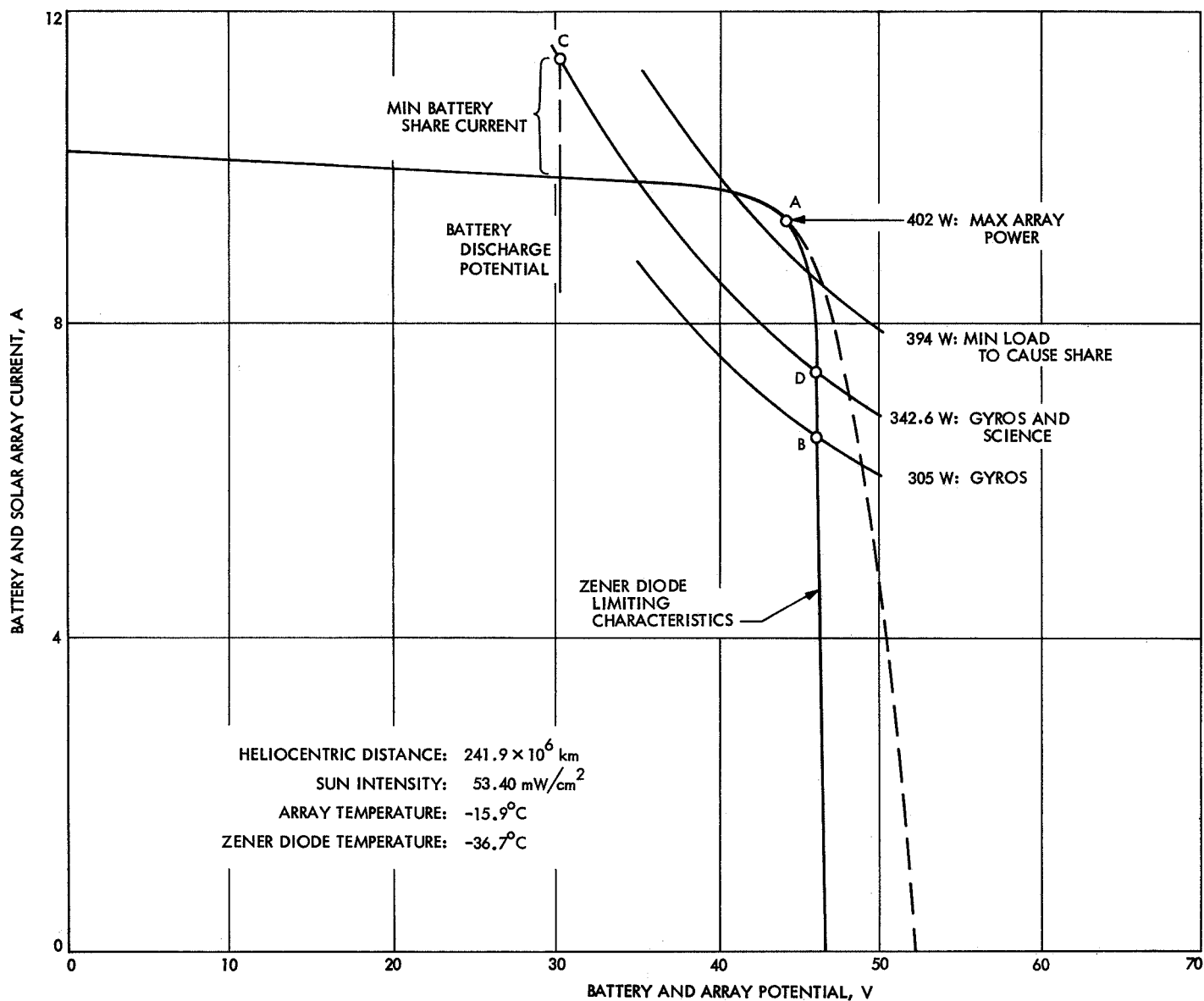


Fig. 71. Mariner VI battery recharge curve after 93% depth of discharge



**Fig. 72. Mariner VI power subsystem performance during unexpected battery-array share on October 8, 1969 with nominal array orientation**

indicate a probable battery discharge current rate of about 1.5 A at point C for the short duration of the share. The share incident did not occur at a time in the spacecraft data stream to permit commutation of the battery discharge current.

The *Mariner VI* telemetry at Mars encounter on July 31, 1969 sampled a portion of a similar power surge when science was turned on for the first time in the mission. At that time, a power transient of 21 W was noted at the array; this value probably did not represent its maximum level. The science instruments at this phase of the *Mariner VI* mission excluded the 4-W infrared spectrometer cooldown motor that was turned on later in the sequence, prior to Mars encounter; the motor operates after encounter whenever science instruments are energized. At encounter, there was no battery share, which would have required a power transient of 127 W at the array when science turned on—this to exceed the threshold requirement for a share mode for the estimated 475-W array at the time. The spacecraft steady-state power requirements with science instruments and the cooldown motor operating were 342.7 W at encounter and 342.6 W on October 8, 69 days later.

It is probable that a boost converter pulse restored the operating point from the share mode potential at point C of Fig. 72 to that at point D at a higher potential where no energy contribution is required from the battery.

The *Mariner VI* attitude adjustment to enable the ultraviolet spectrometer probe of the comet tail on October 8 required the spacecraft to pitch  $-18$  deg and roll  $-26$  deg. The maximum power of the array diminished from 402 to 351 W after the  $-18$  deg pitch turn (shown as the dashed curve in Fig. 73). Two sections on the  $-y$  solar panel were shaded after the pitch, and the spacecraft load level that would cause share reduced to 344 W, compared to the steady-state spacecraft load of 342.6 W. It is probable that this operating condition caused the share mode shown at point A in Fig. 73. The boost converter is made inoperative automatically as the spacecraft is oriented from the Sun vector by more than 6 deg. This prevents wasteful boost pulses (to dislodge operation in a battery-array share mode) to have the array alone support the spacecraft electrical load at a time when the Sun misorientation makes it impossible. The *Mariner VI* battery discharged at about 4.5 A during the period of maximum spacecraft pitch, and the spacecraft load reduced by 6 W (to 337 W) because of decreased dc heater dissipation at battery potential.

One of the two shaded  $-y$  solar panel sections regained full Sun illumination after the  $-26$ -deg roll to complete the comet pointing maneuver, and the maximum power of the array increased from 351 to 369 W (shown as the solid array curve in Fig. 73). The battery discharge rate decreased to about 4.0 A after the roll. Although the array was then capable of supporting the spacecraft load without the aid of the battery, the lack of booster converter pulses prevented regaining this operative mode, and the battery discharged about 4.5 A-h during the comet investigation.

*Second unexpected share event.* *Mariner VI* experienced another unexpected share event on April 9, 1970 when the gyros were commanded on. The event lasted 4–8 s, when the power source logic potential dropped to battery potential for one data frame. Battery discharge current again was not sampled. On this date, the estimated array maximum power point was 351 W, the heliocentric distance was  $256.2 \times 10^6$  km, the Sun intensity was  $47.6 \text{ mW/cm}^2$ , the open-circuit voltage array temperature indication was  $-23.3^\circ\text{C}$ , and the zener diode temperature was  $-43.7^\circ\text{C}$ . The minimum load necessary to have precipitated a share condition on this occasion was 344 W, and the minimum transient was 41 W as the gyros turned on.

*Mariner VII power subsystem operation in the standby power chain.* A C1 stored command was issued by the CC&S to the attitude control subsystem on November 3, 1969 to update the Canopus star tracker cone angle. The desired cone angle setting was not achieved. Instead, the *Mariner VII* power subsystem transferred to its redundant power chain.

Engineering data confirms the occurrence of transients, at about the time the gyros were automatically commanded on, that were similar to those during the July 30–31 anomaly. The transients stepped the scan platform reference potentiometers, caused errors in the flight telemetry subsystem, stepped the spacecraft event counters, and set the CC&S power relay such that its functions were inhibited.

Figure 74 shows the estimated *Mariner VII* power subsystem performance characteristics on November 3, 1969. The array zeners were again limiting on this date. The maximum array power was 408 W (point A in the figure) at a time when the spacecraft heliocentric distance was  $244 \times 10^6$  km, the Sun intensity was  $52.2 \text{ mW/cm}^2$ , and the array temperature was  $-17.4^\circ\text{C}$ . The

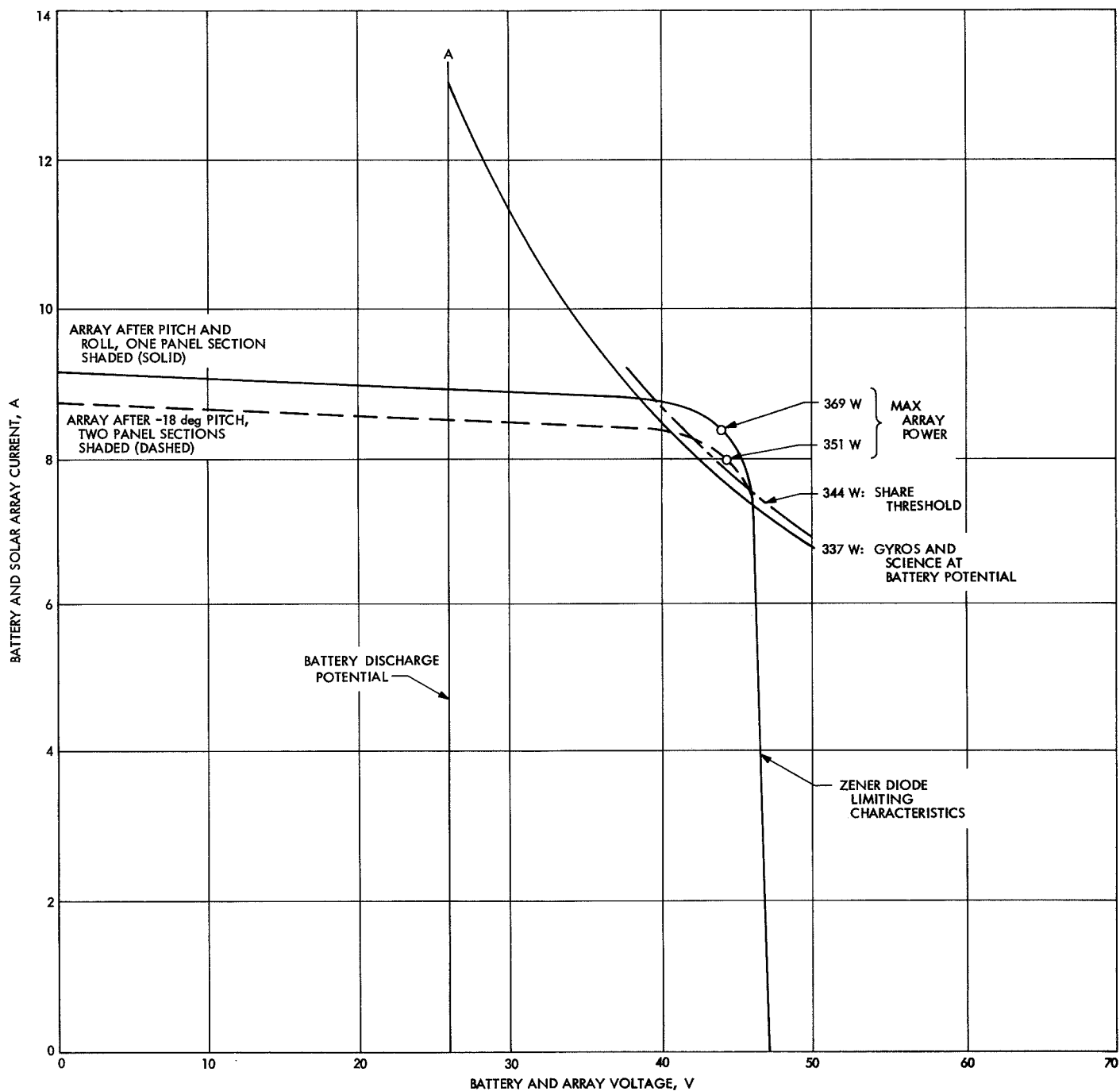
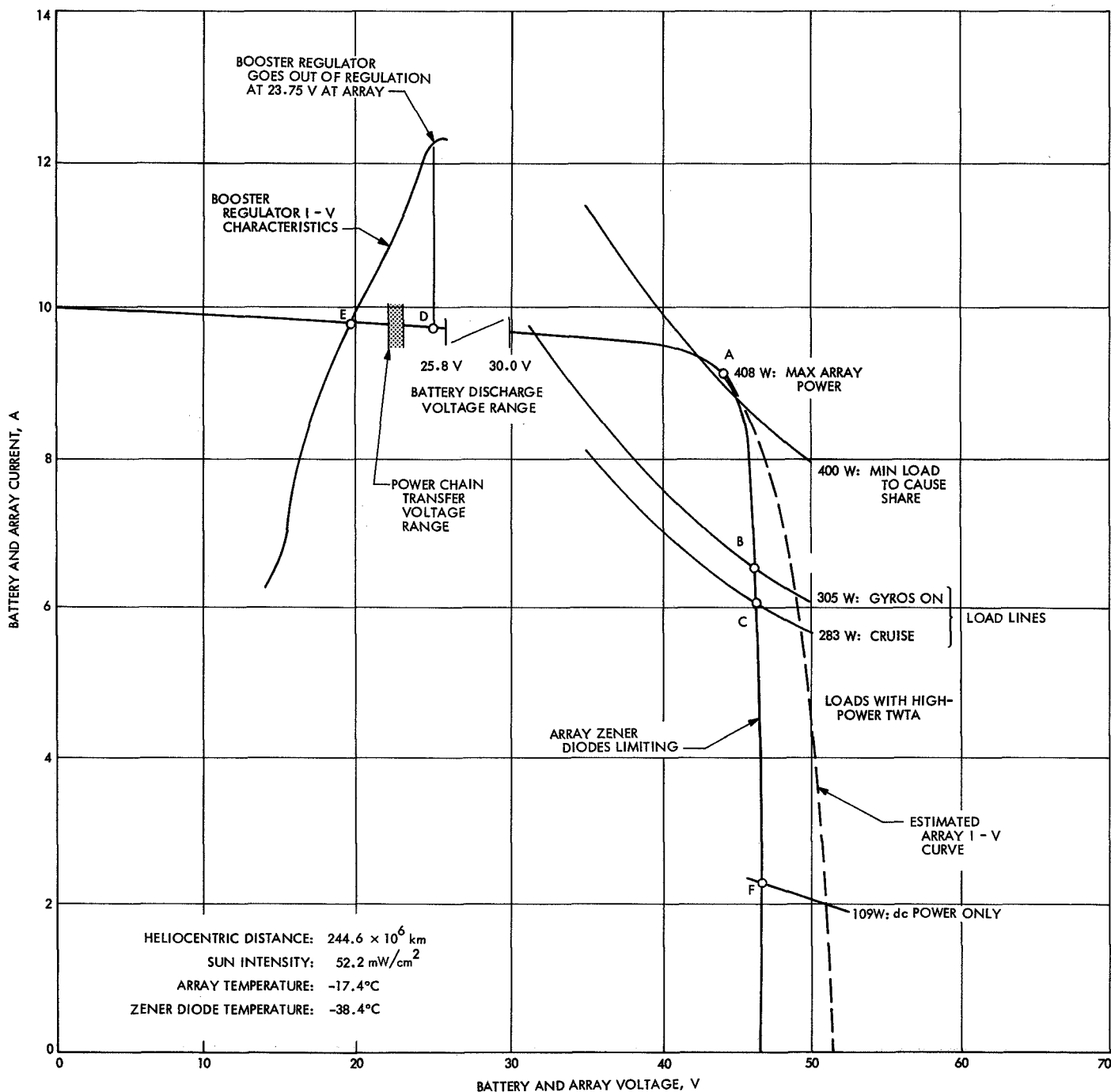


Fig. 73. Mariner VI power subsystem performance on October 8, 1969 with off-Sun array orientation



**Fig. 74. Mariner VII power subsystem power chain transfer on November 3, 1969**

average zener temperature is estimated at  $-38.4^{\circ}\text{C}$ . The *Mariner VII* cruise load was 283 W, operating at point B of the array-zener characteristics.

The anticipated spacecraft steady-state load with gyros operating was 305 W (point C in the figure). However, it is probable a power surge occurred at gyro turn-on that exceeded the steady-state load magnitude and also the 400-W load threshold to precipitate battery-array share (i.e., a share mode if there were an operative battery on *Mariner VII* at this time in the mission). It appears a minimum power surge of about 95 W occurred at the array as the gyroscopes switched on, causing the chain transfer.

The power subsystem was unable to support a spacecraft load of this magnitude solely with the solar array, and the operating point took a path along the array characteristics to a lower potential from point B, passed the maximum array power point, and passed the voltage range of a normally discharging battery as it sought more current. When the battery supports the spacecraft load with the array, the potential of the array operating point is clamped within the battery discharge voltage range. The range lies above the potential at which the booster regulator goes out of regulation. However, having failed, the *Mariner VII* battery provided no clamp, and the operating point declined below the minimum potential required for regulation at point D and stopped at the intersection of the resistive portions of the booster regulator characteristics and the array characteristics at point E.

After the booster regulator no longer regulates the spacecraft load, the load terminates its general constant power characteristics at the array and appears resistive. A portion of the booster regulator current-voltage characteristics (Fig. 75) is shown in Fig. 74. On November 3, the array operating point of *Mariner VII* is estimated to have settled at 190 W, at less than 20 V (point E in Fig. 74), and at a potential below that required to sustain the power subsystem operation in the main power chain. The power subsystem automatically transfers to the standby units if the dc power bus potential seen at the array is at or below  $22.5 \pm 0.5$  V for more than about 1.5 s because the output potential of the booster regulator will decline to standby power chain trip levels. It is probable that this interval was exceeded and that the operating point drifted from point E of Fig. 74 toward point F with just the spacecraft 109-W dc loads operating, for about 60 ms, as the standby power chain electronics warmed. Telemetry indications of power transients had disappeared before the chain transfer, and the operating

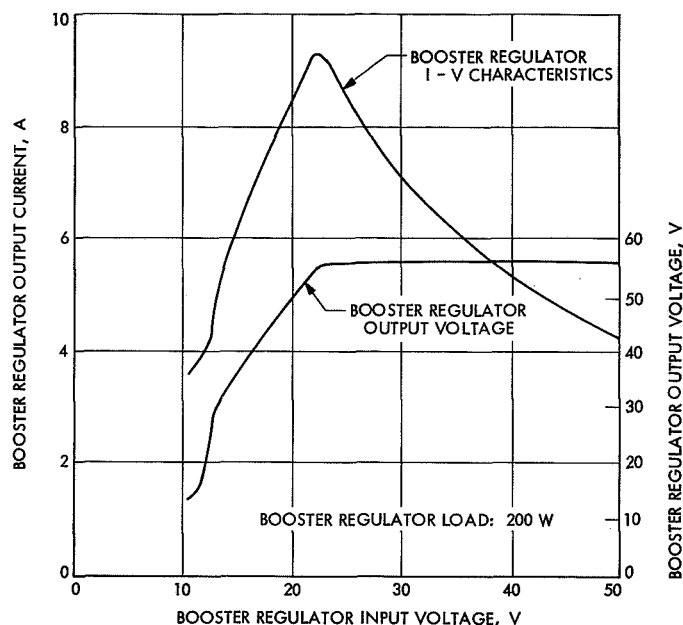


Fig. 75. *Mariner Mars 1969* booster regulator performance characteristics

point of the array resumed its proper location at point C as power was restored to the spacecraft, but with the power subsystem operating with its redundant units. The power chain transfer relay is powered by the dc power bus and will operate at potentials as low as 15 V.

The spacecraft data do not indicate out-of-regulation battery regulator operation, perhaps because of temporary loss of data as the spacecraft reacted to low potentials caused by the transient. An interval of  $4.26 \pm 0.42$  s occurred between the start of the transient and the time of restoration of good spacecraft data that provided the first indication of power chain transfer.

c. *Summary of solar array performance.* Telemetry data received from the solar array short-circuit current-open-circuit voltage ( $I_{sc}$ - $V_{oc}$ ) transducers supplement engineering data from the solar array to assess the array flight performance. The solar cells used to assemble the transducers are typical of those used in the solar array assembly, including cover glass and glass adhesive. Two  $I_{sc}$  transducers are monitored, one of which is pre-irradiated by electron bombardment of  $1 \times 10^{16}$  e/cm<sup>2</sup> at 1 MeV. The short-current output of the irradiated cell ( $I_{ser}$ ) is reduced thereby by about 50% and is rendered relatively insensitive to further radiation damage. Array radiation damage evaluation is consequently aided by data comparison from the short-circuit current transducers during the mission. One  $V_{oc}$  transducer is also monitored.



Evaluation of the  $I_{sc}$ - $V_{oc}$  transducers indicates *Mariner VI* array degradation of 8% after 14 mo in space environment and *Mariner VII* array degradation of 5% after 13 mo. The degradation affected array current output, and, although the cause of the degradation has not been positively identified at this time, it appears that radiation incident to the solar array is the most probable cause. This seems the case because the  $I_{sc}$  transducers degraded on both spacecraft during this interval, whereas the  $I_{scr}$  transducers remained undegraded.

The temperature-sensitive open-circuit voltage transducers of both *Mariner* spacecraft deviated significantly from their prelaunch predicted values on the basis of temperatures indicated by the array temperature transducers. The Sun side array temperatures appeared more reliable, had greater resolution, and were more consistent with spacecraft heliocentric distance when they were derived on the basis of the  $V_{oc}$  output. The  $V_{oc}$  data reduction based upon the revised array temperatures proved more consistent, as did projected array current-voltage and power-voltage characteristics for the various mission phases.

Array surface temperatures derived from the temperature sensors mounted on the rear of the solar panels are more prone to error because: (1) material thermal properties may change with time in space environment and (2) effects on temperature vary as thermal gradients change with heliocentric distance, even with constant thermal properties. On the other hand, array Sun side temperatures based on  $V_{oc}$  data are more representative of true solar cell junction temperature with the noted uncertainties integrated.

The revised *Mariner VI*  $V_{oc}$  data reduction resulted in a small constant deviation from predicted values, which could be explained by the expected small potential change as the cell current output varied with spacecraft heliocentric distance.

The discrepancy of *Mariner VII*  $V_{oc}$  transducer flight data with predicted values remained anomalous despite the use of the revised derivation of array temperature (i.e., anomalous with regard to performance based upon preflight calibration). The cell performance was normal. The *Mariner VII*  $V_{oc}$  cell performance is still under investigation; however, at the time of this report, it appears to track with a constant offset from the *Mariner VI*  $V_{oc}$  cell for a given heliocentric distance. This analysis is derived on the basis of temperatures derived from the *Mariner VI*  $V_{oc}$  at that distance. The constant  $V_{oc}$

offset is 12.1 mV higher for *Mariner VII*; that is, it appears to be 5°C cooler than the  $V_{oc}$  cell on *Mariner VI*.

Figure 76 shows the flight performance and that predicted for  $V_{oc}$  transducers, with data reduction based on array temperatures as indicated by the array temperature transducers. Figure 77 indicates both  $V_{oc}$  flight performance, with array temperatures based on  $V_{oc}$  data, and adjusted predicted performance of the transducer. The predicted performance for the *Mariner VII* transducer (Fig. 76b) is increased (Fig. 77b) by 12.1 mV to compensate for a possible calibration error; the resulting  $V_{oc}$  curves deviate by only the small potential change associated with heliocentric distance and a 1°C temperature error.

Figures 78 and 79 compare the undegraded predicted values of both  $I_{sc}$  transducers with the actual performance until April 30, 1970 and the projected performance. Similar comparisons are made for both transducers in Figs. 80 and 81.

Array voltage limiting by zener diodes started for both *Mariners VI* and *VII* when array temperatures declined to about 10°C on the basis of open-circuit voltage transducer data (see Fig. 82). This array operation occurred about 1-mo before each encounter with Mars (July 2 and 4, 1969 for *Mariner VI* and *VII*, respectively). Heliocentric distance was  $199 \times 10^6$  km. The cruise load for both spacecraft was 274 W at the array at the time, and the average zener diode temperature was estimated at -6.5°C.

Zener diode limiting had been continuous since its start to 14 mo for *Mariner VI* and 13 mo for *Mariner VII*. Predicted orbit parameters indicated zeners were to cease limiting on or about September 9, 1970 for *Mariner VI* and August 7, 1970 for *Mariner VII*, and spacecraft performance indicated this to be the case (spacecraft tracking permitted this time evaluation to be made as close as twice per week).

**6. Extended mission.** *Mariners VI* and *VII* spacecraft data will be used to test the general theory of relativity as the spacecraft approaches superior conjunction with the Sun. The intent is to measure the retardation of the tracking signal as it is affected by the solar gravitational field, and the parameters of the experiment will serve to provide data having the highest resolution to date. *Mariner VI* may be commanded for attitude adjustment to provide optimum high-gain antenna pointing to the Earth for doppler and ranging tracking.

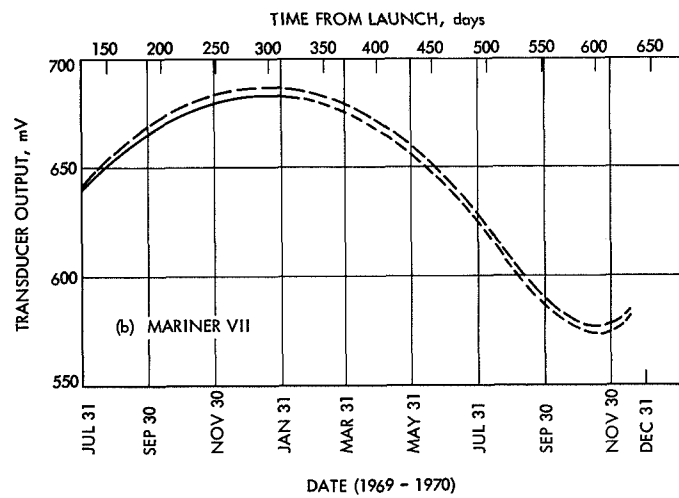
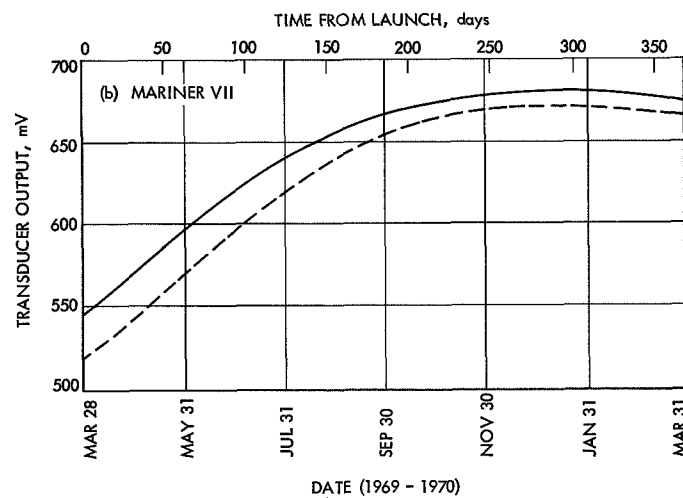
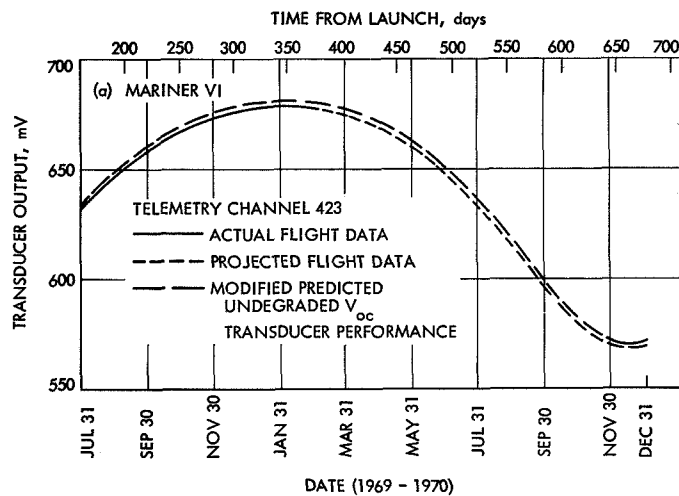
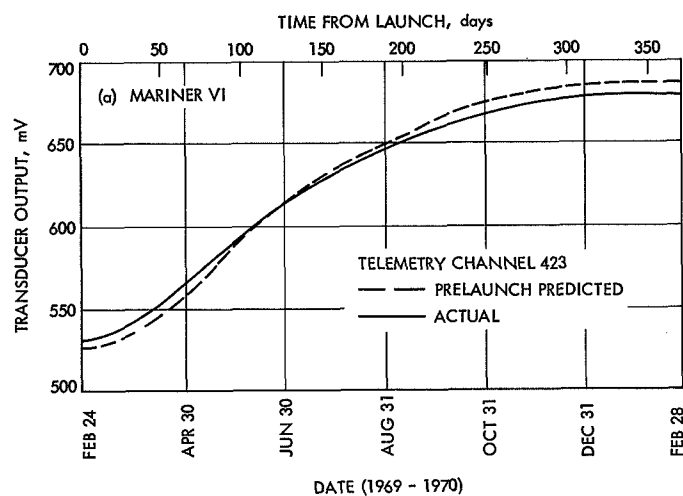


**Fig. 76. Actual vs predicted prelaunch performance of the open-circuit voltage transducer based on array temperature transducer data**

**Fig. 77. Actual and projected vs predicted flight performance of the open-circuit voltage transducer based on  $V_{oc}$  transducer data**

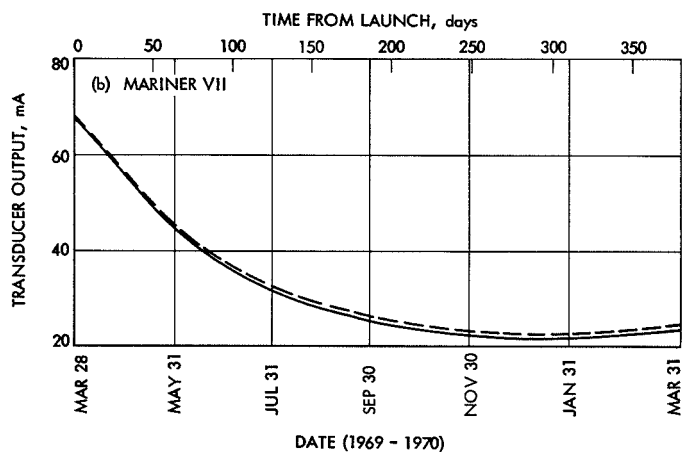
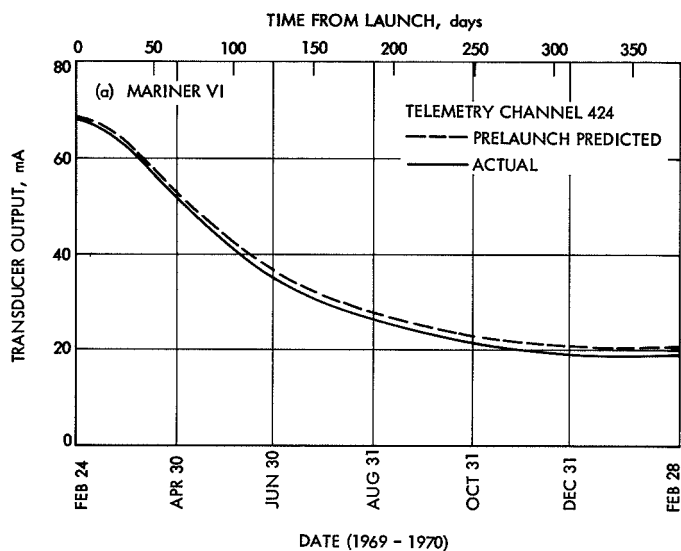


Fig. 78. Actual vs predicted prelaunch performance of the short-circuit current transducer

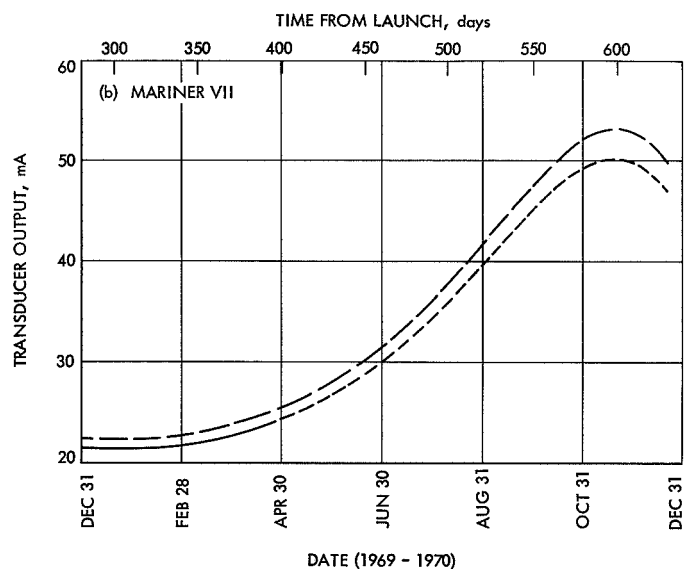
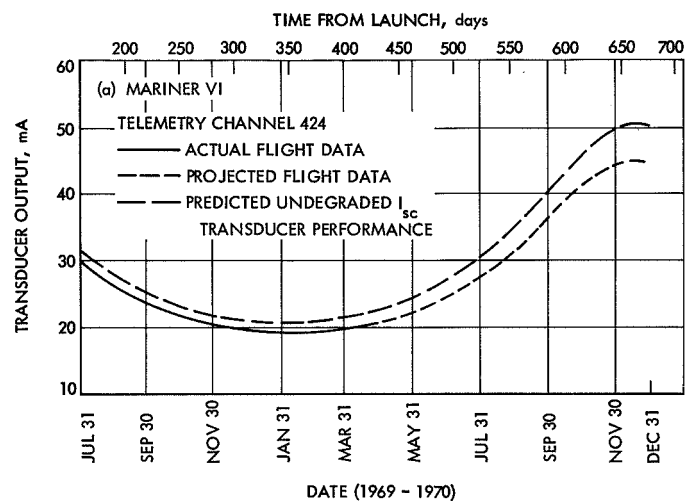


Fig. 79. Actual and projected vs predicted flight performance of the short-circuit current transducer

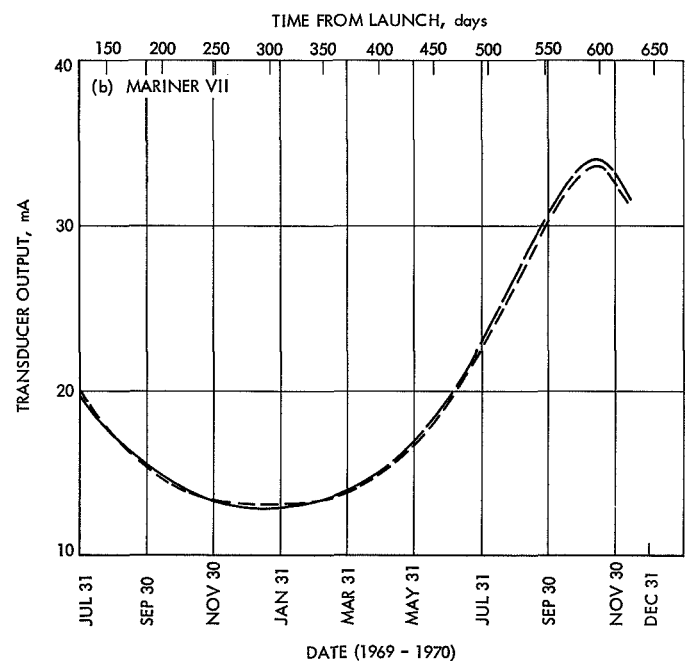
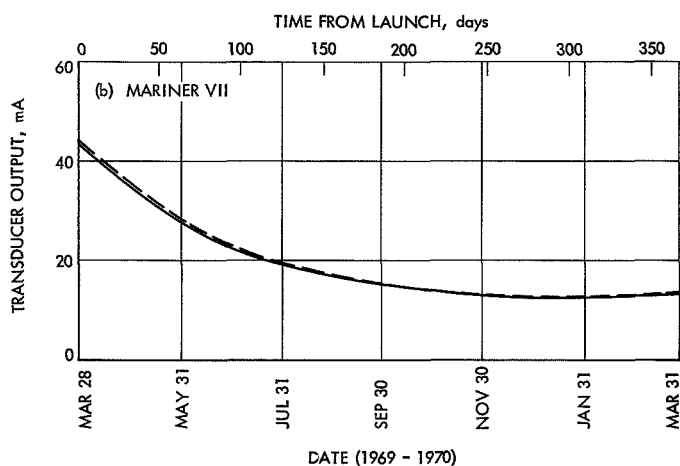
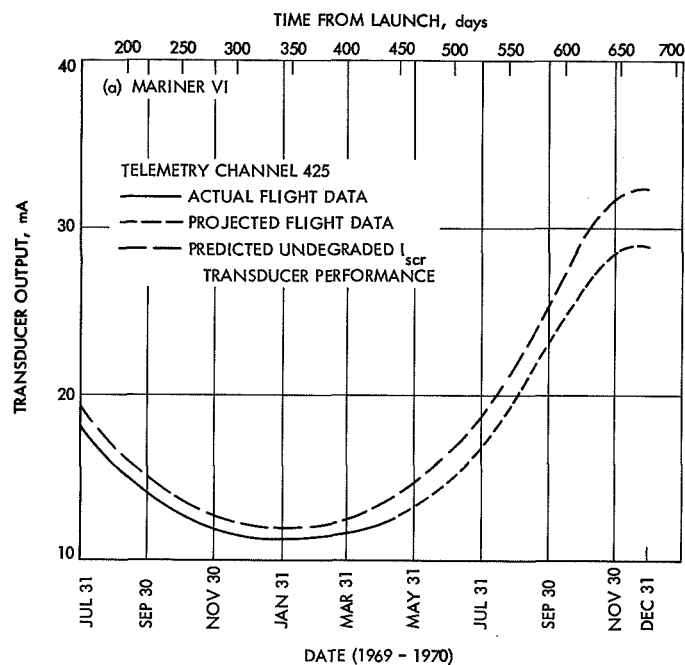
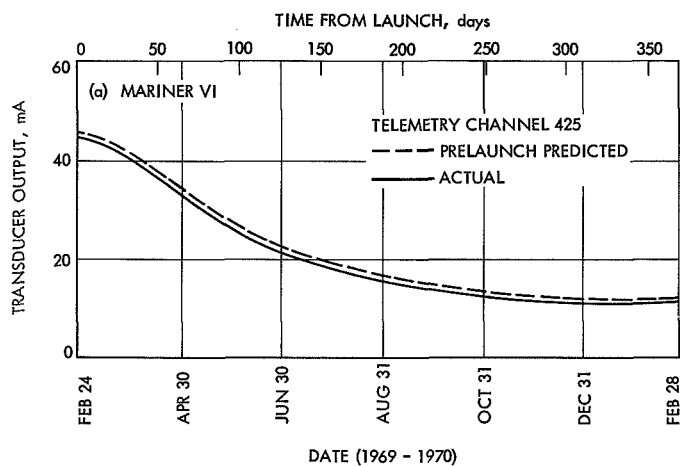
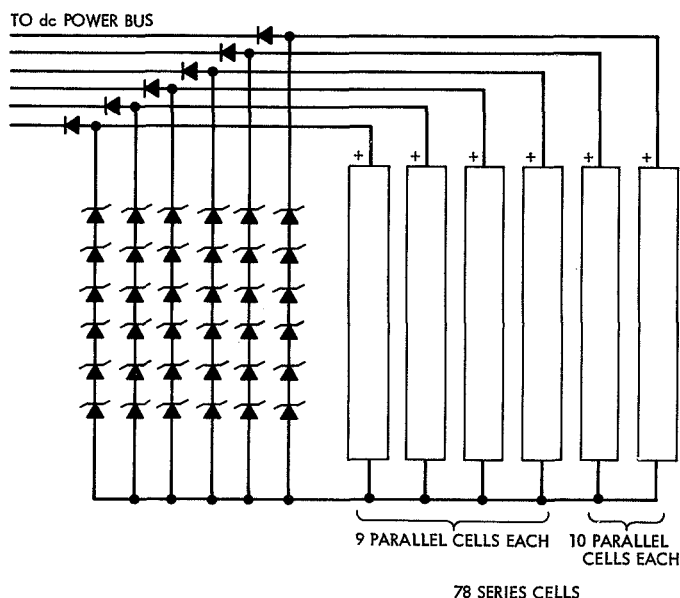
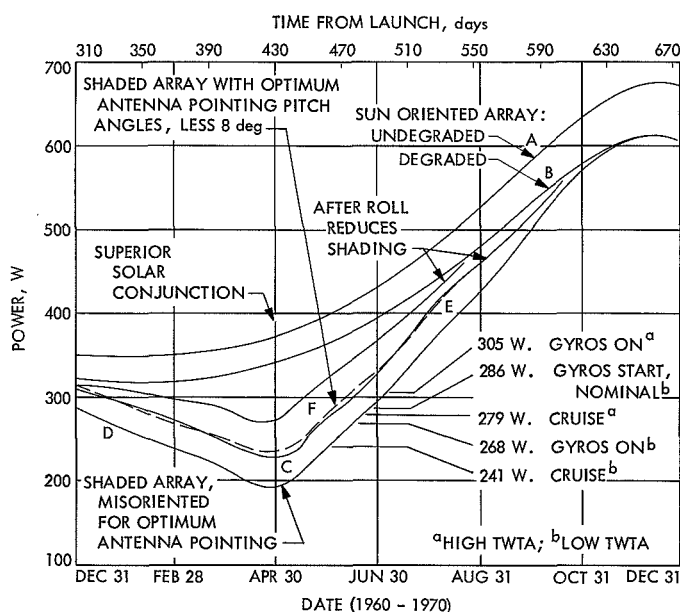


Fig. 80. Actual vs predicted prelaunch performance of the irradiated short-circuit current transducer

Fig. 81. Actual and projected vs predicted flight performance of the irradiated short-circuit current transducer



**Fig. 82. Mariner Mars 1969 solar panel electrical diagram**



**Fig. 83. Projected Mariner VI power subsystem support for extended mission**

Figure 83 shows the projected extended mission power subsystem support for the relativity experiment for *Mariner VI*. Curve A is the estimated Sun oriented undegraded solar array maximum power output as a function of orbit heliocentric distances. Curve B is the normally oriented array as it degraded over this period.

The addition of a 400-kW transmitter to the 210-ft-diam antenna at Goldstone, Calif. was planned to supplement its 20-kW transmitter. Because high-gain antenna pointing to the Earth could have been required if the new transmitter were not operational in time, a study was made to evaluate solar array power output as the spacecraft was maneuvered from the Sun to maintain proper communication.

Spacecraft attitude adjustments for *Mariner VI* Earth antenna pointing are time-variant functions of the spacecraft orbit, and changes in pitch and roll generate a variety of Sun shadow patterns that are cast upon the solar panels by the antennas. The shadows reduce array power output.

Array shadowing tests were conducted at JPL with a *Mariner Mars 1969* spacecraft model in the Celestarium facility. Greater pitch angle magnitudes cause greater power reduction, but roll turn magnitudes that occur after the pitch maneuver redistribute the shadow pattern to cause much of it to fall between solar panels. The roll maneuver thus recovers some of the array power output lost because of antenna shading after pitch. The greater the pitch angle and resulting shadowing, the greater the power recovery after roll.

Curve D in Fig. 83 (*Mariner VI* misoriented from the Sun) shows the estimated maximum power output of the shaded degraded array as it is pitched off the Sun line to start the pitch maneuver that results in maximum shadowing. Curve C shows the estimated maximum power output of the shaded array after the roll turn completes the antenna pointing maneuver and reduces array shadowing. Curves C and D describe array power output as the result of attitude changes to obtain optimum antenna pointing. A similar set of array curves (E and F) are provided for optimum pointing pitch angles that are decreased by 8 deg to obtain greater array power and still maintain adequate spacecraft communication with marginal antenna patterns.

Figure 84 contains estimates of *Mariner VII* solar array performance for the same period, but because of the loss of its battery, this spacecraft is largely restricted to Sun-oriented operation.

Load magnitudes shown for both spacecraft are reflected at the array. The projected maximum power of the curves is decreased by 2% to allow for estimated ripple power that prevents spacecraft operation at the array

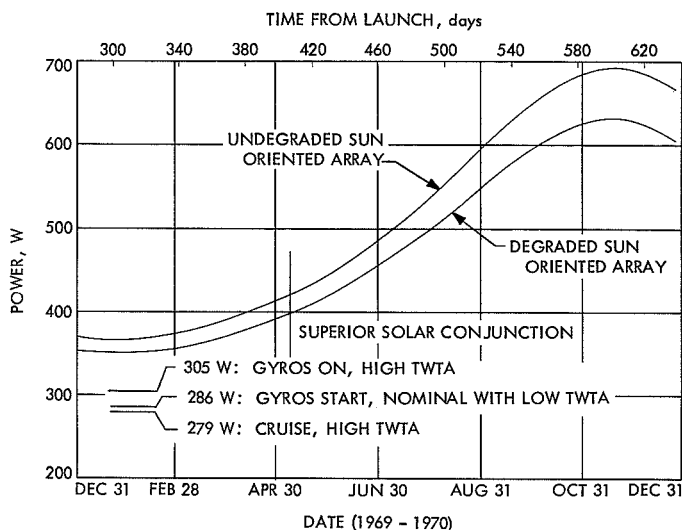


**Fig. 84. Projected Mariner VII power subsystem support for extended mission**

maximum power point. Curves for both spacecraft include a 5% uncertainty factor for possible errors in:

- (1) Shadowing investigation for *Mariner VI*.
- (2) Estimated heliocentric distance and Sun intensity.
- (3) Estimated average array temperature as it is normal to the Sun, and for *Mariner VI* as it is maneuvered from the Sun vector and when shaded.
- (4) Graphic representation of the curves.
- (5) Telemetry.

**7. Conclusions.** Despite the failure of the battery, the power subsystem of *Mariner VII* successfully supported the spacecraft during the 4-month interval to Mars, and beyond (for approximately two years in the space environment). The *Mariner VI* power subsystem had no failure and probably will log a longer lifetime in space because the spacecraft will maintain proper attitude control for a longer period. The *Mariner VII* battery failure fortunately had little effect upon the spacecraft mission performance before and after encounter. The battery of *Mariner VI* had performed nominally and in a predictable manner during the two years in the space environment.

The frequency of the 2.4-kHz inverter has an 0.01% specification and appears to have operated 0.001% slow for the duration of the *Mariner VI* mission. The main 2.4-kHz inverter of *Mariner VII* appears to have oper-

ated 0.0007% slow during a 7-month period of operation, and afterwards, the standby unit was 0.0006% slow for the time it operated. The *Mariner VII* power subsystem automatically switched to its redundant units because of an unusually high power transient when the gyroscopes were switched on (3 November 1969).

**8. Recommendations.** The following improvements to the power subsystem are recommended for future programs.

*a. Charger performance and array operating potential.* The major recommendation for the improvement of the *Mariner* power subsystem regards the interrelation of the design of the solar array and battery charger operation, and the manner that the interrelation was affected by the array operating potential during the mission. The array operating potential has presented design difficulties during the near Earth portion of the mission and has presented undesirable operating characteristics as the spacecraft approached the environment of Mars.

*Series solar cell length.* Battery charging at near Earth with a warm array is one of the important considerations that impacts the design of series configuration of the solar cell circuit on the solar array. The final array design that incorporated 78 series-connected cells would have had an operating potential of 34.5 V, which provided for only partial recharge of the battery at near Earth, for the worst case array temperature of 75°C.

Worst case analyses in the design phase indicated that the slightly short solar cell series length, which provided for partial battery recharge at near Earth, was an acceptable design limitation for the mission. However, in the Mars environment, the solar cell series length proved excessively long, causing the array operating potential to rise to zener cutoff level prior to the planet encounter. The increased array potential was caused by the array operating at cooler temperatures, while the zener limiting voltage decreased as the zener diode junctions cooled.

*Array zener diodes.* The solar array zener diode circuit limited the array voltage at a level that provided about 45.0 V to the input of the booster regulator of *Mariners VI* and *VII*. Array voltage clamping started about a month prior to Mars encounter for both spacecraft, and the zener diode current flow (while the zeners limited the voltage) represented a power loss to the spacecraft during encounter. Future designs should review the requirements for array voltage limiting, and review whether array voltage limiting to obtain a potential as low as 45 V

at the booster regulator input is required to maintain booster regulator loop stability for output power regulation at 56 V. Moreover, the zener component selection should be reviewed for cut-on characteristics at projected diode junction temperatures during the critical mission phases to avoid premature limiting, or account for limiting in the array design.

*Charger design.* The problem regarding the array operating potential appears to center about the battery charger design. Future programs should employ battery charger designs that reduce to a minimum the potential drop across the unit at the full limiting charge rate.

The minimum charger potential drop to attain the limiting charge rate for *Mariner Mars 1969* was 4.0 V. A reduction in the charger potential drop could have required fewer solar cells in series for the array, and still may have enabled full battery recharge at near Earth for the worst case. It may also have resulted in more desirable zener cut-on characteristics, and possibly permitted additional parallel solar cells in the array design to more adequately support the electrical power requirements in the Mars environment, particularly power transients.

*b. Sun gate signal control of boosting.* A greater command flexibility to control the booster converter activity for boosting the power subsystem operation out of a share mode is recommended for future programs. In *Mariner Mars 1969*, the circuit is automatically disabled whenever the array is 6 deg or more from the sun vector. This automatic feature is valuable when the spacecraft is not under ground surveillance, since it could prevent unnecessary battery discharge. A circumstance could arise where the battery continuously powers the boost circuit to pulse the power subsystem out of the share mode to operate solely from the solar array, which may be unable to support the electrical load by itself.

However, future designs should incorporate an added command to enable the boost circuit with significant sun misorientation, if the array could support the spacecraft at the adjusted attitude. This flexibility would prevent a repeat of a circumstance similar to that affecting *Mariner VI* on 8 October 1969, when the pitch portion of a maneuver caused the spacecraft structure to shade the array and precipitate a share mode. A subsequent roll maneuver cast the shadow between solar panels, causing the array power output to increase to the extent that it was again capable of supporting the spacecraft electrical

load, although the spacecraft was still pitched. However, the boost circuit was disabled because of the sun misorientation, and the battery continued to discharge unnecessarily until the sun was reacquired at the termination of the sequence.

*c. Load management.* In future programs, spacecraft command design should avoid the *Mariner Mars 1969* mechanization whereby one command turned on all science instruments, including switching on data automation, data storage, and the scan platform in slew. Not only is there considerable loss of flexibility to manage individual loads during the mission, but the mechanization generates a serious power transient source.

## IV. Engineering Mechanics Subsystem

### A. Structure

The primary function of the *Mariner Mars 1969* spacecraft structure was to integrate the spacecraft subsystems structurally by providing mechanical support and alignment for all flight equipment.

Planet-oriented scientific instruments that required servo-controlled pointing were mounted on a planetary platform (scan platform) located on the lower side of the octagonal framework. The scan platform is a two-degree-of-freedom, gimballed support structure that supplied the articulation and precise mountings necessary to permit the scan-platform instrumentation to acquire and track the planet Mars and for the science instruments to obtain the encounter measurements.

No indications of any failures or anomalies were attributable to structural malfunctions during either the *Mariner VI* or *VII* flight.

### B. Mechanical Devices Performance

The mechanical devices aboard the spacecraft included the following:

- (1) Solar panel boost dampers.
- (2) Solar panel deployment and latch mechanisms, including switch assemblies for indications of deployment of panels.
- (3) Cruise dampers.
- (4) Low-gain antenna dampers.
- (5) Scan-platform release device.

- (6) Pyrotechnic arming switch (PAS).
- (7) Separation-initiated timer (SIT).
- (8) Spacecraft separation mechanisms.
- (9) Spacecraft V-band.

**1. Solar panel boost dampers.** The purpose of the boost dampers, which were pairs of viscously damped struts, was to furnish lateral support between each of the four solar panels during the launch and boost phases of flight. One end of each damper pair was attached through a pyrotechnic pinpuller to a bracket on the tip of the solar panels. The opposite end of each of the damper pairs was attached through a bolted joint to the adjacent panel tip.

**2. Solar panel deployment mechanism.** The solar panels were spring-loaded to deploy from the vertical launch position upon actuation of the pinpullers located on the boost dampers. The spring force was sufficient to ensure deployment without causing the panels to be overstressed when they were stopped in the deployed position. The spring force was supplied by two spirally wound clock springs, located on one hinge of each panel, augmented by booster springs at the damper clevises. Near the fully deployed position, the panel structure momentarily closed an electrical switch that furnished an indication of deployment over the flight telemetry subsystem (FTS).

**3. Cruise dampers.** The cruise dampers were provided to absorb the deployment energy of the solar panels, to locate the panels in the deployed position, and to minimize the interaction between the panels and the autopilot during midcourse maneuvers. The cruise dampers were attached to the outboard face of octagon bays I, III, V, and VII, and latched to the solar panels upon full deployment.

**4. Low-gain antenna dampers.** The low-gain antenna was laterally supported during all phases of flight by two viscously damped struts located about 90 deg apart. One end of each strut was attached to the antenna at approximately one-fourth of its height above the octagon; the other end was attached to the upper surface of the octagon.

**5. Scan platform release device (latch).** The scan platform was latched to the main equipment compartment during the launch and maneuver periods (1) to minimize the design loads for the structure members

and drive mechanisms, and (2) to assure a minimum of dynamic interaction between the platform structure and the autopilot during midcourse maneuvers. The latch mechanism holds the scan platform in its stowed or launch position by means of four pneumatic latch mechanisms manifolded together to obtain parallel release. The latch points are located approximately at the four corners of the basic box structure of the platform, thus forming a broad base for load transfer to the bus structure. Latch preload was applied by pressurizing the manifold to engage T-bar latches at a serrated interface. Piston areas were chosen to give preloads of approximately 5700 lbf at each inboard location and 1600 lbf at the outboard latches when pressurized to 1500 lbf/in.<sup>2</sup> This preload, in conjunction with the serrations, ensured that no joint separation or slippage would occur within the design loads expected at the platform.

Platform latch release was initiated by firing a normally closed pyrotechnic valve to allow manifold venting to space. To minimize the resultant torque reaction on the spacecraft, venting was accomplished through a sintered plug resistor to limit flow rate, and the gas was discharged overboard through a balanced T-fitting. The 4-in. manifold was designed to be vented from 1500 lbf/in.<sup>2</sup> to a nominal unlatching pressure of 24 $\frac{+0}{-1}$  lbf/in.<sup>2</sup> in approximately 60 s upon receipt of the DC-45 (scan-unlatch) command. Piston-return springs were sized to allow the outboard latches to disengage slightly before the inboard latches did.

**6. Pyrotechnic arming switch.** The PAS consisted of a set of electrical switches mounted at the base of the octagon structure. The switches were actuated sequentially when the spacecraft separated from the spacecraft adapter. Switching functions performed were the following: (1) safe-light umbilical function to launch complex equipment (LCE) for the pyrotechnic subsystem before launch; (2) after separation, power turn-on to the pyrotechnic subsystem; and (3) power turn-on to the attitude control subsystem.

**7. Separation-initiated timer.** The SIT provided a means of time-deployed switching to back up the PAS, and also provided other timed events. When the spacecraft was separated from the launch vehicle, an SIT spring-loaded actuation plunger was released to actuate a bank of electrical switches. The switching functions performed were the following: (1) safe-light umbilical function to LCE for the pyrotechnic subsystem before launch; (2) after separation, power turn-on to the



pyrotechnic subsystem; (3) event indication of SIT actuation to flight telemetry subsystem; and (4) command solar panel deployment.

**8. Spacecraft separation mechanisms.** The spacecraft separation mechanisms consisted of four spring-loaded pistons mounted on the spacecraft adapter at alternate corners of the octagon; these were preloaded against pads on the octagon structure to apply to the spacecraft a  $\Delta V$  of  $2.17 \pm 0.33$  ft/s relative to the *Centaur* when the spacecraft was released from the adapter. The spacecraft separation mechanism was designed to impart a tumble rate no greater than 3 deg/s to the spacecraft with respect to inertial space.

**9. Spacecraft V-band.** The spacecraft V-band secured the spacecraft to the adapter by providing a radial force on eight shoes that mated the spacecraft and adapter feet in a V-shaped groove. A V-band tension of approximately 2500 lbf was adjusted by turnbuckles in the band, and monitored by means of strain gages. The V-band was released by two pyrotechnic devices—one each on opposite sides of the spacecraft. Each device made use of two squibs and was individually capable of releasing the spacecraft from the adapter. The V-band was restrained by springs and lanyards to the adapter to ensure unobstructed separation of the spacecraft and a minimum of postseparation free debris.

**10. Performance of mechanical devices.** All mechanical devices on the spacecraft performed extremely well; no anomalies occurred with respect to their function, although the time to unlatch the *Mariner VI* scan platform was considerably longer than predicted. Scan-platform unlatch time was 248 s for *Mariner VI* and 145 s for *Mariner VII*, or about 166 and 65 s longer, respectively, than the preflight predicted time of 80 s. Following the *Mariner VI* event, an investigation of this apparent anomaly revealed that an erroneous unlatch pressure of 50 instead of 24 lbf/in.<sup>2</sup> had been used in calculating the time to unlatch, and that the pressure-discharge resistor was subject to varying degrees of restriction because of debris generated by the pyrovalve. It was found that the 24-lbf/in.<sup>2</sup> unlatch pressure and restricted pressure discharge could combine to produce a total unlatch time up to 250 s. The unlatch time for both flights occurred within this range.

### C. Cabling Subsystem Performance

Physically, the cabling subsystem was separated into three groups according to location: (1) the upper ring

harness, contained by a support structure on the top surface of the octagon; (2) the lower ring harness, supported by the octagonal structure adjacent to the lower periphery of the electronic assembly cases; and (3) the assembly harnesses, used by the seven major electronic assemblies mounted within the octagon to interconnect subassemblies into functional subsystems and to provide connections external to each assembly. External cable harnesses were used to interconnect electronic equipment and devices external to the main assembly bays.

This extensive subsystem performed as designed throughout the mission. The only problem relating to cabling was the discovery, made after launch, that the connections for the bay III solar panel temperature transducers (inboard and outboard) were reversed; this necessitated careful interpretation of the recorded data. An error in the vendor drawing was the cause of this discrepancy, which occurred on both spacecraft.

### D. Temperature Control Subsystem Performance

From the point of view of temperature control, it is convenient to consider the spacecraft as being separable into three main components: the spacecraft bus, the appendages, and the science instrument platform. As on previous *Mariner* spacecraft, temperature control of the bus was accomplished both actively and passively.

Internal power distribution within the bus was such that some bays were completely without power during certain portions of the mission (e.g., bays V and VII except during encounter or playback). For this reason, the previous *Mariner* design philosophy was logically extended to include the use of fixed-resistance ac heaters to provide the bus with substitute power during cruise; this resulted in a more even distribution of power during the entire mission.

The temperature of the appendages (i.e., solar panels, low- and high-gain antennas, Sun sensors, and attitude-control gas jets) was controlled in a manner similar to that used on previous *Mariner* projects; namely, temperatures were passively controlled, wherever possible, by means of thermal shields or appropriate thermo-optical coatings.

Figure 85 shows the location and orientation of the science instruments, the planet sensor, the Mars gates, and the cone-actuator motor on the platform structure.

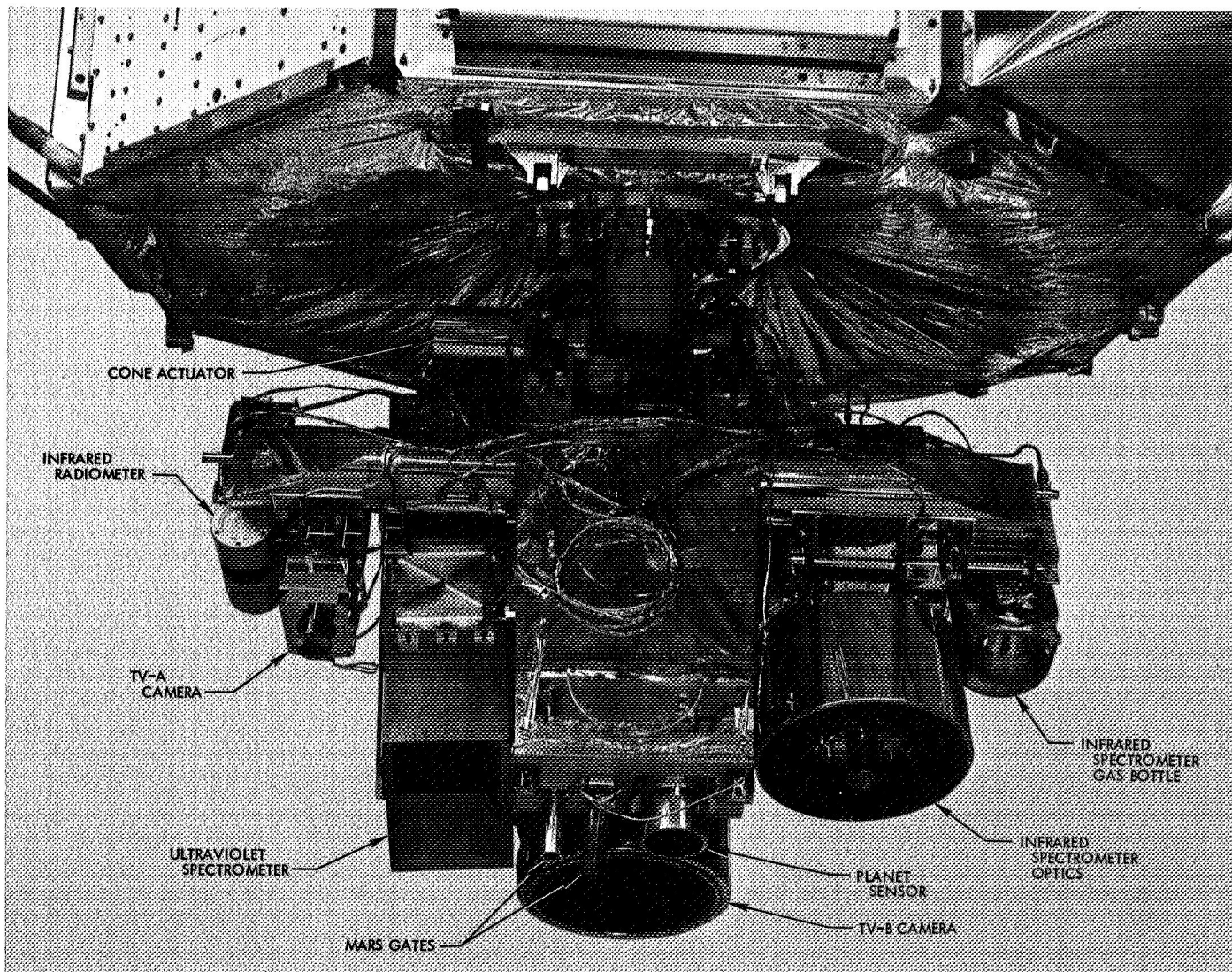


**Fig. 85. Equipment location and orientation on planetary platform**

As mentioned above, the temperature control subsystem used both active and passive methods. Hardware for the active category included thermally activated louver assemblies and both ac and dc heaters; the passive category included superinsulation blankets, polished aluminum shields, and selected surface finishes. Thermal blankets, shields, and louvers covered approximately 95% of the 48-ft<sup>2</sup> surface of the spacecraft bus. Except for the infrared spectrometer (IRS), all instruments on the science platform were enclosed by a thermal blanket with an approximate 18-ft<sup>2</sup> surface area. Items outside the shielding (solar panels, antennas, and attitude-control gas jets) were passively controlled by surface finishes.

**1. Temperature measurement.** The flight telemetry subsystem provided 26 on-board flight temperature measurements. Figure 86 shows the temperature-measurement mechanism. Characteristics of the transducers are listed in Table 24.

**2. Performance.** The temperature control subsystem performed as designed throughout both flights; all equipment was maintained within allowable temperatures, and values were very close to those predicted. Allowable

temperature ranges for both operating and nonoperating periods are listed in Table 25. The predicted and actual flight temperature data are shown in Fig. 87 for *Mariner VI* and in Fig. 88 for *Mariner VII*.

**Table 24. General specifications for temperature transducers**

Parameter	Specification
Operating range	-300 to +300°F
Calibration	
Points	LN <sub>2</sub> , 32°F, 125°F, 212°F
Temperature accuracy	±0.25°F
Resistance accuracy	±0.1 % resistance
Resistance	500 Ω ±1 % at 75°F, types 1 and 2 125 Ω ±1 % at 75°F, type 3
Resistance change over temperature range	606.6 Ω nominal, types 1 and 2 151.6 Ω nominal, type 3
Maximum current (continuous)	20 mA rms
Maximum peak current	40 mA for 3.33 ms or less
Thermal time constant	Less than 2.5 s in agitated water
Insulation resistance	Greater than 10 MΩ at 500 Vdc
Repeatability	±0.25°F
Environment	Capable of passing JPL type-approval and flight-acceptance tests

**Table 25. Equipment operating and nonoperating temperature limits**

Equipment or assembly	Operating limits, °F		Nonoperating limits, °F		Equipment or assembly	Operating limits, °F		Nonoperating limits, °F	
	Min	Max	Min	Max		Min	Max	Min	Max
Bay I (power)	32	130	-4	167	Battery	55	85	32	140
Bay II (propulsion)	40	90	40	90	Sun sensor	-13	130	-50	167
Bay III (gyros and CC&S <sup>a</sup> )	32	130	-4	167	Canopus sensor	20	100	-4	130
Bay IV (telemetry and command)	32	130	-4	167	Solar panels	-175	167	-200	212
Bay V (data storage)	32	130	-4	167	Infrared radiometer	-4	32	-22	122
Bay VI (radio VCO <sup>b</sup> and auxiliary oscillators—TWT <sup>c</sup> 1 and 2)	32	130	-4	167	TV-A camera (wide-angle)	-4	86	-22	122
	50	148	-4	194	TV-B camera (narrow-angle)	-4	86	-22	122
Bay VII (science equipment)	32	130	-4	167	Ultraviolet spectrometer	-4	68	-22	122
Bay VIII (power regulator)	32	130	-4	167	IRS <sup>d</sup> electronics	-54	-27	-60	104
					IRS radiator	-170	-132	-170	104
					Clock cone actuators	-4	131	-40	167

<sup>a</sup>CC&S = central computer and sequencer.

<sup>b</sup>VCO = voltage-controlled oscillator.

<sup>c</sup>TWT = traveling-wave tube.

<sup>d</sup>IRS = infrared spectrometer.

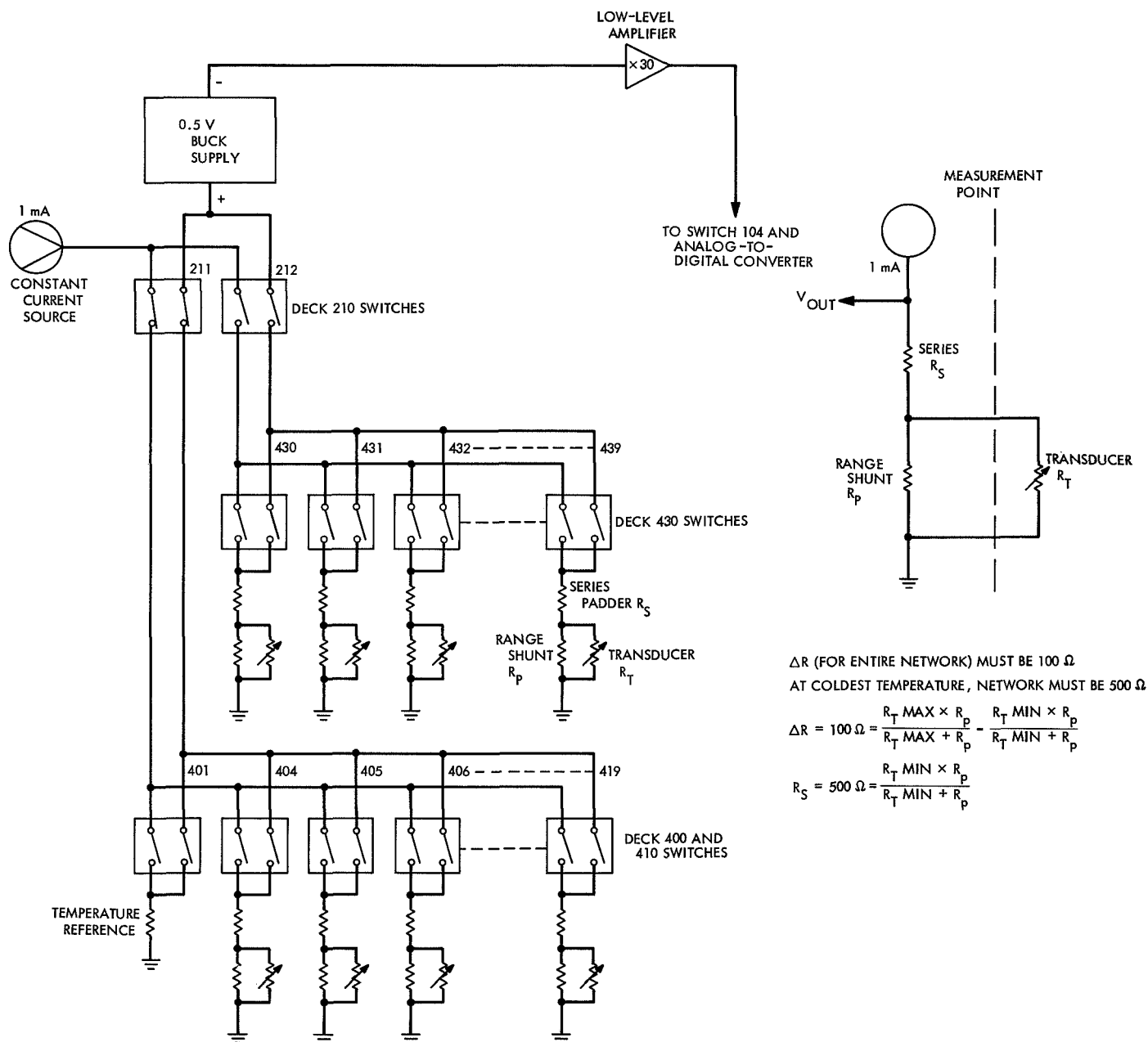


Fig. 86. Temperature measurement mechanism

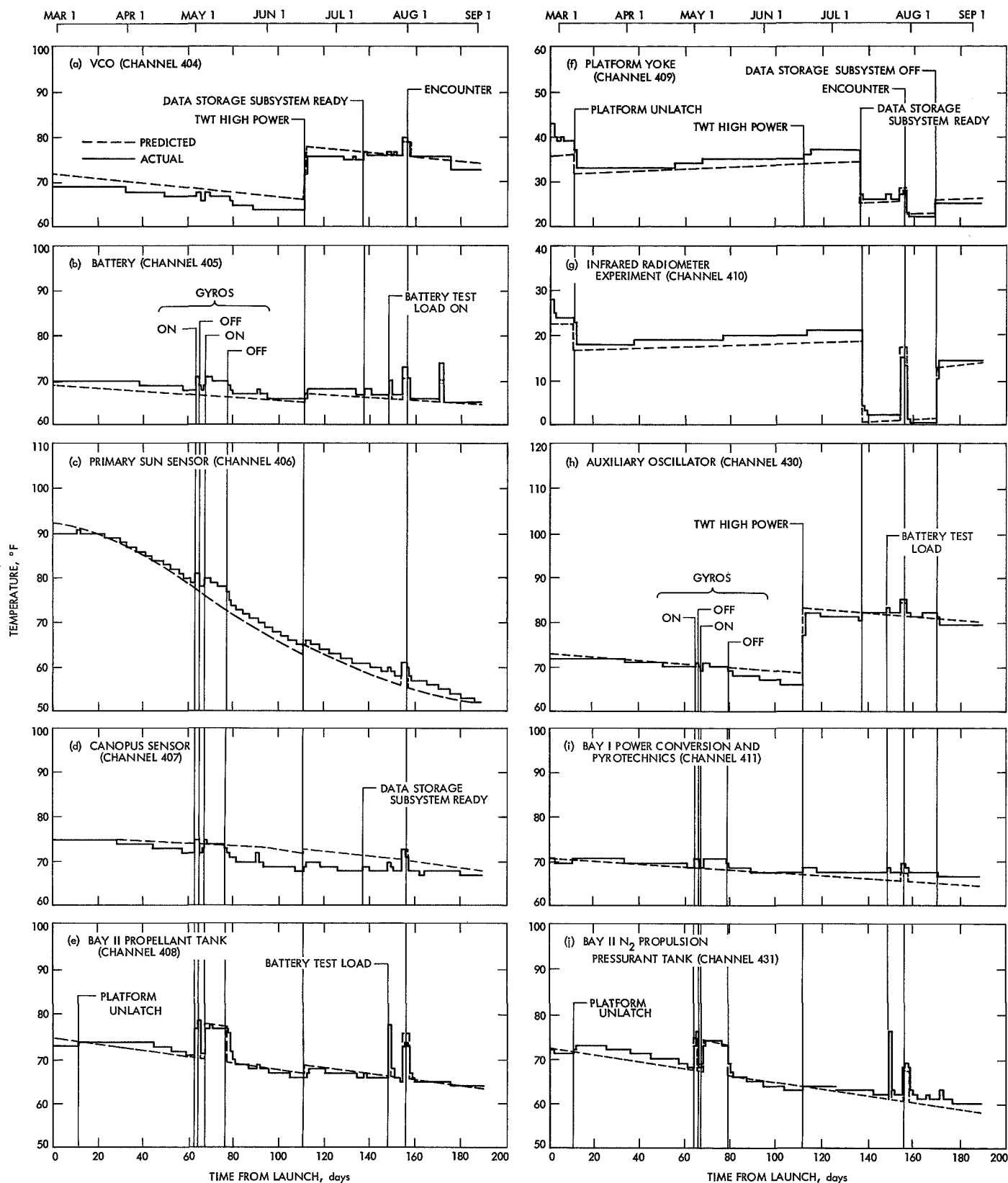


Fig. 87. Mariner VI flight temperatures

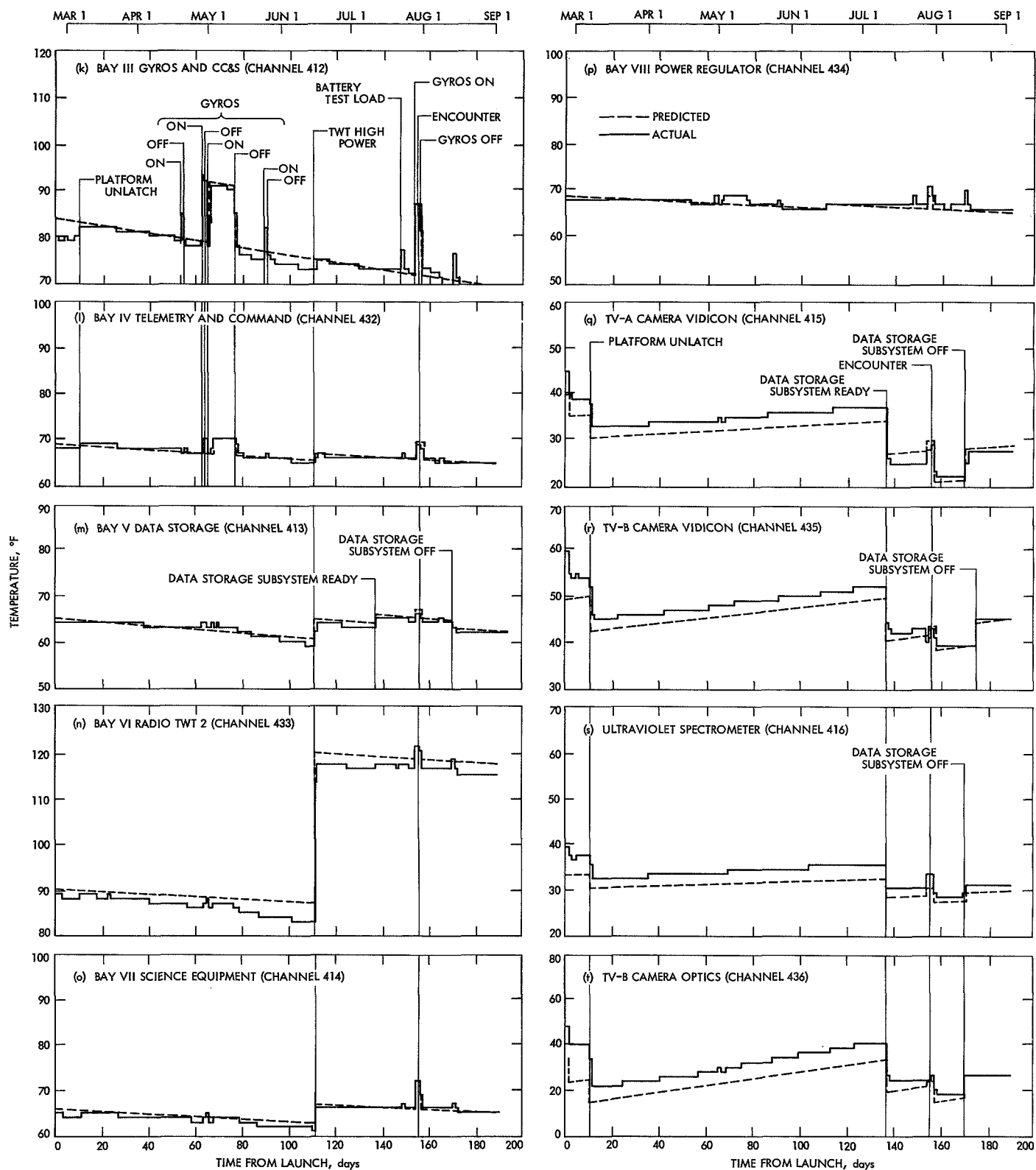


Fig. 87 (contd)

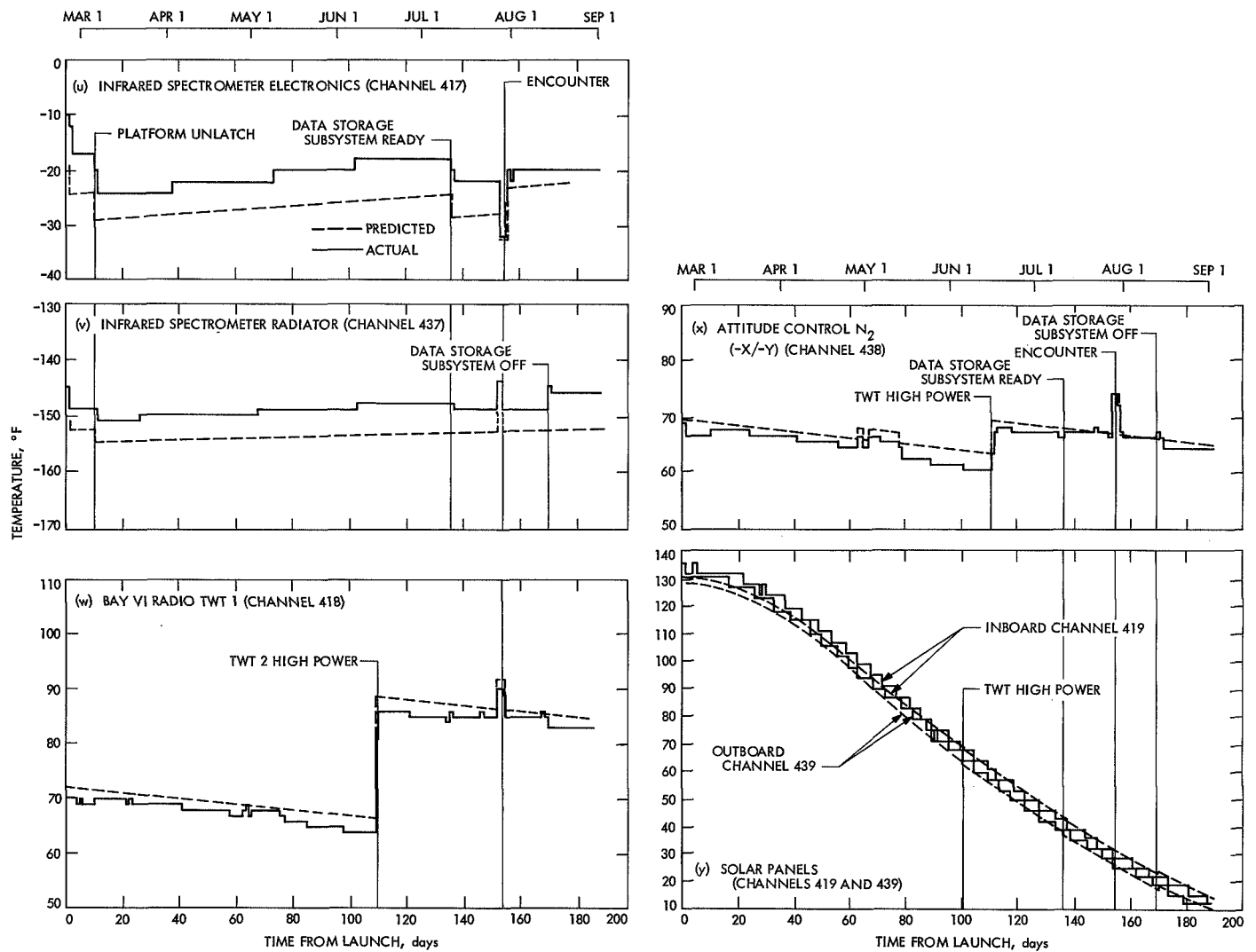


Fig. 87 (contd)

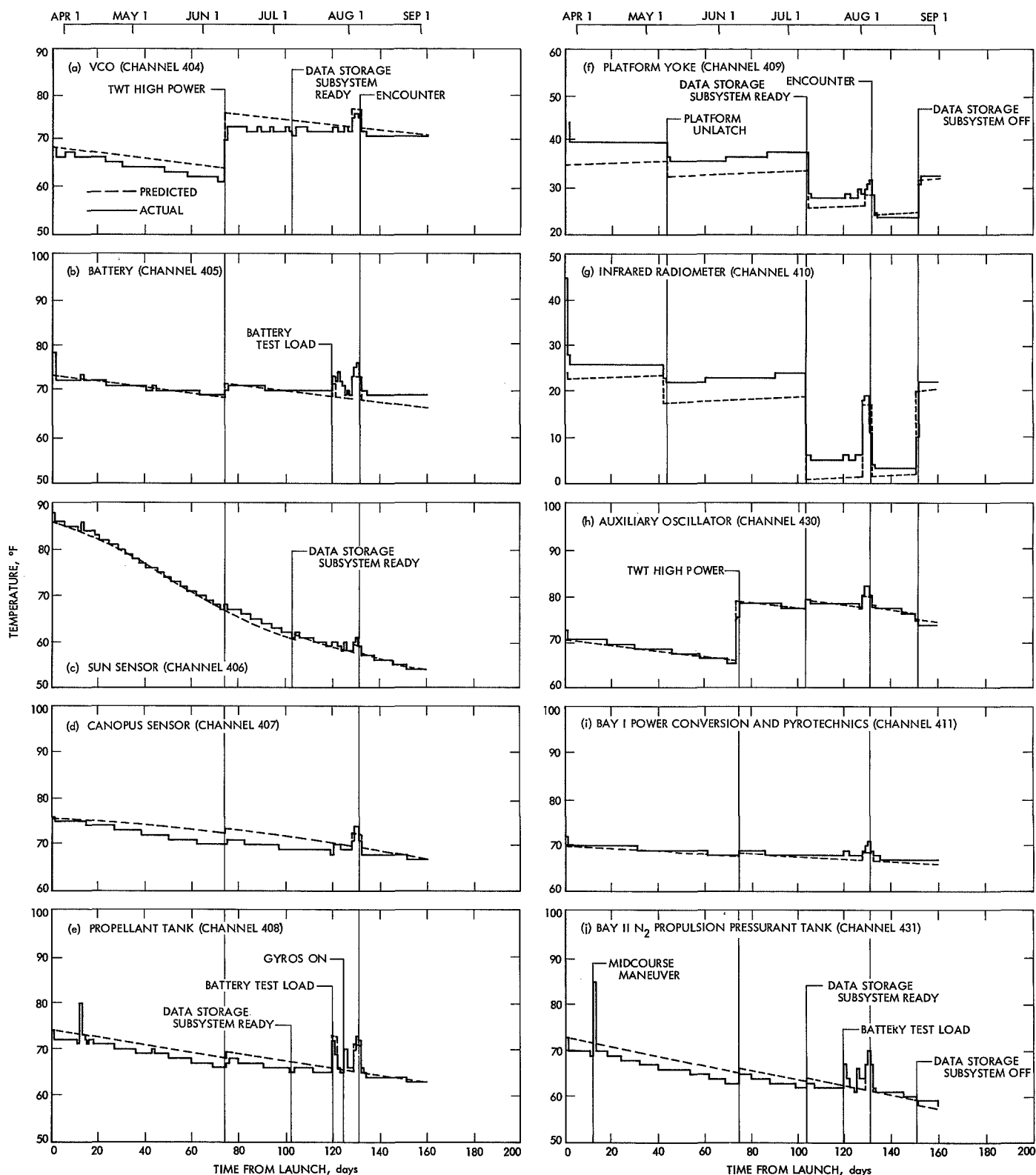


Fig. 88. Mariner VII flight temperatures



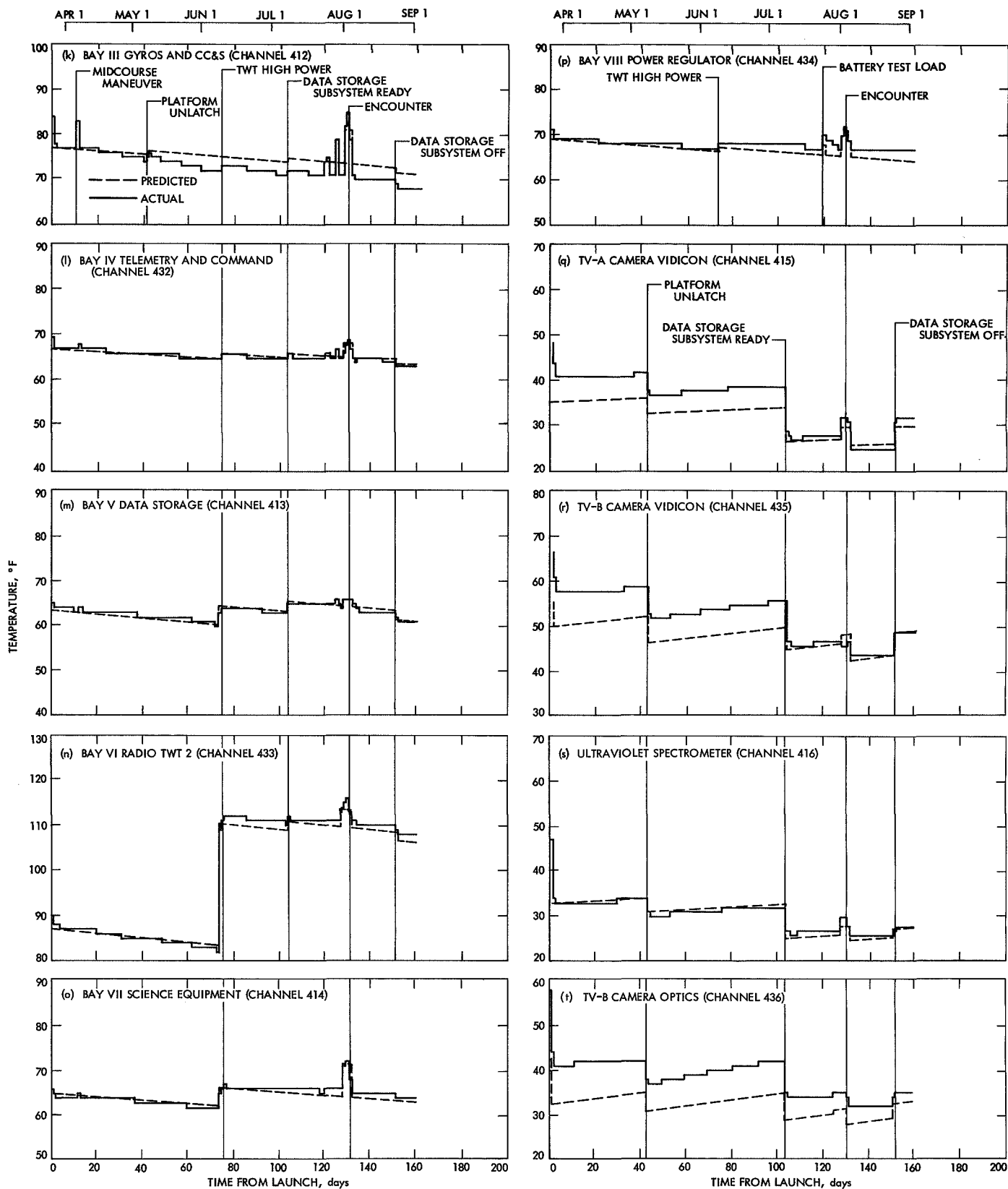


Fig. 88 (contd)

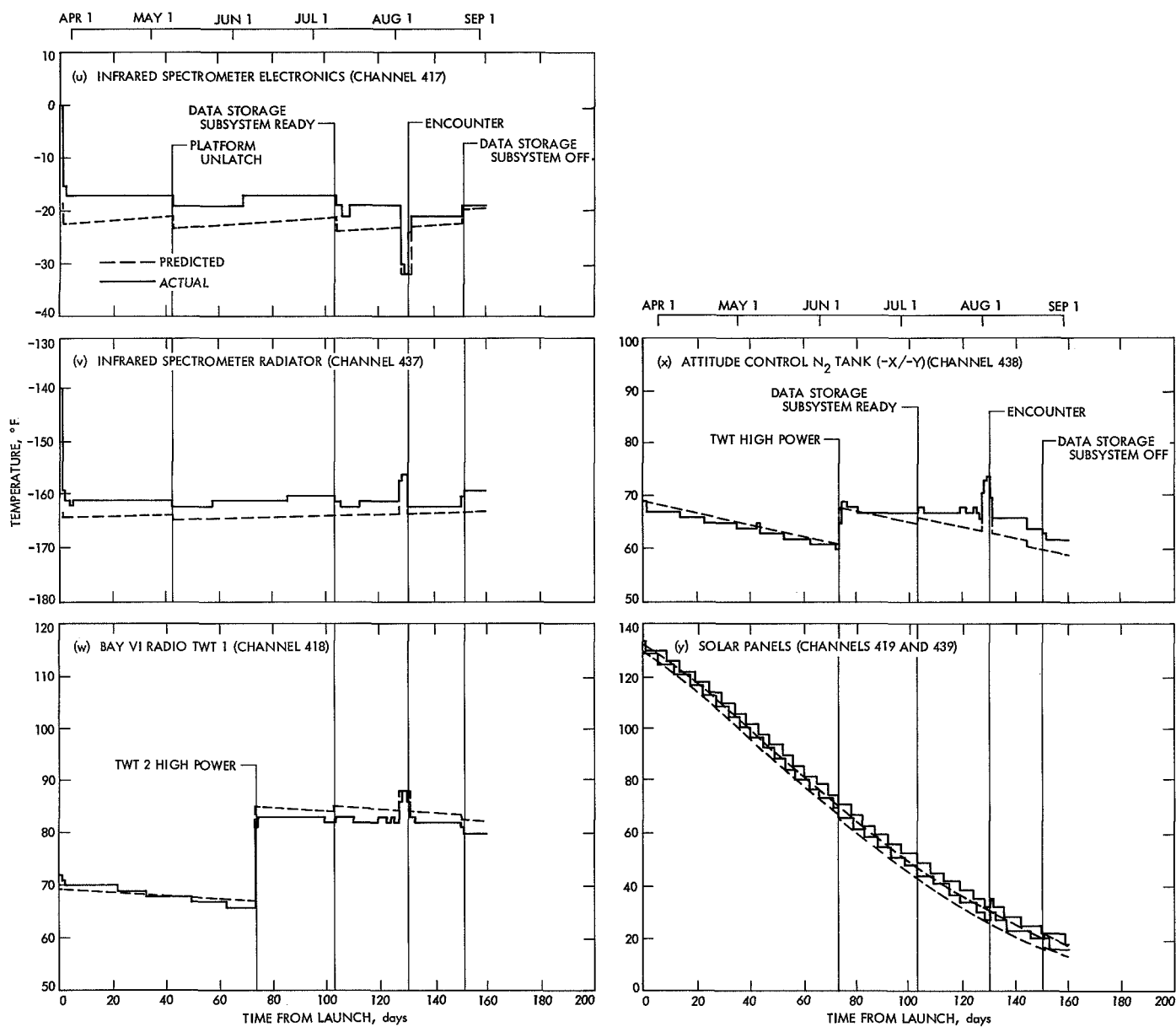


Fig. 88 (contd)

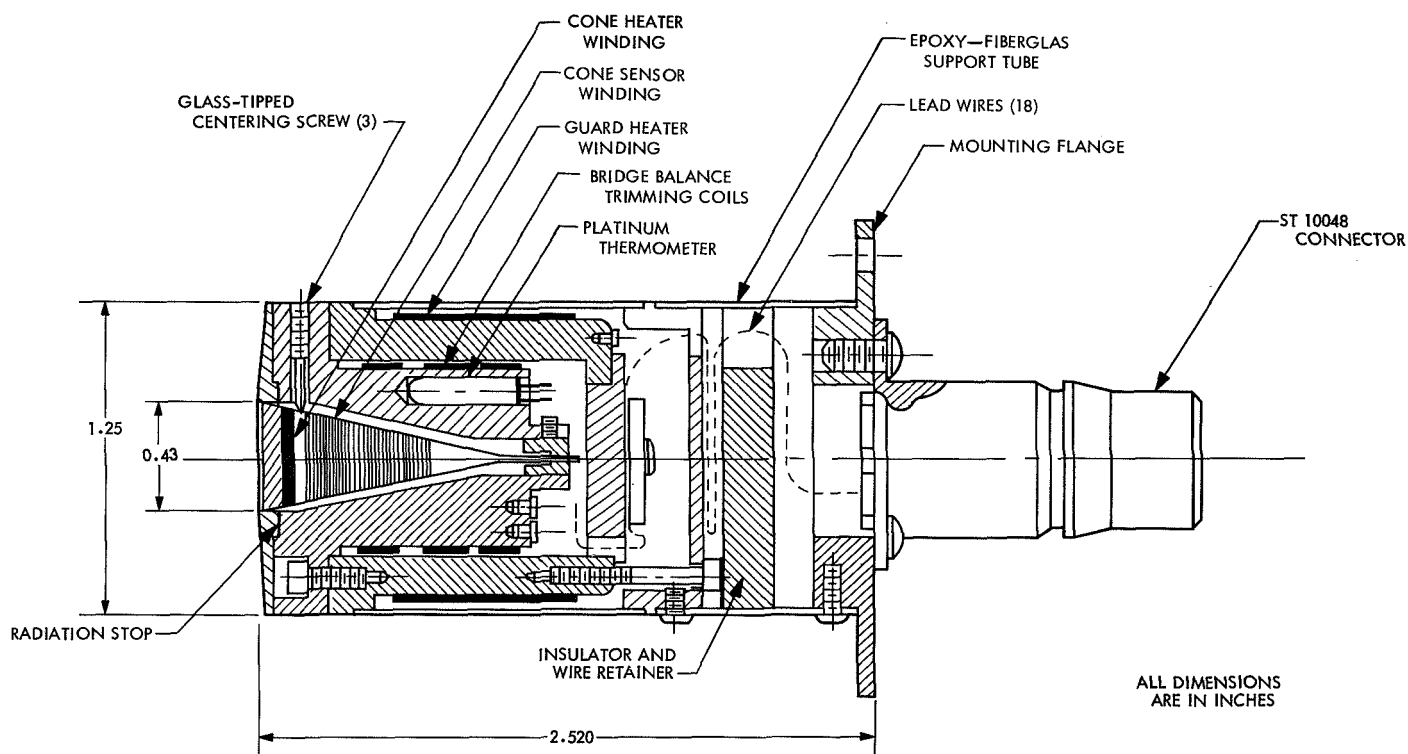


Fig. 89. Temperature control flux monitor transducer

#### E. Temperature Control Flux Monitor Performance

The temperature control flux monitor (TCFM) was flown on *Mariners VI* and *VII* as an engineering experiment designed to make a more accurate determination of the integrated solar flux. The unit consisted of a transducer and necessary supporting electronic circuits to provide power and signal conditioning. The transducer, which weighed 0.25 lb and used 1 W of power, was located at the top of the low-gain antenna; there it received sunlight with a minimum of reflected light from other parts of the spacecraft, and was not shadowed by other spacecraft hardware. The electronics, which weighed 4.5 lb and used 6 W of power, were packaged in the main equipment compartment of bay I. A schematic view of the transducer is shown in Fig. 89.

**1. Temperature measurement.** The TCFM measurements were absolute in the sense that calibration against a radiometric source was not required. The absolute measurement error was less than  $\pm 1.5\%$  and the relative resolution error was  $\pm 0.04\%$ . The sensing or active element of the detector was a conical cavity. Except for the aperture, the cavity was surrounded by a thermal guard for the purpose of providing a controlled environment around the cavity. The transducer body was main-

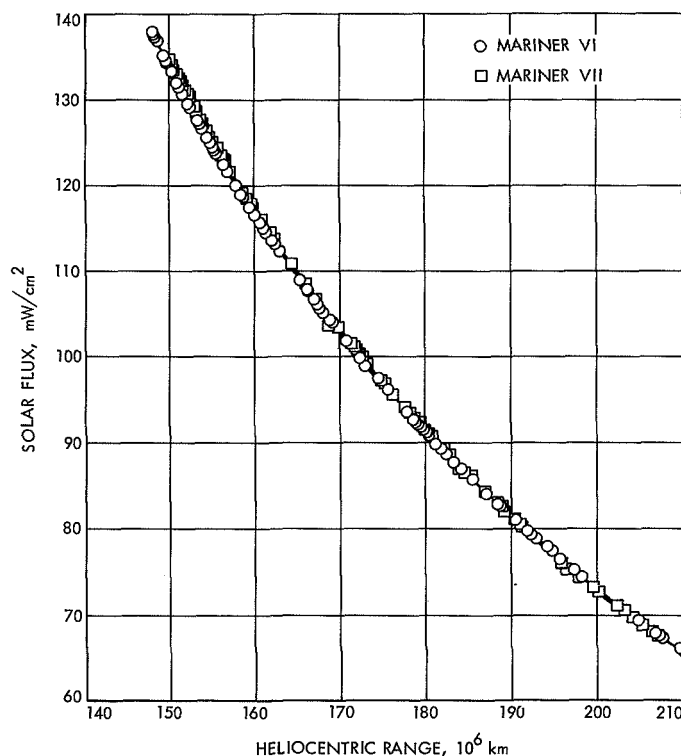


Fig. 90. Solar flux vs heliocentric range, *Mariners VI* and *VII*

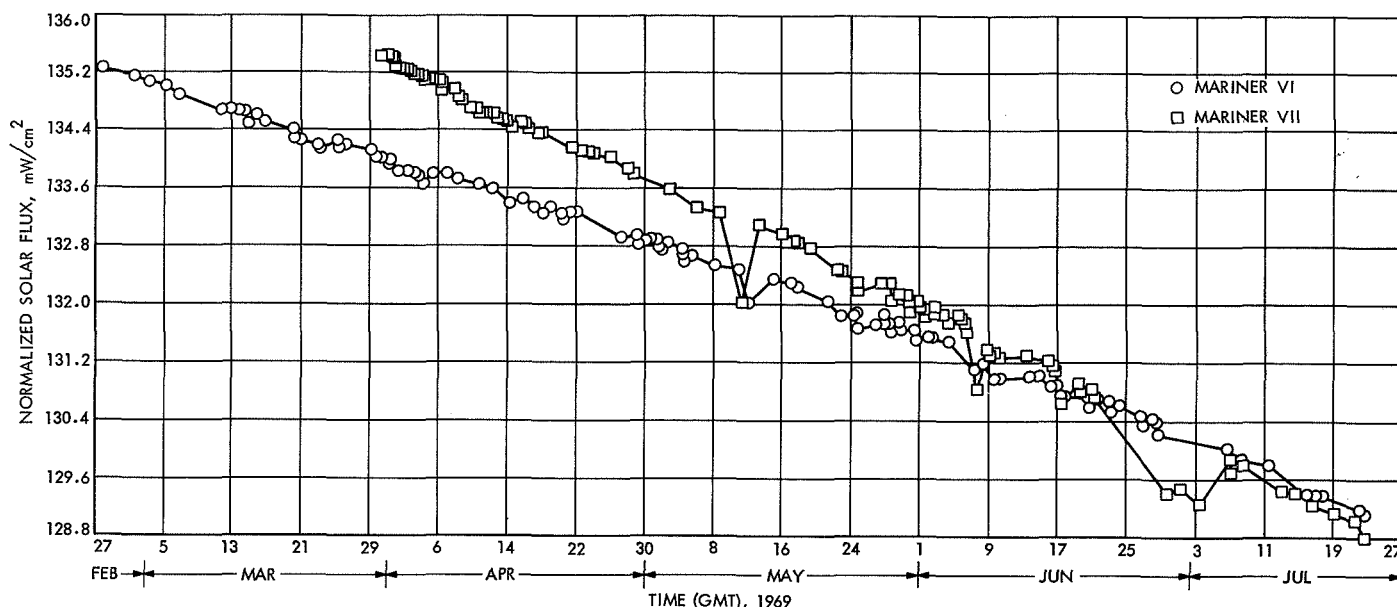


Fig. 91. Solar flux (normalized to 1 AU) vs time for *Mariners VI and VII*

tained within  $\pm 0.1^\circ\text{C}$  of a preselected temperature by an electronic control unit. Electrical power was applied to the cone to slave its temperature to within  $\pm 0.1^\circ\text{C}$  of the guard temperature. The power required to slave to cone temperature was measured, and the unknown radiation entering the cone was determined from

$$I_{\text{unk}} = \frac{\epsilon}{\alpha_s} \sigma T^4 - \frac{P}{\alpha_s A}$$

where

$I_{\text{unk}}$  = unknown radiation

$\sigma$  = Stefan-Boltzmann constant

$T$  = preselected guard temperature

$P$  = electrical power to cone

$A$  = cone aperture area

$\epsilon, \alpha_s$  = effective radiation properties of cone

**2. Performance.** The flight measurements made by the two flight units are presented in Fig. 90 as a function of heliocentric range. Figure 91 indicates the same data normalized or corrected to 1 AU and plotted against time in days. The negative slope of these curves is approximately 5%. These data conflict with the concept of a constant solar intensity vs time and the  $\pm 1.5\%$  error limit of the TCFM.

To resolve this apparent discrepancy, an inflight calibration of the TCFM aboard *Mariner VI* was made. After encounter, a pitch turn of about 100 deg was performed. The calibration obtained showed a significant shift in the zero point of the instrument. By use of this calibration, and the assumption that all of the drift had occurred in the set point of the instrument, a new temperature was computed and an exponential equation for set-point temperature vs time was fitted to the flight data. As shown in Fig. 92, a good horizontal plot resulted, giving an average solar constant of 135.25 mW/cm<sup>2</sup>. This value is 3% less than the heretofore accepted value of 139.6 mW/cm<sup>2</sup>.

A similar recalibration of the *Mariner VII* temperature control flux monitor was not possible, as the spacecraft

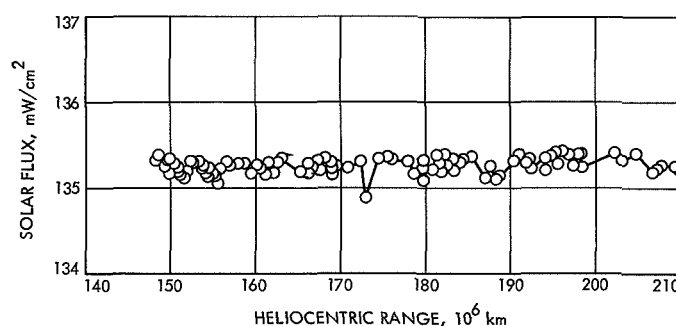


Fig. 92. Normalized solar flux vs heliocentric range for *Mariner VI* (corrected for drift)

could not be pitched off the Sun because of a battery failure.

## V. Propulsion and Pyrotechnics

The *Mariner* Mars 1969 propulsion subsystem provided the impulse required for trajectory-correction maneuvers. Capability to perform two maneuvers was incorporated into the monopropellant hydrazine engine with a nominal thrust of 51 lbf.

The *Mariner* Mars 1969 pyrotechnic subsystem actuated, on command, the solar panel pinpullers, the propulsion start and stop valves, the scan latch valve, and the infrared spectrometer (IRS) gas valves. Simultaneous with the initiation of cooldown, the pyrotechnic subsystem supplied the start command to the IRS scan motor.

### A. Propulsion Subsystem Performance

1. *Mariner VI*. Performance characteristics of the *Mariner VI* propulsion subsystem (Fig. 93) are shown in Table 26. These data were obtained during prelaunch testing and served as the basis for the maneuver burn duration prediction.

During the launch of *Mariner VI*, the thrust chamber pressure transducer measured the expected decline in

**Table 26. Nominal performance characteristics of the Mariners VI and VII propulsion subsystems**

Characteristic	<i>Mariner VI</i>	<i>Mariner VII</i>
<b>Engine performance<sup>a</sup></b>		
Thrust (without jet vanes), lbf	51.10	51.76
Thrust coefficient	1.703	1.716
Characteristic exhaust velocity, ft/s	4349	4371
Specific impulse, lbf-s/lbm	230.2	233.2
Cold throat area, in. <sup>2</sup>	0.1516	0.1498
Regulator set pressure (at 70°F), psia	311.9	302.4
Propellant mass loaded at AFETR, lbm	21.48	21.54
Maximum velocity increment capability at launch (at 70°F), m/s	57.47	58.80
<sup>a</sup> At 70°F, propellant flow rate = 0.222 lbm/s.		

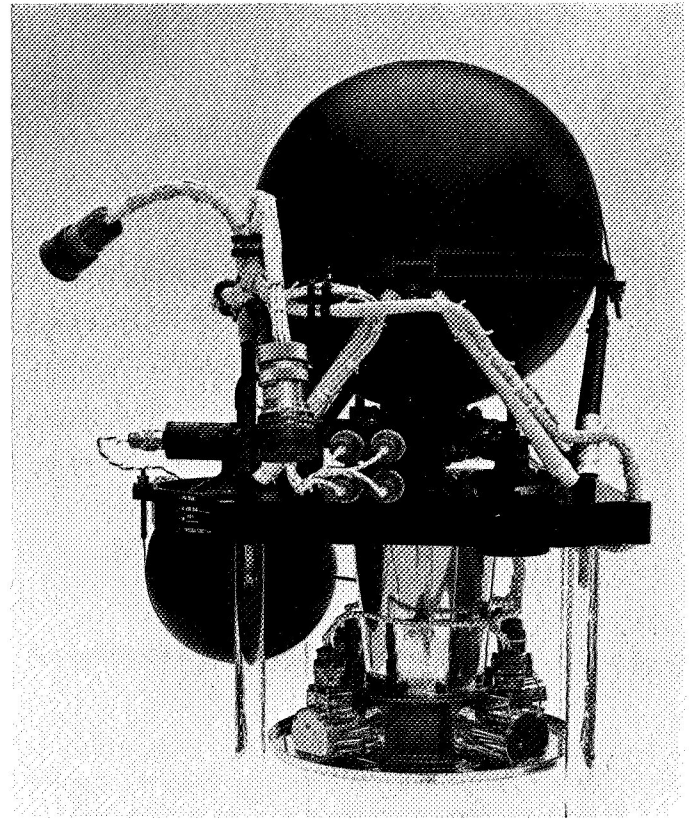


**Fig. 93. Mariner Mars 1969 propulsion subsystem**

ambient pressure as the nose fairing vented. Propellant and nitrogen tank pressures responded to temperature changes as predicted. No evidence of leakage from either tank was detected during this or later stages of the mission.

The planned trajectory-correction maneuver was performed on March 1, 1969, four days after launch. Tracking data indicated that nominal launch vehicle performance had been obtained, and the desired velocity increment for the correction maneuver was very nearly that required to remove the injection bias. The final maneuver calculations gave a desired spacecraft velocity increment of 3.0813 m/s. As shown in Table 27, this corresponded to a predicted engine firing duration of 5.3724 s. The duration was rounded to 5.350 s to provide an integral number of central computer and sequencer (CC&S) timing pulses (at 20 pulses/s). This was the commanded firing duration and corresponded to a predicted velocity increment of 3.0679 m/s.

The DC-27 command used to start the maneuver sequence was timed to insure that the propellant tank

**Table 27. Desired, predicted, and actual Mariner VI trajectory-correction maneuver performance**

Parameter	Desired	Predicted	Actual
Velocity increment, m/s	3.0813	3.0679	3.1456
Burn duration, s	5.3724	5.350	5.350 <sup>a</sup>
Thrust chamber pressure, psia	—	191.8	191.9 ± 1.2
Propellant tank pressure, <sup>b</sup> psia	—	311.9	313.0 ± 2.0
Propulsion N <sub>2</sub> tank pressure, <sup>b</sup> psia	—	2827	2809 ± 15

<sup>a</sup>Rounded to an integral number of CC&S timing pulses at 20 pulses/s.  
<sup>b</sup>After motor burn.

pressure would be sampled immediately after the end of the engine firing. This provided a measure of the regulator operating point at the time the stop valves terminated nitrogen and propellant flow. Since the measurement was in the low-low deck (channel 428) and was sampled only once every 14 min, the transmission of the DC-27 command was timed to place this measurement after shutdown but before thermal soak-back from the hot engine could elevate the tank pressure. As shown in Table 27, the propellant tank pressure, a single measurement of thrust chamber pressure obtained during the engine firing, and the nitrogen tank pressure subsequent to the firing were as predicted.

Analysis of trajectory data indicated that a velocity increment of 3.1456 m/s was actually imparted to the spacecraft. This represented an error of 2.53%, or  $2.01\sigma$ . No specific cause for an error this large was observed in the limited telemetry data obtained. This first maneuver was deemed sufficiently accurate to meet mission objectives, and the remaining correction capability was not used.

Postmaneuver cruise was characterized by a gradual increase in propellant tank pressure as a result of slow decomposition of the hydrazine. Such decomposition, which had been observed on all previous *Mariner* flights, is induced by small amounts of impurities in the butyl rubber bladder. As shown in Fig. 94, decomposition produced a pressure increase totaling 42 psia at encounter. This was well within acceptable limits and posed no threat to the spacecraft. The nitrogen tank pressure-temperature history is shown in Fig. 95.

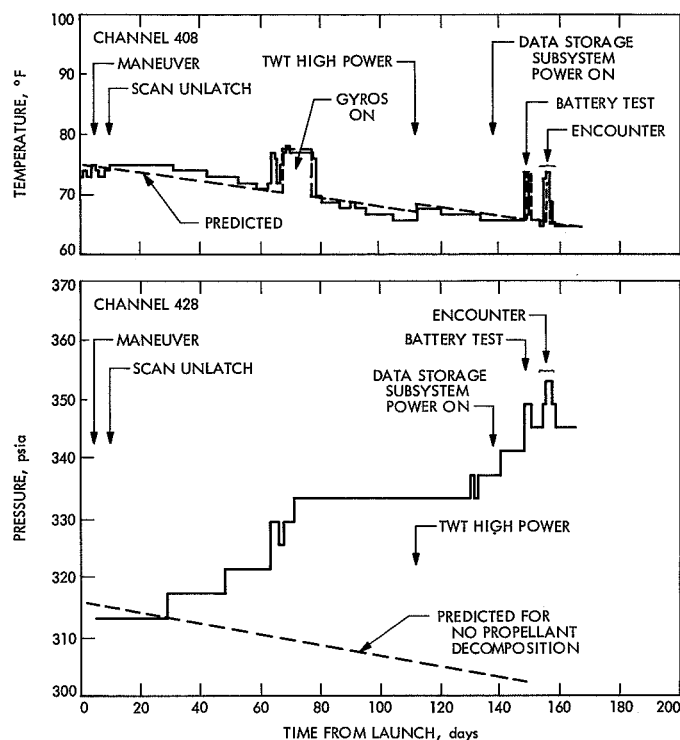


**Fig. 94. Mariner VI propellant tank temperature-pressure history**

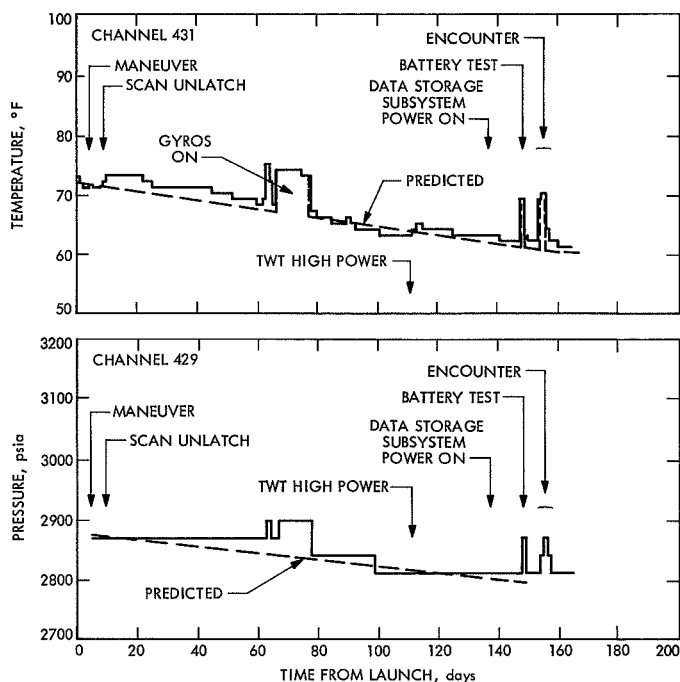


**Fig. 95. Mariner VI propulsion nitrogen tank temperature-pressure history**

**2. Mariner VII.** Performance characteristics of the *Mariner VII* propulsion subsystem are shown in Table 26. These data, which were obtained during prelaunch testing, served as the basis for the maneuver burn duration prediction.

During the launch of *Mariner VII*, the pressure under the nose fairing declined in similar fashion to that observed during the ascent of *Mariner VI*. Propellant and nitrogen pressures responded as predicted to small temperature changes. No evidence of leakage from either tank was observed during the launch phase, and the tanks appeared to remain leak-tight throughout the mission.

The planned trajectory-correction maneuver was performed on April 8, twelve days after launch. As with *Mariner VI*, a near nominal maneuver was required, with a desired spacecraft velocity increment of 4.3111 m/s. As shown in Table 28, this corresponded to an engine firing duration of 7.63 s. This was rounded to 7.60 s to provide an integral number of CC&S timing pulses and resulted in a predicted velocity increment of 4.2920 m/s.

**Table 28. Desired, predicted, and actual *Mariner VII* trajectory-correction maneuver performance**

Parameter	Desired	Predicted	Actual
Velocity increment, m/s	4.3111	4.2920	4.2879
Burn duration, s	7.6325	7.600	7.600 <sup>a</sup>
Thrust chamber pressure, psia			
First sample	—	186.5	183.5 ± 1.2
Second sample	—	192.5	197.5 ± 1.2
Propellant tank pressure, <sup>b</sup> psia	—	303.2	313.4 ± 2.0
Propulsion N <sub>2</sub> tank pressure, <sup>b</sup> psia	—	2751	2735 ± 15

<sup>a</sup>Rounded to an even number of CC&S timing pulses at 20 pulses/s.  
<sup>b</sup>After motor burn.

Procedures developed during the *Mariner VI* maneuver preparations were again used to time the DC-27 command that initiated the maneuver. Proper timing was required to obtain the propellant tank pressure after the firing but before thermal soakback affected the pressure. The timing was also optimized to obtain two thrust chamber pressure readings (channel 117) during engine operation.

As shown in Table 28, the telemetry data obtained deviated slightly from predicted values. The two chamber pressure points appear to bracket the prediction (one high, one low) but are representative of typical pressure fluctuations observed during ground testing of the engine. The propellant tank pressure sample was approximately 10 psi higher than predicted. A similar discrepancy was observed prior to launch when the propellant pressure read 6 psi higher after installation of the propulsion subsystem in the spacecraft than it had read during postloading storage in the explosive safe area at the AFETR. The two offsets are similar in nature, suggesting a problem with the transducer, possibly an increase in hysteresis after flight approval testing. Although the reason for the offsets was never firmly established, there were no indications that the postmaneuver offset was a result of an unusually high regulator operating pressure; the transducer remained the prime suspected cause of the discrepancy. The nitrogen tank pressure telemetry point was as predicted.

Analysis of trajectory data indicated that a velocity increment of 4.2879 m/s was actually imparted to the spacecraft. This represented an error of only 0.10% or

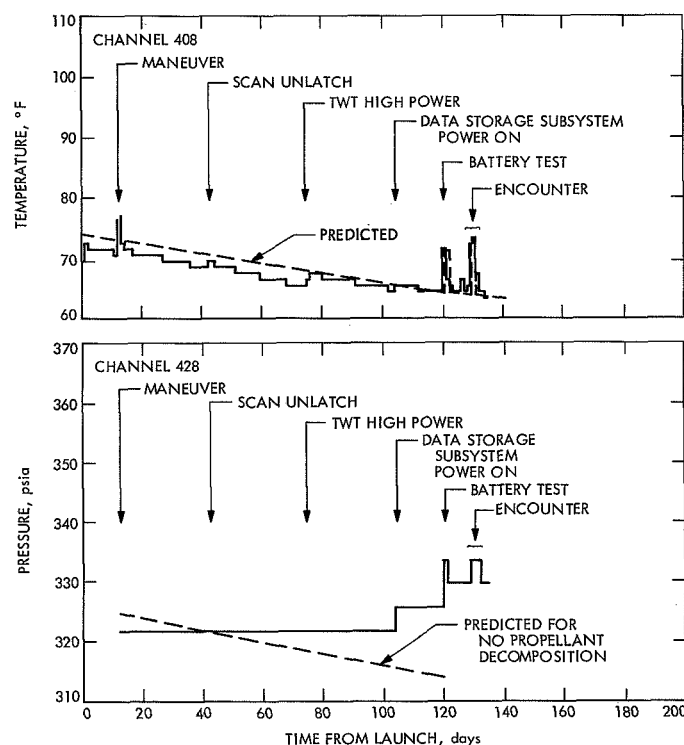


**Fig. 96. *Mariner VII* propellant tank temperature-pressure history**

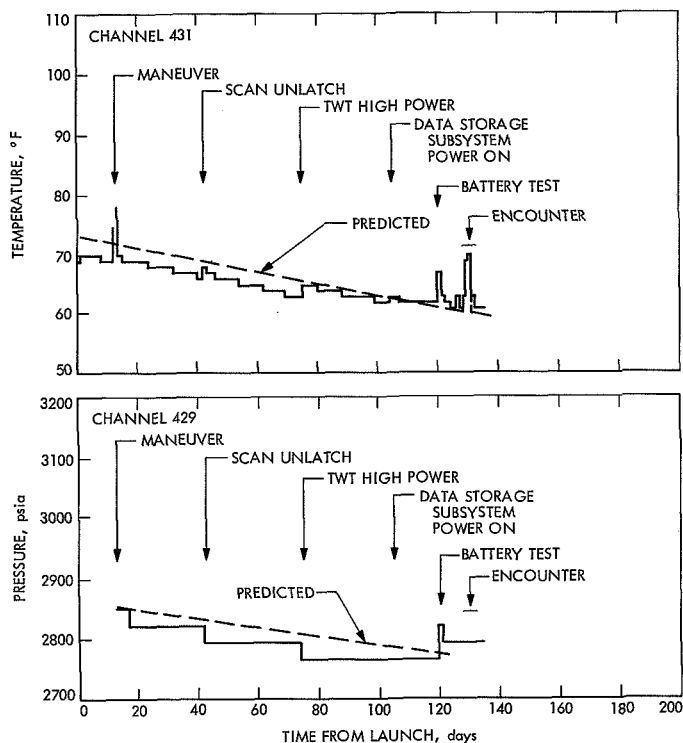


**Fig. 97. Mariner VII propulsion nitrogen tank temperature-pressure history**

0.08 $\sigma$ . This first maneuver met the project requirements, and the remaining correction capability was not used.

As with *Mariner VI*, the postmaneuver *Mariner VII* cruise was characterized by a gradual increase in propellant tank pressure as a result of slow decomposition of the hydrazine. As shown in Fig. 96, decomposition produced a pressure increase totaling 16 psi at encounter. This increase was approximately one-third that experienced by *Mariner VI*. The nitrogen tank pressure-temperature history is shown in Fig. 97.

The propulsion subsystem showed no evidence of involvement in the pre-encounter anomaly. However, temperature excursions typical of a normal gyros-on condition were observed during the anomaly.

**3. Recommendations.** As a result of the limited data returned during the motor burn portion of the *Mariners VI* and *VII* midcourse maneuvers, it is recommended that future spacecraft incorporate a maneuver telemetry mode. An accurate determination of subsystem functional performance in flight is essential to optimize future spacecraft designs as well as to insure that multiple-spacecraft missions such as *Mariner Mars 1969* derive

maximum benefit from the performance of the first spacecraft to enhance success of later arriving spacecraft. In addition, an increased data (bit) rate and an increase in engineering word length (from the present seven bits) are recommended to provide increased data return and resolution. Finally, a change from potentiometric pressure transducers to a strain-gage type is recommended to increase accuracy and reduce hysteresis.

## B. Pyrotechnic Subsystem Performance

**1. Mariner VI.** The pyrotechnic subsystem performed nominally and without incident throughout the *Mariner VI* mission. Subsystem functions and command sources are listed in Table 29, and the flow diagram is shown in Fig. 98.

**Table 29. Pyrotechnic subsystem functions and command sources**

Function	Command source <sup>a</sup>	
	Primary	Backup
Pyrotechnic arming	PAS	SIT
Solar panel deploy	SIT	CC&S L1
Propulsion start	CC&S M6	CC&S tandem command
Propulsion stop	CC&S M7	CC&S tandem command
Scan platform unlatch	CC&S C5	DC-45
IRS <sup>b</sup> cooldown	NAMG-1	DC-49 <sup>c</sup>
Propulsion enable	DC-14	—
Propulsion inhibit	DC-13	—
IRS cooldown enable	CC&S N6	DC-26
IRS cooldown inhibit	DC-1	—

<sup>a</sup>PAS = pyrotechnic arming switch, SIT = separation-initiated timer, CC&S = central computer and sequencer, NAMG-1 = narrow-angle Mars gate.

<sup>b</sup>IRS = infrared spectrometer.

<sup>c</sup>To optimize the *Mariners VI* and *VII* near-encounter strategies, DC-49 was used as the primary infrared spectrometer cooldown command.

The subsystem was armed by the pyrotechnic arming switch at spacecraft/*Centaur* separation. All indications of proper solar panel deployment were received via telemetry. Deployment was initiated by the separation-initiated timer.

Event register changes were observed at the expected times for propulsion start and stop during the midcourse



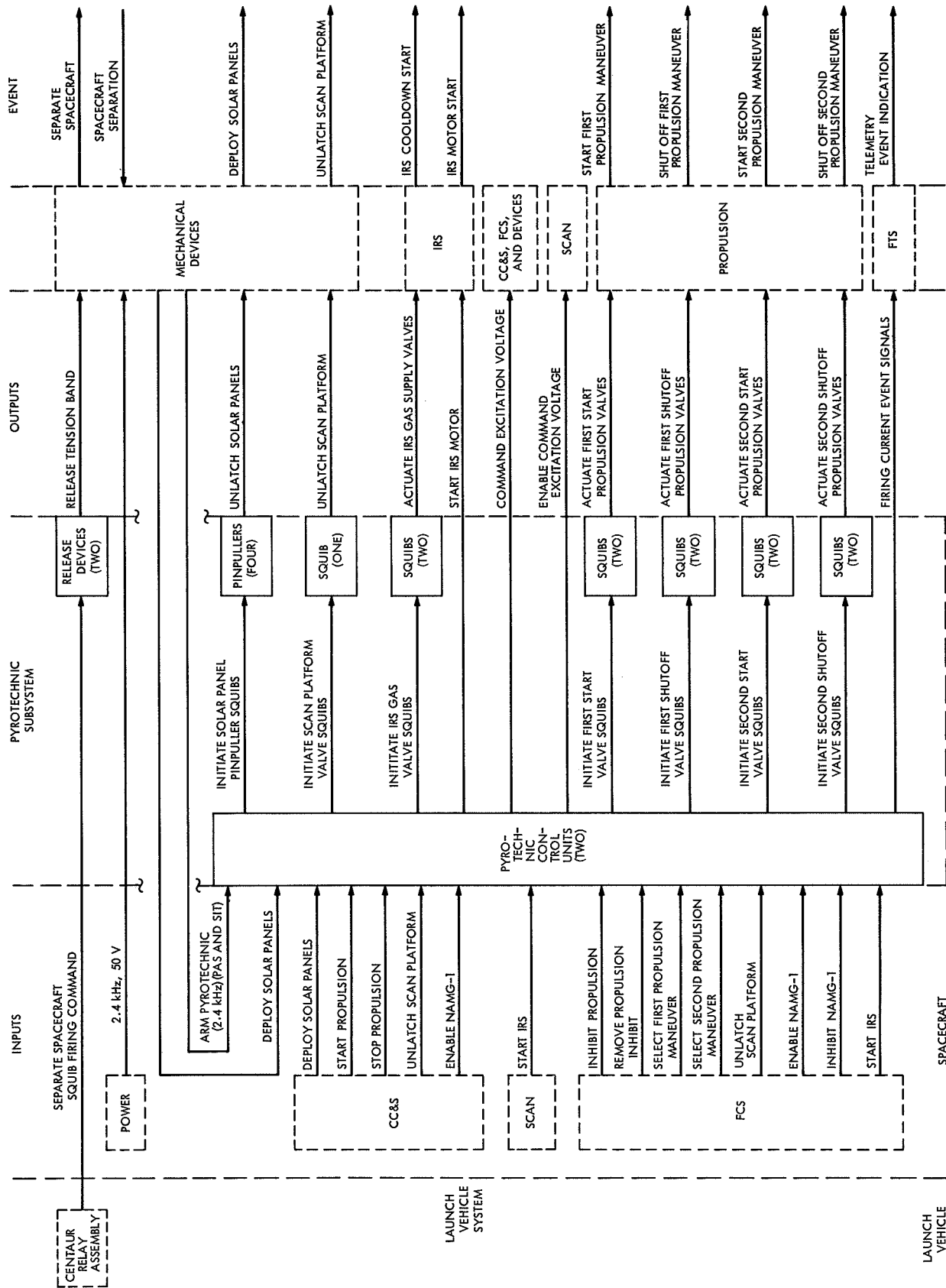


Fig. 98. Pyrotechnic subsystem flow diagram

maneuver. Propulsion telemetry data confirmed proper operation of pyrotechnic valve firing functions. On March 4, three days after the maneuver, a DC-13 command was transmitted to inhibit pyrotechnic maneuver functions. In addition to reducing the probability of initiating an inadvertent maneuver via the CC&S, the maneuver inhibit, by discharging the motor start capacitor banks, protected the spacecraft from an uncontrolled maneuver in the event that either of the silicon controlled rectifiers that trigger the motor-start function failed by shorting. Although considered a low-probability event, an inadvertent motor start would result in a burn to propellant depletion and would be catastrophic to the mission.

The scan platform was unlatched on March 5 by a DC-45 command. All indications of nominal subsystem performance were obtained. A register 1 event, corresponding to a pyrotechnic-current event, was received at the expected time. However, as expected, the register 3 pyrotechnic-current event was masked by the second register 3 event for the direct command. This problem, which had been identified during Spacecraft Assembly Facility system tests, was the result of the command event having a pulse width that overlapped the pyrotechnic telemetry output pulse.

A DC-14 command was transmitted on April 18 to enable the inertial control sequence that was included as a part of the conservative encounter sequence. This command had the undesirable side effect of enabling pyrotechnic maneuver functions and exposing the spacecraft to the failure mode mentioned previously. Except for short periods when the DC-13 command was in effect to condition the CC&S, the pyrotechnic subsystem remained enabled until after encounter when the maneuver inhibit was reinstated by a DC-13 command.

Infrared spectrometer cooldown was enabled during near-encounter by a DC-26 command with CC&S command N6 (pyrotechnic) as backup. Cooldown was initiated by a DC-49 command, as indicated by a pyrotechnic-current event in register 1. (As was the case with scan unlatch, the register 3 pyrotechnic-current event was masked by the final register 3 event for the direct command.) Backup was provided by the narrow-angle Mars gate (NAMG-1) command and by a second DC-49 command; however, neither proved necessary. Although both IRS gas bottle supply valves were actuated, the channel 1 detector was not cooled. This problem was attributed by the experimenter to a plugged

cryostat. The 400-Hz power was properly switched to the IRS scan motor at cooldown start.

**2. *Mariner VII.*** As was the case with *Mariner VI*, the *Mariner VII* pyrotechnic subsystem performed nominally and without incident throughout the mission.

The subsystem was armed by the pyrotechnic arming switch at spacecraft/*Centaur* separation, and all indications of proper solar panel deployment were received via telemetry. Deployment was initiated by the separation-initiated timer.

Event register changes were observed at the expected times for propulsion start and stop during the midcourse maneuver. Propulsion telemetry data confirmed proper operation of pyrotechnic valve-firing functions. Following the maneuver, a DC-13 command was transmitted to inhibit pyrotechnic maneuver functions.

The pyrotechnic subsystem remained inhibited until May 8 when the scan platform was unlatched by a CC&S C5 command. As a test of the inertial hold sequence under consideration for the near-encounter phase of the mission, a DC-14 command was placed in effect during the unlatch exercise to allow the CC&S to issue commands to the attitude control subsystem. All indications of proper pyrotechnic performance, including registers 1 and 3 events for pyrotechnic current, were received when the scan unlatch valve was actuated. Following the exercise, a DC-13 command was transmitted to again inhibit pyrotechnic maneuver functions.

On May 10, a DC-14 command was again transmitted to enable the inertial control portion of the conservative encounter sequence. (The effect of this command on the pyrotechnic subsystem is described in the discussion of *Mariner VI* performance.) However, on July 9, following diagnosis of the CC&S C1 driver failure, which forced a change in encounter strategy, a DC-13 command was again transmitted to inhibit pyrotechnic maneuver functions. The pyrotechnic subsystem remained inhibited for the remainder of the mission, except for the gyro warm-up period prior to near-encounter. This period required the DC-14 command to be in effect to allow the CC&S to command attitude control functions.

Because of the CC&S C1 driver failure, the CC&S N6 (pyrotechnic) enable command for IRS cooldown

could not be used during encounter. For this reason, two DC-26 commands were transmitted during near-encounter to insure that the pyrotechnic subsystem was enabled. Cooldown was successfully initiated by a DC-49 command, as indicated by a register 1 pyrotechnic-current event and by proper operation of the IRS channel 1 detector. (Again, the register 3 pyrotechnic-current event was masked by the second register 3 event for the direct command.) Power was properly switched to the IRS scan motor, as indicated by an increase in channel 205 (400-Hz inverter input) and by proper operation of the instrument. The NAMG-1 command and a second DC-49 command were provided as backups for IRS cooldown, but were not needed.

The pyrotechnic subsystem was apparently unaffected by the pre-encounter anomaly. Propulsion pressures showed no evidence of maneuver commands having been issued and, although the state of the IRS and maneuver inhibit/enable relays cannot be determined from telemetry, it is unlikely that any changes in pyrotechnic states occurred.

**3. Recommendations.** The following changes in implementation to the pyrotechnic subsystem of the *Mariner*

Mars 1969 spacecraft are recommended for future spacecraft:

- (1) Use of the same inhibit/enable commands by more than one subsystem should be avoided. Although intended primarily as maneuver enable/abort commands, DC-14/DC-13 commands were used throughout both missions to change CC&S states and to close and open the CC&S attitude control command lines. Use of DC-14 commands to enable CC&S control of gyro functions exposed the spacecraft to an undesirable failure mode (a short in the pyrotechnic subsystem silicon controlled rectifier that could initiate motor burn) throughout the majority of both missions.
- (2) Critical relay positions should be monitored by telemetry. In the *Mariner* Mars 1969 design, the pyrotechnic maneuver inhibit/enable, first-burn/second-burn, and IRS inhibit/enable relay positions were not monitored. As a result, relay positions could not be positively determined. This was of particular concern after the *Mariner VII* pre-encounter anomaly.

## Scientific Instrument Performance

The *Mariner VI* and *VII* spacecraft each carried four scientific instruments and performed two additional experiments making use of portions of the tracking data. The six scientific experiments associated with each flight were successfully performed. Their results and scientific conclusions are discussed in Volume III of this report and in other documents.\*

The four instruments that were developed and flown in the *Mariner Mars 1969* project were mounted on a two-degree-of-freedom scan platform, and were turned on only at the start of Mars encounter operations. The instruments were supported by a data automation subsystem (DAS), whose performance is described below (see Section V), and by the data storage, flight telemetry, power, and other spacecraft subsystems, whose performance is described above. The instrument subsystems, a description of whose performance follows, are the television subsystem, of which the ground-based image processing laboratory is an essential companion element; the ultraviolet and infrared spectrometers; and the infrared

radiometer. All of the scientific instruments obtained satisfactory planetary data.

### I. Television Subsystem

As an extension of previously developed technologies for planetary photography, the television instrument for *Mariners VI* and *VII* incorporated both digital and analog video data processing to achieve photometric precision and high spatial resolution within the constraints of the storage capacity of the spacecraft tape recorder. This dual-data format, in conjunction with rudimentary data-compression methods, combined to form an instrument whose output data format depended totally on a computer-oriented image-reconstruction process to achieve the scientific objectives.

This instrument (Fig. 1) consists basically of two separate camera heads, each containing a vidicon image sensor, its attendant electronics, and independent optical systems with companion shutter mechanisms. Further, the instrument contains a common set of electronic circuit assemblies, which perform the various amplification, conversion, timing, and scanning functions necessary to

---

\*Refer to articles in *Science* not reprinted in Volume III; also, *Radio Science*, *Journal of Geophysical Research* (January 1971), etc.

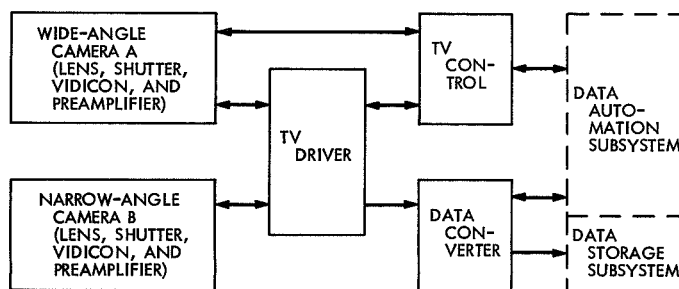


Fig. 1. Television subsystem

derive image data in a form suitable for storage and transmission to the Earth. Companion subsystems to the television instrument are the DAS, which provides basic timing, data processing, and general housekeeping functions for all the scientific instruments, and the data storage subsystem. The data storage subsystem consists of an analog tape recorder and a digital tape recorder, both of which function to store video data before transmission to the Earth.

#### A. Mission Performance

1. *Instrument status.* The four telemetry channels that indicated the temperature of the A and B vidicons, B

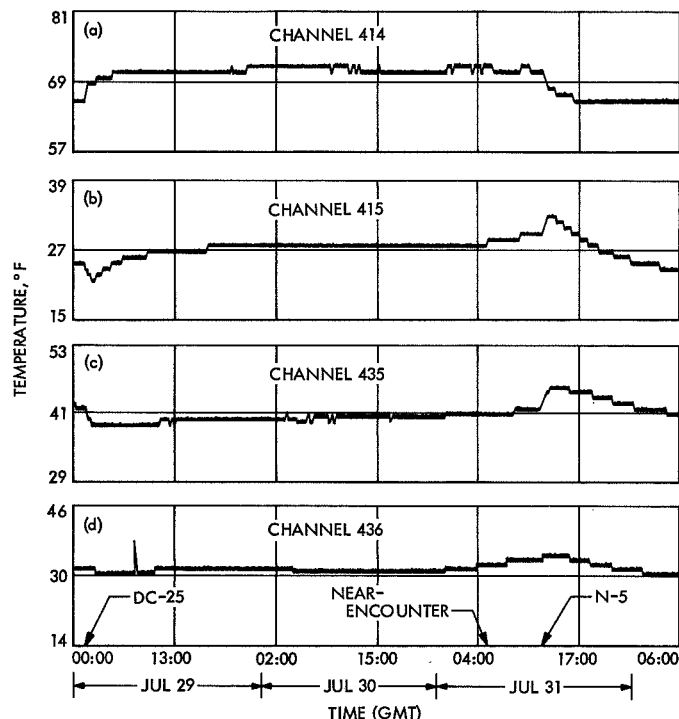


Fig. 2. Encounter temperatures, *Mariner VI*: (a) TV electronics, (b) A vidicon, (c) B vidicon, (d) B optics

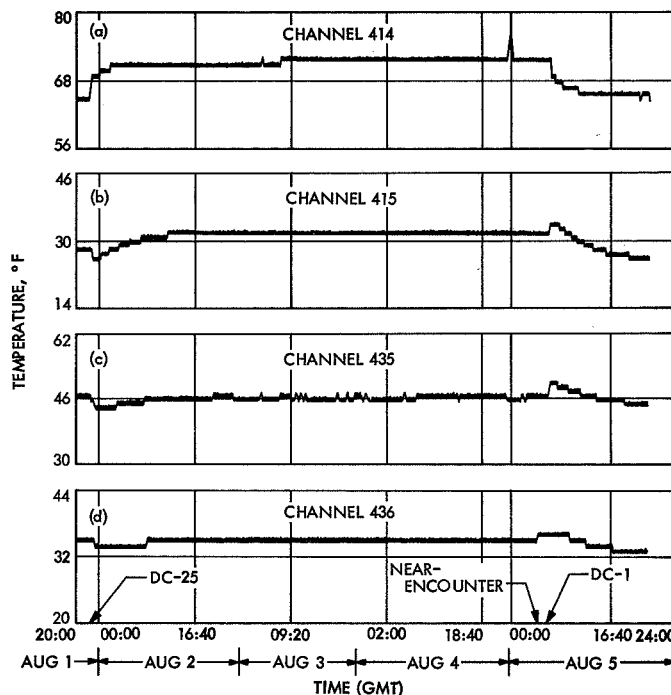


Fig. 3. Encounter temperatures, *Mariner VII*: (a) TV electronics, (b) A vidicon, (c) B vidicon, (d) B optics

optics, and TV electronics during the far- and near-encounter periods are plotted in Figs. 2 and 3. Throughout the encounter period, temperatures of the *Mariner VI* vidicons were approximately 8°F below the predicted value, whereas the *Mariner VII* vidicons were only about 3°F below predictions. However, all temperatures were well within the operating limits.

The video gain as a function of temperature for each camera is shown on the accompanying graph (Fig. 4). Also included are the points at which the gain was set, the predicted temperature, and the actual encounter temperature points. It is obvious from this graph that the gain of the *Mariner VI* camera was reduced (by temperature) substantially more than was the gain of the *Mariner VII* camera.

During far-encounter, the automatic aperture control (AAC) is locked out, and does not function. Both cameras remained in the low-gain state throughout their entire far-encounter sequences. During near-encounter, the AAC performed as had been predicted. As can be seen in Tables 1 and 2 and Fig. 5, its gain was, in most cases, exactly as had been predicted. It varied in a few cases, but never by more than one gain step.

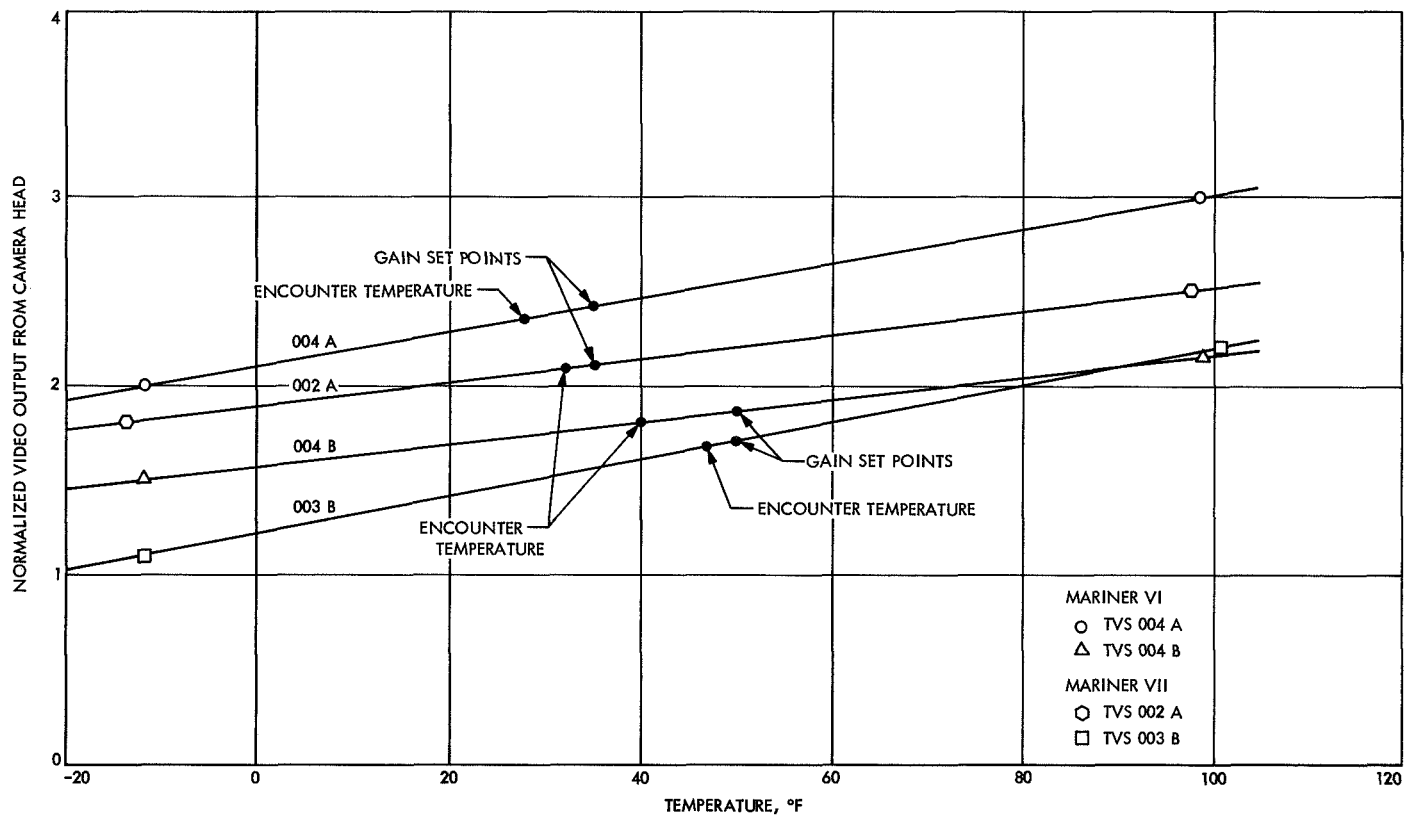


Fig. 4. Television camera gain vs temperature, *Mariners VI and VII*

**Table 1. Mariner VI television camera gain, actual vs predicted**

Near- encounter picture No.	DAS <sup>a</sup> picture count	DAS RTFC <sup>b</sup>	Time (GMT) at Earth	Filter	Actual gain state	Camera	Predicted	Differences (No. of gain states)
1	53	44324	05:10:35	Blue	000	A	000	—
2	54	44334	05:11:17	Top	000	B	000	—
3	55	44344	05:11:59	Green-2	000	A	000	—
4	56	44354	05:12:41	Bottom	000	B	000	—
5	57	44364	05:13:24	Red	000	A	000	—
6	58	44374	05:14:06	Top	010	B	000	1
7	59	44384	05:14:48	Green-1	000	A	000	—
8	60	44394	05:15:30	Bottom	000	B	000	—
9	61	44404	05:16:12	Blue	000	A	000	—
10	62	44414	05:16:54	Top	000	B	000	—
11	63	44424	05:17:37	Green-2	000	A	000	—
12	0	44434	05:18:19	Bottom	000	B	000	—
13	1	44444	05:19:01	Red	000	A	000	—
14	2	44455	05:19:43	Top	000	B	000	—
15	3	44465	05:20:26	Green-1	000	A	000	—
16	4	44475	05:21:08	Bottom	010	B	010	—
17	5	44485	05:21:50	Blue	010	A	010	—
18	6	44495	05:22:32	Top	100	B	010	1
19	7	44505	05:23:15	Green-2	100	A	010	1
20	8	44515	05:23:57	Bottom	100	B	100	—
21	9	44525	05:24:39	Red	100	A	100	—
22	10	44535	05:25:21	Top	010	B	010	—
23	11	44545	05:26:04	Green-1	010	A	010	—
24	12	44555	05:26:46	Bottom	100	B	100	—
25	13	44565	05:27:28	Blue	100	A	100	—
26	14	44575	05:28:10	Top	110	B	110	—
27	15	44585	05:28:52	Green-2	110	A	—	—
28	16	44595	05:29:35	Bottom	111	B	—	—
29	17	44605	05:30:17	Red	111	A	—	—
30	18	44615	05:30:59	Top	111	B	—	—
31	19	44625	05:31:41	Green-1	111	A	—	—
32	20	44635	05:32:23	Bottom	111	B	—	—
33	21	44645	05:33:05	Blue	111	A	—	—

<sup>a</sup>DAS = data automation subsystem.

<sup>b</sup>RTFC = real-time frame count.

**Table 2. Mariner VII television camera gain, actual vs predicted**

Near- encounter picture No.	DAS <sup>a</sup> picture count	DAS RTFC <sup>b</sup>	Time (GMT) at Earth	Filter	Actual gain state	Camera	Predicted	Differences (No. of gain states)
1	34	1632	04:46:03	Blue	000	A	000	—
2	35	1643	04:46:45	Top	000	B	000	—
3	36	1652	04:47:28	Green-2	000	A	000	—
4	37	1662	04:48:10	Bottom	000	B	000	—
5	38	1672	04:48:52	Red	000	A	000	—
6	39	1683	04:49:34	Top	000	B	000	—
7	40	1693	04:50:16	Green-1	000	A	000	—
8	41	1703	04:50:59	Bottom	000	B	000	—
9	42	1713	04:51:41	Blue	000	A	000	—
10	43	1723	04:52:23	Top	000	B	000	—
11	44	1733	04:53:05	Green-2	000	A	000	—
12	45	1743	04:53:48	Bottom	000	B	000	—
13	46	1753	04:54:30	Red	000	A	000	—
14	47	1763	04:55:12	Top	000	B	000	—
15	48	1773	04:55:54	Green-1	000	A	000	—
16	49	1783	04:56:37	Bottom	000	B	000	—
17	50	1793	04:57:19	Blue	000	A	000	—
18	51	1803	04:58:01	Top	000	B	000	—
19	52	1813	04:58:43	Green-2	000	A	000	—
20	53	1823	04:59:26	Bottom	000	B	000	—
21	54	1833	05:00:08	Red	000	A	000	—
22	55	1843	05:00:50	Top	000	B	000	—
23	56	1854	05:01:32	Green-1	000	A	000	—
24	57	1864	05:02:15	Bottom	010	B	010	—
25	58	1874	05:02:57	Blue	010	A	010	—
26	59	1884	05:03:39	Top	100	B	010	1
27	60	1894	05:04:21	Green-2	100	A	010	1
28	61	1904	05:05:04	Bottom	010	B	010	—
29	62	1914	05:05:46	Red	010	A	010	—
30	63	1924	05:06:28	Top	000	B	000	—
31	0	1934	05:07:10	Green-1	000	A	000	—
32	1	1944	05:07:53	Bottom	100	B	010	1
33	2	1954	05:08:35	Blue	100	A	010	1
34	3	1964	05:09:17	Top	110	B	100	1
35	4	1974	05:09:59	Green-2	110	A	100	1

<sup>a</sup>DAS = data automation subsystem.

<sup>b</sup>RTFC = real-time frame count.



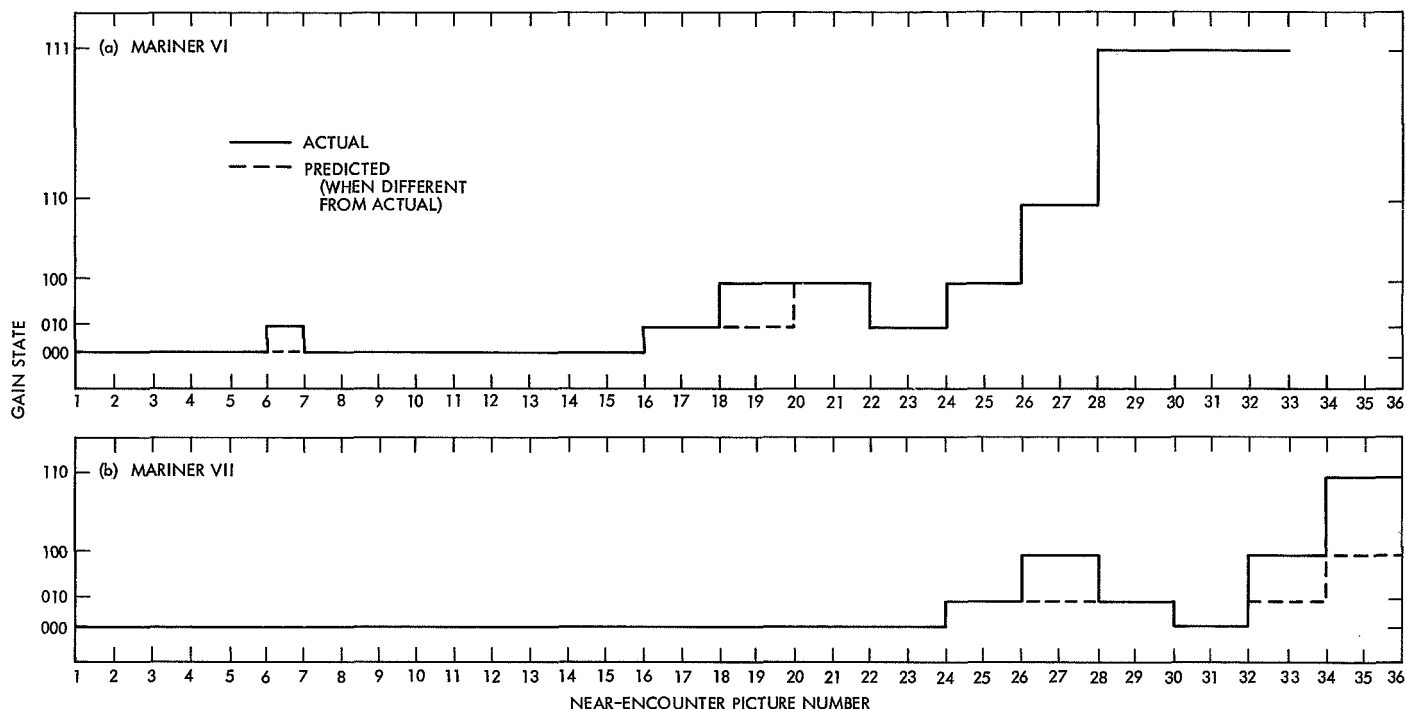


Fig. 5. Near-encounter gain switching, *Mariners VI and VII*

The total number of shutter cycles that occurred in each camera on each spacecraft during the mission, and over the lifetime of the mission, is given in Table 3.

Table 3. Shutter cycles, *Mariners VI and VII*

Spacecraft	Camera	Number of cycles during mission	Lifetime cycles accumulated in system through Aug 5, 1969
<i>Mariner VI</i>	A	2288	$17,703 \pm 20$
<i>Mariner VI</i>	B	2288	$20,878 \pm 20$
<i>Mariner VII</i>	A	3408	$16,298 \pm 20$
<i>Mariner VII</i>	B	3408	$18,388 \pm 20$

There was little variation in other engineering parameters throughout the mission, as shown in Table 4.

2. *Encounter sequences.* From a television point of view, the term *far-encounter* was generally associated with data from the narrow-angle camera. A notable exception was the *Mariner VII* far-encounter real-time digital video, which included data from the wide-angle camera. In the far-encounter mode of operation, both the narrow- and wide-angle cameras viewed the planet, but only the full data from the narrow-angle camera

were stored in the data storage subsystem, and subsequently played back and transmitted to the Earth. During this mode of operation, the pointing angle of the TV cameras, mounted on the movable scan platform, was under control of the far-encounter planet sensor, which tracked the brightness centroid of the planet. During far-encounter, a command was periodically issued from the on-board sequencer (or directly from the Earth) that initiated tape recording of the scene currently being

Table 4. Engineering parameter variation, *Mariners VI and VII*

Parameter	<i>Mariner VI</i>		<i>Mariner VII</i>	
	Camera A	Camera B	Camera A	Camera B
Grid voltage	$297 \pm 1^a$	$250 \pm 1$	$295 \pm 1$	$350 \pm 1$
Anode voltage	$246 \pm 2$	$256 \pm 5$	$246 \pm 2$	$250 \pm 1$
Focus current	$253 \pm 2$	$261 \pm 1$	$252 \pm 2$	$270 \pm 2$
Optics temperature (cover on)	$193 \pm 1$		$202 \pm 1$	
Optics temperature (cover off)	$356 \pm 1$		—	

<sup>a</sup>Units are in data numbers.

viewed by the narrow-angle camera. The frequency of these recordings was so programmed that, because of the rotation of the planet, many different planet meridians were central in the recorded scenes.

The *Mariner VI* and *VII* spacecraft system was designed to provide a high degree of operational flexibility. Both automatic operation (via an on-board sequencer) and Earth-based command capability were provided to control the acquisition, storage, and transmission to the Earth of TV data. The encounter sequences that were ultimately executed exploited the flexibility of the system to greatly exceed the TV data return objectives of the early mission designs.

To ensure science data return if direct command (DC) capability should be lost, instructions for automatically performing the encounter sequence were loaded into the central computer and sequencer (CC&S) aboard the spacecraft. The CC&S was then capable of commanding a completely automatic *conservative encounter sequence*, which would include science data acquisition, recording, and playback. The conservative encounter sequence was as follows:

Time	Event
$E - 24$ h	Turn on science power
$E - 21$ to $E - 11$ h	Record eight narrow-angle pictures at 1-h 22-min intervals
$E - 15$ min	Start near-encounter sequence; record total of 25 wide- and narrow-angle pictures
$E + 20$ min	Start playback

During the long period between launch and encounter, encounter sequences of a much more ambitious nature were designed for each of the *Mariner* spacecraft. These sequences became known as *standard encounter sequences*. Key requisites of the standard encounter sequences were continued direct command capability and satisfactory performance of the high-rate (block-coded) data channel. The standard encounter sequences were designed to revert back to the conservative encounter sequence in case of direct command loss. In contrast to the far-encounter portion of the conservative encounter sequence, which provided for the recording of eight narrow-angle pictures, the standard encounter sequences produced 50 and 93 far-encounter recorded

narrow-angle pictures for *Mariners VI* and *VII*, respectively. The far-encounter events that were of particular significance to the television portion of the mission are listed in Table 5 for *Mariner VI* and in Table 6 for *Mariner VII*.

**Table 5. *Mariner VI* far-encounter sequence of events**

Date (1969)	Time (GMT)	Event
Feb 21	22:54:18	Science power turned off following final precountdown test
Jul 29 ↓ Jul 30 ↓ Jul 30	01:22:30	Science power turned on in space (power had been off for 157 days 2 h 28 min 12 s)
	01:59	Slewed scan platform to far-encounter position
	02:08	First indication of planet observed in real-time data
	02:39	Scan platform to near-encounter position
	02:54	Scan platform to 101-deg cone position
	03:14	Scan platform to near-encounter position
	03:29	Encounter II data mode (real-time digital video)
	03:49	Scan platform to far-encounter position
	04:06	Planet in TV view
	04:49	Enabled 33-picture far-encounter sequence
	05:28	Recorded first of 33 far-encounter pictures taken at 37-min intervals
	06:00	Television A optics cover deployed
	08:32	Encounter I data mode
	22:24	Encounter II data mode
	01:11	Recorded far-encounter picture 33 on ATR <sup>a</sup>
	01:31	Started playback of 33 far-encounter pictures
	04:21	Terminated ATR playback
	04:28	Encounter II data mode
	04:47	Started ATR erase
	05:11	Enabled 17-picture far-encounter sequence
	05:46	ATR advanced to track 3
	07:31	Recorded far-encounter picture 34—17-picture sequence: 6 pictures at 65-min intervals; 2 pictures at 84-s intervals (attempt to photograph Phobos); 9 pictures at 56-min intervals
	08:21	Encounter I data mode
	10:08	Planet visible in A camera real-time data
Jul 30	22:21	Recorded far-encounter picture 50

<sup>a</sup>ATR = analog tape recorder.

Table 5 (contd)

Date (1969)	Time (GMT)	Event
Jul 31	00:56	Started playback of 17 far-encounter pictures
	02:20	Terminated ATR playback; scan platform to near-encounter position
	02:21	Encounter II data mode
Jul 31	02:39	Started ATR erase

Table 6. *Mariner VII* far-encounter sequence of events

Date (1969)	Time (GMT)	Event
Mar 25	20:16:30	Science power turned off following final precountdown test
Aug 1	22:18:43	Science power turned on in space (power had been off for 129 days 2 h 2 min 13 s)
Aug 1	23:21	Encounter II data mode
Aug 2	00:15	Slewed scan platform to far-encounter position
	00:23	First indication of planet in real-time digital video
	01:21	Started scan-platform diagnostic exercise. Television was used to determine scan-platform pointing after position telemetry was lost. Exercise included stepping scan platform to several positions while receiving real-time digital video, recording two B camera pictures on ATR <sup>a</sup> , ATR playback, and ATR erase
Aug 2	09:05	Enabled first 34-picture far-encounter sequence
	09:32	Recorded first of 34 far-encounter pictures taken at 26-min intervals
	23:59	Recorded far-encounter picture 34
Aug 3	01:01	Started ATR playback of first 34 far-encounter pictures
	03:53	Terminated ATR playback
	04:30	Started ATR erase
Aug 3	05:23	Enabled second 34-picture far-encounter sequence (34 pictures at 36-min intervals)
	06:00	Recorded far-encounter picture 35
	01:47	Recorded far-encounter picture 68
Aug 4	02:20	Started ATR playback of second 34 far-encounter pictures
	05:13	Terminated ATR playback
	05:25	Started ATR erase

<sup>a</sup>ATR = analog tape recorder.

Table 6 (contd)

Date (1969)	Time (GMT)	Event
Aug 4	05:46	Enabled 25-picture far-encounter sequence (20 pictures at 47-min intervals, 5 pictures at 12-min intervals)
	05:56	Stepped ATR to track 2
	08:06	Recorded far-encounter picture 69
Aug 4	23:59	Recorded far-encounter picture 93
Aug 5	00:02	Stepped ATR to track 2
	00:08	Started ATR playback of 25 far-encounter pictures
	02:22	Encounter II data mode (real-time digital video of far-encounter pictures close to planet)
Aug 5	02:25	Started ATR erase
	02:37	Television A optics cover deployed
	03:25	Scan platform to near-encounter position

During the near-encounter mode of operation, the data storage subsystem recorded alternately the output from both the narrow- and wide-angle cameras. Recording was of two forms, digital video and analog video, with a separate recorder for each data type. The near-encounter sequences that were ultimately executed provided considerably more TV data return than would have been possible under conditions of the earlier mission designs. The increased TV data return was made possible by two factors that could not be assumed, but had to be demonstrated during the actual missions; namely, acceptable performance of the high-rate data channel (block-coded data) and continuous Earth-based command capability. Acceptable performance of the high-rate data channel allowed playback of all far-encounter data before the start of near-encounter. This provided additional data storage capability for near-encounter TV data. Continuous Earth-based command capability allowed reprogramming of the on-board sequencer after the occurrence of the far-encounter events. Because the on-board sequencer had only a limited instruction memory, reprogramming (as opposed to a completely automatic sequence, which included both far- and near-encounter events) provided additional near-encounter instruction capacity. The end result was a greater number of TV pointing-angle positions and last-minute changes, which enhanced the scientific return from the TV subsystem.

During encounter planning, the TV experiment team stated a preference for a particular TV-A color-filter sequence during near-encounter. Both *Mariner VI* and *VII* near-encounter recording sequences were to start with

A camera views exposed through blue filters. The desirability of specific near-encounter filter sequences had been anticipated, and, during Air Force Eastern Test Range (AFETR) test activities, the TV subsystems were always turned off with the TV-A filter in a known position. Through a knowledge of the TV/DAS turn-on and timing characteristics, it was possible to calculate far-encounter science power turn-on times, which provided the desired near-encounter TV-A filter positions.

The near-encounter events that were of particular significance to the television mission are listed in Table 7 for *Mariner VI* and in Table 8 for *Mariner VII*.

During the near-encounter sequence of each spacecraft, the scan platform was moved to four different

**Table 8. *Mariner VII* near-encounter sequence of events**

Date (1969)	Time (GMT)	Event
Aug 5	04:33:41	Transmission of near-encounter start command (DC-16) initiated
	04:39:06	Planet in A camera field of view
	04:40:10	Calculated arrival time, at spacecraft, of DC-16 command
	04:40:31	Started frame readout of first spacecraft-recorded near-encounter picture (A camera, blue filter); initial scan-platform pointing angles: Cone 135.5 deg Clock 217.5 deg
	04:44:39	Planet limb visible in Earth-received real-time digital video from A camera
	04:46:51	Started frame readout of near-encounter picture 10; scan-platform pointing angles: Cone 144.7 deg Clock 250.0 deg
	04:54:40	Started frame readout of near-encounter picture 21; scan-platform pointing angles: Cone 100.2 deg Clock 233.6 deg
	04:59:31	Started frame readout of near-encounter picture 28; scan-platform pointing angles: Cone 100.2 deg Clock 228.8 deg
	05:04:55	ATR <sup>a</sup> fully loaded (near-encounter picture 35, line 462)—last ATR-recorded data
	06:11:33	Transmission of DC-48 command (TV shutter inhibit) initiated
Aug 5	06:23:39	Science power turned off with DC-1 command
Aug 6	00:24	Started first ATR playback of 35-picture near-encounter sequence
Aug 6	06:05	Terminated second ATR playback of near-encounter pictures

<sup>a</sup>ATR = analog tape recorder.

positions. This was done to maximize the amount of science data obtained, including the number of television pictures taken. Table 9 lists the cone and clock angles of the scan platform for each near-encounter picture.

The *Mariner* Mars 1969 wide-angle TV cameras (A cameras) were equipped with command-deployable, optically flat, quartz optics covers. Their purpose was to prevent deposition of any outgassed or propulsion contamination of the external A camera optical surface. The spectral characteristic of the covers is essentially flat over most of the spectral range of the A camera, with

**Table 7. *Mariner VI* near-encounter sequence of events**

Date (1969)	Time (GMT)	Event
Jul 31	04:58:35	Transmission of near-encounter start command (DC-16) initiated
	05:03:50	Planet in A camera field of view
	05:04:52	Calculated arrival time, at spacecraft, of DC-16 command
	05:05:15	Started frame readout of first near-encounter picture (A camera, blue filter); initial scan-platform pointing angles: Cone 128.4 deg Clock 261.5 deg
	05:10:52	Started frame readout of near-encounter picture 9; scan-platform pointing angles: Cone 128.3 deg Clock 247.7 deg
	05:14:24	Started frame readout of near-encounter picture 14; scan-platform pointing angles: Cone 100.0 deg Clock 266.8 deg
	05:17:13	Started frame readout of near-encounter picture 18; scan-platform pointing angles: Cone 100.0 deg Clock 265.6 deg
	06:59	Transmission of DC-48 command (TV shutter inhibit) initiated
	12:32:50	Science power turned off with N5 from CC&S <sup>a</sup>
	00:32	Started ATR <sup>b</sup> playback of 25 near-encounter pictures
Aug 1	05:46	Terminated second ATR playback of near-encounter pictures

<sup>a</sup>CC&S = central computer and sequencer.  
<sup>b</sup>ATR = analog tape recorder.

**Table 9. Camera orientation**

Near-encounter pictures	Scan platform	
	Cone angle, deg	Clock angle, deg
<i>Mariner VI</i>		
1-8	128.4	261.5
9-13	128.3	247.7
14-17	100.0	267.8
18-25	100.0	265.6
<i>Mariner VII</i>		
1-9	135.5	217.5
10-20	144.7	250.0
21-27	100.2	233.6
28-33	100.2	228.8

transmission of approximately 90%. Because of the large physical dimensions of the narrow-angle camera (B camera) optics, it was impracticable, from a reliability standpoint, to equip the B cameras with optics covers. Instead, the philosophy assumed was to compare the A camera data before and after optics cover deployment to determine whether any contamination effects were present, and then apply the same corrections to the pictures from the B cameras.

Because the *Mariner VI* mission philosophy was somewhat more conservative than that of *Mariner VII*, the *Mariner VI* A camera optics cover was deployed approximately 45 h before encounter. At this range, the planet was quite small in the A camera field of view, and was completely obscured by the digital video data bar. These factors prevented generation of any before/after video data relative to the *Mariner VI* A camera optics cover deployment. This was not the case for *Mariner VII*, whose A camera optics cover remained in place over the A optics until approximately 2 h before encounter. In addition, the camera was viewing the planet and real-time digital video was received for numerous A camera exposures immediately before and after cover deployment.

Comparison of the *Mariner VII* A camera digital video picture exposures immediately before and after optics cover deployment indicates a difference of approximately 10% in video amplitude for all A camera filter positions.

**3. Picture quantity and use of data storage subsystem.** The capability to command spacecraft events from the Earth (as opposed to a completely automatic encounter

sequence) and to obtain satisfactory performance of the high-rate data channel provided a significant increase in TV data return. Use of the high-rate data channel reduced the analog tape recorder playback time by a factor of 60, and provided digital video data transmission in real-time. Conservative encounter sequences would have produced a total of only 32 analog and 24 digital video pictures from each spacecraft by loading each track of the tape recorders only once and transmitting no real-time digital video pictures. The actual picture count for *Mariners VI* and *VII* is given in Table 10.

**Table 10. Television picture count, *Mariners VI* and *VII***

Spacecraft	Far-encounter pictures		Near-encounter pictures	
	Analog	Real-time digital	Analog	Digital
<i>Mariner VI</i>	50	428 <sup>a</sup>	25	26
<i>Mariner VII</i>	93	749 <sup>a</sup>	35	33
Total	143	1177	60	59

<sup>a</sup>A portion of the planet is visible in each picture.

Loading of the four tracks of the analog tape recorder occurred 9 times for *Mariner VI* and 15 times for *Mariner VII*, as shown in Table 11.

**Table 11. Analog tape recorder track loadings**

Track number	Number of times loaded	
	<i>Mariner VI</i>	<i>Mariner VII</i>
1	2	3
2	2	4
3	3	4
4	2	4

*a. Noise.* In all of the *Mariner* Mars 1969 photography, a degree of coherent noise is present. This noise is believed to have been introduced into the television at the most sensitive (and therefore most susceptible) point in the system—the vidicon target lead. The target lead is in close proximity to the focus and deflection coils, which receive their drive power over long leads running parallel to the 2400-Hz power supply leads. A capacitive coupling of the 2400-Hz power into the target lead via the focus and deflection coil leads is believed to be the most probable source of the coherent noise.

*b. Blemishes.* Blemishes in the television pictures are the result of small nonuniformities in the vidicon photoconductor surface. These nonuniformities cause small white spots or blemishes to appear in the pictures. Occasionally, these artifacts are much larger and more readily apparent, as in Fig. 6b (picture 7), taken by *Mariner VI* camera B. These blemishes do not move; therefore, they can be removed by computer processing. Pictures 6-9 (Fig. 6a-d) were obtained by averaging together all near-encounter pictures. Because only 16 pictures were averaged for each camera, all true video information was not removed from the final products; hence, it is possible to observe latent image information in the "averaged" photographs. The white spots representing blemishes are readily apparent, however.

Figure 6a (picture 6) contains a large dark spot just below and to the left of center. This spot is a dust particle on the vidicon faceplate, which probably resided there following the launch-vibration environment. Figure 6b (picture 7) shows a large white spot in the lower right corner, which represents a much larger than average blemish. Figure 6c (picture 8) contains two dark areas, one near the center and one near the top left corner, which are believed to be slight deposition irregularities in the vidicon photoconductor. Figure 6d (picture 9), representing the *Mariner VII* B camera, contains the largest number of blemishes of the four flight cameras. However, although there are a large number of blemishes, these are very small compared to those on the other cameras.

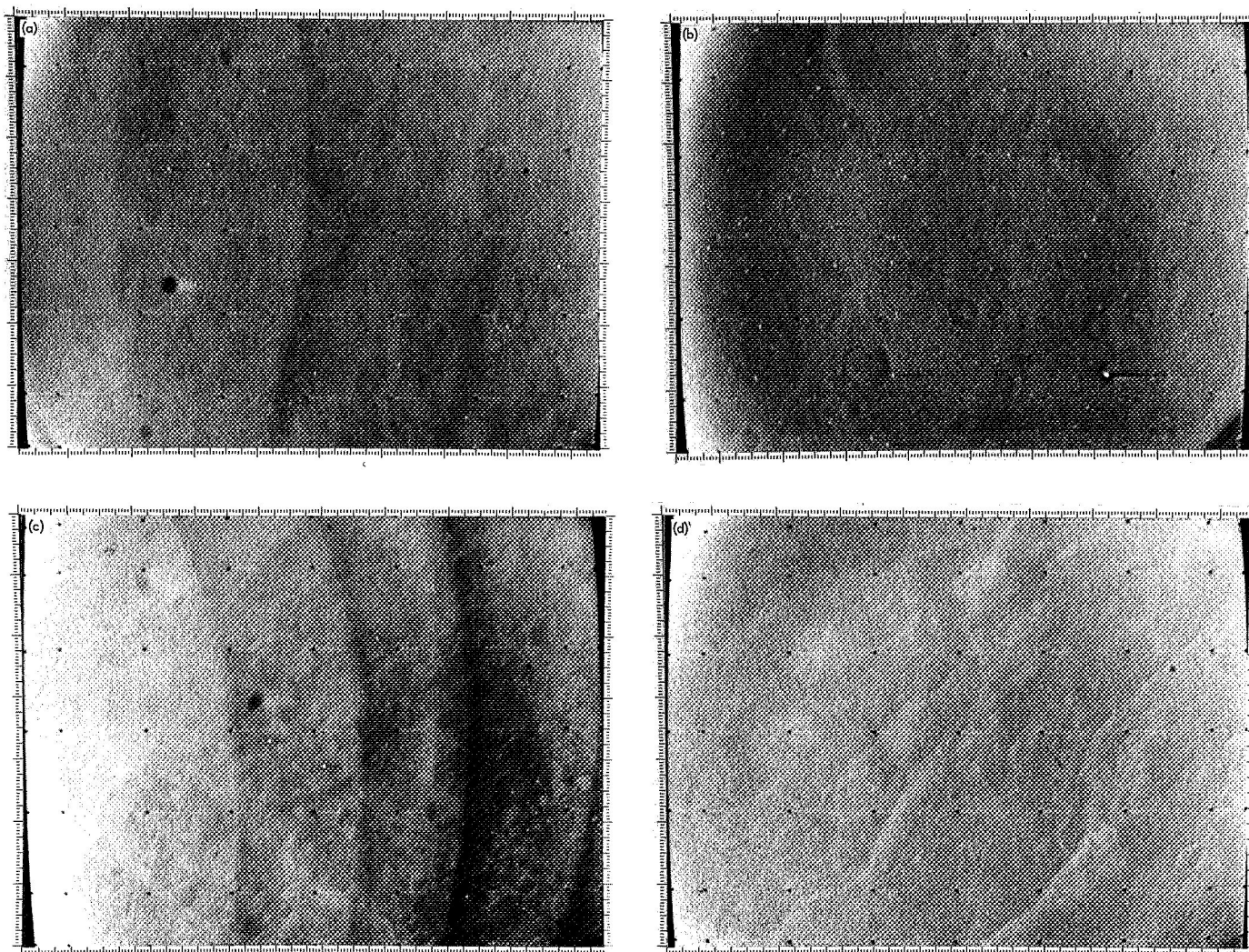


**Fig. 6. Averaged near-encounter photographs: (a) *Mariner VI* A camera (picture 6), (b) *Mariner VI* B camera (picture 7), (c) *Mariner VII* A camera (picture 8), (d) *Mariner VII* B camera (picture 9)**

c. *Distortion.* The primary aberrations in optics include spherical aberration, coma, astigmatism, curvature of field, and distortion. Of these, only distortion was measured in the optical systems of the *Mariner* Mars 1969 television subsystem. Distortion is classified by either a negative or a positive magnification of the image in the object plane. If distortion is present, the image of any straight line in the object plane that meets the optical axis will itself be a straight line, but the image of any other straight line will be curved (Ref. 1). If the effective magnification increases in the outer parts of the field, this distortion is classified as *pincushion* distortion; if the magnification decreases, one obtains *barrel* distortion.

The distortion present in the *Mariner* Mars 1969 TV pictures originated from two separate components. The first of these is the optics. The optical distortion caused by the optics was pincushion distortion, which caused the outside corners to have slightly greater magnification. In the worst case, the corners were displaced about 12 to 15 pixels. The second source of distortion is the electronic optics in the vidicon. This distortion was classified as barrel. The corners were displaced, in the worst case, about 25 pixels. These two distortions actually compensated each other to some degree (this was noted in the optical geometric distortion target used in the calibration). The output pictures showed the grid lines to be rather straight, but the vidicon mask was clearly distorted. The cartographic requirements of "fractions of a pixel" accuracy demand that this distortion be measured and corrected. This measurement will allow the maps produced from the *Mariner* Mars 1969 data to have an accuracy comparable to the maximum resolution in each photograph. The correction will be performed in two stages at the image processing laboratory. The measurements obtained from the calibration will be used in this process of distortion removal.

A phenomenon known as *raster shift* was discovered during the reduction of the calibration data. This raster shift was also evident in the flight pictures. Shifts on the order of 2 pixels are observable in the data.

d. *Brightness assessment.* The prelaunch planet surface radiance predictions were based on data obtained from Earth-based photometry published in the literature. These measurements were quite accurate; because of their poor resolution, however, they served only as an average value for the whole planet disk. These measurements were made at phase angles much smaller than those planned for the *Mariner* Mars 1969 television

cameras. Some Earth-based photometric data were of sufficient resolution to differentiate between a desert area and a dark *mare* area. These data were combined with the calibrated spectral-sensitive characteristics of the *Mariner* Mars 1969 television subsystem (on the assumption that the phase-dependence properties of the surface are Lambertian) to predict the exposures of the far- and near-encounter pictures. These predictions were made for a desert area, the polar cap, the dark *mare* area, and the average disk exposure in far-encounter. An assumption was made that the polar cap has an effective reflectance of 1.5 times that of the desert, and that the dark *mare*-like areas have an effective reflectance of 0.7 times that of the bright deserts.

These predictions were used to make an estimate of the highest expected exposure, which was then used to set the electronic gain so that the maximum dynamic range was available for photography.

All of the *Mariner* VI and VII near-encounter pictures had adequate exposures, with the predicted gain states in good agreement with the actual gain states obtained during encounter (see Table 2). The first six pictures of the *Mariner* VI near-encounter were degraded by a failure in the analog tape recorder (ATR) playback amplifier of track 1. The predicted vs actual gain states (see Table 1) show very good agreement.

e. *Contrast.* During the *Mariner* VII far-encounter, it became evident that the analog TV data being received were of higher contrast, and consequently showed more apparent detail, than the data returned by *Mariner* VI. Later analysis showed that, for *Mariner* VII, bright deserts resulted in higher data numbers and dark *maria* in lower data numbers than for corresponding *Mariner* VI far-encounter data. Paradoxically, however, larger portions of the polar cap saturated ( $DN \geq 254$ ) in the *Mariner* VI data than in the *Mariner* VII data.

After rather careful decalibration of the mission data, it is clear that the characteristics of the B camera of *Mariner* VI changed, whereas the characteristics of the *Mariner* VII B camera did not. Inasmuch as the A and B cameras of the spacecraft use common video-processing electronics following the preamplifiers in each camera, the *Mariner* VI B camera vidicon or preamplifier apparently changed during or after launch and before Mars encounter. It may not be possible to unequivocally identify the component of the *Mariner* VI B camera that



changed, but an investigation is continuing in an attempt to understand this anomaly more thoroughly.

*f. Focus.* An initial analysis of the flight data revealed no evidence to suggest that any of the cameras aboard the two spacecraft were out of optical focus. A comparison with the performance during the calibration tests before launch, as well as the flight data, also reveal no sign of deterioration in focus of any sort. The sharp, bright limb in all of the far-encounter pictures clearly indicates that the cameras were properly focused. Detailed analysis of the data shows this limb or bright disk edge to go from dark sky to a data number indicative of the planet surface, usually within two picture elements. As to the extent of electronic focus of the vidicon read beam in the flight data, further analysis was hindered by the noise in the data. Until these data have been processed, it is not possible to extend any further qualitative or quantitative analysis of the focus.

## B. Postencounter Activities and Performance

After the completion of encounter, and playback of *Mariner VI* and *VII* data, a number of science activities were conducted. Of these, only one exercise for each spacecraft was specifically intended as a television subsystem experiment. These two exercises were virtually identical for each spacecraft.

The TV experiments were attempts to detect certain selected bright (near-0 magnitude) stars within the field of view provided by the scan platform. In each case, 24 pictures were taken by the narrow-angle camera and recorded by the data storage subsystem. The pictures consisted of four frames at platform positions enclosing the direction vector toward the star Vega. The platform was moved to the coordinates of the star Altair, and then of Alpheratz. At each position, the four-picture/position sequence was repeated. The first 12 pictures were taken with the camera electronics at the 000 (minimum) automatic aperture control gain state. The AAC gain was then allowed to step automatically to the 111 (maximum) level, and the sequence was repeated in reverse order.

Throughout these operations, the telemetry parameters and temperatures of both *Mariner VI* and *VII* television subsystems remained at the values and levels observed during the planetary encounter sequences. Although several pointing errors occurred during these star-orientation exercises, it is tentatively concluded that no stars were imaged. The pictures were processed by subtraction to remove noise effects and bright blemishes, and no bright

spots were found at expected star locations. The post-encounter operations during which science power was applied are listed in Table 12.

**Table 12. Postencounter television operations**

Date (1969)	Operation	Duration, <sup>a</sup> h	Spacecraft
Aug 11–12	Southern celestial hemisphere scan by UVS <sup>b</sup> and IRR <sup>c</sup>	2.0	<i>Mariner VI</i>
Aug 12–13	Northern celestial hemisphere scan by UVS and IRR	6.3	<i>Mariner VI</i>
Aug 14	Galactic center scan by UVS and IRR	3.8	<i>Mariner VI</i>
Sep 8	Television star calibration: Vega, Altair, and Alpheratz	3.3	<i>Mariner VI</i>
Sep 10	Television star calibration: Vega, Altair, and Alpheratz	2.1	<i>Mariner VII</i>
Sep 15–16	Radio test sequence; science on for temperature control	0.7	<i>Mariner VII</i>
Sep 22	Milky Way scan by UVS	7.7	<i>Mariner VII</i>
Oct 1	RFS <sup>d</sup> anomaly troubleshooting; science on for temperature control	1.1	<i>Mariner VI</i>
Oct 8–9	Comet 1969B scan by UVS	1.8	<i>Mariner VI</i>

<sup>a</sup>Total postencounter operating time = 18.3 h (*Mariner VI*) + 10.5 h (*Mariner VII*) = 28.8 h.  
<sup>b</sup>UVS = ultraviolet spectrometer.  
<sup>c</sup>IRR = infrared radiometer.  
<sup>d</sup>RFS = radio-frequency subsystem.

## C. Television Image Processing

**1. Introduction.** The function of the image processing laboratory (IPL) in support of the *Mariner* Mars 1969 television experiment was to provide, from the video data returned by *Mariners VI* and *VII*, products usable by the TV experimenters and other interested scientists.

The spacecraft sent back approximately 200 photographs of Mars taken from distances ranging between  $1 \times 10^6$  and  $3 \times 10^3$  km relative to the planet surface.



These images contain true object space information that is distorted to some extent by the signature of the imaging system itself. To maximize the scientific yield of the television data, the nature of the distortions introduced by the imaging system must be quantitatively determined, and techniques developed whereby they can be accurately removed.

Television systems typically exhibit photometric non-uniformities and nonlinearities, geometric distortions (both optical and electronic), and image-retention and spatial-frequency-response limitations. In addition, *Mariner* Mars 1969 specific problems were introduced in the course of on-board processing applied in the interest of data compression and efficient bandwidth utilization. A cubing amplifier and an automatic gain control (AGC) circuit were employed, with photometric "DC reference" supplied in the form of a separately encoded, under-sampled raw signal. The effects of on-board processing can, in principle, be removed by means of combining these separate data streams.

Digital image-processing techniques developed at JPL were used to characterize these various distortions, by use of calibration data, and to remove them from the images of Mars. In addition, these techniques were used to manipulate the data (for example, to improve small-crater detectability) in support of particular interpretive activities.

**2. Data input.** *Mariner VI* returned 50 far-encounter composite analog video (CAV) and 25 near-encounter CAV pictures; for *Mariner VII*, the CAV picture quantities were 93 from far-encounter and 35 from near-encounter. Of the 143 total far-encounter CAV pictures, corresponding digital video (DV) data are available for approximately 10. About 1200 real-time DV images were transmitted by the two spacecraft. All of the near-encounter pictures were recorded and received in DV as well as CAV form.

Data received at DSS 14 and sent to JPL in real-time over the high-rate data link were logged by CTA-21 (the compatibility test area developed for spacecraft telecommunications testing), and converted to quick-look IPL-formatted tapes by the science ground data handling group. All of the IPL first-order processing conducted between July 29 and September 9, 1969, used these tapes as the data source.

The high-rate data logged by DSS 14 and CTA-21 were used to generate experimenter data record tapes

for the use of the TV experimenters and IPL. Final decalibration processing used these data products, which contain the best achievable data, relabeled to indicate spacecraft shutter times for all pictures.

**3. First-order IPL processing.** During the early phases of data analysis, a number of processing steps were applied to the data in a first-order sense, in response to the scientific needs of the TV experiment team. Table 13 is a summary of the processing completed in the interval from July 29 to September 9, 1969. (For an explanation of the listed programs, see Volume I of this report.) It should be noted that not all of the indicated processing produced entirely satisfactory results. This is particularly true in the case of the reconstructions of *Mariner VI* near-encounter pictures 1-8; for these, the low-amplitude signal received from ATR track 1 playback resulted in a very high random noise component, which in turn limited the success of the reconstruction effort. Multiple playback averaging was employed in the course of final processing in an attempt to improve early results. *Mariner VII* noise removal was another example of less than satisfactory processing. It was not as successful as was the noise removal conducted on the *Mariner VI* pictures because the coherent noises project at lower

**Table 13. Image processing laboratory first-order processing of *Mariners VI* and *VII* data, July 29 to September 9, 1969**

Process	Total pictures processed, %			
	<i>Mariner VI</i> encounter		<i>Mariner VII</i> encounter	
	Near (25)	Far (50)	Near (35)	Far (93)
Contrast enhancement	88	60	86	10
ATR <sup>a</sup> dropout removal	100	60	66	8
MSB <sup>b</sup> restoration	96	—	100	—
Noise removal	88	10	66	2
First-order reconstruction	80	—	86	—
Residual image removal	40	—	49	—
First-order photometric decalibration	40	—	54	—
MTF <sup>c</sup> correction	88	30	60	—
First-order geometric distortion removal	—	10	—	4

<sup>a</sup>ATR = analog tape recorder.  
<sup>b</sup>MSB = most significant bit.  
<sup>c</sup>MTF = modulation transfer function.

frequencies on the vertical axis. As a result, the noise-removal technique was modified for application to the *Mariner VII* data.

**4. Summary of final decalibration processing procedures.** Because of the unique design of the *Mariner Mars 1969* television subsystem, photometric decalibration must await the completion of the reconstruction process in which the analog and digital data are combined. This provides an output picture in which the effects of the on-board processing electronics have been removed. This process is discussed in later paragraphs.

Reconstructed photographs contain all of the photometric distortions characteristic of vidicon images. The first of these to be removed in the decalibration procedure is that of residual images. Calibration data provide a measure of retentivity as a function of previous exposure and position in the image format for each of the flight cameras. This information permits the construction of a residual image sensitivity map for each of the cameras, which can be used to modulate the previous picture; the resultant is then subtracted from the photograph containing the residual image to effect the desired correction. Far-encounter pictures contain residual images formed by the immediately previous exposure. However, only widely spaced far-encounter pictures were recorded so that the limited (33-pictures-per-tape load) capacity of the ATR could be efficiently utilized. The technique for residual-image removal for far-encounter, therefore, involved subtraction of the appropriately scaled portion of the picture from itself, after first translating it to coincide with the location of the residual image. The registration of the real to the residual image could be accurately checked by use of difference picture techniques. Because the planet revolves only about  $\frac{1}{2}$  deg per frame time, and the residual image percentage is less than 12% of the previous exposure throughout the image format, photometric errors introduced in this procedure are small. Photometric decalibration also involves the removal of coherent noise superimposed on the video signal; this procedure will be described later.

After noise and residual-image removal had been completed, correction was made for sensitivity variations across the scanned area of the vidicon target. Calibration data provide a light-transfer characteristic function (data number out vs luminance in) for each point in the image format. These data were obtained by use of luminance sources specially constructed to be

uniform to within a few tenths of one percent over the entire region viewed by the vidicon target. Spatial variations in output intensity could, therefore, be accurately described in terms of sensitivity variations on the vidicon surface. Calibration flat-field pictures, properly scaled for temperature coefficients and spectral response, provided the basis for the final sensitometric correction to the flight data.

A major indicator of the accuracy of photometric decalibration is the extent to which vidicon target "shading" is removed in the product pictures. Figure 7a is a contoured (i.e., bit-clipped) version of *Mariner VII* B camera near-encounter reconstructed pictures averaged together. Figure 7b is a similarly averaged and contoured version of those same pictures after photometric decalibration. One intensity cycle (i.e., black-to-black) in each of these figures represents 8 data numbers out of a total range of 256. Data from the four cameras aboard *Mariners VI* and *VII* provide a unique opportunity to evaluate TV system photometric performance and the efficacy of calibration and decalibration techniques, as the pictures contain a number of *in situ* test points; i.e., the same Martian area taken under nearly identical viewing conditions by two (or more) different camera systems. Preliminary analysis of the decalibrated data shows that certain inconsistencies exist. The continued analysis of these data may yield information valuable to the design of future similar experiments.

The removal of geometric distortions from the flight data is required to allow the accurate determination of spatial relationships and scaling in object space. These types of measurement are important in attempts to construct maps of the areas photographed for the guidance of future exploration efforts and for the determination of the figure of the planet in using far-encounter photography. Two types of distortion exist in the data. Optical distortion is present in the image on the vidicon target (as is the case with any camera system). A more significant distortion, termed *electronic*, is introduced in the course of scanning the target to produce the video signal. These effects can be separated and individually corrected by means of *in situ* measurements of a reseau pattern that was accurately deposited on the vidicon target combined with calibration data taken by use of a test target produced from grating engine-scribed glass plate. The procedure followed in *Mariner Mars 1969* geometric correction involved first the normalization of the flight data (based on reseau locations determined for each individual picture) to the same target-space

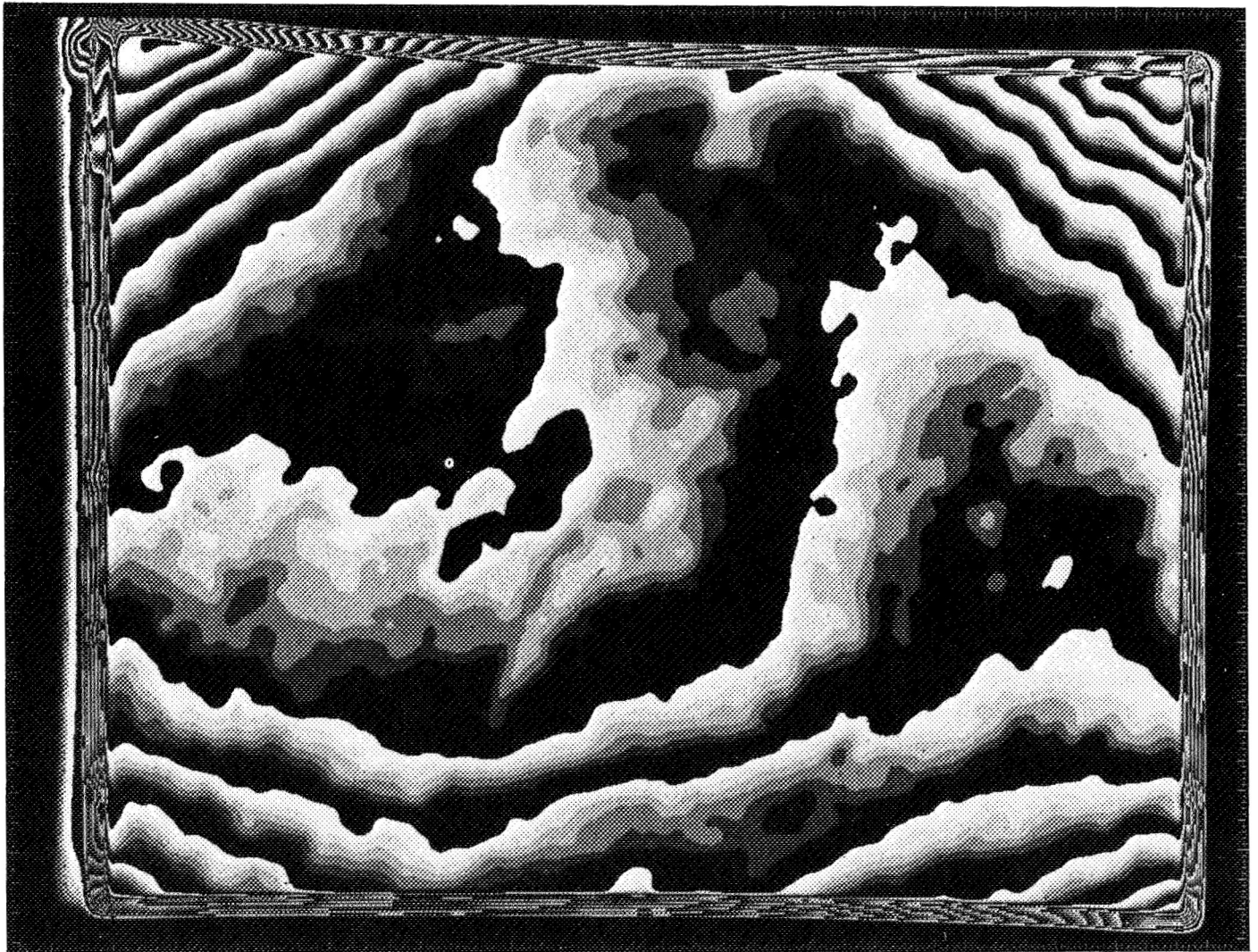
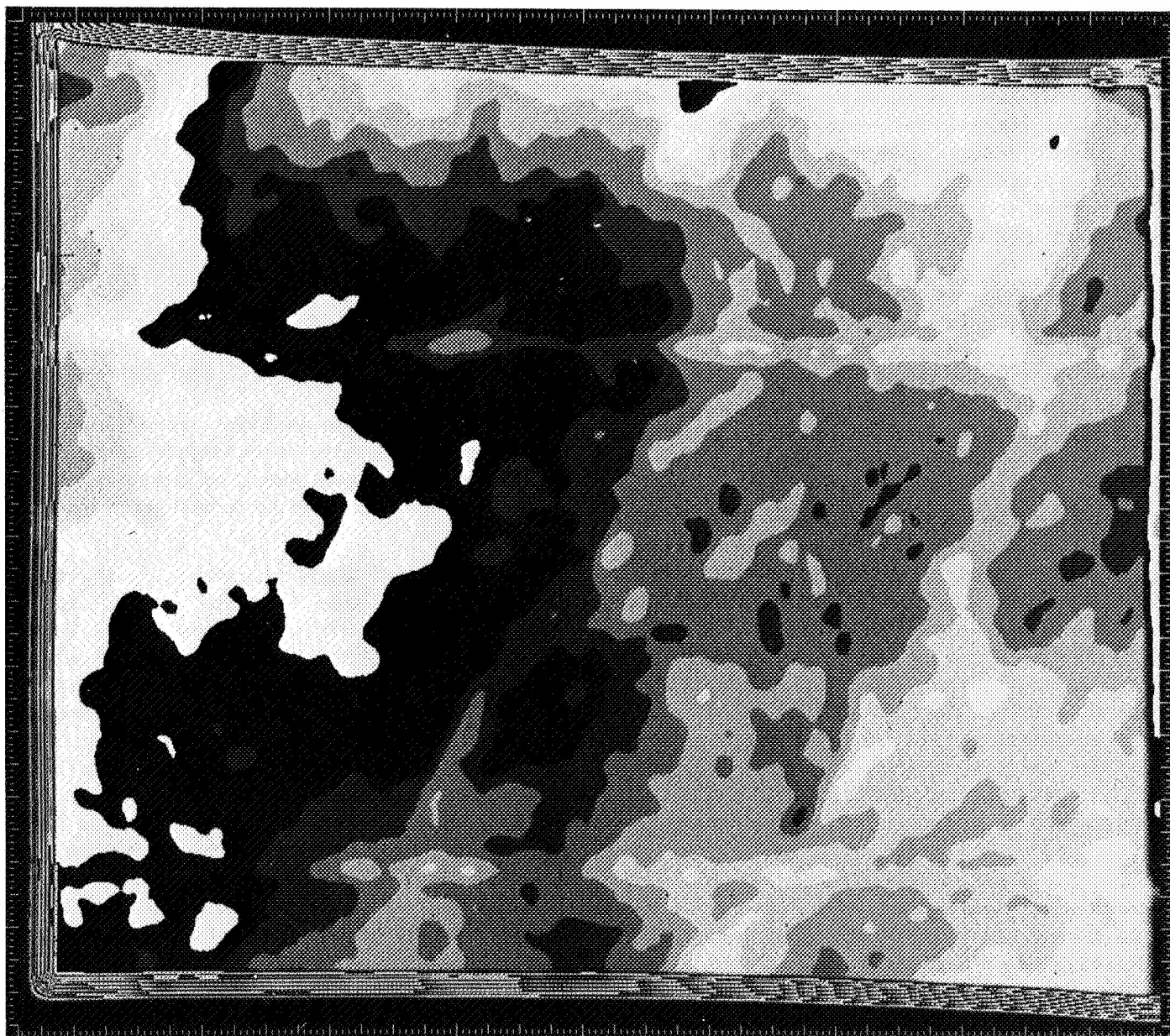


Fig. 7a. Contoured version of *Mariner VII* B camera near-encounter reconstructed pictures averaged together



**Fig. 7b. Same pictures (Fig. 7a) after photometric decalibration**



coordinates as a selected geometric distortion calibration frame. A second geometric correction was then conducted by use of parameters that had been previously determined to correct the image of a geometric distortion test target to its independently measured true shape.

Another correction made to the data involved the restoration of high-spatial-frequency information by means of convolution filtering. Referred to as sine-wave-response filters in recognition of the generally sinusoidal intensity distribution of the scanning beam, the filters were derived from calibration measurements of the modulation-transfer function of the camera systems obtained using computer-generated, variable-frequency, low-contrast, sinusoidal targets.

This brief summary of decalibration procedures touches only the major classes of processing steps, and is intended only to serve as a background for the ensuing discussion of the two procedures that dominated the *Mariner* Mars 1969 decalibration processing at the image processing laboratory. These two procedures are reconstruction and coherent noise removal.

*a. Reconstruction.* As described above, the fully sampled near-encounter data required the restoration of a dc photometric reference before measurements of relative scene luminances could be made. The data formats obtained from the spacecraft are illustrated in Fig. 8. The mottled appearance of Figs. 8a and 8b results from the truncation of the two most significant bits (MSBs) before transmission. The first and most difficult step in the reconstruction process involves the restoration of these bits; this is an iterative operation wherein automatic computations are interleaved with manual adjustments until a satisfactory product is obtained.

The primary tool in the accomplishment of MSB restoration is a program that, in the course of several passes through the picture, attempts to restore MSBs by use of criteria that essentially demand smooth intensity transitions in the output picture. Because two MSBs are missing, the true intensity at any given point in the picture can be in any of four "quadrants" (i.e., 00, 01, 10, or 11). The MSB program, then, first scans the columns in the picture to seek sharp discontinuities, which represent probable quadrant changes; it also seeks lesser discontinuities, termed *ambiguities*, at which a quadrant change may or may not have occurred. The program then selects a column that exhibits the largest number of quadrant changes and the smallest number

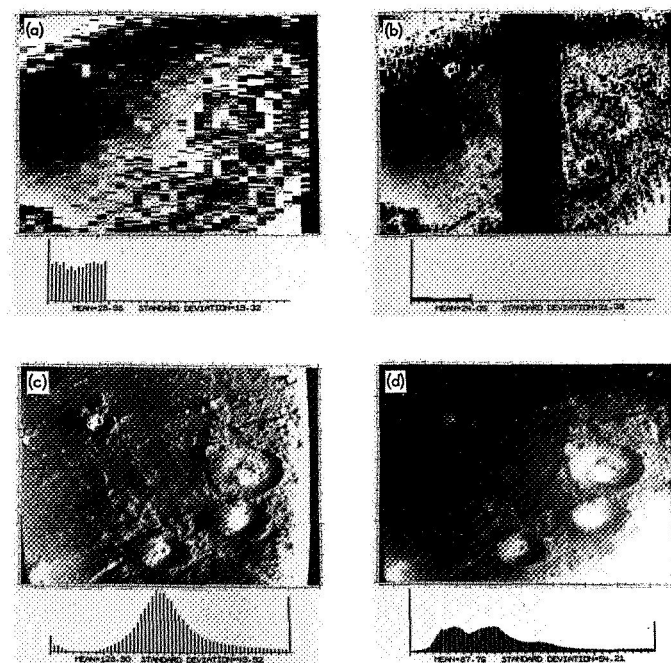


**Fig. 8. *Mariner VII* near-encounter picture 12 (narrow-angle camera): (a) every twenty-eighth digital video, (b) every seventh digital video, (c) composite analog video, (d) product obtained by reconstruction process**

of ambiguities, and begins to correlate across rows in the picture, again using the smoothness criterion to make most probable MSB assignments. The output picture so produced is then examined by an analyst; errors in MSB assignments are noted, and point-by-point adjustments are made to correct MSB assignment errors. This procedure often takes several iterations, particularly in the case of pictures wherein noise bursts have produced anomalous intensity values that perturb the MSB program. Obviously, also, certain true image characteristics (e.g., small, sharp crater shadows) can violate smoothness criteria; therefore, they require manual adjustment of the automatic MSB assignments to produce a true representation of the scene. This, of course, implies the use of the CAV pictures as a guide in the generation of correctly restored DV. An example of MSB restoration, as applied to *Mariner VII* near-encounter picture 20, is given in Fig. 9.

Once MSB restoration has been completed for digital video, these pictures are combined with the composite analog video to produce the reconstructed picture. The technique used is one of multiplicative adjustment of the CAV intensity to match that of the MSB-restored digital value at the corresponding point in the picture.

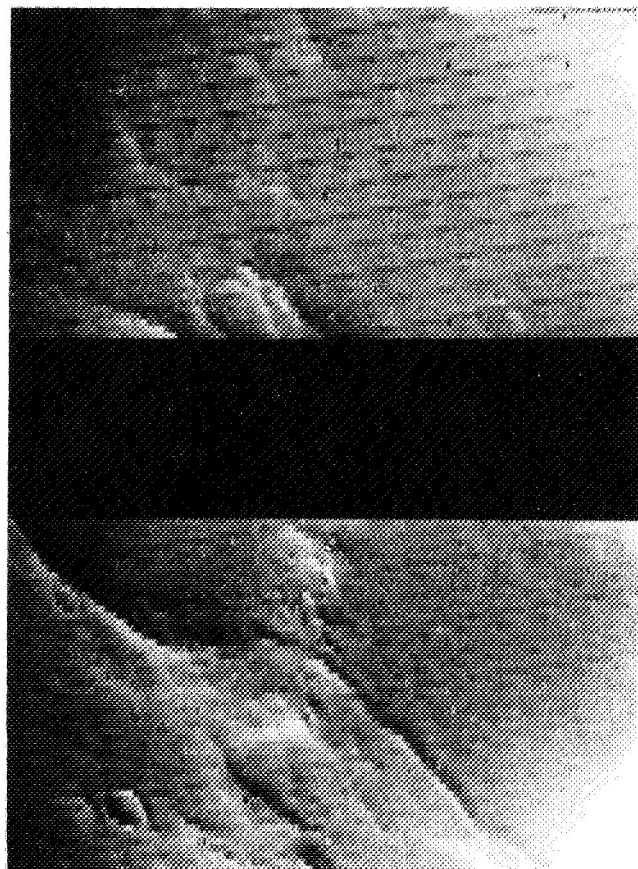
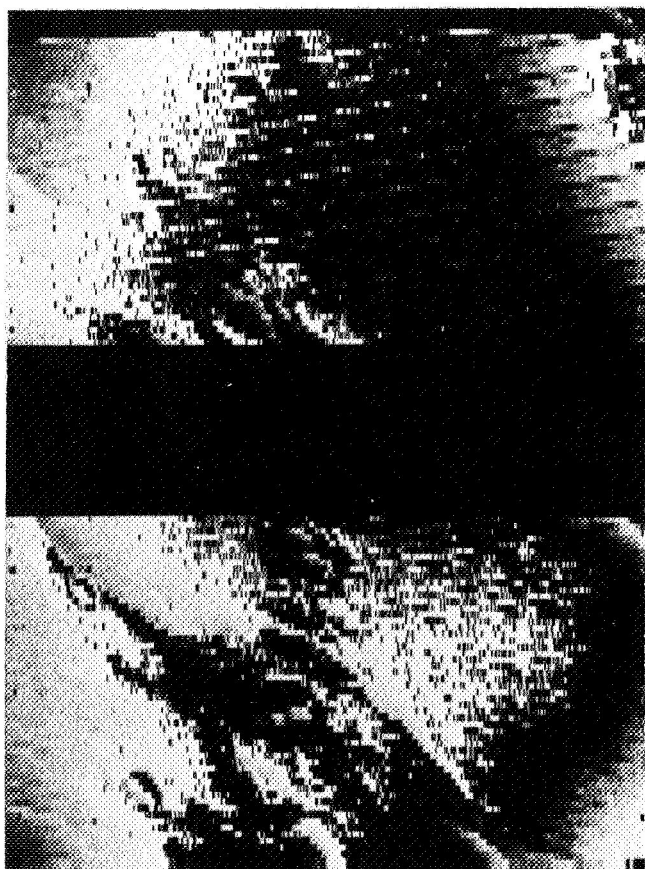


**Fig. 9. Example of most significant bit restoration: *Mariner VII* near-encounter picture 20**

The gain factor used to make this adjustment is then applied to adjacent CAV points, after correction by linear interpolation to vary smoothly between DV-sampled points. The product of this process is again iterated upon by a combination of manual adjustments and discontinuity-recognizing programs to produce the final reconstructed picture. Iterations are required because of errors in either CAV or DV introduced by noise or phase shifts.

Figures 10 and 11 illustrate the effects of the reconstruction process. These figures are mosaics of five *Mariner VII* wide-angle camera pictures of the Martian south polar cap; Fig. 10 is the raw CAV mosaic and Fig. 11 is the reconstructed versions of the same photographs. The photometric distortions in Fig. 10 are notable; the luminance of the desert on the right appears to be nearly equivalent to that of the "snow"-mantled polar-cap region. The true luminance relationships are shown in Fig. 11. The dark collar around the cap-desert interface

should be noted in Fig. 10. This dark band is illustrative of the time constant of the AGC. A comparison of the two mosaics also provides an appreciation of the value of the on-board processing electronics in enhancing visible detail in the raw pictures. The true contrast range on Mars (see Fig. 11) is obviously too great to allow the optimum visibility of surface detail over the whole of the region covered by these mosaics to be shown in a single photographic print. Finally, it should be noted that the residual images of earlier limb pictures (visible in Fig. 10) can be removed only after completion of the reconstruction procedure because this process relies on a knowledge of the true exposure level in the picture that produced the residual image.

*b. Coherent noise removal.* The *Mariner Mars 1969* data are characterized by the presence of a significant amount of structured noise introduced into the video signal by pickup from power supplies, heater wires, etc. The character of these noises is best illustrated in the fre-

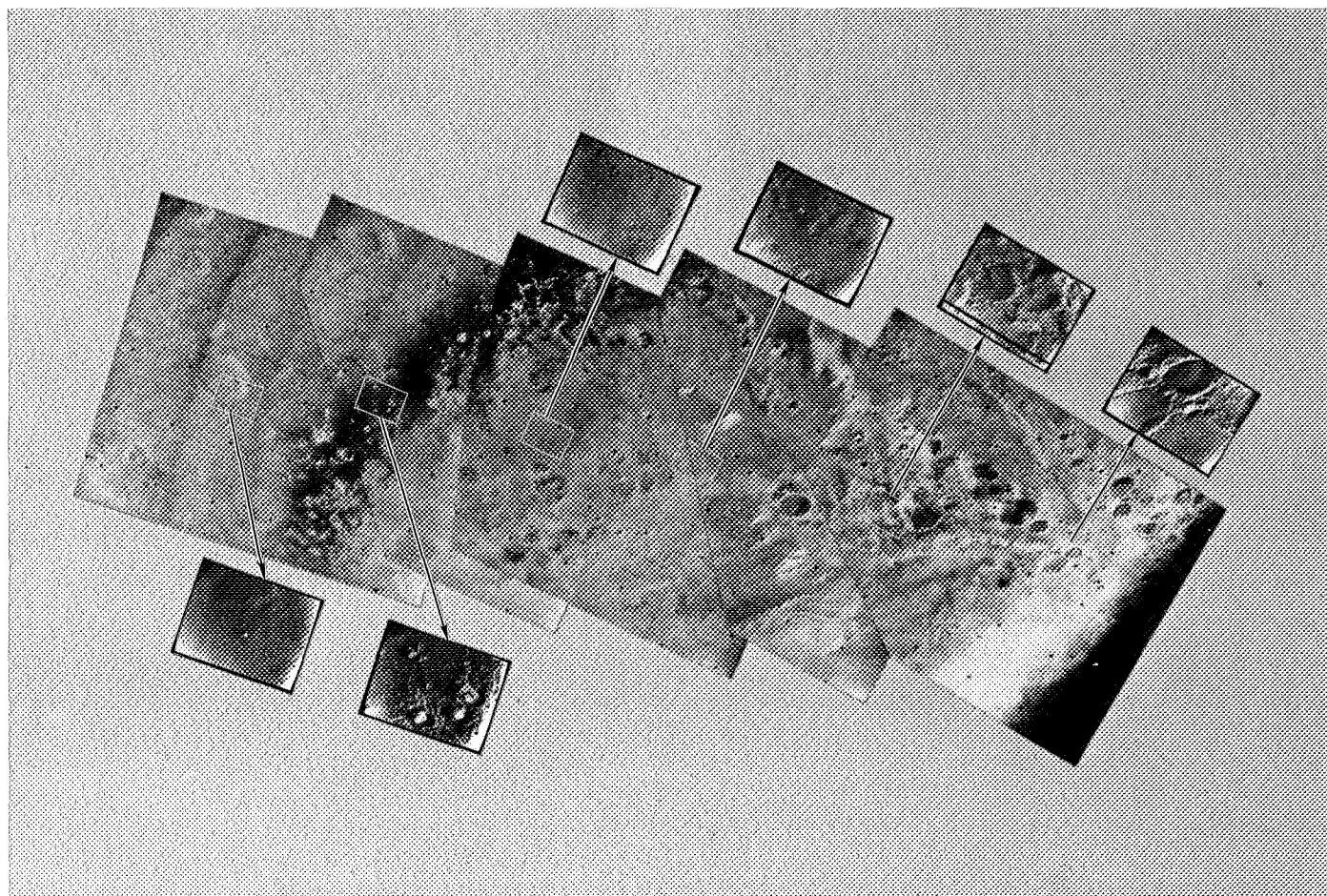


Fig. 10. Raw composite analog video mosaic of *Mariner VII* polar-cap sequence



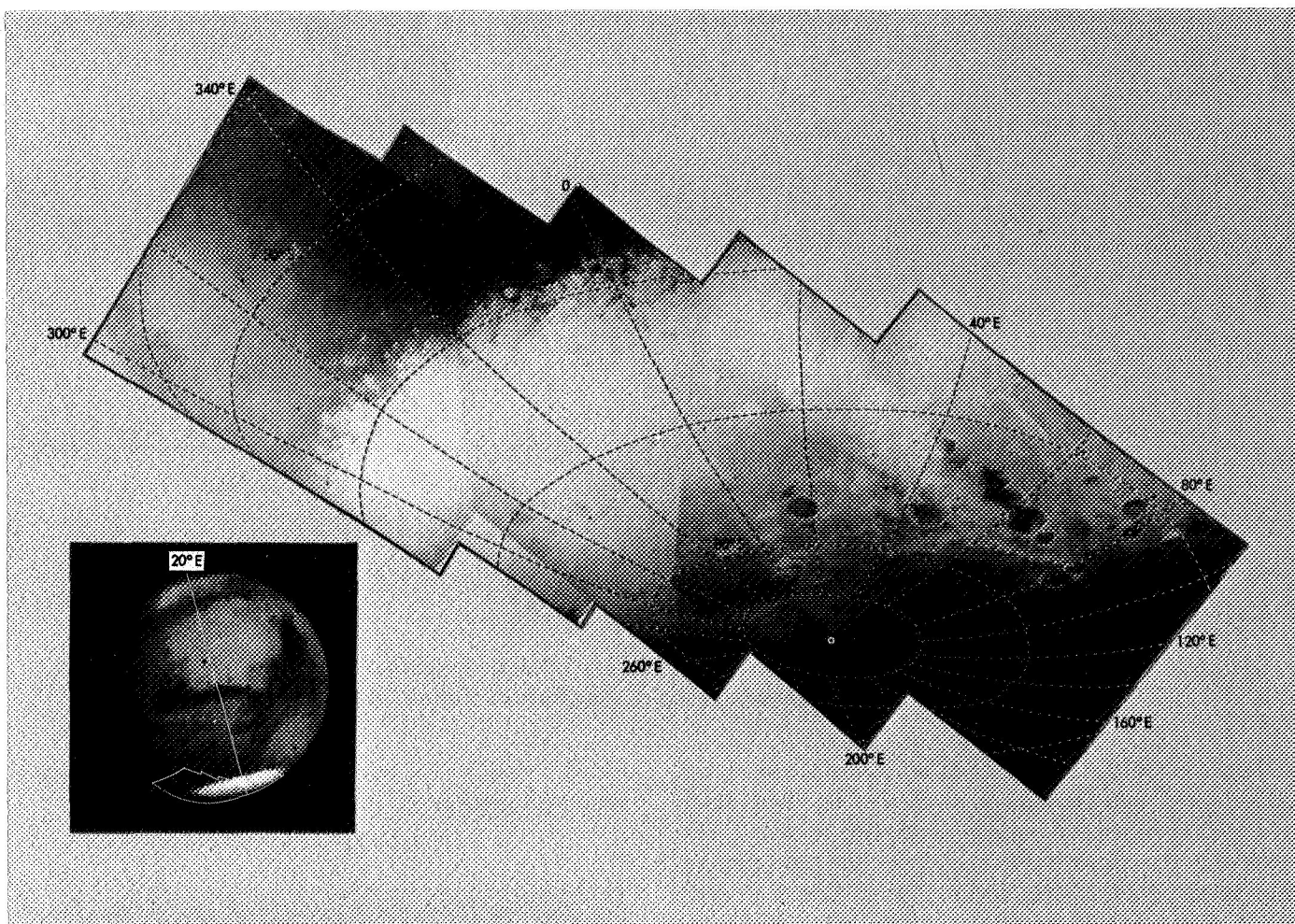


Fig. 11. Mosaic of reconstructed versions of *Mariner VII* polar-cap sequence (wide-angle camera)

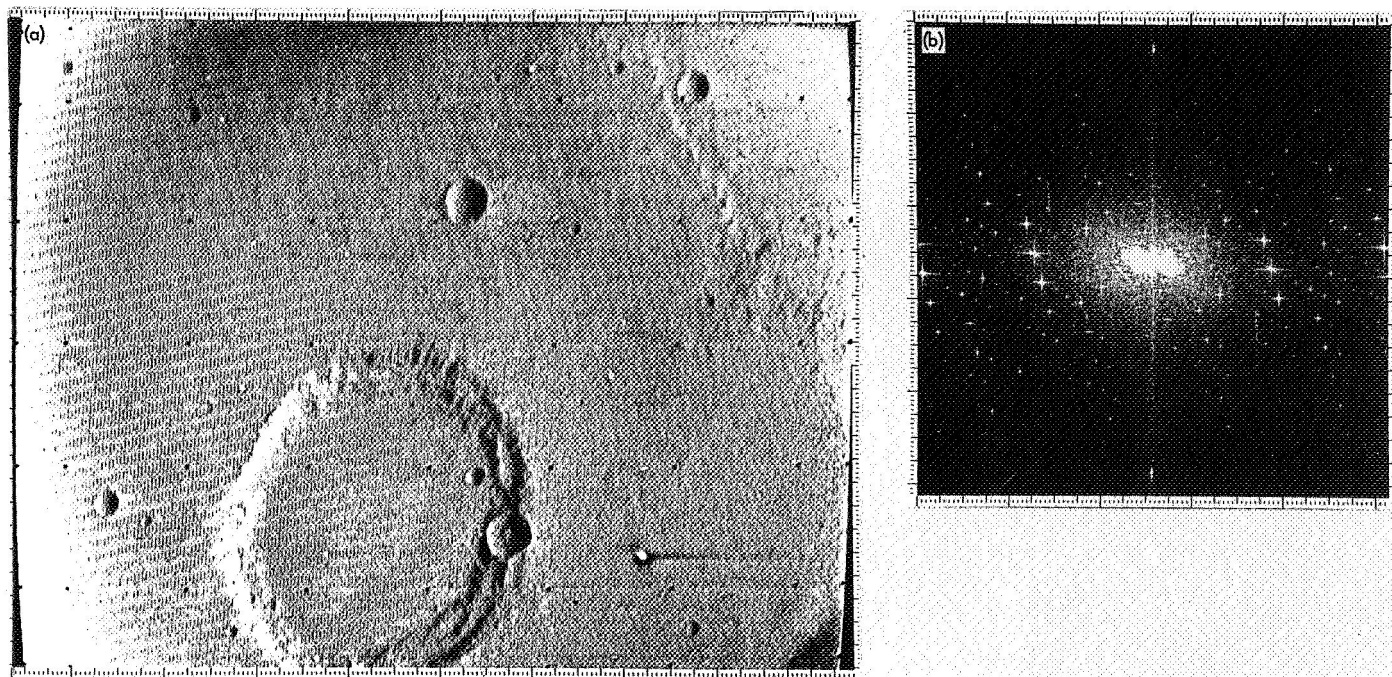
quency domain. Figure 12a shows *Mariner VI* picture 18 and Fig. 12b is a two-dimensional Fourier transform of the same picture. The central region in the transform (dc is at the origin) contains most of the scene modulation or picture power. The sharply defined, star-like maxima occurring throughout two-dimensional-frequency space represent coherent noises.

Figure 13 is a similar two-dimensional Fourier transform of a portion of *Mariner VII* near-encounter picture 19. In this transform, a different quadrant convention is employed than that in Fig. 12, and dc is at the corners. Again, the presence of periodic components superimposed on the smoothly varying image "continuum" is quite evident. These well-defined (in the frequency domain) peaks represent an almost trivial problem from the viewpoint of pattern recognition, and their isolation and removal from picture data are

in principle quite straightforward. The quantitative and accurate removal of these periodic components can be difficult in practice, however, because of their complex phase relationships and amplitude variation throughout the picture format.

Noise removal first requires the acquisition of such two-dimensional frequency information as is shown in Fig. 13. On the basis of measurements made by use of these data, the picture is bandpass-filtered; i.e., only those periodic components that one desires to remove are passed into an output picture. This output picture, then, is essentially the noise pattern that one wishes to extract from the original picture. The next step involves fitting this uniform, idealized pattern to the picture data so that the quantitatively correct amplitude can be subtracted in each area of the picture. The fitting is done by means of least-squares analysis for small ( $30 \times 30$ )



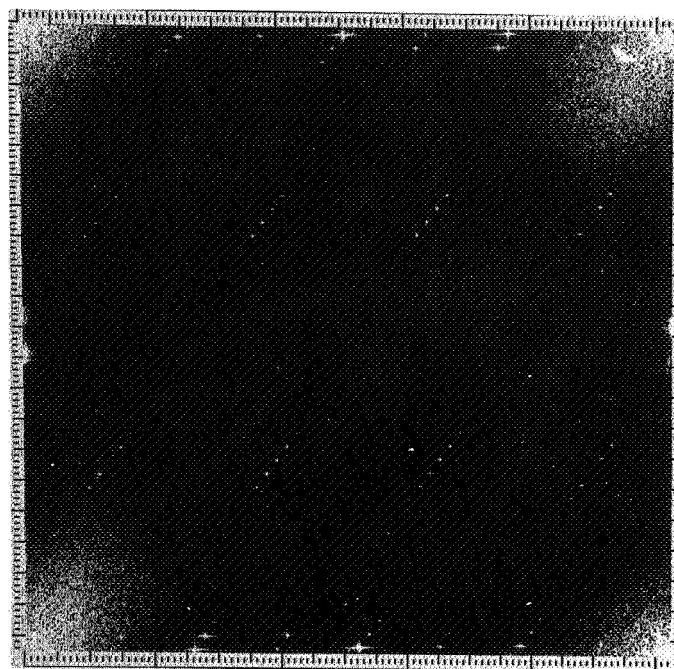


**Fig. 12. Coherent noise removal: (a) *Mariner VI* near-encounter picture 18, (b) two-dimensional Fourier transform of picture 18**

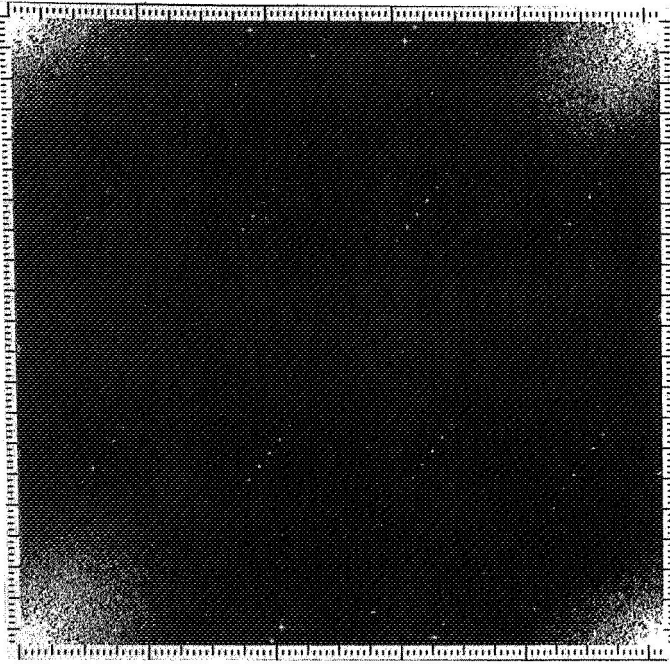
portions of the picture. A modulation-coefficient matrix is calculated that contains a coefficient for each small area so that, when the noise is multiplied by that coefficient and the result subtracted from the raw picture, the variance in that area of the output picture is minimized. The raw picture, noise pattern, and modulation-coefficient matrix are then combined in the final noise-removal step. The operation of this process is shown in Figs. 13–17.

Figure 14 is the two-dimensional Fourier transform of *Mariner VII* near-encounter picture 19 after noise removal. The vacant areas occupied by sharp maxima in the left-hand transform should be noted. Figure 15 shows raw and Fig. 16 noise-removal versions, respectively, of the same small area of picture 19. Figure 17 is a difference picture obtained by subtraction of the noise removed from the raw versions shown in Figs. 15 and 16; it represents, then, the actual noise pattern extracted from this portion of picture 19. The image detail apparent in the noise pattern should be noted. The presence of this nonperiodic modulation may at first seem to suggest the passage of some “picture power” into the noise picture, which would imply the removal of some image detail along with the noise. Actually, the presence of these features in the noise pattern is merely illustrative of the action of the modulation-coefficient matrix, which

found virtually no noise modulation in these nearly saturated portions of the picture.



**Fig. 13. Two-dimensional Fourier transform of *Mariner VII* near-encounter picture 19**



**Fig. 14.** Two-dimensional Fourier transform of *Mariner VII* near-encounter picture 19 after partial removal of coherent noise

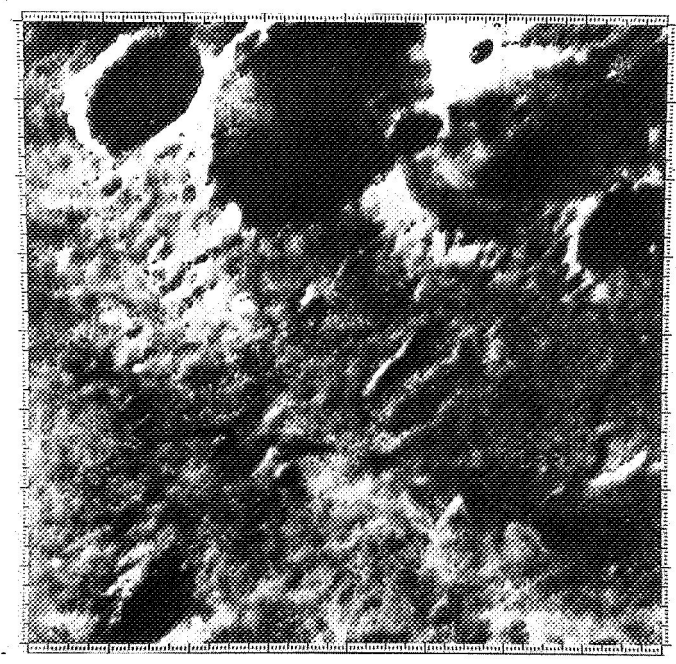


**Fig. 16.** Picture 19 after partial removal of coherent noise



**Fig. 15.** Enlargement of a portion of *Mariner VII* near-encounter picture 19

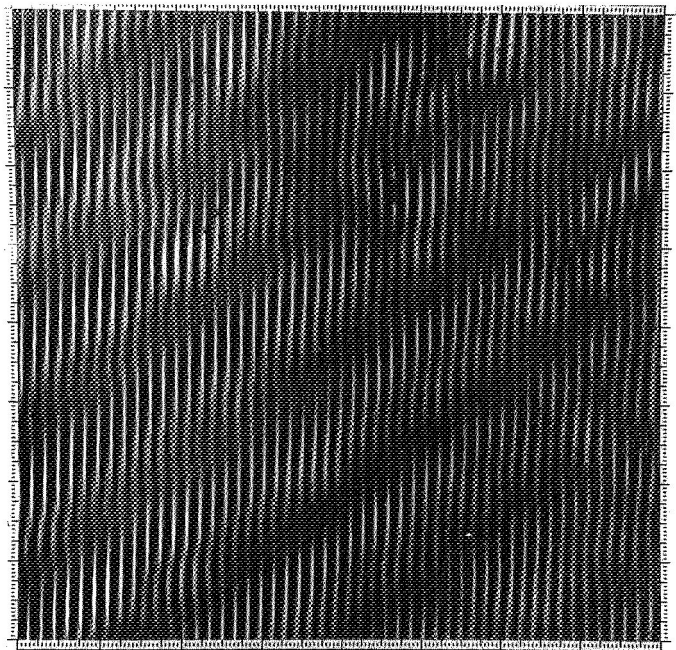


**Fig. 17.** Difference picture obtained by subtraction of Fig. 14 data from data given in Fig. 15 (zero differences appear as a neutral gray shade)



The improvement illustrated in Figs. 15 and 16 resulted (as can be seen by comparing Figs. 13 and 14) from the removal of a small number of frequency components. This limitation is imposed by the nature of the bandpass technique employed, which operates on a picture one line at a time because of core limitations. This requires a two-step filtering procedure—once horizontal and once vertical. The areas removed in two-dimensional-frequency space are, therefore, determined by the intersections of bands projected parallel to the axes. To avoid the loss of image information, the number of such bands must be kept to a minimum; therefore, only a few rectangles can be removed in a single "pass." Final processing employed a direct, two-dimensional bandpass technique by use of a larger machine (IBM 360/75). This method permits the removal of virtually all periodic components in a single pass, and produces an output picture with a significantly lower residual noise content than is evident in Fig. 16. Figures 18–20 show the operation of this technique on a portion of *Mariner VI* near-encounter picture 13. Figure 21 is representative of data after final noise removal. Two additional algorithms operated on these data to remove ATR "streaking" and to isolate "spike" noises, respectively.



**Fig. 18. Enlargement of a portion of *Mariner VI* near-encounter picture 13**



**Fig. 19. Figure 18 after final two-dimensional coherent noise removal**

The removal of coherent noise enhances the visibility of fine detail in these pictures. Furthermore, greater improvement is made possible by the removal of these noises, in that edge enhancement by means of convolution filtering becomes practicable once the sharply defined coherent noises have been removed. Such filtering is not practicable in the presence of the fine-structured noises characteristic of the unprocessed *Mariner Mars 1969* data.

*c. Final products.* In the course of decalibration processing, prints of preliminary and significant intermediate products were continuously made available to the members of the experiment team, as were numerical listings of specific areas of pictures (as requested). Final products (maximum-discriminability and photometrically decalibrated pictures) were generated in a number of different versions (stretches) to assist in interpretation. Prints and negatives of the versions considered optimal by the experiment team were provided to the National

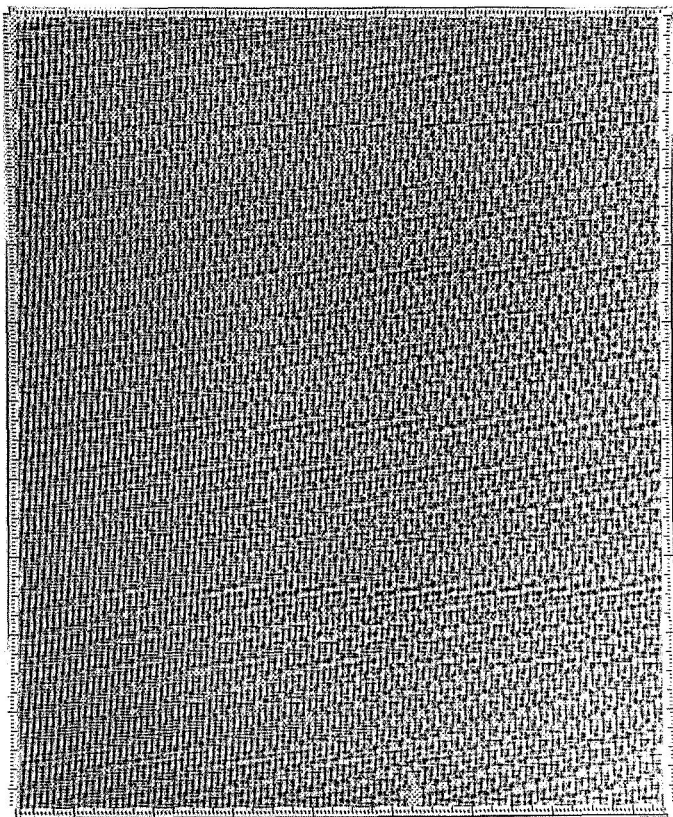


**Fig. 20. Coherent noise pattern extracted from Fig. 18**



**Fig. 21. Final version of Fig. 18 with coherent and nonperiodic noises removed**

Space Science Data Center (NSSDC), GSFC, Greenbelt, Md., for all final products. Included in the final products for the decalibrated data were magnetic tapes.

*Magnetic tapes.* Image processing laboratory formatted tapes containing final products (maximum-discriminability and photometrically decalibrated data) have been sent to NSSDC and to those experimenters who requested them. Archival and working copies of final-product tapes and certain critical intermediate products will be retained by the IPL until July 1, 1971, at which time they will be transferred to the science ground data handling library for archival storage.

*Maximum-discriminability pictures.* The CAV near-encounter pictures discussed above display high-spatial-frequency image data in an optimal manner because of the action of the AGC and cuber. For the recognition of surface morphological features on a fine scale, then, suitably processed versions of these pictures are most desirable. For this reason, the maximum-discriminability version is identified as a major product type. All

maximum-discriminability pictures have been processed in the manner described in Section I-C-4-b. Additionally, near-encounter maximum-discriminability pictures are sine wave response filtered by use of convolution filter weights derived from calibration data to enhance high-frequency detail. As indicated earlier, maximum-discriminability pictures were produced with a range of contrast-enhancement parameters to assist in interpretability; however, a single "optimal" stretch has been used to generate the photographic version of this final product type for general distribution.

*Photometrically decalibrated pictures.* This final product represents the best available photometric representation of the area photographed. Its principal value will be in the conduct of quantitative photometric measurements by use of numerical printouts derived from the data tapes. However, contrast-enhanced versions have been made available in the form of photographic prints to aid in the identification and interpretation of true scene intensity variations.

## II. Infrared Spectrometer Subsystem

### A. Objectives

The objectives of the infrared spectrometer (IRS) subsystem were to make use of measurements of the spectral radiance of the thermally emitted radiation from the Martian atmosphere and surface to infer atmospheric and surface parameters. These parameters will be used in (1) studies of the vertical temperature structure, composition, physical behavior, and dynamics of the Martian atmosphere, and in (2) investigations of surface types, composition, and structure.

### B. Performance

1. *Launch to far-encounter.* From launch until science power was turned on, 2 or 3 days before Mars encounter, the IRS instrument was passive, and the only indication of the condition of the instrument was the data from the two flight telemetry subsystem (FTS) engineering measurements of the electronics and radiator temperatures. Both instruments cooled to the proper temperatures shortly after launch, and remained so until encounter. The observed temperatures at  $L + 36$  h, science turn-on, and the corresponding design temperatures are given in Table 14.

Table 14. Infrared spectrometer flight temperatures

Source	$L + 36$ h, °K	Science turn-on, °K	Design, °K
Mariner VI electronics	245.4	243.3	241
Mariner VI radiator	172.7	172.7	167
Mariner VII electronics	245.9	244.9	241
Mariner VII radiator	165.9	165.9	160

2. *Far-encounter.* The far-encounter sequence started when science power was turned on, which was approximately 2 days from Mars encounter for *Mariner VI* and approximately 3 days from Mars encounter for *Mariner VII*. With science on, the 10 IRS engineering words and the 2 science channels were read out by the DAS, and then transmitted to the Space Flight Operations Facility (SFOF) at JPL.

Both *Mariner VI* and *VII* engineering temperature measurements were within the expected tolerances, and the log stacks in each instrument started cycling after about 1.5 h, as expected. Also, the voltage measurements for each instrument were the same as they had been

at launch, indicating good thermal stabilization of the power supply. Good far-encounter engineering data were received from both the *Mariner VI* and *VII* instruments, indicating that they were in good condition and ready for near-encounter.

3. *Near-encounter.* The near-encounter sequence for the IRS started approximately 35 min before encounter with the squib firing that released the  $N_2$  and  $H_2$  gases for cooling of the cryostat associated with channel 1. The cooling period was expected to require about 15 min.

The cooling gases were properly released on both *Mariners VI* and *VII*; however, on *Mariner VI*, it appeared that the cryostat became plugged and failed to cool to the proper temperature, resulting in loss of channel 1 data. The plugging of the cryostat was assumed to be the cause of this failure because a number of cryostats had plugged during testing under much the same conditions as those on *Mariner VI*. The instrument operated well in all other respects, and good data were obtained from channel 2 (the failed cryostat affected only the channel 1 data).

The *Mariner VII* IRS performed as designed. Shortly after release of the cryostat cooling gases, the temperature of the two gas bottles slowly decreased, indicating that the cryostat was being cooled. This was followed by a sudden decrease of about 200 data numbers in the channel 1 detector temperature, indicating that the cooling process had worked satisfactorily. At 11 min after the  $N_2$  and  $H_2$  gases were released, the cryostat had cooled to the proper temperature. As the spacecraft flew by Mars, adequate channel 1 and 2 data were received.

## III. Ultraviolet Spectrometer Subsystem

### A. Objectives

The purpose of the ultraviolet spectrometer subsystem (UVS) was to measure the density and scale height of atoms, ions, and molecules in the upper atmosphere of Mars (60- to 600-mi range); the Rayleigh scattering from the lower atmosphere; and the ultraviolet reflectivity of the planet surface.

### B. Performance

The UVS instrument on both *Mariners VI* and *VII* performed as designed, with only one minor anomaly—a small shift in the data zero level of the *Mariner VII*

instrument (described below). The predicted temperature of the instrument at encounter was 30°F. The actual temperature was 33°F for *Mariner VI* and 30°F for *Mariner VII*.

**1. Data modes.** The UVS power application was coincidental with that of the other science instruments. The UVS itself had only one operational mode; that is, its operation was unaffected by transmitted data rates and orbital positions. For encounter Mode I (the 66%-bits/s data mode), only the real-time Lyman-Alpha (1216-Å atomic hydrogen resonance line) was extracted by the DAS for radio transmission, along with the engineering data. In the real-time high-rate telemetry mode at 16.2 kbits/s (encounter Mode II), the complete spectral data were transmitted, but only the Lyman-Alpha data were displayed in real-time. The full UVS spectrum data were recorded on tape, and small segments (2 or 3 min) were available upon request (within about 4 h) in a decimal-dump format and in spectral plots (time vs amplitude in decimal data number). Recorded magnetic tapes of the high-rate data were to be used for data reduction and processing. In the spacecraft playback mode, the UVS spectral printout in decimal-dump form was available from the 1219 printer. Because there were such large amounts of data (about 600 readouts per 3-s spectral scan), only the UVS flyby temperature, voltage, and calibration measurements were noted and verified.

## 2. Lyman-Alpha data.

**a. Mariner VI.** At all times other than during the near-encounter phase (including postencounter), the integrated real-time Lyman-Alpha data varied in random fashion between data numbers of 11 and 20. The averaged UVS analog output in this data-number range is about 250 to 500 mV above the data zero level. Occasionally, a single reading spike would occur that was created by a cosmic ray colliding with the phototube sensor. Such events are statistical, and the occurrences (rates and amplitudes) were as predicted. At approximately 5 h before closest approach, the Lyman-Alpha data rise became significant. When the spacecraft platform was slewed so that the UVS was viewing closer to Mars (the platform position from far- to near-encounter), the averaged analog voltage increased by 50 to 100 mV (2 to 4 DN). The characteristic of these data is that, as the ultraviolet light source increases in brilliance, the data samples will not only increase the averaged level, but also increase the peak-to-peak excursion. Figure 22 is a time history of the Lyman-Alpha readings. During the period that the UVS viewed the Martian atmosphere (from 100 km above the Martian surface to the planet limb), the Lyman-Alpha readings rose sharply from an averaged DN of about 20 (about 0.50 V analog above data zero) to a peak DN of 235 (analog signal level of about 5 V) at the limb. The platform was slewed at this point so that the UVS again

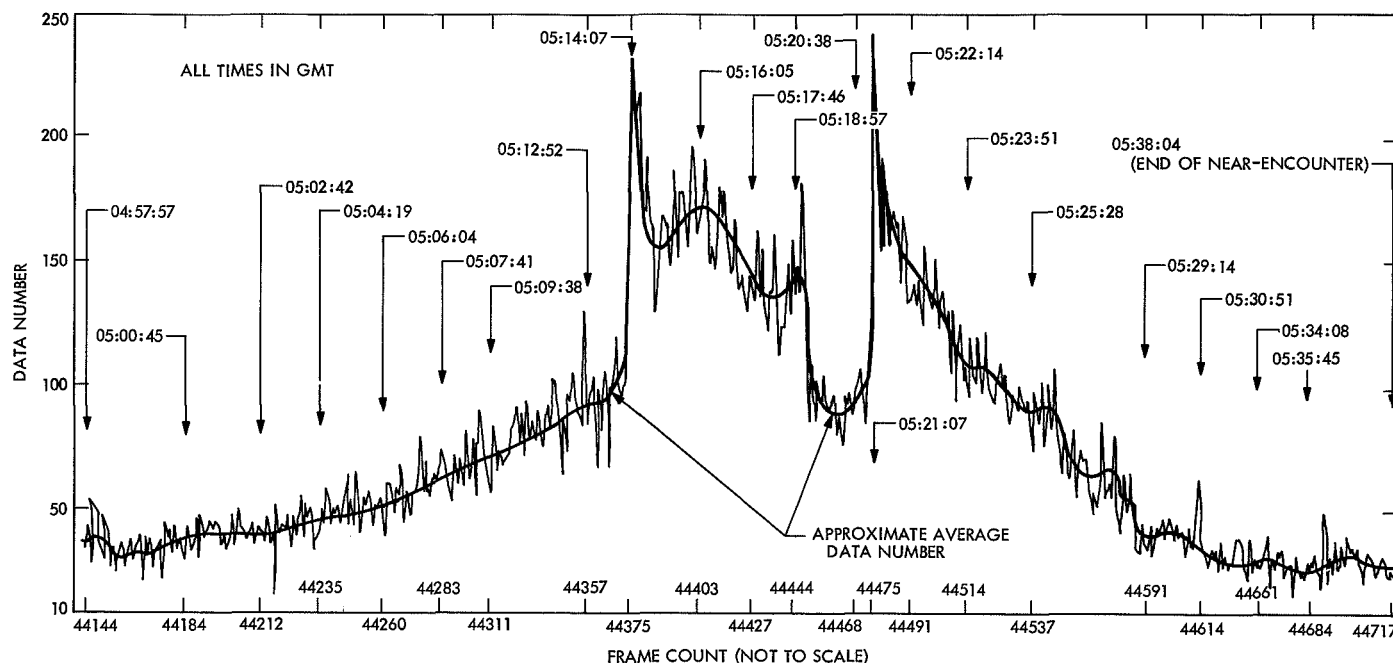


Fig. 22. Hand plots of UVS telemetry data, *Mariner VI* encounter, July 31, 1969

viewed the upper atmosphere, and the second set of Lyman-Alpha data agreed with the first. The spacecraft was switched to playback mode within 15 min of the second data peak, and real-time data were no longer available. The last reading was a DN of 23.

*b. Mariner VII.* From power turn-on to completion of the mission, the integrated real-time data ranged from 5 to 12 DN. During the on-pad testing before launch, the readings were from DN 11 to 20. Spectrum data extracts from the 16.2-kbits/s real-time data show the data zero level varying from 0 to 3 DN instead of a normal DN of 4 to 7. The UVS analog-to-pulse widths (APWs) are bipolar, and negative analog voltage readings to  $-0.5$  V are not degraded throughout the spacecraft and data systems; however, polarity information is not in the DAS format. Data plots showed a smooth transition from the last UVS engineering measurement, channel 1 photomultiplier tube (PMT) high voltage, to the data zero level without approaching zero. The analog gain measurement did not change, indicating that the data zero level shift was small (a few data numbers only) and that the level probably did not shift to a negative polarity. The zero level shift was the result of some unknown occurrence or disturbance between launch and science turn-on. A similar event occurred in Florida during systems testing as a result of an analog amplifier input field-effect transistor gate current leakage increase. In that case, however, because

it was a component part current leakage increase, the analog output offset continued to increase with time. Because the analog amplifier input impedance is very high ( $10^9 \Omega$ ), an increase in input current leakage at the phototube sensor could have been caused by some unknown change in its environment.

The Lyman-Alpha hand plots shown in Fig. 23 indicate data very similar to those of *Mariner VI*. The peak amplitude at the planet limb, however, reached a DN of only 150 (analog signal voltage of about 3.75 V).

**3. Spectrum data.** During the far-encounter phase for both *Mariners VI* and *VII*, the only spectral activity occurred at the Lyman-Alpha wavelength. The only noise spikes occurred on the N-tube (channel 2) PMT analog output. While the instrument was viewing the Martian atmosphere, the activity in both analog channels was appropriate. All 10 engineering measurements (Table 15) on both spacecraft were consistently correct in all data received at the SFOF.

All of the high-rate real-time data were rerecorded from the IPL-formatted tapes, and flown to Colorado University, where the spectrum data were reduced by computer, the plots recorded on 35-mm photographic film, and the film returned to the SFOF at JPL within about 6 h. With one exception, all of the plots were in agreement with one another and with the electrical

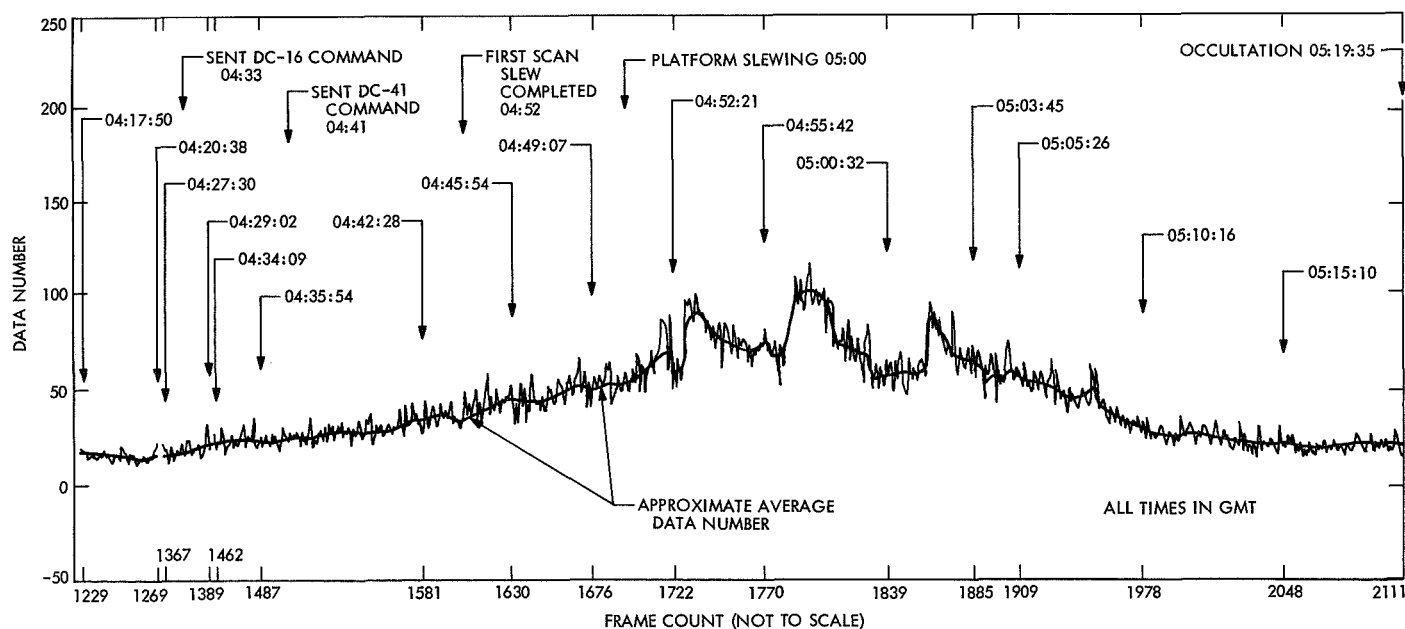


Fig. 23. Hand plots of UVS telemetry data, *Mariner VII* encounter, August 5, 1969



**Table 15. Ultraviolet spectrometer engineering measurements**

Measurement	Analog output		Duration, ms	Number of APW <sup>b</sup> readouts
	DN <sup>a</sup>	Voltage, V		
Channel 1				
Zero data level	6	0.141	40	8
Gain calibrate	190	4.471	40	8
Optical temperature 1	189	4.447	20	4
Optical temperature 2	189	4.447	20	4
PMT <sup>c</sup> high voltage	194	4.565	20	4
Channel 2				
Zero data level	5	0.118	40	8
Gain calibrate	182	4.282	40	8
PMT temperature	190	4.471	20	4
Regulated +15-V supply	202	4.753	20	4
PMT high voltage (normal)	145	3.412	20	4
PMT high voltage (when UVS viewing lighted surface of Mars)	50	1.177	—	—
<sup>a</sup> DN = data number.				
<sup>b</sup> APW = analog-to-pulse width.				
<sup>c</sup> PMT = photomultiplier tube.				

calibrations made on the Earth; the sole exception was the *Mariner VII* data zero level shift.

In addition to the optical and PMT temperatures (see Table 15), a UVS instrument temperature was transmitted by the FTS on channel 416 throughout both flights. During the cruise mode, when the UVS and other science instruments were off, an electrical heater was used to maintain the proper temperature.

**4. Limb sensor results.** Both the *Mariner VI* and *VII* limb sensors operated as designed. The rectangular-shaped projected field of view (ratio of length to width is 10) was essentially parallel to the Martian limb at the first limb encounter of *Mariner VI*. During one UVS atmospheric scan by *Mariner VII*, one limb sensor had remained excited by viewing the south polar cap while the other limb sensor continued to view the atmosphere and did not trigger. This unplanned condition permitted some channel 2 data amplitudes (e.g., CO<sub>2</sub><sup>+</sup>) to be obtained that otherwise would have been off scale.

**5. Postcounter tests.** Only real-time Lyman-Alpha data were received on the Earth from the three *Mariner VI* postcounter tests. No significant changes in the background data were apparent from the hand plots that were taken in real-time. The postcounter tests were arranged so that the UVS could view atomic hydrogen activity in the Milky Way and the Magellanic clouds.

## IV. Infrared Radiometer Subsystem

### A. Objectives

The purpose of the infrared radiometer (IRR) subsystem was to provide temperature measurements of the surface of Mars by detection of thermal radiation in the infrared portion of the electromagnetic spectrum. The IRR was boresighted with the TV-B camera to allow correlation of surface temperatures with terrain features and clouds, thus providing a means of mapping the planet surface by relating temperature variations to surface features. The instruments aboard both spacecraft scanned the Martian surface across the sunlit portion and into the dark side (in effect, from late morning to late evening). The data obtained will yield cooling rates that show the daily variations in temperature as the surface absorbs heat from the sun during the day and loses heat during the night. Data on the dark side of Mars, which are not obtainable from the Earth, will be of particular value.

Each of two detectors in the instrument provided 30 readings every 63 s. Of the 30 readings, 27 were of planetary temperature, 2 were calibration readings, and 1 was a temperature and voltage engineering measurement. The calibration readings were made from an internal source of known temperature and from deep space (the latter representing a zero reference point).

### B. Cruise Performance

The *Mariner VI* IRR cruise temperature rose from 19.3 to 21.3°F by June 18, 1969, and remained at that point until July 11; at that time, a DC-47 command was sent to activate the data storage subsystem and turn the IRR cruise heater off. By July 12, the temperature had dropped to 4.2°F; on July 13, it was 3.3°F; and, by July 14, it had settled at 2.3°F, where it remained until the IRR was activated for far-encounter. After activation (power turn-on), it took 30 h for the temperature of the unit to become stable. All planet-measurement



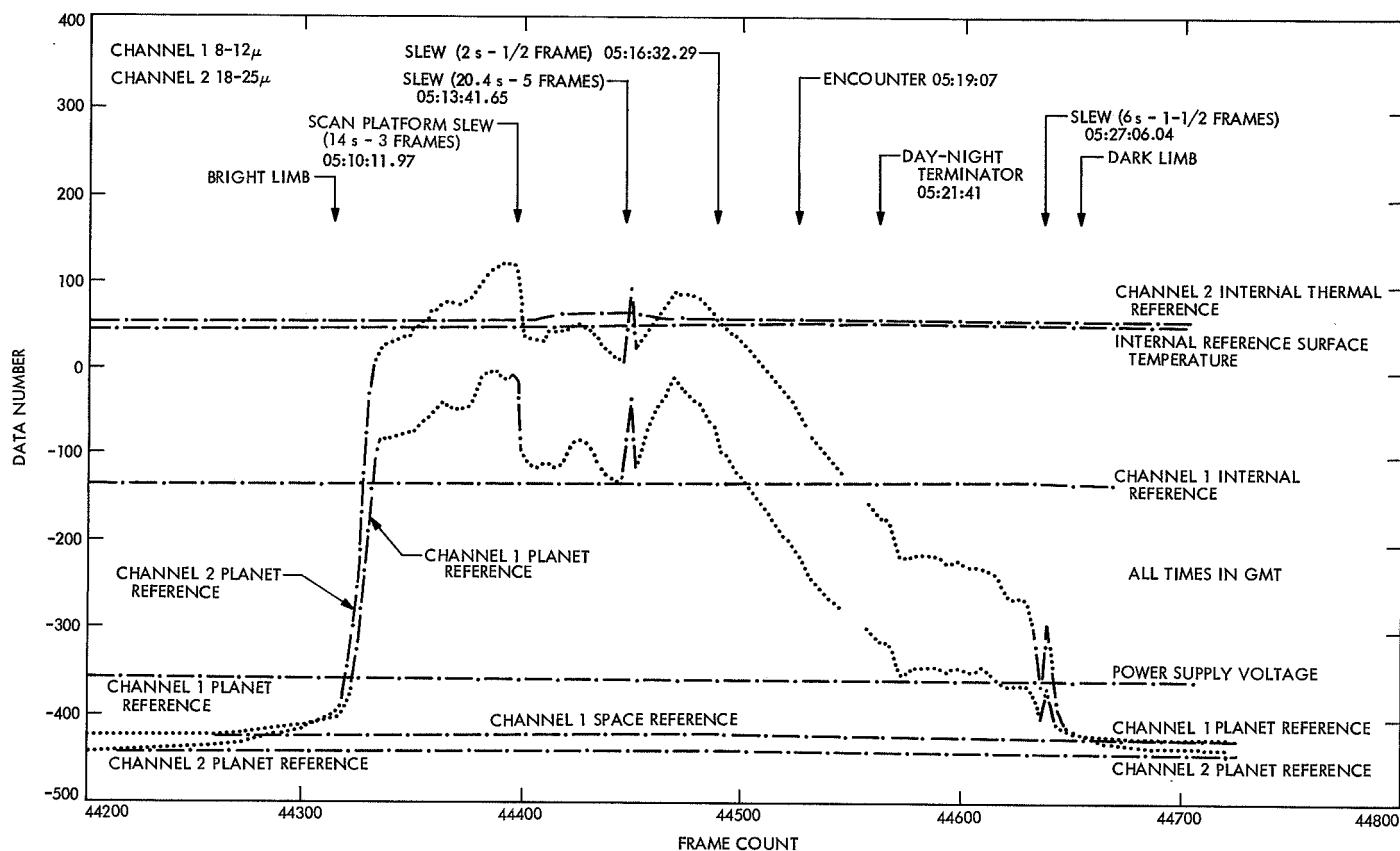


Fig. 24. Temperature history of *Mariner VI* infrared radiometer at encounter

data were usable, even with the changing reference temperature during this 30-h period. The change in reference temperature was caused by a fabrication error that placed the IRR cruise heater on the back of the data storage subsystem on-off relay. This location error was detected during preflight tests; however, it was felt to be more expeditious to leave it in that location, and not to rework the cabling, as the unit would normally have enough time to stabilize while in far-encounter.

The *Mariner VII* IRR cruise temperature was maintained at a stable 26.1°F by the cruise heater until the platform-unlatch event on May 8, 1969, when its temperature dropped to 22.0°F. By June 25, the temperature had risen to 24.0°F, and remained stable at this temperature until July 8, when a DC-47 command was sent to turn on the data storage subsystem and turn off the IRR cruise heater. The temperature of the IRR dropped to 6.1°F by July 9 and to 5.0°F by July 10. The IRR remained at this temperature until activation for far-encounter. With power turn-on, it took the unit 31 h to come to a stable temperature. Temperature histories

of the IRR instruments on *Mariners VI* and *VII* are given in Figs. 24 and 25, respectively.

### C. Far-Encounter Performance

The *Mariner VI* IRR was activated by science power turn-on at 01:27:40 GMT, and the first synchronized data were received at 01:31:00 (frame count 46), on July 28, 1969. Each IRR data channel read data every 2.1 s, and these data were returned in real-time. (The IRR was boresighted with the TV-B camera.) The moment of contact with the planet was readily seen. The unit operated normally, with a noise level of approximately  $\pm 1$  DN at all times, except during scan-platform slews. Deviations occurred during slews between near- and far-encounter positions. Channel 2 seemed to be more susceptible to these deviations than was channel 1. For example, when the CC&S originated an F1 command to slew from near- to far-encounter, the channel 2 readings varied from -442 to -456 DN during the slew. Except for such deviations during slews, as the IRR field of view was filled more completely by the planet, the data followed a predicted curve. The

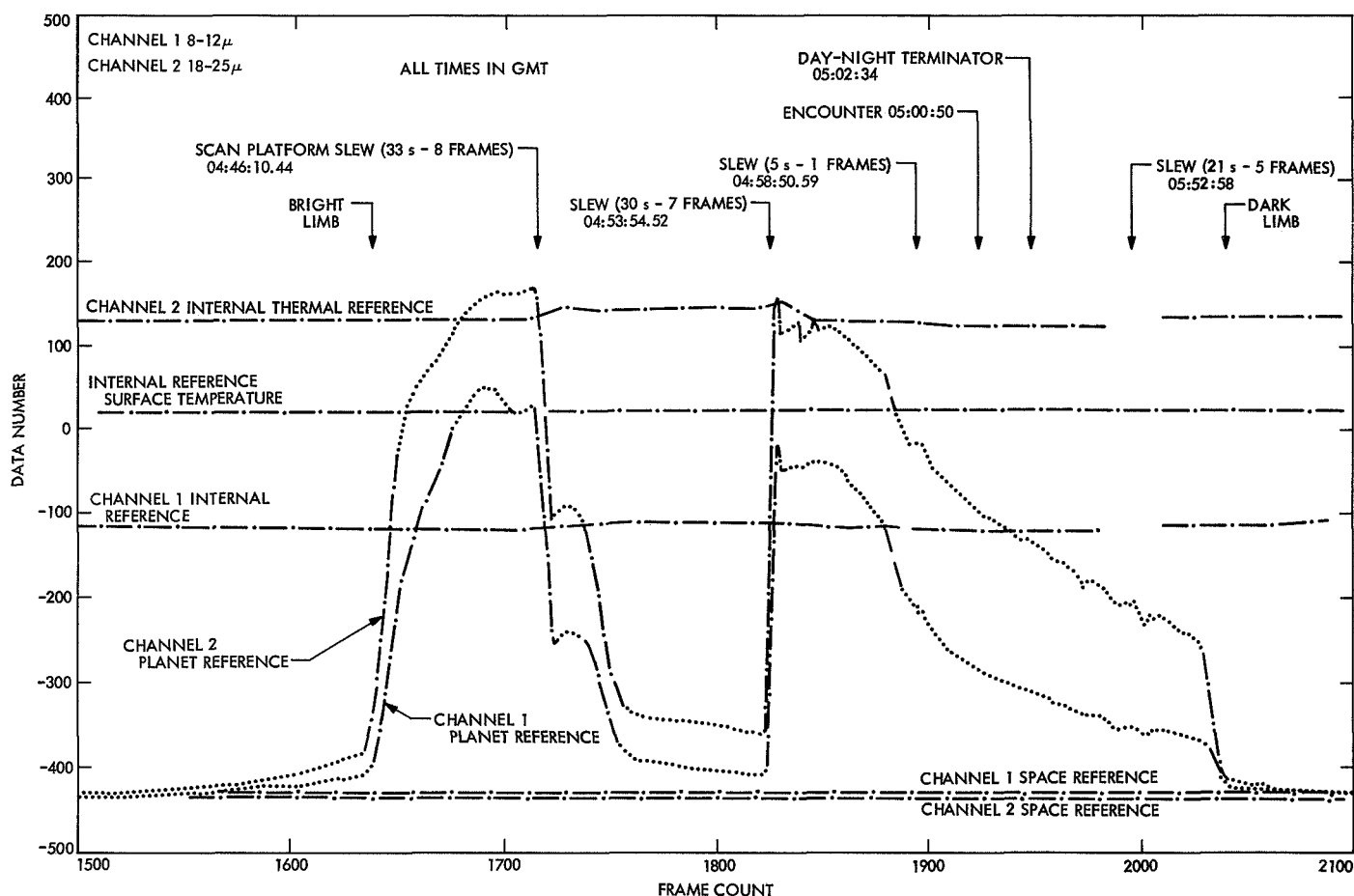


Fig. 25. Temperature history of Mariner VII infrared radiometer at encounter

cause of measurement deviations during scan-platform slews is under investigation.

After the recovery of *Mariner VII* following loss of contact during cruise, a special pre-encounter test was run for the purpose of reorienting the spacecraft. As *Mariner VII* moved across the planet, a change from a nominal space reading in the planet-view position to a warmer or more positive data number was very prominent, indicating that Mars was in the IRR field of view. Television pictures were taken and, with the IRR bore-sighted with the TV to within 0.3 deg and the optical alignment between the TV and the IRR known to  $\pm 0.1$  deg, orientation of the spacecraft was verified.

The IRR operated normally, with a noise level of approximately  $\pm 1$  DN at all times except during the scan-platform slews. Variances were noted in the data during these slews. As the spacecraft approached the planet, the data again followed a predicted curve.

#### D. Near-Encounter Performance

The *Mariner VI* IRR performed satisfactorily during near-encounter. All step functions were normal, and no out-of-sequence stepping was experienced. A good temperature profile of the planet was obtained. The temperatures appeared to be capable of correlation with areas seen during the pass. For hand plots of the telemetry data obtained during *Mariner VI* near-encounter, see Fig. 24.

The *Mariner VII* IRR also performed satisfactorily during near-encounter. All step functions were normal, and no out-of-sequence stepping was experienced. The temperature profile of the polar pass was good. During the scan-platform slew at the end of the south-polar-cap swath, the variances in the data were again noted. These were most prominent in frame 1831, when the reference reading on channel 2 read 154 DN instead of the proper reading of 131 DN.

After encounter, the IRR instruments on both spacecraft responded correctly to the DC-48 command to stow the mirror in a position pointing toward the internal thermal reference. This was done to prevent damage by sunlight during spacecraft roll maneuvers. Correct response to the DC-48 command was verified by receipt of only the normal internal-reference readings. For hand plots of the telemetry data obtained during the *Mariner VII* near-encounter period, see Fig. 25.

The *Mariner VI* IRR was reactivated on August 12, 1969, for postencounter exercises. Scans of the galactic plane were made that necessitated a 1-deg scan-platform slew every 4 s. The resulting channel 2 readings (nominally  $-442 \pm 1$  DN) varied from  $-452$  to  $-432$  DN, which was a variance of  $\pm 10$  DN from the nominal. This large variance is attributable to the noise caused by the platform slews, as previously noted during the encounter phase. (The *Mariner VII* IRR was not used in postencounter exercises.) The expected readings of the galactic plane would probably not have deviated more than 5 DN from the nominal value; therefore, they would have been completely lost in this noise. Consequently, the IRR scans of the galactic plane were considered unsuccessful.

## V. Data Automation Subsystem

### A. Objectives

The data automation subsystem provided the data handling and control for the science instruments. The science data were converted into digital form, stored, and routed to both the flight telemetry subsystem and the data storage subsystem for transmission to the Earth. Except for the data required during the occultation and celestial mechanics experiments, the science data were not obtained during the cruise portion of the flights.

### B. Performance

The performance of the data automation subsystem was excellent on both the *Mariner VI* and *VII* spacecraft. All far- and near-encounter functions were executed as designed.

The *Mariner VI* DAS was energized approximately 52 h before encounter, and the *Mariner VII* DAS was energized about 76 h before encounter, by receipt of the DC-25 command that turned science power on. The temperature of the DAS followed the predicted curve throughout both flights. During the encounter period, the temperature reached approximately 80°F for *Mariner VI* and 65°F for *Mariner VII*.

On July 30, 1969, at 12:28:47 GMT, the *Mariner VI* DAS received the first NAMG-2 signal from the narrow-angle Mars gate detector to start the near-encounter science data recording sequence. The signal was not expected until about 14 min before encounter, and receipt of the signal some 15 h early was cause for some concern. However, it was determined that the planet brightness of 0.039 ft-cd had exceeded the detector threshold level of 0.034 ft-cd, so that the signal should indeed have occurred when it did. For *Mariner VI*, the early NAMG-2 signal did not disturb the programmed sequence because the necessary companion signal N6 from the CC&S (or its backup signal DC-26 from the FTS) was not present.

The *Mariner VI* DAS did not lose sync throughout the entire mission, nor was the frame count upset. The length of the mission was insufficient to cause frame-count recycling. The *Mariner VII* DAS also did not lose sync nor experience frame-count upset during the mission. The length of this mission, however, was sufficient to cause the DAS frame count to recycle to zero. The recycling occurred on August 5 at 02:38 GMT (frame count = 65536), and was at the proper time.

The *Mariner Mars 1969* DAS was found to be much less sensitive to external noise than the previous designs flown. This improvement was the result of much stricter logic design rules, larger functional blocks of logic contained in each subassembly, and fewer interconnections between logic subassemblies.

No anomalous conditions occurred during either the *Mariner VI* or *VII* flights that could be attributed to the data automation subsystem.

## Reference

1. Born, M., and Wolf, E., *Principles of Optics*. Pergamon Press, New York, 1959.

## Glossary

AAC	automatic aperture control	LMC	Large Magellanic Cloud
A/DC	analog-to-digital converter	LOS	loss of signal
AEOT	analog end of tape	MCR	midcourse correction requirement
AFETR	Air Force Eastern Test Range	MECO	main engine cutoff ( <i>Centaur</i> )
AGC	automatic gain control	MES	main engine start
ATR	analog tape recorder	MSB	most significant bit
BECO	booster engine cutoff ( <i>Atlas</i> )	MSFN	Manned Space Flight Network
BER	bit error rate	MTF	modulation transfer function
CAP	cone angle position	NAMG	narrow-angle Mars gate
CAV	composite analog video	PAS	pyrotechnic arming switch
CCA	Canopus cone angle	PIFOV	planet in field of view
CC&S	central computer and sequencer	PMT	photomultiplier tube
DAP	digital antenna pattern	RFS	radio frequency subsystem
DAS	data automation subsystem	SAF	Spacecraft Assembly Facility
DEOT	digital end of tape	SCA	scan control actuator
DPODP	double-precision orbit determination program	SECO	sustainer engine cutoff
DSIF	Deep Space Instrumentation Facility	SIPM	star identification program for <i>Mariner</i>
DSN	Deep Space Network	SIT	separation-initiated timer
DSS	Deep Space Station	SNR	signal-to-noise ratio
DTR	digital tape recorder	SPAC	spacecraft performance analysis and command
DV	digital video	SPE	static phase error
EOT	Earth-observed time	TCA	time of closest approach
FCS	flight command subsystem	TCAT	telecommunications analysis team
FEPS	far-encounter planet sensor	TCFM	temperature control flux monitor
FPAC	flight-path analysis and command	TCP	telemetry and command processor
FTS	flight telemetry subsystem	TWT	traveling-wave tube
HRTS	high-rate telemetry subsystem	TWTA	traveling-wave tube amplifier
IPL	image processing laboratory	UVS	ultraviolet spectrometer subsystem
IRR	infrared radiometer subsystem	VCO	voltage-controlled oscillator
IRS	infrared spectrometer subsystem	VECO	vernier engine cutoff
LCE	launch complex equipment	VSWR	voltage standing-wave ratio

N71-20460

## TECHNICAL REPORT STANDARD TITLE PAGE

1. Report No. 32-1460, Vol. II	2. Government Accession No.	3. Recipient's Catalog No.	
4. Title and Subtitle  MARINER MARS 1969 PROJECT REPORT PERFORMANCE		5. Report Date March 1, 1971	
		6. Performing Organization Code	
7. Author(s) JPL Staff		8. Performing Organization Report No.	
9. Performing Organization Name and Address  JET PROPULSION LABORATORY California Institute of Technology 4800 Oak Grove Drive Pasadena, California 91103		10. Work Unit No.	
		11. Contract or Grant No. NAS 7-100	
		13. Type of Report and Period Covered  Technical Report	
12. Sponsoring Agency Name and Address  NATIONAL AERONAUTICS AND SPACE ADMINISTRATION Washington, D.C. 20546		14. Sponsoring Agency Code	
15. Supplementary Notes			
16. Abstract  <p>This second of three volumes of the Mariner Mars 1969 Project Report describes the performance of the mission by flight and Earth-based elements during the launch and space flight phases. The first volume describes the pre-operational activities, including planning, development and design, manufacture, and testing; the third volume deals with the scientific program, including experiment results.</p> <p>The dual-spacecraft (Mariners VI and VII) Mars flyby mission was successfully conducted according to plan. A number of flight anomalies were observed, including a major incident involving the Mariner VII spacecraft shortly before its Mars encounter, but these difficulties were overcome. The performance of all elements was generally excellent, and copious scientific data were returned to the Earth, including television pictures, ultraviolet and infrared spectral data, surface-temperature measurements, and other information.</p> <p>The flight performance of each element is analyzed, problems are discussed, and recommendations based on the experience are presented.</p>			
17. Key Words (Selected by Author(s))  Mariner Mars 1969 Project Scientific Instruments Telemetry and Command Tracking		18. Distribution Statement  Unclassified -- Unlimited	
19. Security Classif. (of this report)  Unclassified	20. Security Classif. (of this page)  Unclassified	21. No. of Pages  311	22. Price

## HOW TO FILL OUT THE TECHNICAL REPORT STANDARD TITLE PAGE

Make items 1, 4, 5, 9, 12, and 13 agree with the corresponding information on the report cover. Use all capital letters for title (item 4). Leave items 2, 6, and 14 blank. Complete the remaining items as follows:

3. Recipient's Catalog No. Reserved for use by report recipients.
7. Author(s). Include corresponding information from the report cover. In addition, list the affiliation of an author if it differs from that of the performing organization.
8. Performing Organization Report No. Insert if performing organization wishes to assign this number.
10. Work Unit No. Use the agency-wide code (for example, 923-50-10-06-72), which uniquely identifies the work unit under which the work was authorized. Non-NASA performing organizations will leave this blank.
11. Insert the number of the contract or grant under which the report was prepared.
15. Supplementary Notes. Enter information not included elsewhere but useful, such as: Prepared in cooperation with... Translation of (or by)... Presented at conference of... To be published in...
16. Abstract. Include a brief (not to exceed 200 words) factual summary of the most significant information contained in the report. If possible, the abstract of a classified report should be unclassified. If the report contains a significant bibliography or literature survey, mention it here.
17. Key Words. Insert terms or short phrases selected by the author that identify the principal subjects covered in the report, and that are sufficiently specific and precise to be used for cataloging.
18. Distribution Statement. Enter one of the authorized statements used to denote releasability to the public or a limitation on dissemination for reasons other than security of defense information. Authorized statements are "Unclassified-Unlimited," "U. S. Government and Contractors only," "U. S. Government Agencies only," and "NASA and NASA Contractors only."
19. Security Classification (of report). NOTE: Reports carrying a security classification will require additional markings giving security and downgrading information as specified by the Security Requirements Checklist and the DoD Industrial Security Manual (DoD 5220.22-M).
20. Security Classification (of this page). NOTE: Because this page may be used in preparing announcements, bibliographies, and data banks, it should be unclassified if possible. If a classification is required, indicate separately the classification of the title and the abstract by following these items with either "(U)" for unclassified, or "(C)" or "(S)" as applicable for classified items.
21. No. of Pages. Insert the number of pages.
22. Price. Insert the price set by the Clearinghouse for Federal Scientific and Technical Information or the Government Printing Office, if known.